New Methods for the Synthesis of

Pharmaceutical Azacycles

PhD Thesis

Peter Clark

Supervised by

Dr Glynn D. Williams

Chemical Development, GlaxoSmithKline

and

Professor Nicholas. C. O. Tomkinson

Department of Pure and Applied Chemistry, University of Strathclyde

February 2020

Declaration

This thesis is the result of the author's original research. It has been composed by the author and has not been previously submitted for examination which has led to the award of a degree. The author supervised an Industrial Placement student (S. J. M. Patterson) for 3 months and guided the direction of the research to synthesise several compounds in Section **3.10**.

The copyright of this thesis belongs to the author under the terms of the United Kingdom Copyright Acts as qualified by University of Strathclyde Regulations. Due acknowledgement must always be made of the use of any material contained in, or derived from, this thesis.

Peter R Clark

February 2020

Acknowledgements

I am incredibly grateful to both Glynn and Nick for your help, patience and guidance over the past 3.5 years. I would also like to thank the Chemical Development department at GlaxoSmithKline and the occupants of 2G135 for being supportive and encouraging of my research. I would personally like to thank Jerome Hayes for initial project guidance and Mike Anson for valuable conversations, career advice and for funding my research and travel within your unit. Harry Kelly for providing financial support for my attendance at international conferences, along with a continued passion and interest in my research. Katherine Wheelhouse for being particularly supportive and offering valuable conversations, both technical and personal. Susanne Davies for offering valuable insight for DoE analysis and James Wickens for aid with HRMS analysis and interpretation.

I would particularly like to thank Sarah for being an exceptionally motivated and driven student who I had the pleasure to supervise for 3 months during her Industrial Placement at GSK.

All the people I have shared the lab with over the past 3.5 years and been able to call my friends.

Finally, Rebecca. Thank you for your constant support, kindness and love.

Abstract

New methods for the synthesis of heterocyclic compounds are constantly required and sought after by the chemical industry. Specific heterocycles, including 1,2,3-triazoles and benzimidazoles are present in a multitude of pharmaceutical and agrochemical compounds.

Contained within this thesis is the discovery, optimisation and exemplification of a highly general method for the synthesis of 1,2,3-triazoles and a new methodology for the synthesis of a specific class of benzimidazole.

Chapter 1 concerns the synthesis of 1,2,3-triazoles. The state-of-the-art reaction to synthesise 1,2,3-triazoles uses high energy azides and alkynes, which require elaborate and lengthy synthetic procedures to incorporate these functional handles into the substrate. Moreover, the use of metal catalysts to furnish specific regioisomers of the 1,2,3-triazole product renders these reactions non-ideal from a financial, environmental and practical perspective. A new procedure has been designed which bypasses the use of azides and directly converts primary amines into 1,2,3-triazoles. The reaction is a 3-component coupling between α-ketoacetals, *p*-toluene sulfonylhydrazide and a primary amine and does not require a metal catalyst. Issues such as chemoselectivity, regiospecificity and scalability have all been addressed. An orthogonal set of conditions have been developed which allow for the chemoselective conversion of either aliphatic amines or aromatic amines into a 1,2,3-triazole depending on the utilised reaction conditions. The reaction has been exemplified multiple times to be highly efficient in the synthesis of 1,2,3-triazoles on a large scale in both batch and flow reactors. The reaction has been shown to give regiospecific access to 4-, 1,4-, 1,5-, 4,5-, 1,4,5- and 1-substituted systems and is often complete within less than 10 minutes. The desired triazoles can be isolated without chromatography in yields of up to 98% and the reaction has been exemplified on greater than 70 examples.

Chapter 2 concerns the synthesis of 2-aminobenzimidazoles. Current methods to synthesise benzimidazoles largely rely on the use of 1,2-diaminobenzenes whereby a series of synthetic procedures furnish the benzimidazole. A new C–H functionalisation reaction to form

2-aminobenzimidazoles has been developed which directly targets the synthesis of this heterocycle in one-step from aryl-guanidines. High throughput screening and statistical Design of Experiments have enabled the discovery of an efficient system which uses a simple copper salt as a catalyst to mediate a C–H functionalisation event using pivalic acid as an additive. Empirical examination of this additive reveals that increased steric bulk around the carboxylate moiety plays a key role in delivering useful yields of the desired benzimidazole, providing a potential explanation as to why pivalic acid is an effective mediator. The developed methodology has been applied to the synthesis of Emedastine, a marketed pharmaceutical compound, in which the key step was performed on a gram-scale, highlighting the practical utility of the developed procedure.

Abbreviations

°C	Denotes the temperature scale in degrees centigrade
δ	Chemical shift
λ	Wavelength
ν	Frequency (IR)
AAC	Azide Alkyne Cycloaddition
Ac	Denotes an acyl, or CH_3CO group
acac	Acetylacetonate anion
amu	Daltons, Atomic Mass Unit
app.	Apparent. Used to denote a chemical shift resembling a specific multiplet. *e.g. "app.* d" indicates an apparent doublet
aq	Aqueous
bar	Bar. Absolute pressure. Defined as 10^5 kPa
BINAP	2,2′-bis(diphenylphosphino)-1,1′-binaphthyl
Bn	Denotes a benzyl, or CH_2Ph group
Boc	Denotes a *tert*-butyloxycarbonyl, or $NCO_2C(CH_3)_3$ group
bpy	2,2'-bipyridine
Bz	Denotes a benzoyl, or PhCO group
cal	Calories, a unit of energy. Defined as 4.184 joules
CDI	Carbonyldiimidazole
CMD	Concerted metalation deprotonation
COD	1,5-cyclooctadiiene
Concn.	Concentration
Cp*	Pentamethylcyclopentadienyl anion
CSA	Camphor sulfonic acid
Cy	Denotes a cyclohexyl group
d.r.	Diastereomeric ratio
dba	Dibenzylideneacetone
DCB	Dichlorobenzene. Preceded by a numbering assignment to indicate relative positioning of chlorine atoms
DCM	Dichloromethane
DFT	Density Functional Theory
DG	Denotes a directing group
DIBALH	Di-*iso*-butylaluminium hydride
DIPEA	Di-*iso*-propylethylamine
DMA	*N,N*-dimethylacetamide
DME	Dimethoxyethane
DMF	*N,N*-dimethylformamide
DMSO	Dimethylsulfoxide
DNA	Deoxyribonucleic acid
DoE	Design of Experiments
E	Denotes the stereochemical assignment of an internal alkene in which the Cahn-Ingold highest priority substituents are on the opposite sides of the double bond
e.r.	Enantiomeric ratio
EAA	Ethyl acetoacetate anion
EH	2-ethylhexanoate
equiv.	Molar equivalents

Et	Denotes an ethyl, or CH_2CH_3 group
FDA	Food and Drug Administration
FT	Fourier Transform
Gly	Glycine
GSK	GlaxoSmithKline
h	Hour(s)
HFIP	Hexafluoroisopropanol
HOMO	Highest Occupied Molecular Orbital
HPLC	High-Performance Liquid Chromatography
HRMS	High-Resolution Mass Spectrometry
IPA	Isopropyl alcohol
^{i}Pr	Denotes an *iso*-propyl, or $CH(CH_3)_2$ group
IR	Infrared (spectroscopy)
J	Denotes the magnitude (in Hz) of the NMR coupling constants in a multiplet
KHMDS	Potassium bis(trimethylsilyl)amide
KIE	Kinetic Isotope Effect
LCMS	Liquid Chromatography Mass Spectrometry
LG	Leaving group
LUMO	Lowest Unoccupied Molecular Orbital
M. pt.	Melting point
m/z	Mass to charge ratio
MDAP	Mass-Directed Auto-Purification
Me	Denotes a methyl, or CH_3 group
min	Minute(s)
MO	Molecular Orbital
mol	Mole, molar amount
m_r	Reduced mass
Ms	Denotes a methanesulfonyl, or SO_2Me group
NMP	*N*-methyl-2-pyrrolidone
NMR	Nuclear Magnetic Resonance
^{n}Pr	Denotes a linear propyl, or $CH_2CH_2CH_3$ group
PFP	Pentafluorophenol
Ph	Denotes a phenyl, or C_6H_5 group
phen	Phenanthroline. Preceded by a numbering assignment to indicate relative positioning of nitrogen atoms
Piv	Denotes a pivaloyl, or $(CH_3)_3CO$ group
pKa	$-\log_{10}(K_a)$, where K_a is the acid dissociation constant of a specified Brønsted acid in aqueous conditions at 25 °C
PPA	Polyphosphoric acid
ppm	Parts per million
Py	Pyridine
R	Denotes a generic group which may be specified in context
r.t.	Room temperature
RDS	Rate-determining step
s	Second(s)
Sal	Salicylic acid
S_NAr	Nucleophilic aromatic substitution
STING	Stimulator of Interferon Genes
T	Temperature
t	Time

TBAI	Tetrabutyl ammonium iodide
TBME	*tert*-butyl methylether
TBPB	*tert*-butylperoxybenzoate
Tert	Tertiary
^{t}Bu	Denotes a *tert*-butyl, or $C(CH_3)_3$ group
TC	Thiophene 2-carboxylic acid
Tf	Denotes a trifluoromethylsulfonyl, or SO_2CF_3 group
TFA	Trifluoroacetic acid
THF	Tetrahydrofuran
tmp	Tetramethylpiperidine
TMS	Denotes a trimethylsilyl, or $Si(CH_3)_3$ group
Ts	Denotes a *p*-toluenesulfonyl, or $SO_2C_6H_4CH_3$ group
USD	United States Dollar
WHO	World Health Organisation
w.r.t	With respect to
Z	Denotes the stereochemical assignment of an internal alkene in which the highest priority substituents are on the same side of the double bond

Contents

0. General Introduction

0.1 The importance of nitrogen-containing heterocycles

Nitrogen-containing heterocycles are the cornerstone to the development of life. Deoxyribonucleic acid (DNA) is fundamentally constructed by the interaction of nitrogen-containing heterocycles and the intermolecular hydrogen bonding these species adopt.[1,2] The DNA base-pairs Guanine (**1**), Cytosine (**2**), Adenine (**3**) and Thymine (**4**), and the respective paired adducts they adopt, constitute the core nucleobase structure of DNA (Figure 1).
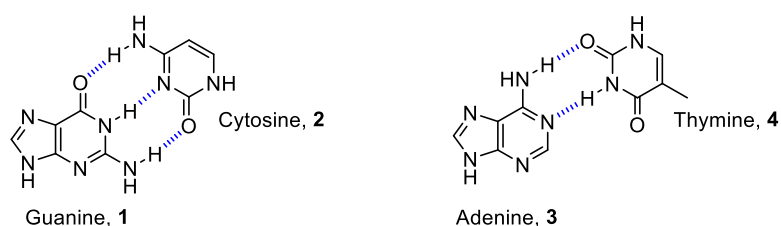

Figure 1: Guanine, Cytosine, Adenine and Thymine, the base-pairs of DNA

Further nitrogen-containing heterocycles are present in a plethora of essential natural biochemical processes, such as Pyridoxine (**5**, Vitamin B_6) and Cobalamin (**6**, Vitamin B_{12}) (Figure 2), two species in which the heterocyclic moiety (pyridine and benzimidazole respectively) are central to their biochemical roles.[3,4]
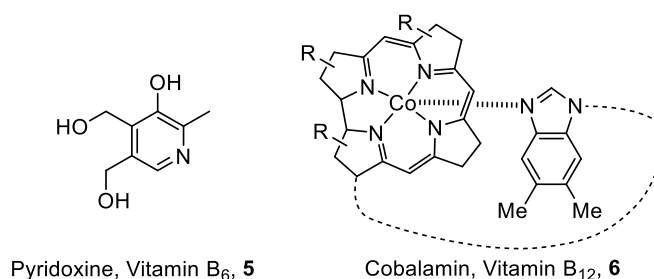

Figure 2: Vitamin B_6 and B_{12}, two important biological nitrogen heterocycles

Owing to the importance of these species, it is unsurprising that numerous industries have capitalised on the ability of nitrogen-containing heterocycles to elicit useful and valuable biological responses. Nitrogen-based heterocycles are often key features of modern pharmaceutical compounds, highlighted by a recent analysis of FDA approved drugs in the

U.S.A. summarising that 59% of all unique small-molecule drugs contain a nitrogen heterocycle (from herein described as an azacycle).[5] This indicates that the public health sector is dependent on the advancement of novel and improved methodologies to develop the next-generation of pharmaceutical compounds.

In particular, one of the most common types of heterocycle adopted by the pharmaceutical industry are 5-membered azacycles.[6] Nitrogen can be incorporated into a range of 5-membered rings in which the positioning and number of the nitrogen atom(s) result in different physiological responses. Displayed in Figure 3 are the different 5-membered azacycles which are possible. Pyrrole (**7**), a 5-membered species containing one nitrogen atom is present in a range of important biochemicals, including haemoglobin.[7] Increasing the number of nitrogen atoms in the ring to two gives rise to two different regioisomeric heterocycles, these being pyrazole (**8**) and imidazole (**9**). Pyrazole is the chemical structure obtained when the two nitrogen atoms are adjacent to each other, and imidazole is obtained when the nitrogen atoms are separated by a carbon unit. Histidine, one of the 20 proteogenic amino acids, contains an imidazole unit.[8] Adding a third nitrogen atom gives rise to two regioisomeric triazole motifs; 1,2,3-triazole (**10**) and 1,2,4-triazole (**11**). Adding a fourth nitrogen atom results in the formation of tetrazole (**12**). Finally, although strictly not an *organic* azacycle, the last in this series is pentazole (**13**), a 5-membered compound in which all the atoms within the ring-system are nitrogen. Examples and applications of pentazole are rare and only recently has the parent heterocycle (**13**) been synthesised.[9]
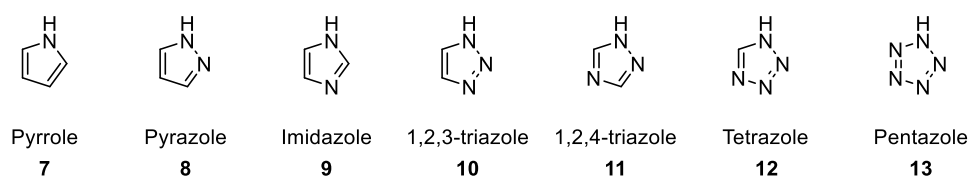
Pyrrole	Pyrazole	Imidazole	1,2,3-triazole	1,2,4-triazole	Tetrazole	Pentazole
7	**8**	**9**	**10**	**11**	**12**	**13**

Figure 3: The 5-membered azacycles

Key examples of these heterocycles are presented in Figure 4 in which the displayed drug products elicit a range of valuable pharmaceutical responses. Atorvastatin (**14**) is arguably the best example of a 5-membered azacycle and at the "core" of the drug is contained the pyrrole

heterocycle. This is one of the best-selling drugs of the last 16 years and generated sales of nearly $13 billion USD in its best-selling year (2006).[10] Celecoxib (**15**) is an example of a pyrazole-containing pharmaceutical compound. This species is a nonsteroidal anti-inflammatory drug and is used for the treatment of rheumatoid arthritis.[11] Midazoloam (**16**) contains an imidazole and is often used to elicit an analgesic response.[12] Tazobactam (**17**), an antibiotic[13] and Anastrozole (**18**), a breast-cancer treatment[14] are triazole regioisomers, being a 1,2,3-triazole and 1,2,4-triazole respectively. Finally, Candesartan (**19**), which is used to treat elevated blood pressure and heart failure, contains both a tetrazole and an imidazole motif.[15] These six examples offer an important insight as to why 5-membered azacycles are highly important and sought-after moieties by chemical industries. This thesis is concerned with the preparation of two specific azacycles: 1,2,3-triazoles and 2-aminobenzimidazoles.
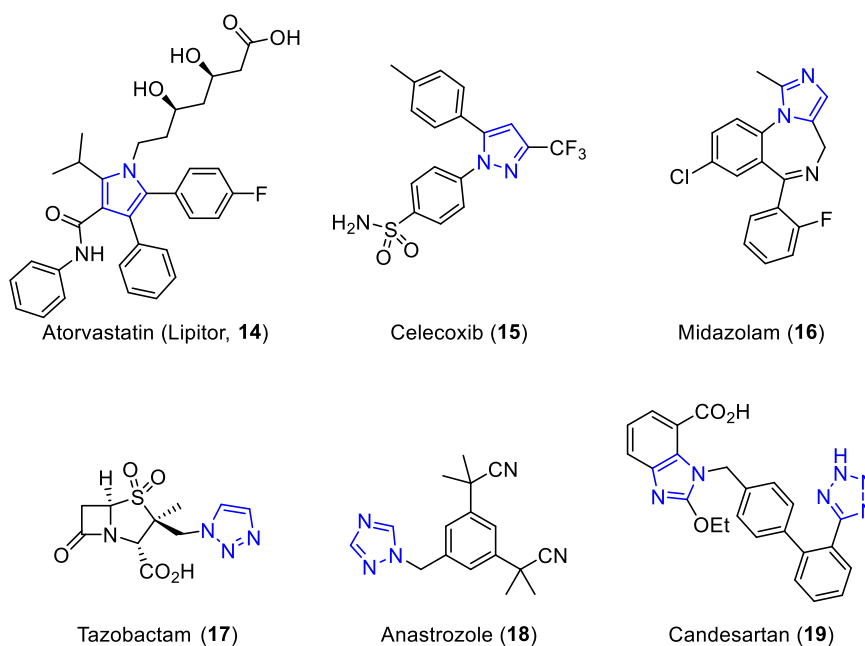

Figure 4: Important examples of the 5-membered azacycle series within pharmaceutical compounds

Chapter one

1. Introduction

1.1 The importance of 1,2,3-triazoles

The 1,2,3-triazole heterocycle is a 5-membered azacycle with three adjacent nitrogen atoms (Figure 5). Undoubtedly this chemical scaffold has been popularised through the development of one of the most prominent "Click" reactions; the [3+2] dipolar cycloaddition of an alkyne with an organic azide. The copper-catalysed azide-alkyne cycloaddition (CuAAC) was reported in two papers published in 2002 by Sharpless and Meldal.[16,17]
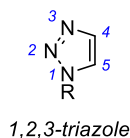

1,2,3-triazole

Figure 5: 1,2,3-triazole

The 1,2,3-triazole has a range of applications in functional coatings, DNA modification and is present within medicinal compounds.[18-20] 1,2,3-triazoles have further been shown to display potency as antivirals, antihistamines, antioxidants and antibacterials, as well as displaying activity for the treatment of Parkinson's disease and obesity-related illnesses.[21-25] Examples of the 1,2,3-triazole structure in marketed drugs include Tazobactam (**17**), Rufinamide (**20**) and Mubritinib **21** (Figure 6). In recent years, it has been shown that the 1,2,3-triazole is bioisosteric with the *trans*-conformation of an amide bond. This has provided medicinal chemists with a new avenue to pursue when exploring the structure-activity relationship of new pharmaceutical compounds (Figure 6).[26,27] These factors considered, it would be unsurprising if a number of new compounds containing a 1,2,3-triazole moiety progress through the pharmaceutical and agrochemical pipelines, given the favourable properties of this heterocyclic scaffold.
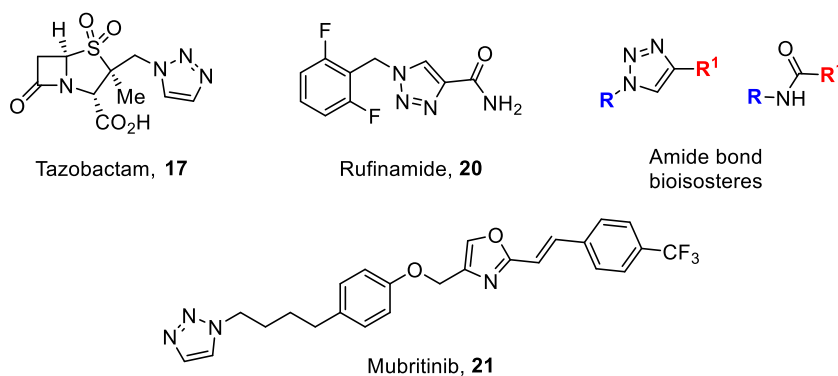
Figure 6: Applications of the 1,2,3-triazole

Arguably however, the 1,2,3-triazole to-date has seen its largest impact as a molecular scaffold within chemical biology and target identification.[28-33] The reactions which are adopted by chemical biologists to be used *in-vivo* are required to be fast, have extremely high functional group tolerance, be stable under biological conditions and result in the formation of little-to-no waste by-products. Fulfilling these criteria, and as such being one of the most utilised reactions in a chemical biologist's toolkit, is the CuAAC reaction.[29]
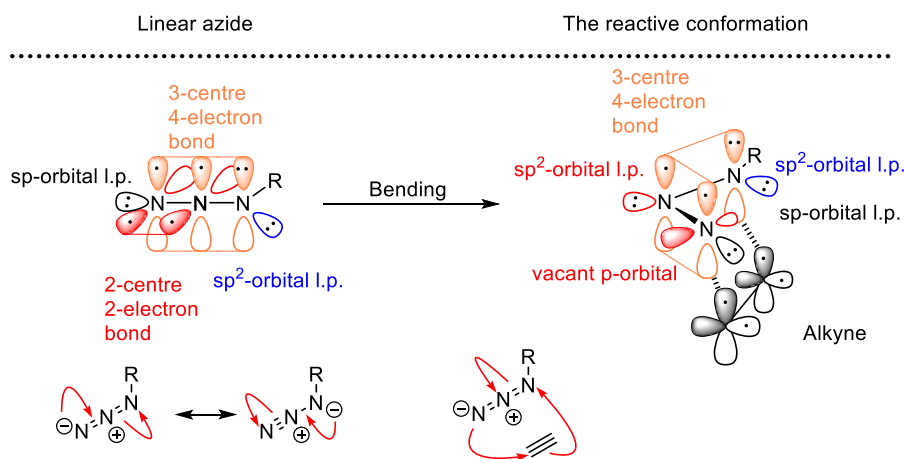
1.2 The azide-alkyne cycloaddition

The thermal [3+2] dipolar cycloaddition between an azide and an alkyne was initially reported in a relatively uncited & uncredited report by Dimroth in 1902.[34] However, Dimroth's main research interests were focussed on the unusual rearrangements that certain substitution patterns of 1,2,3-triazoles undergo, now termed the Dimroth rearrangement.[35,36] The cycloaddition was also picked up in a review from Smith in 1938. It was reported that acetylene (**22**) reacts with hydrazoic acid (**23**) and phenylazide (**24**) to form the corresponding triazoles (Scheme 1).[37] However, the generality and scope of this procedure were not examined, so the reaction and its potential remained unexplored.

22 R = H, **23** R = H, **25**
   R = Ph, **24** R = Ph, **26**
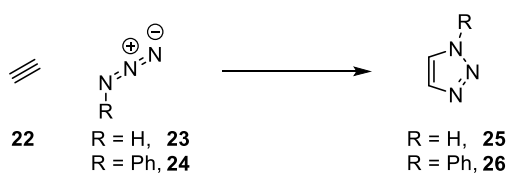
Scheme 1: The azide-alkyne cycloaddition (AAC)

It wasn't until the 1960s when Hüisgen reported his findings on 1,3-dipolar cycloadditions that this reaction to form 1,2,3-triazoles started to gain interest.[38,39] Hüisgen detailed an in-depth analysis of a number of [3+2] dipolar cycloadditions, including the use of azides and alkynes as substrates. A major artefact of the report was the in-depth mechanistic studies, including molecular orbital (MO) descriptions of the substrates and overall reaction mechanism.[40] Hüisgen concluded that the reaction proceeds through a concerted addition, "*in which the two new σ-bonds are formed simultaneously.*"[40] Scheme 2 details Hüisgen's MO description of the reaction mechanism. The first major point to note is that the geometric configuration of an azide constitutes a linear N–N–N system. Secondly, the MO description of an azide is a 3-centre, 4-electron (3c,4e) π-bond and a regular π-bond (shown in orange and red respectively). This 3c,4e-bonding is impossible to describe in one skeletal structure, but the two resonance forms of an azide accurately describe this (Scheme 2). For the cycloaddition to occur, the azide needs to bend for the π-systems of the alkyne and the azide to efficiently overlap. To achieve the reactive configuration of 120 °, the regular π-bond (shown in red) is required to break. In doing so, the π-bond electrons are described as having to reside in an sp^2 orbital on the central nitrogen, leaving a vacant p orbital on the terminal nitrogen. The energy lost from breaking of the π-bond is somewhat compensated by rehybridisation of the central nitrogen atom and containment of the resultant lone pair in an sp^2 orbital of high 's' character. This energy payback enables effective bending of the azide to engage in the concerted addition with the π-system of the alkyne. This report by Hüisgen was the first accurate description of the reaction mechanism for [3+2] dipolar cycloadditions and to this day remains the largely favoured mechanism based on experimental and computational observations.

Linear azide

The reactive conformation

3-centre
4-electron
bond

sp-orbital l.p.

2-centre
2-electron
bond

sp²-orbital l.p.

3-centre
4-electron
bond

sp²-orbital l.p.

sp²-orbital l.p.

sp-orbital l.p.

Bending

vacant p-orbital

Alkyne

R

Scheme 2: The mechanism and molecular orbital description of the azide-alkyne cycloaddition

Despite offering a huge scope and excellent mechanistic understanding, the thermal dipolar cycloaddition presents two key problems. Arguably the main problem resides in the fact that the reaction displays poor regioselectivity. Often reactions give mixtures of the 1,4- and 1,5-substituted triazoles, which can be difficult to separate and therefore would result in lower yields of the desired regioisomer. An example is given in Scheme 3 using phenylacetylene (**27**) and phenylazide (**24**) resulting in regioisomeric products **28** & **29** in 43% and 52% isolated yield respectively.[39]

$R-N_3$ R^1

R^1

24 **27**

Toluene

Reflux

28, 43% **29**, 52%

1,4-substituted 1,5-substituted
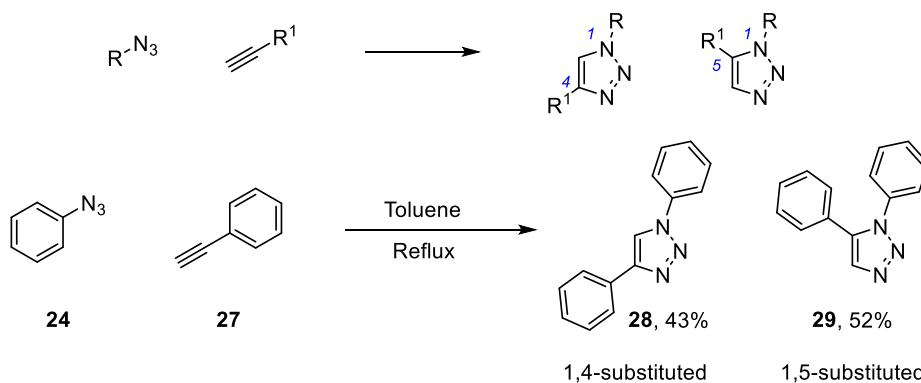
Scheme 3: Regiochemical challenges with the AAC

Moreover, owing to the high activation energy of the transformation, the reactions often require heating for long reaction times.[16] The transition state energies for the 1,4- and 1,5-substituted products between methyl azide and propyne have high activation energies of 25.7 and 26.0 kcal mol⁻¹.[41,42] The small difference between these two barriers (0.3 kJ mol⁻¹) explains the poor

regioselectivity. Figure 7 describes the optimised transition-state structures for the formation of both regioisomers, highlighting the poor differentiation between the formation of either regioisomer.
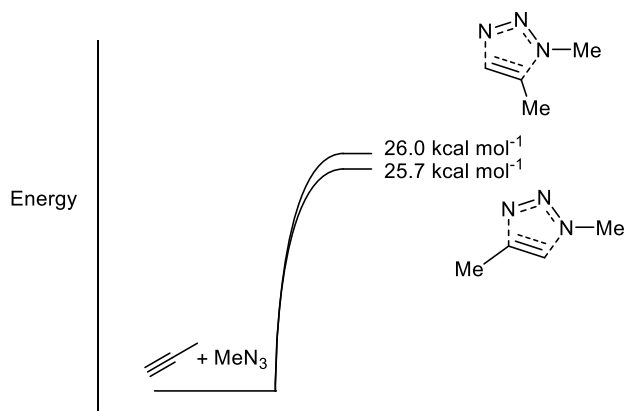

Figure 7: Poor energetic differentiation between the regioisomeric transition states

1.3 The copper-catalysed azide-alkyne cycloaddition (CuAAC)

Owing to the highlighted regiochemistry problems, in 2002 when Sharpless and Meldal published their independent reports of the CuAAC, it is unsurprising that the chemical community were quick to adopt these processes.[16,17] With a catalytic amount of a copper salt (Cu(I) being the active catalyst, produced *in-situ* by reduction of Cu(II) using sodium ascorbate), terminal alkynes and organic azides react to give 1,4-substituted triazoles with complete regioselectivity (Scheme 4). The functional group tolerance of the reaction proved remarkable, and the reported conditions were incredibly mild.
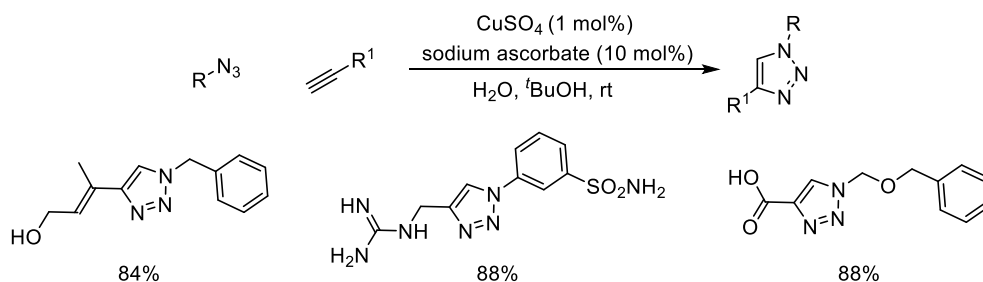
Scheme 4: Copper-catalysed AAC (CuAAC). Regioselective 1,4-triazole synthesis

1.3.1 The mechanism for the CuAAC

The mechanism for the CuAAC proved very challenging to study, not least owing to the small redox potentials for Cu(II)/Cu(I), the propensity for Cu(II) species to disproportionate *in-situ* and the tendency for copper-complexes to aggregate.[43] It quickly became apparent that the CuAAC was not concerted, unlike the uncatalysed variant described by Hüisgen: this reaction proceeds *via* a polar, stepwise mechanism.[44] Moreover, early DFT evidence suggested that the reaction involved one copper species and the cyclisation proceeded through subsequent annulation steps after predicting a number of unprecedented intermediates.[42] In a mechanism proposed by Sharpless (Figure 8), copper acetylide **32** (*c.f.* Sonogashira reaction[45]) coordinates to the azide (**33**) to give intermediate **34**, displacing a ligand on the copper (not shown in Figure 8 for clarity). The distal nitrogen of the azide then attacks the acetylide to give **35**, whereby subsequent rearrangement gives the desired copper-triazolide **36** which subsequently undergoes protodecupration to give the desired triazole.
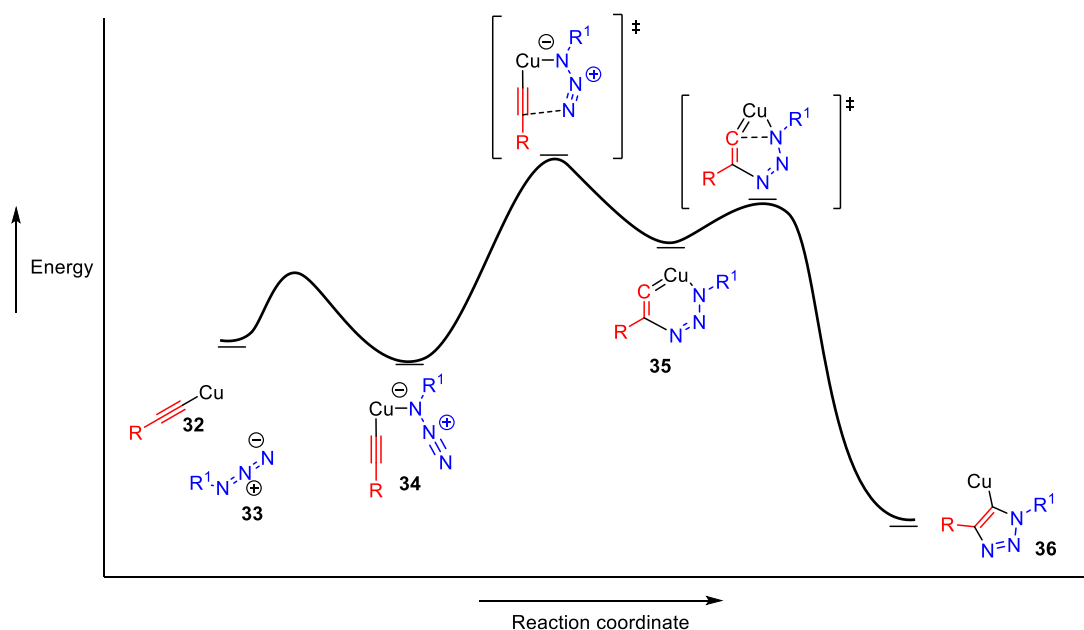

Figure 8: The first suggested CuAAC mechanism

However, several papers published after Sharpless' work suggested that the reaction involves two separate copper species operating through a dinuclear mechanism. This essentially ruled out the mechanism described in Figure 8.[46,47] In 2013, Fokin published the now widely-accepted mechanism for the CuAAC.[48] Through a series of control reactions using an isolable

and stable copper-acetylide, it was shown that in the absence of an exogenous copper source, copper-acetylides and azides do not undergo the [3+2] dipolar cycloaddition. On addition of an exogenous copper source to a copper-acetylide and an azide, the reaction was observed by real-time heat-flow reaction calorimetry to quickly and smoothly undergo the desired reaction to form the triazole. This showed that a binuclear mechanism was at play. The new, adjusted mechanism proposed by Fokin is presented in Scheme 5. Starting with alkyne **37**, the first copper atom engages in π-coordination with the alkyne (**38**), to then readily undergo formation of a copper acetylide. The copper acetylide rapidly engages in weak π-coordination with a second copper species to form **39**. At this point, coordination of the azide to the non-acetylenic copper forms intermediate **40** which is primed to undergo the first C–N bond-forming step to form binuclear species **41**. This is the step in which the exquisite regioselectivity is obtained; the current understanding is that R and R^1 are orientated apart, as supported by DFT studies,[49] which ultimately results in formation of the 1,4-substituted product **43**. Through isotopic labelling of the copper species, the first C–N bond-forming step was shown to produce intermediate **41**, a species which contains a plane of symmetry (i.e., with indistinguishable copper atoms). The second C–N bond-forming step forms copper triazolide **42** and protonation of this yields the final triazole (**43**).
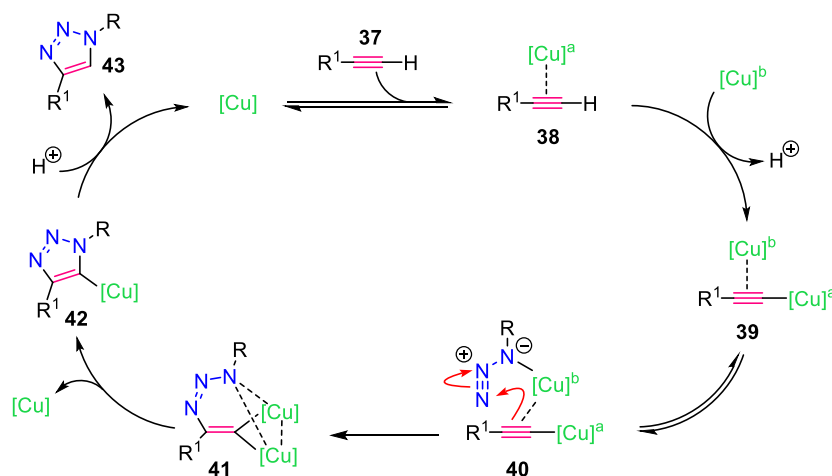

Scheme 5: The generally accepted CuAAC mechanism based on experimental and theoretical observations

Within chemical sciences, the advancements of the synthetic application and mechanistic understanding of the CuAAC have been high-impacting and wide spanning in application. These reactions have enabled a completely regioselective synthesis of 1,4-substituted 1,2,3-triazoles from azides and terminal alkynes through the addition of catalytic quantities of a simple copper salt. However, this methodology does not allow for the synthesis of 1,5-substituted or 1,4,5-trisubstituted triazoles.

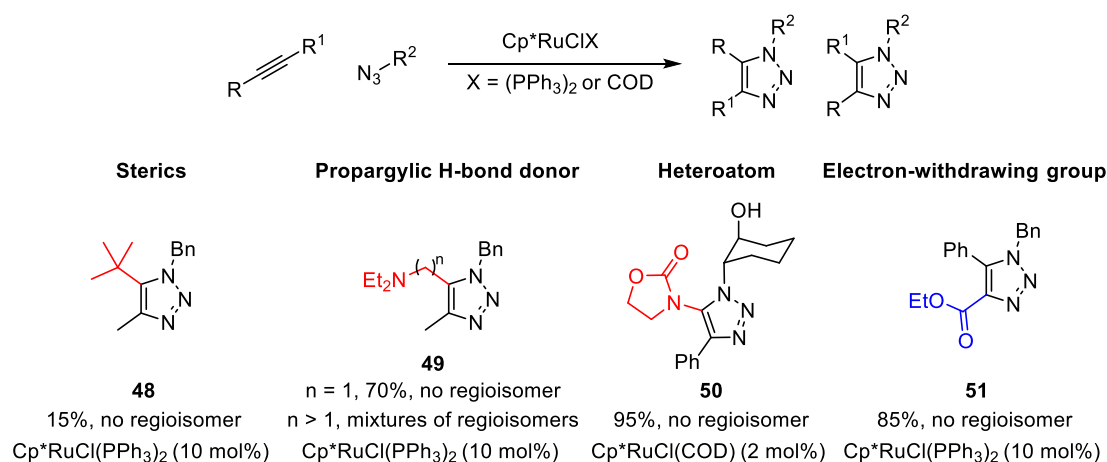## 1.4 The ruthenium-catalysed azide-alkyne cycloaddition (RuAAC)

The regioselective synthesis of 1,5-triazoles was reported in 2005 by Sharpless and Fokin (**44–46**, Scheme 6).[50] This procedure, which complements the CuAAC reaction, gives exclusive access to 1,5-triazole products, with a similarly high level of functional group compatibility to the CuAAC. Moreover, the protocol allows for internal alkynes to react to give a 1,4,5-trisubstituted triazoles, providing access to products such as 4,5-diphenyl triazole **47** in a quantitative yield. The reaction to form 1,5-triazoles is highly dependent on the ligand environment on the ruthenium centre, with the Cp* ligand being crucial to impart the high-level of regiocontrol on the reaction. When Ru(OAc)$_2$(PPh$_3$)$_2$ was used, the major product was the 1,4-substituted product. The triphenylphosphine ligand proved to be a spectator ligand only – when this was replaced with other ligands (such as COD, NBD and chloride), the reaction remains unaffected.
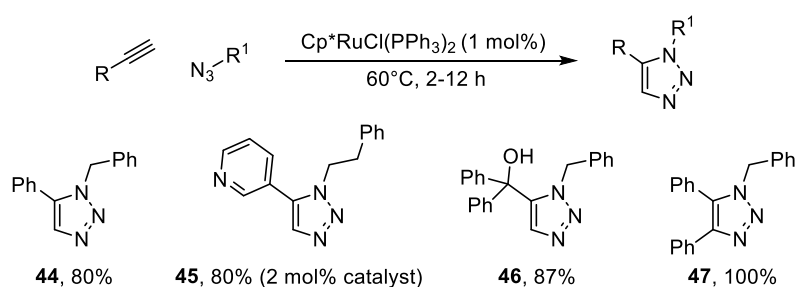
Scheme 6: Ruthenium-catalysed AAC (RuAAC). Regioselective 1,5-substiututed triazole and 1,4,5-substituted triazoles

1.4.1 Regiochemical observations

Internal alkynes give access to 4,5-substituted triazole products.[41] The reaction proceeds efficiently when a symmetrical alkyne is used, however, when using an unsymmetrical internal alkyne, the reaction can give rise to regioisomers of the triazole product. A summary of the empirical observations made in the literature are highlighted in Scheme 7. When an alkyl-disubstituted internal alkyne is used (R, R^1 = alkyl), mixtures of regioisomers are obtained. This is only biased when the steric differentiation is large, exemplified by ^{t}Bu triazole **48** being observed in a 15% yield as the exclusive regioisomer. If R = aryl and R^1 = alkyl, poor regioselectivity is also observed. Where the alkyne starting material contains a propargylic H-bond donor as in **49** (n=1), exclusive positioning of this group into the 5-position of the triazole product is observed. Moving the H-bond donor further away (n>1) results in the formation of regioisomeric triazoles. Next, introducing a heteroatom into the alkyne positions this group into the 5-position of the triazole (**50**). Finally, electron-withdrawing groups are placed in the 4-position of the triazole product (**51**).[41,51-53]

| Sterics	Propargylic H-bond donor	Heteroatom	Electron-withdrawing group
48	**49**	**50**	**51**
15%, no regioisomer	n = 1, 70%, no regioisomer	95%, no regioisomer	85%, no regioisomer
Cp*RuCl(PPh$_3$)$_2$ (10 mol%)	n > 1, mixtures of regioisomers	Cp*RuCl(COD) (2 mol%)	Cp*RuCl(PPh$_3$)$_2$ (10 mol%)
	Cp*RuCl(PPh$_3$)$_2$ (10 mol%)		

Scheme 7: Regiochemical observations for RuAAC

The regiochemical determination of the RuAAC of internal alkynes is thus challenging to predict. Unless the system is heavily biased towards these empirical observations, it is likely that mixtures of regioisomeric triazoles will be obtained.

1.4.2 The mechanism for the RuAAC

The mechanism for RuAAC is fundamentally different from CuAAC. This is implied by the successful formation of 4,5-substituted products which indicates that formation of a metal-acetylide is not an active mechanistic pathway in these transformations. Several mechanistic and theoretical studies have been performed and the generally accepted mechanism for the RuAAC is displayed in (Scheme 8).[41,50,51] Coordination of the alkyne to the ruthenium centre locates the 'R' group away from the azide to minimise steric interactions. Metalocyclopropene intermediate **52** then adds to the electrophilic terminal end of the azide to form the new carbon-nitrogen bond (**53**). The reductive elimination to form the second carbon-nitrogen bond (**54**) has been suggested to be the rate-determining step. Finally, decomplexation of the triazole (**55**) from the ruthenium completes the catalytic cycle to form **56**, the active catalyst.
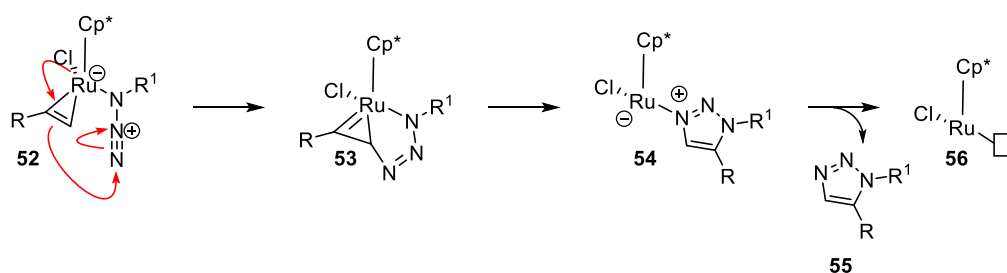

Scheme 8: The generally accepted mechanism for the RuAAC

The current challenges with RuAAC are emphasised when a regioselective synthesis of a triazole is required in which poor differentiation with an internal alkyne is observed. Moreover, the fundamental requirement for the use of azides in CuAAC and RuAAC necessitates synthetic procedures to incorporate these functional groups into organic compounds.

1.5 1-Substituted triazoles

To access 1-substituted triazoles the required alkyne is acetylene. These reactions can often be performed in the absence of a catalyst and use acetylene gas directly.[54] However, the use of acetylene gas presents an inherent safety concern and requires specialist equipment to handle safely.[55,56]

Alternatives to the use of acetylene have been presented in the literature, many of which are "protected" acetylene equivalents.[57-60] Scheme 9 displays a range of acetylene surrogates that have been reported in the literature. These include TMS (**57**), acetone (**58**) and carboxylate-protected species (**59**), along with the use of an inorganic source of acetylene, calcium carbide (**60**). Often the isolated triazoles from these reactions still contain the protecting group, which later needs to be removed, adding a synthetic step and an inevitable loss in yield associated with the deprotection. Recently, ethenesulfonyl floride (**61**) has been reported as an effective acetylene surrogate which smoothly undergoes reaction with an azide to form a 1-substituted triazole.[61]

Acetylene analogues
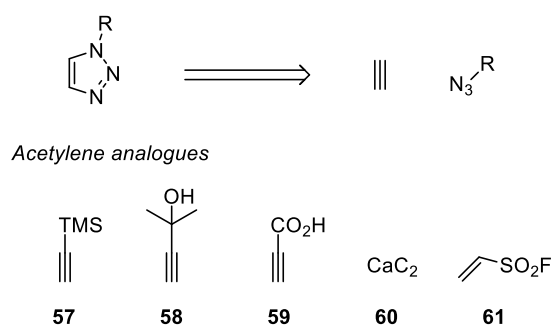
Scheme 9: 1-substituted triazole retrosynthesis

1.6 The challenges with azides

1.6.1 Azide incorporation into give an organic compound

The most common method for the introduction of an alkyl azide (**62**) is through displacement of a leaving group (**63**, chloride, bromide, tosylate) with sodium azide (Scheme 10, left).[62] Aromatic azides (**64**) are most commonly prepared by diazotisation of an aniline (**65**) followed by S_NAr with sodium azide, or directly from anilines with diazo-transfer reagents (Scheme 10, right).[63,64]
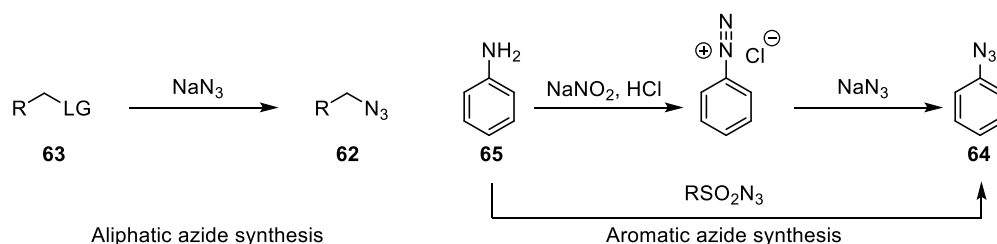
Scheme 10: Incorporation of azides into organic compounds

Very recently, Sharpless reported the direct conversion of primary amines into organic azides with the diazo-transfer reagent fluorosulfuryl azide (FSO_2N_3, **66**) in which the azide product does not require purification (Scheme 11).[65] The authors were able to directly convert primary amines into azides with **66**, followed by *in-situ* CuAAC to form a diverse triazole library. The addition of this synthetic step however, decreases the overall efficiency of the resultant synthesis of a triazole product.
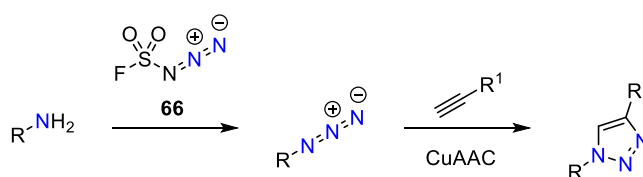
Scheme 11: Sharpless' azide synthesis from primary amines using fluorosulfuryl azide

1.6.2 Azide safety concerns

A second factor to consider is the high energy associated with organic azides. Azides are known to decompose under thermal conditions or prolonged exposure to light.[66,67] This

decomposition releases nitrogen; an uncontrolled release of this gas can be dangerous when performing reactions with azides on scale.[68] Moreover, there are safety concerns associated with the toxicity of sodium azide.[69] These factors explain why, realistically, an azide is produced *in-situ* through the introduction and consumption of this species within two consecutive synthetic steps to minimise handling.

1.6.2.1 The scalability of the CuAAC

After introduction of the azide, the products are often used directly in the subsequent triazole forming step without purification. The CuAAC has been examined as a method for the feasible construction of 1,2,3-triazoles on scale, and the Early Chemical Development team at AstraZeneca were apprehensive about the potential to generate copper azide.[70] Scheme 12 describes the synthetic sequence undertaken to form ester-containing triazole **67**. The azide was introduced from α-bromoester **68** by an S_N2 reaction to form alkyl-azide **69**. The risk with using azide **69** directly in the subsequent CuAAC with alkyne **70** was that any residual sodium azide could then undergo a salt metathesis with the copper catalyst to form copper azide. The AstraZeneca chemists used real time in-line monitoring of the reaction by FTIR to examine the levels of sodium azide remaining after the S_N2 reaction. Sodium azide has a strong IR absorption band at 2050 cm^{-1} and monitoring of this window gave a qualitative understanding of the residual levels of sodium azide before bringing it into contact with a copper catalyst. However, monitoring of this window does not give quantitative proof of total consumption of sodium azide. The detection threshold of sodium azide by the FTIR probe was not determined and so there remained the risk of producing copper azide.
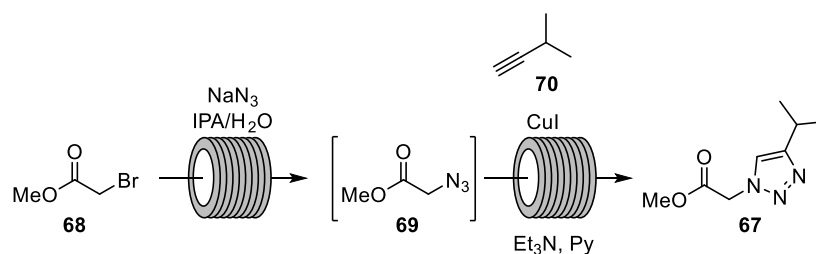
Scheme 12: AstraZeneca's telescoped triazole synthesis which was monitored by FTIR

Copper azide is a detonator and as such a primary explosive.[71-73] Process safety departments are quick to highlight the CuAAC as a 'red-flag' reaction and enforce stringent safety controls to mitigate the formation of copper-azide. In 1976 the National Institute for Occupational Safety & Health issued an explosion warning to hospitals and clinical laboratories about the disposal of sodium azide waste.[73] Solutions of sodium azide (concentrations of <0.1%) were used as a diluent for automatic blood cell counters and these were routinely disposed of through the plumbing systems of the labs. These plumbing systems contained lead, copper and brass that, when exposed to sodium azide, could form accumulations of lead and copper azide, both of which are shock sensitive primary explosives. Copper(I) azide has a very low friction sensitivity before detonation (2.66 N cm^{-2}), lower than that of any other metal-azide tested in a military examination of primary explosives.[74] This emphasises the significant safety concern associated with the production of copper azide and arguably indicates that reactions which are at risk of forming this species should be avoided for large-scale purposes.

An alternative to this inherent safety problem would be to circumvent the use of azides to make triazoles altogether, through direct conversion of a primary amine into the desired triazole (Scheme 13). Primary amines are the most widely available functional group from commercial suppliers,[75] making it desirable to use these substrates directly as the functional handle. It is therefore unsurprising that the direct conversion of a primary amine into triazoles has received the attention of synthetic chemists.
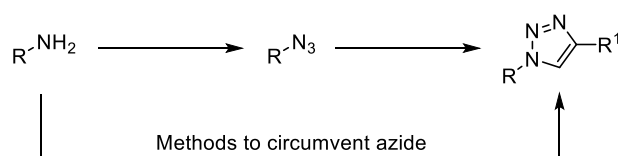

Scheme 13: 1,2,3-triazole synthesis circumventing an azide

## 1.7 1,2,3-triazoles from primary amines

1.7.1 Oxidative methodologies

Several methods to directly convert a primary amine into a triazole have been reported. Wang and Ji published an oxidative method to synthesise 1,4-diaryl substituted triazoles **73** from acetophenone-derived tosylhydrazones **71** and anilines **72** (Scheme 14).[76] The procedure uses an oxidative mediator (I_2) and the terminal oxidant *tert*-butyl peroxybenzoate (TBPB) to regenerate I_2 *in-situ*. The procedure proved to be robust in the synthesis of diaryl substituted triazoles, but the authors do not report the formation of products which are not derived from acetophenones. This is likely to do with the proposed mechanism which involves enolisation of acetophenone and trapping with I_2. A ketone substrate with two enolisable positions would therefore give regioisomeric triazoles.
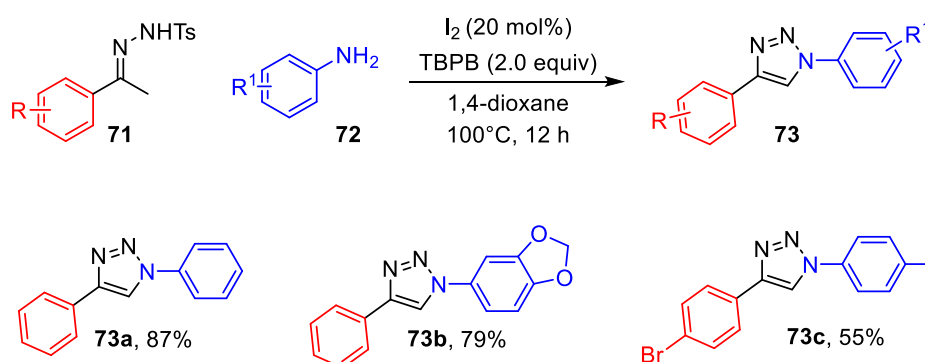

Scheme 14: Wang and Ji's oxidative methodology to form triazoles from hydrazones and aromatic amines

At the same time, Zhang published a very similar study using hydrazones (**71**) and anilines (**72**), with stoichiometric iodine as the oxidant, in which the scope and observed yields were virtually identical to Wang and Ji's report (Scheme 15).[77] Zhang noted that aliphatic amines behaved worse under the reaction conditions giving poor yields of the desired triazole. No explanation was offered other than the observation that reaction mixtures contained a complex mixture of products.
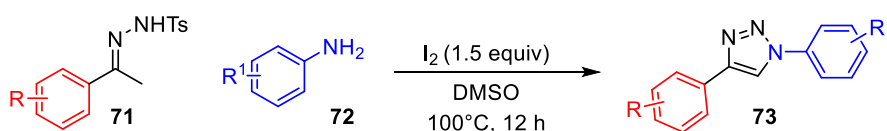
*Scheme 15: Zhang's oxidative triazole synthesis from hydrazones and aromatic amines*

In 2013, Zhang further revealed an oxidative copper-promoted triazole formation using tosylhydrazones (**74**) and aromatic amines (**75**) under aerobic conditions (Scheme 16).[78] The procedure exhibited excellent functional group tolerance and an extensive range of aromatic amine substrates were explored (**76**). Moreover, the reaction could generate 1,4,5-substituted triazoles, providing access to products such as **76c** which would be challenging to access *via* traditional AAC chemistry. One key problem with this methodology, as was noted by the authors, was that aliphatic amines were not tolerated; such reactions generated very complicated mixtures of products.

76a, 73%   **76b**, 63%   **76c**, 50%
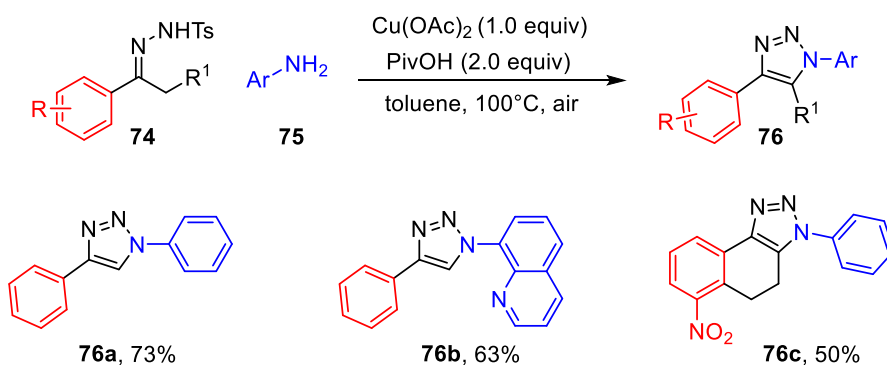
*Scheme 16: Zhang's oxidative copper(II) acetate methodology to form triazoles*

Zhang furthered this research using modified conditions with tosylhydrazones (**77**) and allowed for the use of aliphatic amines (**78**) to give *N*-alkyl triazoles (**79**, Scheme 17).[79] This system used stoichiometric copper as a terminal oxidant with an amino acid derived ligand, ultimately the addition of the ligand and the change of additive (NaOAc from PivOH) allowed for this improvement to tolerate aliphatic amines. The procedure showed tolerance of a range of heterocycles in the 4-position of the triazole from the hydrazone starting materials. However, this procedure still relied on the use of ketones which only contain one set of enolisable protons and so is ineffective at producing 4-alkyl substituted products. Furthermore, the use of

superstoichiometric copper is undesirable from a sustainability perspective and will likely not be attractive as a scalable procedure.
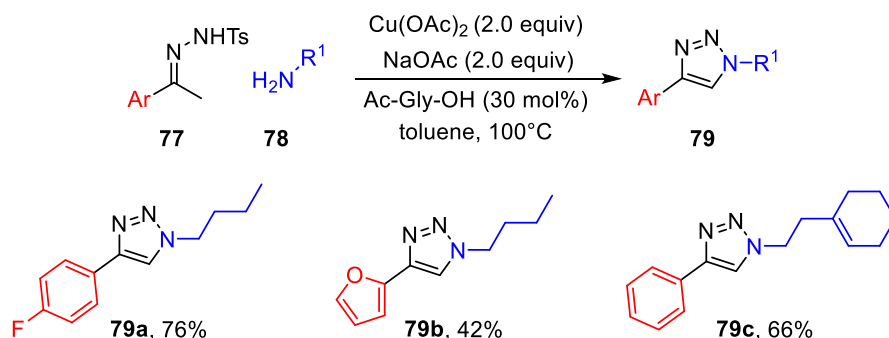
Scheme 17: Zhang's improved method to allow for aliphatic amines

In 2015, Wang and Ji reported a powerful method for the synthesis of 1,4- and 1,5-substituted triazoles from the corresponding α-chlorotosylhydrazone which offers moderate-to-good yields of the desired product (Scheme 18).[80] Moreover, the regiospecific access to triazoles by this method was unprecedented. 1,4-substituted triazoles (**82a**) were accessed from ketone substrates, and 1,5-substituted triazoles (**82b**) were accessed from aldehyde substrates. Access to 1,4,5-trisubstituted triazoles (**82c**) was not possible by this method and aliphatic amines were ineffective in providing *N*-alkyl triazoles.
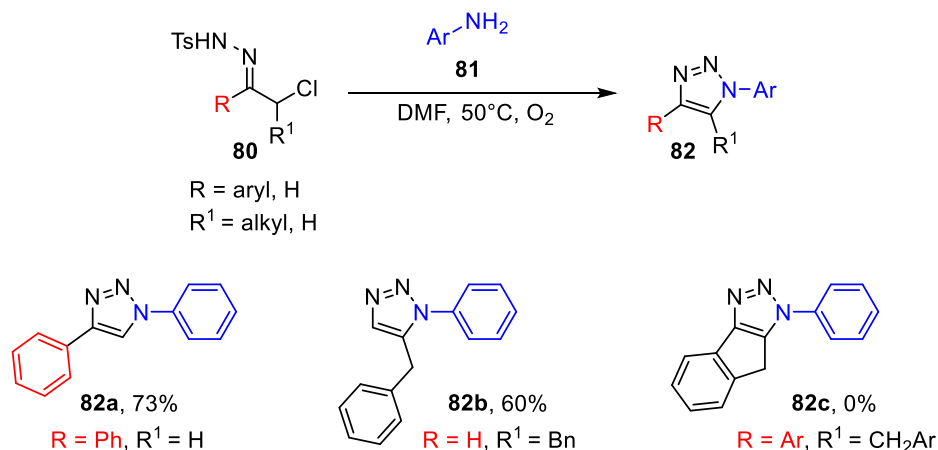

Scheme 18: Wang and Ji's method allow for 1,4- and 1,5-substituted triazoles

The above examples highlight recent advancements in the direct conversion of an amine into a 1,2,3-triazole. Each method presents individual advantages and disadvantages. For a

method to really compare with the CuAAC reaction, several hurdles need to be overcome. Firstly, the conditions need to be considered mild – many of the above protocols use high temperatures for long reaction times. Secondly, one of the main advantages of the CuAAC is the "additive" nature of the reaction; waste products are minimised or very easy to remove. In many of the above examples, the use of stoichiometric oxidants and the production of halogenated waste result in laborious work-up procedures and poor mass efficiency. Thirdly, a general protocol for the synthesis of all substitution patterns of 1,2,3-triazoles is desirable. A single methodology which gives access to all substitution patterns would be necessary from a synthetic diversity viewpoint and a wide-spanning application.
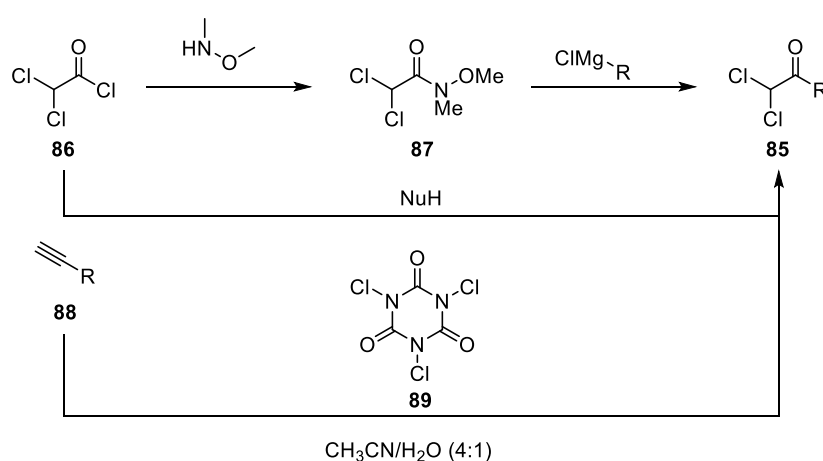
1.8 The Sakai Reaction

A procedure which fulfils many of these criteria is the reaction of an α,α-dichlorotosylhydrazone (**83**) with a primary amine, known as the Sakai reaction.[81] Sakai's original 1986 report highlighted this interesting reaction, but the scope of the reaction wasn't explored until a 2012 publication from Westermann (Scheme 19).[82] The mild conditions allowed for a reaction with an incredibly wide substrate scope. Amines with stereocentres were retained with no erosion of enantiopurity (**84a**), sensitive functional groups (ketones **84b**, acetals **84c**) remained stable and importantly the conditions tolerate both aromatic and aliphatic amines. A remarkable display of the tolerance of the method was displayed by the 48% yield observed of a product derived from psychosine, a highly bioactive substrate, to give elaborate triazole **84e**. This displayed the power of the methodology in derivatising primary amines directly, without first the need to convert them into an azide. However, the reaction offered poor differentiation between aliphatic and aromatic amines, as evidenced by compound **84f** being isolated from a bifunctional amine baring both an aliphatic and an aromatic amine in 69% yield.
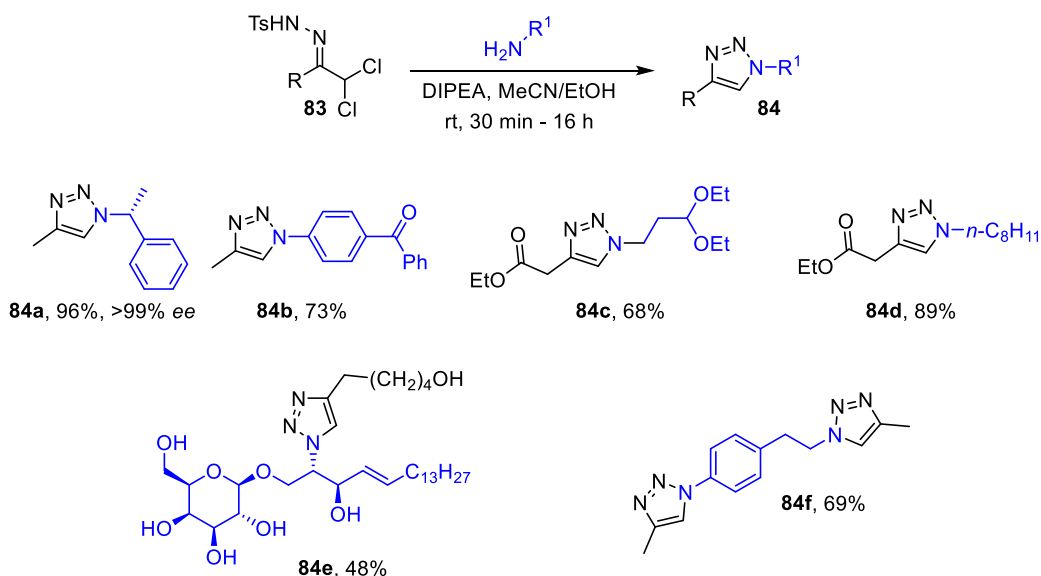
*Scheme 19: The Sakai reaction of α,α-dichlorotosylhydrazones with a primary amine*

α,α-Dichlorotosylhydrazones can be prepared from α,α-dichloroketones (**85**), which themselves are prepared in either one or two steps from dichloroacetyl chloride (**86**, Scheme 20). The first reaction involves the formation of the Weinreb amide **87**, followed by addition of an organometallic reagent, such as a Grignard.[83] In some cases, the products can be prepared in one step from the acyl chloride **86**.[84] A one-step oxidative method to access α,α-dichloroketones was reported by Sheppard in 2014 from the treatment of a terminal alkyne **88** with trichloroisocyanuric acid (**89**).[85] The ease of preparation of these substrates makes the Sakai reaction highly accessible for the synthesis of triazoles.

Scheme 20: Synthesis of α,α-dichloroketones

**1.8.1 The Sakai reaction on a large scale**

Rib-X, an American biopharmaceutical company focussing on the development of antibiotics, explored the Sakai reaction as a method of scaling up the synthesis of one of their key antibacterial macrolides (**90**, Scheme 21). This method was used because the chemists were concerned about the risk of producing copper azide and handling azides on scale which emphasises the length that pharmaceutical companies will go to in order to avoid the CuAAC reaction on scale. Starting from chiral amine **91**, the reaction with hydrazone **92** gave the desired triazole **93**. This example further displays the exquisite functional group compatibility of the reaction, through the retention of two stereocentres, a free-amine baring pyrimidine, and an ester functionality. Moreover, the mild conditions (35 °C, short reaction times) ultimately allowed the reaction to be conducted on a large scale, safely delivering over 3 kg of triazole **93** in an 80% yield.
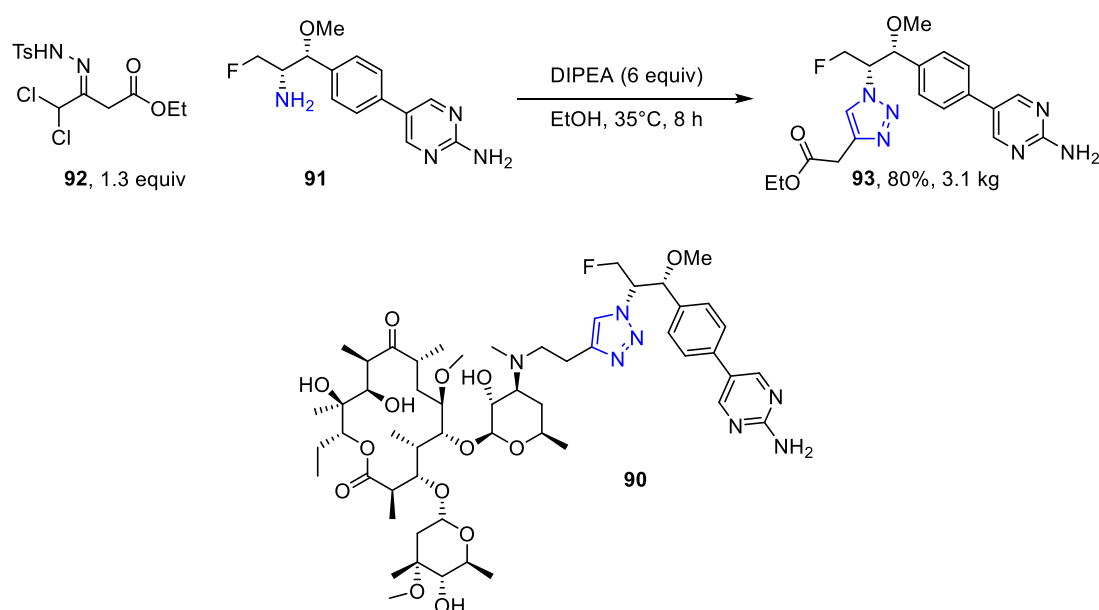
Scheme 21: Rib-X's antibiotic triazole synthesis using a Sakai reaction

One of the key challenges with this transformation is the 2-step nature of the reaction which starts from ketone **94**, the reasoning for this is displayed in Table 1. During the formation of hydrazone **92** from ketone **94**, the authors noted the production of bishydrazone species **96**. The relative ratio of the desired monohydrazone to bishydrazone varied depending on the

solvent used. The solvent that resulted in the highest formation of monohydrazone was propionic acid as reported by Sakai in the original publication (9:1 ratio, Entry 1).[81] However, it was known that the cyclisation to the triazole required basic conditions (DIPEA), and so the required solvent-swap into a non-acidic solvent for the subsequent step was undesirable owing to the time taken when conducting the chemistry on scale. Consequently, the authors undertook a small screen of solvents including ethyl acetate, toluene, acetonitrile and methanol (Table 1, Entries 2–5). The production of the bishydrazone **96** varied between 6:1 in toluene and 1:1 in methanol. It was observed that the bishydrazone was insoluble in both toluene and acetonitrile, and the resultant filtrate contained >99:1 of the desired α,α-dichlorotosylhydrazone **92** (Entries 3 and 4). Acetonitrile gave the best isolated yield of the desired product, with excellent purging of the bishydrazone. Moreover, it was noted that using the hydrazone crude (*i.e.* without purging of the bishydrazone), the impurity profile for the subsequent step was poor, giving lower yields of the desired triazole. These factors explain why the hydrazone formation and triazole formation and conducted over 2 separate synthetic steps.
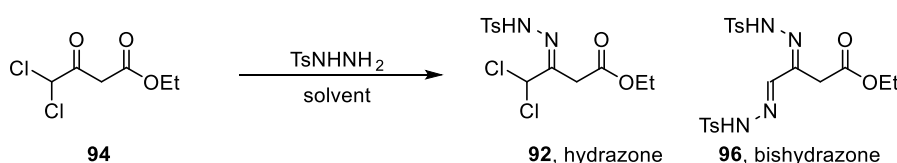

Entry	Solvent	Ratio of **92:96**		Yield **92** (%)[b]
		Crude	Filtrate	
1	Propionic acid	9:1	N/A[a]	N/A
2	EtOAc	5:1	6:1	90
3	Toluene	6:1	>99:1	56
4	MeCN	5:1	>99:1	80
5	MeOH	1:1	3:1	59

Table 1: Solvent effect for monohydrazone and bishydrazone formation
*[a]No precipitation observed. [b]Solution yield of **92** in the filtrate by HPLC*

1.8.2 Access to 1-substituted triazoles *via* the Sakai reaction

Both Singh and Harada have published the use of *α,α*-dichloroacetaldehyde to furnish 1-substituted triazoles (Scheme 22).[86-88] This transformation involves condensation of *α,α*-dichloroacetaldehyde (**97**) with *p*-toluene sulfonylhydrazide and isolating hydrazone **98**. This is followed by exposure of the hydrazone to a primary amine which results in formation of a 1-substituted 1,2,3-triazole (**99**). This reaction offers the opportunity to produce 1-substituted triazoles without the need to use acetylene gas, which often requires specialist equipment and presents a safety concern.
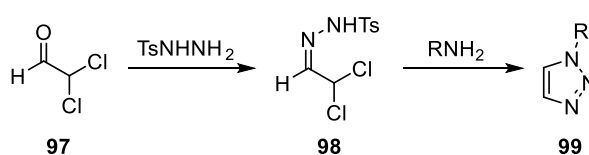
Scheme 22: Singh and Harada's adaption of the Sakai reaction to access 1-substituted triazoles using α,α-dichloroacetaldehyde

Section **1.5** presented methods to access 1-substituted triazoles using protected acetylene surrogates. The Sakai reaction offers an alternative "traceless" activating group strategy in which the resultant triazole does not require deprotecting. The advantages with this method include triazole products are obtained more quickly, in higher yields and without the need for high-energy azides. This results in a shorter synthesis, allowing the direct conversion of primary amines into a triazoles.

However, the procedure using *α,α*-dichloroacetaldehyde is affected with many of the same concerns as the Sakai reaction, including the requirement to isolate the hydrazone. Moreover, dichloroacetaldehyde is highly toxic and there is a drive to move away from halogenated compounds as functional handles. These factors necessitate the development of new synthetic methods.

1.8.3 The Sakai reaction to access different substitution patterns

The apparent power of using *α,α*-dichlorotosylhydrazones to make triazoles lies in the potential to access all different regioisomers of substituted triazoles (Scheme 23). 1,4-substituted

triazoles have been extensively reported, as discussed in Section **1.8** (Method A). However, the use of *α,α*-dichloroaldehydes (Method B) to furnish 1,5-substituted triazoles, and the use of *α,α*-dichloro, *α*-substituted ketones to furnish 1,4,5-trisubstituted triazoles (Method C) have never been reported. Given the power of the Sakai method for 1,4-substituted triazole synthesis, it is surprising that this hasn't been explored. Finally, the preparation of 1-substituted triazoles has been shown by Singh and Harada (Method D). However, there remains scope to expand this methodology to enable a one-pot procedure.
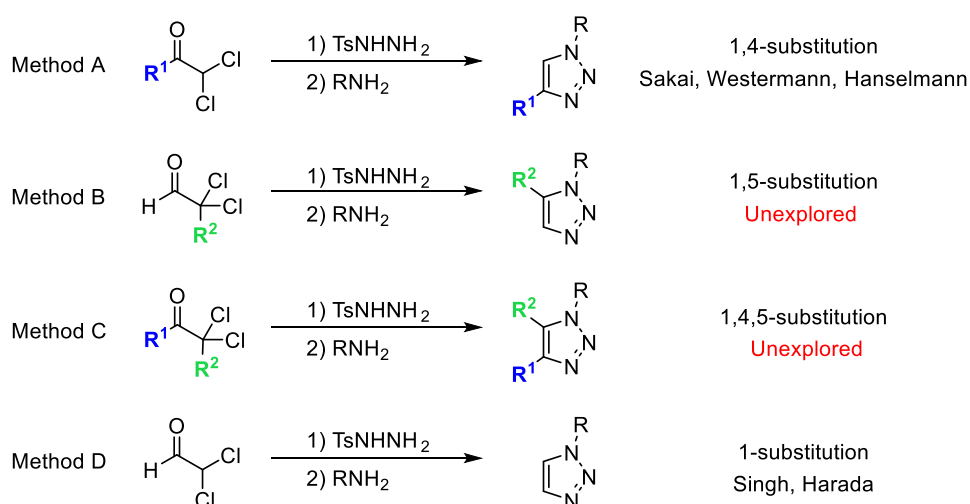
Scheme 23: Methods to access different substitution patterns of 1,2,3-triazoles using α,α-dichloroketones. 1,5- and 1,4,5-substitution remains unexplored

2. Aims and Objectives

The overall aim of this chapter was to expand on the potential of the Sakai reaction as a method of directly converting a primary amine into a 1,2,3-triazole, thus removing the requirement to use azides.

The Sakai reaction has been shown as a versatile alternative to the CuAAC reaction in preparing highly functionalised triazoles under mild conditions. Moreover, the method has been shown to present a safer alternative to the CuAAC in producing triazoles on scale.[82,84] However, the Sakai reaction is yet to be considered general for the synthesis of all substitution patterns of triazoles.

The key objectives were to develop a method which regiospecifically targets the synthesis of most substitution patterns of triazoles by appropriate selection of starting materials (Figure 9). This will be achieved by developing a method which does not necessitate isolation of the intermediate hydrazone, by eliminating the formation of a problematic and limiting bishydrazone. Achieving quantitative conversion to the desired hydrazone will allow for the development of a 1-pot, 3-component coupling to access these important products. Developing a reaction which has these characteristics brings the reaction into the realms of being considered a "Click" reaction, closer to having applications within biological systems as well as providing a valuable synthetic tool.[89] Moreover, showing scalability of the procedure would further add weight to this synthetic method for preparing triazoles on a preparative scale.

Once these conditions had been developed, the objective was to exemplify the method for the synthesis of a range of substitution patterns of 1,2,3-triazoles, including 1,4-, 4,-, 1,5-, 1,4,5-, 4,5- and 1- substituted triazoles (Figure 9). This would present a highly general, redox-neutral, azide- alkyne- and halogen-free synthesis of 1,2,3-triazoles which has not yet been reported.
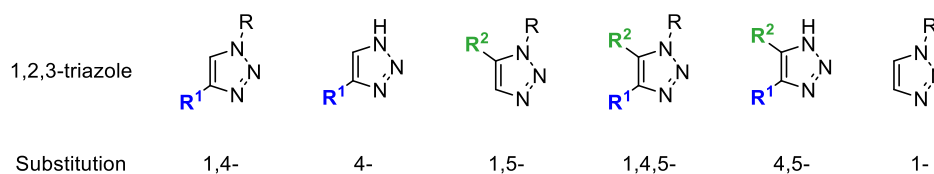
1,2,3-triazole

| Substitution | 1,4- | 4- | 1,5- | 1,4,5- | 4,5- | 1- |

Figure 9: The various substitution patterns of 1,2,3-triazoles which are targeted within this thesis

Finally, current methods do not offer chemoselectivity for aliphatic or aromatic amines.[82] It would be ideal to develop a complementary set of conditions which allow for the functionalisation of an aromatic amine in the presence of an aliphatic amine, or *vice versa*, without protecting groups (Scheme 24). Two sets of orthogonal conditions to selectively convert aromatic or aliphatic amines into a corresponding triazole would be desirable and would have a range of potential applications.
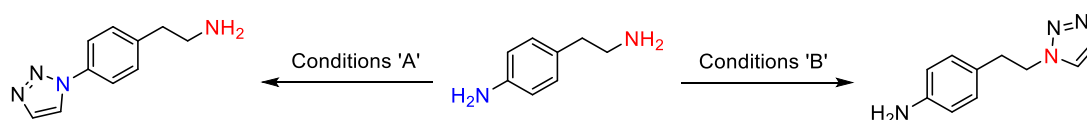
Scheme 24: The proposed chemoselectivity to develop orthogonal conditions for either aromatic or aliphatic amine conversion

3. Results and Discussion

The main aim of this chapter was to achieve a one-pot hydrazone formation which can be telescoped into the subsequent cyclisation to a 1,2,3-triazole. The Sakai reaction involves two steps, the first being the formation of the hydrazone, which needs to be isolated owing to the significant formation of a bishydrazone.[81,82,84] The proposed mechanism for the Sakai reaction involves the desired α,α-dichlorotosylhydrazone **101** eliminating an equivalent of HCl to form vinyldiazene species **102** (Scheme 25). This species, described as being highly electrophilic, readily undergoes 1,4-addition with a primary amine. This leads to iminohydrazone **103**, which cyclises to form the triazole, eliminating a sulfinic acid by-product.

During the formation of α,α-dichlorotosylhydrazone **101**, if the vinyldiazene (**102**) is formed by elimination of HCl, then any excess tosylhydrazide will react with the vinyldiazene (**102**) to form the undesired bishydrazone (**104**, Scheme 25). If the rate of vinyldiazene formation can be decreased, there will be a lower concentration of this reactive intermediate, removing the potential to form the bishydrazone. Replacing the dichloro handle with a poorer leaving group, such as dimethoxy (an acetal functional group), the forward rate of vinyldiazene formation would be expected to be slower, making intermediate hydrazone **105** more stable. This should reduce the formation of bishydrazone **104** and allow for the potential of a one-pot, 3-component reaction without the need to isolate the hydrazone.

This hypothesis

- Decrease rate of vinyldiazene formation
- If a poorer leaving group is used, the intermediate will be more stable
- Propose replacing the dichloride handle with an acetal (alkoxide leaving group)
- A more stable intermediate should produce less/no bishydrazone
- This should then allow for a telescoped procedure
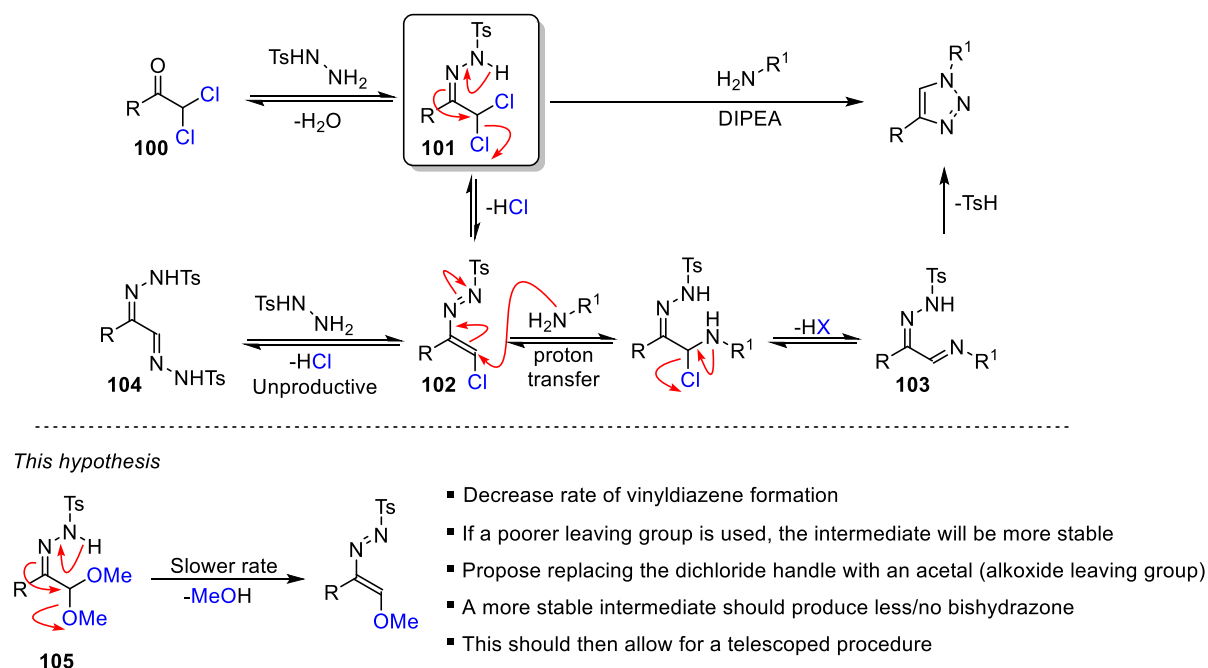
Scheme 25: The hypothesis. Use of α-ketoacetals as precursors to 1,2,3-triazoles

3.1 Development of conditions for hydrazone formation

At the outset of the study, the conditions for the formation of a hydrazone between an α-ketoacetal and *p*-toluene sulfonylhydrazide were examined. As had been previously reported in the Sakai reaction (Section **1.8.1**), the solvent in which the hydrazone was formed had a large effect on the relative production of the desired hydrazone and side-products.[84] 1,1,dimethoxypropan-2-one **106** is a commercial and readily available α-ketoacetal and so this was chosen as a model substrate. Dissolving α-ketoacetal **106** in acetonitrile, tetrahydrofuran, 1,4-dioxane, dimethyl sulfoxide and methanol and adding 1 equivalent of *p*-toluene sulfonylhydrazide **107** gave the results shown in Table 2 after 30 minutes at room temperature. The formation of two new products was observed. The mass-ions of hydrazone **108** (*m/z*, M−H 285) and bishydrazone **109** (*m/z*, M+H 409) were observed by LCMS. Interestingly, at 10 minutes in acetonitrile two species were observed which were consistent in mass with the hydrazone **108** at a ratio of 1:1. These two species are likely the two stereoisomers of the hydrazone (**108** and **108a**). After 30 minutes, the ratio had changed to 4:1 indicating that interconversion of these two species is facile and that one of the stereoisomers is thermodynamically more stable. Only one stereoisomer was observed in all other solvents.

In all cases the reaction had gone to near completion after 30 minutes, resulting in < 5% residual *p*-toluene sulfonylhydrazide by HPLC and LCMS analysis of the reaction mixture (Entries 1–5). However, the relative ratio of reaction components varied with solvent. Bishydrazone **109** formed in up to 12% in acetonitrile but was not observed at all in either dimethylsulfoxide or methanol.


107, 1 equiv   **106**, 1 equiv   **108**, *m/z* (M⁻) = 285   **109**, *m/z* (M⁺) = 409

108   **108a**
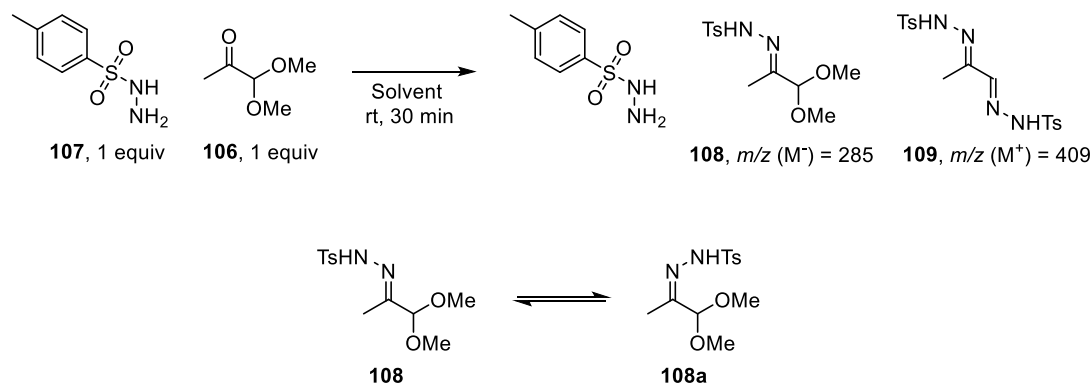
Entry	Solvent	Residual hydrazide **107** /%	Hydrazone **108** /%	Bishydrazone **109** /%
1	MeCN	0	88	12
2	THF	2	87	4
3	1,4-dioxane	0	80	9
4	DMSO	3	91	0
5	MeOH	1	95	0

Table 2: The solvent effect on the ratio of mono and bishydrazone
Percentages given are of HPLC & LCMS analysis of the reaction mixture.
Where mass balances are < 100%, no individual impurity was greater than 0.5%.
*Hydrazone **108** percentages are the combined peak area percentages of both stereoisomers.*

The observed selectivity for the formation of the desired hydrazone **108** over bishydrazone **109** was highly encouraging considering the objective to achieve a one-pot triazole formation. In both dimethylsulfoxide and methanol, no formation of bishydrazone **109** was observed after 30 minutes (Entries 4 & 5). Compared to the α,α-dichloroketone system in Table 1 (Section **1.8.1**) no solvent gave better than a 5:1 ratio of mono:bishydrazone, and methanol gave very poor results yielding a 1:1 ratio in the crude reaction mixture. Despite not being an exact comparison owing to the different ketone substrate, this potentially eludes to the increased stability of a hydrazone derived from an α-ketoacetal over that of an α,α-dichloroketone.

In methanol, 95% of the desired hydrazone was observed after 30 minutes, with no formation of the bishydrazone. Moving forward, the aim was to design a procedure to encourage formation of an iminohydrazone **110** (Scheme 26). This intermediate is classically invoked in the mechanism for the Sakai reaction, and so if this could be accessed the triazole formation should proceed accordingly.[84,90] The initial aim was to develop selective conditions to hydrolyse the acetal whilst retaining the hydrazone, to form aldehyde **111**. This aldehyde should then react with a primary amine to form the desired iminohydrazone **110**.
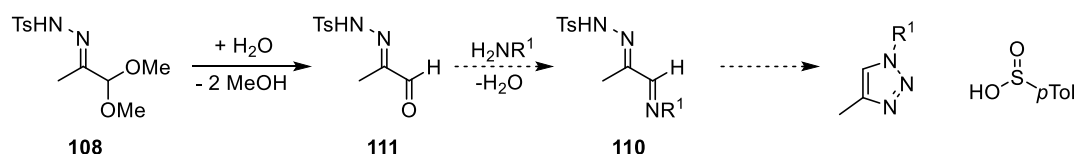
*Scheme 26: The proposed selective hydrolysis to furnish an aldehyde with the aim of forming iminohydrazone **110** on the way to forming a triazole*

3.2 A model system

A literature search to selectively hydrolyse an acetal in the α-position of a hydrazone to an aldehyde returned limited results, with the only comparable transformation shown in Scheme 27.[91] The conditions use 2 equivalents of lithium tetrafluoroborate in acetonitrile:water (98:2) to form **113** from **112**. This looked problematic for two reasons. If this procedure was adopted to access the aldehyde, it was known that the formation of the hydrazone in acetonitrile was poor (Section **3.1**). This would necessitate swapping from methanol into acetonitrile, removing the potential of a one-pot procedure. Secondly, the low yield of **113** (24%) did not look promising from the perspective of developing a high-yielding methodology. This suggested that the hydrolysis step would require significant optimisation.
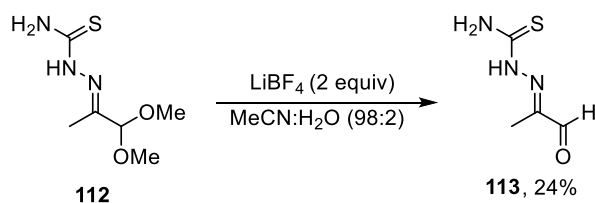
Scheme 27: Literature result for a selective hydrolysis of an acetal in the presence of a hydrazone

Therefore, before pursuing what appeared to be a highly challenging hydrolysis, a model system was designed to examine whether this was a feasible strategy. Using 1,2-dicarbonyl compound **115** would examine whether the selective hydrolysis strategy could give access to the desired imine intermediate **117**. To pursue this, 1,2-diketone **115** was reacted with *p*-toluene sulfonylhydrazide in methanol. After 1 hour, by HPLC & LCMS a species consistent in mass with hydrazone **116** was observed at 84%, with 4% bishydrazone present (not shown for clarity). On addition of benzylamine, no imine intermediate **117** or triazole **118** was observed. Instead, the formation of *p*-toluene sulfinic acid **119** was observed and 66% of α-diazocarbonyl species **120** was isolated.
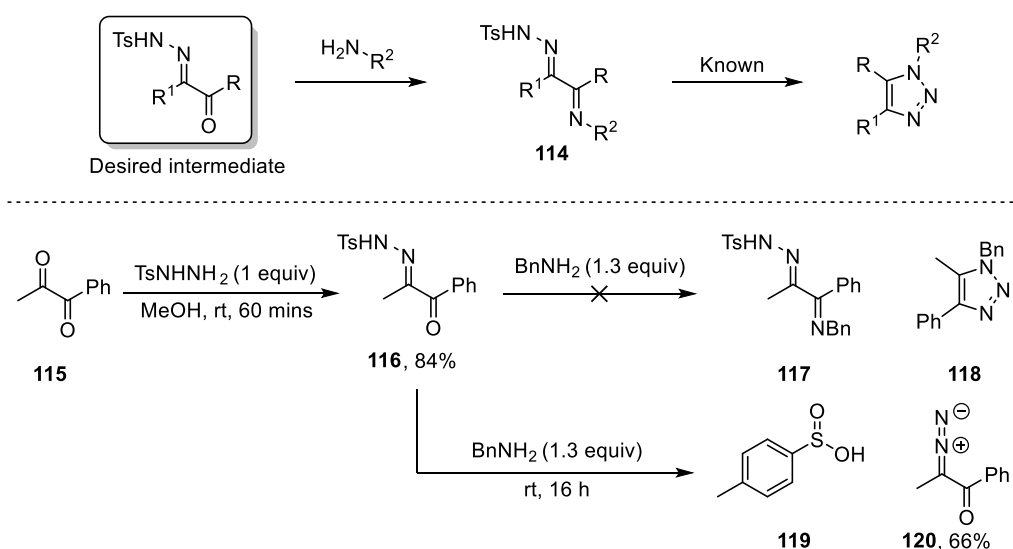
Scheme 28: α-diazocarbonyl formation from a hydrazone

The collapse of the hydrazone follows the first part of a Shapiro or Bamford-Stevens mechanism.[92,93] Deprotonation of the sulfonamide NH on **121** by base (benzylamine, triethylamine) gives azo-enolate **122** (Scheme 29). This compound is stabilised by conjugation of the anion throughout the carbonyl and the sulfonamide, explaining the ease of deprotonation. At this point the anion can push through, eliminating *p*-toluene sulfinate to give α-diazocarbonyl **120**.
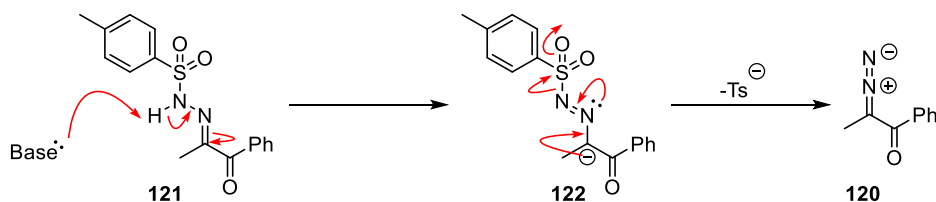
Scheme 29: The elimination of p-toluene sulfinic acid to give an α-diazocarbonyl

Unfortunately, α-diazocarbonyl **120** did not undergo formation of an imine (**123**) on addition of benzylamine (Scheme 30). This is unsurprising considering the resonance structure of the diazo compound decreases the electrophilicity of the carbonyl group owing to its enolate-type nature.
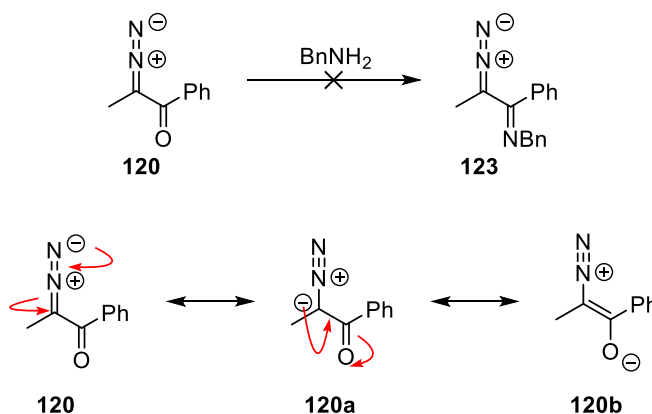
*Scheme 30: Resonance structures of an α-diazocarbonyl, explaining the poor reactivity towards an amine*

The above observations suggest that α-carbonyl hydrazones are not a suitable intermediate to target for the synthesis of 1,2,3-triazoles. This is because the collapse of the intermediate hydrazone to an α-diazocarbonyl compound — which is unreactive — occurs preferentially over imine formation. These factors suggested that pursuing the aldehyde as an intermediate was not going to be productive.

3.3 A surprisingly labile acetal

With these observations, the hydrazone formation and resultant steps were examined in more detail. Using tosylhydrazide (**107**) as the limiting reagent and α-ketoacetal **106** in deuterated methanol, the reaction was monitored by ^{1}H NMR spectroscopy. After 5 minutes *p*-toluene

sulfonylhydrazide (**107**) had been fully consumed, resulting in near quantitative formation of hydrazone **108** (Scheme 31).
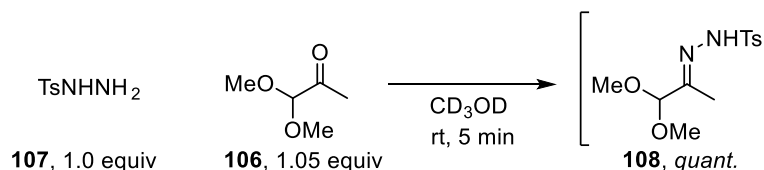
Scheme 31: Quantitative hydrazone formation in deuterated methanol

However, on leaving the same reaction to stand for 2 hours at room temperature, by LCMS analysis of the reaction mixture the mass ion (*m/z* M$^-$) of the hydrazone increased from 285 to 288 and to 291 (Figure 10). This increase in multiples of 3 suggested the exchange of 3H's for 3D's. The absence of integers other than 3 or 6 indicated that the deuterium atoms are associated with CD$_3$ group of the deuterated solvent rather than multiple sequential additions of individual deuterium atoms.

Figure 10: Mass spec trace of the hydrazone over a 120-minute period.
Left = 5 minutes, middle = 50 minutes, right = 120 minutes

Interpretation of these results likely suggest that the dimethyl acetal of the hydrazone substrate **108** is being exchanged with a deuteriomethoxy acetal from the solvent. After 2 hours at room temperature, greater than 90% incorporation of the OCD$_3$ acetal was observed by ^{1}H NMR spectroscopy (Scheme 32). This explains the sequential increase in mass observed in the M$^-$ by the formation of deuterated acetals **124**, **125** and **126**.
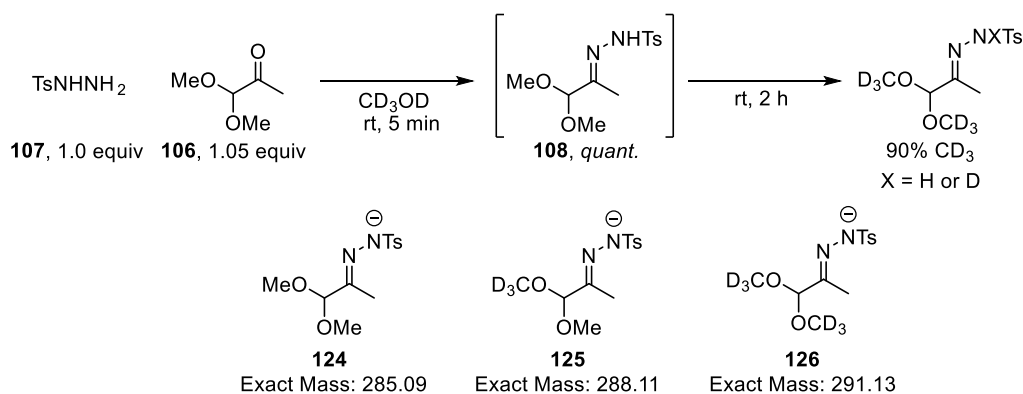
Scheme 32: The lability of the acetal towards exchange with the deuterated solvent

Reaction of α-ketoacetal **106** in deuterated methanol and leaving at room temperature for 2 hours resulted in complete recovery of the ketoacetal with no deuterium incorporation (Scheme 33). This shows that the hydrazone is crucial to the lability of the acetal.
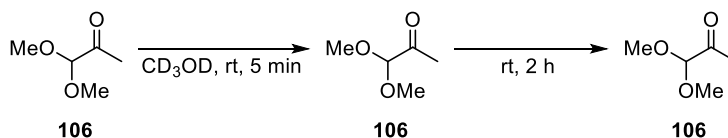
Scheme 33: Control reaction of α-ketoacetal in deuterated methanol

If benzylamine (**127**) was added as soon as the hydrazone had formed, the acetal-exchange almost entirely shut-down. The hydrazone containing 90% CH_3 acetal was observed after 2 hours, with the remaining 10% being mono-methoxy, mono-deuteriomethoxy acetal. No bis-deuteriomethoxy acetal was observed even after 2 hours (Scheme 34).
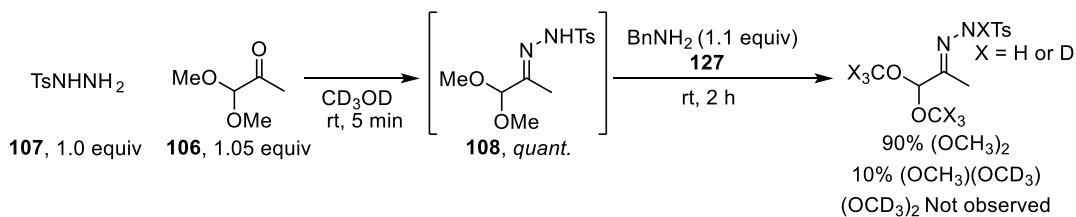
Scheme 34: Suppressed acetal exchange under basic conditions

Moreover, the ^1H NMR analysis showed that the NCH_2 signal of benzylamine undergoes a downfield shift from 3.77 ppm to 3.88 ppm (Scheme 35). This downfield shift is highly indicative of a proton transfer between the hydrazone substrate and benzylamine. The complete

protonation of benzylamine (evidenced by disappearance of singlet at 3.77 ppm) suggested that the hydrazone was remarkably acidic. The pK$_a$H in water of benzylamine is 9.34,[94] implying that the pK$_a$ of the hydrazone must be at least 3 pK$_a$ units lower than benzylamine to leave no observable neutral benzylamine by ^{1}H NMR analysis (Figure 11). The pKa of *p*-toluene sulfonylhydrazide is 1.09 (measured in a water:DMSO mixture)[95] which also suggests the hydrazone would be similarly acidic.
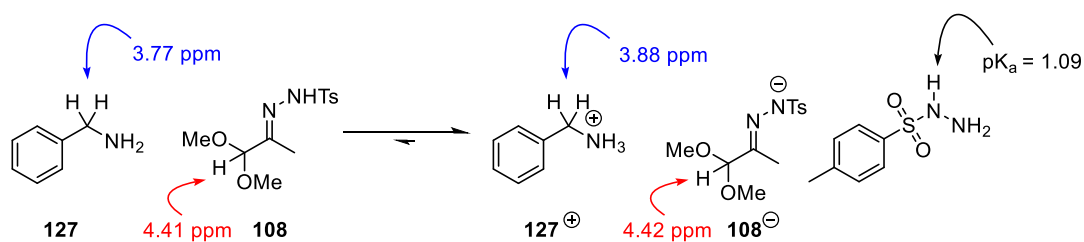
*Scheme 35: Acid-base equilibrium between hydrazone **108** and benzylamine (**127**)*
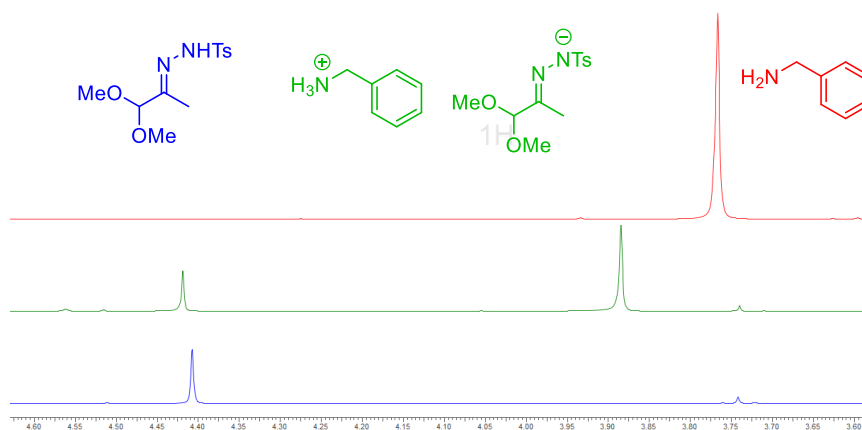
Figure 11. Red = benzylamine reference, green = reaction mixture 2 hours after benzylamine addition, blue = reaction mixture before benzylamine addition

This observation has implications for the mechanism in which the acetal collapses. If the hydrazone contains the N–H bond, *i.e* without base, then a 6-membered species can be drawn (**128**, Scheme 36). This intramolecular H-bonding arrangement would facilitate acetal collapse and an intramolecular proton transfer, eliminating methanol to form enoldiazene **129**. Evidence for the formation of the enoldiazene species was seen in the LCMS trace. Only one species

was observable by liquid chromatography which had the mass-ion of *m/z*=285 in the ES- (hydrazone **108**/**128**). However, a fragment-ion of the same species was observed with an *m/z*=255 in the ES+ (Scheme 36). This suggests that the formation of an enoldiazene is mechanistically feasible, even though this species has not been observed by ^{1}H NMR analysis. This could suggest that the enoldiazene intermediate is fleeting and is rapidly trapped by any pendant nucleophiles (CD$_3$OD/MeOH).

128, Exact Mass: 286.10   **129**, Exact Mass: 254.07   Exact Mass: 290.12
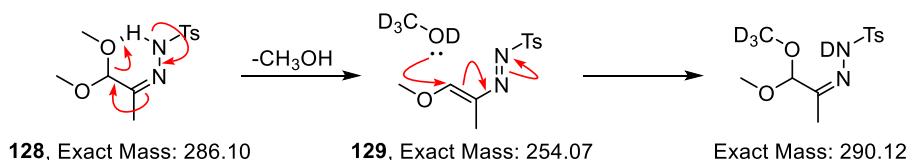
Scheme 36: Intramolecular elimination of methanol and trapping of an enoldiazene
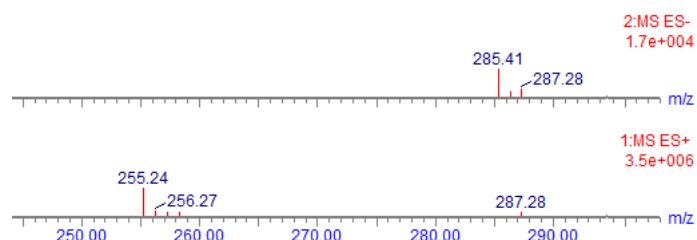
Figure 12: Mass-spectrometry trace of hydrazone, showing a fragment ion consistent in mass with enoldiazene 129

On addition of benzylamine, the discussed intramolecular hydrogen bond is disrupted (as evidenced in Figure 11) resulting in the deprotonation of hydrazone **108** by benzylamine. The decrease in OCD$_3$ incorporation into the acetal can be explained through the equilibrium obtained between the hydrazone and benzylamine (Scheme 37). The hydrazone substrate (**108**) and benzylamine (**127**) engage in an acid-base equilibrium which, as shown by ^{1}H NMR spectroscopy, the position of equilibrium lies on the left-hand side of the arrow. This results in a very low concentration of neutral benzylamine, and by effect, neutral hydrazone. However, as discussed, Scheme 34 shows that after 2 hours with benzylamine 10% acetal exchange had occurred. This therefore suggests that the anionic hydrazone (**108**⁻) can very slowly eliminate methoxide to form the enoldiazene **129**. The absence of a separate species with a different retention time in the LCMS and the lack of evidence for enoldiazene **129** by ^{1}H NMR suggest that trapping of this intermediate by a nucleophile is rapid.
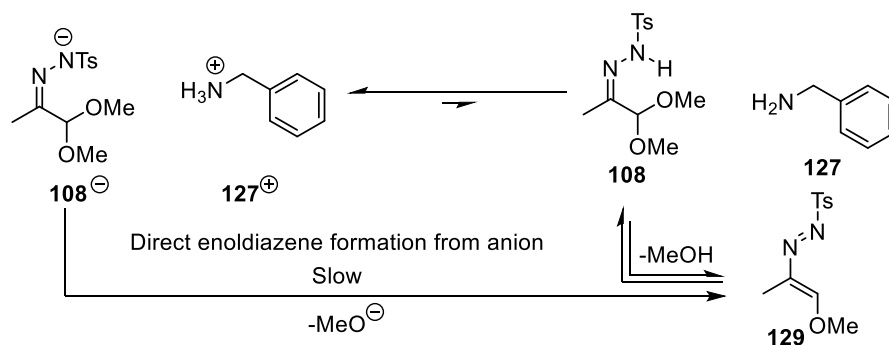
Scheme 37: Proposed mechanism for enoldiazene formation

The elimination of an alkoxide α to a hydrazone is commonly exploited in the Eschenmoser fragmentation (Scheme 38). The Eschenmoser reaction is a fragmentation in which an α,β-epoxy *N*-tosylhydrazone **131** ring-opens the epoxide to give **132**, which subsequently collapses to give an alkyne **133** and a carbonyl product **134**.[96] The first step of the reaction after hydrazone formation involves the ring-opening of the epoxide which can occur under basic conditions.[97] The comparison between the Eschenmoser fragmentation and the observation of the acetal lability is not a totally fair comparison however; the Eschenmoser reaction relies on the opening of a strained 3-membered ring to liberate an alkoxide – this ring-strain is not present in the case of hydrazone **108**. However, this does imply that the direct enoldiazene formation for the hydrazone anion **108⁻** could be possible.
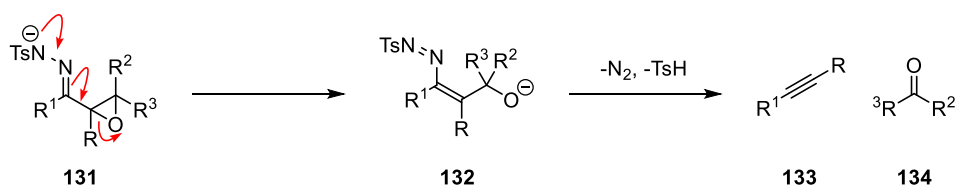
Scheme 38: The Eschenmoser fragmentation

On leaving the reaction with benzylamine at room temperature overnight, singlets at 5.53 ppm and at 7.68 ppm in the ^{1}H NMR spectrum were observed. This was believed to be due the CH_2 and the CH protons of the desired triazole product **135** (Figure 13). This was further supported by the LCMS trace showing a species consistent in mass with the desired triazole.
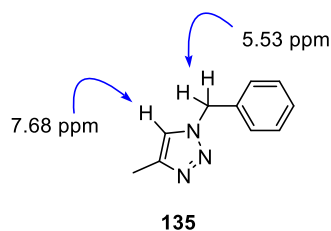
Figure 13: Observation of the triazole

On repeating this reaction, 1-benzyl-4-methyl-1,2,3-triazole **135** was isolated in 47% yield (Scheme 39) with 25% hydrazone **108** remaining. This indicates that the intermediate enoldiazene **129** could be trapped by the amine directly. Again, no species consistent in mass with the enoldiazene **129** or any further subsequent intermediates were observed. This suggests that the slow step is elimination of methoxide from the anionic hydrazone to give enoldiazene. Evidence suggests that trapping of this species is rapid. The methoxide can then deprotonate the ammonium to generate the free-base *in-situ* which reacts with the enoldiazene **129**.
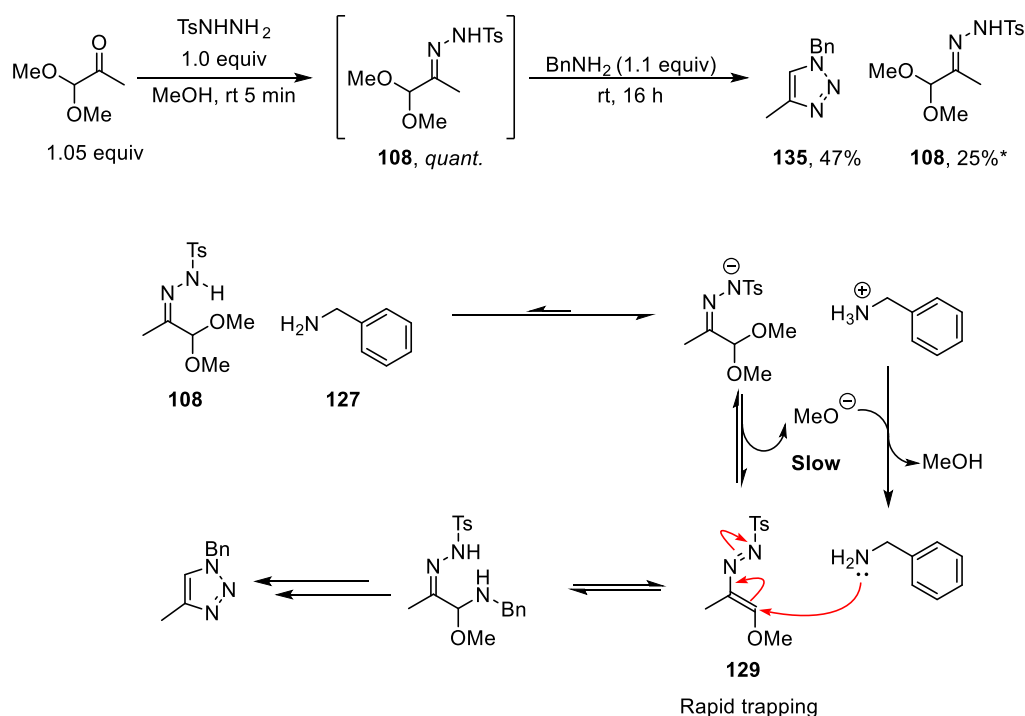
*Scheme 39: Formation of triazole **135** at room temperature.*
25% remaining by ^{1}H NMR analysis of the crude reaction mixture

3.4 Trapping of enoldiazene 129 with benzylamine

Encouraged by the formation of triazole **135** in 47% yield (Entry 1, Table 3), methods to improve the observed yield were examined. On heating the reaction under reflux for 16 hours, a 75% solution yield of **135** was obtained by ^{1}H NMR analysis using 1,3,5-trimethoxybenzene as an internal standard (Entry 2). Further encouraged by the positive effect of heating the reaction, an 83% solution yield of **135** was observed when heating the reaction in a sealed vial under microwave irradiation at 120 °C for 20 minutes (Entry 3). This indicated that a hotter reaction was beneficial for increased product formation. Increasing amine equivalents did not increase the observed yield of the product, where an 84% solution yield was observed, and 77% of the product was isolated (Entry 4). A reduced reaction time of 5 minutes also did not have a marked effect on the observed yield giving 82% (Entry 5). This showed that the reaction was complete within 5 minutes with no hydrazone remaining. Increasing the temperature further to 140 °C for 5 minutes gave a further increase in solution yield increase to 89%, further supporting the idea that a hotter, faster reaction is beneficial (Entry 6). The temperature was not increased further owing to the maximum recommended pressure limitation with the microwave equipment.
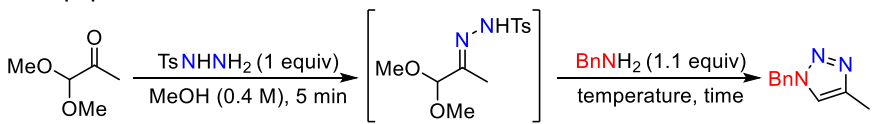

Entry	Temperature	Time	Variations	**135** yield[a]
1	rt	16 h	-	47% (47% isolated)
2	Reflux	16 h	-	75%
3[b]	120 °C	20 min	-	83%
4[b]	120 °C	20 min	BnNH$_2$ (2.0 equiv)	84% (77% isolated)
5[b]	120 °C	5 min	-	82%
6[b]	140 °C	5 min	-	89%
7[b]	140 °C	5 min	+ Et$_3$N (1.1 equiv)	88% (88% isolated)

Table 3: Optimisation table for triazole synthesis. [a]Solution yield calculated using 1,3,5-trimethoxybenzene by ^{1}H NMR analysis. [b]Reaction performed in a sealed vial under microwave irradiation

Throughout the course of the optimisation, the production of an impurity by LCMS and HPLC was observed. The impurity could not be removed by aqueous washes and the only way of separating it was by chromatography. Exposure of the triazole to the reaction conditions did not result in any degradation of the triazole and the unknown impurity was not formed (Scheme 40). This showed that the impurity was not related to the triazole.
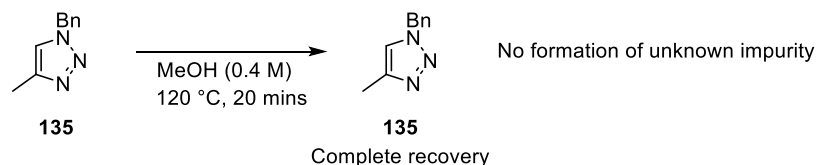

Scheme 40: Control reaction examining triazole stability

Exposing the triazole and *p*-toluene sulfinic acid (**137**) to the reaction conditions also led to full recovery of triazole **135**, however the formation of *p*-toluene sulfonic acid (**138**) and the unknown impurity was observed (Scheme 41) suggesting that the impurity was derived from the sulfinic acid byproduct (**137**).
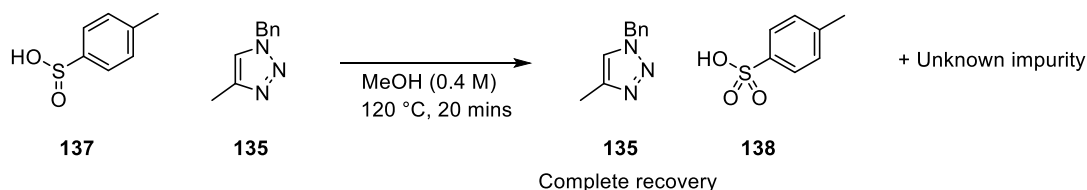
*Scheme 41: Control reaction with p-toluene sulfinic acid (137) and triazole 135*

Finally, to prove the impurity was associated with a degradation product of the sulfinic acid by-product, exposure of this to the reaction conditions gave full conversion of the sulfinic acid. This yielded the unknown impurity with trace quantities of *p*-toluene sulfonic acid. Isolation of the impurity proved it to be methyl 4-methylbenzenesulfonate (**139**) in 84% yield.
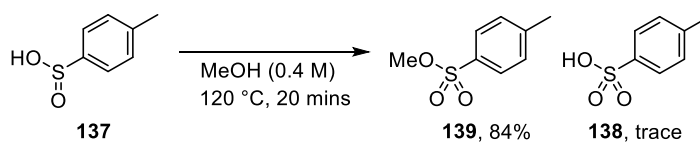
*Scheme 42: Control reactions with p-toluene sulfinic acid (137), showing impurity 139*

The formation of the sulfonic acid (**138**) is likely a result of oxidation of the sulfinic acid side-product. No precautions were made to degas the solvent or to make the headspace of the reaction inert, meaning the reaction would have contained oxygen, facilitating oxidation of the sulfinic acid by-product. Secondly, heating the sulfinic acid in methanol forms the methyl sulfonate product. In order to develop scalable reaction conditions which do not rely on chromatography for purification, a procedure was designed which trapped the *p*-toluene sulfinic acid by-product as the triethylamine salt. Scheme 43 shows the developed conditions where adding 1.1 equivalents of triethylamine shuts down the degradation pathway of the sulfinic acid **137** and traps this species as the triethylamine sulfinate salt.
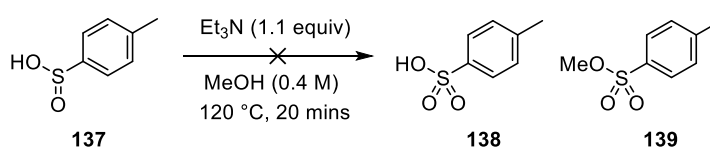
Scheme 43: Triethylamine stops degradation of the sulfinic acid byproduct

With this learning, Entry 7 in Table 3 shows how adding 1.1 equivalents of triethylamine to the reaction mixture gives (within error) the same yield of triazole **135** (88% yield). This procedure allows for the separation of the sulfinate by-product from the triazole by a simple aqueous wash. Even though the material could be isolated in acceptable purity (93% by LCMS), analytically clean material was isolated by chromatography. The final optimised conditions are displayed in Scheme 44. These conditions give access to the triazole in an excellent yield in 10 minutes from α-ketoacetal **106**.
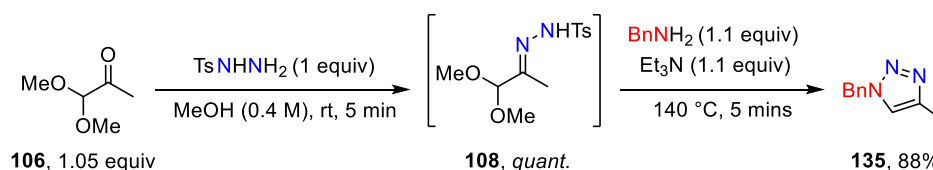

Scheme 44: The optimised reaction conditions

3.5 Exploration of the substrate scope for 1,2,3-triazole synthesis

3.5.1 Simple aliphatic amines

Having seen that triazole **135** could be isolated in excellent yield, the scope of the primary amine was next explored. Scheme 45 displays the results of using simple aliphatic primary amines. Using *n*-propylamine, triazole **140** was isolated in a 98% yield after a simple aqueous wash of the triazole in CH_2Cl_2. The formation of *N*-methyl triazole **141** under these high-pressure conditions is interesting; the high volatility of methylamine (boiling point = −6 °C) suggests this species may largely exist in the headspace of the reaction. However, the high pressure and temperature of the reaction forces the methylamine into solution to react. More likely, however, is that the methylamine is protonated on reaction with the hydrazone (as evidenced in Figure 11 Section **3.3**), suppressing the volatility and ensuring retention of this substrate in solution. Secondly, a 40% aqueous solution of methylamine was used, showing that the reaction is highly tolerant towards the presence of water. Other amines, including *iso*-propylamine, cyclopropylamine, cyclohexylamine and *tert*-butylamine gave triazoles **142–145** in 79%, 97%, 91% and 90% respectively. Highly sterically hindered amine substrates such as cyclohexylamine and *tert*-butylamine behaved excellently. All the triazole products presented here afforded analytically clean material without chromatography.
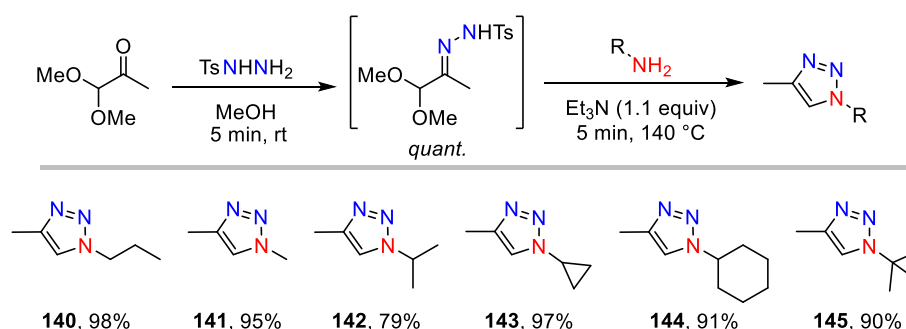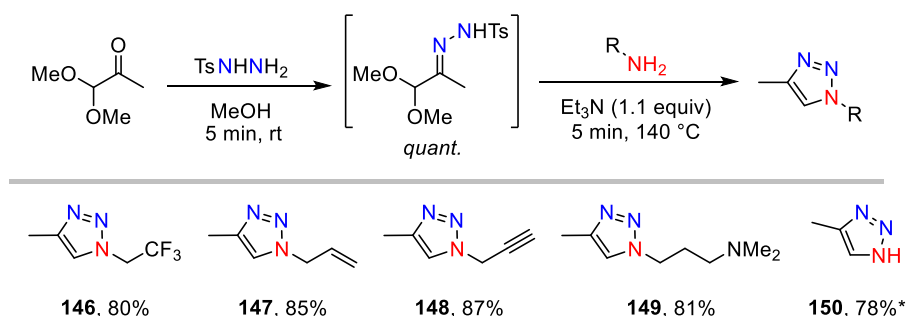

Scheme 45: Scope of simple aliphatic amines

3.5.2 Functionalised aliphatic amines

To further explore the functional group compatibility of the amine substrate, a series of aliphatic amines baring various functional groups were exposed to the reaction conditions and the

results are displayed in Scheme 46. Fluorinated triazole **146** was isolated in 80% yield using 2,2,2-trifluoroethylamine, a highly volatile amine reagent (boiling point 37 °C[98]). This further supports the claim that these high-pressure conditions are suitable for the conversion of volatile, low molecular weight amines. *N*-alkenyl and *N*-alkynyl triazoles **147** & **148** were isolated in 85% and 87% yield using allylamine and propargylamine respectively. The formation of these two products strongly emphasises the orthogonality of this reaction when compared to AAC's. Both alkenes and alkynes participate in cycloadditions with azides.[99] This shows that this approach is a complementary method to the AAC synthesis of triazoles, in which alkenes and alkynes are not tolerated reagents. A primary amine attached to a pendent tertiary amine resulted in triazole **149** in 81% yield. Next, to explore whether an NH triazole (**150**) could be synthesised, it was proposed that using a solution of ammonia in methanol would be suitable. Unfortunately, under the conditions displayed in Scheme 46 with 1.1 equivalents triethylamine, compound **150** could not be separated from several impurities including the triethylamine salt. The product could not be recovered by chromatography and the product decomposed under vacuum distillation. However, a slight modification of the reaction conditions using 2.2 equiv ammonia as a solution in methanol with the omission of triethylamine allowed for clean isolation of NH triazole **150** in 78% yield. This observation is notable as a Click reaction using sodium azide to give an NH triazole is highly challenging. Hydrazoic acid can be used,[37] however this presents a significant safety concern. This method presents a chemist with the ability to install an NH triazole simply from ammonia.

*Scheme 46: Scope of functionalised aliphatic amines. *2.2 equiv ammonia in MeOH*

**3.5.3 Elaborated amine substrates**

In attempts to stretch the reaction, functionalised benzylamine derivatives were examined (Scheme 47). Benzylamine gave 88% triazole **135** as discussed previously, and both electron withdrawing and donating substituents on the aromatic ring were tolerated. For example, 4-methoxybenzylamine and 4-cyanobenzylamine also gave triazoles **151** & **152** in 84% and 91% respectively. Further, bromo-containing triazole **153** was isolated in 80% yield, providing a potential handle for further elaboration. This, despite not being an exhaustive examination, suggested that the electronics of a benzylamine substrate do not affect its ability to undergo the desired reaction. Primary amines baring heterocyclic functional groups were next examined. Pyridines, furans and *N*-Boc protected azetidines proved to be synthetically versatile substrates giving the triazoles **154–156** in 68%, 96% and 92% yield respectively. It is also worth noting that both **155** and **156** yielded analytically clean material without chromatography, adding weight to the claim that this reaction could be deemed a "Click" process. Aniline provided *N*-phenyl triazole **157** in 74% yield, showing that aromatic amines also prove to be suitable substrates for the synthesis of triazoles. Finally, a 2-aminopyrazole derived triazole **158** was isolated in 91% yield. This shows how complex heterocyclic products which resemble pharmaceutical compounds can be synthesised using this methodology.
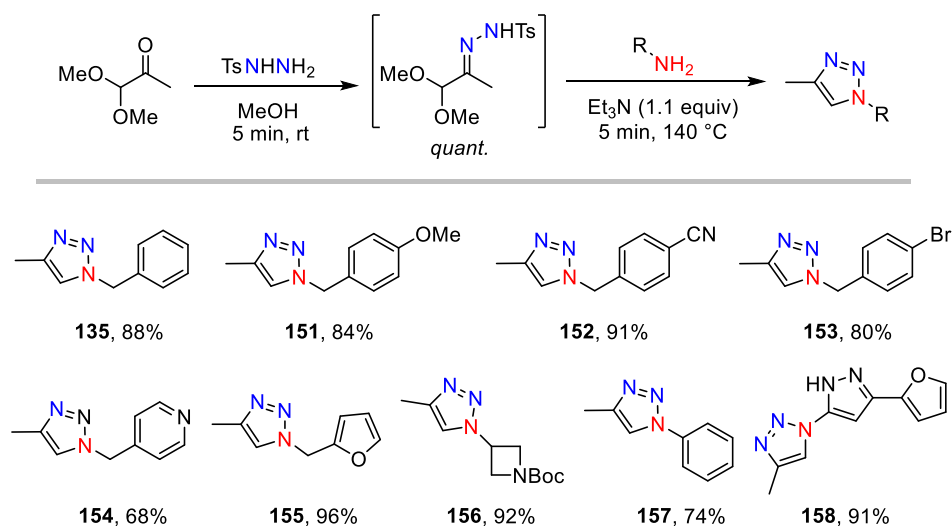
*Scheme 47: Scope of benzylamines, heterocyclic aliphatic amines and aromatic amines*

3.5.4 Enantiomerically enriched amine substrates

In attempts to examine how chiral amines behave under the reaction conditions, a *cis*-1,2-amino alcohol was exposed to the reaction conditions to give triazole **159** in 80% yield (Scheme 48). Under the standard conditions the product was isolated with no erosion of diastereomeric purity which was determined by ^{1}H NMR analysis. The NC<u>H</u> proton of **159** was observed as a sharp doublet at 6.13 ppm with a coupling constant of 5.9 Hz, which is consistent with the *cis*-configuration of a 2-amino-1-indanol.[100] *Trans*-2-amino-1-indanols have a coupling constant of >6.5 Hz[101] and no 6.5 Hz doublet was observed.
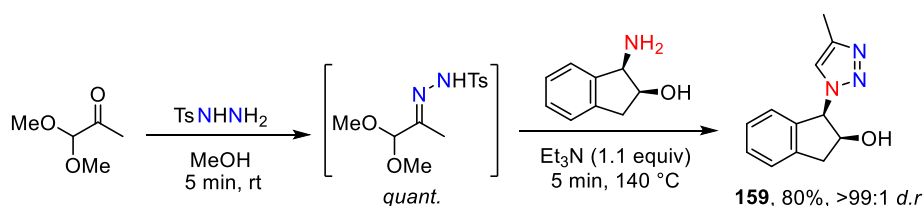

Scheme 48: Retention of diastereomeric purity in an indanol substrate

An alanine amino acid derivative was exposed to slightly modified conditions using 2 equivalents of triethylamine (Scheme 49). The reason for this was that alanine-ethyl ester was provided as the hydrochloride salt. The excess of triethylamine was to free-base the alanine-ethyl ester *in-situ*. The triazole product **160** was isolated in 84% yield. However, when the triazole was analysed by HPLC on a chiral stationary phase, an 80:20 enantiomeric ratio was observed (referenced to a racemic marker). Unsurprisingly, under the basic conditions of the reaction some erosion of enantiomeric purity was observed. The ester moiety in either the starting material, product or an intermediate can convert to an enol or an enolate under the reaction conditions (drawn as an enol owing to the weakly basic reaction conditions). This results in a prochiral enol which is unselectively protonated on either the *Re* or *Si* face, resulting in erosion of enantiomeric purity.
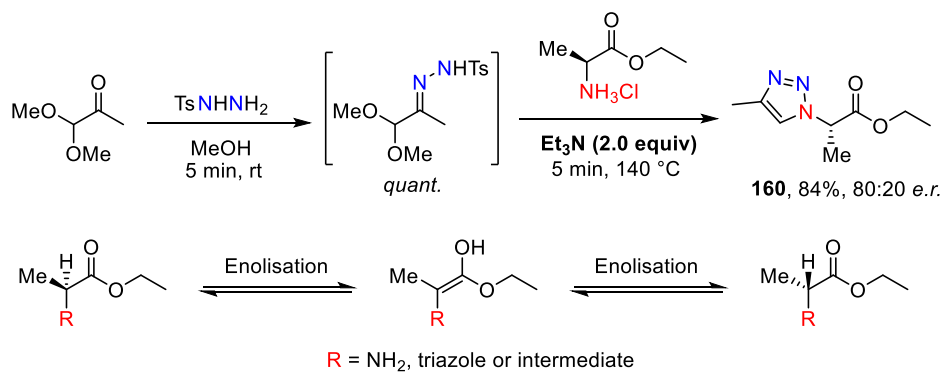
*Scheme 49: Erosion of enantiomeric purity under high-temperature conditions*

To improve the enantiomeric purity of triazole **160**, modification of the reaction conditions was pursued. By lowering the reaction temperature to 75 °C and extending the reaction time to 18 hours, whilst using only one equivalent of triethylamine, the enantiomeric purity was greatly improved to 98:2 (by HPLC analysis using a chiral stationary phase) and the product **160** was isolated in 84% yield (Scheme 50).
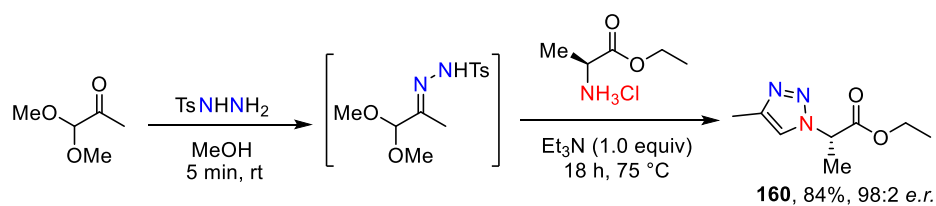
*Scheme 50: Modification of reaction conditions to improve enantiomeric purity of **160***

3.5.5 Unsuccessful nucleophiles

To further probe the reaction to examine the scope of the amine nucleophile, benzamide was exposed to the reaction conditions (Scheme 51). No *N*-benzoyl triazole **161** was observed. Instead, the sealed reaction vial remained pressured after heating to the reaction temperature for 5 minutes. By LCMS analysis, benzamide remained unreacted, however, the residual pressure in the microwave vial highlighted that the hydrazone had undergone decomposition. This suggested that the hydrazone would decompose with particularly poor amine nucleophiles such as benzamide.
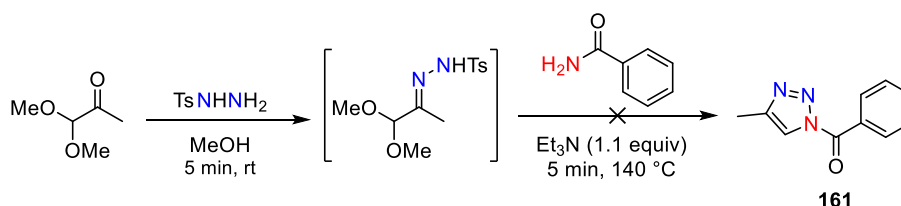
Scheme 51: Unsuccessful nucleophile

## 3.6 Synthesis of triazole 144 on a multi-gram scale

Moving forward, to exemplify this procedure as a synthetically valuable protocol to access triazoles on a preparative scale, cyclohexylamine was treated with the *in-situ* formed hydrazone under reflux (Scheme 52). After 16 hours at reflux, 7.4 g of triazole **144** was isolated in an 81% yield. This compares favourably with a 91% yield under the optimised super-heating conditions. This suggests that the process will be a practical method to synthesis 1,2,3-triazoles on a preparative scale.
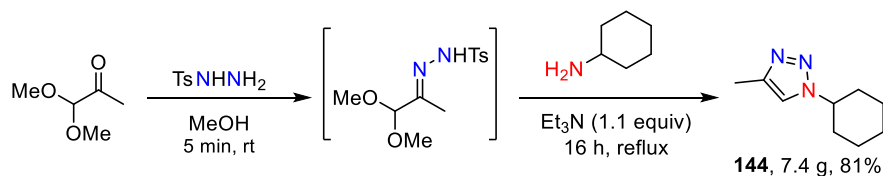
*Scheme 52: Multi-gram scale synthesis of triazole **144** from cyclohexylamine under typical batch conditions*

From here, to further show scalability, a two-stage flow process was designed (Scheme 53). A 0.43 M solution of *p*-toluene sulfonylhydrazide (**107**) was combined with a 0.979 M solution of α-ketoketal **106** at flow rates of 4.60 mL min^{-1} and 2.02 mL min^{-1} respectively. This results in a molar flow rate of 1.978 mol min^{-1} of both solutions, which was passed through a 20 mL reactor at 20 °C. The residence time for this process was 3.02 minutes. After this, the hydrazone solution and a 1:1 solution of cyclohexylamine and triethylamine were combined in a T-piece, whereby the reaction was superheated to 145 °C through a 50 mL reactor. After a residence time of 7 minutes, the solution was passed through a back-pressure regulator and the solution collected. 73 grams of triazole **144** was isolated in an 82% yield after a processing time of 4.5 hours. This flow-process exemplifies the power of the designed synthetic procedure to rapidly access triazoles on a preparative and process chemistry relevant scale.
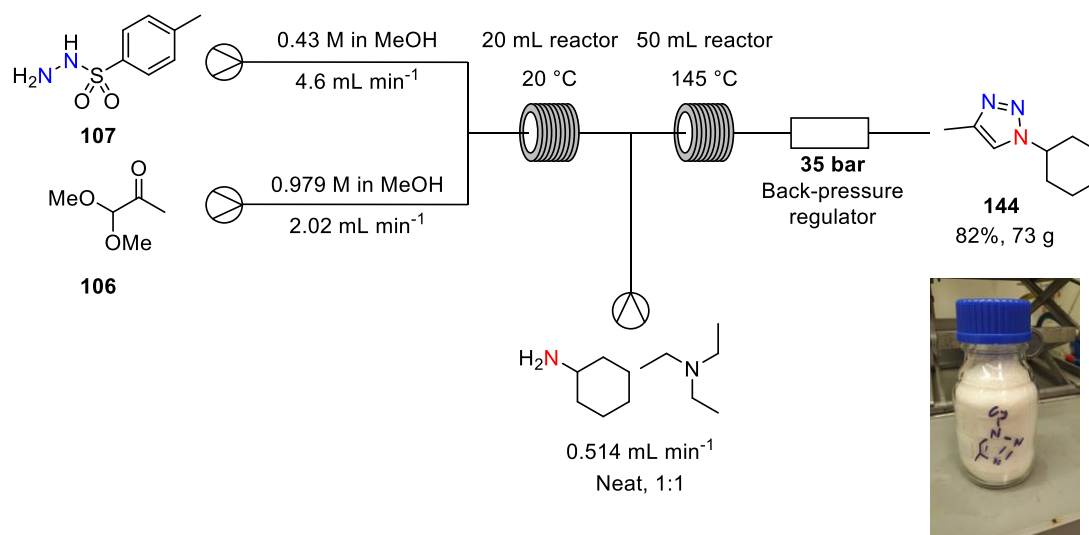
Scheme 53: The designed flow-sequence to synthesise triazoles under the optimised conditions on a large scale

3.7 Exploration of the α-ketoacetal

To examine the compatibility of substitution on the 4-position of the triazole, a synthetic route to access a series of α-ketoacetals (**162**) was required (Scheme 54). Literature methods often rely on the use of Weinreb amides (**163**) as precursors, whereby addition of an organometallic reagent (Grignard, organolithium) forms the desired α-ketoacetal.[102] Weinreb amides are often not commercially available and require synthesising, likely from an acid chloride which in-turn is made from the carboxylic acid. Another, arguably more attractive method uses simple α-esteracetals such as ethyl diethoxyacetate (**164**). These species are commercial, and so looked like an attractive option to gain rapid access to a series of α-ketoacetals.
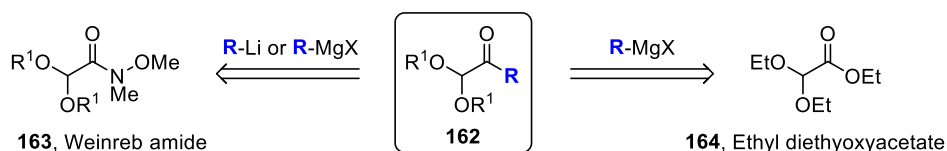
*Scheme 54: Retrosynthesis of functionalised α-ketoacetals*

3.7.1 Grignard additions to esters

Traditionally, the reaction of Grignard reagents with esters gives poor selectivity when the desired product is the ketone; the major product from this reaction is the tertiary alcohol (Scheme 55). The initial Grignard addition to the ester (**165**) gives tetrahedral intermediate **166**. This intermediate rapidly collapses, even at low temperatures, expelling an alkoxide to give a ketone **167**. The instability of the tetrahedral intermediate means that the ketone is formed when there is a Grignard reagent remaining. Ketones are more electrophilic than esters, meaning that there is a lower activation barrier to the addition of a nucleophile. As such, a Grignard reagent will preferentially add to the ketone over the ester, resulting in the formation of a tertiary alcohol. As a result, when 1 equivalent of a Grignard reagent is added to a simple ester (**165**), in most cases the observed products are the tertiary alcohol (**168**) and residual starting material (**165**) in a 1:1 ratio.[103,104]

165 **166** **167** **168**

165 **168** **165**

1 : 1
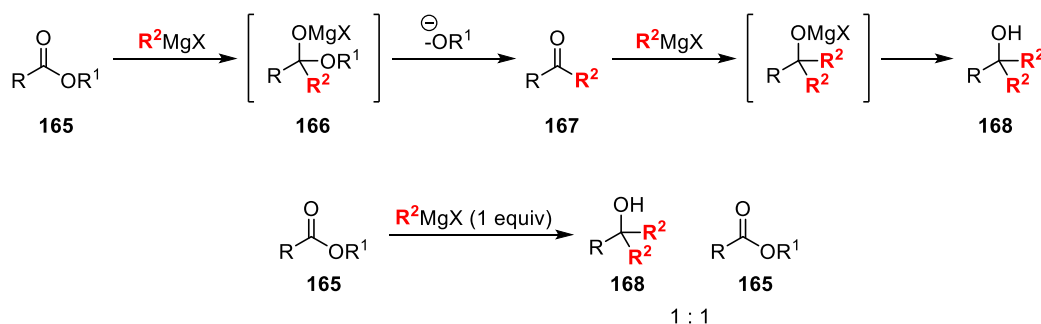
*Scheme 55: The challenge with Grignard additions to esters*

It was believed that addition of a Grignard reagent to ethyl diethoxyacetate (**164**) would result

in the formation of a stabilised tetrahedral intermediate (**169**) in which the pendant acetal would

coordinate to the magnesium centre, resulting in the formation of the ketone (**170**) as a major

product. A literature search indicates that this idea has been pursued and successfully applied

to the synthesis of a range of α-ketoacetals.[105]

164 **169** **170**
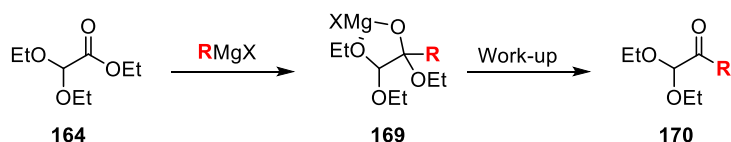
Scheme 56: Grignard addition to an acetal-containing ester

### 3.7.2 Preparation of a library of α-ketoacetals

This method enabled the synthesis of a variety of α-ketoacetals to examine the tolerance of

the ketoacetal in the triazole-forming reaction. Addition of a Grignard reagent to

ethyl diethoxyacetate at −78 °C in THF gave the α-ketoacetals displayed in Scheme 57. Allyl,

homoallyl, cyclohexyl and homobenzyl substrates (**171**, **172**, **174** and **175**) were prepared in

47%, 58%, 49% and 64% respectively. Substrate **173** was used as sourced from a commercial

supplier.
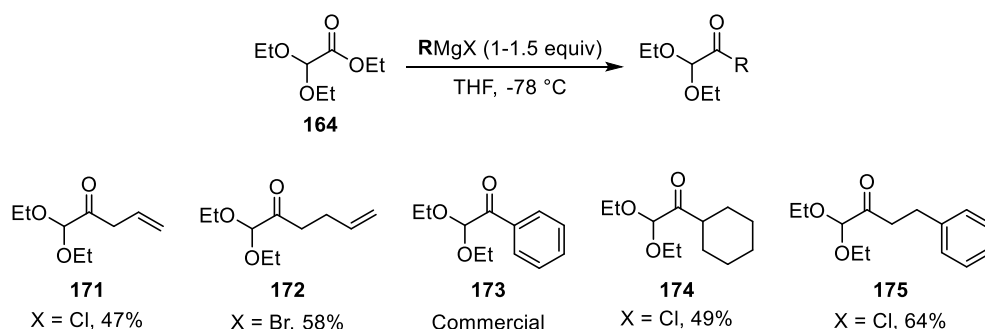
Scheme 57: The synthesised α-ketoacetals and the commercial substrate 173

3.7.3 The reaction of allyl substrate 171

On exposure of allyl-ketoacetal **171** to *p*-toluene sulfonylhydrazide in methanol, after 10 minutes the reaction gave a species consistent in mass with hydrazone **176** by LCMS analysis. Addition of benzylamine and triethylamine followed by heating to 140 °C for 5 minutes gave a mixture of products. 4-allyl triazole **177** was isolated in 39% yield and a 4:1 mixture of the stereoisomeric internal alkene triazoles **178** were isolated in 24% combined yield. The internal alkene products could not be separated by chromatography or preparative HPLC but were isolated as a mixture of both *E* and *Z* isomers as determined by ^{1}H NMR analysis.
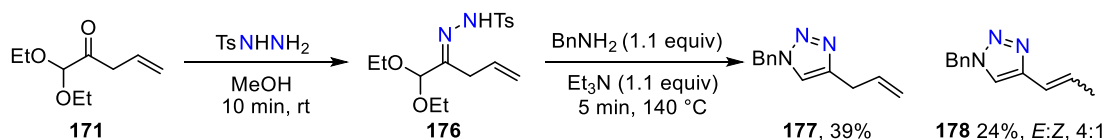
Scheme 58: The reaction of 171. Alkene migration under the optimised conditions

The internal alkene products **178a** and **178b** could form as a result of alkene migration in the product. The internal alkene is more substituted and is conjugated into the triazole aromatic π-system, providing a thermodynamic driving-force for the migration (Scheme 59).[106] An alternative option is the intermediate hydrazone undergoes alkene migration by the formation of an enamine intermediate **178** from **176**. However, the described deuteration experiments in Section **3.3** have provided no evidence for the formation of an enamine under the reaction conditions.

57
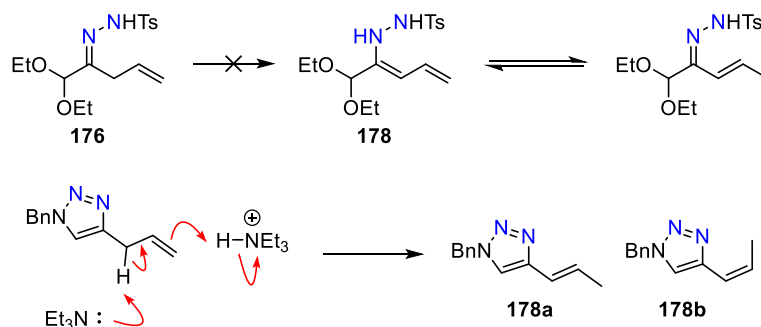
Scheme 59: Postulated mechanism for alkene migration

3.7.4 Homologation of allyl substrate

By homologating α-ketoacetal **171** from allyl to homoallyl to give substrate **172**, on exposure to the same reaction conditions, hydrazone **180** was obtained and no migration of the alkene in the triazole product was observed, providing a product solely containing a terminal alkene. Benzylamine, aniline, methylamine, cyclohexylamine and ammonia all underwent efficient cyclisation to the alkene-baring triazoles **181**–**185** in 75%, 81%, 82%, 84% and 75% (Scheme 60).
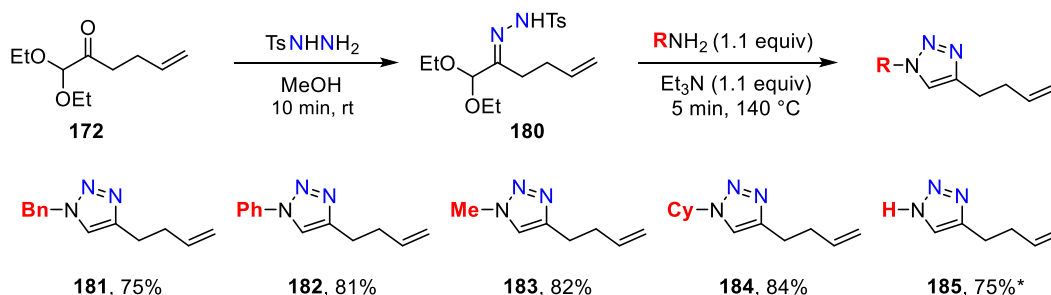

Scheme 60: Homologation of alkene, scope with 5 representative amines.
*No Et₃N, 2.2 equiv NH₃

With the alkene triazoles displayed above in Scheme 60, it is worth noting the formation of a side-product. The triazoles derived from benzylamine, methylamine and ammonia, after standard-phase chromatography were isolated containing between 3–6% of their saturated alkane analogue and the yields shown above are of clean alkene product isolated after preparative HPLC. Standard phase chromatography was able to separate the alkane-side products of the triazoles derived from aniline and cyclohexylamine (**182** & **184**). The formation of an alkane under these conditions is interesting. On considering the methylamine derived

triazole, standard phase chromatography gave a mixture of the alkene and alkane products in a 13:1 ratio (78% **183** and 6% **186** respectively) (Scheme 61). Moreover, through studying the hydrazone formation by HPLC, no *p*-toluene sulfonylhydrazide was observed on completion of hydrazone formation. This highlights the reversibility of the hydrazone formation.
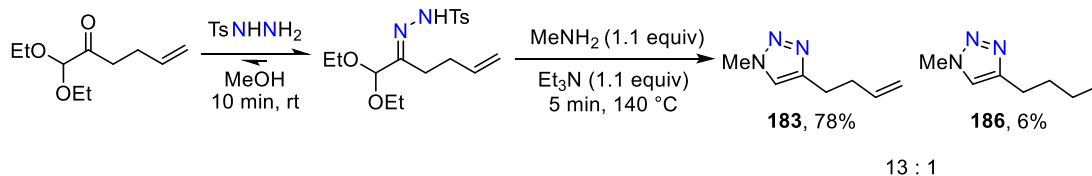

Scheme 61: Background reduction of the alkene

To investigate the formation of the alkane, a series of experiments were conducted. Exposing the mixture of alkane **186** and alkene **183** shown in Scheme 60 to 1 equivalent of *p*-toluene sulfonylhydrazide altered the ratio of alkene to alkane to 1:6 (Scheme 62).
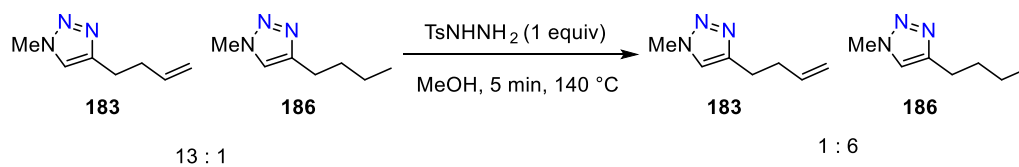
Scheme 62: Control reaction to elucidate the reductant

Adding 1 equivalent of either triethylamine or methylamine gave complete conversion to the alkane (Scheme 63).
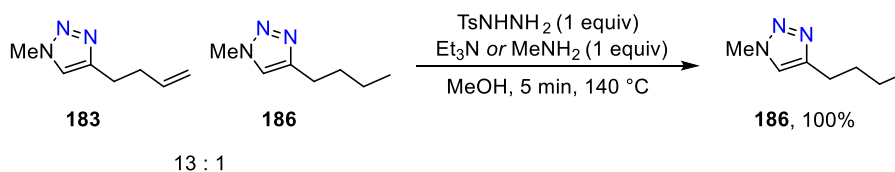
*Scheme 63: Second control reaction to elucidate the reductant. Quantitative conversion to alkane product **186**.*

These experiments suggest that the responsible reductant is diimide (**187**), derived from either the thermal or base-promoted decomposition of *p*-toluene sulfonylhydrazide , a known process to reduce unhindered, unpolarised alkenes (Scheme 64).[107] The initial hydrazone formation

was monitored closely by HPLC analysis and no residual *p*-toluene sulfonylhydrazide was remaining before the amine was added and the reaction heated. This suggested that the hydrazone formation is reversible under the reaction conditions. At elevated temperatures any free *p*-toluene sulfonylhydrazide can eliminate to form diimide, which then engages with the reduction of the alkene.

187
Diimide formation
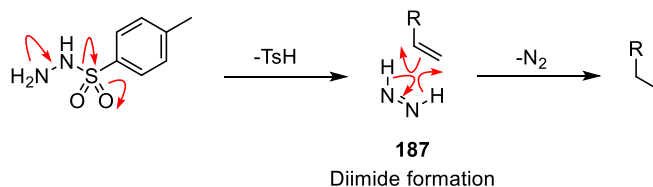
Scheme 64: Diimide reduction of unhindered alkenes

3.7.5 Further α-ketoacetal substrates

Phenyl α-ketoacetal **173** took 2 hours to form the desired hydrazone (**188**) smoothly by LCMS analysis of the reaction mixture. The longer length of time taken for hydrazone formation is likely due to the increased steric encumbrance around the ketone. After this time, the desired amine was added and the reaction submitted to the optimised conditions to give triazoles **189−193** in 72%, 67%, 86%, 73% and 74% respectively (Scheme 65).
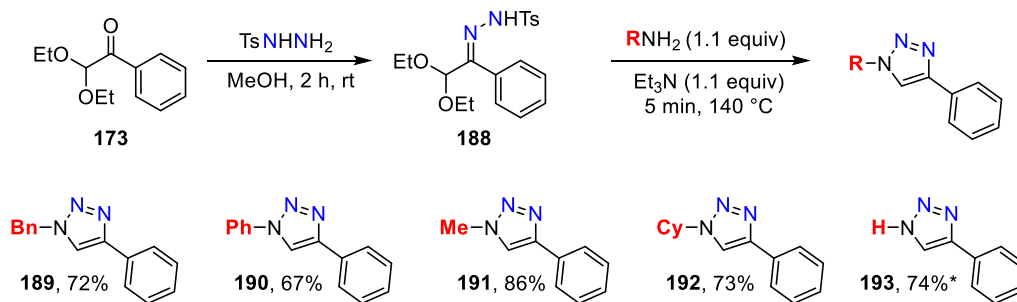
*Scheme 65: Phenyl substrate **173**, scope with 5 representative amines. *No Et₃N, 2.2 equiv NH₃*

Cyclohexyl substrate **174** underwent smooth formation to hydrazone **194** in 90 minutes. This longer length of time before complete hydrazone formation was observed is again attributed to increased steric encumbrance around the carbonyl group. Triazoles **195−199** derived from benzylamine, aniline, methylamine, cyclohexylamine and ammonia were formed in 84%, 69%, 90%, 85% and 58% respectively (Scheme 66).
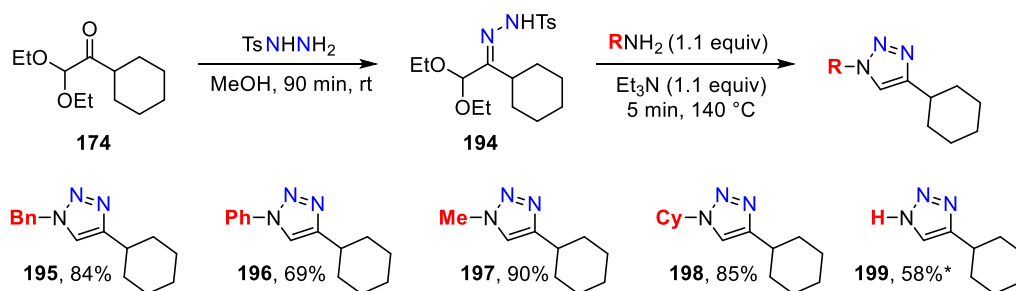
*Scheme 66: Cyclohexyl substrate **174**, scope with 5 representative amines. *No Et₃N, 2.2 equiv NH₃*

Finally, homobenzyl α-ketoacetal **175** underwent smooth conversion to the hydrazone (**200**) within 5 minutes and triazoles **201**–**205** were isolated in 83%, 77%, 88%, 85% and 82% respectively (Scheme 67).
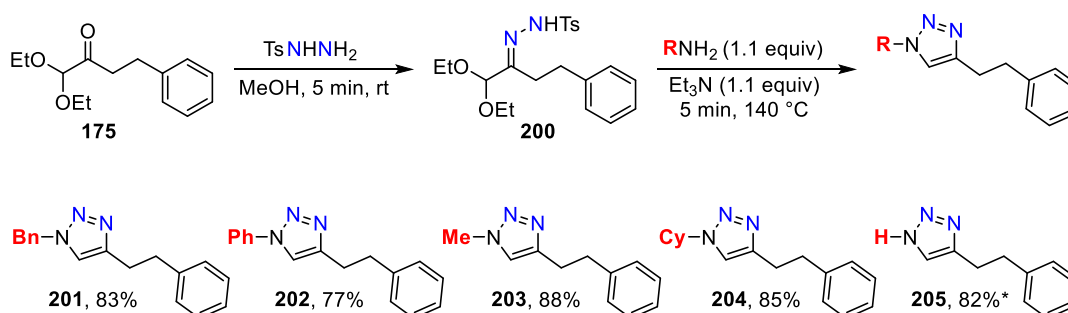
*Scheme 67: Homobenzyl substrate **175**, scope with 5 representative amines. *No Et₃N, 2.2 equiv NH₃*

A thorough examination of the use of α-ketoacetals as a method to synthesise 1,4-substituted triazoles as a direct comparison to the Sakai reaction of α,α-dichlorotosylhydrazones with primary amines has been established. The tolerance of the amine has been shown to be remarkable, aliphatic and aromatic amines are tolerated giving the triazoles in excellent yields. Chiral amines give access to enantioenriched products with excellent retention of enantiomeric purity and ammonia can give access to NH triazoles, a species which cannot be directly accessed *via* an AAC without using hydrazoic acid. Furthermore, the 4-position of the resultant triazole has been shown to be easily functionalised with a range of alkyl-, aryl- and alkenyl groups *via* the preparation of different α-ketoacetals by a Grignard addition to commercial ethyl diethoxyacetate. Up until this point the new method is directly comparable to the Sakai reaction in terms of functional group compatibility and ease of substitution at the 4-posititon (Figure 14). The developed method is beneficial when compared to the Sakai reaction by not needing to

isolate and purify the intermediate hydrazone as a problematic and limiting bishydrazone has been eliminated. The developed procedure provides rapid access to triazoles in a 3-component coupling which can be exemplified on large scale using both batch (7-gram exemplification) and flow techniques (73-gram exemplification). Moving forward, attempts to further differentiate this method from the Sakai reaction was attempted by examining the effectiveness of this procedure to synthesise different substitution patterns of triazoles (Figure 14).
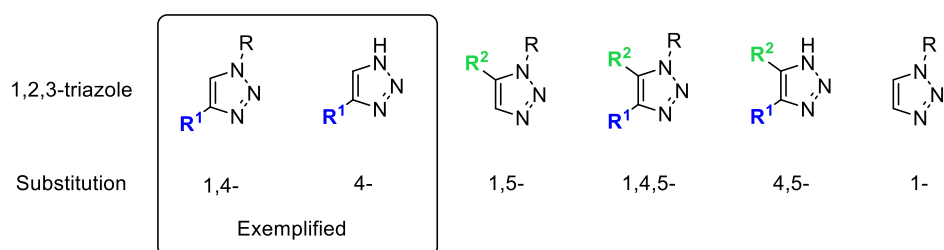

*Figure 14: The exemplified 1,2,3-triazoles (boxed). Unboxed are triazoles left to exemplify*

3.8 1,5-Substituted triazoles

3.8.1 Accessing aldehyde 211

In order to access 1,5-substituted triazoles, the required substrate is an α-ketal aldehyde (**206**, Scheme 68). The proposed retrosynthesis for such a compound stemmed back to a 1,2-diketone, in which the two carbonyls are differentiated by the inclusion of an ester and a ketone (such as **207**). Differentiation between the carbonyls is required to enable selective protection of one carbonyl over the other, whereby a functional group interconversion of the ketone to a ketal introduces the required functional group. The aldehyde is then accessed by a selective reduction of the ester. A literature search of differentiated 1,2-dicarbonyl in which one carbonyl is an ethyl ester and the other is a ketone generated greater than 50 examples with numerous commercial suppliers in which R is alkyl, aryl or heteroaryl (**208**). This suggests that these 1,2-dicarbonyl starting materials would be a suitable starting point for accessing α-ketal aldehydes.
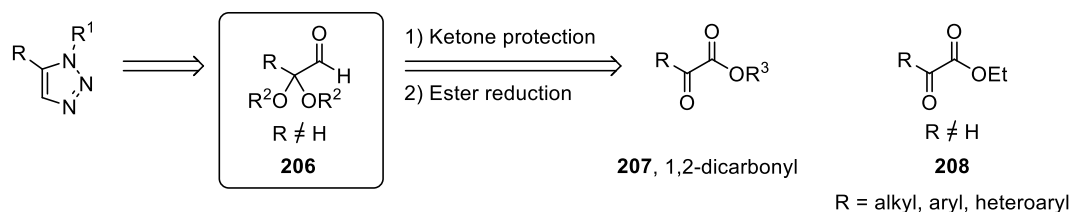
Scheme 68: Retrosynthesis of an α-ketalaldehyde

As a starting point, ethyl pyruvate (**209**) was reacted with triethyl*ortho*formate to give ketal ester **210** in a 93% yield on a >40 g scale (Scheme 69). From here, reduction of the ester using diisobutyl aluminium hydride at −78 °C gave aldehyde **211** in a moderate yield of 43%. Isolation of the aldehyde proved challenging as this species did not survive chromatography or a rapid filtration through a small plug of silica as the literature suggested.[108] The 43% quoted yield in Scheme 69 was from the product isolated by Kugelrohr distillation at 10 mbar and 45 °C. Even with careful handling and manipulation, subsequent decomposition of **211** occurred rapidly, meaning manipulations were performed quickly and under an inert atmosphere. However, this method enabled access to aldehyde **211** which could be used in the subsequent reactions.
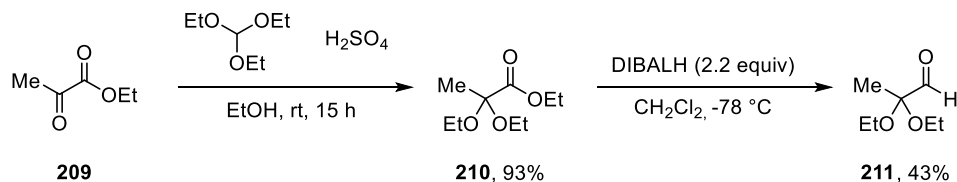
*Scheme 69: The synthesis of aldehyde **211***

3.8.2 Cyclisation of aldehyde 211 to give 1,5-triazoles

With aldehyde **211** in hand and an understanding of how to appropriately handle this substrate, the formation of a 1,5-triazole was pursued (Scheme 70). Full conversion of *p*-toluene sulfonylhydrazide (**107**) was observed after less than 5 minutes by LCMS analysis of the reaction mixture. The only observed component was a species consistent in mass with the desired hydrazone (**212**). The high reactivity of this aldehyde is unsurprising given its instability and the electron-deficiency of aldehydes, as exemplified by the in the ^{13}C chemical shift of the

aldehyde carbon (199.7 ppm). The highly electron-deficient nature of the aldehyde manifests itself in a very fast rate of hydrazone formation. To hydrazone **212** was then added a selection of primary amines, including benzylamine, cyclohexylamine, propargylamine, aniline and *tert*-butylamine. The mixtures were then subject to the optimised reaction conditions of 140 °C for 5 minutes to give 1,5-substituted triazoles **213−217** in 72%, 77%, 75%, 68% and 77% respectively. Importantly, only the 1,5-substituted triazole was observed, highlighting the regiospecificity of the process.
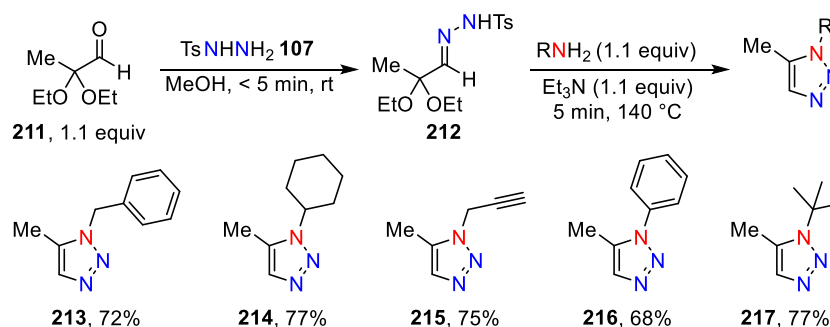
*Scheme 70: Examination of the regiospecific 1,5-substituted triazole synthesis from aldehyde **211***

3.8.3 Regiochemistry determination

As a general trend, as described in a review of 1,2,3-triazoles, the C5 carbon of a 1,4-disubstituted triazole displays a signal in the ^{13}C NMR at 120 ± 3 ppm. The corresponding C4 carbon of the 1,5-disubstituted isomer instead appears at 133 ± 3 ppm.[51] This is exemplified in Figure 15 in which the aromatic region of the ^{13}C NMR spectra of cyclohexyl triazoles **144** and **214** (1,4- and 1,5-substituted) are displayed. In the 1,4- isomer (**144**), the C5 carbon has a chemical shift of 118.8 ppm, and in the 1,5-isomer (**214**) the C4 has a chemical shift of 132.7 ppm. Since the ^{13}C chemical shifts in the observed products described above fall within the ranges provided, this offers strong evidence for the regiospecific formation of either 1,4- or 1,5-substituted triazoles depending on starting material.
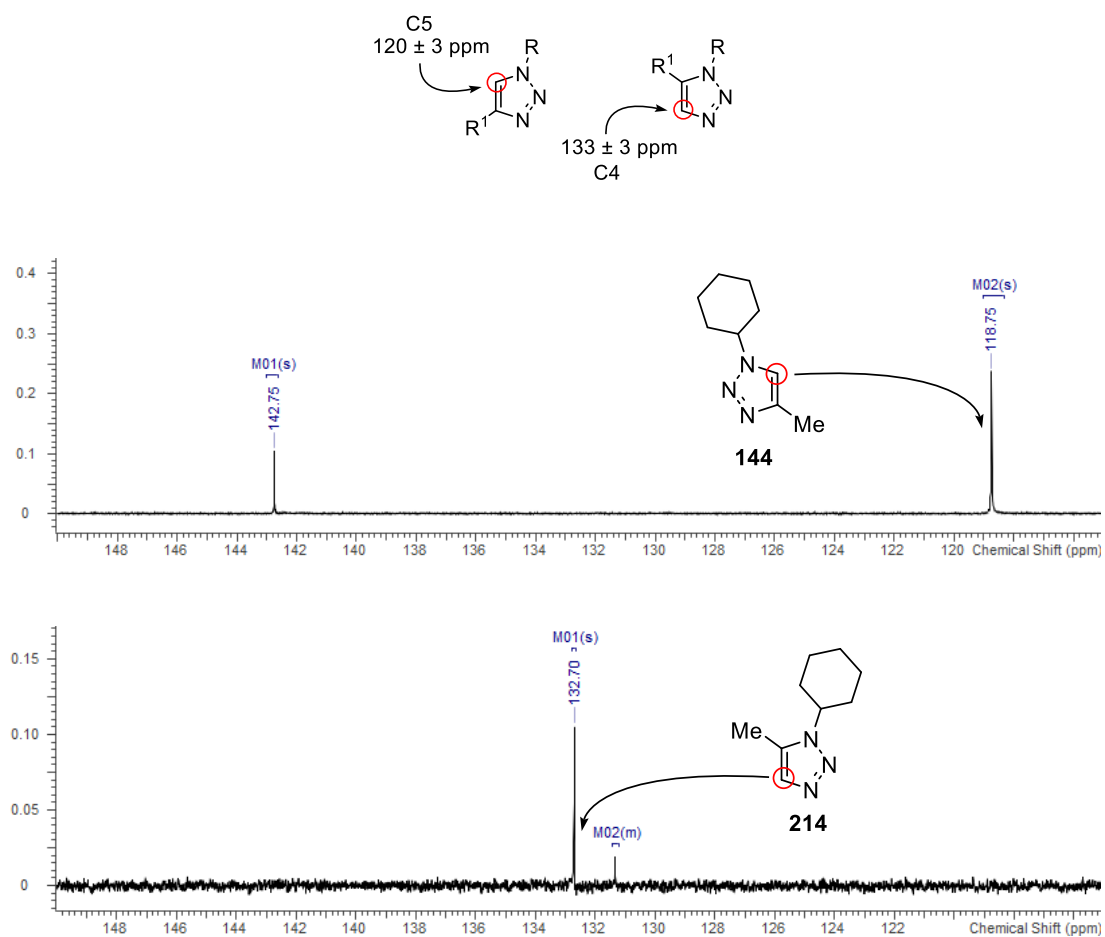
Figure 15: Regiochemistry determination by ^{13}C chemical shift of the triazole products. Top, 1,4-isomer (**144**), bottom, 1,5-isomer (**214**).

3.9 (1),4,5-Substituted triazoles

3.9.1 Acyclic systems

To access (1),4,5-substituted triazoles, the proposed starting material is an α-ketoketal (**218**, Scheme 71). The nomenclature (1),4,5 is used to include the formation of NH triazoles, which are formally not substituted on the 1-position. There are a number of these substrates commercially available (**219**, **220**) often derived from a symmetrical 1,2-diketone. As a starting point, 3,3-dimethoxybutan-2-one **219** was examined.
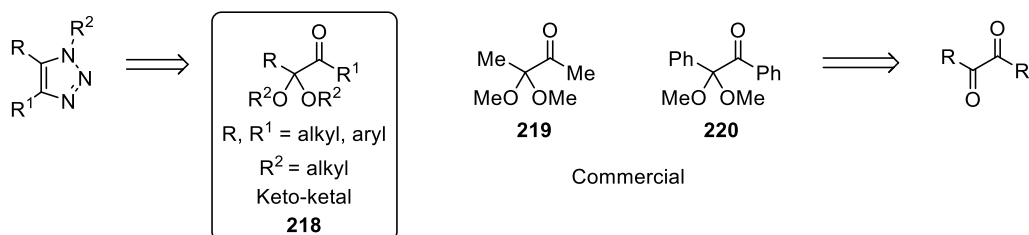
Scheme 71: The proposed retrosynthesis of 1,4,5-substituted triazoles from α-ketoketals

Addition of *p*-toluene sulfonylhydrazide to 1.05 equiv ketoketal **219** in deuterated methanol gave a mixture of 3 products after 60 minutes by LCMS analysis. The ratios of the 3 species are shown in Scheme 72. Hydrazone **221**, bishydrazone **222** and ketone **223** were observed in a 3.5 : 1.4 : 1 ratio respectively after 60 minutes. On leaving the same reaction for a further 60 minutes at room temperature, the ratio of **221:222:223** had changed to 1 : 1.6 : 4.3.

	221	222	223
t = 60 min	3.5	1.4	1
t = 120 min	1	1.6	4.3
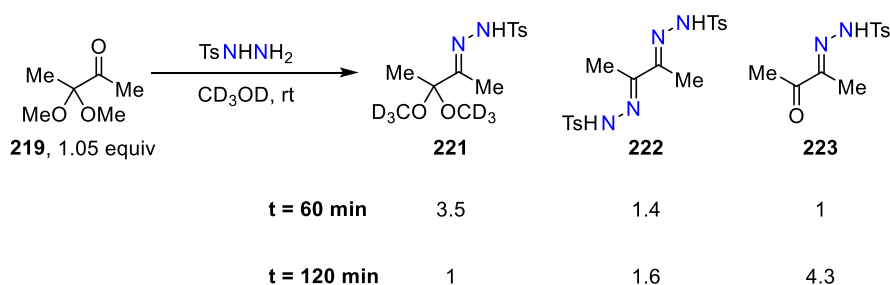
Scheme 72: The instability of a hydrazone derived from an α-ketoketal with substantial bishydrazone formation. Values shown are relative ratios

The above result suggests that the ketal-hydrazone intermediate (**221**) is unstable with respect to water (Scheme 73). Water is present from the initial hydrazone-formation or from residual

water in the solvent. This could add into enoldiazene intermediate **224** to form hemiacetal **225** which then collapses to ketone **223**.
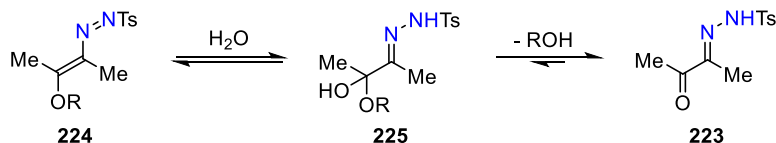
*Scheme 73: A proposed hydrolysis mechanism of the enoldiazene*

It was observed that heating the hydrazone formation reaction to 60 °C resulted in a different product distribution (Scheme 74). No desired ketal-hydrazone **221** was observed after 15 minutes, and the bishydrazone **222** and the hydrolysed ketal **223** were observed in a 1.4 : 1 ratio. This suggests that bishydrazone **222** is a thermodynamic product, and to preferentially form the ketal hydrazone **221** over the bishydrazone then the rate of formation of the ketal hydrazone **221** needs to be increased.
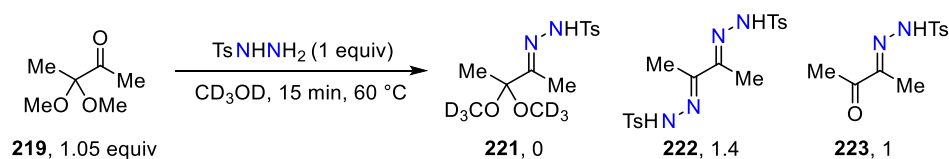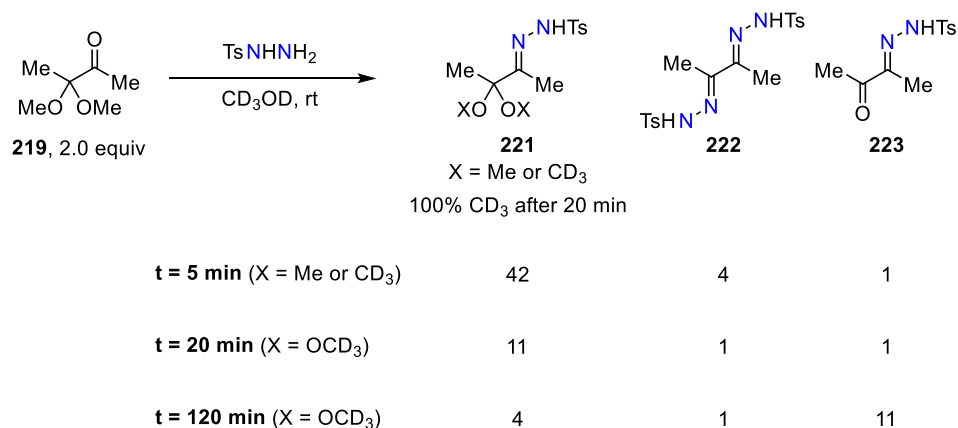

*Scheme 74: Higher temperature increases the formation of the bishydrazone **222***

In order to preferentially form the hydrazone over the bishydrazone, 2 equivalents of **219** was used. Under these conditions after 5 minutes, the ketal hydrazone **221,** bishydrazone **222** and ketone **223** were observed in a 42 : 4 : 1 ratio respectively (Scheme 75). After 20 minutes, the ratio had changed to 11 : 1 : 1 respectively. On leaving for a further 100 minutes, the ratio had further changed to 4 : 1 : 11 respectively. These points indicated a couple of factors which were taken into consideration. Firstly, the formation of a hydrazone with α-ketoketals is slower than with α-ketoacetals. This is likely because the ketone is *neo*-pentylic and as such is more sterically hindered, making attack onto the carbonyl group by a nucleophile slower. Secondly, the hydrazone derived from an α-ketoketal is remarkably more labile than that derived from an α-ketoacetal. Based on evidence by LCMS, the hydrazone-ketal hydrolyses to a hydrazone-ketone, and on consideration, this hydrolysis — in methanol — is surprising.

Secondly, complete incorporation of the OCD_3 ketal within 20 minutes further emphasises this increased lability. Scheme 32 (Section **3.3**) showed that the hydrazone derived from an α-ketoacetal undergoes 90% OCD_3 incorporation within 2 hours. The results from α-ketoketal **219** show that within 20 minutes, complete OCD_3 incorporation into the ketal was observed (Scheme 75).

|	**221**	**222**	**223**
t = 5 min (X = Me or CD_3)	42	4	1
t = 20 min (X = OCD_3)	11	1	1
t = 120 min (X = OCD_3)	4	1	11

*Scheme 75: Increased equivalents of α-ketoketal **219** increases the rate of formation of hydrazone **221** which decomposes over time*

The rationale for this observation can be explained by the Thorpe-Ingold effect.[109] The Thorpe-Ingold effect is a kinetic effect in which a quaternary carbon contained within a ring system promotes intramolecular interactions. Hydrazone **226** is proposed to undergo collapse to enoldiazene **227**, mediated by an intramolecular hydrogen bond between the hydrazone NH and the acetal (Scheme 76). In the case of a hydrazone derived from an α-ketoketal (**226**) the methyl group and OMe group (both shown in red) will have a larger bond angle between them compared with the proton and OMe group from the α-ketoacetal hydrazone (**228**) (both shown in blue) owing to increased steric interaction. An MOE calculation of the bond angle between the hydrazone and methoxy group in substrate **226** returned a bond-angle of 115.1 °, whereas the calculated value for substrate **228** was 115.6 °, providing support for this Thorpe-Ingold hypothesis. This decrease in bond angle in **226** favours the intramolecular interaction and thus the elimination of methanol to form the enoldiazene (**227**) over that of **229** (from **227**). This provides an explanation for the faster rate of enoldiazene formation with α-ketoketals than α-ketoacetals.
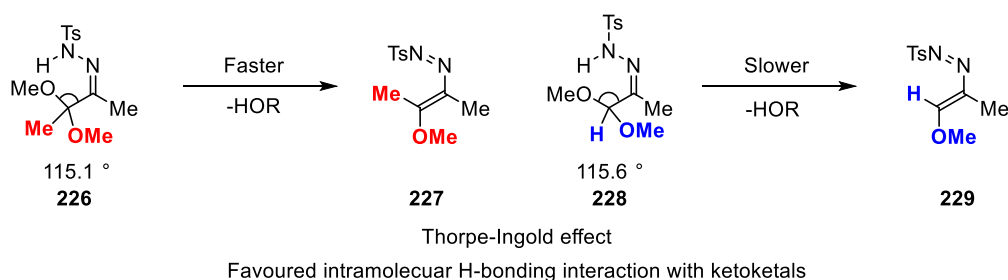
Scheme 76: A potential explanation of the increased lability of hydrazone **226**. Thorpe-Ingold effect

Another possibility to consider with α-ketoketals is the potential to form an enol-ether (**230**) under the reaction conditions. It is known that under acidic reaction conditions methyl-ketals undergo conversion to methyl enol-ethers.[110] Scheme 77 displays an elimination which could theoretically occur under the reaction conditions. In this example the intramolecular hydrogen bond between the hydrazone and the ketal (**226**) could facilitate the elimination to enol-ether **230** by weakening the carbon−oxygen bond. This species could then undergo oxonium formation (**231**) which is trapped by solvent to form the deuterated species (**232**).
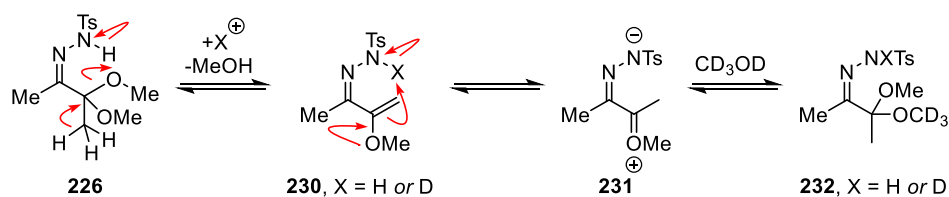
Scheme 77: Hypothesis of the potential for enol-ether formation. X = H or D

To search for evidence of this enol-ether the hydrazone formation was conducted in CH_3OD in order to separate the changes from incorporation of an OCD_3 group into the acetal from sequential M+1, M+2, M+3 peaks involving incorporation of individual deuterium atoms. Isolating the two different mechanisms for deuterium incorporation allows for an understanding of the equilibrium processes which the hydrazone intermediate is undergoing. By LCMS analysis, sequential M+1, M+2, M+3 mass changes were not observed (Scheme 78). If an enol ether (**230**) is formed, an increase in mass of M+1 should be observed by LCMS analysis resulting from protonation of this species to give deuterated ketal **233**. The mass ion of the hydrazone remained at 299 in the MS$^-$, suggesting that an enol ether is not a species present in solution.
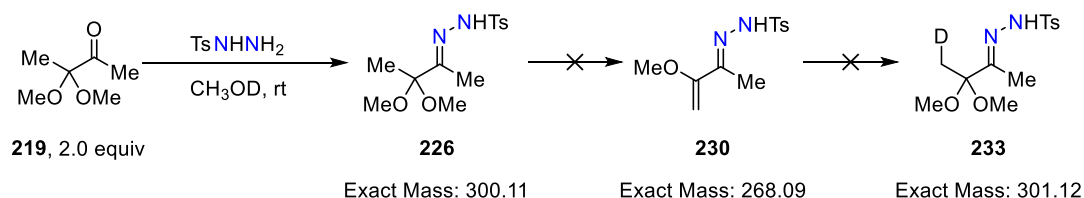
Scheme 78: Examination of enol-ether formation.
Deuterium labelling suggests that an enol-ether is not formed

As a result of the slow hydrazone formation owing to the ketone being neopentylic, and this effect being compounded by the intermediate hydrazone being significantly less stable owing to a potential Thorpe-Ingold effect, it became apparent that the intermediate hydrazone should not be held for prolonged periods before adding an amine and cyclising to the triazole. With these considerations, 1,4,5-trisubstituted triazoles **234** & **235** derived from benzylamine and aniline were isolated in a 75% and 91% yield respectively in which the amine was added as soon as complete hydrazone formation was observed (Scheme 79).
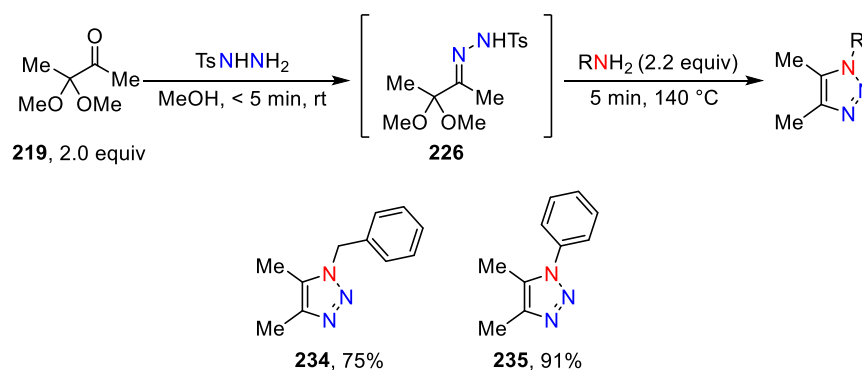
Scheme 79: Synthesis of 1,4,5-substituted triazoles from α-ketoketals

To further explore the scope of the α-ketoketal, diphenyl substrate **220** was investigated. This substrate did not undergo a reaction with *p*-toluene sulfonylhydrazide to form **236** or **237** at either room temperature or under reflux (Scheme 80). In fact, decomposition of *p*-toluene sulfonylhydrazide occurred before any consumption of the α-ketoketal was observed by LCMS analysis.
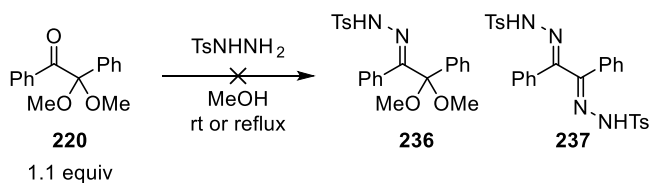
Scheme 80: Hindered α-ketoketals are ineffective substrates

The above result likely indicates that this ketone is too sterically hindered to undergo a reaction with *p*-toluene sulfonylhydrazide. A literature search for the reaction of a hydrazide or hydrazine with this α-ketoketal substrate does not yield any results, highlighting the difficulty of this reaction. In fact, a recent publication detailing a similar transformation with substrate **238** shows the highly forcing conditions required to encourage nucleophilic attack onto a neopentylic benzoic ketone to form heterocyclic species **239** (Scheme 81).[111] Considering the nucleophile in this example is hydrazine, which is known to be highly nucleophilic,[112] the highly forcing conditions demonstrate the challenge with nucleophilic attack onto a neopentylic benzoic ketone.
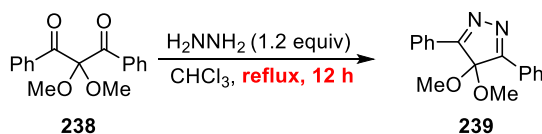
Scheme 81: Literature evidence highlighting the challenge with nucleophilic addition onto hindered neopentylic benzoic ketones

3.9.2 Attempts to access 1,4,5-substituted triazoles with different 4 & 5 groups

Being able to access 1,4,5-substituted triazoles in which the R & R^1 groups are different would be desirable (Figure 16). The CuAAC reaction has never been shown to afford 4,5-substituted triazoles, however RuAAC has shown promise in affording these products as discussed in Section **1.4**, however, regioisomers are often observed.[51] Moreover, the Sakai reaction of an α,α-dichlorotosylhydrazone has never been shown to access 4,5-substituted triazoles. Being able to access these products in a metal- and azide-free manner would be a significant advancement in this field.
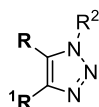
Figure 16: Differentially substituted 4,5-substituted triazoles

Methods of accessing an α-ketoketal (such as **241**) which would be derived from an unsymmetrical 1,2-diketone were examined in a manner analogous to Section **3.7.2** in which the α-ketoacetals were accessed *via* a Grignard addition to an ester (**240**, Scheme 82).
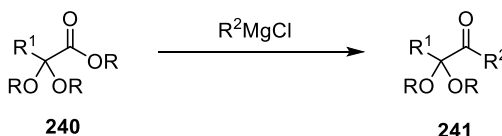
Scheme 82: The proposed addition of a Grignard reagent to an α-ketalester

Unfortunately, using the same procedure as described in Section **3.7.2**, the corresponding addition of Grignard reagent **242** to ketal-ester **243** resulted in full recovery of the starting material after 3 hours at −78 °C (Scheme 83). This was surprising; however, it was perhaps an indication of the challenging addition of a nucleophile to a neopentylic carbonyl compound. The Newman projection indicates that an incoming nucleophile and the pendant groups α to the carbonyl experience a large steric repulsion, disfavouring addition to the ester (Scheme 83).
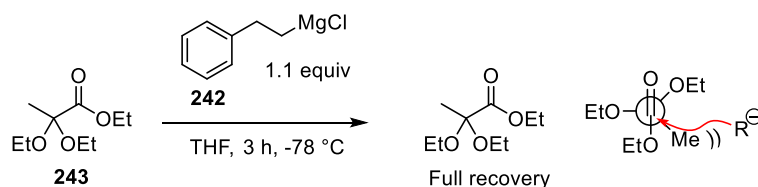
*Scheme 83: Full recovery of ester **243**, highlighting challenging nucleophilic addition to neopentyl ester*

In order to encourage Grignard addition to the sterically hindered ester, the reaction was gradually allowed to warm to room temperature overnight (Scheme 84). After 15 hours, 10% of clean α-ketoketal **244** was isolated with 30% unreacted starting **243** material. This procedure ultimately gave enough material to use for subsequent transformations but highlights how this route may not be suitable for future synthesis of these α-ketoketals without substantial optimisation.
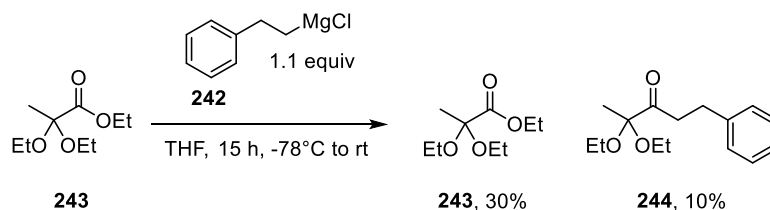
*Scheme 84: Synthesis of α-ketoketal **243***

α-Ketoketal **244** (1.5 equivalents) was exposed to *p*-toluene sulfonylhydrazide in methanol (Scheme 85). After 1 hour at room temperature, LCMS analysis of the reaction mixture showed no observable hydrazone product **245**, with 16% bishydrazone **246**; the rest of the mass balance being unreacted *p*-toluene sulfonylhydrazide. This can be explained by a very slow hydrazone formation as a result of the neopentylic carbonyl effect, as described previously. Under the current hypothesis the bishydrazone forms from enoldiazene intermediate **247**. This would suggest that the hydrazone formation is slower than the subsequent conversion to the bishydrazone, explaining why no intermediate hydrazone (**245**) was observed (Scheme 85). The increased steric encumbrance of this substrate when compared to α-ketoketal **219** is described by the Newmann projection in Scheme 85, where the homobenzyl group hinders an incoming nucleophile more than the proton in α-ketoketal **219**.
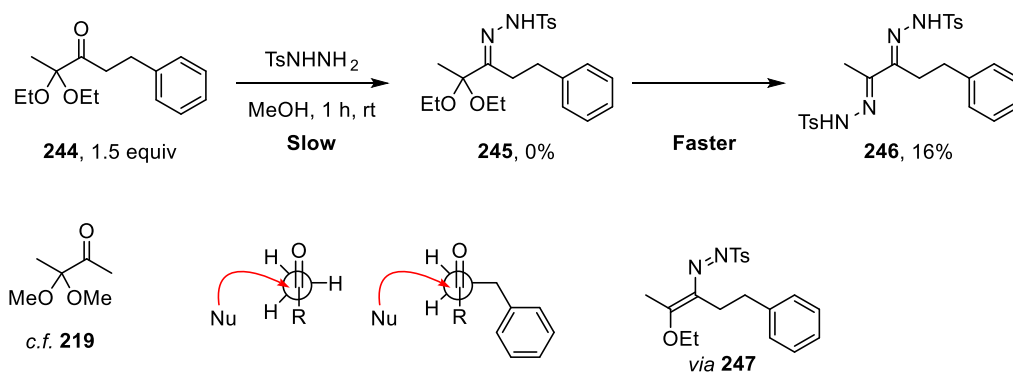
*Scheme 85: Poor selectivity for hydrazone formation with α-ketoketal **244**.
Percentages shown are LCMS peak area, discounting for residual starting material **244**.
The remaining 84% is p-toluene sulfonylhydrazide*

In attempts to increase the rate of hydrazone formation, acetic acid was added (Scheme 86). Complete consumption of *p*-toluene sulfonylhydrazide was observed under these conditions, suggesting that the addition of acetic acid did catalyse formation of the hydrazone. However, the only observed products by LCMS analysis were the hydrolysed ketal-hydrazone **248** and bishydrazone **246**. This further demonstrated the challenging preparation of the hydrazone.
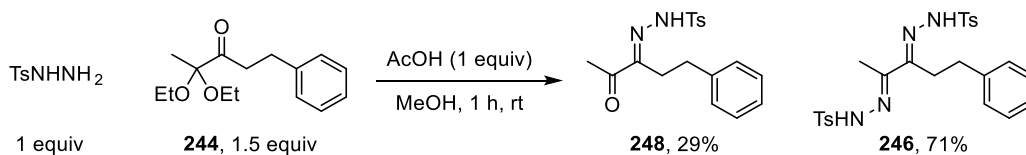
*Scheme 86: Acid-catalysed hydrazone formation.
Percentages shown are LCMS peak area, discounting for residual starting material **244***

The methoxy-ketal analogue of **244** was next synthesised in order to gain a direct comparison to Scheme 75. Two point-changes are currently present: the first is the ethoxy *vs.* methoxy ketal, and the second is the replacement of a proton with a benzyl group. As such a fair comparison between ethoxy α-ketoketal **244** and α-ketoketal **219** could not be made (Figure 17). The reason for exploring this was to elucidate whether the reason for the slower hydrazone formation was associated with the larger ethoxy ketal or the presence of the homobenzyl group.
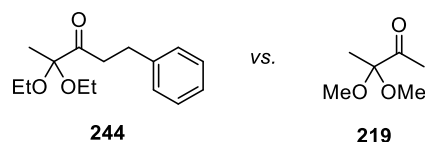
Figure 17: Comparison between α-ketoketals 244 and 219

The analogous Grignard addition to ketal ester **249** did not give any observable product **250** (Scheme 87). However, **250** was accessed *via* an aldol-elimination-reduction sequence. The α,β-unsaturated ketone **251** was obtained in 95% yield from an aldol reaction with α-ketoketal **219** and benzaldehyde. Subsequent reduction of this species with hydrogen and palladium on carbon gave the desired α-ketoketal **250** in 43% yield.
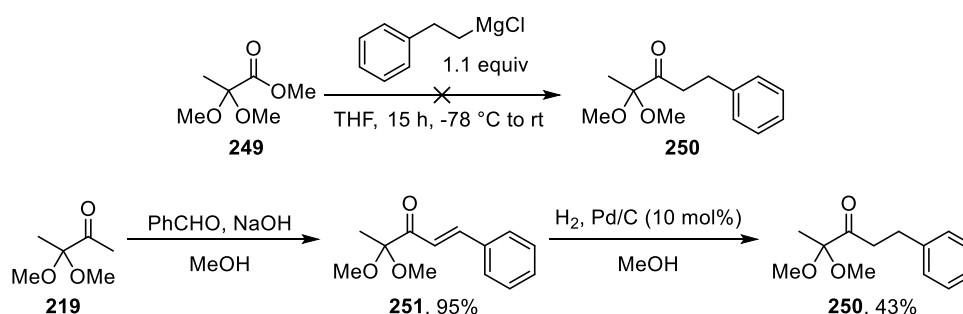
Scheme 87: Synthesis of α-ketoketal 250

Adding *p*-toluene sulfonylhydrazide to 2 equivalents of α-ketoketal **250** gave a substantially different result to Scheme 75. No hydrazone ketal **253** was observed by LCMS. A species consistent in mass with the hydrolysed ketal **248** was observed at 11% and bishydrazone **246** was observed at 17%. This experiment, in combination with Scheme 75, compares the size of a proton with a benzyl group. The results suggest that increasing substitution on the α-position of the ketone substrate substantially decreases the rate of hydrazone formation owing to increased steric congestion around the ketone. This therefore does not allow for clean formation of the hydrazone and thus is a present limitation of this methodology.
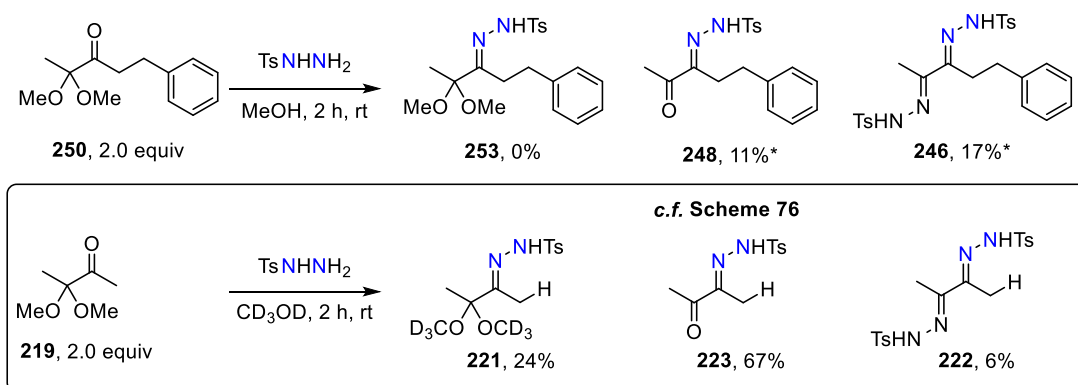
Scheme 88: Hydrazone comparison between *α-ketoketals* **250** and **219**.
*LCMS area% discounting for residual **250**

These factors point towards the conclusion that acylic α-ketoketals remain a challenge using this methodology and significant further work is required to address this problem. See Future Work Section **4.2** for ideas to improve this reactivity.

3.9.3 Cyclic systems

To examine the effect of using a cyclic α-ketoketal, cyclohexane-1,2-dione (**256**) was reacted in acidified methanol to give cyclic α-ketoketal **257** in 24% yield.[113]
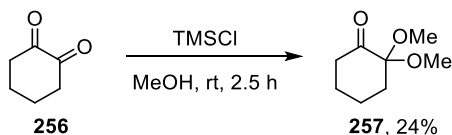
*Scheme 89: Cyclic α-ketoketal **257** synthesis*

With cyclic α-ketoketal **257** in hand, it was quickly observed that the desired ketal hydrazone **258** formed smoothly within 10 minutes using only a slight excess of **257** (Scheme 90). No bishydrazone formed under these conditions. This could indicate that the hydrazone formation is substantially faster in a cyclic system, or that the intermediate hydrazone of a cyclic α-ketoketal is more stable than an acyclic counterpart. In the acyclic system, the formation of the bishydrazone was a major constituent under the same conditions (see Scheme 72). This suggested that cyclic α-ketoketals would be more suitable substrates than acyclic variants. With smooth conversion to the hydrazone using cyclic substrate **257**, triazoles **259** and **260** were isolated by addition of either benzylamine or ammonia in 79% and 87% yield respectively (Scheme 90). An extensive substrate scope of the amine was not pursued; the assumption being that the scope of the amine would not change under these conditions.
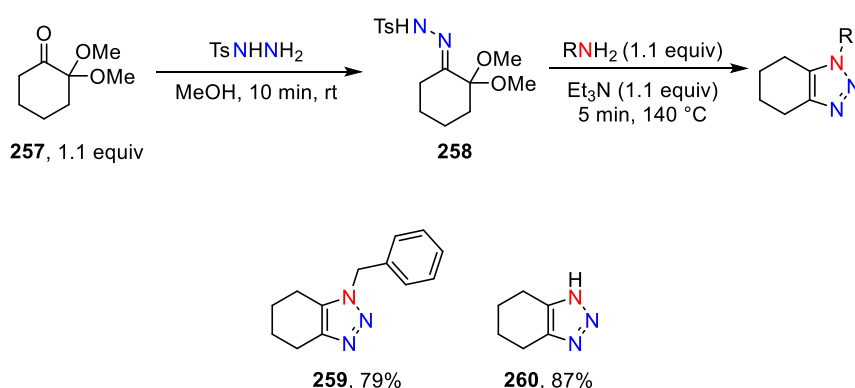
*Scheme 90: Exemplification of 1,2,3-triazole synthesis from cyclic α-ketoketal **257***

These tetrahydrobenzotriazole products are very interesting from an accessibility point of view. If AAC chemistry was used to access these products, the required alkyne would be cyclohexyne (**262**); a highly strained, energetic compound which is challenging to prepare.[114] The use of cyclohexyne to access tetrahydrobenzotriazoles is known (Scheme 91),[115] however, the starting materials are tetrasubstituted cyclic alkenes such as **261**, which are non-trivial to synthesise.[116] The method presented above is the first example of a redox-neutral, azide-free synthesis of tetrahydrobenzotriazoles. This could therefore prove to be a valuable tool in the synthesis of these products.
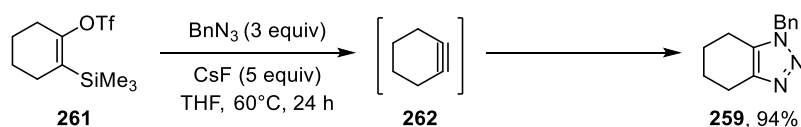
*Scheme 91: The traditional synthesis of tetrahydrobenzotriazoles; benzyne (**262**) is the required precursor*

3.10 1-Substituted triazoles

3.10.1 *N*–Alkyl Triazoles

1-substituted triazoles are often accessed from an azide and acetylene.[56] These reactions either necessitate an acetylene atmosphere which presents a fundamental safety concern, or require the use of specialist equipment to safely handle acetylene. As such, the use of protected acetylene analogues has garnered attention.[57-61] The protecting groups introduced often require a further synthetic step post-triazole formation to remove. As a solution, both Singh and Harada have reported an adaption of the Sakai reaction to furnish 1-substituted triazoles using either dichloroacetaldehyde or dichloroacetaldehyde-hydrate (**263** & **264**, Scheme 92).[86,88] This procedure offers a traceless alternative to the use of protected acetylenes in which the triazole is isolated without a residual protecting group. However, dichloroacetaldehyde and the hydrate are both highly reactive species and have extremely high associated toxicity concerns. Moreover, the intermediate hydrazone still required isolation, meaning this procedure was two-steps and couldn't be considered a "Click" reaction.
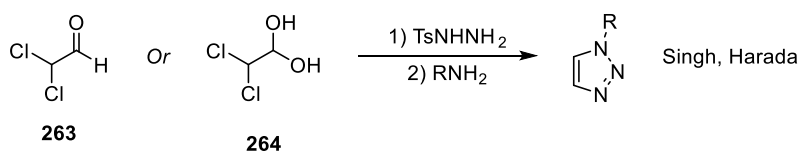
Scheme 92: Singh and Harada's 1-substituted triazole synthesis

The hypothesis presented here, an extension of the previously discussed methodology, would enable the use of 1,1-dimethoxyacetaldehyde (**265**) as a precursor to 1-substituted triazoles (Scheme 93). The benefits offered with this procedure would be the neutral reaction conditions as HCl would not be produced throughout the reaction, the use of a safer, more stable aldehyde starting material and the one-pot nature of the reaction. If this procedure behaves as previously described, the hydrazone would not need to be isolated and could rapidly gain access to 1-substituted triazoles.
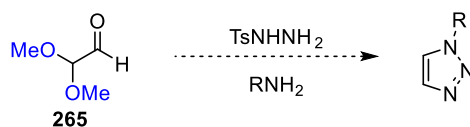
Scheme 93: The proposed adaption of the procedure using 1,1,-dimethoxyacetaldehyde

At the outset it was observed that the reaction between *p*-toluene sulfonylhydrazide and 1,1-dimethoxyacetaldehyde to form hydrazone **266** took two hours before full consumption of *p*-toluene sulfonylhydrazide was observed. The increased length of time for hydrazone formation is likely due to the form in which the aldehyde was obtained. An aqueous solution of aldehyde **265** was used and so it is likely that the aldehyde exists in an equilibrium with hydrate **267**. This aldehyde-hydrate will be unreactive with *p*-toluene sulfonylhydrazide, providing an explanation for the slower hydrazone formation. The important point to note is that no bishydrazone **268** was observed under these conditions.
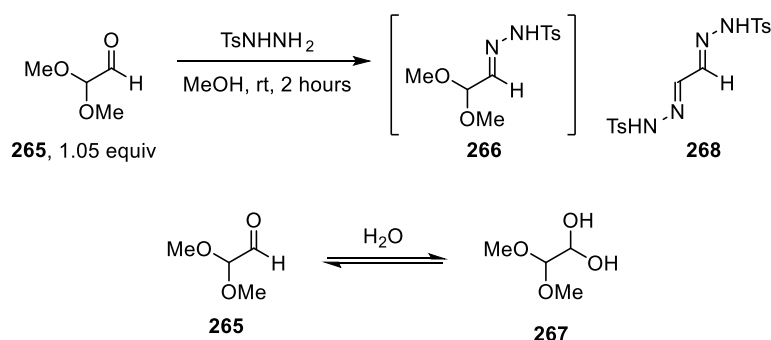
Scheme 94: An explanation for the slow hydrazone formation

3.10.2 Optimisation

Hydrazone **266** was exposed to the optimised conditions from the previous investigations using 1.1 equivalents of both the primary amine and triethylamine at 140 °C for 5 minutes. By LCMS analysis, the reaction profile was very messy and isolation of triazole **269** was challenging (Scheme 95).

265, 1.05 equiv   **266**   **269**, Messy
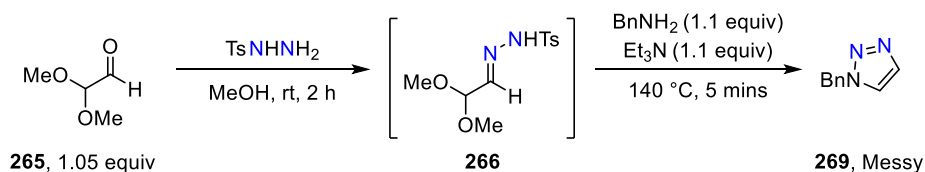
*Scheme 95: Poor selectivity for triazole **269** formation under previously optimised conditions*

In order to improve the reaction profile, the temperature was lowered to 75 °C in a sealed tube (Scheme 96). After 16 hours under these conditions a 57% solution yield the triazole **269** was observed by ^{1}H NMR spectroscopy using 1,3,5-trimethoxybenzene as an internal standard.

265, 1.05 equiv   **266**   **269**, 57%
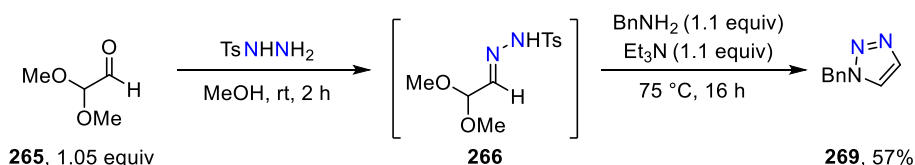
*Scheme 96: Improved triazole **269** formation under milder conditions*

Table 4 displays the results of an optimisation procedure. The author would like to highlight the significant contribution of S. J. M. Patterson in the optimisation and synthesis of the triazoles contained within this Section. Entries 1, 2 and 6 were conducted by the author, S. J. M. P. performed the remaining entries with guidance from the author. Entry 1 is described in Scheme 96 where a 57% solution yield of **269** was observed. Interestingly, the solution yield of triazole **269** was 65% in the absence of any additives suggesting that basic reaction conditions were suboptimal for the desired transformation. Adding 0.05 equivalents of acetic acid (Entry 3) gave a yield increase to 69%. This may be encouraging collapse of the acetal; a species which is known to be labile under acidic conditions.[117] Gradually increasing the number of equivalents of acetic acid from 0.1 equivalents through 0.2 equivalents, 1 equivalent and 3 equivalents led to a concurrent increase in solution yield of the triazole (Entries 4–7, 72%–79%). When 5 equivalents of acetic acid were added the yield dropped to 74% (Entry 8). Lowering the temperature resulted in a loss in yield to 60% at 40 °C and 54% at 30 °C respectively after 72 hours (Entries 9 & 10). Stronger acids (methane sulfonic acid, Entries 11–13) completely shut off the desired reactivity. The pKa of the additive was next examined and found that less acidic additives including pentafluorophenol (pKa = 5.5)[118] and

hexofluoroisopropanol (pKa ~9)[119] were also advantageous over no additive giving 76% and

72% yield respectively (Entries 14 & 15). These factors suggest that weak acids are the best

additives for the desired transformation. With this, triazole **269** was isolated in 76% yield from

the conditions shown in Entry 6 on a 1 g scale.
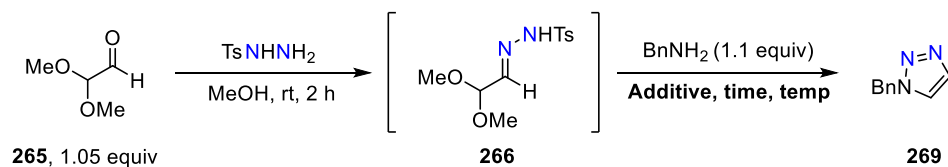
Entry	Temp. / °C	Additive (equiv)	Time / h	**269** yield /%[a]
1[b]	75	Et$_3$N (1.1)	16	57
2[b]	75	–	16	65
3	75	AcOH (0.05)	16	69
4	75	AcOH (0.1)	16	72
5	75	AcOH (0.2)	16	76
6[b]	75	AcOH (1.0)	16	78 (76)
7	75	AcOH (3.0)	16	79
8	75	AcOH (5.0)	16	74
9	40	AcOH (1.0)	72	60
10	30	AcOH (1.0)	72	54
11	75	MsOH (1.0)	16	2
12	75	MsOH (3.0)	16	0
13	75	MsOH (5.0)	16	0
14	75	PFP (1.0)	16	76
15	75	HFIP (1.0)	16	72

Table 4: Optimisation of 1-substituted triazole synthesis.
[a]Solution yield using 1,3,5-trimethoxybenzene by ^{1}H NMR spectroscopy.
[b]The reported solution yield is the mean average of 3 experiments.
PFP = pentafluorophenol. HFIP = hexafluoroisopropanol. Yields in parenthesis are isolated yields.

3.10.3 *N*-alkyl triazoles

Having developed optimised conditions, the scope of the primary amine was explored. Triazoles derived from benzylamine, propargylamine, cyclohexylamine and hexylamine were isolated in 76%, 33%, 54% and 57% yield respectively (**269−272**, Scheme 97). It is proposed that the moderate yields observed were associated with the acid-base equilibrium obtained on mixing the amine with acetic acid.
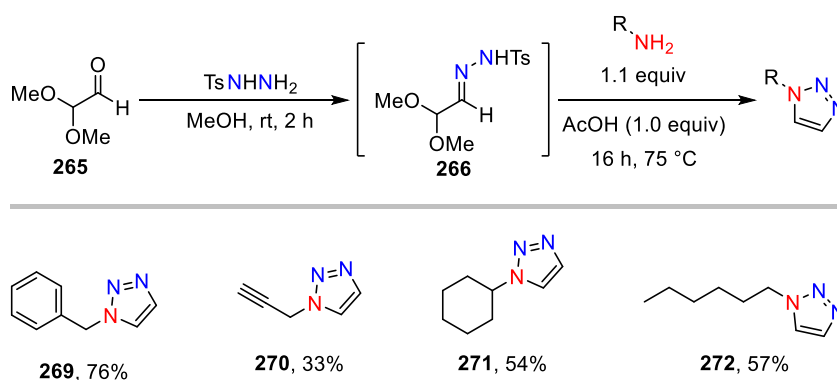
Scheme 97: Scope of aliphatic amines to give N-alkyl triazoles

3.10.4 *N–*Aryl Triazoles

Aliphatic amines provided triazoles in poor to moderate yields. It was proposed that less basic nucleophiles would counterintuitively be better substrates under the acidic conditions. A less basic nucleophile would result in a higher concentration of free, unprotonated amine which would be able to engage in the desired reaction. Anilines (aniline pK_aH = 4.63[120]) were thus proposed to be suitable substrates. Gratifyingly, when aniline was used as the nucleophile, *N*-phenyl triazole **273** was isolated in a 97% yield confirming the hypothesis (Scheme 98). A range of halogenated anilines were then reacted to give halogenated triazoles **274−277** in 82%, 75%, 75% and 78% respectively.

3. Results and Discussion

273, 97%   **274**, 82%   **275**, 75%   **276**, 75%   **277**, 78%
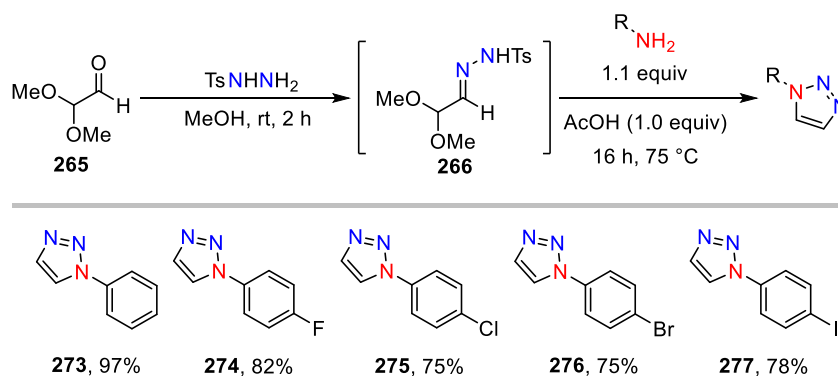
Scheme 98: Scope of aniline and halogenated substrates

Examination of the electronics of the aniline partner indicated that electron-rich anilines, including 4-methoxy- and 4-dimethylamino aniline yield triazoles **278** & **279** in 90% and 78% yields respectively (Scheme 99). Electron-deficient anilines also provided the triazoles in excellent yields, with ketone- and ester-containing anilines giving triazoles **280** & **281** in a 95% and 98% yield, along with 4-nitroaniline providing a surprisingly high yield of triazole **282** in 81% yield. This seeming independence of electronic nature of the amine partner suggests a very wide substrate scope for the presented transformation.

278, 90%   **279**, 78%   **280**, 95%   **281**, 98%   **282**, 81%
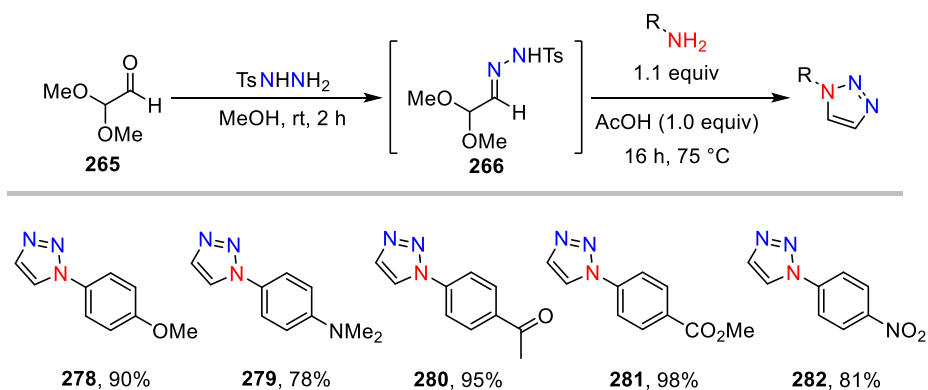
Scheme 99: Scope of electron-rich and electron-deficient anilines

Sterically hindered 2,6-dimethylaniline was exposed to the reaction conditions and the triazole **283** was isolated in an 82% yield (Scheme 100). This shows the tolerance of highly sterically hindered amine partners. An unprotected phenol substrate provided triazole **284** in 84% yield, showing how phenols can be carried through without protecting groups. 2- and 3-amino pyridine also underwent cyclisation in moderate to good yields, giving triazoles **285** and **286**

in 38% and 67% yield respectively – this was highly encouraging owing to poor nucleophilicity of these species. Finally, highly substituted complex anilines baring a range of functional groups could also be successful manipulated into the desired triazoles **287** and **288** in 90% and 24% yield.
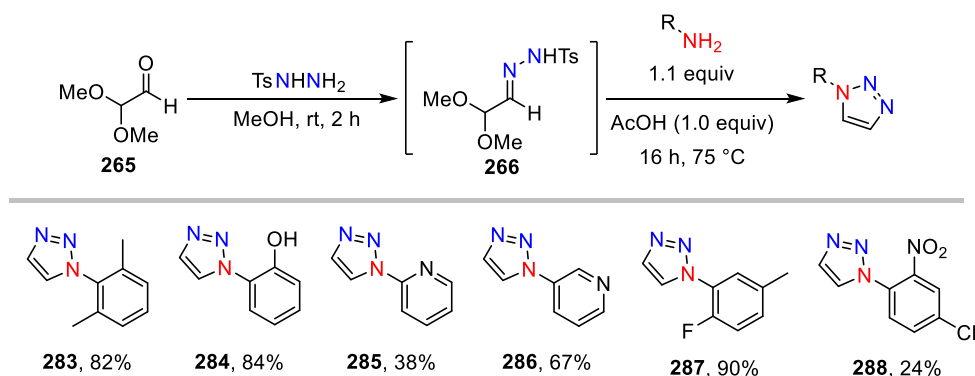
Scheme 100: Scope of functionalised aromatic amines

To exemplify the scalability of this method, the triazole synthesis was performed on a 13.35-gram scale. Triazole **281** was isolated in an 85% yield without chromatography (Scheme 101). After the reaction was complete, the reaction mixture was concentrated in volume such that ~20 mL of methanol remained. At this point, an antisolvent addition (TBME) resulted in the precipitation of the triazole whilst all impurities were retained in the organic solution. This procedure highlights the potential for this method to access 1-substituted triazoles on a preparative scale.
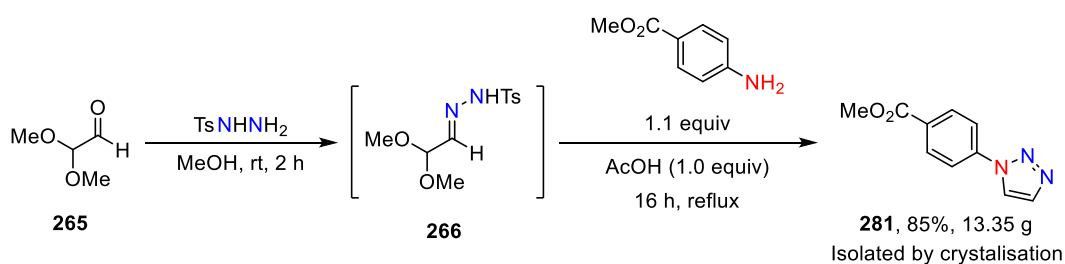
*Scheme 101: Scalability of the procedure, delivering triazole **281** on 13 g scale*

3.11 Mechanistic considerations

3.11.1 Examination of the role of the N–H bond

Throughout the optimisation procedure, using deuterated methanol proved to be an effective tool to monitor the stability and reactivity of the intermediate hydrazone. Deuterated methanol allowed for monitoring of the rate of exchange of the acetal. As a general 'rule-of-thumb' it has been observed that the faster the rate of acetal-exchange, the more bishydrazone is observed. This implies that the bishydrazone forms from a species in the acetal-exchange pathway.

When using α-ketoketals, the rate of acetal-exchange is so fast that complete exchange is observed after 20 minutes (Scheme 75, Section **3.9.1**). In order to examine the underlying principle behind this acetal-exchange, *N*-methyl tosylhydrazide (**289**) was synthesised by reacting *N*-methylhydrazine (**290**) with *p*-toluenesulfonyl chloride (**291**) in a biphasic mixture to give the product in 81% yield (Scheme 102). The reason for preparing this molecule was to monitor the hydrazone formation and the subsequent acetal-exchange to examine whether the N–H bond was key for this lability.
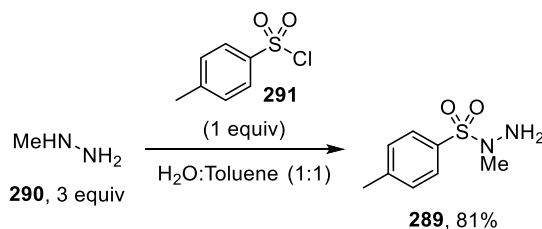
*Scheme 102: Synthesis of N-methyl p-toluene sulfonylhydrazide (**289**)*

Exposure of *N*-methyl tosylhydrazide **289** to α-ketoacetal **106** in deuterated methanol led to the following observations. The hydrazone (**292**) formation was substantially slower; with the unmethylated hydrazide, the hydrazone formation was complete in less than 5 minutes. The *N*-methylated analogue was incomplete after 20 minutes, leaving 13% *N*-methyl tosylhydrazide (**289**) remaining (Scheme 103). This suggests that the acidity of the *p*-toluene sulfonylhydrazide acts as a catalyst to increase the rate of hydrazone formation, or the hydrazone product self-catalyses the hydrazone formation by the presence of the acidic

proton. Secondly, a fragment-ion of the hydrazone was also consistent in mass with that of an enoldiazonium intermediate **293**, the species which is invoked as the reactive intermediate (Scheme 103). This species is now formally positively charged and so a mass ion of *m/z*=269 was observed in the MS+. The observation of this species provides further evidence that this species is present and can be invoked as a reactive intermediate in the triazole formation.
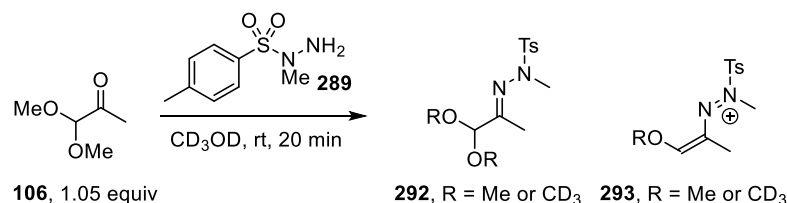
Scheme 103: Slower hydrazone formation and observation of enoldiazonium cation

A key difference with the methylated hydrazide was observed after 2 hours. The hydrazone (**292**) and bishydrazone (**294**) were observed in a 4.7:1 ratio (Scheme 104) with full consumption of the hydrazide. With the NH hydrazide, no bishydrazone was observed after the same reaction time.
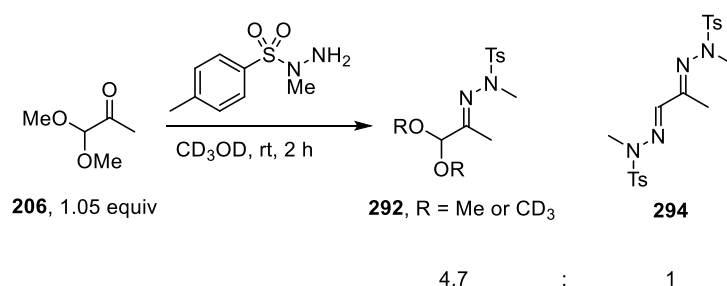
Scheme 104: Bishydrazone formation with N-methyl p-toluene sulfonylhydrazide

Further, the mass spectrometry trace suggested that the hydrazone had undergone a series of proton-deuterium exchanges. This had been observed previously in which the mass of the hydrazone increased by 3 and 6 Daltons, indicating incorporation of the deuteriomethoxy acetal. However, in this reaction all mass-ion integers from M^+ through to $M+10^+$ (301 to 311) were observed (**292** and **295**, Scheme 105). This suggested that all labile protons had undergone exchange. This was further supported by the fragment enoldiazene cation also

displaying this sequential incorporation of deuterium showing an increase in mass-ion from 269 up to 276 (**293** and **296**, Scheme 105).
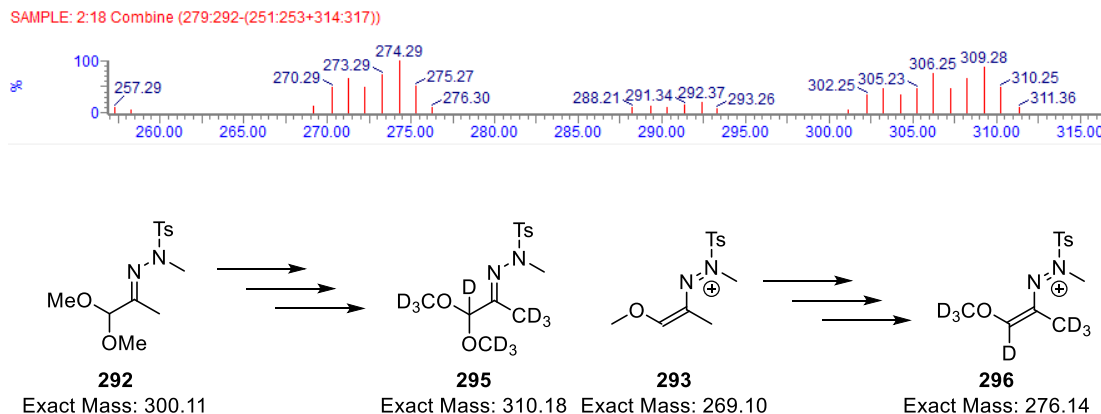
*Scheme 105: Deuterium incorporation into hydrazone **292***

Further evidence for the deuteration of the labile protons was also observed in the mass spectrum of the bishydrazone **294**. A species with a mass of 437 up to 441 was observed, which is consistent in mass with incorporation of 4 deuterium atoms in the bishydrazone (**294** and **297**, Scheme 106).
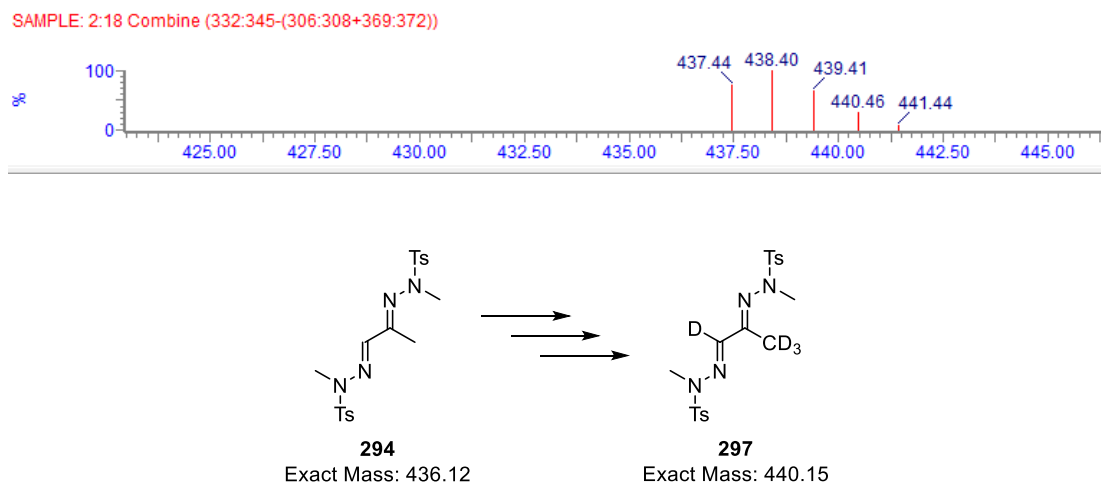
*Scheme 106: Incorporation of deuterium into bishydrazone **294***

The rationale for this sequential incorporation of deuterium atoms can be explained through a combination of factors. The acetal exchange with OCD_3 accounts for integers +3 and +6. However, the integers of +1, +2… could occur from the formation of enamine type

intermediates including **298** and **299**. Subsequent redeuteration accounts for the incorporation of individual deuterium atoms (Scheme 107).
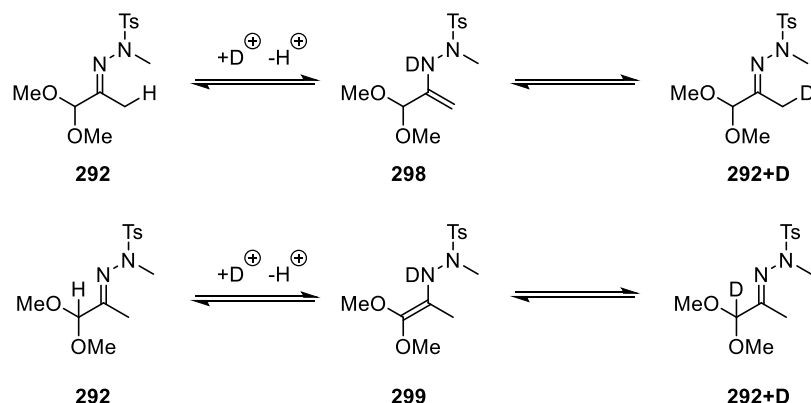
*Scheme 107: Sequential deuteration of hydrazone **292** by enamine formation*

No evidence has been observed for the formation of an enamine species when using *p*-toluene sulfonylhydrazide. Enamine substrates are nucleophilic, meaning the formation of an enamine in the triazole forming reaction would be detrimental. The N–H bond appears to be vital in limiting the formation of an enamine intermediate (Scheme 108).
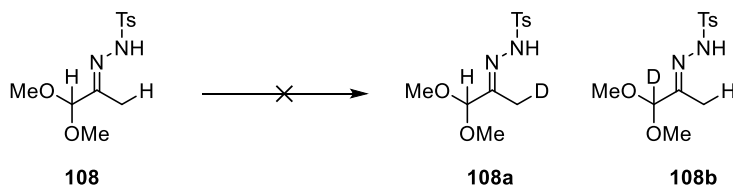
Scheme 108: Enamine formation is not present with the NH hydrazone

Having the *N*-methyl group on the hydrazone will increase the basicity of the neighbouring nitrogen atom, favouring formation of an enamine. On the contrary, with an N–H hydrazone, the hydrazone substrates are acidic, not basic. This therefore suggests that the hydrazone anion (**300**) is unable to undergo formation of an enamine, and instead is primed to undergo elimination of methoxide, to give enoldiazene intermediate **129** (Scheme 109).

300   **129**
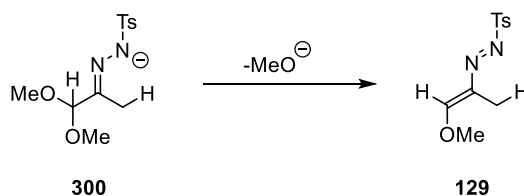
Scheme 109: The NH hydrazone is essential to invoke elimination of methoxide

3.11.2 Attempts at probing the N–S bond cleavage

As no intermediates after the enoldiazene had been observed, an alternative mechanistic pathway was considered which involved elimination of *p*-toluene sulfinate from enoldiazene **301** to form diazonium species **302** (Scheme 110). This diazonium species can react with an amine to give vinyl triazene species **303**. This species is then primed to undergo an addition-elimination reaction to form the triazole whilst eliminating methanol.

301   **302**   **303**
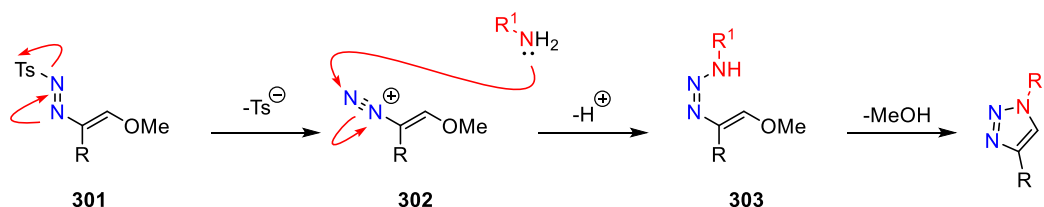
Scheme 110: A proposed alternative reaction mechanism to form triazoles, involving formation of a diazonium species

Evidence for the formation of such enoldiaznoiums can be traced back to a report from 1975 by Bott (Scheme 111). It was reported that tosylhydrazones derived from α-ketoacetals (**108**) can undergo conversion to the diazonium (**304**) by treatment with Lewis acids, such as tin(IV) chloride (Scheme 111).[121] It was shown that α-acetal tosylhydrazone **108** could eliminate PTSA to form the diazonium salt **304** which could be isolated and was thermally stable. In part, this remarkable stability was attributed to resonance forms of this species in which the electron rich alkene conjugates through the π* orbital (**304a** and **304b**).
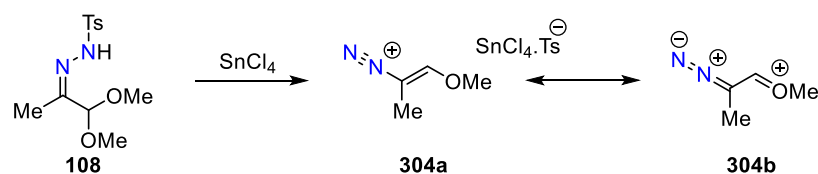
*Scheme 111: Bott's observation of diazonium **304***

To examine the potential formation for such a diazonium species, **304** was proposed which could be trapped with a secondary amine (Scheme 112). The addition of morpholine (**305**) would allow for the determination as to whether a diazonium forms under the reaction conditions. The diazonium **304** would be trapped by morpholine to give an enoltriazene species **306**, which would be unable to cyclise to a triazole. Moreover, formation of the diazonium **304** from the enoldiazene would likely be an irreversible process.
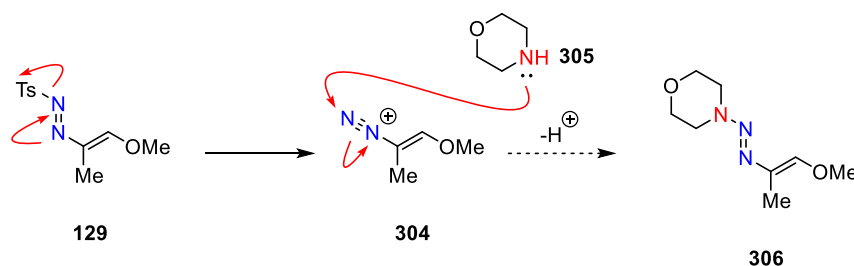
*Scheme 112: The examination for the formation of diazonium **304** by trapping with morpholine*

After adding morpholine (**305**) to the reaction mixture and stirring at 30 °C for 3 days, 40% PTSA was observed with 60% hydrazone **108** remaining by LCMS analysis of the reaction mixture (Scheme 113). However, by ^{1}H NMR only one set of signals corresponding to a morpholine were observed. The ^{1}H NMR signals of morpholine are highly characteristic. This suggested that the morpholine was unrelated to the production of PTSA and that all the morpholine in the reaction remained as a single species. The morpholine signals observed were deshielded with respect to morpholine, suggesting that the only species present was a protonated morpholine. This result suggested that the formation of a diazonium and enoltriazene (**306**) is not involved in the mechanistic pathway.
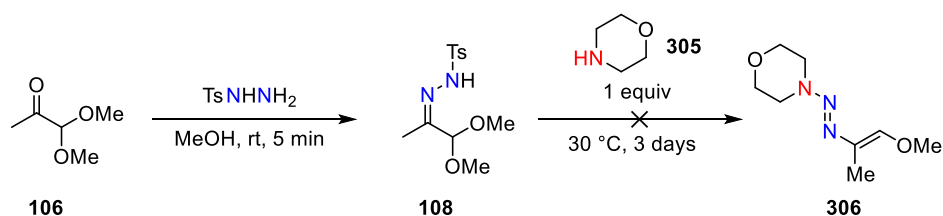
*Scheme 113: No formation of triazene **306** by addition of morpholine, suggesting a diazonium is not present*

The observation of only one morpholine species by ^{1}H NMR spectroscopy indicates that the diazonium pathway is not active. This therefore suggests that the addition of morpholine to enoldiazene species **129** is a reversible process forming hemiaminal species **307** (Scheme 114). This species was not observed by either ^{1}H NMR or LCMS. This reaction pathway does not have a thermodynamic driving force as an aromatic product cannot be formed. Therefore, it can be invoked that the addition of an amine to an enoldiazene is reversible, and the position of equilibrium lies on the side of the enoldiazene **129** and acetal hydrazone **108**. Moreover, intermediate **307** will likely remain protonated on the red nitrogen owing to the acidity of the hydrazone, which would further shift the position of equilibrium to the left-hand side.
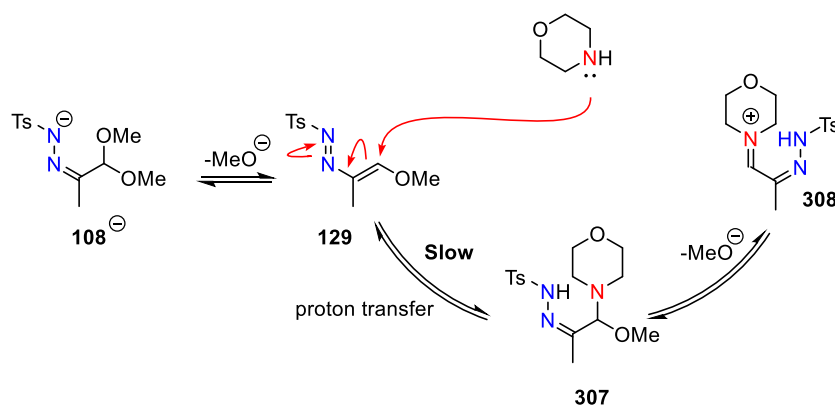
Scheme 114: A rationale for the lack of observation of any intermediates

To further probe the N–S bond cleavage, an experiment was designed which compared the rate of formation of triazole **144** using the standard hydrazone (R = Me, **108**) and an activated hydrazone (R = NO$_2$, **310**, Scheme 115). Placing an electron-withdrawing group on the hydrazone would be expected to facilitate cleavage of the N–S bond. However, if the rate-determining step of the reaction happens before cleavage of the N–S bond, the rate of formation of triazole **144** should be the same using either hydrazone **108** or **310**. Therefore, in two separate reactions α-ketoacetal **106** was treated with either hydrazide **107** or **309**. In methanol, nitrohydrazone **310** was insoluble, so a 4:1 solvent system of methanol:DMSO was utilised in both cases (Scheme 115). The rate of formation of hydrazones **108** and **310** was virtually identical using hydrazides **107** or **309** respectively, indicating that the electronics of the arene play a small role in the formation of the hydrazone.
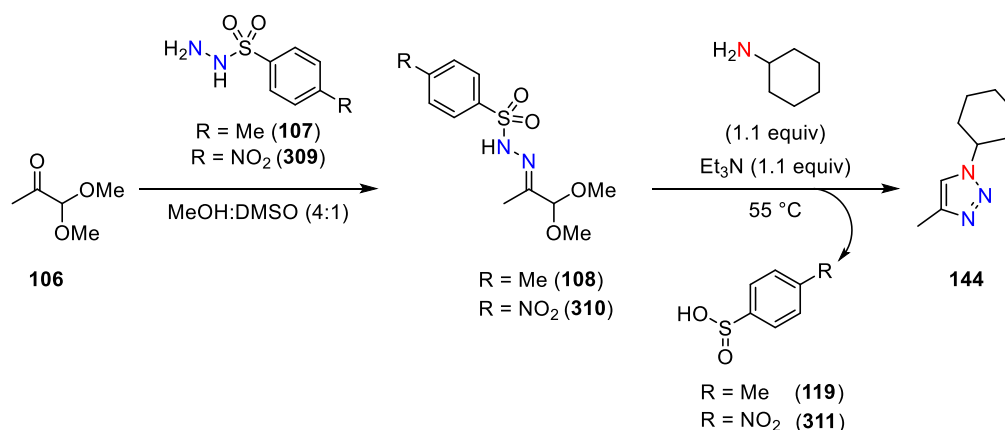
*Scheme 115: Comparison in rate of triazole **144** formation using either **108** or **310**.*
Reactions performed with anisole as an internal standard.

To the hydrazone was then added 1.1 equivalents of both cyclohexylamine and triethylamine and the reactions were heated to 55 °C. The reactions were monitored by HPLC analysis using anisole as an internal standard. Samples were taken at frequent time-points and the ratio of triazole **144**:anisole was plotted against time to give Figure 18. The rate of triazole formation is virtually identical in both cases, suggesting that an electron-withdrawing group on the sulfonylhydrazone does not increase the rate of triazole formation. This suggests that cleavage of the N–S bond is not rate-limiting, and as such indicates that the rate-limiting step happens before cleavage of the N–S bond.

3. Results and Discussion

Comparison of the rate of formation of triazole **144**
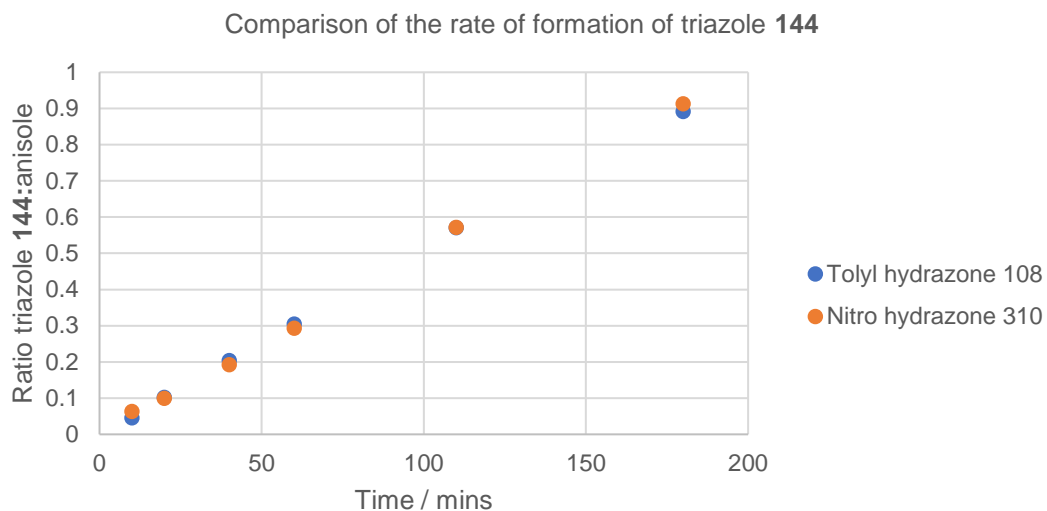
*Figure 18: Rate of formation of triazole **144** using hydrazone **108** or **310***

3.11.3 A proposed mechanism for the formation of triazoles from α-ketoacetals

With the observations discussed within the previous Sections, also in combination with literature evidence from the Sakai reaction of α,α-dichlorotosylhydrazones, a mechanism can be proposed for the synthesis of 1,2,3-triazoles from α-ketoacetals (Scheme 116). The hydrazone formation from α-ketoacetal **312** proceeds smoothly, catalysed by the presence of the acidic proton on *p*-toluene sulfonylhydrazide (Section **3.11.1**). At this point, hydrazone **313** and the added amine undergo a proton transfer, as indicated by ^{1}H NMR spectroscopy in Figure 11, Section **3.3**. The anionic hydrazone **314** can then eliminate methoxide in a reversible step to form enoldiazene **315** which can be invoked owing to the presence of a species consistent in mass as a fragment ion of the hydrazone by LCMS (Figure 12, Section **3.3**). This process is reversible, as evidenced by the acetal exchange with deuterated methanol (Figure 10, Section **3.3**). Moreover, based on the lack of direct observation of this species by ^{1}H NMR or as a separate fragment by LCMS and HPLC, it is proposed that this is the slow step of the reaction. The methoxide liberated in this step would readily deprotonate the ammonium salt which formed in the first step to give a free amine. After this point in the mechanism, no intermediates have been observed by LCMS analysis or ^{1}H NMR spectroscopy. This observation is not consistent with the reports of Hanselmann who studied

the mechanism with α,α-dichlorotosylhydrazones. Intermediates analogous with aminal **316** and iminohydrazone **317** were observed by LCMS.[84] The observation of these species therefore suggests that the rate-limiting step with α,α-dichlorotosylhydrazones occurs after the formation of iminohydrazone **317**. This is unsurprising given that an enoldiazene is more electron rich than a chlorovinyldiazene which is invoked in Sakai chemistry. Furthermore, section **3.11.2** indicates that the rate of triazole formation is not affected by placing electron-withdrawing groups on the hydrazone, which would be expected to facilitate cleavage of the N–S bond. This therefore suggests that there is a change in rate-determining step between the use of α,α-dichloroketones and α-ketoacetals. After the addition of the amine to enoldiazene **315**, the hemiaminal intermediate **316** can collapse to an iminohydrazone **317**, the same species invoked in Sakai chemistry. After this point, a [1,5] H-shift can occur to give enamine-type species **318** as has been previously suggested in the literature.[90] Results obtained in this work indicate that cleavage of the N–S bond is not the slow step, however the exact mechanism for the N–N bond formation still requires further work to be understood in more detail. However, an addition-elimination of the enamine to the diazene **318** can be invoked, whereby elimination of the sulfinate by-product **319** furnishes the triazole product **320**.

Scheme 116: The proposed reaction mechanism for triazole synthesis from α-ketoacetals

3.12 Chemoselective triazole synthesis

The results contained in Section **3.10** highlighted how *N*-aryl triazoles formed in higher yields

than *N*-alkyl triazoles under the acidic conditions examined. This suggested that an orthogonal

set of reaction conditions could be developed to selectively functionalise either an aromatic or

an aliphatic amine. Amine **321**, a bifunctional compound containing both an aliphatic and an

aromatic primary amine was chosen as a model substrate to examine this hypothesis (Scheme

117).
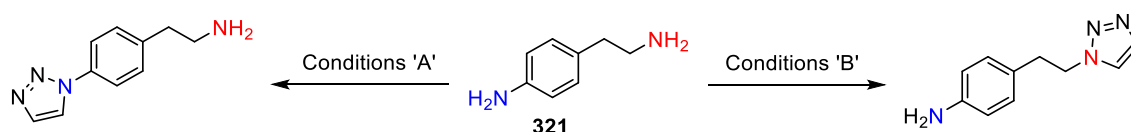
Scheme 117: Postulated chemoselectivity for either aromatic or aliphatic amine conversion

3.12.1 Aliphatic amine functionalisation

As an initial starting point to test for chemoselectivity, α-ketoacetal **106** was reacted with

p-toluene sulfonylhydrazide to give hydrazone **108**, in an identical procedure to that described

in Section **3.3**. From here, adding bifunctional amine **321** and using the conditions developed

in Section **3.4** (NEt$_3$ (1 equiv), 140 °C, 5 min) the only observed product was triazole **322**,

derived from functionalisation of the aliphatic amine, which was isolated in an 83% yield

(Scheme 118). By ^{1}H NMR analysis of the crude reaction mixture, no product derived from

functionalisation of the aromatic amine was observed.
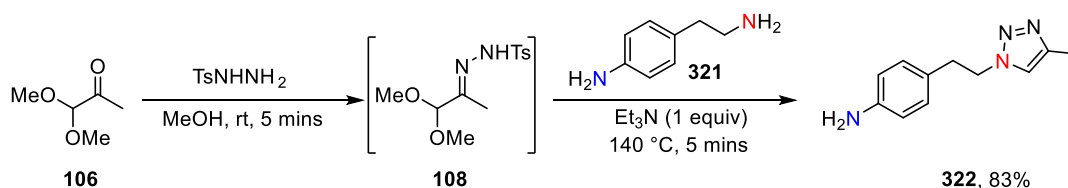
Scheme 118: Complete chemoselectivity for aliphatic amines under basic conditions with bifunctional amine 321

Interestingly, the use of dichlorotosylhydrazone **323** and the same bifunctional amine **321** has

been reported by Westermann (Section **1.8** & Scheme 119).[82] Under the optimised reaction

conditions it was reported that no chemoselectivity for either an aliphatic or an aromatic amine was observed giving bis-triazole **84f** in 69% yield. The reason for this is likely a combination of factors; the method presented by Westermann requires 1.7 equivalents of dichlorotosylhydrazone **323**, presenting the system with an excess of the intermediate for both pendant amines to react with. Secondly, it is possible that the intermediate in the dichloro system is more reactive, resulting in poor differentiation between aromatic and aliphatic amines. Under the conditions developed for ketoacetal **106**, not requiring an excess of the hydrazone, complete chemoselectivity for the aliphatic amine was observed.
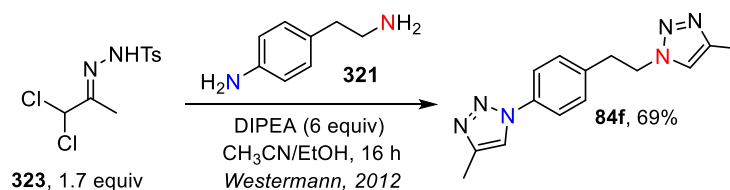
Scheme 119: Westermann's report of poor chemoselectivity with bifunctional amine 321

The difference in chemoselectivity between the dichloroketones and α-ketoacetals could be explained by the reactive intermediate proposed in both cases. Chlorovinyldiazene species **324** has been invoked as the reactive intermediate which undergoes a 1,4-addition with the primary amine nucleophile (Figure 19). This chlorovinyldiazene is unsurprisingly electrophilic, as the electronegative chlorine atom will inductively withdraw electron density from the π-system *via* the inductive effect, making the alkene electron-deficient and susceptible to nucleophilic attack. Based on the mechanistic considerations contained within this report, it is likely that this reaction proceeds by a similar mechanism. Therefore, the enoldiazene **129** can be invoked as a reactive intermediate. This species is reminiscent of an enol-ether which are electron rich and formally nucleophilic, often invoked as a masked enolate species.[106] The increased electron density of the enoldiazene with respect to the chlorovinyldiazene will thus increase the energy of the LUMO, resulting in an increase in the differentiation between attack from either an aliphatic or an aromatic amine.
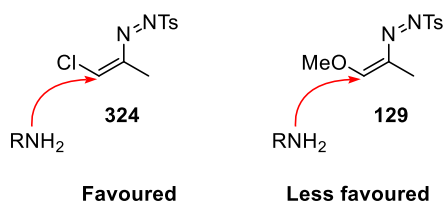
Figure 19: The differentiation between addition to a chlorovinyldiazene and an enoldiazene

The observed chemoselectivity for this process is a new observation. If dichlorotosylhydrazones were employed to selectively functionalise either the aromatic or the aliphatic amine, protecting groups would need to be utilised. Under these new conditions, the aliphatic amine can be selectively functionalised over the aromatic amine in the absence of protecting groups. The reaction solely relies on the inherent difference in the nucleophilicities of an aromatic *vs.* an aliphatic amine.

3.12.2 Aromatic amine functionalisation

The conditions presented in Section **3.10** appeared to be a good starting point for the development of conditions to selectively functionalise an aromatic amine. The acidic conditions allow for the formation of *N*-aryl triazoles in excellent yields whilst *N*-alkyl triazoles behaved poorly, giving lower yields of the triazoles products. Exposure of bifunctional amine **321** to the hydrazone derived from dimethoxy acetaldehyde with 1 equivalent of acetic acid gave triazoles **325** and **326** in a 1:3 ratio by ^{1}H NMR analysis of the crude reaction mixture (Scheme 120). **325** forms from functionalisation of the aliphatic amine, whilst **326** forms from functionalisation of the aromatic amine. This switch in chemoselectivity shows that the acidic conditions favour the formation of the *N*-aryl triazole over the *N*-alkyl triazole. Increasing the amount acetic acid to 3 equivalents increased the ratio of products to 1:4, showing how more acid offered increased chemoselectivity.
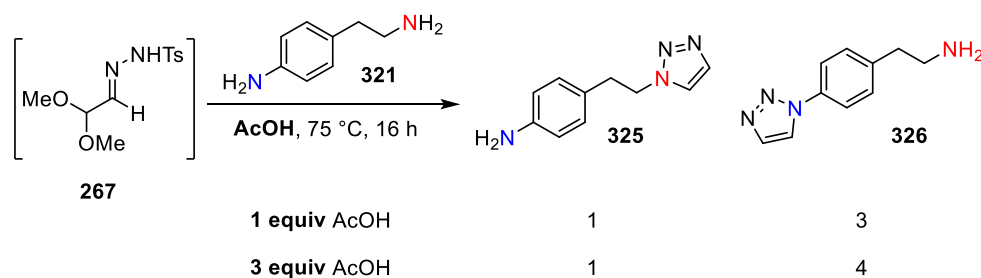
Scheme 120: Observation of chemoselectivity for aromatic amines under acidic conditions

It was hypothesised that stronger acids would further increase this chemoselectivity. In the presence of benzoic acid, the chemoselectivity further increased to 1:5 for triazoles **325**:**326** (Scheme 121). Increasing the acidity of the additive further by using trifluoroacetic acid increased the observed ratio to greater than 1:50 by ^{1}H NMR analysis. The general trend observed is that the chemoselectivity for aromatic amines over aliphatic amines increases with more acidic additives. Acetic acid (pKa = 4.76)[122] gave a 1:3 ratio, benzoic acid (pKa = 4.31)[122] gave a 1:5 ratio and trifluoroacetic acid (pKa = 0.25)[122] gave a greater than 1:50 ratio.
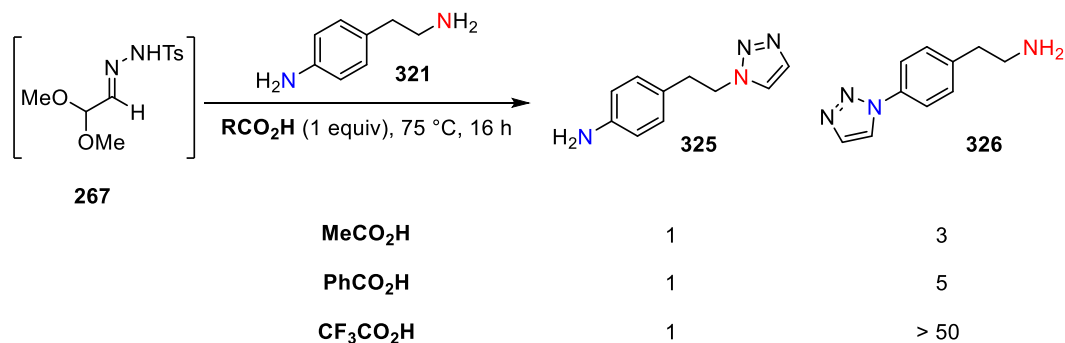
Scheme 121: Stronger acids improve chemoselectivity

To validate this result, the triazole **326** formed in an 88% solution yield when TFA was used and was isolated in an 81% yield (Scheme 122). The product derived from functionalisation of the primary amine, **325**, was observed in < 2% yield by ^{1}H NMR analysis of the crude reaction mixture. This switch in chemoselectivity can be explained by considering that the aliphatic amine, owing to its increased basicity, is transiently "protected" as the ammonium salt **328**, leaving it unable to participate in the triazole formation. The increased basicity of an aliphatic amine over an aromatic amine is highlighted in the pKaH values. The pKaH value of

methylamine is 10.63, and the pKaH of aniline is 4.63, highlighting that aliphatic amines are ~10^6 times more basic than aromatic amines.[120] This transient protonation consequentially removes the aliphatic amine as a reactive partner, resulting in the aromatic amine being the only available nucleophile.
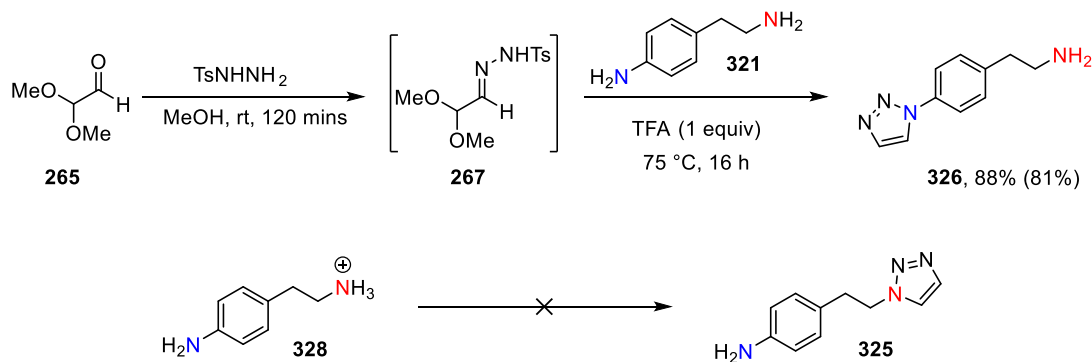
Scheme 122: Functionalisation of an aromatic amine under acidic conditions

In attempts to highlight the generality of this procedure and show the starting material was not limited to dimethoxy acetaldehyde, 1,4-substituted triazole **329** was synthesised with an excellent degree of chemoselectivity, giving the triazole product in 87% isolated yield using TFA as an additive within the reaction (Scheme 123).
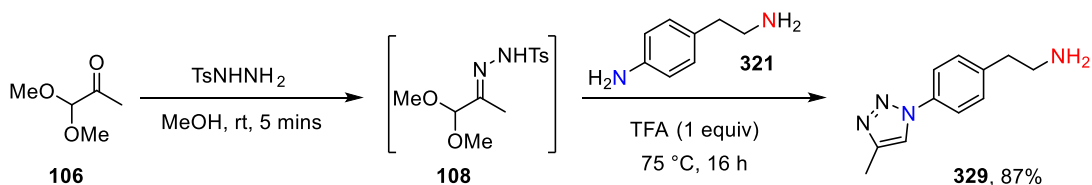
Scheme 123: Functionalisation of an aromatic amine with an α-ketalacetal

3.12.3 A note on regiochemistry determination

The above regiochemistry of the triazole formation is easily elucidated by the chemical shifts of the alkyl protons. The alkyl protons in *N*-aryl triazole **329** are at 2.96 and 2.87 ppm, whereas in the *N*-alkyl triazole **322** the alkyl protons undergo a substantial downfield shift to 4.52 and 3.05 ppm (Figure 20). This downfield shift can be explained by the protons in the *N*-alkyl triazole being in the vicinity of an electron-deficient heterocycle, in which the alkyl protons are deshielded with respect to the protons on amine **329**.
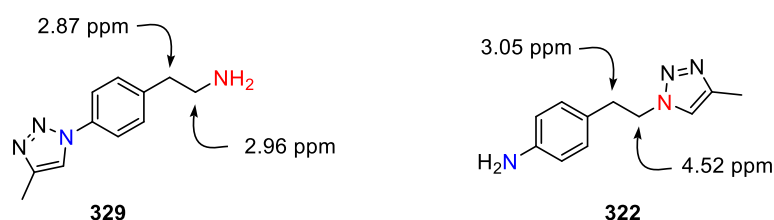
Figure 20: Regiochemistry determination

The developed processes are therefore an orthogonal set of reaction conditions to selectively functionalise either an aromatic amine or an aliphatic amine (Scheme 124). This offers many advantages, including obviating the use of protecting groups which could be challenging to chemoselectively introduce selectively in the first place.
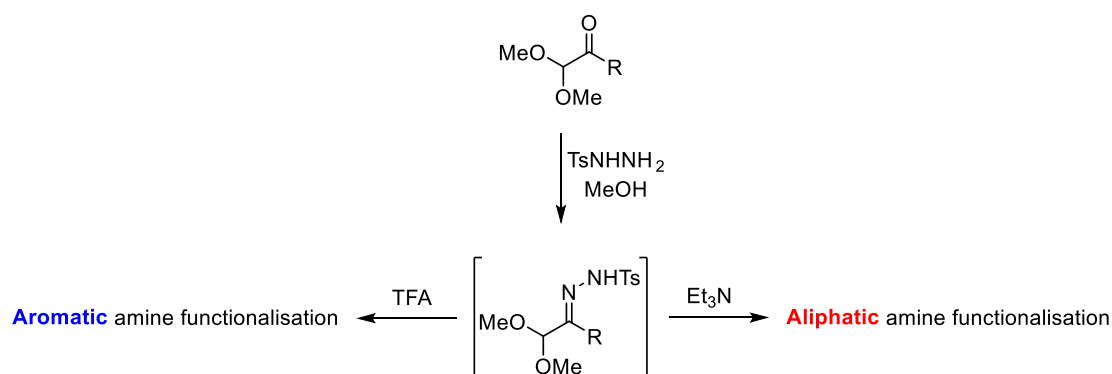
Scheme 124: A general scheme showing conditions to functionalise aromatic or aliphatic amines

3.12.4 A one-pot, multi-stage telescoped synthesis of bis-triazoles

To exemplify the potential of these orthogonal reaction conditions, a one-pot, multi-stage telescoped reaction procedure to form bis-triazole **330** was designed (Scheme 125). Starting from dimethoxy acetaldehyde **265**, hydrazone **267** was formed as per Section **3.10**. Telescoping hydrazone **267** into the triazole formation gave *N*-aryl triazole **326**. To a separate vial containing the α-ketoacetal **106** was added *p*-toluene sulfonylhydrazide to make hydrazone **108** *in-situ*. The reaction mixture containing *N*-aryl triazole **326** was then added to the hydrazone **108**, which was basified with 2.2 equivalents of triethylamine, followed by exposure to the optimised reaction conditions to give bis-triazole **330** in 69% yield. These four telescoped steps, with a midway point of convergence, exemplify the potential for this reaction to enable a rapid, chemoselective, regiospecific synthesis of substituted triazoles.
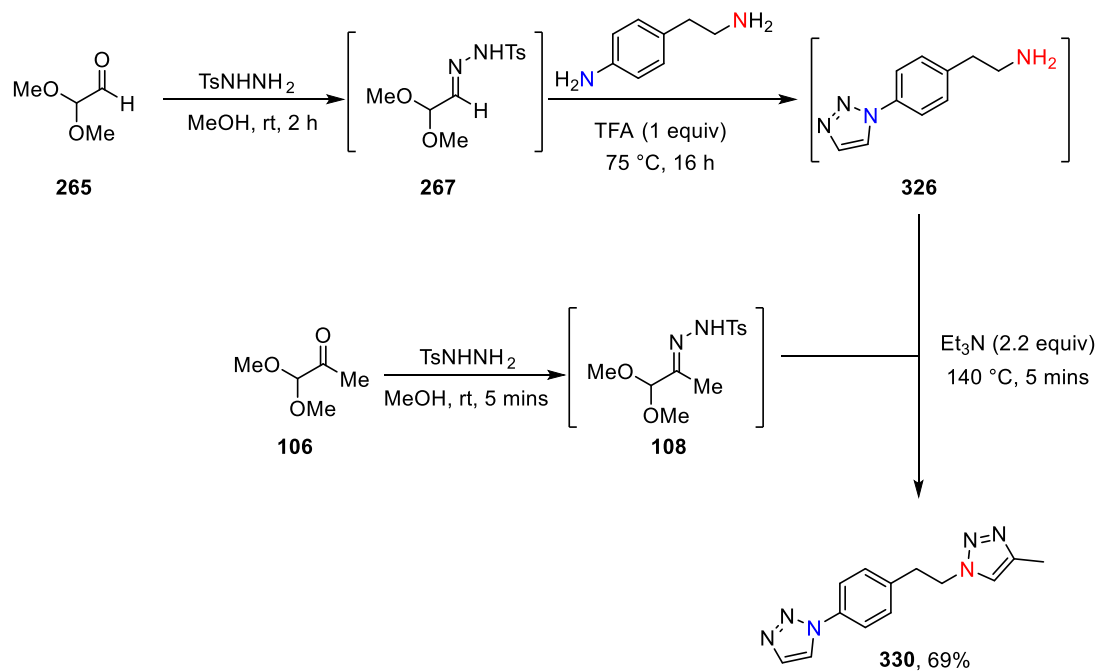
*Scheme 125: A one-pot, 4-stage telescoped process to synthesise differentiated bis-triazole **330***

4. Conclusions and Future Work

4.1 Conclusion

In conclusion, α-ketoacetals have been shown to impart a higher degree of selectivity in the reaction with *p*-toluene sulfonylhydrazide when compared with α,α-dichloroketones. This enables formation of the intermediate hydrazone with complete selectivity over the formation of a bishydrazone which does not undergo cyclisation to a triazole. As a result, 1,2,3-triazoles can be synthesised directly in one-pot from α-ketoacetals, without the required isolation of an intermediate hydrazone. This enables a faster, cleaner synthesis of 1,2,3-triazoles on scale, often enabling isolation of the triazole product without the requirement for chromatography. This is exemplified by the synthesis of triazoles **144** & **281** on a multi-gram scale. A two-stage flow chemistry set-up has been exemplified as an effective tool to perform the high-temperature reaction on a large scale, isolating 73 grams of triazole **144**. This strongly emphasises the utility of the new method as an efficient synthetic tool to form 1,2,3-triazoles on a preparative scale.

Sakai reaction
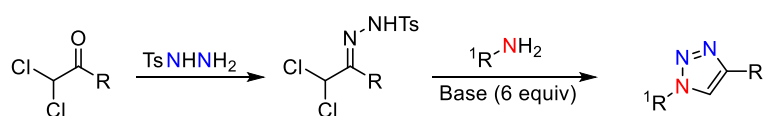
Pros
Mild conditions
Azide-free
Amine partner has exceptional functional group tolerance
Access to 1- and 1,4-substituted triazoles

Challenges
Two step process
Potentially toxic chlorinated reagent and intermediate
4-, 1,5- and (1),4,5-substituted triazoles not known
No chemoselectivity for aromatic or aliphatic amines

This variant
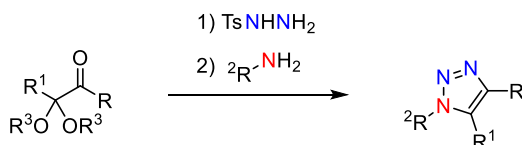
Benefits
Works under neutral conditions
Regiospecific access to
   4-, 1,4-, 1,5-, (1),4,5- and 1-substituted triazoles
Scalable in batch and flow reactors
One-pot process – hydrazone isolation removed
Clean reaction – products can easily be isolated
   without chromatography
Chemoselective conditions for the conversion of aromatic
   or aliphatic amines

Challenges
Optimum conditions require high temperature
Acyclic 1,4,5-substituted triazoles with large R^1
   groups are currently inaccessible

It has been shown that this procedure can access a multitude of substitution patterns of 1,2,3-triazoles, including 4-, 1,4-, 1,5-, 1,4,5-, 4,5- and 1-substituted triazoles. This methodology has been exemplified by synthesising >70 1,2,3-triazoles. The amine coupling partner has a wide-spanning scope, including the use of aliphatic, aromatic and heteroaromatic amines. Amines containing a range of functional groups including esters, ketones, halogens, alkynes, sterically hindered groups and chiral groups all undergo efficient cyclisation with retention of chemical information, indicating that the developed procedure is highly general. Further, α-ketoacetals have been shown to be readily accessed *via* a Grignard addition to commercial starting materials. This indicates that substitution of the carbon skeleton of the triazole is facile and the substrates can be readily prepared in one-step from commercial starting materials. (1),4,5-substituted 1,2,3-triazoles have been shown to be accessible using this methodology, however, the current limitation is that the intermediate hydrazone of these substrates is unstable with respect to hydrolysis and conversion to the unreactive bishydrazone. Ideas to solve this have been presented in a future work section.

Mechanistic studies allude to a change in rate-determining step between the use of α,α-dichloroketones or α-ketoacetals as precursors to 1,2,3-triazoles. Experimental evidence suggests that cleavage of the N–S bond is not rate-determining when α-ketoacetals are used as precursors to 1,2,3-triazoles. This is mechanistically different to the use of α,α-dichloroketones as the synthetic precursor in which the N–S bond-cleavage event is proposed to be rate-determining. Based on the findings in this work, the rate-determining step appears to be the elimination of methoxide from an intermediate hydrazone, to form a reactive enoldiazene.

Finally, an orthogonal set of reaction conditions have been developed to selectively functionalise either an aromatic or an aliphatic amine, further showing the potential of the developed synthetic method. The use of trifluoroacetic acid as an additive gave exclusive access to *N*-aryl triazoles, whilst basic conditions using triethylamine give exclusive access to *N*-alkyl triazoles. This has been exemplified by the synthesis of *N*-aryl, *N*-alkyl bistriazole **330**, which was synthesised in 4 telescoped reaction steps.

330, 69%
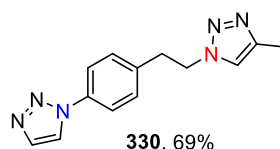
This is the first reported example of a redox-neutral, azide-, alkyne- and halogen-free synthesis of triazoles which can be considered general by giving access to almost all substitution patterns of 1,2,3-triazoles. This procedure offers scalable, rapid, chemoselective and regiospecific access to triazoles which will likely attract significant interest in the synthetic chemistry community and have applications across a wide-range of chemical sciences.[123]

4.2 Future work

Section **3.9** detailed the challenges with using α-ketoketals as substrates to access (1),4,5-substituted triazoles. The problem largely appears to be two-fold. Firstly, nucleophilic addition onto an α-ketoketal is slow owing to the increased steric hindrance around the ketone. As R^1 (**331**) increases in size, the rate of hydrazone formation decreases. This is explained as the neopentylic effect. Secondly, the intermediate hydrazone (**332**) is less stable with respect to elimination of methanol to form enoldiazene **333**. Therefore, a major product in these reactions is the bishydrazone **334**, especially as R^2 increases in size (Scheme 126).
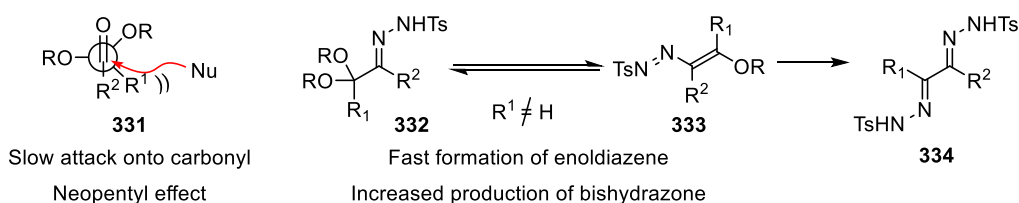
Scheme 126: An explanation for the poor results obtained with α-ketoketals

A proposed solution to this is to use a cyclic ketal (**335**) or a tetrahydroimidazole (**337**) instead of the acyclic ketals presented in this thesis. The incorporation of a cyclic ketal would change the position of equilibrium and should disfavour formation of the diazene **336** or **338** in high concentrations. The reverse reaction, involving intramolecular attack of the pendant alcohol or secondary amine onto the enoldiazene would be a favoured process over an intermolecular

reaction. This should therefore result in smoother formation of an intermediate hydrazone, enabling access to 4,5-substituted triazoles in which R^1 and R^2 are different.
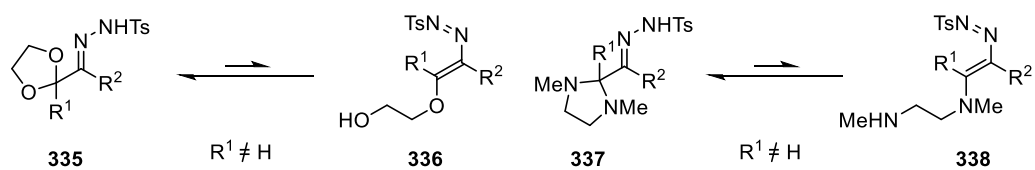
*Scheme 127: A proposal to use a cyclic ketal **335** or a tetrahydroimidazole **337** protecting group*

Chapter Two

5. Introduction

5.1 The importance and synthesis of benzimidazoles

Further azacycles of importance to the pharmaceutical industry include benzimidazoles (**339**) – imidazoles which are fused to a benzene ring (Figure 21). A meta-analysis of over 1,000,000,000 prescribed medicinal drug products was published in the British Journal of Clinical Pharmacology in 2018.[124] The results of this analysis reveal that the number one 'drug-group' prescribed by British clinicians were proton-pump inhibitors. Within this category, Omeprazole, a benzimidazole-containing compound (**340**, Figure 22) was the most prescribed drug.

Figure 21: Benzimidazole nomenclature

Most benzimidazole-derived pharmaceutical compounds on the market are proton-pump inhibitors.[6] Omeprazole (**340**) and Pantoprazole (**341**) are sold as treatments for a range of disorders, including peptic ulcer disease, gastroesophageal reflux disease and Zollinger-Ellison syndrome.[125] Omeprazole is deemed by the World Health Organisation (WHO) as one of the world's most essential medicines for a functional healthcare system.[126] Telmisartan (**342**) is used for the treatment of high blood pressure[127] and contains two benzimidazole motifs (Figure 22).

Figure 22: Examples of benzimidazole-containing pharmaceutical compounds
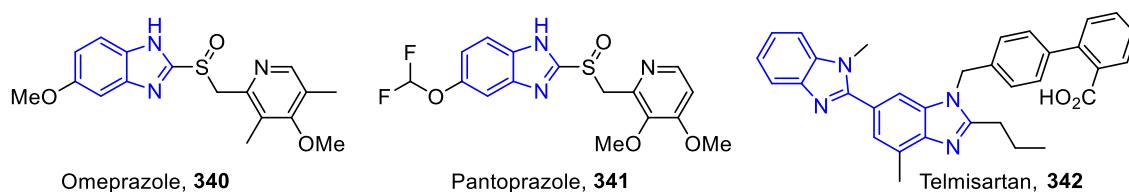
Benzimidazole (**343**) can be formed by the condensation reaction between 1,2-diamino benzene (**344**) with formic acid or trimethyl *ortho*formate (Scheme 128).[128] 1,2-diamines will often require preparation from the *o*-nitroaniline (**345**) by means of reductive methods.
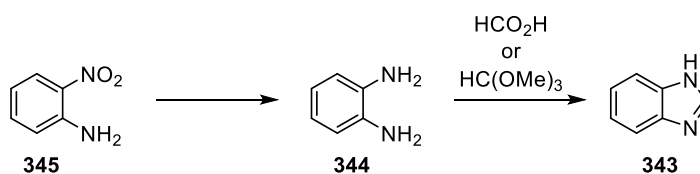
Scheme 128: Synthesis of a benzimidazole from 1,2-diaminobenzene with formic acid or an orthoformate

2-substituted benzimidazoles (**346**) are synthesised by the reaction of a 1,2-diamine (**344**) with either an aldehyde and oxidant, or the condensation reaction with an ester, acid or a nitrile (Scheme 129).[129-131] This necessitates the use of 1,2-difunctionalised arenes for the synthesis of these moieties.
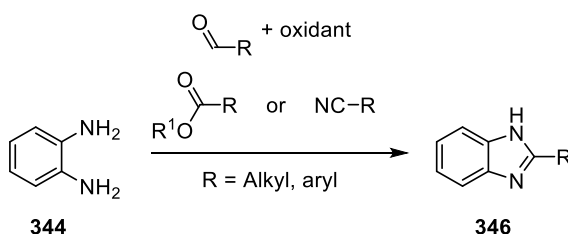
Scheme 129: Synthesis of 2-substituted benzimidazoles by the condensation reaction of a 1,2-diaminobenzene with an ester or aldehyde

On considering the commercial synthesis of Telmisartan, a nitration-reduction-condensation sequence was utilised (Scheme 130).[132] The trifunctionalised arene **347** was nitrated using HNO_3/H_2SO_4 to give **348**, followed by heterogeneous hydrogenation with a palladium-on-carbon catalyst to give 1,2-diamine **349**. Upon one-pot saponification-cyclisation of methyl-ester **349**, the furnished carboxylic acid **350** behaves as the condensation partner for 1,2-diamine **351** to give the second benzimidazole **352**. Indeed, almost all benzimidazole motifs are synthesised in the manner of nitration-reduction-condensation, largely owing to the easily accessible starting materials.[131]

*Scheme 130: The partial synthesis of Telmisartan **342** using a double condensation sequence*

This method of using 1,2-diamines remains the standard method for the synthesis of other benzimidazoles, including Omeprazole. The reaction sequence to form the ring and introduce the sulfur atom relies on the condensation of 1,2-diaminobenzene **353** with potassium ethylxanthate to give 2-thiobenzimidazole **354** (Scheme 131).[133]

Scheme 131: The synthesis of the benzimidazole ring in Omeprazole
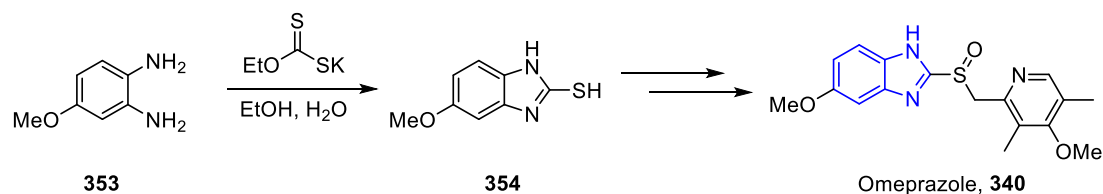
The challenge with the nitration-reduction sequence to access benzimidazoles originates with the nitration reaction. Aniline (**355**) itself is challenging to nitrate under standard nitrating conditions (HNO₃, H₂SO₄), since protonation of the nitrogen atom results in the formation of anilinium **356** (Scheme 132). The strongly electron-withdrawing nature of the NH_3^+ group deactivates this species with respect to electrophilic aromatic substitution, making the nitration of aniline to give nitroaniline **357** challenging.[134]

Scheme 132: Explaining the challenge with the nitration of aniline
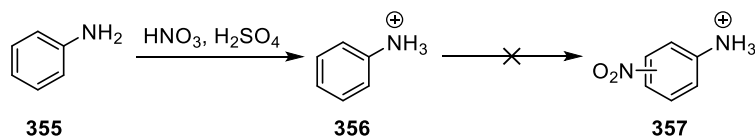
To solve the above issues, the nitrogen atom can be protected by means of an *N*-acyl or *N*-sulfonyl aniline to inhibit formation of the anilinium, upon which the nitration reaction proceeds readily.[134] When considering a substituted aniline derivative, in which the *ortho*-, *meta*- and *para*-positions are substituted with an 'R' group (Scheme 133), the nitration reaction can lead to a mixture of regioisomeric nitroanilines. *Ortho*- and *meta*-substituted anilines (**358**, **359**) could theoretically result in the formation of four regioisomeric products, whilst a *para*-substituted aniline (**360**) can result in the formation of two regioisomeric products. The regioselectivity can be controlled by an appropriately directing 'R' group and many of the theoretical isomers are not observed, however, in a lot of cases the formation of more than one nitration product is observed, resulting in lower yields of the desired nitration product.
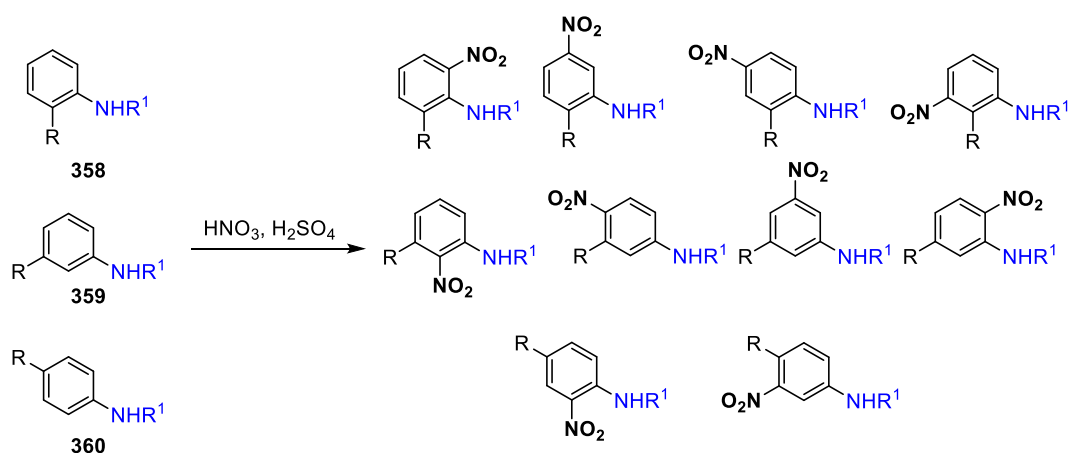
Scheme 133: Regioselectivity issues with nitration reactions

5.2 The importance of 2-aminobenzimidazoles

As of 2014, 77% of all marketed unique small-molecule drugs which contain a benzimidazole are substituted with a heteroatom (N, O or S) at the C_2 position (Figure 23).[5] Emedastine (**361**), Albendazole (**362**) and Astemizole (**363**) are three marketed examples of this substitution in which the 2-position is functionalised with an amine.
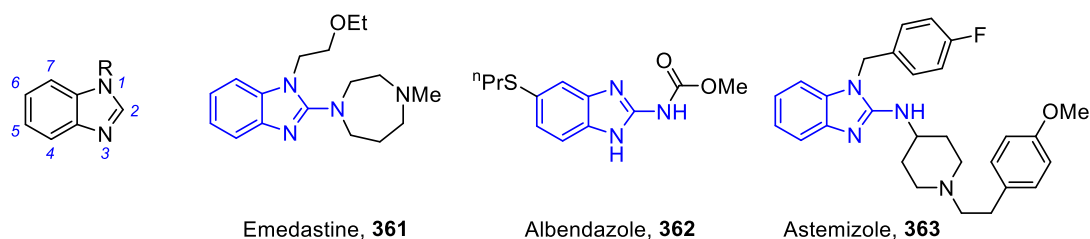
Figure 23: Examples of 2-aminobenzimidazoles

Emedastine (**361**) is a second-generation antihistamine developed by Alcon for the treatment of allergic conjunctivitis. This compound displays vastly improved binding affinity to the target protein over first-generation alternatives.[135]

Albendazole (**362**) is a GlaxoSmithKline (GSK) marketed drug, patented in 1975,[136] and is used for the treatment of numerous parasitic worm infections. These include enterobiasis, filariasis and ascariasis. These conditions result in rashes, skin thickening, abdominal pain and can cause down-stream effects such as blindness. Largely, these parasitic infections are tropical diseases which are carried by mosquitoes or through poor sanitation, and as such are prevalent in warm, arid climates.[137,138] Up to 1 billion people are potentially at risk of contracting these parasites across 82 countries, of which the most susceptible population are infants.[139] In 2013 GSK had donated 763 million Albendazole doses to the developing world, with a pledge to bring this total to over 2 billion by 2020.[140] This equates to 800 tonnes of Albendazole at an average dose of 400 mg.[141] This particularly emphasises the importance of this class of azacycle and why efficient synthetic methodologies are required for the preparation of 2-aminobenzimidazoles.

2-Aminobenzimidazoles have shown significant promise within medicinal chemistry for their use as use as antibacterials, immunosuppressives, antidiabetics, antivirals and analgesic compounds.[142-149] Furthermore, in recent years, 2-aminobenzimidazoles have become highly promising targets for STING receptor agonists (Stimulator of Interferon Genes), an example of which is the experimental dimeric aminobenzimidazole **364** (Figure 24). STING is a signalling molecule located in the endoplasmic reticulum and is essential for regulating transcription of a host's defensive genes.[150] As such, there is an intensive research effort to capitalise on these observations to find applications within oncology and infectious diseases.[151-153]

364
STING receptor agonist
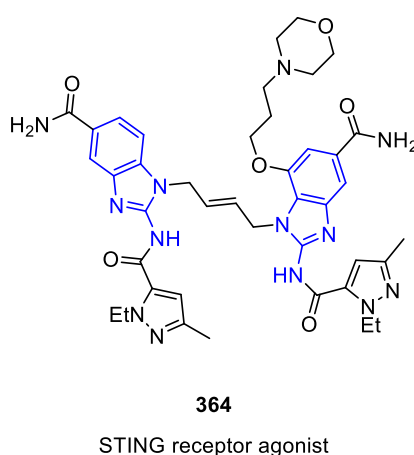
Figure 24: GSK's 2-aminobenzimidazole candidate for STING receptor agonists

5.3 The synthesis of 2-aminobenzimidazoles

5.3.1 From 1,2-diaminobenzenes

The original method for the formation of 2-aminobenzimidazole can be traced back to a report by Pierron from the early 20th century.[154] The reaction involves the condensation of a 1,2-diamine (**365**) with cyanogen bromide to give species **366** which rapidly collapses to cyanamide **367** by elimination of bromide. Intramolecular addition of the aniline to this species furnishes the unsubstituted 2-aminobenzimidazole **368** (Scheme 134).[155-157] This procedure is practically simple to perform and high-yielding, however, the products are limited to those baring an NH_2 in the C_2 position of the benzimidazole.
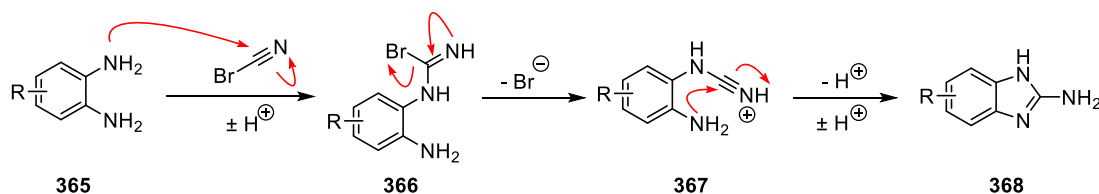
Scheme 134: The Pierron method for 2-aminobenzimidazole synthesis

Alternative methods which allow for substitution on the C2 position include the phosphorous oxychloride mediated dehydration-cyclisation of aryl urea-containing substrates such as **369** (Left, Scheme 135). This proceeds through the formation of an intermediary chloroamidinium species **370**, whereby this highly reactive species is trapped by the intramolecular aniline, yielding the benzimidazole.[158,159] Other similar methods include the cyclodesulfuration of thioureas (**371**) with mercury or lead salts, which are assumed to occur through formation of an intermediary diimide, although the evidence for this species is inconclusive (Right, Scheme 135).[160] Medicinal chemistry programmes have been supported by this cyclodesulfuration technique,[161] however, the method is operationally unpragmatic owing to the use of either lead or mercury. One-pot procedures using other cyclodesulfuration agents (carbodiimide) have more recently been reported.[162] The use of stoichiometric agents to affect the cyclodesulfuration, including mercury and lead, render this procedure unattractive towards scale-up.
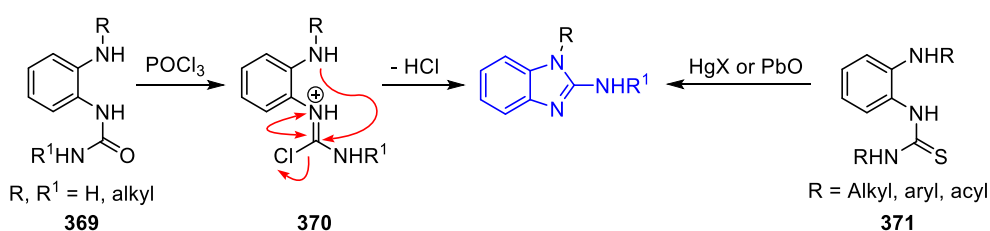
Scheme 135: Synthesis of 2-aminobenzimidazoles using POCl₃ or mercury and lead mediated methods

In 1975, Lugosi and Hornyak studied the spontaneous cyclisation of *o*-amino arylguanidines (Scheme 136).[163] These reactions involve the functionalisation of an *o*-nitroaniline (**372**) into the corresponding nitroguanidine **373**. The guanidinylation agent (**374**) is prepared by phosphorous oxychloride mediated dehydration of a urea. This highly electrophilic reagent

reacts with the aniline to form the guanidine. Upon catalytic reduction of the nitro group to aniline **375**, the guanidine free-base undergoes cyclisation to the 2-aminobenzimidazole, liberating an amine. These thermolysis reaction conditions superficially appear to be more pragmatic than the mercury and lead mediated cyclodesulfuration, however, they only occur in the solid-state or when heated at significantly elevated temperatures. Moreover, when the 'R' groups on the aryl-guanidine are different, the procedure offers little to no selectivity for elimination of different amines. This presents a challenge when 'R' is highly elaborate or expensive, as half of the 'R' group present in substrate **373** would be lost.
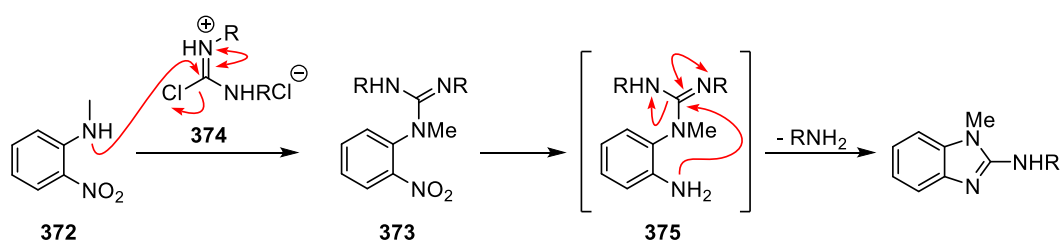
Scheme 136: Intramolecular cyclisation of o-aminoarylguanidines

In 2013, Wang and Ji published a transition-metal catalysed procedure using 1,2-diamines (**376**) and an isocyanide (**377**) to synthesise 2-aminobenzimidazoles (**378**) (Scheme 137).[164] This obviates the need for strong dehydrating conditions. However, the procedure is limited to the accessibility of isocyanides as coupling partners, which despite a number being commercial, these species require synthesising when the 2-amino group requires increased complexity. It was also noted that reactions with aromatic amines afforded poor to moderate yields of the desired 2-aminobenzimidazole, exemplified by a 51% yield of **378b**.
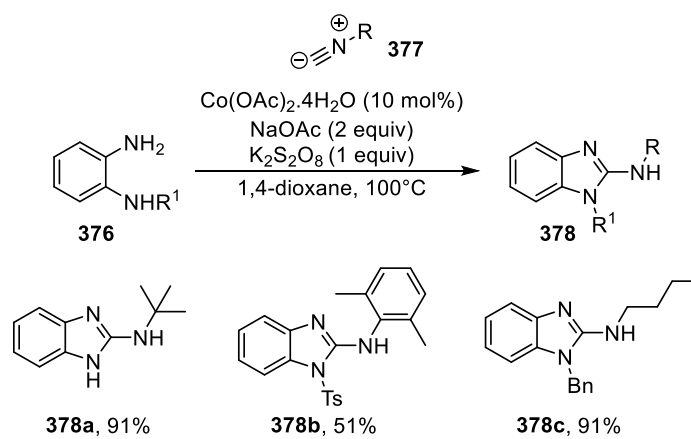
Scheme 137: Wang and Ji's 2-aminobenzimidazole synthesis from isocyanides

5.3.2 From 2-chloro benzimidazoles

The substitution of a chloride at the 2-position of a benzimidazole (**379**) by an amine was first reported in 1912 by Kim and Ratner (Left, Scheme 138).[165] This nucleophilic aromatic substitution (S$_N$Ar) method is arguably the most adopted method for the synthesis of 2-aminobenzimidazoles and various adaptions of this method have recently been reviewed.[166] The reactivity of 2-chlorobenzimidazoles (**380a**) with a secondary amine (piperidine) has been shown to be less than that of 2-chlorobenzoxazole (**380b**) and 2-chlorobenzothiazole (**380c**) analogues (Right, Scheme 138).[166] The exact mechanism for this S$_N$Ar reaction has not been studied extensively, however, this observation would be consistent with a slow formation of the Meisenheimer intermediate (often invoked as the rate-determining step in S$_N$Ar reactions[167,168]) owing to the increased electron density in a benzimidazole compared with benzoxazoles and benzothiazoles. A concerted S$_N$Ar mechanism can't be ruled out however.[169] This is represented in the forcing conditions required to substitute the chloride with the desired amine, often under high pressures at elevated temperatures.[170] The temperature of these reactions can be lowered by using lithium amides instead of the amine,[171] however, the preparation and handling of lithium amides require extra steps and can restrict the tolerance of certain base-sensitive functional groups.
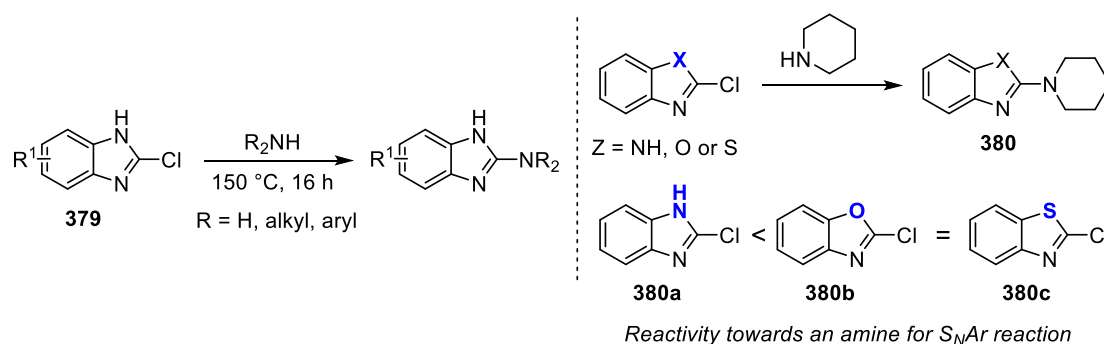
Scheme 138: S$_N$Ar reactivity comparison between 2-chlorobenzimidazoles, 2-chlorobenzoxazoles and 2-chlorobenzothiazoles with an amine

It has been shown using flow chemistry that with high temperature (225 °C) and pressures (120 bar) S$_N$Ar reactions can be realised to give significantly shorter reaction times (Scheme 139).[172] 2-chlorobenzimidazole (**381**) was shown to undergo an S$_N$Ar to give benzimidazole **382** in 78% yield. This procedure offers a scalable method to furnish 2-aminobenzimidazoles

through an S$_N$Ar reaction. However, the requirement for specific flow technologies does not make this method widely accessible.
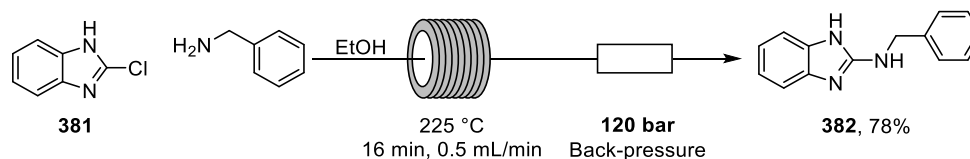
Scheme 139: S$_N$Ar reactions in flow to decrease the reaction times

Transition metal catalysis has proved to be an effective tool to couple 2-chlorobenzimidazoles with primary amines.[173] Sennanyake and co-workers developed a novel procedure to form Norastemizole **383**, a closely related analogue of the marketed drug, Astemizole **363** (Scheme 140). The procedure involves a Buchwald-Hartwig amination[174,175] of 2-chlorobenzimidazole **384** with primary amine **385** to give **383**. This procedure offers milder reaction conditions than the S$_N$Ar protocol with shorter reaction times, giving the desired product in one hour at reduced temperatures.
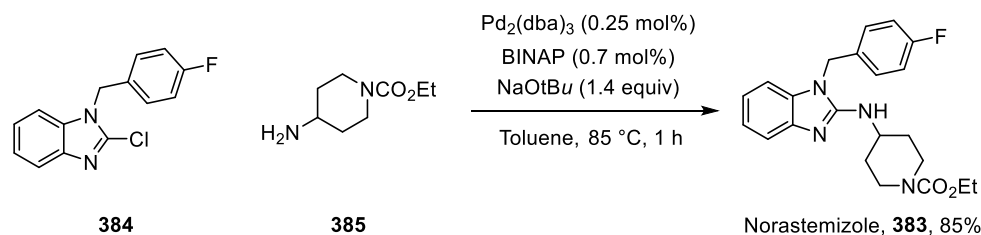
Scheme 140: Palladium-catalysed aminations of 2-chlorobenzimidazoles and the application towards Norastemizole

The challenge with using 2-chlorobenzimidazoles lies in the preparation of the starting materials. 2-chlorobenzimidazoles (**386**) are accessed from chloro-dehydration of a benzimidazolone (**387**), which itself is prepared by ring-closure of a 1,2-diamine (**388**) with phosgene (COCl$_2$) or carbonyl diimidazole (CDI) (Scheme 141).[176] Thus, 2-chlorobenzimidazole materials are the product of two separate synthetic steps. With simple starting materials (*e.g.* R = H), these materials are commercially available and easily accessible. However, when R ≠ H or the starting materials contain functional groups which are

unstable with respect to either CDI or POCl$_3$ (amines, amides, ureas, pyridiones), this synthetic sequence will likely make the synthesis of 2-chlorobenzimidazoles highly challenging.
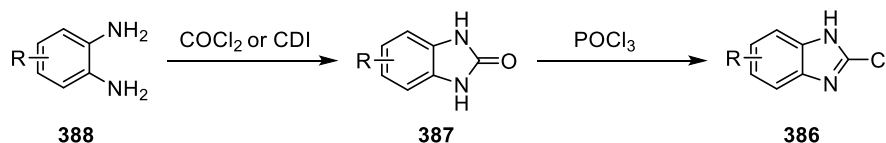
Scheme 141: The two synthetic steps to access 2-chlorobenzimidazole

5.3.3 From 2H benzimidazoles

The direct C–H amination of an aromatic species presents a significant advantage over the functionalisation of C–X bonds (where X ≠ H). There are several reasons for this: time and material are saved by not needing to introduce a synthetic handle, and the elimination of these handles reduces the consequential production of waste. C–H bonds are ubiquitous in organic compounds, and the capability to directly convert these to C–N bonds has drawn significant attention from synthetic chemists in recent years. These elegant and impactful transformations have been reviewed in detail, emphasising the efforts of the chemistry community to realise C–H amination as a realistic and practical synthetic technique.[177-179] A fundamental consideration with C–H amination is the requirement for an oxidant. The electrons in the C–H bond either leave as molecular hydrogen or are shuttled through to a terminal oxidant.[177] Described herein are a number of C–H amination procedures to form 2-aminobenzimidazoles (**389**) from benzimidazoles (**390**) (Scheme 142).
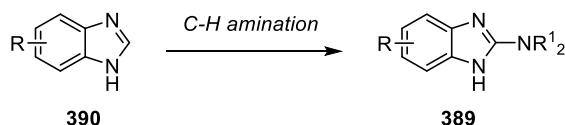
Scheme 142: A general scheme to consider the C–H amination of benzimidazole

The Chichibabin reaction was reported in 1914 as a simple method to substitute the 2-position of a pyridine (**391**) using sodium amide to give 2-aminopyridine (**392**, Left, Scheme 143).[180] This unusual reactivity invokes a hydride as a leaving group, which remained of synthetic and mechanistic interest throughout the 20th century.[181] An adaption of this method was reported

throughout the 1960s–1970s to form 2-aminobenzimidazoles (**394**) from the corresponding

C−H benzimidazole (**393**, Right, Scheme 143).[182] This is a highly elegant procedure as it is a

metal- and oxidant-free method to access these products. However, the high basicity of the

nucleophiles (pKa of NH_3 = 38)[183] renders the functional group compatibility towards

base-sensitive groups (ketones, aldehydes, acids) poor. Moreover, the presence of these

functional groups would consume the nucleophile, removing the desired reactivity altogether.
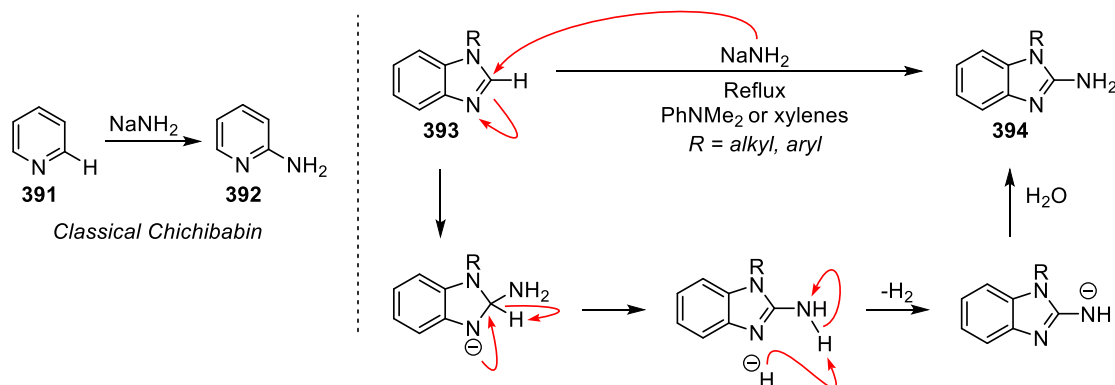
Scheme 143: The Chichibabin reaction

Modifications of the Chichibabin reaction have recently been reported by Roy in 2018 (Scheme

144).[184] Acylation of *N*-methyl benzimidazole (**395**) gives cationic species **396**, which acidifies

the C2H position, allowing for smooth carbene formation and trapping of this with iodine to give

an intermediate 2-iodobenzimidazolium **397**. This species is suggested to undergo an

S$_N$Ar-type reaction with sodium amide to give an imine intermediate **398**. Despite aryl-iodides

being well known to be poor S$_N$Ar substrates,[185,186] this likely attests to the high reactivity of

the benzimidazolium species **397** towards nucleophilic attack. The iminium substrate **398** is

then exposed to hydrolysis conditions to cleave the carbamate, revealing the desired

2-aminobenzimidazole (**399**). The advantage of this procedure is the removal of the

requirement to use sodium amide under reflux and removes the production of hydrogen, both

of which present a significant safety concern.[187] This method again suffers from the same

functional group challenges as the standard Chichibabin reaction owing to the use of highly

basic sodium amide. Secondly, these reactions have not been reported with complex alkyl or

aryl amides, suggesting poor generality of the procedure. Ultimately, the Chichibabin reaction

and the associated modifications are limited to the synthesis of compounds baring an NH_2 group in this position and suffer from poor substrate scope compatibility.
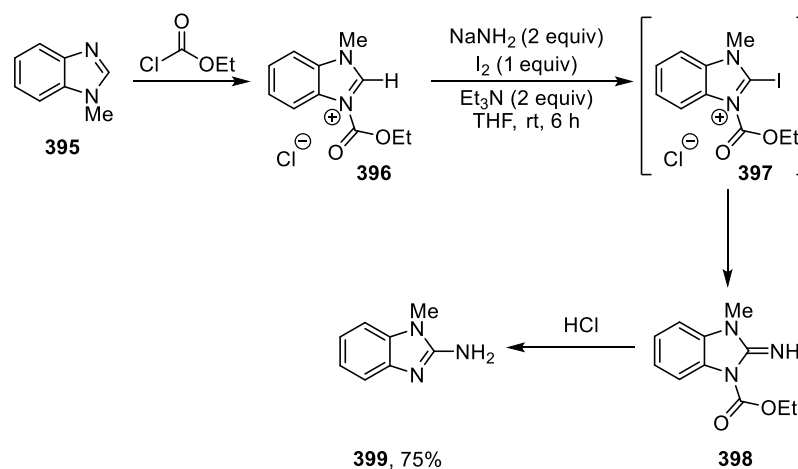
Scheme 144: Roy's adaption of the Chichibabin reaction

Various other strategies which directly functionalise the C–H bond in the 2-position have been reported using transition metal catalysis. The first example of the direct C–H amination of the 2-position of benzimidazole using copper-catalysis was reported in 2009 by Mori (Scheme 145).[188] The catalytic system uses copper(II) acetate and triphenylphosphine in xylene under an oxygen atmosphere which acts as the terminal oxidant. The paper only reports one example of an aminobenzimidazole (**400**, 51%), but this seminal report highlighted the potential for this interesting transformation. This was later followed up in 2014 by Bhanage showing how the use of copper(acac)$_2$ proved beneficial, affording the benzimidazole **400** in 84% yield without triphenyl phosphine under otherwise identical conditions.[189] This suggests that the ligand environment on the copper-catalyst plays an important role in the transformation. Furthermore, only one example of a 2-aminobenzimidazole was reported in this publication using *N*-methyl benzylamine. As such, a true examination of the substrate generality was not obtained.
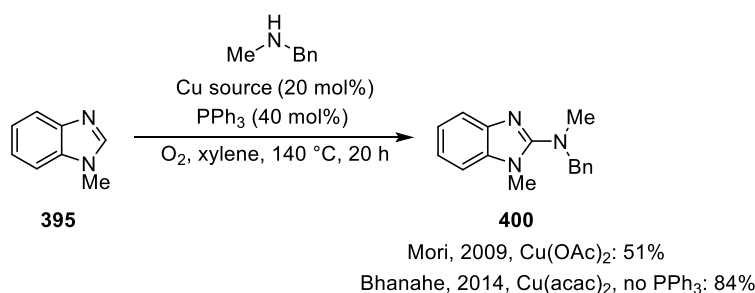
Scheme 145: Mori and Bhanage's report of the direct C–H amination of benzimidazole using a copper catalyst under oxygen

In 2014 Schreiber reported an elegant methodology to couple benzimidazoles with nitrogen nucleophiles (Scheme 146).[190] Using *N*-methylbenzimidazole (**395**), the scope of the amine partner was extensively examined and resulted in the formation of products in good yield, exemplified by species **401a–c**. The procedure was limited to substrates baring moderately acidic NH bonds, (primary and secondary amines were not tolerated) however, this efficient reaction paved the way for the next advancement for the C–H amination of benzimidazoles.
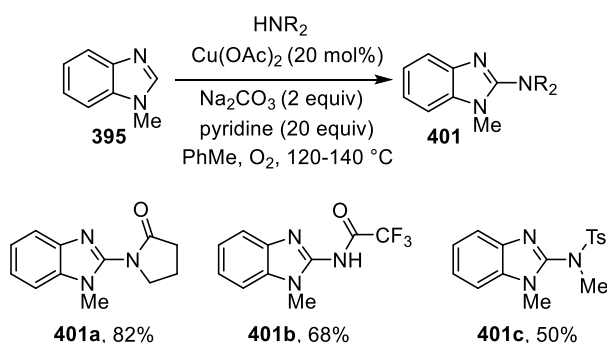
Scheme 146: Schreiber's report of the C–H amination of benzimidazoles using acidic amine coupling partners

In 2013, Shi published an interesting stoichiometric study using the copper-adducts of simple aliphatic amines. This showed how non-acidic amine partners can be efficiently coupled to give 2-aminobenzimidazoles (Scheme 147) under remarkably mild reaction conditions.[191] The reaction proceeds with both primary and secondary amines, along with anilines to furnish a variety of substituted 2-aminobenzimidazoles (**402a–c**). The conditions offered in this report (lower temperatures, shorter reaction times, the use of air and not oxygen) offer a great improvement over the previous methodologies, and the scope of the amine partner is

dramatically improved. This publication also offers an interesting mechanistic insight into these transformations by suggesting that once an amine and the aryl partner are both coordinated to the copper-centre, the reaction readily occurs, emphasised by the mild reaction conditions. However, little mechanistic insight was offered into either the C–H functionalisation or the C−N bond-forming step.
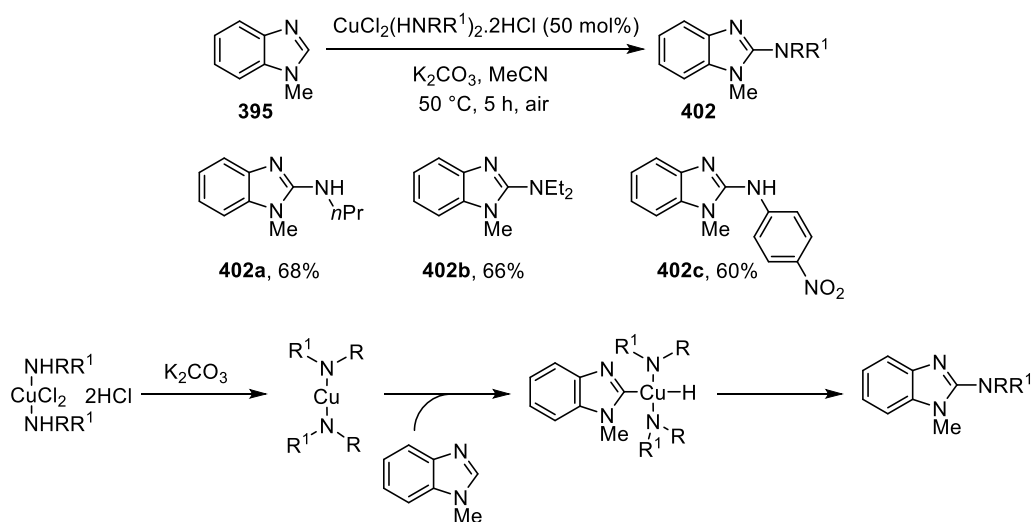
Scheme 147: Shi's methodology using copper-amine salt complexes

A novel zincation-amination strategy was reported by Wang in 2014 which involved transmetalation of an *in-situ* generated benzimidazole-2-zincate onto a copper catalyst, ultimately giving the 2-aminobenzimidazole (Scheme 148).[192] This strategy opened the door to a range of amine partners which weren't accessible by Schreiber's methodology (**403a–c**). This paper also highlighted the use of an endogenous oxidant, in which the imported N–O bond on the amine acts as an oxidant, without the requirement to add exogenous oxidising species. However, these substrates require elaborate synthetic preparation, and when a more complex amine partner is required this strategy would become less feasible owing to the preparation of the hydroxylamine derived substrate.
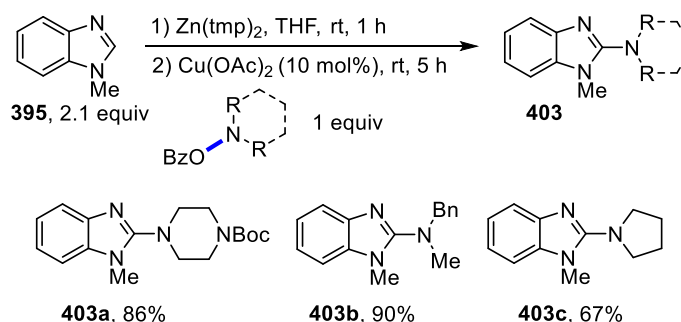
Scheme 148: Wang's zincation-amination using an internal oxidant in the form of an activated hydroxylamine

There remains a significant challenge with the C–H amination of benzimidazoles. The reactions are currently limited to nitrogen-based nucleophiles baring acidic NH bonds and often use very forcing conditions, or, use amine substrates which are activated in the form of hydroxylamines. Given the abundance of similar methodologies to aminate the C_2 position of benzoxazoles by transition-metal catalysis[193-200] and under metal-free conditions,[201-206] other strategies are required to target 2-aminobenzimidazoles.

While progress in the C–H amination of benzimidazole has developed in recent years to become a powerful methodology, the substrates require the heterocycle to be pre-formed. This ultimately results in lengthened syntheses of the final products, especially when highly substituted benzimidazoles are required. The use of 1,2-diaminobenzenes is therefore essential for all the discussed methods up until this point. For simple substrates, many are likely to be commercially available. However, given the increasing complexity of pharmaceutical and agrochemical compounds, it is likely that the heterocycle would require assembly. This would necessitate the use of a nitration-reduction sequence which increases the length of the resultant synthesis of the desired benzimidazole. Furthermore, the required synthetic sequence of a nitration limits functional group compatibility when other aromatic systems are present, along with the regiochemical challenges for the nitration reaction. The second synthetic step, involving reduction of a nitro group, further limits the substrate scope. These factors therefore necessitate other synthetic methodologies which directly target the formation of the heterocycle, removing the nitration-reduction sequence.

5.4 2-aminobenzimidazoles from other 1,2-disubstituted arenes

5.4.1 Intramolecular examples

Owing to the challenges associated with the C–H amination of the preconstructed benzimidazole core, as described in Section **5.3**, it is unsurprising that other methods are desirable for the construction of the heterocycle in one step. An intramolecular copper-catalysed C–N bond formation was reported by Batey which transforms α-halo aryl-guanidines (**404**) into the corresponding 2-aminobenzimidazoles (**405a–c**, Scheme 149).[207] This reaction offers access to products which are challenging to access by C–H amination methods (aliphatic amines) and quickly allows efficient construction of the desired heterocycle.
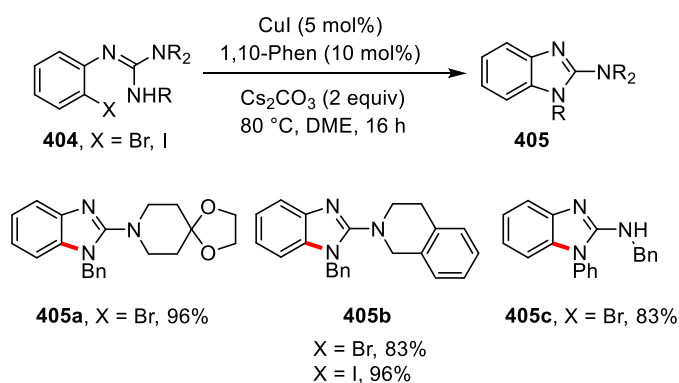
Scheme 149: Intramolecular amination of 2-haloarylguanidines using a homogenous catalyst

A similar method was later published by Punniyamurthy *et al* using heterogenous copper catalysis with α-bromo aryl-guanidines (**406**) which largely gives access to the analogous species obtained by Batey in comparable yields (**407a–c**, Scheme 150).[208] The advantage of this procedure is that the simple, ligand-free catalytic system could easily be recycled which offers practical advantages and restricts metal-contamination in the isolated products.
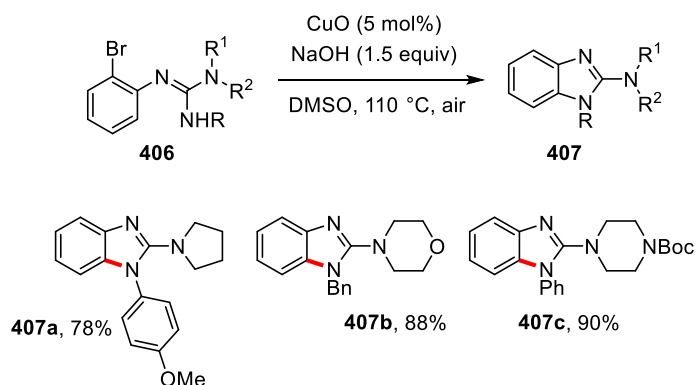
Scheme 150: Punniyamurthy's heterogenous intramolecular amination of 2-haloarylguanidines

5.4.2 Intermolecular examples

In 2009, an intermolecular bis-functionalisation of 1,2-dihalo arenes (**408**) with guanidines (**409**) was reported by Deng, a strategy which offers theoretical advantages over the intramolecular examples above (**410a–c**, Scheme 151).[209] By use of a simple ligand system and taking advantage of the intermolecular nature of the reaction, it allows for a variety of products to be assembled through a late convergence point, without substrate preparation as in the above examples. However, the highly forcing conditions (>150 °C, long reaction times) and low yields do not lend well to providing a reliable method to access these products. Moreover, the use of heavy halogens (bromine, iodine) consequently lower the atom economy of the procedure, and 1,2-dihaloarenes represent a non-trivial synthetic target to access. These factors limit the applicability of this method in providing a scalable synthesis of these compounds.
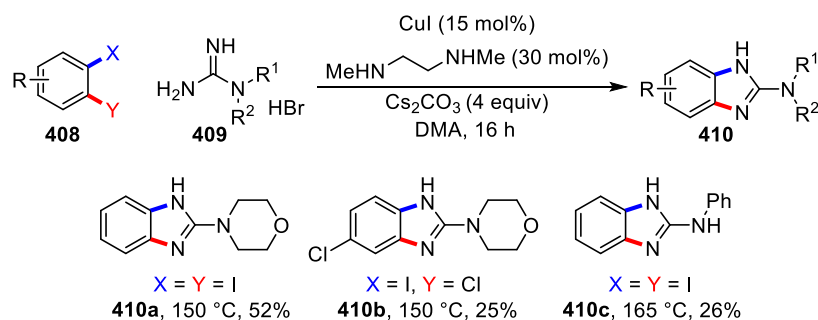
Scheme 151: Deng's copper-catalysed guanidinylation of 1,2-dihaloarenes

Bao and co-workers published the use of aryl-diimides (**411**) as an intermolecular example of 2-aminobenzimidazole formation.[210] The reaction proceeds under similar conditions and offers comparable yields to the reports in Section **5.4.1**. The authors showed that the reaction went *via* guanidine **413**, but the slight advantage offered by this adaption is that it telescopes the guanidine-formation through to the cyclisation event. The diimide substrates can be readily prepared by dehydration of a urea,[211] however, this is a limitation of the methodology as diimides are strongly dehydrating substrates. This limits functional group compatibility towards dehydrating sensitive groups (carboxylic acids, primary amides, amines).
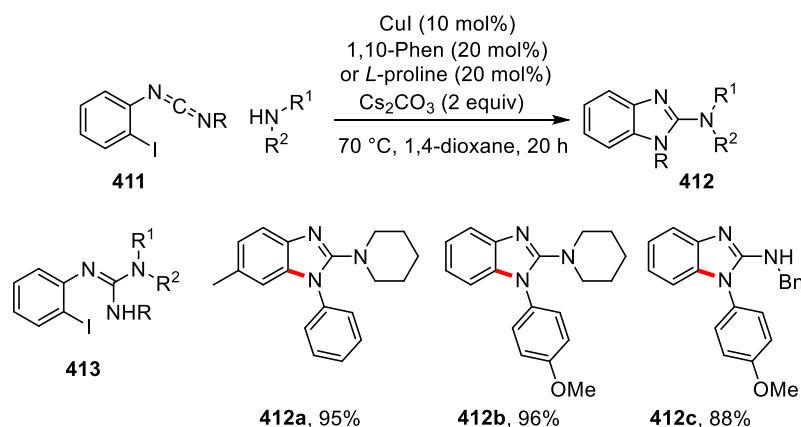
Scheme 152: The use of aryldiimides as precursors to 2-aminobenzimidazoles

This diimide strategy was later extended by switching the diimide and amine partner. Two sequential publications detailing the intermolecular reaction between *o*-haloanilines (**413**) and exogenous carbodiimides (**414**) to give 2-aminobenzimidazoles (**415**) were reported in 2010/2011 by Xi and Bao (Scheme 153).[212,213] These diimide procedures offer improved yields over other intermolecular examples and the ligand-free design in this example makes for an operationally simple protocol. The authors noted that unsymmetrical aryl-alkyl diimides give N_1-aryl benzimidazole products **415e** & **415f**, indicating a good level of regioselectivity for these specific products. However, the functional group tolerance is limited by using highly reactive dehydrating diimide substrates[214] and the use of a strong base (NaO^{t}Bu). Furthermore, the reaction class is limited to products with specific substitution patterns, and aniline substrates baring electron donating groups were not tolerated.
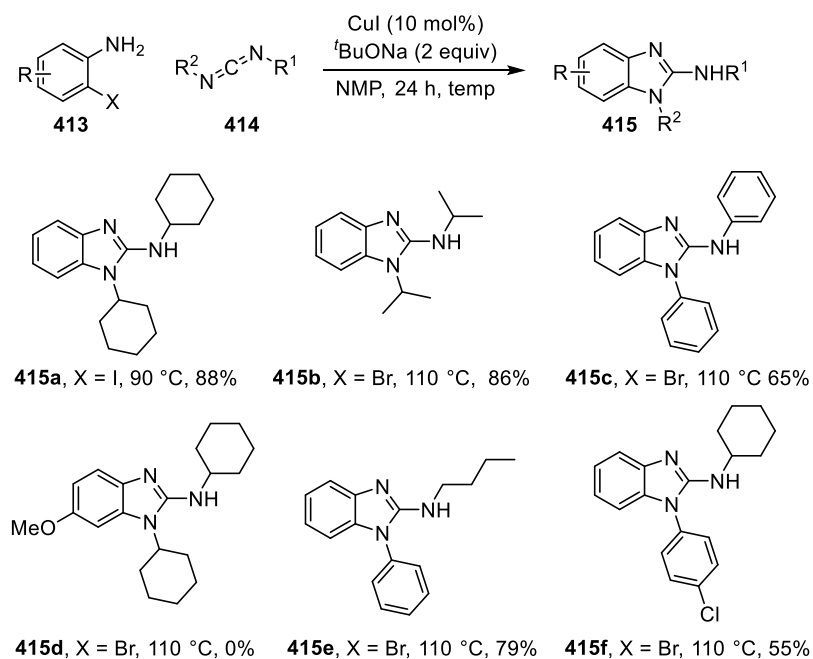
Scheme 153: The coupling of o-haloanilines with diimides to form 2-aminobenzimidazoles

The procedures discussed in this section use *o*-halo arylguanidines to synthesise 2-aminobenzimidazoles. This offers an advantage as the heterocycle can be directly synthesised in one step. However, the substrates for these transformations are synthesised from *ortho*-haloanilines, which are not trivial synthetic targets to access.

5.5 Direct heterocycle synthesis by C–H functionalisation

5.5.1 The challenge with 1,2-substituted arenes

Ultimately, the requirement for 1,2-disubstitution on the arene portion of the substrate is essential for all the examples discussed up until this point. Various limitations exist to this strategy; however, the overarching problem is access to the required 1,2-disubstituted starting materials. The most common method of accessing 1,2-diamines comes from the reduction of a 2-nitroaniline[128] and 2-haloanilines are likely products of a Sandmeyer reaction.[215-218]

The commercial production of 2-nitroaniline (**417**) is performed by aminolysis of 2-chloronitrobenzene (Scheme 154).[219] On further consideration, 2-chloronitrobenzene itself is synthesised through the nitration of chlorobenzene, of which the desired *ortho*-substituted product **418** is not the major product from this reaction. The nitration reaction gives 35% of the desired *ortho*-isomer with the major product being the *para*-isomer **420** in 64% yield.[106] Despite these reactions being commercialised and conducted on a huge scale, the desired 1,2-diamine for benzimidazole synthesis is likely the minor product of 4 separate synthetic steps from crude petroleum/benzene (chlorination, nitration, aminolysis, reduction). All of which before even considering further substitution on the arene backbone.
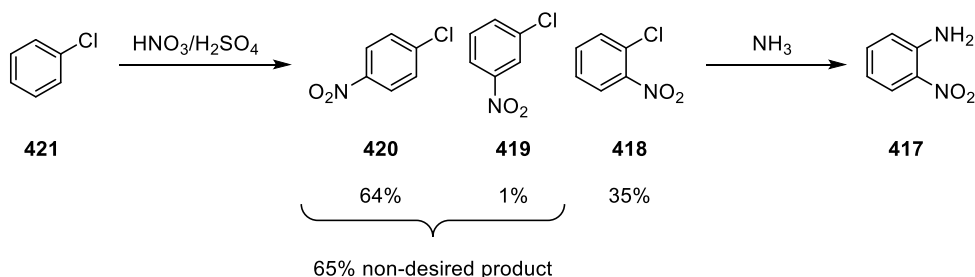
Scheme 154: Regioselectivity problems with the nitration reaction

When considering the synthesis of 2-haloanilines, a versatile synthetic precursor to 2-aminobenzimidazoles as discussed in Section **5.4**, a common method to do so is the Sandmeyer reaction of a 2-nitroaniline (**417**, Scheme 155). This reaction involves diazotisation of the aniline and then CuX (X = Cl, Br) mediated halogenation.[215] This synthetic sequence to access *o*-haloanilines is an indirect series of transformations. 2-nitroanilines (**417**) are

themselves versatile substrates to access 2-aminobenzimidazoles as described by methods in Section **5.3.1**. Adding two further transformations to manipulate 2-nitroanilines (**417**) into 2-haloanilines (**423**) thus adds unnecessary synthetic complexity.
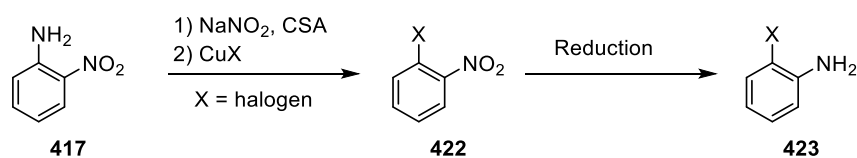
Scheme 155: Synthesis of o-haloanilines via a Sandmeyer reaction

A significant advantage in the synthesis of 2-amionobenzimidazoles would be realised by obviating the requirement to go through this multi-step reaction sequence. A result of this would be lower cost of goods, less waste and access to starting materials on a larger scale.

5.5.2 C–H functionalisation methods with endogenous oxidants

The first intramolecular C–H amination to form 2-aminobenzimidazoles from aryl-guanidines was reported by Schubert in 1973 (Scheme 156). This proceeded in a similar vein to Partridge and Turner's observation of benzimidazole formation in 1958 from aryl-amidines.[220,221] This report described how when briefly heated to the melting point, N–O acylated guanidines (**424**, guanidoximes) spontaneously cyclise to the corresponding 2-aminobenzimidazoles (**425**). The authors state that it is likely the reaction proceeds through the formation of nitrenoid species **426**. However, the low yields (<30%) and neat reaction conditions limit the practical application of this methodology.
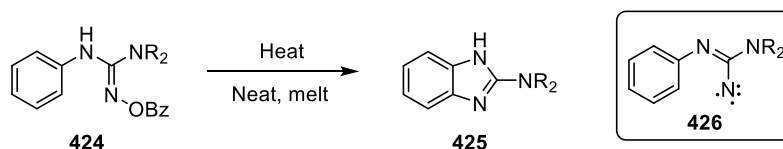
Scheme 156: The use of guanidoximes as internal oxidants to form 2-aminobenzimidazoles

It was reported by Esser in the 1990's that N–O bond containing substrates (**427**) can undergo a vicarious nucleophilic substitution to give 2-aminobenzimidazoles (Scheme 157).[222] Vicarious nucleophilic substitution is a subset of S_NAr in which the addition-elimination sequence results in elimination of a leaving group which is bonded to the incoming nucleophile, as opposed to the aromatic ring being substituted.[223] Under significantly milder conditions to those offered above, substrates which are 'loaded' with an appropriately positioned activating group (nitro) under basic conditions result in cyclisation to the 2-aminobenzimidazole. The anionic guanidine's (**428**) nucleophilic N–O nitrogen adds into the π-system where the negative charge is stabilised by the highly electron-withdrawing nitro group to form **429**. Under the basic conditions of the reaction, the 'vicarious' leaving group (methoxy in the shown example) is eliminated to give intermediate **430**. The final product (**431**) is formed after protonation of **430**. Despite offering an elegant route into these products, the starting materials require a multi-step sequence to assemble and the requirement for suitable activating groups, such as a nitro, remain essential for this vicarious substitution reaction to occur.
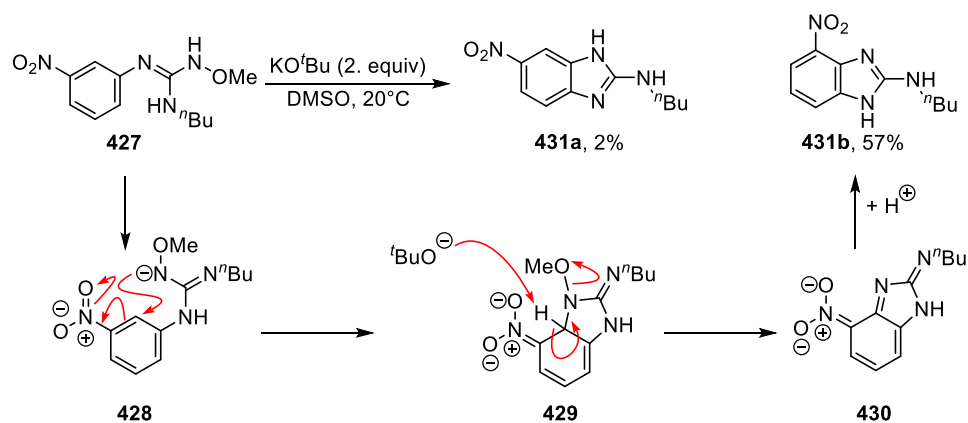
Scheme 157: Vicarious S$_N$Ar to form 2-aminobenzimidazoles

Owing to the elaborate synthesis required for N–OR substrates, it is desirable to use free amines, or unactivated amino-containing substrates, to improve synthetic tractability. In light of this, Esser further reported that *meta*-substituted nitro-aryl guanidines **432** cyclise under basic conditions to give substituted benzimidazoles **433** in 58% yield in the absence of a vicarious leaving group or oxidant (Scheme 158).[224] This reaction highlighted that guanidines such as **432** are self-oxidising, by the formation of reduced aza-oxy compounds **434a** & **434b** in 20% and 6% respectively. Attempts to control this redox pathway by adding exogenous oxidants did not result in improved yields or suppressed formation of undesired aza-oxy species, highlighting that this would be a challenging procedure to harness. Moreover, the specific substitution pattern of highly electron-withdrawing groups limits the generality of this procedure.
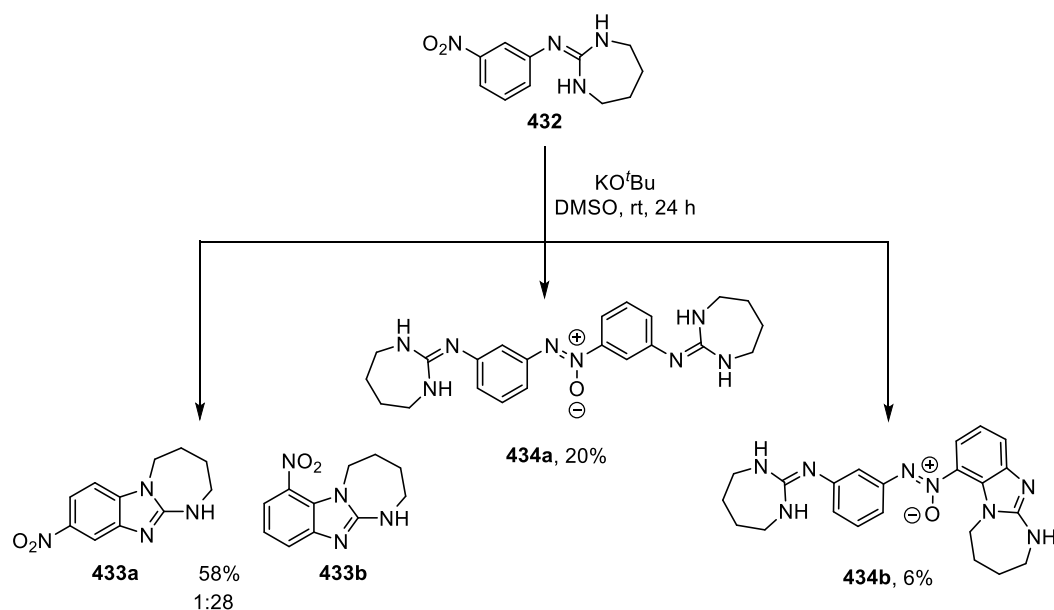
Scheme 158: The self-oxidising ability of nitroguanidines

Endogenous oxidants, *i.e* substrates which contain an internal oxidant, are beneficial owing to the relatively benign side-products which are formed along with not having to add stoichiometric amounts of an exogenous species. However, the challenging synthesis of the N−O containing fragment results in a long synthesis which uses hazardous reagents (HgO, hydroxylamines).[222] Ultimately, this limits the uptake of the methodology. As a result, the development of simple methodologies to form 2-aminobenzimidazoles using exogenous oxidants has drawn the attention of synthetic chemists.

5.5.3 C–H functionalisation methods with exogenous oxidants

A strategy using an aryl-guanidine (**435**) and a hypervalent iodine oxidant was published by Zhang in 2014.[225] Initial S_N2 substitution of the guanidine onto the iodine(III) species liberates trifluoroacetate, forming iodinated-guanidine intermediate **436**. This species is then primed to undergo an electrophilic aromatic substitution reaction with the arene, liberating the reduced iodine(I) compound and intermediate **437** which after deprotonation yields the product (**438**). Strong evidence for this mechanism was given by poorly behaving electron deficient substrates (as exemplified by **438b**, R = CN, 37%). The authors noted good selectivity for the formation of 1-aryl products, emphasised by the product of **438c** in 83% yield. This selectivity is interesting, suggesting that when R^2 = aryl, an anilinic nitrogen preferentially displaces the trifluoroacetate in the first step of the mechanism, as opposed to the more nucleophilic cyclopentyl-baring nitrogen.

Despite the advantages offered in this method, this procedure raises the question of the choice of oxidant for these transformations. The reaction requires the TFA-derived oxidant **439**, other hypervalent iodine species, for example $PhI(OAc)_2$, result in the formation of different products (**438d**). This selectivity concern results in the need to fine-tune the oxidant, and the relatively high cost, high molecular weights and the poor atom-efficiency of hypervalent iodine oxidants renders these protocols unattractive towards industrial requirements.
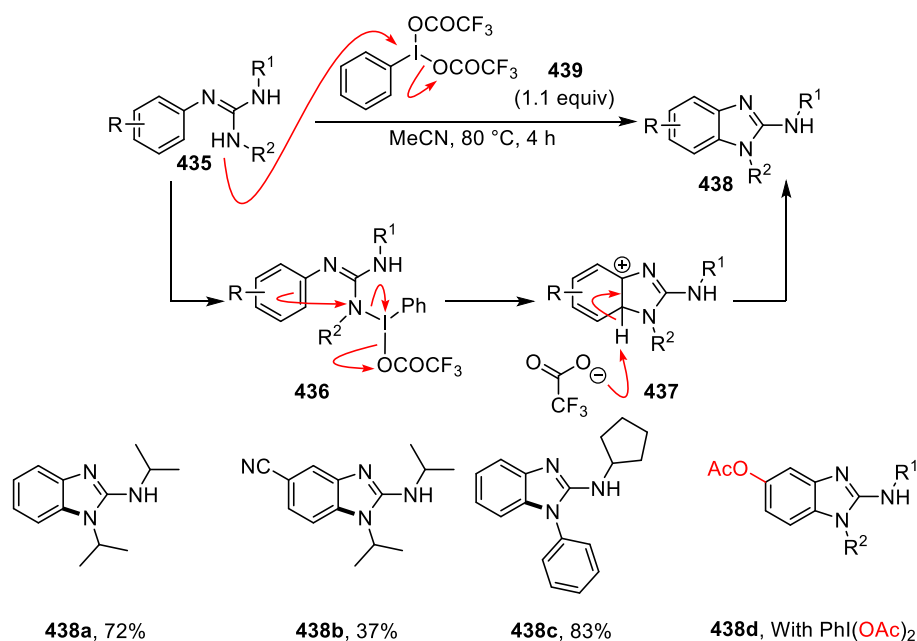
Scheme 159: Hypervalent iodine derived oxidants give access to 2-aminobenzimidazoles

An alternative to the use of hypervalent iodine oxidants is the use of a transition metal catalyst with a sacrificial 'turnover limiting' reagent acting as the exogenous oxidant. The combination of copper and an atmosphere of oxygen as a terminal 'green' oxidant has received significant interest. Bao reported that bis-aromatic carbodiimides (**440**) with a copper(II) catalyst in the presence of an amine result in the formation of 2-aminobenzimidazoles (**442** Scheme 160).[226] The reaction proceeds *via* an intermediate guanidine species **441**, whereby following a C–H functionalisation event, the desired 2-aminobenzimidazole is formed. This was the first report of a copper-catalysed C–H functionalisation to form 2-aminobenzimidazoles under aerobic conditions. However, the requirement for symmetrical diimide substrates restricts the products to those where the arene portion of the benzimidazole and the N_1-aryl group are equivalent. In cases where an unsymmetrical diimide is used, the benzimidazole is isolated as a mixture of regioisomers (as exemplified by **441b**).
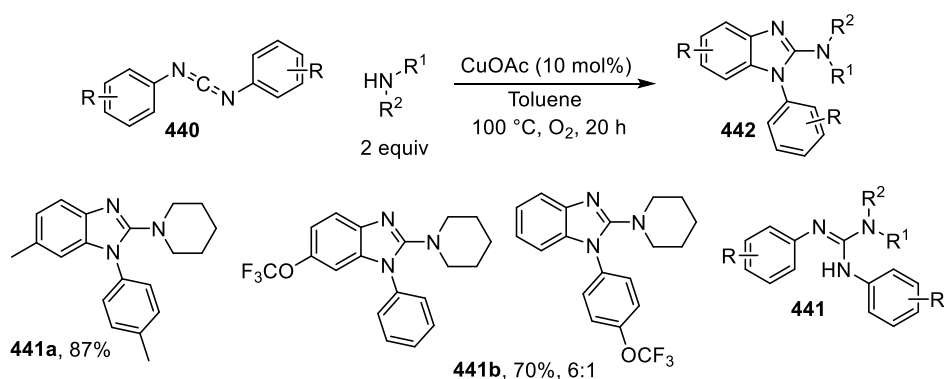
Scheme 160: The copper-catalysed C–H amination of diaryldiimides and an amine

A double-oxidation procedure to form 2-aminobenzimidazoles from amines (**443**), aryl boronic acids (**444**) and aryl cyanamides (**445**) was reported by Neuville (Scheme 161).[227] This tandem Chan-Evans-Lam *N*-arylation/C–H functionalisation highlights the potential for the combination of copper and air to be a highly effective and efficient method for the synthesis of 2-aminobenzimidazoles. Despite the rapid assembly of the benzimidazole core from relatively unfunctionalised starting materials, the problems with this procedure are comparable to the method of Xi and Bao (Scheme 152 and Scheme 153). Often the 2 aryl groups must be equivalent, as mixtures of regioisomers are isolated otherwise (**446c**). Further concerns are presented with aryl boronic acids. These species are often synthesised from feedstock materials, either by metalation of haloarenes and trapping with a boronate ester,[228] or transition metal catalysed borylations, both of which increase the length of the synthesis.[229,230] Further challenges with using boronic acids are presented in their reported toxicological concerns, where a number of common aryl-boronic acids have been shown to be mutagenic in the Ames assay.[231,232] These concerns often present a hurdle to process chemists, and methods which negate the use of mutagenic compounds are desirable from a safety perspective.
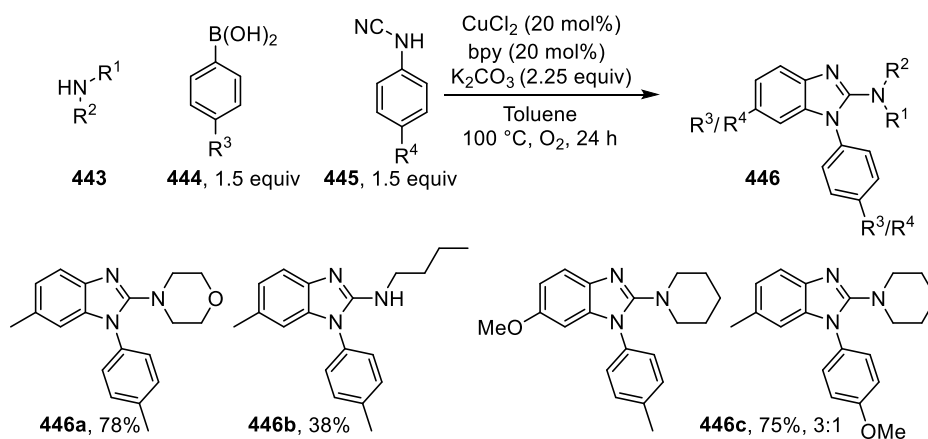
Scheme 161: A 3-component coupling of amines, aryl-boronic acids and a cyanamide

The direct conversion of C–H bonds to 2-aminobenzimidazoles has received significant interest in recent years. The progress made in this field has made access to these species from simple starting materials efficient and attractive to a synthetic chemist for several reasons. There is no longer a requirement to synthesise the benzimidazole heterocycle and undergo a series of laborious post-formation modifications to incorporate the amino group into the 2-position. This ultimately saves time, effort and resources to develop new benzimidazole containing compounds. The key to the success of these methodologies has been the development of powerful and user-friendly oxidation procedures which harness the potential of a successful C–H functionalisation. However, the use of stoichiometric oxidising reagents lowers the appeal of these protocols owing to the formation of substantial waste products, or challenging chemoselectivity problems with the synthesis of 2-aminobenzimidazoles depending on the choice of oxidant. The opportunities presented through the combination of copper as a catalyst and air as exogenous oxidant, whereby the oxidation by-products are easy to remove and handle, have the potential to solve several of the related concerns with the discussed oxidation procedures.

5.6 Copper-catalysed aerobic oxidations

5.6.1 Oxidations and the use of O_2

An oxidation is an event in which a species undergoes a loss of electrons. These reactions are crucial for several processes, including, but not limited to, metabolism, energy generation and the synthesis of organic compounds.[233]

The key requirement of an oxidant is the presence of empty orbitals that are low-lying in energy.[234] These empty orbitals, on oxidation of the substrate, become occupied, reducing the oxidant and completing the redox transfer. Given in Figure 25 is a molecular orbital diagram for diatomic oxygen and the peroxide ion. The regions shown are those associated with the redox properties of these molecules.[235] The $2p\pi_g^*$ orbitals are two low lying anti-bonding π-orbitals. In O_2, contained within these two degenerate orbitals are two electrons, which are distributed evenly in a manner to maximise the spin multiplicity of the system according to Hund's rule.[236] This triplet state, termed due to the two unpaired electrons, is the ground state of diatomic oxygen (O_2), a highly unusual example of a stable diradical species. On 2-electron reduction of O_2, the two new electrons occupy the half-filled $2p\pi_g^*$ orbitals, spin-pairing with the unpaired electrons from O_2. The processes decreases the bond order from 2 to 1 to give peroxide (O_2^{2-}) resulting in an elongation of the bond length. This bond-lengthening is often interpreted as a sign of the reduction of oxygen in mechanistic studies.
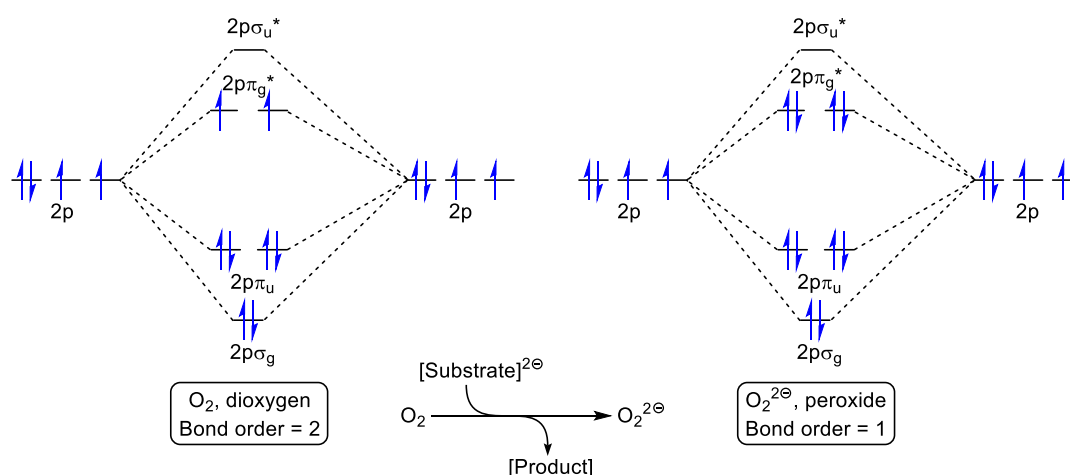
Figure 25: Molecular orbital diagram of diatomic oxygen. Note 1sσ and 2sσ orbitals are omitted for clarity. g=gerade, u=ungerade.

The reasons that oxygen is desirable as an oxidant in synthetic organic chemistry are relatively apparent. Chemical industries often strive to use oxygen as an oxidant owing to the high atom-economy offered and the untaxing effect on the environment.[237] Oxygen constitutes 21% of the earth's atmosphere and is constantly being renewed by photosynthesis.[238] Because of these factors, it is considered a green, renewable oxidant which is available in vast quantities.[238] Furthermore, when used directly as air, it comes at essentially no cost to the chemist. This has been capitalised on by the commodity chemicals industry, and several feedstock materials are produced by way of an aerobic oxidation. Formaldehyde (from methanol), ethylene oxide (from ethene), 1,2-dichloroethane (from ethene & hydrochloric acid), vinyl acetate (from ethene & acetic acid), phenol (from cumene) and caprolactam (from cyclohexanone) are all produced using air or oxygen as the oxidant (Scheme 162).[239]
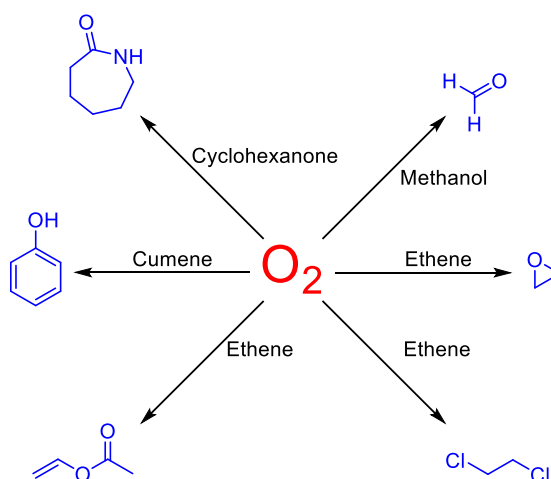
Scheme 162: The use of oxygen as a terminal oxidant to form a range of commodity chemicals

Traditionally, however, the pharmaceutical industry has remained cautious of the use of oxygen. In most cases, the organic solvents which are used in chemical reactions are volatile and highly flammable. This presents an inherent risk of fire or explosion when performing reactions under an atmosphere of oxygen.[240,241]

In recent years, many elegant engineering solutions have been developed which present solutions to the flammability concerns through the development of bespoke reaction vessels. For example, systems which directly bubble oxygen into the solvent and allow for rapid dissolution and consumption of oxygen have been developed.[242] This prevents the build-up of oxygen in the headspace of the reaction, removing the risk of explosion in batch reactors. Other solutions are presented by the use of flow chemistry, which often present huge advantages in biphasic reactions owing to superior mixing abilities.[243,244] These solutions to the risks associated with using oxygen as an oxidant have allowed industries to look upon, and pursue aerobic oxidations as a viable, safe alternative to the use of other, more hazardous oxidants. In recent years the pharmaceutical industry has adopted aerobic oxidations for the synthesis of important pharmaceutical compounds, perhaps indicating a change of mindset to the use of aerobic oxidations given appropriate understanding of the safety of the process.[245]

5.6.2 The combination of copper and oxygen as an oxidation method

The combination of copper and oxygen as a feasible oxidation method is neither new nor an exclusive synthetic method. The combination has roles associated with, but not limited to, metabolism, energy conversion and storage, and synthetic methods to form organic compounds.[246] The interaction of copper and oxygen is extensively exploited by natural systems, with important enzymatic and biochemical process harnessing these important interactions. For example, haemocyanin is a bimetallic copper-containing oxygen transport protein in arthropods and mollusks[247] and a range of monooxygenase enzymes contain copper-ions.[233]

A key synthetic example of an industrialised process in which copper and oxygen are combined is the Wacker process (Scheme 163).[248] The production of acetaldehyde from ethene and oxygen supplies world-wide markets with two million metric tonnes per year. The reaction mechanism has been studied extensively[249] and will not be discussed in detail. However, the important interaction is the role of copper and oxygen in the transformation. After the formation of acetaldehyde, the palladium catalyst is reduced to a Pd^0 species (**447**) which is unable to re-engage in the catalytic cycle, necessitating a stoichiometric loading of palladium for full conversion. The Wacker process uses a substoichiometric quantity of Cu(II) chloride which efficiently oxidises the palladium centre back to the active Pd^{II} complex **448**. The reduced CuCl then undergoes aerobic oxidation with O_2, forming water and regenerating $CuCl_2$ to re-engage in the catalytic cycle. The use of oxygen in combination with copper enables the industrial route to utilise catalytic quantities of both palladium and copper, whereby the resultant process is very cost, atom and mass efficient.
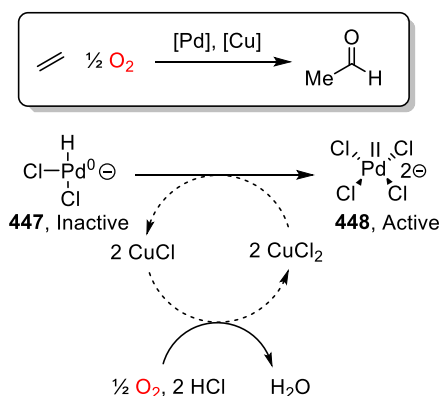
Scheme 163: The importance of the combination of air and copper in the Wacker reaction

The binding of oxygen to copper and the subsequent interactions has been studied extensively by computational methods and using heterogeneous copper-bound supports (zeolites).[250] Oxygen can bind a copper centre either *end-on* or *side-on*, providing an indication of the coordination properties of O_2.[251,252] Further, on binding to a zeolite-bound copper species, the oxygen–oxygen bond length increases from 1.22 Å (free O_2) to between 1.27–1.32 Å, which, compared to the O–O bond length in hydrogen peroxide (1.46–1.48 Å dependant on the source) suggests a bond-weakening effect.[251,252] This bond lengthening is highly indicative of increasing the electronic population of the $2p\pi_g{}^*$ orbitals, whereby the π-bond is weakening, which results in a longer oxygen–oxygen bond. Finally, computational methods have shown the charge-transfer of ~0.3 eV from a copper 3^d orbital onto oxygen.[251] Despite zeolite structures not being representative of what is occurring in a homogenous catalytic system, they do provide a powerful and insightful mechanistic model onto the activation of O_2 by coordination to a copper atom.

Copper exhibits four different oxidation states, Cu(0), Cu(I), Cu(II) and Cu(III), allowing it to act by one-electron or two-electron redox processes.[242] Moreover, the different oxidation states allow it to form favourable Lewis acid interactions with organic substrates, facilitating a range of powerful chemistry, including the reactions discussed in Sections **5.4** and **5.5**. Given the correct arrangements of ligands and organic groups bound to an active complex, Cu(III) can readily undergo reductive elimination to Cu(I), forming a range of valuable C–C and C–X bonds, in many cases from the functionalisation of C–H bonds.[242] The Cu(I) species which

forms as a result of the reductive elimination is then readily oxidised by O_2 back to Cu(II), allowing copper to be used in catalytic quantities. Given in Figure 26 are the standard electrode potentials of the half-reactions associated with an aerobic oxidation of copper.[253,254] The values displayed in Figure 26a show the redox half-equations and potentials for the reduction of O_2 to water (E° = +0.401 V) and in Figure 26b the one-electron reduction of Cu(II) to Cu(I) (E° = +0.153 V). Both values are positive, indicating that the position of equilibrium shifts to the right-hand side of the arrow. Moreover, the low value for Cu(II)/Cu(I) indicates that interconversion between Cu(II) and Cu(I) is facile. On considering the oxidation of Cu(I) to Cu(II), the reverse direction of the equilibrium arrow is followed, whereby the magnitude of the value remains identical, with a change in sign. Therefore, the redox potential for the oxidation of Cu(I) becomes E° = −0.153 V (Figure 26c). Finally, on combining both equations to develop the electrode potential for the electrochemical cell between O_2 and Cu(I), it is observed that E_{cell} = +0.248 V (Figure 26d). Despite these being ideal equations for "free" copper, (i.e, not ligated with organic ligands and substrates), these equations do not provide a quantitative numerical value for what is happening in organic reactions.[254] However, taken in isolation, the values provide a sense of the feasibility for the forward reaction to occur. The positive value of E_{cell} indicates that the forward reaction is favourable (i.e ΔG < 0 according to the Nernst equation, Figure 26e) showing that the aerobic oxidation of Cu(I) ions by oxygen is favourable.

a) $O_2 + 4H^+ + 4e^- \rightleftharpoons 2H_2O$ E° = +0.401 V

b) $Cu(II) + e^- \rightleftharpoons Cu(I)$ E° = +0.153 V

c) $Cu(I) \rightleftharpoons Cu(II) + e^-$ E° = -0.153 V

d) $O_2 + 4H^+ + 4Cu(I) \rightleftharpoons 4Cu(II) + 2H_2O$ E_{cell} = + 0.248 V
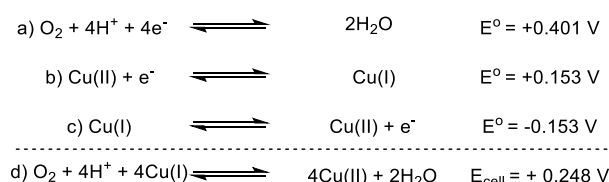
$$e)\ \Delta G = -nFE_{cell}$$

Figure 26: A thermodynamic explanation for the oxidation of Cu(I) by oxygen. Standard E° values, at 298.15 K (25 °C), and at a pressure of 101.325 kPa (1 atm). Values are referenced relative to the standard hydrogen electrode ($2H^+ + 2e^- \rightarrow H_2$. E° = 0.000 V)

6. Aims and Objectives

New methods for the synthesis of important azacycles are constantly desired by chemical industries. Specific species, such as 2-aminobenzimidazoles, remain highly challenging to access by traditional methods.[154,156,160]

Over the past 20 years, the development of oxidative copper-catalysed methodologies which utilise oxygen as a terminal oxidant have received substantial interest. New methods developed include the Chan-Evans-Lam C–N bond-forming reaction of amines with aryl and vinyl bornate species,[255-258] the Stahl oxidation of alcohols to ketones/aldehydes[259-261] and direct heterocycle forming reactions by methods previously discussed in Sections **5.4** and **5.5**.

The current copper-catalysed aerobic oxidation methods to form 2-aminobenzimidazoles suffer with poor generality and the products are highly restricted to specific substitution patterns.[226,227] The aims of this chapter are to develop a set of general conditions to synthesise 2-aminobenzimidazoles (**450**) through an intramolecular C−H functionalisation protocol of aryl guanidines (**449**) using a copper-catalyst and air as a terminal oxidant (Scheme 164).
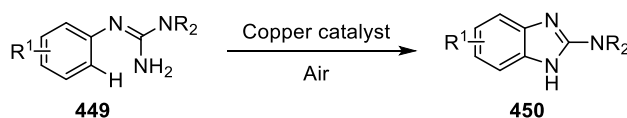
Scheme 164: The proposed copper-catalysed intramolecular C–H amination of aryl guanidines

The reasons for this are because the starting materials required for C–H functionalisations are cheaper, more sustainable, and more available than the required alternatives.[128] Once a suitable method for the synthesis of 2−aminobenzimidazoles through an intramolecular C−H functionalisation has been developed, the aim is to explore the substrate scope of the developed reaction to examine the generality of the procedure. Once examined, the method will be applied to the synthesis of an important pharmaceutical compound to highlight the procedure as a viable alternative to traditional methods.

Moreover, with the development of new methodologies comes improved understanding of the mechanisms by which these products are formed. The intramolecular copper-catalysed C−H functionalisation has received relatively little mechanistic investigation, specifically including the role of key additives within the reaction system. Through a series of control reactions, the aim was to improve the understanding of key additives and the mechanistic role these species play. This provided an improved mechanistic understanding of the C−H functionalisation event.

7. Results and Discussion

7.1 Reaction scouting and optimisation

Inspiration for an intramolecular C–H functionalisation to target 2-aminobenzimidazoles was garnered from a seminal report by Buchwald in 2008.[262] It was reported that aryl-amidines (**451**) baring an arene in the R^2 position which was *ortho*-substituted underwent cyclisation to a benzimidazole (**452**) in the presence of copper(II) acetate and acetic acid (Scheme 165). It was clear that there were unknowns in the reaction mechanism owing to the highly restricted substrate scope requiring a specific substitution pattern, however, these conditions offered a promising starting point. Within the publication, it was mentioned that functionalisation of an electron-rich substrate proceeded slightly faster than an electron-deficient substrate.
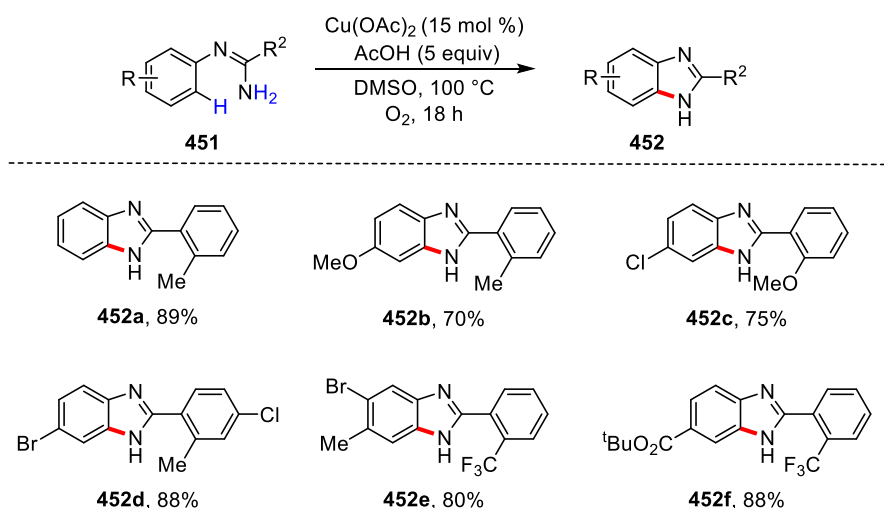
Scheme 165: Inspiration for the transformation, taken from a 2008 report by Buchwald

With the observation that functionalisation of an electron rich substrate was faster, a model guanidine substrate was designed which was electron rich and would give access to a 2-aminobenzimidazole. 3-methoxyaniline (**453**) was deprotonated with sodium hydride in DMSO and reacted with *N,N*-dimethyl cyanamide to give electron-rich aryl-guanidine **454** in 52% yield on a multi-gram scale (Scheme 166).
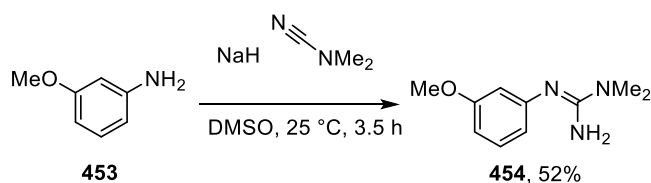
*Scheme 166: Synthesis of electron-rich aryl guanidine **454***

An initial experiment using the conditions presented in Buchwald's publication using 15 mol% copper(II) acetate and 5 equivalents of acetic acid in DMSO at 100 °C gave starting guanidine **454** and only trace quantities of benzimidazole **455** after 16 hours.

Trace quantities
73% guanidine remaining

Scheme 167: Initial screening using literature conditions

Lowering the equivalents of acetic acid from 5 to 1, the observed HPLC area% of benzimidazole **455** did not change (*c.f.* Entry 1 vs 2 Table 5). However, replacing acetic acid for pivalic acid gave an increase in formation of benzimidazole **455** to 13% (Entry 3) and using copper(I) acetate further increased the yield to 31% (Entry 4). Finally, changing reaction solvent from DMSO to NMP gave an increase in benzimidazole formation to 41% (Entry 5).
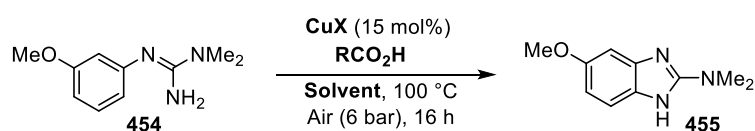
Entry	Copper salt	Acid	Solvent	Benzimidazole **455** / HPLC area%	Guanidine **454** / HPLC area%
1	Cu(OAc)$_2$	AcOH (5 equiv)	DMSO	8	73
2	Cu(OAc)$_2$	AcOH (1 equiv)	DMSO	8	66
3	Cu(OAc)$_2$	PivOH (1 equiv)	DMSO	13	53
4	CuOAc	PivOH (1 equiv)	DMSO	31	38
5	CuOAc	PivOH (1 equiv)	NMP	41	14

Table 5: Initial catalyst and additive variation

When NMP was employed as the reaction solvent, the formation of benzimidazole **455** increased to 41% (Entry 5 Table 6). Under these conditions, the formation of a dimeric benzimidazole was observed which was retrospectively isolated and characterised as **456** (Table 6). This species was a major side-product when using NMP as the reaction solvent and so understanding the factors which affect its formation would be beneficial in optimising the reaction conditions. Lowering the temperature of the reaction from 100 °C to 80 °C substantially lowered the formation of the dimeric species **456** from 10% to 2% (Entries 1 *vs.* 2). Secondly, gradually increasing the loading of the copper salt from 15 mol% up to 100 mol% resulted in a gradual increase in the production of this dimeric species **456** from 2% to 25% (Entries 2–6). This increase in the formation of dimer **456** at higher copper loadings ultimately begins to negatively affect the yield of the benzimidazole **455**. Entries 4, 5 & 6 use 25 mol%, 50 mol% and 100 mol% copper(I) acetate respectively. The observed formation of benzimidazole **455** decreases from 42% down to 20% as the loading of the copper salt increases. The formation of the benzimidazole **455** requires one intramolecular oxidation event. Dimer **456** forms as a result of a second oxidation event in an intermolecular reaction, requiring a second oxidative turnover of the copper catalyst with oxygen. It was therefore proposed that limiting the oxygen in the reaction would limit the formation of the dimeric impurity. Entry 7 shows the result of a reaction performed without stirring. The observed formation of benzimidazole **455** increased from 20% with stirring (Entry 6) to 59% without stirring. This observation came with a concurrent decrease in formation of dimer **456** (10% down from 25%). Oxygen can only enter the reaction by diffusion from the reaction headspace through the gas:liquid interface; a process which is facilitated by mixing and disturbance of the solvent surface. Not stirring the reaction therefore decreases the rate of dissolution of oxygen and limits the formation of the dimeric species which forms from a second oxidation event.

Entry	CuOAc	Temperature	Benzimidazole **455** / HPLC area%	Guanidine **454** / HPLC area%	Dimer **456** / HPLC area%
1	15 mol%	100 °C	41	14	10
2	15 mol%	80 °C	35	47	2
3	20 mol%	80 °C	37	40	4
4	25 mol%	80 °C	42	31	5
5	50 mol%	80 °C	33	25	13
6	100 mol%	80 °C	20	5	25
7[a]	100 mol%	80 °C	59	8	10

Table 6: Product variation with catalyst loading. [a] Reaction performed without stirring

The effect observed above in which limiting the oxygen in solution appears to result in a cleaner reaction was examined further. The reaction was next performed under an inert atmosphere taking precaution to exclude all oxygen using freeze-pump-thaw degassed NMP. Exposing aryl-guanidine **454** to 25 mol% copper(I) acetate and 1 equivalent of pivalic acid in NMP at 80 °C without stirring gave a 15% solution yield of the benzimidazole **455** and 20% consumption of the guanidine after 16 hours (Scheme 168). Interestingly, the characteristic green colour of the reaction mixture had disappeared after this reaction time, resulting in a pale-yellow solution (Left, Figure 26). This colour change is highly indicative of an oxidation-state change of the copper-catalyst. On opening the reaction to expose it to air, a green band formed at the gas:liquid interface which slowly spread through the reaction (Right, Figure 26). At this point, the reaction headspace was exposed to vacuum and placed under an inert atmosphere. Again, after leaving the reaction for 23 hours, the reaction turned pale-yellow. On repeating this process four times, a 53% solution yield was observed at 70% conversion of the guanidine. Importantly, formation of the dimeric benzimidazole was not formed under these reaction conditions, signifying that the production of this species is intimately linked with the oxygen dissolution in the reaction system.
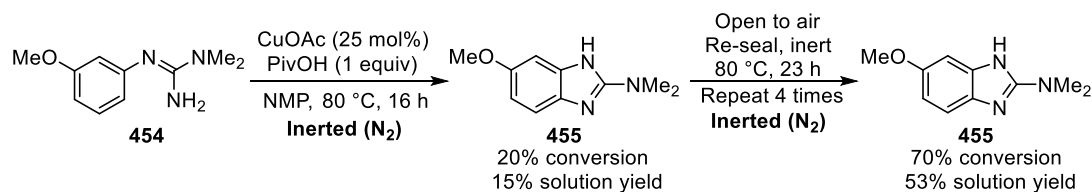
Scheme 168: Oxygen-starved reaction, reaction stalls
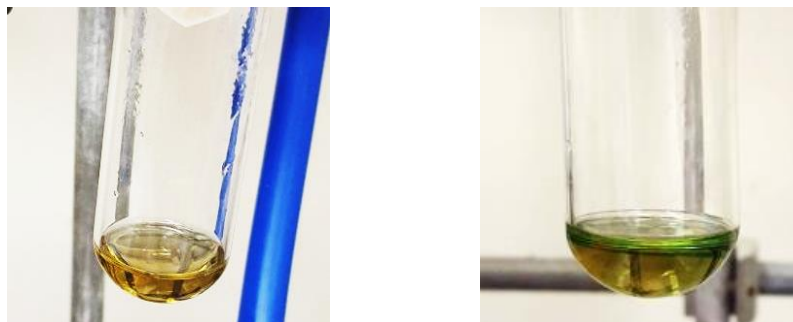
*Figure 27: Left, reaction after 16 hours at 80 °C, characteristic green colour disappeared.
Right, reaction exposed to air, initiating oxidation of catalyst*

In attempts to improve the yield of benzimidazole **455**, it was proposed that a stoichiometric loading of the copper salt would result in equally good, if not better yields of the benzimidazole. As such, guanidine **454** was treated with 1 equivalent of copper(I) acetate and pivalic acid in degassed NMP under an inert atmosphere. Benzimidazole **455** was observed to form in an 80% solution yield at 90% conversion of the guanidine. From this reaction, 64% of benzimidazole **455** was isolated by chromatography (Scheme 169).
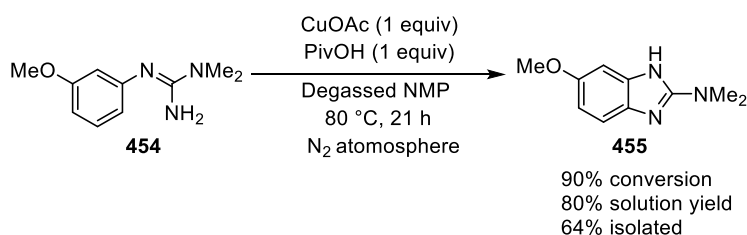
*Scheme 169: Cyclisation of guanidine **454** using 1 equivalent of copper*

At this point, guanidine **458** was synthesised to examine the effect of an electron deficient guanidine in the cyclisation reaction. Deprotonation of 3-trifluoromethylaniline (**457**) with sodium hydride in DMSO and addition of *N*,*N*-dimethyl cyanamide gave guanidine **458** in 65% yield (Scheme 170).
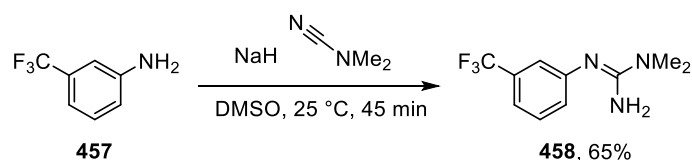
*Scheme 170: Synthesis of electron-deficient aryl guanidine **458***

When the electron-deficient trifluoromethyl guanidine **458** was exposed to the conditions developed above, only 17% benzimidazole **459** was isolated as a single regioisomer after 48 hours with very low conversion of guanidine **458** (Scheme 171). This observation is consistent with Buchwald's report who noted that insertion into an electron deficient C–H bond is slower than insertion into an electron-rich aromatic.[262]
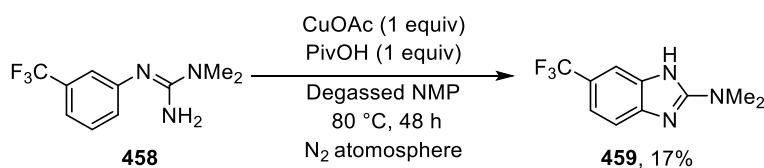
*Scheme 171: Poor conversion of guanidine **458***

This dependence on the electronics of the system was further probed by synthesising highly electron-deficient pyridyl guanidine **461**, through deprotonation of 4-aminopyridine (**460**) and treatment of the anion with *N,N*-dimethyl cyanamide to give pyridyl guanidine **461** in 10% yield (Scheme 172).
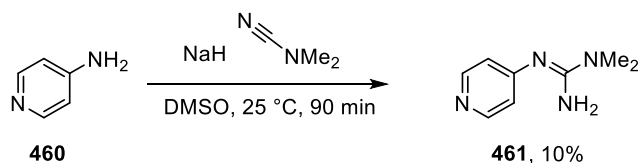
Scheme 172: Synthesis of an electron-deficient pyridine-derived guanidine

Under the same conditions, 4-pyridiyl guanidine **461** did not undergo any conversion to the imidazopyridine product **462** after one week, returning only starting material after this time (Scheme 173). This further suggested that the developed system using 1 equivalent of copper(I) acetate cannot undergo insertion into electron deficient C–H bonds. As such, the reaction did not offer a general procedure to access a range of 2-aminobenzimidazoles.
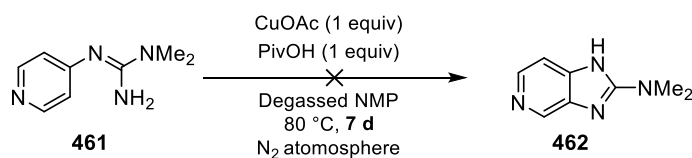
*Scheme 173: No cyclisation of guanidine **461***

Despite conditions being developed which allow for the synthesis of 2-aminobenzimidazole **455** in a 64% isolated from an aryl-guanidine *via* a C–H functionalisation, the developed conditions did not appear to be general.

7.2 Discrete variable determination

The goal of the project was to achieve a catalytic transformation of aryl-guanidines to give 2-aminobenzimidazoles using sub-stoichiometric copper with oxygen as a terminal oxidant; the conditions presented up until this point did not fulfil that goal. Anaerobic conditions were required to improve the selectivity for the formation of an aminobenzimidazole over that of over-oxidised dimeric species **456**. A fair assumption was that, under aerobic conditions, the formation of dimeric species such as **456** resulted from the coordination of two benzimidazole products to the copper-centre. It was postulated that a copper-salt with a coordinating ligand would disfavour the formation of dimeric species such as **456** by restricting coordination of multiple benzimidazole products to the catalyst. As such, a series of copper-salts with coordinating ligands were chosen for examination to determine whether a catalytic-system could be developed, using air/oxygen as a re-oxidant.

Three copper(II) sources with 2-ethylhexanoate, hexafluoroacetylacetonate and ethylacetoacetate as coordinating ligands and three copper(I) sources with 3-methylsalicylate, thiophene 2-carboxylate and copper(I) acetate (control) were examined (Figure 28). These salts have seen applications in a range of homogenous catalysis in which coordinating ligands were required to improve the desired reactivity.[263-268] Moreover, Bhanage showed how 1,3-dicarbonyl ligands display improved reactivity for similar transformations (Scheme 145, Section **5.3.3**) suggesting that variation of the ligand could prove to be beneficial.

Copper(II) 2-ethylhexanoate
Cu(EH)$_2$

Cu(II) hexafluoroacetylacetonate
Cu(acac-F$_6$)$_2$

Cu(II) ethylacetoacetate
Cu(EAA)$_2$

CuOAc

Cu(I) 3-methylsalicylate
CuMeSal
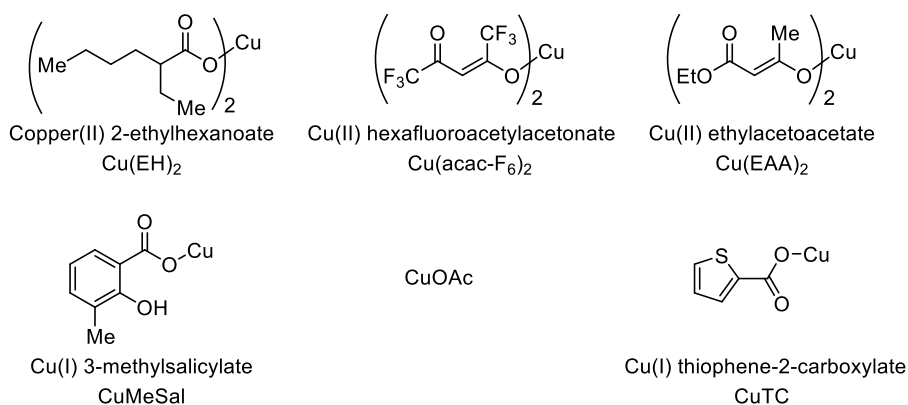
Cu(I) thiophene-2-carboxylate
CuTC

Figure 28: Examination of various ligand-stabilised copper-salts

Secondly, an examination of solvents with high flash points was performed. High flash point solvents are necessary from an industrial perspective when performing high temperature reactions in the presence of oxygen.[245] The flash point of a compound is defined as the temperature at which a species' vapour pressure reaches a level at which it will ignite when given a suitable source of ignition.[269] Any reaction which heats the solvent in an oxidising atmosphere above its flash point is susceptible to fire and/or explosion. Therefore, when designing a methodology which is targeted at an industrial environment the consideration of the solvent properties is vital. DMSO, NMP and sulfolane were considered obvious choices owing to their high flashpoints of 89 °C, 86 °C and 177 °C respectively.[270]

Table 7 and Table 8 display an abridged results section of a screen examining copper source, additive and solvent (see experimental, Section **9.4** for the full results of the screen containing 84 reactions). Copper salts were examined at 50 mol% loading, with 1 equivalent of an additive in a solvent at a concentration of 0.3 M. Reactions were placed under 6 bar pressure of air for 16 hours at 80 °C. The values presented in Table 7 and Table 8 correspond to the HPLC area percentages. Entry 1 in Table 7 displays the control reaction using copper(I) acetate with pivalic acid in NMP (see Entry 5 Table 6) which gave 33% benzimidazole with 25% guanidine remaining, forming dimeric species **456** at 13%. The most obvious trend from the screen was the large solvent effect. DMSO gave 19% product **455** with 45% guanidine **454** remaining (Entry 2). However, a noticeable increase in product **455** was observed when sulfolane was used, giving 45% benzimidazole **455** (Entry 3). Also interesting was the suppression of dimeric

species **456** down to 5% when sulfolane was used. Entries 3 and 4 shows how pivalic acid only offers a marginal increase in benzimidazole **455** yield compared with acetic acid (*cf.* 45% vs. 42% product respectively). The poor conversion obtained with sodium pivalate indicates that the presence of H^+ in the reaction is important to encourage high conversion of guanidine **454**, leaving 79% unreacted guanidine after 16 hours (Entry 5).
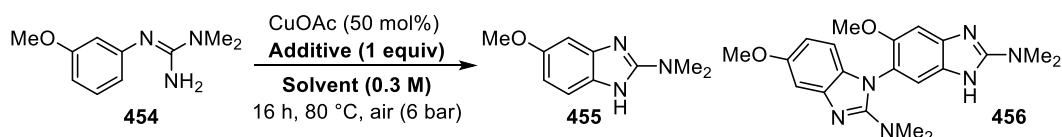
Entry	Additive	Solvent	Benzimidazole **455** / HPLC area%	Guanidine **454** / HPLC area%	Dimer **456** / HPLC area%
1	PivOH	NMP	33	25	13
2	PivOH	DMSO	19	45	6
3	PivOH	Sulfolane	45	30	5
4	AcOH	Sulfolane	42	33	6
5	PivONa	Sulfolane	9	79	1

Table 7: Examination of solvent and additive

Moving forward, the comparison between copper salts is presented using pivalic acid and sulfolane. Entry 1 Table 8 uses CuOAc with PivOH/sulfolane and gave 45% **455**, 30% starting material **454** and 5% dimeric species **456**. Changing to copper(II) 2-ethylhexanoate gave significantly poorer conversion of guanidine **454**, with 63% remaining after 16 hours, albeit with good formation of product at 30% with this poor conversion (Entry 2). This implies a high level of selectivity for the desired transformation using $Cu(EH)_2$. More importantly, the formation of dimeric product **456** was almost eliminated using $Cu(EH)_2$ (<1%) potentially due to the increased size of the coordinating ligand restricting coordination of multiple benzimidazole species to the copper centre. Electron-deficient 1,3-dicarbonyl ligated copper salt (hexafluoroacetylacetonate) also gave poor conversion of the guanidine with 68% remaining after 16 hours (Entry 4). Increasing the electron-density of the 1,3-dicarbonyl ligand, using ethylacetoacetate ligated copper salt gave a substantial increase in benzimidazole **455** to 54% with 25% guanidine remaining (Entry 4). The dimeric species was still produced at low enough quantities for the reaction to be synthetically useful (2%). Both 3-methyl salicylate and

thiophene 2-carboxylate delivered poor formation of benzimidazole (29% and 27% respectively, Entries 5 and 6).
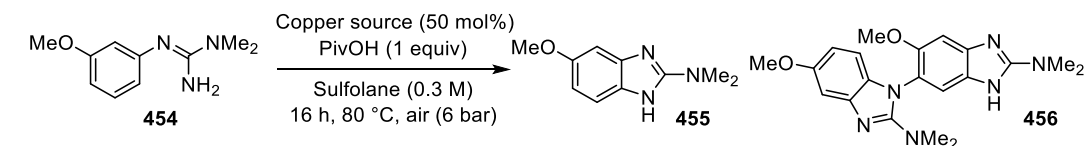
Entry	Copper source	Benzimidazole 455 / HPLC area%	Guanidine 454 / HPLC area%	Dimer 456 / HPLC area%
1	CuOAc	45	30	5
2	Cu(EH)$_2$	30	63	< 1
3	Cu(acac-F$_6$)$_2$	17	68	< 1
4	Cu(EAA)$_2$	54	25	2
5	CuMeSal	29	55	1
6	CuTC	27	34	7

Table 8: Variation of catalyst

7.3 Non-discrete variable determination

Cu(EAA)$_2$ enabled increased production of benzimidazole 455 and supressed the formation of dimeric species 456. Pivalic acid offered increased formation of product 455 and sulfolane further supressed the formation of 456 whilst delivering increased formation of 455. Moving forward, to determine an optimum set of non-discrete continuous variables, an in-depth statistical optimisation procedure was designed using Design of Experiments. Design of Experiments (DoE) is regularly used for the optimisation of reaction conditions and to gain an understanding of factors that influence the product distribution.[271,272]

Electron-deficient aryl-guanidine 458 was chosen, in order to optimise the system around a challenging substrate. This would enable the development of conditions which should be applicable to a range of substituted aryl-guanidines. A factorial design using four factors was performed. The factors selected were concentration (A), pivalic acid loading (B), catalyst loading (C) and temperature (D). The process design involved setting predetermined continuous variable windows for the discrete variables in which the experimental design took place. The windows for reaction concentration (A) were set between 0.1–0.4 M, pivalic acid (B) between 1–2 equivalents, copper loading (C) between 5–25 mol% and temperature (D)

between 100–130 °C. The reactions were performed for 4 hours before sampling for HPLC

analysis and the results of the DoE are presented in Table 9.
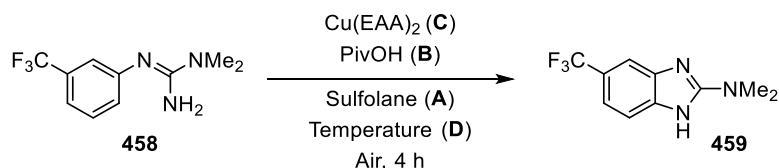
Entry	Reaction Type	Concn. (M) (**A**)	PivOH (equiv) (**B**)	Copper (mol%) (**C**)	Temp. (°C) (**D**)	Product **459*** (%)
1	Factorial	0.1	1	5	100	9
2	Factorial	0.1	1	25	130	74
3	Factorial	0.1	2	5	130	23
4	Factorial	0.4	2	25	130	74
5	Factorial	0.1	2	25	100	60
6	Centre Point	0.25	1.5	15	115	74
7	Factorial	0.4	2	5	100	23
8	Factorial	0.4	1	25	100	67
9	Centre Point	0.25	1.5	15	115	75
10	Factorial	0.4	1	5	130	26

*Table 9: DoE experimental design at 4 hours. *HPLC Area%*

The above data was inputted into the DoE software (Design-Expert 10®, DX10) which

generated a statistically significant model for the formation of product in the reaction at 4 hours

(R^2 = 0.9735, Adj R^2 = 0.9647). From this model was generated a half-normal plot which is

displayed in Figure 29. A half-normal plot is a graphical representation of the most important

factors in eliciting a desired response; in this case maximising the formation of product. The

factors which are further to the right-hand side of the plot are the factors which elicit the largest

response of the desired outcome (product yield). The loading of copper was by far the most

important factor at increasing the formation of benzimidazole **459**, second most important was

the reaction temperature. Concentration has less of an affect and pivalic acid equivalents has

a very small, if not negligible impact on increasing the formation of product.
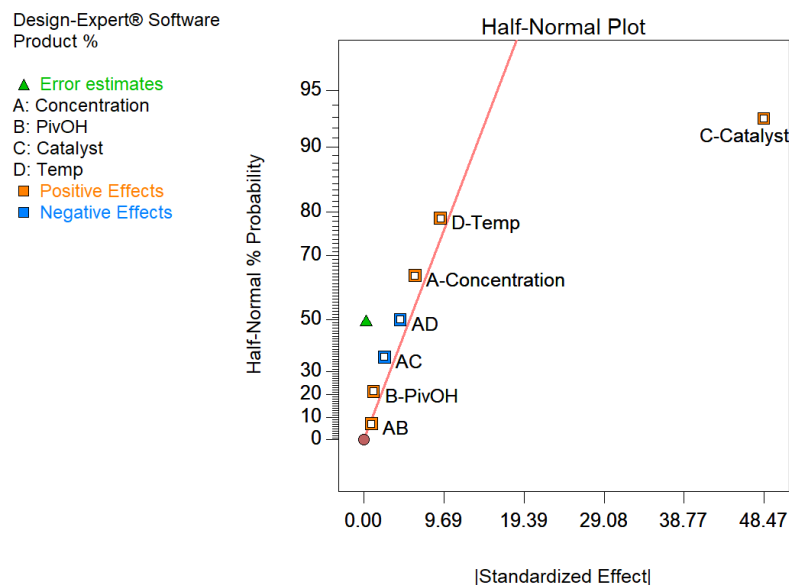
Figure 29: Half-normal plot of DoE analysis

In attempts to further drive the reaction, the DoE was repeated for 21 hours, of which the results are presented in Table 10. A model from this dataset could not be obtained without significant curvature, and as such a valid statistical model could not be generated. However, what was interesting to observe was that the reactions which had the largest product formation at 4 hours (Entries 2, 4, 6 and 9 gave 74%, 74%, 74% and 75% respectively in Table 9), at 21 hours the product had decreased to 52%, 32%, 64% and 66% respectively (Entries 2, 4, 6 and 9 Table 10). These entries all use both high catalyst loadings and high temperatures. This indicates that under these conditions the product is unstable. Entry 8 uses 25 mol% $Cu(EAA)_2$ at 100 °C and at 21 hours this reaction returned 80% indicating that under these conditions the product is more stable and affords a better yield.
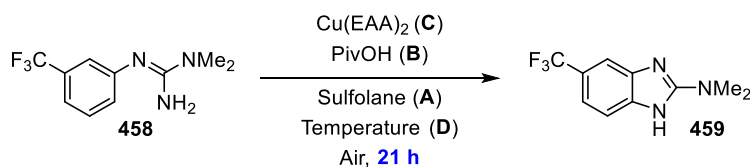
| Entry	Reaction Type	Concn. (M) (**A**)	PivOH (equiv) (**B**)	Copper (mol%) (**C**)	Temp. (°C) (**D**)	Product **459*** (%)
1	Factorial	0.1	1	5	100	12
2	Factorial	0.1	1	25	130	52
3	Factorial	0.1	2	5	130	22
4	Factorial	0.4	2	25	130	32
5	Factorial	0.1	2	25	100	76
6	Centre Point	0.25	1.5	15	115	64
7	Factorial	0.4	2	5	100	54
8	Factorial	0.4	1	25	100	80
9	Centre Point	0.25	1.5	15	115	66
10	Factorial	0.4	1	5	130	21

Table 10: DoE experimental design at 21 hours.
*HPLC Area%

7.4 Validation of DoE and formation of 2-aminobenzimidazole 459

With this observation in mind, Entry 8 Table 10 was scaled up. Using 25 mol% Cu(EAA)$_2$, 1 equivalent of pivalic acid, in sulfolane, 54% of 2-aminobenzimidazole **459** was isolated after 24 hours (Scheme 174). This was a significant improvement on the 17% isolated yield with stoichiometric copper(I) acetate in NMP as described in Scheme 171 Section **7.1**.
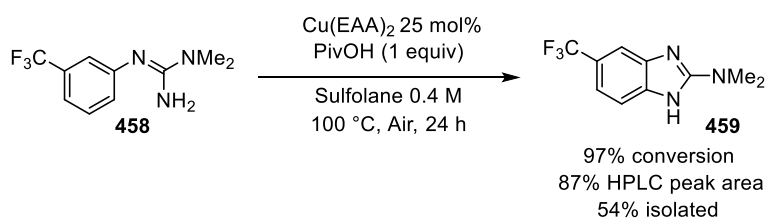

Scheme 174: Validation of DoE results

7.5 Examination of the scope of the reaction

7.5.1 Synthesis of *N,N*-dimethyl aryl-guanidines

To examine the generality of the developed copper-catalysed intramolecular C–H functionalisation to form 2-aminobenzimidazoles, a selection of substituted anilines were

deprotonated with sodium hydride in DMSO and reacted with *N,N*-dimethyl cyanamide. The resultant *N,N*-dimethyl arylguanidines, **463–471** are displayed in Scheme 175. Guanidines derived from electron-deficient and electron-rich anilines with various functional groups were synthesised.
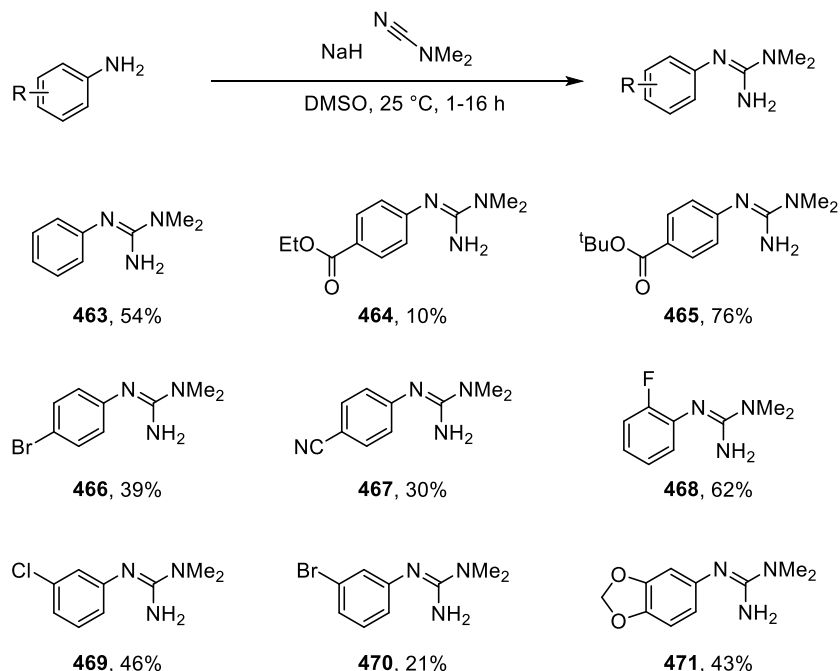
Scheme 175: Synthesis of a variety of aryl guandines

7.5.2 Synthesis of 2-dimethylamino benzimidazoles

Initially, the 4-substituted aryl-guanidines were exposed to the reaction conditions. Benzimidazoles **472–476** were isolated in 65%, 63%, 53%, 58% and 40% yield respectively (Scheme 176). The tolerance of esters, halogens and nitriles indicate that this method could be used to access species which can undergo subsequent synthetic transformations common with the pharmaceutical and agrochemical industry. Moreover, the formation of brominated benzimidazole **475** shows that the developed conditions are selective over Ullmann-type chemistry which involves copper insertion into the carbon–bromine bond.[273] No debrominated starting material or benzimidazole was observed under the reaction conditions. *Ortho*-fluoro guanidine **468** gave fluorinated benzimidazole **477** in 46% yield.
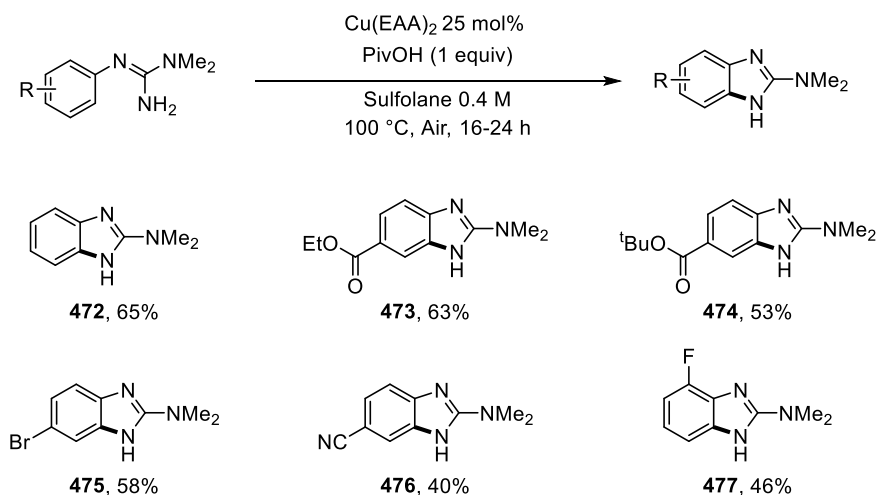
Scheme 176: Synthesis of 2-aminobenzimidazoles under optimised conditions derived from para- and ortho-substituted anilines

Meta-substituted aryl-guanidines **469–471** were then exposed to the reaction conditions (Scheme 177). In this example the system has an option as to which C–H bond is functionalised, and could result in the formation of regioisomeric benzimidazole products. Reaction of H_a (as shown in Scheme 177) gives rise to products where the less hindered C–H bond has been functionalised (**459**, **475**, **479** and **481**). Whereas, functionalisation of H_b gives rise to products where the more hindered C–H bond has been functionalised (**478**, **480** and **482**). With trifluoromethyl guanidine **458**, only one product was observed by HPLC and ^{1}H NMR: no product corresponding to functionalisation of the more-hindered C–H bond was observed. This suggests that the "H_b" proton in this substrate is too sterically hindered owing to the large neighbouring CF_3 group. 3-bromoguanidine substrate **470** however, underwent cyclisation to give a 4:1 mixture of regioisomeric benzimidazoles by HPLC analysis in which the products **475** and **478** were isolated in 65% and 25% yield respectively. 3-chloroguanidine substrate **469** underwent cyclisation to give benzimidazoles **479** and **480** in a 3:1 ratio by HPLC analysis. The decrease in differentiation in this series can likely be attributed to the decrease in size in the order CF_3 > Br > Cl. The smaller group presents less of a steric block to the functionalisation of H_b.
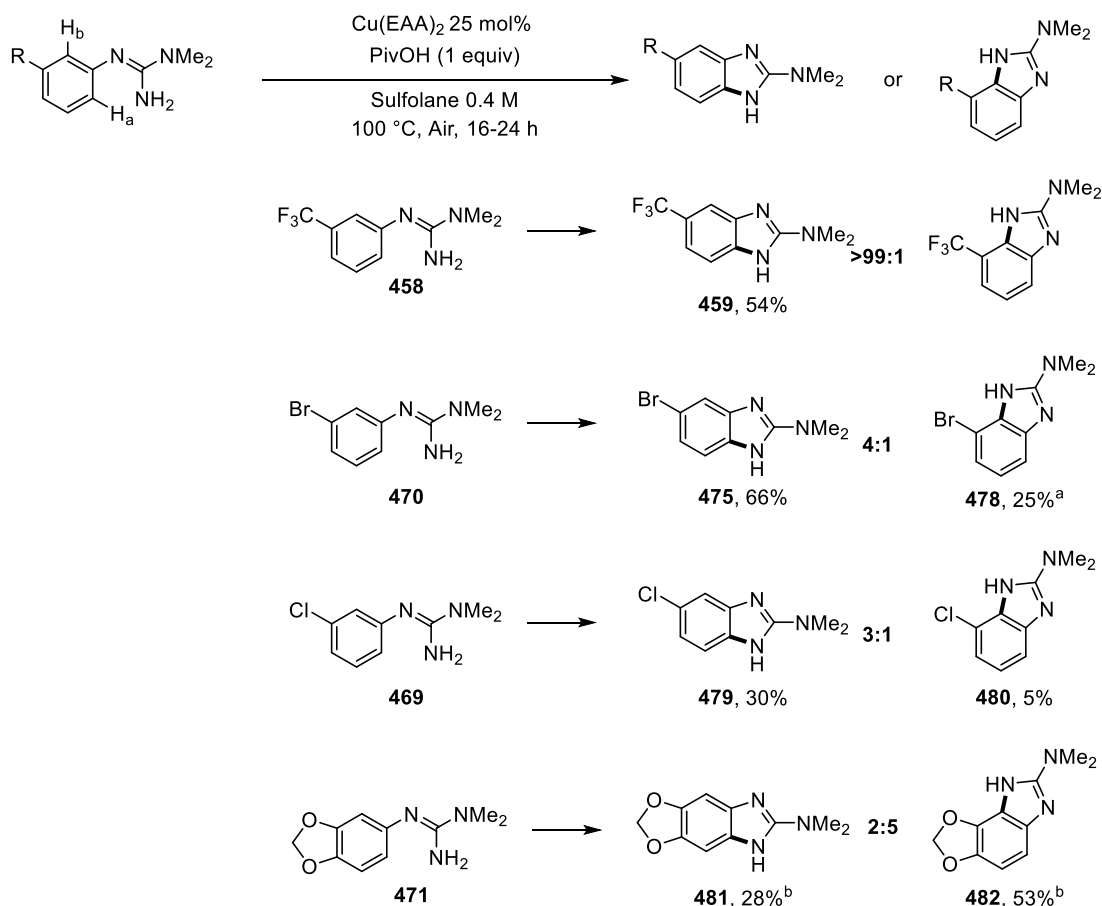
Scheme 177: Regioisomeric benzimidazole products derived from meta-substituted anilines.
[a]product isolated in 78% purity by HPLC analysis containing an unknown impurity which could not be separated.
[b]Reaction performed at 90 °C.

Interestingly, however, with benzodioxole guanidine **471**, a switch in regioselectivity was observed. The observed ratio was 5:2 in favour of H_b functionalisation, yielding benzimidazoles **481** and **482** in 28% and 53% (Scheme 177). A literature search for this effect returned a report by the Nagasawa group from 2009.[274] The paper highlighted how *N*-aryl amides undergo an *ortho* C–H functionalisation to form benzoxazoles using a copper-catalyst, in which a *meta*-directing group on the substrate facilitated functionalisation of the more hindered proton (Scheme 178). It is feasible that the pendant dioxole can act as a directing group (**483**), facilitating insertion into the more hindered proton and thus providing an explanation for the switch in selectivity to give **482** as the major product.
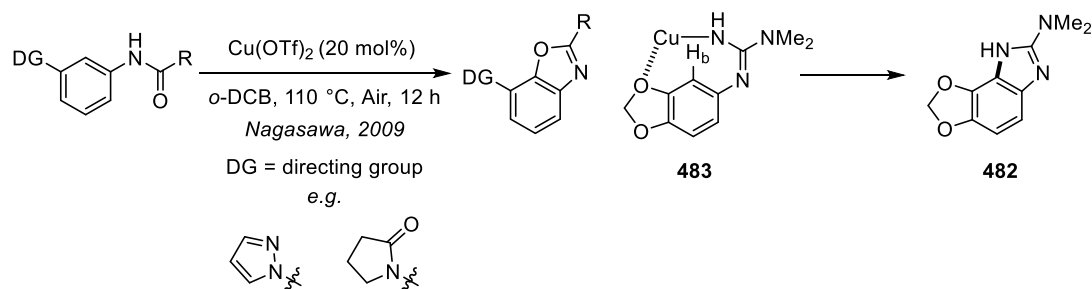
Scheme 178: Directing-group facilitated C–H functionalisation of more hindered protons

At this point, to explore the generality of the 2-amino portion of the product, simple commercial cyanamides *N,N*-diethylcyanamide, piperidine-1-carbonitrile and morpholine-4-carbonitrile were reacted with anilines to give aryl-guanidines **484**–**488** in 35%, 18%, 21%, 34% and 70% yield respectively (Scheme 179).
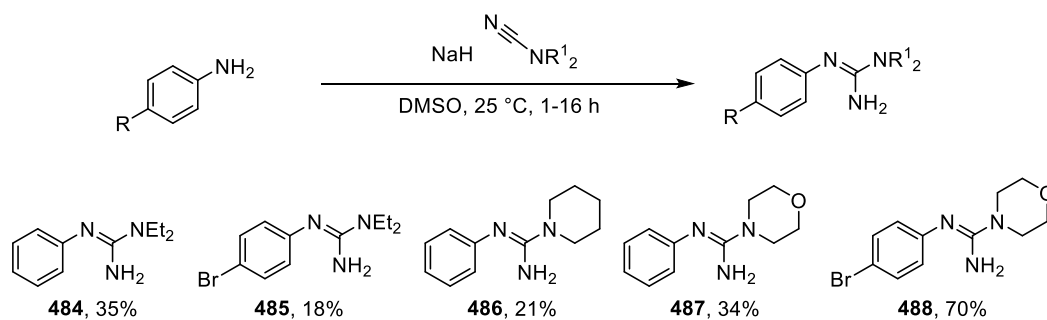
Scheme 179: Synthesis of aryl-guanidines from different cyanamides

Exposure of *N,N*-disubstituted guanidines **484**–**488** to the optimised conditions ultimately returned 2-aminobenzimidazoles **489**–**493** in 46%, 74%, 41%, 52% and 59% (Scheme 180). This short examination of the 2-amino portion suggests that *N,N*-dialkyl arylguanidines will be effective substrates for the presented transformation.
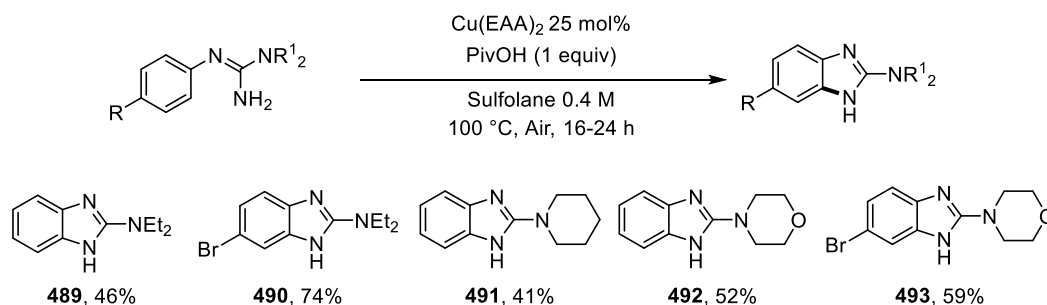
Scheme 180: Synthesis of 2-aminobenzimidazoles from guanidines 489–493

7.5.3 C–H *vs.* C–Hal functionalisation

The examples provided in Section **5.4.1** show how aryl-guanidines with *ortho*-bromides undergo C–Br functionalisation to form 2-aminobenzimidazoles with a copper source. To examine whether the developed procedure offers selectivity for C–H functionalisation over C–halo functionalisation, *ortho*-halo substituted aryl-guanidines **494–496** were prepared in 43%, 45% and 36% yield.
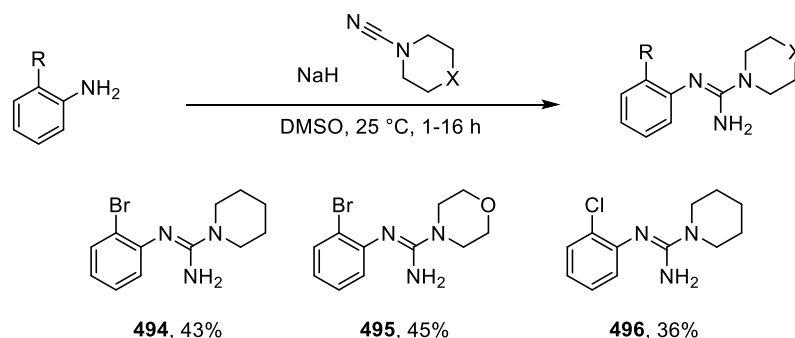
Scheme 181: Synthesis of ortho-substituted aryl guanidines

Exposure of *ortho*-brominated guanidines **494** and **495** to the reaction conditions showed no chemoselectivity for C–H functionalisation over C–Br functionalisation. The only products observed were debrominated benzimidazoles **491** and **492** in 74% and 71% yield (Scheme 182). With *meta-* and *para*-substituted bromo-guanidines (Section **7.5.2**), no debromination was observed. This suggests that coordination of the guanidine to the copper facilitates the oxidative addition into the C–Br bond through the formation of intermediates such as **497** and **498**.

491, 74%   **492**, 71%
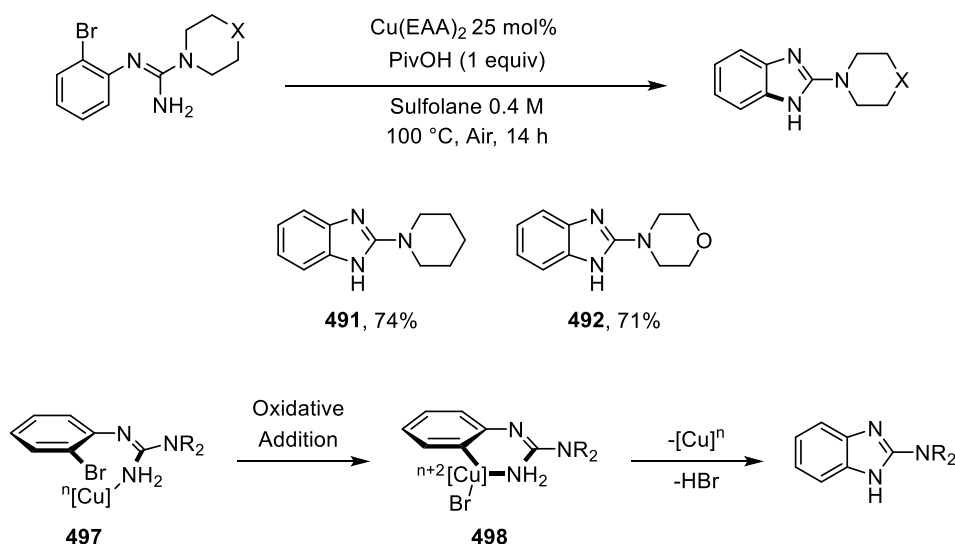
Scheme 182: Selectivity for C–Br functionalisation over C–H functionalisation

When the reaction was repeated with *ortho*-chlorine substituted guanidine **498** however, the major product observed in the reaction mixture was chlorinated benzimidazole **499**. The chlorinated and dechlorinated product were observed in a 6:1 ratio by HPLC analysis and chlorinated benzimidazole **499** was isolated in 51% yield. This result suggests that C–H insertion by the copper catalyst is favoured over C–Cl insertion by retention of the chloride in the product. It is worth noting that **491** could form from **499** by protodehalogenation, however this was not investigated in detail.
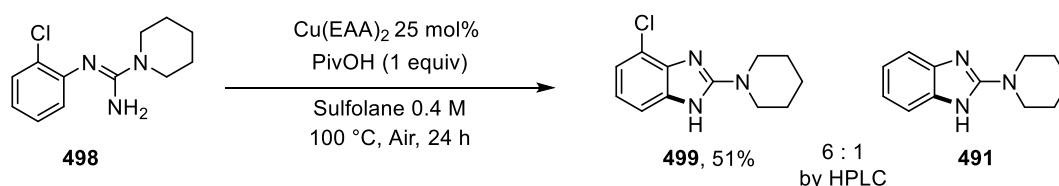
Scheme 183: Reverse selectivity for C–H functionalisation over C–Cl functionalisation

7.6 Mechanistic studies

7.6.1 Kinetic isotope effect

In order to gain an understanding of the mechanistic events which lead to the formation of the benzimidazole, an experiment was devised in which a kinetic isotope effect (KIE) could be measured. In general, there are three main established experimental designs for the calculation of a KIE. The KIE derived from type A (Scheme 184) is derived from two independent reactions in which the rate of consumption of a protonated and deuterated substrate (such as **463** and **500**) are independently monitored to give products **472** and **501** (Scheme 184). The subsequent rates are then plotted against each other and the KIE is derived from the ratio of one to the other. This experimental design is the only one that provides conclusive evidence that C–H bond-cleavage is in the RDS.[275]

A) KIE derived from two parallel reactions

$rate_1 = k_1X$

Cu(EAA)$_2$ 25 mol%
PivOH (1 equiv)

Sulfolane 0.4 M
100 °C, Air, 24 h

$rate_2 = k_2X$

KIE = rate$_1$/rate$_2$
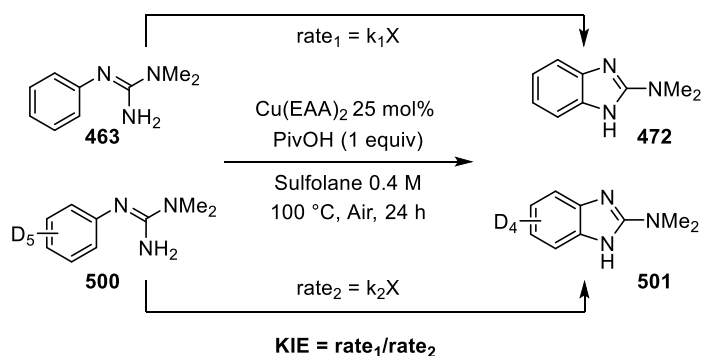
Scheme 184: Kinetic isotope effect from parallel reactions

Type B involves an intermolecular competition example of a reaction containing both a protonated and a deuterated substrate (such as **463** and **500**) in the same reaction vessel, as opposed to type A in which the substrates are in separate vessels. The KIE is then derived from obtaining the ratio of the C–H derived product to the C–D derived product at 50% conversion (Scheme 185).

B) KIE derived from an intermolecular competition
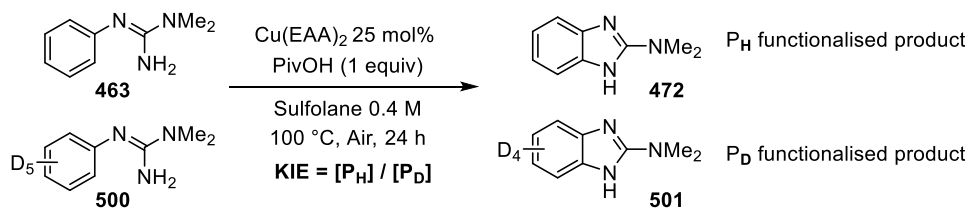
Scheme 185: Kinetic isotope effect from an intermolecular competition reaction

The final KIE experiment (type C) can be derived from an intramolecular reaction of a substrate containing a choice of either a C–H bond or a C–D bond (such as **502**). The KIE is then derived from the relative ratio of protonated (**472**) and deuterated product (**503**) (Scheme 186).

C) KIE derived from an intramolecular competition
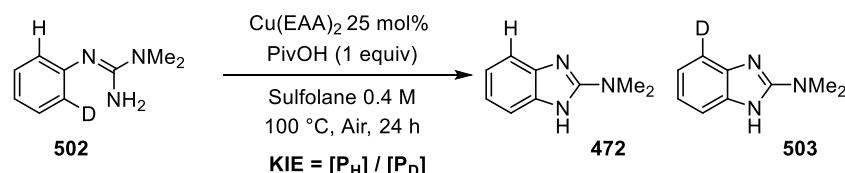
Scheme 186: Kinetic isotope effect from an intramolecular competition reaction

Considering the above experimental designs, the only method which allows for determination as to whether C–H cleavage is rate determining is type A.[275] As such, this was the experimental design chosen. Synthesis of the D_5 deuterated guanidine was performed in an analogous manner to the previous guanidines. D_5-aniline (**504**) was deprotonated with sodium hydride in DMSO and the resultant anion was reacted with *N,N*-dimethyl cyanamide to give deuterated guanidine **500** in 25% yield (Scheme 186).
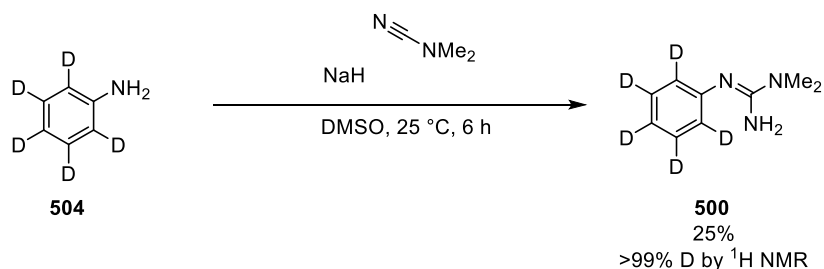
Scheme 187: Synthesis of deuterated guanidine 500

170

From here, guanidine **463** and the deuterated variant **500** were exposed to the reaction conditions in separate reaction flasks. The reactions were monitored by HPLC analysis and the conversion was quantitatively monitored by comparison to an internal standard (biphenyl).

The plots in Figure 30 correspond to the percentage of guanidine remaining over time and the corresponding log-plot – Log(aryl-guanidine) *vs*. time is shown in Figure 31. The blue and grey data-points signify consumption of H_5 guanidine **463** and the yellow and orange data-points signify consumption of D_5 guanidine **500**, *i.e* – each reaction was performed in duplicate. The close overlay of these repeats indicate that the results are reliable. Firstly, from a non-quantitative perspective there is an inherent different in rate of consumption of the guanidines. The H_5 guanidine **463** is consumed at a faster rate than the D_5 guanidine **500**.
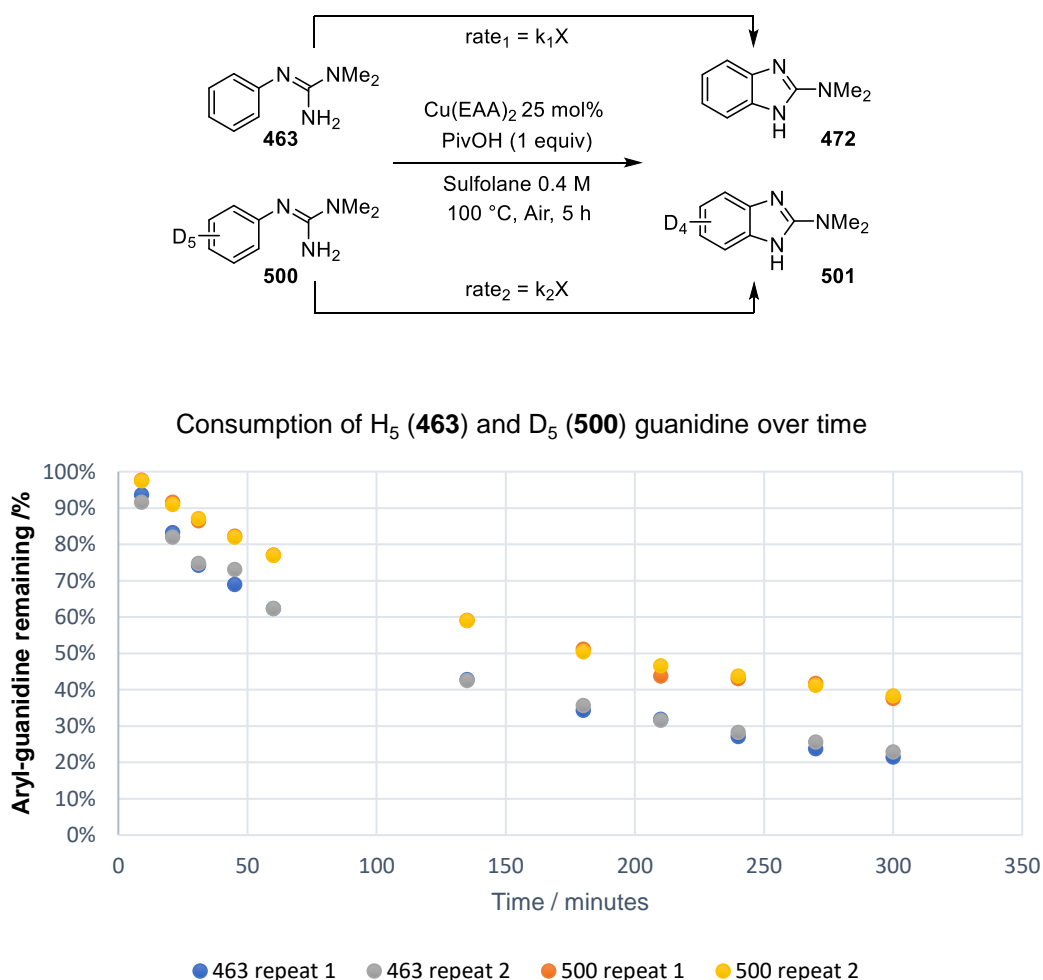
Figure 30: Rate of consumption of protonated and deuterated aryl guanidines

From here, plotting the average of the two repeats as $\log_{10}$ of (% guanidine remaining) against time gives Figure 31. The calculated straight-line equations for the H_5 substrate **463** results in a gradient of -0.0021 min^{-1} and the gradient for the D_5 substrate **500** is -0.0014 min^{-1}. The ratio of H_5/D_5 gives a value of 1.5 which can be interpreted as the KIE value. Interpretation of this value of 1.5 can have mechanistic implications.

Log-plot. Consumption of H5 and D5 guanidine over time
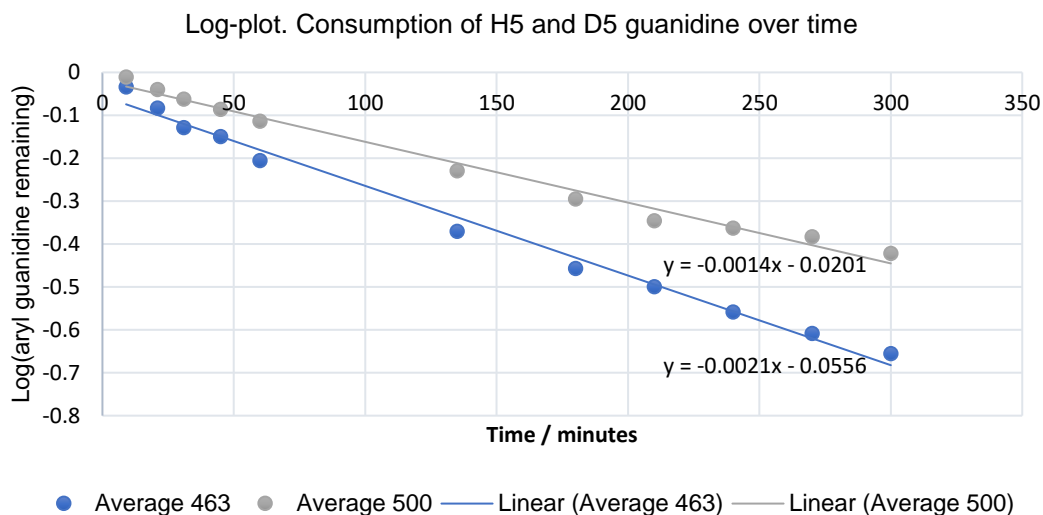
Figure 31: Log-plot of aryl guanidine consumption

The magnitude of a KIE is intimately linked to the changes in the vibrational modes of the C−H or C−D bond as the reactants approach the transition state for the transformation. C−D bonds are stronger than C−H bonds, i.e. the zero-point energy of a C−D bond is lower than that of a C−H bond. This is simplistically explained by considering a chemical bond to be a harmonic oscillator, mathematically exemplified by Hooke's law (Equation 1) in which ν is the vibrational stretching frequency of a bond (C−X, X = H or D in this example).[276] The stretching vibration of a bond is related to k (the bond force constant) and m_r (the reduced mass of the stretching bond). As m_r increases, *i.e.* the difference in mass between m_1 and m_2 decrease, as does the stretching frequency (ν). This therefore results in more energy being required to elongate the C−D bond to the dissociation limit; the origin in the change of rate between C−H cleavage and C−D cleavage.[277]

$$v = \frac{1}{2\pi}\sqrt{\frac{k}{m_r}} \quad \text{where } m_r = \frac{m_1 m_2}{m_1 + m_2}$$

Equation 1: Hooke's law

A KIE value of 1 indicates that there is no change in transition-state energy in the RDS for a substrate baring either a C–H or C–D bond – *i.e.* the cleavage of the bond is not involved in the RDS. A value > 1 indicates that the C–H or C–D bond undergoes a change during the RDS. Values of 1 < KIE < 1.4 can also be considered as secondary effects, with a KIE of 1.4 being considered the maximum theoretical value for a secondary kinetic isotope effect.[277]

Secondary KIEs can have several mechanistic origins. Generally, these are only observed when the isotopically labelled bond is not broken in the RDS but experiences a change in the transition state *i.e.* a change in hybridisation state of the carbon the isotopically labelled species is attached to.[277] Primary KIEs (> 1.4) are observed when cleavage of the isotopically labelled bond is directly involved in the rate determining step.

On considering the magnitude of the KIE value observed here, the measured value of 1.5 lies on the boundary between "primary" and "secondary" kinetic effects. Typically, experimentally derived values of normal secondary KIEs are usually around 1.1–1.2.[277] Therefore, it would be surprising if the calculated value lies exactly on the theoretical maximum of a secondary effect. As such, the value of 1.5 can be interpreted as being a primary, albeit very weak, KIE value.

Three distinct mechanistic pathways for the intramolecular copper-catalysed C–H functionalisation to form benzimidazoles have been proposed, the first of which is presented in Scheme 188.[262] This pathway invokes an electrophilic aromatic substitution-type mechanism, in effect considering this nitrogen to be electrophilic (**505**). The copper species then leaves in an [n−2] reduced form which is then re-oxidised by air to re-engage in the catalytic cycle. The C–H bond is then cleaved in a deprotonation event to give the benzimidazole product, which would be assumed to be fast. A KIE value for this experiment would not give a primary KIE, as the C–H bond is cleaved in a deprotonation event, which

would likely be fast. However, a secondary effect could be observed in the RDS if the electrophilic aromatic substitution is rate-limiting. Intermediate **506** has changed hybridisation state from sp^2 to sp^3. This results in a build-up of positive charge on the neighbouring carbon atom. The hyperconjugative-stabilisation that the carbocation would receive from the isotopically labelled proton could give rise to a normal secondary KIE.[277] However, it is also known that a hybridisation change from sp^2 to sp^3 often give rises to an inverse KIE value (*i.e.* < 1).[277] The formation of this intermediate therefore has a combination of hyperconjugative effects and rehybridisation effects which suggests either a normal *or* an inverse KIE should be observed. If the measured value of 1.5 is indeed a secondary KIE, the above contradictory factors make it challenging to invoke or exclude this mechanism based on the evidence. If, however, the observed value of 1.5 is indeed a small, primary KIE, this suggests that cleavage of the C−H bond is rate-limiting and therefore Scheme 188 is not the active mechanism in this chemistry.
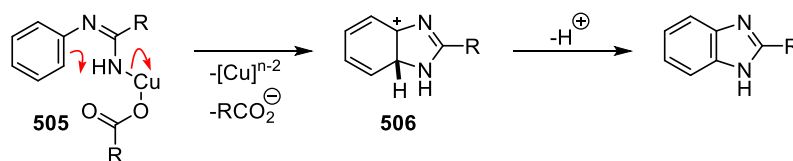
Scheme 188: A mechanistic proposal from Buchwald. Akin to an electrophilic source of nitrogen

A second mechanism proposed in Buchwald's 2008 publication suggested that the arene could attack the copper-centre (**507**) to form cationic species **508**, where the C–H bond is again broken in a deprotonation event to give a 6-membered organocopper intermediate **509** (Scheme 189). The benzimidazole is formed after reductive elimination of the copper species to form a Cu^{n-2} species, which could be reoxidised by air to engage in the catalytic cycle. The factors mentioned in the previous paragraph, including change in hybridisation state and hyperconjugation are also applicable here. The results of a KIE experiment would be hard to distinguish between these two mechanistic pathways. However, the observed KIE of 1.5, if a small primary KIE, would also suggest that this is also not the active mechanism.
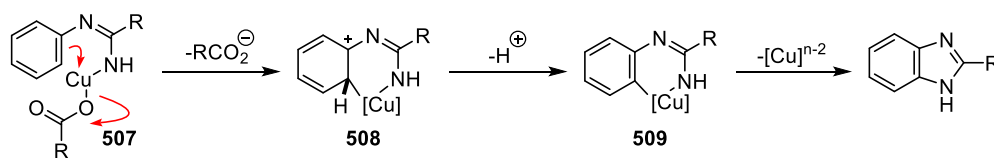
Scheme 189: Formation of an organo-copper cycle

The formation of a copper-nitrenoid intermediate (**510**) has been ruled out computationally by Fu *et al.*[278] The formation of a nitrene (R = Ph, Scheme 190) from a copper-bound substrate was calculated to be highly endergonic (+35.2 kcal mol^{-1}) and so this mechanism is suggested as being highly unfavourable.

510
Copper-nitrenoid
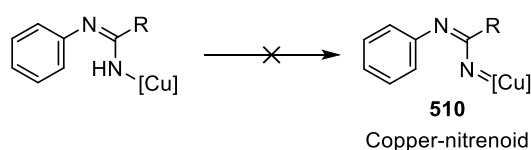
Scheme 190: Copper-nitrenoid

The observed evidence of a small primary KIE does not correlate with any of the previously proposed mechanisms. The experimentally measured KIE value of 1.5 suggests that this value is unlikely to be a secondary effect, owing to the maximum theoretical value of a secondary KIE being 1.4. Most experimentally measured KIEs are between 1.1–1.2.[277] As such, the measured value of 1.5 suggests that cleavage of the C–H bond occurs during the rate-determining step of the reaction.

The lack of experimental and literature evidence to support any of the above mechanisms for the C–H functionalisation prompted a search for a different mechanism to fulfil the experimental observations. Concerted-metalation-deprotonation (CMD) was a mechanistic artefact first discovered by Winstein and Traylor in 1955.[279] The application of this reactivity for the direct conversion of C–H bonds to C–X (X = N, C) bonds was studied and exemplified extensively by Fagnou.[280] The mechanism involves the metalation event of an arene occurring in a concerted manner as the C–H bond is broken (Scheme 191). Often the catalysts utilised are heavy metals (palladium, rhodium) in combination with a carboxylate ligand.[281-283]
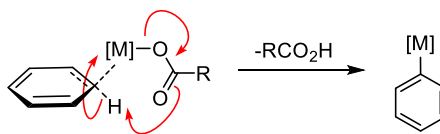
Scheme 191: General scheme for a CMD

The mechanism of palladium-catalysed *ortho* C–H insertions by a CMD mechanism was studied extensively by Ryabov in 1965. Reaction intermediates were observed by NMR spectroscopy and in combination with a Hammett plot, a valid reaction pathway was proposed (Scheme 192).[284] The C–H insertion of palladium(II) acetate into *N,N*-dimethylbenzylamine was shown to be rate-limiting by the presence of a primary kinetic isotope effect. Furthermore, the carboxylate species plays a key role in the C–H insertion event by 1) mediating the puckering of the C–H bond to the reactive configuration, and 2) facilitating a concerted deprotonation (exemplified in **511**). Unfortunately, in the context of this work, no intermediates have been observed or characterised by NMR spectroscopy due to extensive signal broadening of multiplets by the presence of a paramagnetic copper species. As such, no direct evidence of a copper-arene has been observed.
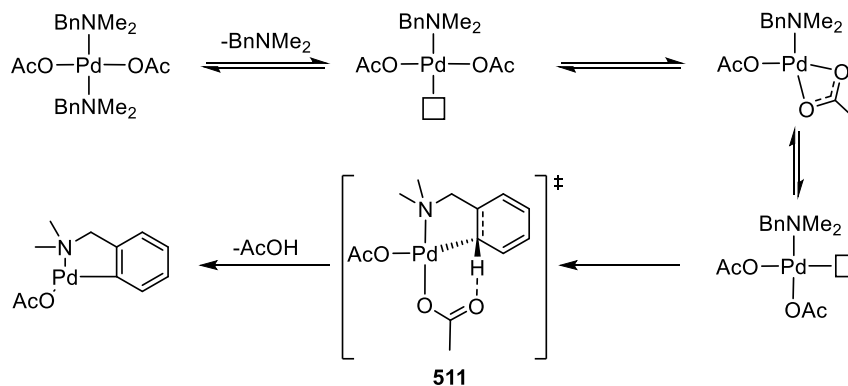
Scheme 192: CMD functionalisation of a benzylamine derivative by palladium

There are several similarities between the conditions developed in this thesis – namely the use of a transition metal catalyst and a carboxylic acid as an additive/ligand – and the conditions for concerted-metalation-deprotonations to be invoked. Moreover, the observed primary kinetic isotope effect suggests that cleavage of the C–H bond is rate-limiting. Scheme 193 provides a depiction of a CMD mechanism within the presented transformation where a

proposed copper-guanidine-carboxylate (**512**) mediates the C–H insertion event. Within similar transformations presented within the literature, there has been very little mechanistic explanation as to what role the carboxylic acid plays. To examine the effect of changing the carboxylate group, a series of experiments were designed to examine the role that the carboxylic acid played in the transformation.
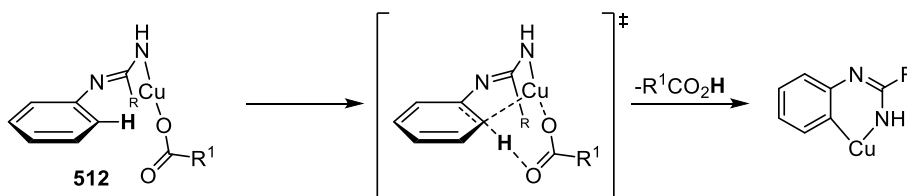
Scheme 193: Hypothesised CMD mechanism within the presented transformation

7.6.2 Examination of the reaction additive

Examining the additive (pivalic acid) and applying systematic variations could shed light on the role played by this species. Table 11 describes a series of additives which were examined to gain an empirical understanding of the importance of this species. Control reactions with no additive, pivalic acid and ethyl acetoacetate highlight the importance of pivalic acid within the transformation (Entries 1–3). Without pivalic acid the desired reaction pathway almost entirely shuts down. Acetic acid remains effective, whilst delivering an inferior yield to pivalic acid (41%, Entry 4). More acidic additives such as trifluoroacetic acid entirely inhibit the desired reaction (Entry 5). Sulfonic acids (methane sulfonic, *p*-toluene sulfonic acid, Entries 6 and 7) also result in no formation of product, and in fact the guanidine was fully recovered from these reactions, likely indicating little interaction of the substrate with the catalyst. Phosphonic acids also result in no formation of product (Entry 8) and the reaction in this case contained a large quantity of a precipitate, indicating either a copper-phosphonate complex or a guanidine-phosphonate salt was insoluble. Oxalic acid, a species known to be a bidentate ligand for copper through both carboxylate moieties[285] also resulted in no formation of the desired product (Entry 9). This effect could be due to the high acidity of oxalic acid giving a comparable result to trifluoroacetic acid (TFA pKa = 0.25, Oxalic acid pKa_1 = 1.25, pKa_2 = 4.10).[122,286]

Entry	Additive	Time / hours	**459** /%[a]
1	None	24	12
2	Pivalic acid	24	54
3	Ethyl acetoacetate	16	3
4	Acetic acid	24	41
5	Trifluoroacetic acid	16	< 1
6	MsOH	16	0[b]
7	TsOH	16	0[b]
8	Phenylphosphonic acid	16	0[c]
9	Oxalic acid	16	0

Table 11: Variation of the acidic additive. [a]Solution yield using 4,4'-di-tert-butyl 1,1'-biphenyl
[b]No conversion of starting material
[c]Precipitate in reaction mixture

It was proposed that bidentate carboxylic acids would result in the carboxylate carbonyl group being too far away from the C–H bond which is being functionalised (**513**). As such, the CMD mechanism would be less feasible owing to the increased distance between the C–H bond and the carbonyl group coordinated to the reactive copper species (Scheme 194).
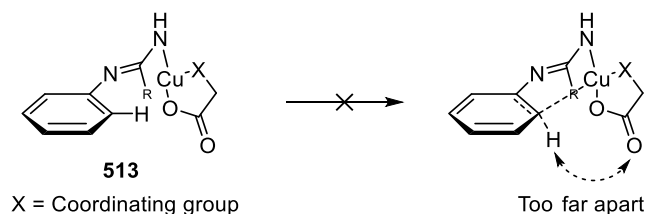
Scheme 194: Bidentate acids should be ineffective at CMD

To probe the effect of having a bidentate carboxylic acid, using carboxylic acids which would have the potential to form the 5 membered organocopper cycle were examined, as depicted in Scheme 194. Oxalic acid, 2-hydroxypropanoic acid (lactic acid), alanine and 2-aminoisobutyric acid all had very poor efficiencies in the desired transformation (Entries 1−4 Table 12). These results initially confirm the above hypothesis, however on considering the pKas of the additives (lactic acid pKa = 3.69, alanine pKa = 2.55, 2-aminoisobutyric acid

pKa = 2.48 respectively)[287,288,289] it is difficult to separate the pKa effect from the bidentate

nature of the additive onto a copper centre.

Entry	Additive	459 /%[a]
1	oxalic acid	0
2	2-hydroxypropanoic acid	9
3	alanine	0
4	2-aminoisobutyric acid	0

Table 12: Examination of acids with the potential to be a bidentate ligand
[a]Solution yield using 4,4'-di-tert-butyl 1,1'-biphenyl

As discussed above, a key consideration to remain aware of is the acid-base equilibrium

obtained when an acid and the substrate are mixed together. Guanidines are highly basic

compounds, with the pKaH of guanidine being 13.7.[290] Compared with triethylamine, in which

the pKaH is 10.7,[291] this shows that that guanidines are ~10^3 times more basic than simple

tertiary amines (Figure 32).
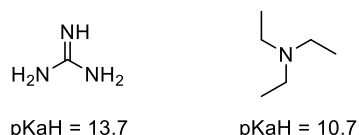
Figure 32: pKaH comparison of a guanidine with a tertiary amine

Therefore, the reaction between a guanidine substrate (**463**) and a carboxylic acid results in

an acid-base equilibrium, as depicted in Scheme 195. Weaker acids therefore shift the position

of equilibrium marginally towards the left-hand side of the arrow, meaning that there is more

unprotonated guanidine in the reaction system. However, assuming the pKa of the

aryl-guanidine substrates presented here are comparable to guanidine, based on the pKa of

the substrate being ~13.7 and a carboxylic acid additive being ~4, roughly 1 in every $10^{9.7}$

guanidine compounds are in their neutral form.
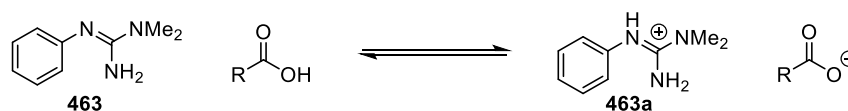
Scheme 195: Acid-base equilibrium obtained between a carboxylic acid and a guanidine

To probe the pKa effect, less acidic species were next examined. Phenol (**514a**, pKa = 10.09),[292] 2-hydroxypyridine (**514b**, pKa = 11.6),[293] benzamidine (**514c**, pKaH = 11.6)[294] and benzamidine hydrochloride (**514d**) were examined to span additives with larger pKa values (Scheme 196). The yield of benzimidazole **459** in all cases was low, giving 1%, 14%, 12% and 1% for the additives respectively.
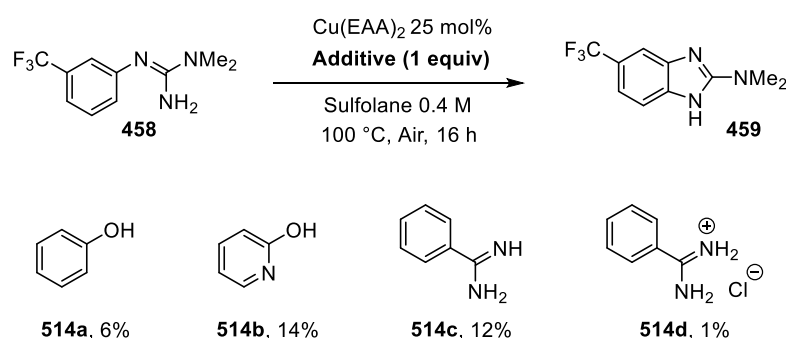
Scheme 196: The use of less acidic additives

Based on the presented results, it appeared that aliphatic carboxylic acids were the best at affording increased yields of the desired product (see Table 11, PivOH = 54%, AcOH = 41%). A series of benzoic acids were next examined, owing to the ease of manipulating both pKa and steric effects by variation of the ring-substituents. Benzoic acid (**515**) gave a yield of 21%, whilst 2,4,6-trimethylbenzoic acid (**516**) gave a yield of 37% (Scheme 197). This eluded to the potential that sterically encumbered carboxylic acids offer a yield benefit over less hindered alternatives.
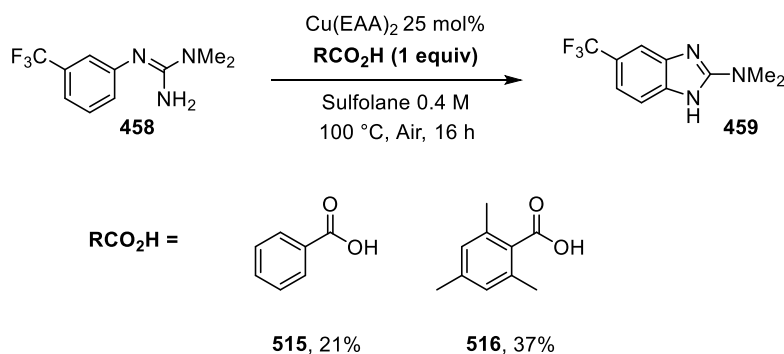
Scheme 197: Comparison between benzoic acid and 2,4,6-trimethylbenzoic acid

From here, 2,4,6-triethylbenzoic acid was synthesised to further examine this effect. Starting from 1,3,5-triethylbenzene (**517**), electrophilic aromatic substitution with bromine gave 1-bromo,2,4,6-triethylbenzene (**518**) in 88% yield. Metalation of bromo-arene **518** with magnesium and subsequent trapping of the Grignard reagent with carbon dioxide gave 2,4,6-triethylbenzoic acid (**519**) in 52% yield.
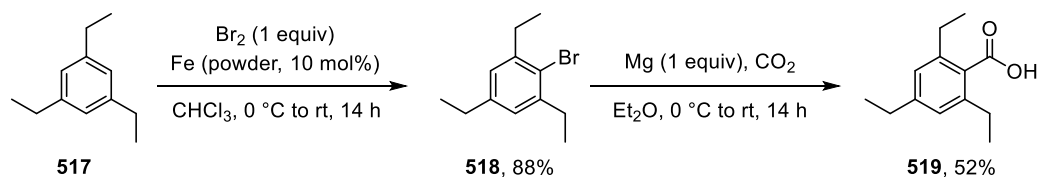
Scheme 198: Synthesis of 1,3,5-triethylbenzoic acid

In continuation, 1-bromo, 2,4,6-tri-*tert*-butylbenzene (**520**) was treated with *n*-butyllithium at room temperature in a lithium-halogen exchange reaction. The aryl-lithium was then trapped with carbon dioxide to give 2,4,6-tri-*tert*-butyl benzoic acid (**521**) in 26% yield.
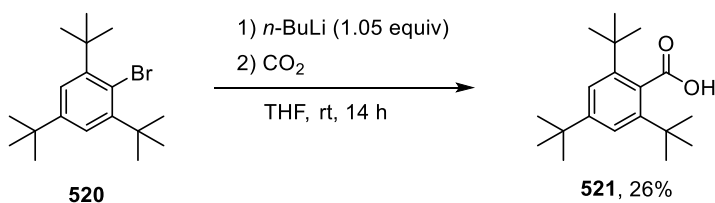
Scheme 199: Synthesis of 1,3,5-tri-tert-butyl-benzoic acid

Using the synthesised carboxylic acids as the reaction additive gave the results presented in Scheme 200. Triethylbenzoic acid (**519**) gave a 44% yield of benzimidazole **459**, and

2,4,6-tri-*tert*-butyl benzoic acid (**521**) gave a yield of 53% benzimidazole **459**. These results show that sterically hindered carboxylic acids are more effective additives at the presented transformation.
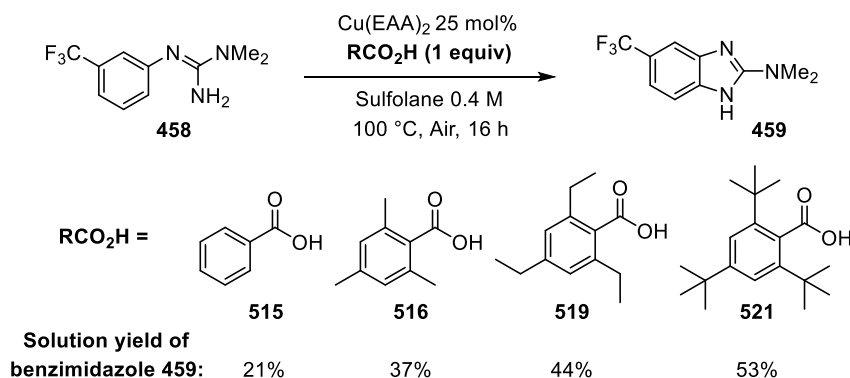
Scheme 200: The use of hindered additives in the presented transformation

A potential explanation for this result can be offered when considering the CMD mechanism, (Scheme 201). As R^1 increases in size (H < Me < Et < *t*Bu in the case of the substituted benzoic acids), as does the steric interaction between R^1 groups and the copper catalyst, especially with spectator ligands on the catalyst. Therefore, the elimination of a larger carboxylic acid would be favoured to decrease the steric repulsion between the carboxylate and the catalyst, and as such the C–H insertion is favoured. This could be considered an entropic driving force. Steric hindrance, by definition, lowers vibrational and rotational degrees-of-freedom, and as such, on elimination of the carboxylic acid the system will gain more degrees-of-freedom, providing an increased entropic driving force for the elimination of more hindered carboxylic acids. Previous reports have also shown the benefit of using highly sterically-hindered carboxylic acids in intramolecular C–H functionalisation reactions proceeding *via* a CMD mechanism.[295]
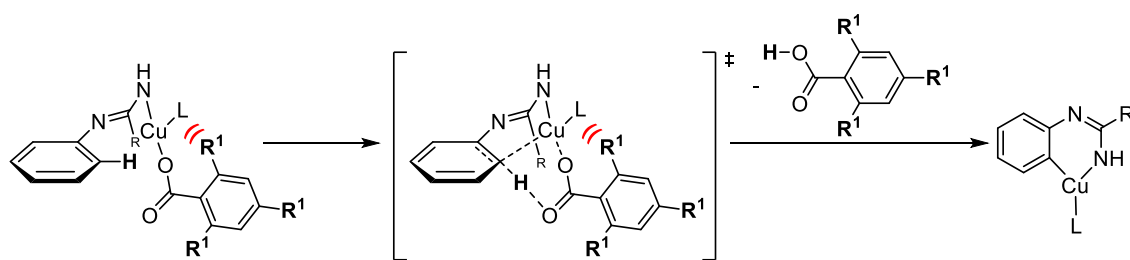
Scheme 201: An explanation for the better efficiency of hindered acids

Pivalic acid is a hindered acid with a relatively high pKa of 5.05.[296] The above observations offer an explanation as to why pivalic acid is the most effective additive; sterically hindered carboxylic acids with high pKas offer the highest yields of the desired benzimidazole. Furthermore, CMD is often the rate-determining step in transition metal C–H functionalisation owing to the high energy associated with puckering the C–H bond to achieve the reactive conformation (Scheme 192).[282,297] Therefore, based on the observations presented in this section, including the experimentally determined KIE value of 1.5 and the observed trends with systematically varying the reaction additive, a concerted-metalation-deprotonation event is a feasible mechanistic pathway for functionalisation of the C–H bond by the copper catalyst.

7.6.3 *N*-Capped aryl guanidines

The synthesis of 2-aminobenzimidazoles containing an R group in the 1 position through a copper-catalysed C–H functionalisation has been indirectly studied by Bao and Neuville (Scheme 202), as described in Section **5.5.3**.[213,227] The R group originates from the non-anilinic nitrogen in the aryl-guanidine starting material (**522**, Left, Scheme 202). However, the formation of a 1-substituted 2-aminobenzimidazole from a starting material which contains an R group on the anilinic nitrogen has not been reported (**523**, Right, Scheme 202). Moreover, a search of a similar transformation to form benzimidazoles without the 2-amino group also returns no result for the presented transformation. Despite the two transformations in Scheme 202 giving access to equivalent products, the presented example would add to a chemical toolkit for making these structures.
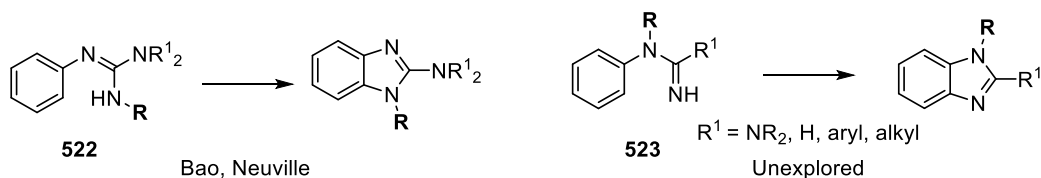
Scheme 202: Anilinic-substituted nitrogen

At the outset *N*-methyl, *N*-benzyl, *N*-tosyl and *N*-benzoyl guanidines **524**–**527** were targeted as model substrates to examine the feasibility for the presented transformation (Figure 33). Discussed below are the synthetic sequences performed to access guanidines with substitution on the anilinic nitrogen.
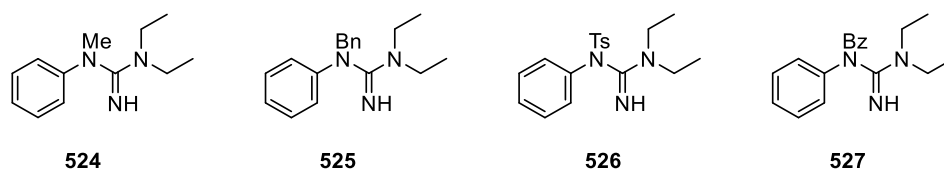
Figure 33: Targeted guanidines

In attempts to prepare *N*-methyl and *N*-benzyl guanidines, *N*-methyl aniline (**528a**) and *N*-benzylaniline (**528b**) were treated with sodium hydride and diethylcyanamide in DMSO, in an analogous manner to the preparation of aryl guanidines in Section **7.5.1**. Interestingly, no

conversion of the aniline was observed under these reaction conditions and starting material was recovered (Scheme 203).
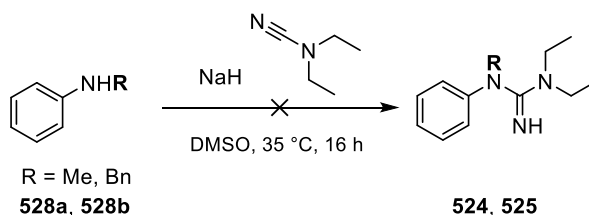
Scheme 203: Attempted synthesis of N-methyl and N-benzyl guanidines

The poor reactivity of *N*-alkyl anilines with *N*,*N*-diethylcyanamide indicated that a new route to these guanidines was required. Switching the cyanamide partner proved to be effective. Treatment of *N*-methyl aniline (**528a**) with cyanogen bromide in THF:Et$_2$O (1:1) afforded *N*-phenyl, *N*-methyl cyanamide (**529**) in 74% yield (Scheme 204). Treatment of cyanamide **529** with diethylamine in the presence of aluminium trichloride as a Lewis acid afforded *N*-methyl guanidine **524** in 33% yield.
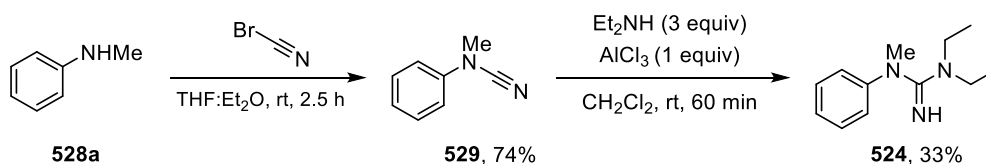
*Scheme 204: Synthesis of N-methyl guanidine **524***

The synthesis of *N*-tosyl cyanamide **530** proceeded in an interesting transformation from phenylurea (**531**) with tosyl chloride in pyridine resulting in the product in 73% yield. However, treatment of **530** with ethylamine and aluminium trichloride did not return any of the target guanidine **526**. Instead, the only observed product observed by LCMS was *N*-tosylaniline **532** suggesting the a cyano-transfer had occured. This is perhaps unsurprising given that *N*-tosyl cyanamide **530** is a powerful *N*-cyanating agent.[298,299] This indicated that the guanidine **526** is unstable with respect to elimination of N-tosylaniline **532**, suggesting that this substrate may not be an appropriate target.
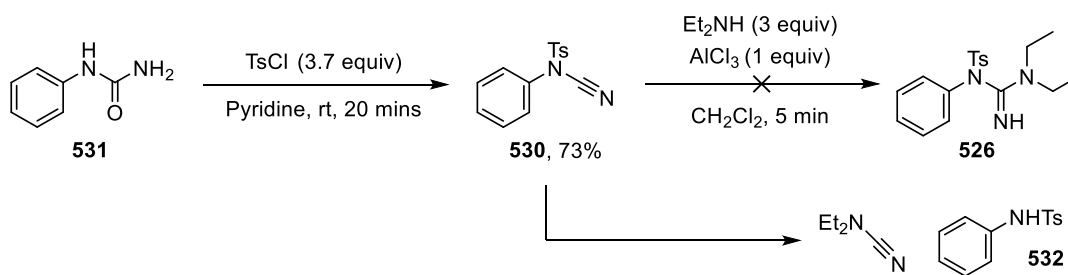
Scheme 205: Unable to access N-tosylguanidine

To examine whether *N*-tosyl cyanamide **530** could act as a cyano-transfer reagent to form the

N-benzoylcyanamide **534**, *N*-phenyl benzamide (**533**) was deprotonated with sodium hydride.

Addition of *N*-tosyl cyanamide **530** did not afford any of the desired product (Scheme 206). No

conversion of either *N*-tosyl cyanamide **530** or *N*-phenyl benzamide (**533**) was observed,

suggesting that the amide anion is unable to act as a nucleophile in the cyano-transfer

reaction.
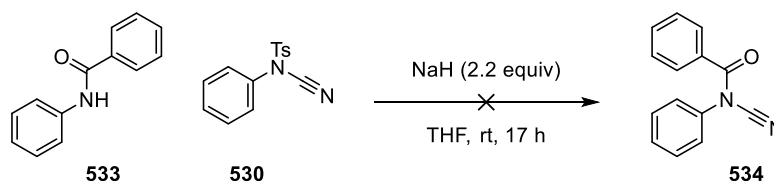
Scheme 206: No reaction between N-phenylbenzamide and NCTS (530)

In further attempts to access *N*-benzoyl cyanamide (**534**), a two-step procedure was

undertaken. Treatment of phenyl isothiocyanate (**535**) with KHMDS in THF gave the potassium

diimide salt **536** (Scheme 207). The potassium diimide intermediate was taken straight into

the next reaction with benzoyl chloride.[300] The *N*-benzoyl cyanamide **534** was isolated in 37%

yield from phenyl isothiocyanate.
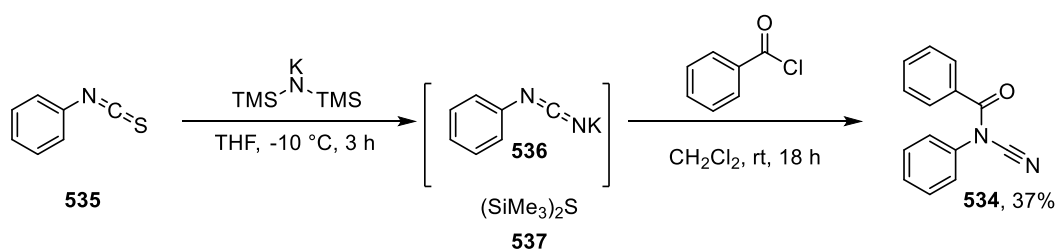
*Scheme 207: Synthesis of N-benzoyl cyanamide **534***

Unfortunately, treatment of N-benzoyl cyanamide **534** with diethylamine and aluminium chloride only returned trace quantities of the desired guanidine **527**. The major product by LCMS was *N*-phenylbenzamide (**533**), suggesting that **534** also acts as a cyano-transfer reagent and that the desired guanidine was unstable (Scheme 208).
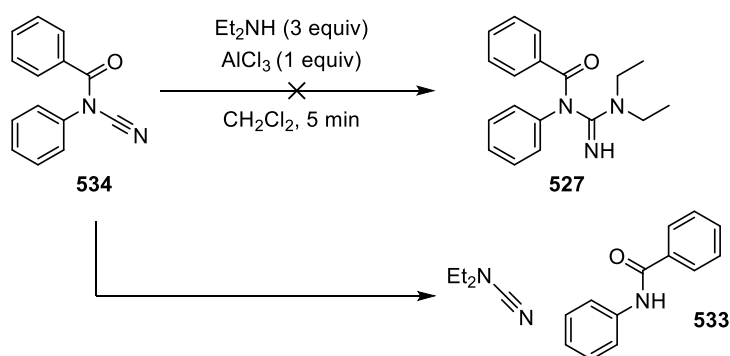
*Scheme 208: Attempted synthesis of N-benzoylguanidine **527***

N-benzyl cyanamide **538** was accessed by an N–S bond-cleavage reaction designed by Morrill.[299] Compound **538** was isolated in 72% yield from *N*-tosyl cyanamide **530** and benzyl alcohol (**539**). Addition of diethylamine and aluminium chloride gave *N*-benzyl guanidine **525** in 95% yield.
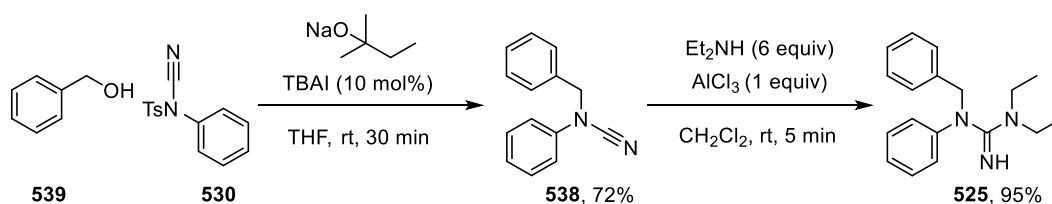
Scheme 209: Access to N-benzyl guanidine

Subjecting guanidines **524** and **525** to the optimised reactions conditions gave negligible formation of products **540** and **541** after 16 hours (Scheme 210). Greater than 20 species were observed by HPLC analysis of the reaction mixture indicating very poor selectivity for the desired reaction.

R = Me, **524**
R = Bn, **525**

Cu(EAA)$_2$ 25 mol%
PivOH (1 equiv)

Sulfolane 0.4 M
100 °C, Air, 16 h
R = Me, Bn

R = Me, **540**
R = Bn, **541**
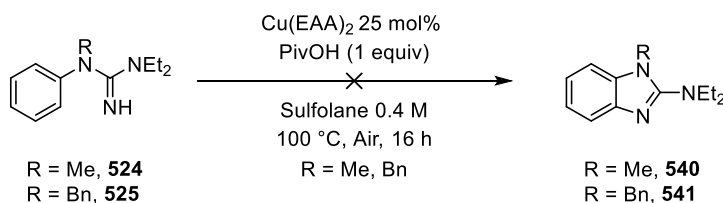
Scheme 210: Poor reactivity of N-methyl and N-benzyl guanidines

The above observation may have an implication for the understanding of the reaction mechanism. After a C–H insertion event has occurred, potentially by a CMD mechanism as discussed in Section **7.6.4**, a 6-membered organocopper species is obtained (**542a** and **542b**, Scheme 211). As the anilinic nitrogen is forced to adopt a more sp^3-type geometry when R ≠ H, the nitrogen which is required to undergo reductive elimination is forced into a more formal sp^2 hybridised geometry. The lack of formation of product with the anilinic-capped guanidines could be explained by the fact that the reductive elimination from the sp^2 hybridised nitrogen is disfavoured (Left, Scheme 211). Therefore, with the optimised system it can be invoked that the reductive elimination occurs from an sp^3 hybridised nitrogen, as shown on the right in Scheme 211. When R = H, the sp^3 hybridised geometry is more favourable on the blue nitrogen owing to the lack of charge separation in the proposed intermediate.

542a
sp^2 C–N reductive elimination
disfavoured

542b
sp^3 C–N reductive elimination
favoured
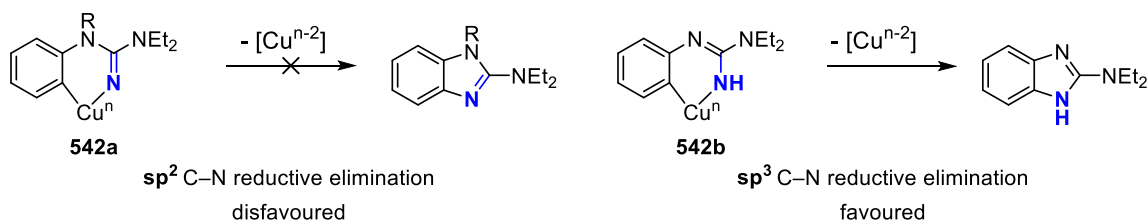
Scheme 211: A potential explanation for the poor reactivity of 524 and 525

To search for any catalytic intermediates to invoke within a mechanistic cycle, several analytical techniques were examined. NMR spectroscopy of the reaction mixture proved to be

challenging. Poor signal resolution owing to extensive signal broadening meant that multiplets could not be resolved and were observed as broad singlets.

7.6.4 Reaction examination by High-Resolution Mass-Spectrometry

High resolution mass spectrometry (HRMS) has recently proved to be a valuable tool to identify potential catalytic intermediates with copper-catalysed reactions.[256] Copper has two stable isotopes, ^{63}Cu and ^{65}Cu at abundances of 69.17% and 30.83% respectively.[301,302] As such, a HRMS analysis of a copper-bound analyte will display a characteristic double-peak in a mass spectrum with relative intensities of 69% and 31%. This makes determination as to whether an observed species contains a copper-ion simple. Therefore, analysis of the reaction mixture by direct-injection HRMS was pursued.

Sulfolane is a very high-boiling solvent (287 °C)[270] and as such volatilising this species for HRMS analysis resulted in a poor mass spectrum. Therefore, a test reaction using a stoichiometric loading of copper in acetonitrile under an inert atmosphere was performed (Scheme 212). Product **459** was still observed to form under these conditions, and so these conditions were utilised for HRMS experiments.
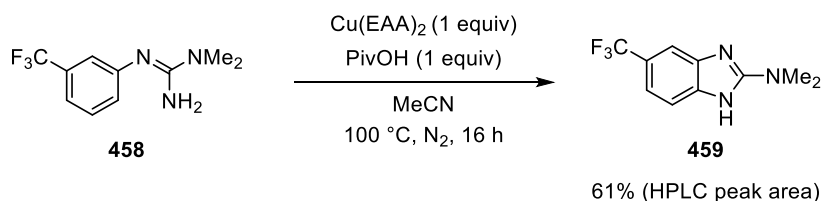
Scheme 212: A stoichiometric reaction in acetonitrile

Using HRMS to discover intermediate structures which concur with the observed mass-ions appeared to be a feasible starting point throughout this part of the study. Several logical decisions lead to the structural formulae which matched the observed mass-ions. With substrate **458**, the number of fluorine atoms could be limited to multiples of 3 owing to the presence of a CF_3 group. In addition, the number of nitrogen atoms could also be limited to multiples of 3 owing to the number of nitrogen atoms in the starting material. These parameters

lead to a small number of theoretical chemical formulae which matched with an observed m/z and intermediates could be proposed from these chemical formulae.

Scheme 213 details the result of a HRMS experiment with trifluoromethyl-guanidine **458**. The reaction was heated to 100 °C for 60 minutes before cooling to room temperature and analysing by direct-injection of the reaction mixture into a high-resolution mass-spectrometer. Several mass ions containing a copper-ion were observed and these will be discussed sequentially. First, a species containing a copper ion with an m/z of 525.1241 was observed in the mass spectrum. On consideration, a bis-guanidine copper complex (**543a**, $C_{20}H_{24}CuF_6N_6$) gives a theoretical monoisotopic mass-ion of 525.1263, which lies 4.12 ppm from the observed mass-ion. The HRMS instrument was calibrated to be accurate within a window of ± 5 ppm and so any theoretical formula which falls within this 5 ppm window could be assumed accurate. Assuming the copper ion is in the +1 oxidation state, this would concur with the observed m/z of 525.1241. To search for further evidence that the observed species was the bis-guanidine adduct, the un-fluorinated guanidine (**463**) was subjected to the same reaction conditions. A mass ion of 389.1496 was observed, which is consistent with the bis-guanidine adduct (**543b**, $C_{18}H_{26}CuN_6$) within 4.88 ppm. Guanidines are known to coordinate to a copper species in a bidentate fashion,[303] which explains why they have been drawn in this manner. Section **7.6.3** also highlighted that the anilinic nitrogen was required to be unsubstituted, suggesting that this nitrogen may be important and required to coordinate to the copper species, hence why it has been drawn in this coordination mode. The dimethylamino group has been drawn coordinating to the copper centre, however, this could equally be the NH_2 group – HRMS would not distinguish between these coordination modes and no evidence has been observed in this thesis or the literature to suggest otherwise. These results suggest that the bis-guanidine adduct appears to be a species present in solution, although the mechanistic implications for the presence of this species remain unclear.

R = CF$_3$ = **458**
R = H = **463**

HRMS analysis of the reaction mixture
R = CF$_3$, Observed m/z = **525.1241**
R = H, Observed m/z = **389.1496**

R = CF$_3$, 543a

Chemical Formula: C$_{20}$H$_{24}$CuF$_6$N$_6$

Monoisotopic mass: 525.1263

+4.12 ppm (*from 525.1241*)

R = H, 543b

Chemical Formula: C$_{18}$H$_{26}$CuN$_6$

Monoisotopic mass: 389.1515

+4.88 ppm (*from 389.1496*)
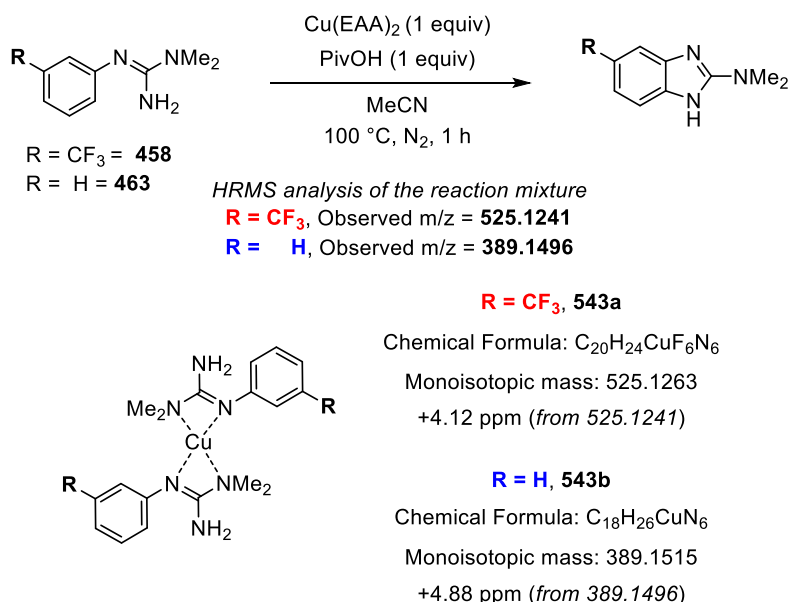
Scheme 213: Observation of a bis-guanidine copper complex

A second species was observed with a mass-ion of 523.1085 (Scheme 214). This [M−2] peak of intermediate **543** described in Scheme 213 could correspond to C$_{20}$H$_{22}$CuF$_6$N$_6$. This could be interpreted as either a C–H insertion product to form cyclic organo-copper intermediate (**544a**) or a copper species ligated with a benzimidazole product and a second guanidine ligand (**544b**). This proposed structure lies 4.04 ppm away from the observed mass-ion (Scheme 214). Isolation of any of these intermediates was unsuccessful and as such characterisation of which intermediate the *m/z* ion of 523.1085 corresponds to is impossible to determine from the mass-ion alone.
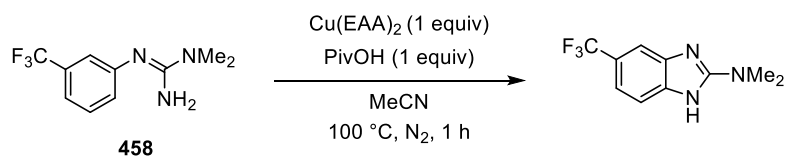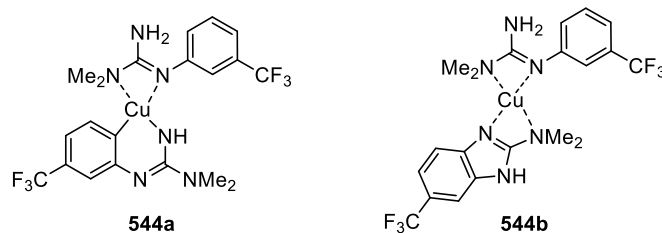
Scheme 214: Observation of an M−2 peak of bis-guanidine species

A final mass ion observed had an *m/z* of 521.0957 (Scheme 215). The chemical formula that this species corresponds to could be the bis-benzimidazole copper adduct **545** ($C_{20}H_{20}CuF_6N_6$). This proposed chemical formula lies 1.40 ppm away from the observed mass, indicating that this is likely the species observed in solution.
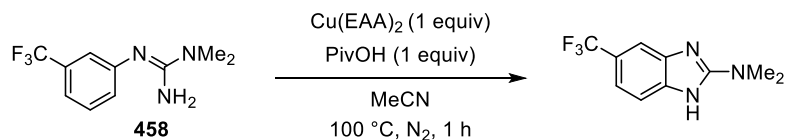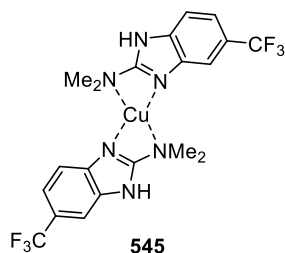
Scheme 215: Observation of an M−4 peak of bis-guanidine species

Empirical evidence obtained in Section **7.2** suggests that the ethyl acetoacetate counter-ion and pivalic acid should play an active role in the catalytic transformation based on the benefit that these species offer. However, in none of the above examples could a sensible structure be drawn which contains a guanidine, pivalate and ethyl acetoacetate ligand (such as **546**, Figure 34).

546
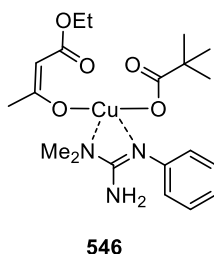
Figure 34: The proposed intermediate based on empirical evidence

The mechanistic implications for the above observations are therefore challenging to rationalise. Empirical evidence from the screening of copper-sources and reaction additives indicate that the additive plays a crucial role in the transformation (Section **7.2**). The ethyl acetoacetate counter-ion increases product formation and suppresses the formation of a dimeric benzimidazole (**456**). The reaction additive (PivOH) is essential for promoting the desired reactivity and evidence suggests that the active mechanism for C–H functionalisation is a concerted-metalation-deprotonation. Therefore, a species should likely be present which contains a copper ion bound by both a guanidine substrate and the carboxylate; no evidence for such an intermediate has been observed by HRMS. Nevertheless, not observing this intermediate does not mean that it is not present in solution, it could simply be unstable under the HRMS conditions. However, what the HRMS experiments do suggest is that the C–H functionalisation event does take place on the copper centre, as species such as **543a**, **544b** and **545** have been observed by HRMS (Figure 35).

543a
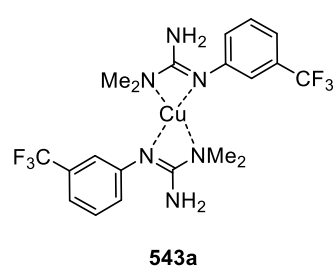
Observed m/z = 525.1241

Chemical Formula: $C_{20}H_{24}CuF_6N_6$

Monoisotopic mass: 525.1263

+4.12 ppm (*from 525.1241*)

544b
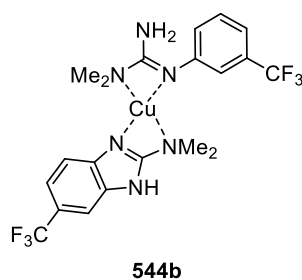
Observed m/z = 523.1085

Chemical Formula: $C_{20}H_{22}CuF_6N_6$

Monoisotopic mass: 523.1106

+4.04 ppm (*from 523.1085*)

545
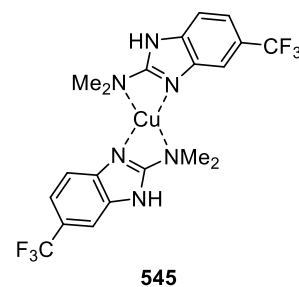
Observed m/z = 521.0957

Chemical Formula: $C_{20}H_{20}CuF_6N_6$

Monoisotopic mass: 521.0950

-1.40 ppm (*from 521.0957*)

Figure 35: Observed species by HRMS

7.6.5 Mechanistic conclusions

The ligand environment on the copper centre has been challenging to study and as such the exact coordination states of the copper catalyst remains unknown. Moreover, specific reaction intermediates could not be observed by any spectroscopic techniques. Therefore, the results obtained and presented within this thesis have not provided substantial evidence to propose a complete mechanistic cycle for the transformation.

Several mechanistic factors can be addressed by the results obtained within this thesis. Electron-deficient 1,3-dicarbonyl groups (hexafluoroacetylacetonate) result in poor conversion of the guanidine when compared to electron-donating 1,3-dicarbonyl groups under otherwise identical conditions (Section **7.2**). Within copper catalysis, reductive eliminations are often invoked from a Cu(III) centre.[256] In the context of this transformation, if a Cu(III) species such as **547** (Figure 36) is obtained after a C–H insertion event, this species will be stabilised by an electron-donating ligand, such as ethyl acetoacetate. This could explain the poor conversion obtained with an electron-deficient ligand, such as hexafluoroacetylacetonate (*cf.* 68% guanidine remaining *vs* 25%, Table 8, Section **7.2**).

547

If L_n is electron-donating, this species is stabilised

Figure 36: The requirement for an electron-donating counterion/ligand

When the anilinic nitrogen is "capped" with an alkyl group (benzyl, methyl, Section **7.6.3**), the developed conditions display very poor reactivity, resulting in significant degradation of the starting material to several unidentified species, and negligible benzimidazole formation was observed. This could suggest several factors. First, coordination of the anilinic nitrogen to the copper centre could play a vital mechanistic role (such as **548**). Second, this result could indicate that reductive elimination from an sp^2-hybridised nitrogen is disfavoured (**542a**, Scheme 216).

R = Alkyl

548
Important binding mode

542a
Disfavoured sp^2 reductive elimination
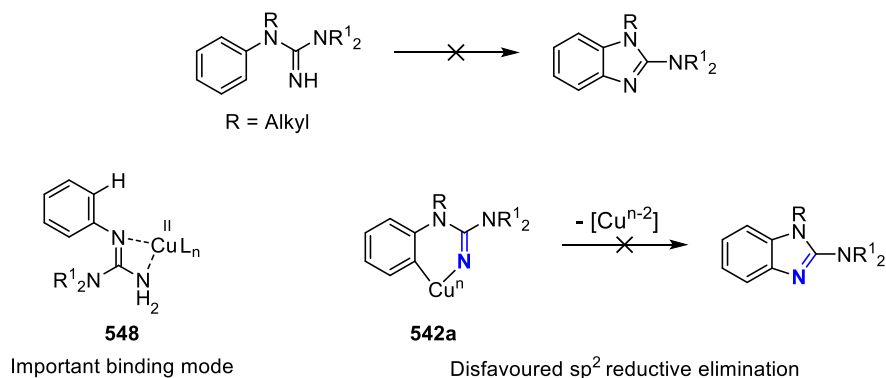
Scheme 216: Reductive elimination for an sp^3-hybridised nitrogen

Finally, a small primary KIE has been observed, suggesting that cleavage of the aromatic C−H bond is rate-limiting (Scheme 217). This suggests that several previously proposed mechanistic steps from within the literature for the C–H insertion event can be discounted.[262,278] Through systematic examination of the reaction additive, a concerted-metalation-deprotonation event, analogous with those often proposed in palladium and ruthenium catalysis, has been invoked.[280,297,304,305]

548   →   **547**
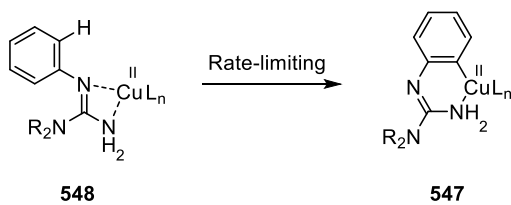
Scheme 217: Cleavage of the C–H bond appears to be rate-limiting

7.7 Application to the synthesis of a known pharmaceutical compound

Several marketed 2-aminobenzimidazoles are known and have been described in Section **5.2**. To demonstrate the relevance of the methodology, Emedastine (**361**) was selected as an appropriate target. The proposed retrosynthesis is shown in Scheme 218. Disconnection across the red C–N bond would give guanidine **549**. Strong evidence was presented in Section **7.6.3** that this transformation would not be feasible. Therefore, a functional group interconversion to N–Boc benzimidazole **550** was proposed, followed by removal of the ether side chain. This traced back to NH benzimidazole **551**, which appeared to be a feasible synthetic target. The key disconnection back to aryl-guanidine **552** was proposed. This guanidine could then be synthesised by the reaction of cyanamide **553** with aniline (**554**).
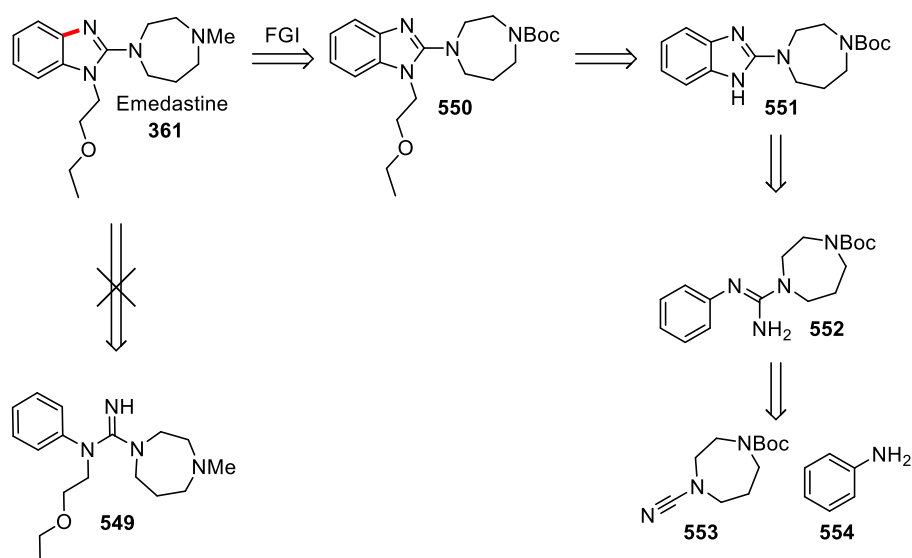
*Scheme 218: Proposed retrosynthesis of Emedastine (**361**) using the developed procedure*

The forward synthesis for Emedastine is described as follows. Treatment of *N*-Boc homopiperazine (**555**) with cyanogen bromide (**556**) in chloroform and di-*iso*-propylethylamine gave cyanamide **553** in 70% yield (Scheme 219).
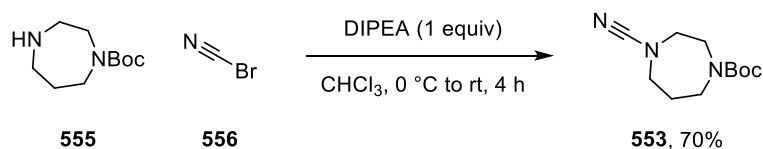
*Scheme 219: Synthesis of cyanamide **553***

Next, aniline was deprotonated in DMSO using sodium hydride and then reacted with cyanamide **553**. Guanidine **552** was isolated in a 67% yield (Scheme 220).
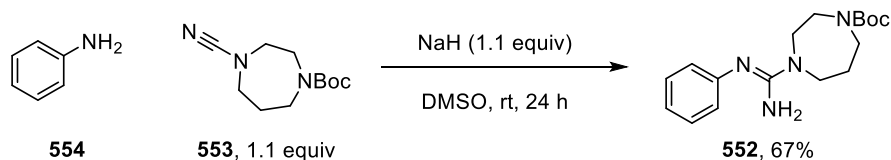
*Scheme 220: Synthesis of guanidine **552***

Subjecting guanidine **552** to modified conditions in which the copper loading could be lowered to 12.5 mol% without a loss of yield gave the benzimidazole core of Emedastine, **551**, in 71% yield on a 1.7 g scale (Scheme 221).
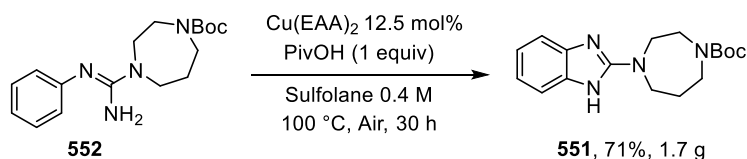
*Scheme 221: Gram-scale synthesis of 2-aminobenzimidazole **551***

Attempted alkylation of the benzimidazole **551** with alkyl chloride **557** did not result in any formation of the *N*-alkyl benzimidazole **550**. The use of various aprotic solvents (DMSO, THF, DMF) did not show any product formation and adding sodium iodide to affect an *in-situ* Finkelstein reaction[306] also did not promote product formation (Scheme 222).
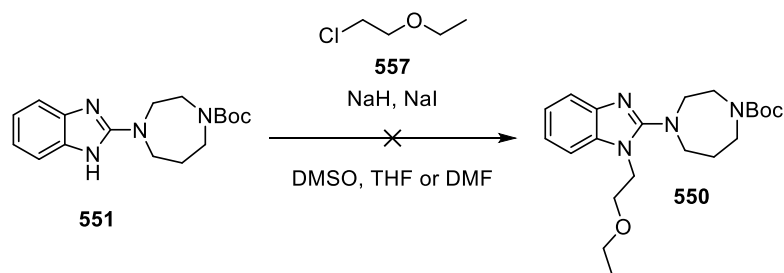
*Scheme 222: Unsuccessful alkylation of benzimidazole **551** with alkyl chloride **557***

A Finkelstein reaction of alkyl chloride **557** with sodium iodide in acetone was performed and after 16 hours under reflux, alkyl iodide **558** was isolated in a 19% yield (Scheme 223).
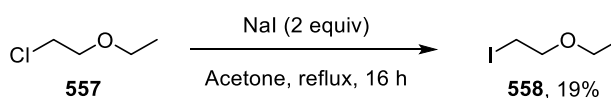
*Scheme 223: Finkelstein reaction to give alkyl iodide **558***

Deprotonation of benzimidazole **551** with sodium hydride in THF and treatment of the anion with alkyl iodide **558** gave the desired *N*-alkyl benzimidazole **550** after 18 hours under reflux (Scheme 224).
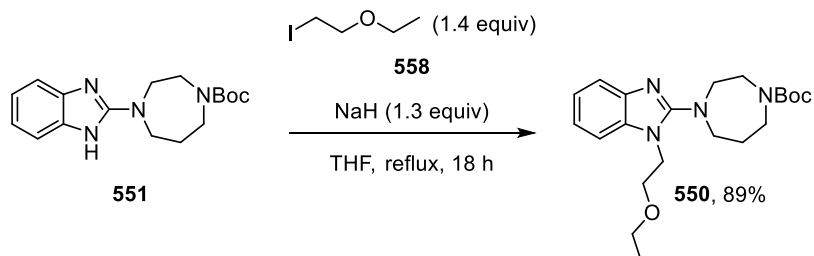
*Scheme 224: Alkylation of benzimidazole **551** with alkyl iodide **558***

N–Boc deprotection of **550** with hydrochloric acid in ethyl acetate gave the NH benzimidazole **559** in 93% yield. Finally, Eschweiler-Clarke methylation[307] of **559** with formaldehyde and formic acid gave Emedastine (**361**) in 86% yield.
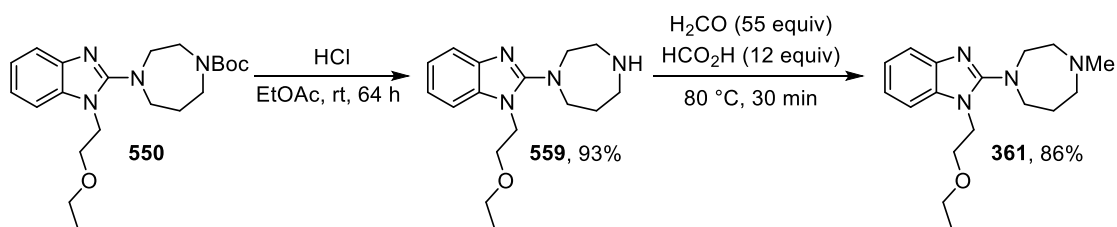
Scheme 225: Functional group interconversions to give Emedastine (361)

The presented new route to Emedastine is a 5-step synthesis from aniline in 34% overall yield, not including the synthesis of alkyl iodide **558** and cyanamide **553**. When compared to the discovery route for Emedastine (Scheme 226) this fragment was synthesised from 2-fluoronitrobenzene (**560**).[308] An S_NAr reaction was used to introduce the ether side chain with primary amine **561** to give **562**, whereby reduction of the nitro group with hydrogen and palladium on carbon gave the 1,2-diamine **563**. Ring-closure with urea gave benzimidazolone **564**. Dehydration of **564** with phosphorous oxychloride gave 2-chlorobenzimidazole **566**, where reaction with *N*-methyl homopiperazine (**567**) gave Emedastine (**361**). The discovery route gave a 43% yield from *o*-nitroaniline **562**.
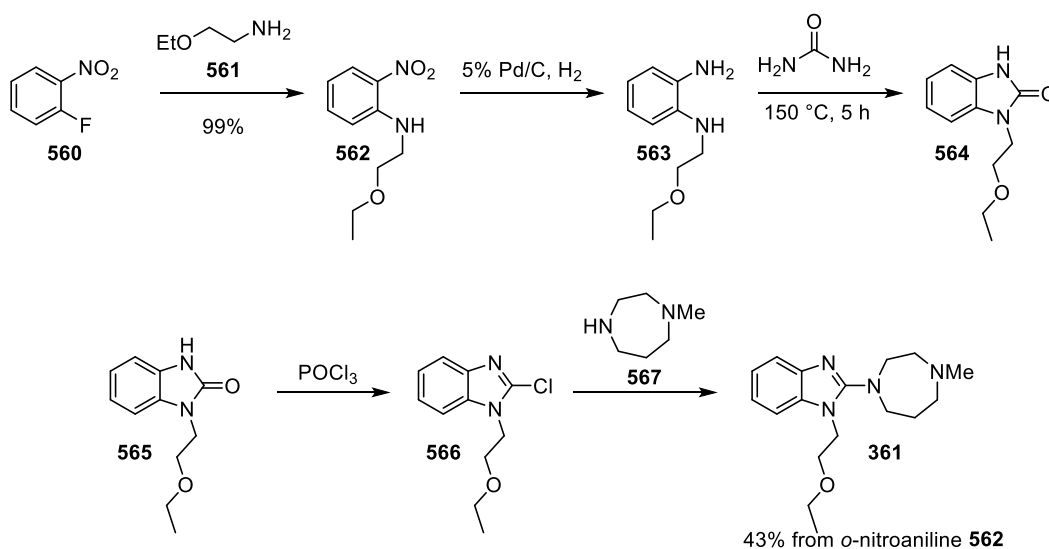
Scheme 226: Discovery route to Emedastine, employing nitro-group reduction, cyclisation, dehydration and S_NAr

8. Conclusions

In conclusion, a new copper-catalysed C–H functionalisation reaction has been developed to form 2-aminobenzimidazoles from aryl-guanidines. The reaction drew inspiration from a 2008 publication, in which the conditions were poorly applicable to this substructure of heterocycle. Through the combination of high throughput screening and statistical design of experiments, a catalytic system was developed to form a range of functionalised 2-aminobenzimidazoles in moderate-to-good yields. The functional group compatibility proved to be good, and the reaction could tolerate functional groups including esters, carbamates, nitriles, halogens and both electron donating and withdrawing substituents on the arene backbone. The developed methodology was then applied to the synthesis of Emedastine, a marketed pharmaceutical compound in which the key-step was performed on a gram-scale.[309]

The system uses a sub-stoichiometric loading of a copper(II) salt complexed with an ethyl acetoacetate ligand. The exact role of the ethyl acetoacetate counterion remains unclear, with spectroscopic evidence being unable to detect a copper intermediate ligated by the ligand in the reaction mixture. However, empirical evidence from a high throughput screen of copper sources indicate that electron-donating 1,3-dicarbonyl ligands are more effective at the transformation than electron-withdrawing 1,3-dicarbonyl ligands. This points towards a disproportionation mechanism in which an intermediate Cu(III) species — which is stabilised by the electron-donating nature of the ligand — can be invoked to facilitate a reductive elimination.

Experimental evidence suggests that a small primary kinetic isotope effect is present in the formation of the aminobenzimidazole. This indicates that cleavage of the C–H bond occurs during the rate-limiting step of the reaction. From this observation, a concerted-metalation-deprotonation mechanism has been invoked. Empirical examination of the reaction additive reveals that sterically encumbered carboxylic acids with decreased acidity (*i.e.* the carboxylates are more basic) are more effective at the transformation. These results concur with other findings of intramolecular C–H functionalisations in which a concerted-metalation-deprotonation is invoked.

9. Experimental

9.1 General comments and considerations

All catalysts, reagents and solvents were supplied by commercial sources and used without further purification, unless otherwise stated. Glassware was used without drying unless stated otherwise. Reactions requiring a headspace of air were simply performed without stoppering. The CAT96 reactor was developed by Hel group. Sulfolane was purchased from AlfaAesar and was melted in a buchi-path heated to 50 °C before use. When degassed solvent was required, a sample was sealed in a microwave vial and frozen in a dry ice/acetone bath at −78 °C, before being exposed to vacuum and warmed in a room temperature water bath. This process was repeated three times, or until bubbles no longer form on melting of the sample. 2,2-dimethoxyacetaldehyde was used as supplied from a commercial supplier as a 60% wt solution in water.

NMR spectra were recorded using a Bruker AV-400 (^{1}H = 400 MHz, ^{13}C = 101 MHz, ^{19}F = 376 MHz). Chemical shifts (δ) are reported in parts per million (ppm) relative to tetramethylsilane, $(CD_3)_2SO$, $CDCl_3$ or CD_3OD and coupling constants (J) in Hz. The following abbreviations are used for multiplicities: s = singlet; d = doublet; t = triplet; q = quartet; m = multiplet; dd = doublet of doublets; dt = doublet of triplets. When a prefix of "*br*" is used, this indicates a broad signal. If not specifically stated, the NMR experiments were run at 30 °C and ^{19}F and ^{13}C were run in {^{1}H}-decoupled mode. All NMR spectra were processed using either ACD Spectrus or ACDLabs.

Automated column chromatography was performed on a Biotage SP4, Isolera 1 or Isolera 4 purification system monitored by UV (λ = 200–400 nm, λ = 254 nm and 220 nm) using, unless stated otherwise, Biotage® SNAP Ultra pre-packed cartridges or Biotage SNAP K*P*-NH cartridges. Reverse phase column chromatography was performed on a CombiFlash automated system using Biotage® SNAP K*P*-C$_{18}$-HS pre-packed cartridge.

Mass spectra were recorded on a Waters ZQ mass spectrometer using alternate-scan positive and negative electrospray ionisation (ES$^+$ and ES$^-$) with a scan range of 100 to 1500 amu,

scan time of 0.50 s and an inter-scan delay of 0.25 s. The analysis software used was FractionLynx 4.1.

Chromatographic solvents were standard HPLC grade provided by Honeywell, and when a modifier was required it was added in-house. Melting points were measured on an OptiMelt melting point apparatus and monitored manually. IR spectra were recorded using a PerkinElmer Spectrum One spectrometer and the data processed using Perkim Elmer Spectrum software. Absorption frequencies (ν max) are reported in wavenumbers (cm^{-1}). The Mettler-Toledo Quantos QB5 or QX96 was used to weigh out desired solids for high throughput screening in preloaded dispensing heads using the supplied dispensing algorithms. Reactions requiring microwave heating were performed in a Biotage Initiator Microwave Reactor.

9.2 Analytical methods

Method	LCMS Method			
General Comments	Attached to this was a Waters ZQ mass spectrometer, running in positive and negative electrospray ionisation mode with a quadrupole detector.			
Column	Acquity UPLC CSH C18 (50 mm × 2.1 mm ×1.7 μm)			
Mobile Phase	A	Aqueous ammonium bicarbonate (10 mM) adjusted to pH 10 with ammonia solution		
	B	Acetonitrile		
Flow Rate	1 mL min^{-1}			
Gradient Profile	Time / min	0	1.5	1.9	2.0
	% A	0	3	3	100
	% B	100	97	97	0
Column Temperature	40 °C			
UV Detection	Summed over 210–350 nm			
Injection Volume	0.2 μL			

Method	HPLC Method			
Column	Waters CSH column (30 mm × 2.0 mm × 8.5 μm)			
Mobile Phase	A	Water + 0.05% v/v trifluoroacetic acid		
	B	Acetonitrile + 0.05% v/v trifluoroacetic acid.		
Flow Rate	1 mL min^{-1}			
Gradient Profile	Time / min	0	3.7	4.0	5.0
	% A	97	5	5	97
	% B	3	95	95	3
Column Temperature	40 °C			
UV Detection	220 nm			
Injection Volume	0.2 μL			

Method	MDAP Purification					
General Comments	Waters FractionLynx system comprising of a Waters 600 pump with extended pump heads, Waters 2700 autosampler, Waters 996 diode array and Gilson 202 fraction collector.					
Column	XSelect CSH C18 (150 mm × 30 mm × 5 µm)					
Mobile Phase	A	Aqueous ammonium bicarbonate (10 mM) adjusted to pH 10 with ammonia solution				
	B	Acetonitrile				
Flow Rate	40 mL min^{-1}					
Gradient Profile	Time / min	0	1	20	20.5	25
	% A	85	85	45	45	45
	% B	15	15	55	55	55
Column Temperature	Ambient					
UV Detection	Summer over 220–350 nm					
Injection Volume	1 mL					

Method	High-Resolution Mass Spectrometry					
Mass Spectrometer	Micromass Q-ToF Ultima hybrid quadrupole time-of-flight					
Column	Phenomenex Luna C18 column (100 mm x 2.1 mm, 3 µm packing diameter).					
Mobile Phase	A	Water + 0.1% v/v formic acid				
	B	Acetonitrile + 0.1% v/v formic acid				
Flow Rate	0.5 mL min^{-1}					
Gradient Profile	Time / min	0	6	8.5	9.5	12
	% A	95	0	0	95	95
	% B	5	100	100	5	5
Column Temperature	35 °C					
UV Detection	Summer over 220–350 nm					
Injection Volume	0.2 µL					

Method	Chiral HPLC	
Column	Chiralpak IC column (250 mm × 4.6 mm × 5 µm	
Mobile Phase	A	Ethanol (+ 0.1% IPA)
	B	Heptane (+ 0.1% IPA)
Flow Rate	0.1 mL min^{-1}	
Gradient Profile	Isochratic. 30% A, 70% B	
Column Temperature	40 °C	
UV Detection	230 nm	
Injection Volume	0.2 µL	

9.3 Chapter One Experimental

Examination of solvent for hydrazone formation
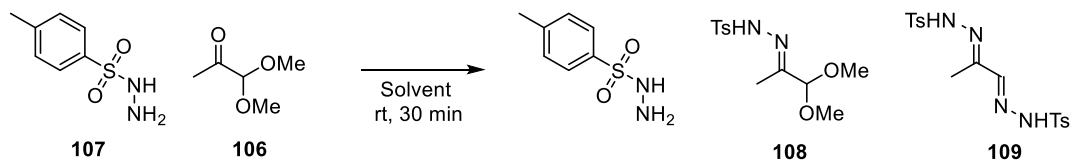
To 4 mL vials were added the below masses of **106**. To the vials were added a stirring flea and 2 mL of the quoted solvent. After 60 seconds, the quoted mass of **107** was added and the reactions stirred at room temperature. After 30 minutes, the results displayed in Table 2 were obtained after removing 10 µL of the reaction mixture and diluting into 1.5 mL acetonitrile and analysing by LCMS analysis.

Entry	**106** / mg (mmol)	Solvent	**107** / mg (mmol)
1	199 (1.68)	MeCN	312 (1.68)
2	204 (1.72)	THF	322 (1.73)
3	199 (1.68)	1,4-dioxane	316 (1.70)
4	204 (1.72)	DMSO	327 (1.76)
5	196 (1.66)	MeOH	312 (1.68)

Bishydrazone 109 and diazo compound 120

N',N'''-propane-1,2-diylidene)bis(4-methylbenzenesulfonohydrazide) 109
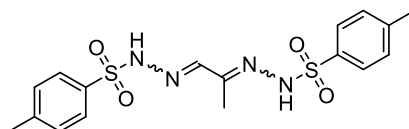
To a solution of 1,1-dimethoxypropan-2-one **106** (5.007 g, 42.40 mmol, 1.0 equiv) in MeOH (50 mL) was added 4-methylbenzenesulfonohydrazide (7.900 g, 42.40 mmol, 1.0 equiv). The reaction was stirred at room temperature for 30 minutes before concentrating *in vacuo.* CH_2Cl_2 (15 mL) was added and the resultant precipitate filtered and washed with cold tBME (3 × 5 mL) to yield *N',N'''-*propane-1,2-diylidene)bis(4-methylbenzenesulfonohydrazide) (**109**) as a fluffy white solid. (2.330 g, 5.70 mmol, 13%).

Appearance: White solid

M.pt: 100 °C (decomposed).

v (neat): 3217, 2995, 1717, 1596, 1338, 1161 914 cm^{-1}

^{1}H NMR (400 MHz, (CD$_3$)$_2$SO) δ ppm 11.59 (1H, *br.* s), 10.93 (1H, *br.* s), 7.63–7.73 (4H, m), 7.33–7.41 (4H, m), 7.30 (1H, s), 2.35 (6H, s), 1.85 (3H, s)

^{13}C NMR (101 MHz, (CD$_3$)$_2$SO) δ ppm 151.0, 146.1, 143.6, 143.6, 135.9, 135.7, 129.7, 129.6, 127.3, 127.0, 21.0, 11.0. *One signal missing. The benzylic methyl groups on the p-toluenesulfonyl group are indistinguishable by NMR, as indicated by the 6H singlet at 2.35 ppm in the 1H.*

HRMS (ESI Orbitrap) *m/z: Unable to detect mass*

2-Diazo-1-phenylpropan-1-one (120)
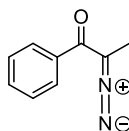
To a solution of 4-methylbenzenesulfonohydrazide (252 mg, 1.35 mmol, 1 equiv) in MeOH (1.5 mL) under nitrogen was added 1-phenylpropane-1,2-dione (202 mg, 1.36 mmol, 1.0 equiv) as a solution in MeOH (3 mL) over 60 minutes. 30 minutes after the addition was complete, benzylamine (196 mg, 1.83 mmol, 1.34 equiv) was added, at which point the colourless solution turned orange and the reaction was stirred at room temperature. After 16 hours, the reaction was concentrated *in vacuo* to give an orange solid which was dissolved in CH$_2$Cl$_2$ (20 mL), washed with water (20 mL), brine (10 mL) and dried over a hydrophobic frit before concentrating *in vacuo*. The crude material was purified by chromatography (100% heptane to 100% EtOAc) to give 2-diazo-1-phenylpropan-1-one (**120**) as an orange oil (144 mg, 0.90 mmol, 66%).

Appearance: Orange oil

^{1}H NMR (400 MHz, CDCl$_3$) δ ppm 7.56–7.61 (2H, m), 7.47–7.53 (1H, m), 7.40–7.47 (2H, m), 2.16 (3H, s)

^{13}C NMR (101 MHz, CDCl$_3$) δ ppm 190.1, 137.7, 131.3, 128.5, 127.2, 62.8 (*br*), 9.6 (*br*)

The spectroscopic data is concurrent with the literature.[310]

Optimisation data for triazole synthesis

To a 5 mL microwave vial was added the quantity of **106** shown in the table below. To this, methanol (2.5 mL) was added and the reaction stirred at room temperature for 60 seconds, after which the specified quantity of **107** was added and the reaction stirred at room temperature for a further 5 minutes. If necessary, the hydrazone formation was monitored by removing 5 µL and diluting into 1.5 mL acetonitrile and analysing by LCMS. The hydrazone formation was complete after 5 minutes. To each reaction was added benzylamine (119 mg, 1.11 mmol, 1.1 equiv) except Entry 4, where (216 mg, 2.01 mmol, 2.0 equiv) was added. Entry 1 was sealed and allow to stir at room temperature for the specified time. All other reactions were sealed and heated to the specified temperature using either a heating mantle (Entry 2) or the Biotage Microwave Initiator for the stated reaction time. After which, each reaction was concentrated *in vacuo* and to the crude material was added the specified quantity of 1,3,5-trimethoxybenzene. Each reaction was homogenised in CD$_3$OD (~3 mL) and analysed by quantitative ^{1}H NMR to give the yields shown in Table 3 and below. When isolation was stated (Entries 1, 4 & 7), it was performed by chromatography (2% Et$_3$N in CH$_2$Cl$_2$). Analytical data for triazole **135** is given below.
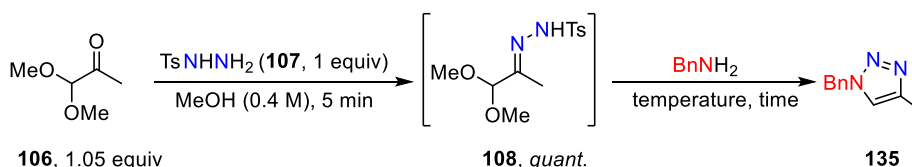
Entry	**106** / mg (mmol)	**107** / mg (mmol)	Temp / °C	Time / mins	1,3,5- TMB / mg	Yield
1	124 (1.05)	188 (1.01)	r.t.	960	52.1	47% (47%)
2	123 (1.04)	187 (1.00)	reflux	960	57.6	75%
3	123 (1.04)	187 (1.00)	120	20	49.6	83%
4	123 (1.04)	187 (1.00)	120	20	59.3	84% (77%)
5	123 (1.04)	188 (1.01)	120	5	56.1	82%
6	125 (1.06)	187 (1.00)	140	5	54.8	89%
7*	123 (1.04)	188 (1.01)	140	5	53.2	88% (88%)

*Reaction performed with triethylamine (109 mg, 1.08 mmol, 1.1 equiv). TMB = trimethoxybenzene

Methyl 4-methylbenzenesulfonate (139)
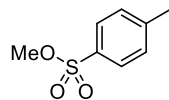
A solution of 4-methylbenzene sulfinic acid (29 mg, 0.19 mmol, 1 equiv) in methanol (0.47 mL) was heated to 120 °C for 20 minutes before cooling to room temperature and concentrating *in vacuo*. The crude material was purified by chromatography (5% EtOAc in heptane) to give methyl 4-methylbenzenesulfonate (**139**) as a colourless oil (29 mg, 0.16 mmol, 84%).

Appearance: Colourless oil

^{1}H NMR (400 MHz, CDCl$_3$) δ ppm 7.80 (2H, d, *J* = 8.0 Hz), 7.36 (2H, d, *J* = 8.0 Hz), 3.74 (3H, s), 2.47 (3H, s)

^{13}C NMR (101 MHz, CDCl$_3$) δ ppm 145.1, 132.2, 130.0, 128.1, 56.2, 21.4

The spectroscopic data is concurrent with the literature.[311]

9.3.2 4-methyl triazole synthesis

General procedure 1 for triazole synthesis
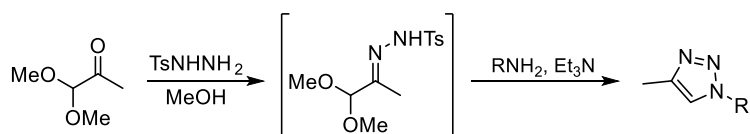
To a microwave vial was added 1,1-dimethoxypropan-2-one **106** (1.05 equiv) and MeOH (to make a ketone solution of 0.4 M). 4-methylbenzenesulfonohydrazide (1.0 equiv) was added and the reaction stirred at room temperature for 5 minutes (LCMS indicated complete hydrazone formation after 5 minutes) before addition of the desired primary amine (1.1 equiv) and triethylamine (1.1 equiv). The reaction vial was sealed and heated to 140 °C for 5 minutes in the Biotage Initiator Microwave Synthesiser.

1-Benzyl-4-methyl-1,2,3-triazole (135)
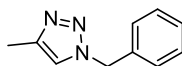
Using General Procedure 1 with 1,1-dimethoxypropan-2-one (494 mg, 4.18 mmol, 1.0 equiv) in methanol (10 mL) with 4-methylbenzenesulfonohydrazide (751 mg, 4.03 mmol, 1 equiv), benzylamine (481 mg, 4.43 mmol, 1.1 equiv) and triethylamine (450 mg, 4.43 mmol, 1.1 equiv). After 5 minutes at 140 °C and cooling to room temperature, the reaction mixture was concentrated *in vacuo* to give an orange oil. The oil was portioned between CH_2Cl_2:water (40 mL, 1:1) and the organic layer separated. The aqueous was extracted with CH_2Cl_2 (2 × 15 mL) and the combined organic extracts washed with brine (20 mL), dried over a hydrophobic frit and concentrated *in vacuo*. The crude material was purified by chromatography (2% MeOH in CH_2Cl_2 with 1% triethylamine in the CH_2Cl_2 portion) to yield 1-benzyl-4-methyl-1,2,3-triazole (**135**) as a white solid (617 mg, 3.56 mmol, 88%).

Appearance: White solid

^{1}H NMR (400 MHz, CD$_3$OD) δ ppm 7.68 (1H, s), 7.29–7.42 (5H, m), 5.53 (2H, s), 2.31 (3H, s)

^{13}C NMR (101 MHz, CD$_3$OD) δ ppm 143.3, 135.5, 128.6, 128.1, 127.6, 122.1, 53.4, 9.0

The spectroscopic data is concurrent with the literature.[312]

4-Methyl-1-propyl-1,2,3-triazole (140)

Using General Procedure 1 with 1,1-dimethoxypropan-2-one (248 mg, 2.10 mmol, 1.0 equiv) in methanol (5 mL) with 4-methylbenzenesulfonohydrazide (380 mg, 2.04 mmol, 1 equiv), propylamine (137 mg, 2.31 mmol, 1.1 equiv) and triethylamine (232 mg, 2.29 mmol, 1.1 equiv). After 5 minutes at 140 °C and cooling to room temperature, the reaction mixture was concentrated *in vacuo* to give an orange oil. The oil was portioned between CH_2Cl_2:water (40 mL, 1:1) and the organic layer separated. The aqueous was extracted with CH_2Cl_2 (2 × 15 mL) and the combined organic extracts washed with brine (20 mL), dried over a hydrophobic frit

and concentrated *in vacuo* to yield 4-methyl-1-propyl-1,2,3-triazole (**140**) as a pale-yellow oil (250 mg, 2.00 mmol, 98%).

Appearance: Pale-yellow oil

ν (neat): 2967, 2937, 1557, 1460, 1386, 1336, 1215 , 1052 cm^{-1}

^{1}H NMR (400 MHz, CD$_3$OD) δ ppm 7.68 (1H, s), 4.31 (2H, t, J = 7.3 Hz), 2.30 (3H,s), 1.90 (2H, sxt, J = 7.3 Hz), 0.92 (3H, t, J = 7.3 Hz)

^{13}C NMR (101 MHz, CD$_3$OD) δ ppm 142.8, 122.0, 51.4, 23.3, 9.8, 9.0

HRMS (ESI Orbitrap) *m/z*: Calcd for C$_6$H$_{12}$N$_3$ [M+H]$^+$ 126.1026; found [M+H]$^+$ 126.1026

1,4-Dimethyl-1,2,3-triazole (141)
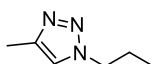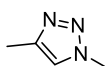

Using General Procedure 1 with 1,1-dimethoxypropan-2-one (249 mg, 2.11 mmol, 1.0 equiv) in methanol (5 mL) with 4-methylbenzenesulfonohydrazide (379 mg, 2.03 mmol, 1 equiv), methylamine (40 wt% solution in water, 179 mg, 0.2 mL, 2.30 mmol, 1.1 equiv) and triethylamine (232 mg, 2.30 mmol, 1.1 equiv). After 5 minutes at 140 °C and cooling to room temperature, the reaction mixture was concentrated *in vacuo* to give an orange oil. The oil was portioned between CH$_2$Cl$_2$:water (40 mL, 1:1) and the organic layer separated. The aqueous was extracted with CH$_2$Cl$_2$ (2 × 15 mL) and the combined organic extracts washed with brine (20 mL), dried over a hydrophobic frit and concentrated *in vacuo* to yield **141** as a pale-yellow oil (188 mg, 1.94 mmol, 95%).

Appearance: Pale-yellow oil

^{1}H NMR (400 MHz, CDCl$_3$) δ ppm 7.25 (1H, s), 4.02 (3H, s), 2.31 (3H, s)

^{13}C NMR (101 MHz, CDCl$_3$) δ ppm 143.5, 122.1, 36.4, 10.7

The spectroscopic data is concurrent with the literature.[313]

1-Isopropyl-4-methyl-1,2,3-triazole (142)

Using General Procedure 1 with 1,1-dimethoxypropan-2-one (248 mg, 2.10 mmol, 1.0 equiv) in methanol (5 mL) with 4-methylbenzenesulfonohydrazide (382 mg, 2.05 mmol, 1 equiv), *iso*-propylamine (138 mg, 2.33 mmol, 1.1 equiv) and triethylamine (232 mg, 2.30 mmol, 1.1 equiv). After 5 minutes at 140 °C and cooling to room temperature, the reaction mixture was concentrated *in vacuo* to give an orange oil. The oil was portioned between CH_2Cl_2:water (40 mL, 1:1) and the organic layer separated. The aqueous was extracted with CH_2Cl_2 (2 × 15 mL) and the combined organic extracts washed with brine (20 mL), dried over a hydrophobic frit and concentrated *in vacuo* to yield **142** as a pale-yellow oil (202 mg, 1.61 mmol, 79%).

Appearance: Pale-yellow oil

ν (neat): 2981, 2939, 1555, 1457, 1345, 1045 cm^{-1}

^{1}H NMR (400 MHz, CD$_3$OD) δ ppm 7.74 (1H, s), 4.81 (1H, spt, *J* = 6.8 Hz), 2.32 (3H, s), 1.56 (6H, d, *J* = 6.8 Hz)

^{13}C NMR (101 MHz, CD$_3$OD) δ ppm 142.6, 119.8, 53.0, 21.7, 9.1

HRMS (ESI Orbitrap) *m/z*: Calcd for $C_6H_{12}N_3$ [M+H]$^+$ 126.1026; found [M+H]$^+$ 126.1023
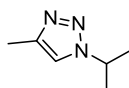
1-Cyclopropyl-4-methyl-1,2,3-triazole (143)
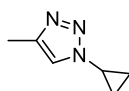
Using General Procedure 1 with 1,1-dimethoxypropan-2-one (250 mg, 2.12 mmol, 1.0 equiv) in methanol (5 mL) with 4-methylbenzenesulfonohydrazide (379 mg, 2.04 mmol, 1 equiv), cyclopropylamine (132 mg, 2.26 mmol, 1.1 equiv) and triethylamine (232 mg, 2.30 mmol, 1.1 equiv). After 5 minutes at 140 °C and cooling to room temperature, the reaction mixture was concentrated *in vacuo* to give an orange oil. The oil was portioned between CH_2Cl_2:water (40

mL, 1:1) and the organic layer separated. The aqueous was extracted with CH_2Cl_2 (2 × 15 mL) and the combined organic extracts washed with brine (20 mL), dried over a hydrophobic frit and concentrated *in vacuo* to yield **143** as a pale-yellow oil (244 mg, 2.00 mmol, 97%).

Appearance: Pale-yellow oil

ν (neat): 1557, 1435, 1215, 1046 cm^{-1}

^{1}H NMR (400 MHz, CDCl$_3$) δ ppm 7.31 (1H, s), 3.71 (1H, tt, *J* = 7.4, 3.8 Hz), 2.32 (3H, s), 1.07–1.27 (4H, m)

^{13}C NMR (101 MHz, CDCl$_3$) δ ppm 142.9, 121.8, 31.0, 10.8, 6.7

HRMS (ESI Orbitrap) *m/z*: Calcd for $C_6H_{10}N_3$ [M+H]$^+$ 124.0869; found [M+H]$^+$ 124.0868

1-Cyclohexyl-4-methyl-1,2,3-triazole (144)
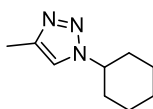
Using General Procedure 1 with 1,1-dimethoxypropan-2-one (249 mg, 2.10 mmol, 1.0 equiv) in methanol (5 mL) with 4-methylbenzenesulfonohydrazide (382 mg, 2.05 mmol, 1 equiv), cyclohexylamine (225 mg, 2.27 mmol, 1.1 equiv) and triethylamine (232 mg, 2.30 mmol, 1.1 equiv). After 5 minutes at 140 °C and cooling to room temperature, the reaction mixture was concentrated *in vacuo* to give an orange oil. The oil was portioned between CH_2Cl_2:water (40 mL, 1:1) and the organic layer separated. The aqueous was extracted with CH_2Cl_2 (2 × 15 mL) and the combined organic extracts washed with brine (20 mL), dried over a hydrophobic frit and concentrated *in vacuo* to yield **144** as a white solid (308 mg, 1.87 mmol, 91%).

Appearance: White solid

M.pt: 80–81 °C

ν (neat): 2935, 2858, 1556, 1451, 1334, 1212 cm^{-1}

^{1}H NMR (400 MHz, CDCl$_3$) δ ppm 7.28 (1H, s), 4.41 (1H, tt, J = 11.8, 3.8 Hz), 2.35 (3H, s), 2.13–2.24 (2H, m), 1.92 (2H, dt, J = 13.7, 3.1 Hz), 1.65–1.83 (3H, m), 1.46 (2H, qt, J = 13.0, 3.3 Hz), 1.18–1.35 (3H, m)

^{13}C NMR (101 MHz, CDCl$_3$) δ ppm 142.8, 118.7, 59.8, 33.6, 25.2, 25.2, 10.9

HRMS (ESI Orbitrap) m/z: Calcd for C$_9$H$_{16}$N$_3$ [M+H]$^+$ 166.1339; found [M+H]$^+$ 166.1339

1-(*Tert*-butyl)-4-methyl-1,2,3-triazole (145)
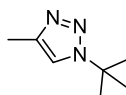
Using General Procedure 1 with 1,1-dimethoxypropan-2-one (247 mg, 2.09 mmol, 1.0 equiv) in methanol (5 mL) with 4-methylbenzenesulfonohydrazide (379 mg, 2.03 mmol, 1 equiv), *tert*-butylamine (166 mg, 2.26 mmol, 1.1 equiv) and triethylamine (232 mg, 2.30 mmol, 1.1 equiv). After 5 minutes at 140 °C and cooling to room temperature, the reaction mixture was concentrated *in vacuo* to give an orange oil. The oil was portioned between CH$_2$Cl$_2$:water (40 mL, 1:1) and the organic layer separated. The aqueous was extracted with CH$_2$Cl$_2$ (2 × 15 mL) and the combined organic extracts washed with brine (20 mL), dried over a hydrophobic frit and concentrated *in vacuo* to yield **145** as a pale-yellow oil (256 mg, 1.84 mmol, 90%).

Appearance: Pale-yellow oil

ν (neat): 2980, 1557, 1462, 1371, 1227, 1205, 1048 cm^{-1}

^{1}H NMR (400 MHz, CD$_3$OD) δ ppm 7.80 (1H, s), 2.32 (3H, s), 1.67 (9H, s)

^{13}C NMR (101 MHz, CD$_3$OD) δ ppm 142.3, 119.3, 59.2, 28.7, 9.0

HRMS (ESI Orbitrap) m/z: Calcd for C$_7$H$_{14}$N$_3$ [M+H]$^+$ 140.1182; found [M+H]$^+$ 140.1182

4-Methyl-1-(2,2,2-trifluoroethyl)-1,2,3-triazole (146)
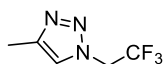
Using General Procedure 1 with 1,1-dimethoxypropan-2-one (249 mg, 2.10 mmol, 1.0 equiv) in methanol (5 mL) with 4-methylbenzenesulfonohydrazide (381 mg, 2.05 mmol, 1 equiv), trifluoroethylamine (227 mg, 2.29 mmol, 1.1 equiv) and triethylamine (232 mg, 2.30 mmol, 1.1 equiv). After 5 minutes at 140 °C and cooling to room temperature, the reaction mixture was concentrated *in vacuo* to give an orange oil. The oil was portioned between CH_2Cl_2:water (40 mL, 1:1) and the organic layer separated. The aqueous was extracted with CH_2Cl_2 (2 × 15 mL) and the combined organic extracts washed with brine (20 mL), dried over a hydrophobic frit and concentrated *in vacuo* to yield **146** as a white solid (271 mg, 1.64 mmol, 80%).

Appearance: White solid

M.pt: 45–47 °C

ν (neat): 1267, 1246, 1167, 1055, 936 cm^{-1}

^{1}H NMR (400 MHz, CD$_3$OD) δ ppm 7.87 (1H, s), 5.28 (2H, q, *J* = 8.9 Hz), 2.36 (3H, s)

^{19}F NMR (376 MHz, CD$_3$OD) δ ppm −73.16 (1F, s)

^{13}C NMR (101 MHz, CD$_3$OD) δ ppm 143.6, 123.6, 122.9 (q, *J* = 278.5 Hz), 49.8 (q, *J* = 35.9 Hz), 8.9

HRMS (ESI Orbitrap) *m/z*: Calcd for $C_5H_7F_3N_3$ [M+H]$^+$ 166.0587; found [M+H]$^+$ 166.0581

1-Allyl-4-methyl-1,2,3-triazole (147)
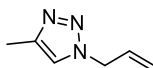
Using General Procedure 1 with 1,1-dimethoxypropan-2-one (248 mg, 2.10 mmol, 1.0 equiv) in methanol (5 mL) with 4-methylbenzenesulfonohydrazide (382 mg, 2.05 mmol, 1 equiv),

allylamine (129 mg, 2.27 mmol, 1.1 equiv) and triethylamine (232 mg, 2.30 mmol, 1.1 equiv).

After 5 minutes at 140 °C and cooling to room temperature, the reaction mixture was concentrated *in vacuo* to give an orange oil. The oil was portioned between CH_2Cl_2:water (40 mL, 1:1) and the organic layer separated. The aqueous was extracted with CH_2Cl_2 (2 × 15 mL) and the combined organic extracts washed with brine (20 mL), dried over a hydrophobic frit and concentrated *in vacuo* to give an orange oil. The crude material was purified by preparative high-performance liquid chromatography (15–55% MeCN in water, 0.05% ammonium bicarbonate buffer). The fractions containing product were concentrated under reduced pressure to remove the volatile organics and the resulting aqueous portion was extracted into CH_2Cl_2 (3 × 50 mL). The combined organics were washed with brine (50 mL) and dried over a hydrophobic frit to yield (**147**) as a colourless oil (218 mg, 1.74 mmol, 85%).

Appearance: Colourless oil

^{1}H NMR (400 MHz, CDCl$_3$) δ ppm 7.29 (1H, s), 6.02 (1H, ddt, *J* = 16.9, 10.5, 6.2, 6.2 Hz), 5.23–5.38 (2H, m), 4.87–5.01 (2H, m), 2.36 (3H, s)

^{13}C NMR (101 MHz, CDCl$_3$) δ ppm 143.6, 131.6, 120.9, 119.7, 52.5, 10.8

The spectroscopic data is concurrent with the literature.[81]

4-Methyl-1-(pro*p*-2-yn-1-yl)-1,2,3-triazole (148)
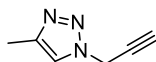
Using General Procedure 1 with 1,1-dimethoxypropan-2-one (250 mg, 2.20 mmol, 1.0 equiv) in methanol (5 mL) with 4-methylbenzenesulfonohydrazide (388 mg, 2.08 mmol, 1 equiv), propargylamine (129 mg, 2.29 mmol, 1.1 equiv) and triethylamine (232 mg, 2.30 mmol, 1.1 equiv). After 5 minutes at 140 °C and cooling to room temperature, the reaction mixture was concentrated *in vacuo* to give an orange oil. The oil was portioned between CH_2Cl_2:water (40 mL, 1:1) and the organic layer separated. The aqueous was extracted with CH_2Cl_2 (2 × 15 mL) and the combined organic extracts washed with brine (20 mL), dried over a hydrophobic frit and concentrated *in vacuo* to give an orange oil. The crude material was purified by

chromatography (50–100% EtOAc in heptane) to yield **148** as a colourless oil (219 mg, 1.81 mmol, 87%).

Appearance: Colourless oil

ν (neat): 3290, 2129, 1557, 1443, 1346, 1217, 1128, 1051, 775 cm^{-1}

^{1}H NMR (400 MHz, CD$_3$OD) δ ppm 7.82 (1H, s), 5.25 (2H, d, J = 2.7 Hz), 3.06 (1H, t, J = 2.7 Hz), 2.34 (3H, s)

^{13}C NMR (101 MHz, CD$_3$OD) δ ppm 143.3, 121.9, 75.6, 75.0, 39.0, 9.0

HRMS (ESI Orbitrap) *m/z*: Calcd for C$_5$H$_7$F$_3$N$_3$ [M+H]$^+$ 166.0587; found [M+H]$^+$ 166.0581

N,N-dimethyl-3-(4-methyl-1,2,3-triazol-1-yl)propan-1-amine (149)
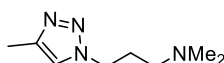
Using General Procedure 1 with 1,1-dimethoxypropan-2-one (250 mg, 2.12 mmol, 1.0 equiv) in methanol (5 mL) with 4-methylbenzenesulfonohydrazide (385 mg, 2.07 mmol, 1 equiv), N^1,N^1-dimethylpropane-1,3-diamine (237 mg, 2.32 mmol, 1.1 equiv) and triethylamine (232 mg, 2.30 mmol, 1.1 equiv). After 5 minutes at 140 °C and cooling to room temperature, the reaction mixture was concentrated *in vacuo* to give an orange oil. The oil was portioned between CH$_2$Cl$_2$:water (40 mL, 1:1) and the organic layer separated. The pH of the aqueous layer was increased to 13 by addition of NaOH (2 M) and extracted with CH$_2$Cl$_2$ (6 × 15 mL). The combined organic extracts were washed with brine (20 mL), dried over a hydrophobic frit and concentrated *in vacuo* to give an orange oil. The crude material was purified by chromatography (5% MeOH in CH$_2$Cl$_2$ with 1% triethylamine in the CH$_2$Cl$_2$ portion) to yield **149** as a colourless oil (281 mg, 1.67 mmol, 81%).

Appearance: Colourless oil

ν (neat): 2945, 2819, 2768, 1557, 1461, 1215, 1047 cm^{-1}

^{1}H NMR (400 MHz, CDCl$_3$) δ ppm 7.29 (1H, s), 4.38 (2H, t, J = 7.0 Hz), 2.35 (3H, s), 2.24–2.29 (2H, m), 2.20–2.24 (6H, s), 1.99–2.09 (2H, m)

^{13}C NMR (101 MHz, CDCl$_3$) δ ppm 143.1, 121.4, 55.9, 47.8, 45.3, 28.3, 10.8

HRMS (ESI Orbitrap) *m/z*: Calcd for C$_8$H$_{17}$N$_4$ [M+H]$^+$ 169.1448; found [M+H]$^+$ 169.1444

4-Methyl-1H-1,2,3-triazole (150)
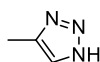
Following a modification of General Procedure 1 with 1,1-dimethoxypropan-2-one (252 mg, 2.13 mmol, 1.0 equiv) in methanol (4.3 mL) with 4-methylbenzenesulfonohydrazide (385 mg, 2.07 mmol, 1 equiv) and ammonia (7 M solution in MeOH) (0.65 mL, 4.6 mmol, 2.2 equiv) *note triethylamine omitted to aid isolation.* After 5 minutes at 140 °C and cooling to room temperature, the reaction mixture was flushed through a 5 g SCX-2 ion exchange cartridge with MeOH (75 mL) and methanolic ammonia (7 M, 20 mL). The methanolic ammonia portion was concentrated in vacuo to yield **150** as a colourless oil (134 mg, 1.61 mmol, 78%).

Appearance: Colourless oil

^{1}H NMR (400 MHz, CDCl$_3$) δ ppm 7.52 (1H, s), 2.41 (3H, s)

The spectroscopic data is concurrent with the literature.[314]

1-(4-Methoxybenzyl)-4-methyl-1,2,3-triazole (151)

Using General Procedure 1 with 1,1-dimethoxypropan-2-one (249 mg, 2.11 mmol, 1.0 equiv) in methanol (5 mL) with 4-methylbenzenesulfonohydrazide (387 mg, 2.08 mmol, 1 equiv), 4-methoxybenzylamine (315 mg, 2.25 mmol, 1.1 equiv) and triethylamine (232 mg, 2.30 mmol,

1.1 equiv After 5 minutes at 140 °C and cooling to room temperature, the reaction mixture was concentrated *in vacuo* to give an orange oil. The oil was portioned between CH$_2$Cl$_2$:water (40 mL, 1:1) and the organic layer separated. The aqueous was extracted with CH$_2$Cl$_2$ (2 × 15 mL) and the combined organic extracts washed with brine (20 mL), dried over a hydrophobic frit and concentrated *in vacuo* to give an orange oil. The crude material was purified by chromatography (50–100% EtOAc in heptane) to yield **151** as a white solid (355 mg, 1.75 mmol, 84%).

Appearance: White solid

M.pt: 74–75 °C

ν (neat): 1610, 1513, 1446, 1334, 1294, 1244, 1025, 772 cm^{-1}

^{1}H NMR (400 MHz, CD$_3$OD) δ ppm 7.62 (1H, s), 7.27 (2H, d, *J* = 8.6 Hz), 6.87–6.95 (2H, m), 5.45 (2H, s), 3.78 (3H, s), 2.28 (3H, s)

^{13}C NMR (101 MHz, CD$_3$OD) δ ppm 159.9, 143.2, 129.2, 127.4, 121.9, 113.9, 54.4, 53.0, 9.0

HRMS (ESI Orbitrap) *m/z*: Calcd for C$_{11}$H$_{14}$N$_3$O [M+H]$^+$ 204.1131; found [M+H]$^+$ 204.1127
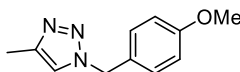
4-((4-Methyl-1,2,3-triazol-1-yl)methyl)benzonitrile (152)
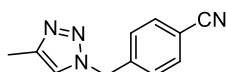
Using General Procedure 1 with 1,1-dimethoxypropan-2-one (248 mg, 2.10 mmol, 1.0 equiv) in methanol (5 mL) with 4-methylbenzenesulfonohydrazide (380 mg, 2.04 mmol, 1 equiv), 4-cyanobenzylamine (309 mg, 2.29 mmol, 1.1 equiv) and triethylamine (232 mg, 2.30 mmol, 1.1 equiv). After 5 minutes at 140 °C and cooling to room temperature, the reaction mixture was concentrated *in vacuo* to give an orange oil. The oil was portioned between CH$_2$Cl$_2$:water (40 mL, 1:1) and the organic layer separated. The aqueous was extracted with CH$_2$Cl$_2$ (2 × 15 mL) and the combined organic extracts washed with brine (20 mL), dried over a hydrophobic frit and concentrated *in vacuo* to give an orange oil. The crude material was purified by

chromatography (50–100% EtOAc in heptane) to yield **152** as a white solid (369 mg, 1.86 mmol, 91%).

Appearance: White solid

M.pt: 87–88 °C

ν (neat): 2233, 1330, 1215, 1052, 772 cm^{-1}

^{1}H NMR (400 MHz, CD$_3$OD) δ ppm 7.76 (2H, d, J = 8.4 Hz), 7.73 (1H, s), 7.45 (2H, d, J = 8.1 Hz), 5.67 (2H, s), 2.32 (3H, s)

^{13}C NMR (101 MHz, CD$_3$OD) δ ppm 143.5, 141.1, 132.5, 128.3, 122.6, 117.9, 111.9, 52.6, 9.1

HRMS (ESI Orbitrap) *m/z*: Calcd for C$_{11}$H$_{11}$N$_4$ [M+H]$^+$ 199.0978; found [M+H]$^+$ 199.0973

1-(4-Bromobenzyl)-4-methyl-1,2,3-triazole (153)
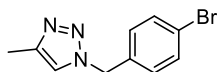
Using General Procedure 1 with 1,1-dimethoxypropan-2-one (249 mg, 2.11 mmol, 1.0 equiv) in methanol (5 mL) with 4-methylbenzenesulfonohydrazide (382 mg, 2.05 mmol, 1 equiv), 4-bromobenzylamine (430 mg, 2.27 mmol, 1.1 equiv) and triethylamine (232 mg, 2.30 mmol, 1.1 equiv). After 5 minutes at 140 °C and cooling to room temperature, the reaction mixture was concentrated *in vacuo* to give an orange oil. The oil was portioned between CH$_2$Cl$_2$:water (40 mL, 1:1) and the organic layer separated. The aqueous was extracted with CH$_2$Cl$_2$ (2 × 15 mL) and the combined organic extracts washed with brine (20 mL), dried over a hydrophobic frit and concentrated *in vacuo* to give an orange oil. The crude material was purified by chromatography (1% MeOH in CH$_2$Cl$_2$ with 1% triethylamine in the CH$_2$Cl$_2$ portion) to yield **153** as a white solid (412 mg, 1.64 mmol, 80%).

Appearance: White solid

M.pt: 98–99 °C

ν (neat): 3139, 1556, 1488, 1333, 1213, 1056, 806, 758 cm^{-1}

^{1}H NMR (400 MHz, CD$_3$OD) δ ppm 7.70 (1H, s), 7.49–7.56 (2H, m), 7.19–7.28 (2H, m), 5.52 (2H, s), 2.31 (3H, s)

^{13}C NMR (101 MHz, CD$_3$OD) δ ppm 143.4, 134.8, 131.7, 129.6, 122.3, 122.0, 52.6, 9.1

HRMS (ESI Orbitrap) *m/z*: Calcd for C$_{10}$H$_{11}$^{79}BrN$_3$ [M+H]$^+$ 252.0131; found [M+H]$^+$ 252.0130

4-((4-Methyl-1,2,3-triazol-1-yl)methyl)pyridine (154)
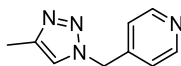
Using General Procedure 1 with 1,1-dimethoxypropan-2-one (249 mg, 2.11 mmol, 1.0 equiv) in methanol (5 mL) with 4-methylbenzenesulfonohydrazide (381 mg, 2.05 mmol, 1 equiv), pyridin-4-ylmethanamine (224 mg, 2.07 mmol, 1.0 equiv) and triethylamine (232 mg, 2.30 mmol, 1.1 equiv). After 5 minutes at 140 °C and cooling to room temperature, the reaction mixture was concentrated *in vacuo* to give an orange oil. The oil was portioned between CH$_2$Cl$_2$:water (40 mL, 1:1) and the organic layer separated. The aqueous was extracted with CH$_2$Cl$_2$ (2 × 15 mL) and the combined organic extracts washed with brine (20 mL), dried over a hydrophobic frit and concentrated *in vacuo* to give an orange oil. The crude material was purified by chromatography (50–100% EtOAc in heptane) to yield **154** as a white solid (241 mg, 1.38 mmol, 68%).

Appearance: White solid

M.pt: 84–85 °C

ν (neat): 2966, 1601, 1542, 1418, 1218, 1053, 782 cm^{-1}

^{1}H NMR (400 MHz, CD$_3$OD) δ ppm 8.49–8.59 (2H, m), 7.81 (1H, s), 7.21–7.31 (2H, m), 5.68 (2H, s), 2.35 (3H, s)

^{13}C NMR (101 MHz, CD$_3$OD) δ ppm 149.3, 146.0, 143.6, 122.8, 122.5, 51.8, 9.1

HRMS (ESI Orbitrap) *m/z*: Calcd for C$_9$H$_{11}$N$_4$ [M+H]$^+$ 175.0978; found [M+H]$^+$ 175.0974

1-(Furan-2-ylmethyl)-4-methyl-1,2,3-triazole (155)
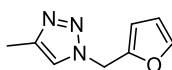
Using General Procedure 1 with 1,1-dimethoxypropan-2-one (248 mg, 2.10 mmol, 1.0 equiv) in methanol (5 mL) with 4-methylbenzenesulfonohydrazide (379 mg, 2.04 mmol, 1 equiv), furfurylamine (220 mg, 2.26 mmol, 1.1 equiv) and triethylamine (232 mg, 2.30 mmol, 1.1 equiv). After 5 minutes at 140 °C and cooling to room temperature, the reaction mixture was concentrated *in vacuo* to give an orange oil. The oil was portioned between CH_2Cl_2:water (40 mL, 1:1) and the organic layer separated. The aqueous was extracted with CH_2Cl_2 (2 × 15 mL) and the combined organic extracts washed with brine (20 mL), dried over a hydrophobic frit and concentrated *in vacuo* to give **155** as a yellow oil (318 mg, 1.95 mmol, 96%).

Appearance: Yellow oil

ν (neat): 1557, 1504, 1334, 1216, 1148, 1050, 1012, 778 cm^{-1}

^{1}H NMR (400 MHz, CD$_3$OD) δ ppm 7.67 (1H, s), 7.52 (1H, s), 6.53 (1H, d, *J* = 2.7 Hz), 6.43 (1H, s), 5.57 (2H, s), 2.30 (3H, s)

^{13}C NMR (101 MHz, CD$_3$OD) δ ppm 148.2, 143.4, 143.2, 121.9, 110.4, 109.5, 46.0, 9.0

HRMS (ESI Orbitrap) *m/z*: Calcd for $C_8H_{10}ON_3$ [M+H]$^+$ 164.0818; found [M+H]$^+$ 164.0813

***Tert*-butyl 3-(4-methyl-1,2,3-triazol-1-yl)azetidine-1-carboxylate (156)**
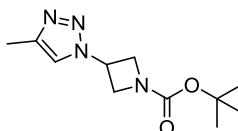
Using General Procedure 1 with 1,1-dimethoxypropan-2-one (247 mg, 2.09 mmol, 1.0 equiv) in methanol (5 mL) with 4-methylbenzenesulfonohydrazide (379 mg, 2.03 mmol, 1 equiv), *tert*-butyl 3-aminoazetidine-1-carboxylate (350 mg, 2.03 mmol, 1.0 equiv) and triethylamine (232 mg, 2.30 mmol, 1.1 equiv). After 5 minutes at 140 °C and cooling to room temperature, the

reaction mixture was concentrated *in vacuo* to give an orange oil. The oil was portioned between CH$_2$Cl$_2$:water (40 mL, 1:1) and the organic layer separated. The aqueous was extracted with CH$_2$Cl$_2$ (2 × 15 mL) and the combined organic extracts washed with brine (20 mL), dried over anhydrous MgSO$_4$ and concentrated *in vacuo* to give **156** as a sticky gum (456 mg, 1.88 mmol, 92%).

Appearance: Colourless gum

ν (neat): 2975, 1696, 1557, 1391, 1366, 1124 cm^{-1}

^{1}H NMR (400 MHz, CD$_3$OD) δ ppm 7.89 (1H, s), 5.43 (1H, tt, *J* = 8.4, 5.1 Hz), 4.49 (2H, t, *J* = 8.4 Hz), 4.24–4.34 (2H, m), 2.35 (3H, s), 1.49 (95, s)

^{13}C NMR (101 MHz, CD$_3$OD) δ ppm 156.6, 143.3, 121.6, 80.3, 56.1, 48.7, 27.2, 9.1

HRMS (ESI Orbitrap) *m/z*: Calcd for C$_{11}$H$_{19}$O$_2$N$_4$ [M+H]$^+$ 239.1503; found [M+H]$^+$ 239.1502

4-Methyl-1-phenyl-1,2,3-triazole (157)
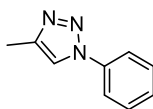
Using General Procedure 1 with 1,1-dimethoxypropan-2-one (248 mg, 2.10 mmol, 1.0 equiv) in methanol (5 mL) with 4-methylbenzenesulfonohydrazide (382 mg, 2.05 mmol, 1 equiv), aniline (214 mg, 2.30 mmol, 1.1 equiv) and triethylamine (232 mg, 2.30 mmol, 1.1 equiv. After 5 minutes at 140 °C and cooling to room temperature, the reaction mixture was concentrated *in vacuo* to give an orange oil. The oil was portioned between CH$_2$Cl$_2$:water (40 mL, 1:1) and the organic layer separated. The aqueous was extracted with CH$_2$Cl$_2$ (2 × 15 mL) and the combined organic extracts washed with brine (20 mL), dried over a hydrophobic frit and concentrated *in vacuo* to give an off-white solid. The crude material was purified by chromatography (CH$_2$Cl$_2$ with 1% triethylamine) to yield **157** as a white solid (242 mg, 1.52 mmol, 74%).

Appearance: White solid

M.pt: 79–80 °C

ν (neat): 1596, 1500, 1343, 1223, 1047, 762 cm^{-1}

^{1}H NMR (400 MHz, CD$_3$OD) δ ppm 8.26 (1H, s), 7.80–7.86 (2H, m), 7.55–7.62 (2H, m), 7.45–7.52 (1H, m), 2.42 (3H, s)

^{13}C NMR (101 MHz, CD$_3$OD) δ ppm 143.8, 137.1, 129.5, 128.5, 120.3, 120.0, 9.1

HRMS (ESI Orbitrap) *m/z*: Calcd for C$_9$H$_{10}$N$_3$ [M+H]$^+$ 160.0869; found [M+H]$^+$ 160.0868

1-(3-(Furan-2-yl)-1*H*-pyrazol-5-yl)-4-methyl-1,2,3-triazole (158)
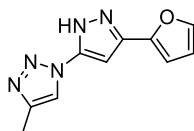
Using General Procedure 1 with 1,1-dimethoxypropan-2-one (247 mg, 2.09 mmol, 1.0 equiv) in methanol (5 mL) with 4-methylbenzenesulfonohydrazide (379 mg, 2.03 mmol, 1 equiv), 3-(furan-2-yl)-1*H*-pyrazol-5-amine (303 mg, 2.03 mmol, 1.0 equiv) and triethylamine (232 mg, 2.30 mmol, 1.1 equiv). After 5 minutes at 140 °C and cooling to room temperature, the reaction mixture was concentrated *in vacuo* to a yellow solid. The solid was dissolved in CH$_2$Cl$_2$ (25 mL), washed with water (20 mL) and the organic layer separated. The aqueous layer was extracted two further times with EtOAc (15 mL) and the combined organic extracts washed with brine (20 mL) and dried over anhydrous MgSO$_4$ before concentrating *in vacuo* to give **158** as a beige powder (400 mg, 1.86 mmol, 91%).

Appearance: Beige powder

M.pt: 218–220 °C

ν (neat): 2850, 1552, 1540, 1228, 980, 948, 748 cm^{-1}

^{1}H NMR (400 MHz, (CD$_3$)$_2$SO) δ ppm 13.71 (1H, br. s), 8.35 (1H, s), 7.85 (1H, d, *J* = 1.4 Hz), 6.99 (1H, d, *J* = 3.4 Hz), 6.93 (1H, s), 6.68 (1H, dd, *J* = 3.4, 1.4 Hz), 2.33 (3H, s)

^{13}C NMR (101 MHz, (CD$_3$)$_2$SO) δ ppm 147.2, 144.1, 143.2, 136.1, 120.6, 112.4, 108.6, 93.2, 10.9. One signal missing.

HRMS (ESI Orbitrap) *m/z*: Calcd for C$_{10}$H$_{10}$ON$_5$ [M+H]$^+$ 216.0880; found [M+H]$^+$ 216.0873

(1*R*,2*S*)-1-(4-Methyl-1,2,3-triazol-1-yl)-2,3-dihydro-1*H*-inden-2-ol (159)
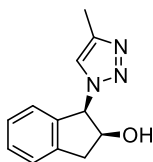
Using General Procedure 1 with 1,1-dimethoxypropan-2-one (247 mg, 2.09 mmol, 1.0 equiv) in methanol (5 mL) with 4-methylbenzenesulfonohydrazide (379 mg, 2.03 mmol, 1 equiv), (1*R*,2*S*)-1-amino-2,3-dihydro-1*H*-inden-2-ol (303 mg, 2.03 mmol, 1.0 equiv) and triethylamine (232 mg, 2.30 mmol, 1.1 equiv). After 5 minutes at 140 °C and cooling to room temperature, the reaction mixture was concentrated *in vacuo* to give an orange oil. The oil was portioned between CH$_2$Cl$_2$:water (40 mL, 1:1) and the organic layer separated. The aqueous was extracted with CH$_2$Cl$_2$ (2 × 15 mL) and the combined organic extracts washed with brine (20 mL), dried over anhydrous MgSO$_4$ and concentrated *in vacuo* to give **159** as a pale-yellow oil that slowly crystallised (355 mg, 1.62 mmol, 80%).

Appearance: White solid

M.pt: 133–135 °C

ν (neat): 3164, 155, 1365, 1058, 748 cm^{-1}

^{1}H NMR (400 MHz, CD$_3$OD) δ ppm 7.34–7.45 (3H, m), 7.24–7.31 (1H, m), 7.13 (1H, d, *J* = 7.6 Hz), 6.14 (1H, d, *J* = 5.9 Hz), 4.77–4.82 (1H, m), 3.27–3.31 (1H, m), 3.09 (1H, dd, *J* = 16.2, 4.4 Hz), 2.32 (3H, s)

^{13}C NMR (101 MHz, CD$_3$OD) δ ppm 142.3, 141.2, 137.9, 129.1, 127.1, 125.2, 124.6, 122.4, 72.8, 67.8, 38.8, 9.1

HRMS (ESI Orbitrap) *m/z*: Calcd for C$_{12}$H$_{14}$ON$_3$ [M+H]$^+$ 216.1131; found [M+H]$^+$ 216.1132

(*S*)-Ethyl 2-(4-methyl-1,2,3-triazol-1-yl)propanoate (160)
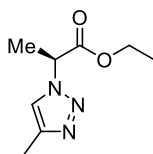
Following a modification of General Procedure 1 using 1,1-dimethoxypropan-2-one (194 mg, 1.64 mmol, 1.1 equiv) in methanol (4.1 mL) with 4-methylbenzenesulfonohydrazide (280 mg, 1.50 mmol, 1 equiv), ethyl-*L*-alaninate hydrochloride (280 mg, 1.82 mmol, 1.2 equiv) and triethylamine (152 mg, 1.51 mmol, 1.0 equiv). After 16 h at 75 °C and cooling to room temperature, the reaction mixture was concentrated *in vacuo* to give an orange oil. The oil was portioned between CH_2Cl_2:water (40 mL, 1:1) and the organic layer separated. The aqueous was extracted with CH_2Cl_2 (2 × 15 mL) and the combined organic extracts washed with brine (20 mL), dried over a hydrophobic frit and concentrated *in vacuo* to give an orange oil. The crude material was purified by chromatography (50–100% EtOAc in heptane) to yield **160** as a colourless oil (231 mg, 1.26 mmol, 84%).

Appearance: Colourless oil

ν (neat): 1741, 1558, 1162, 1193, 1048 cm^{-1}

^{1}H NMR (400 MHz, CD$_3$OD) δ ppm 7.84 (1H, s), 5.51 (1H, q, *J* = 7.4 Hz), 4.23 (2H, q, *J* = 7.1 Hz), 2.35 (3H, s), 1.83 (3H, d, *J* = 7.4 Hz), 1.27 (3H, t, *J* = 7.1 Hz)

^{13}C NMR (101 MHz, CD$_3$OD) δ ppm 169.4, 142.8, 121.8, 61.8, 58.1, 16.4, 12.9, 9.1

HRMS (ESI Orbitrap) *m/z*: Calcd for $C_8H_{14}N_3O_2$ [M+H]$^+$ 184.1081; found [M+H]$^+$ 184.1075

Chiral HPLC data:

Racemic marker using racemic starting material.
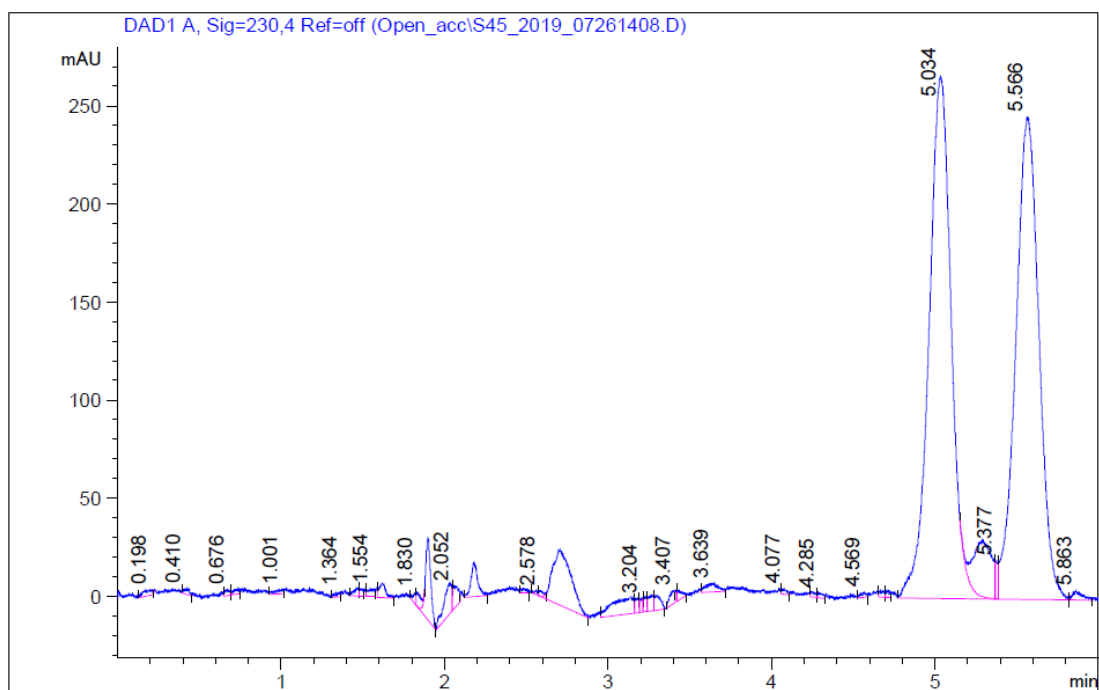
80:20 e.r. using microwave conditions
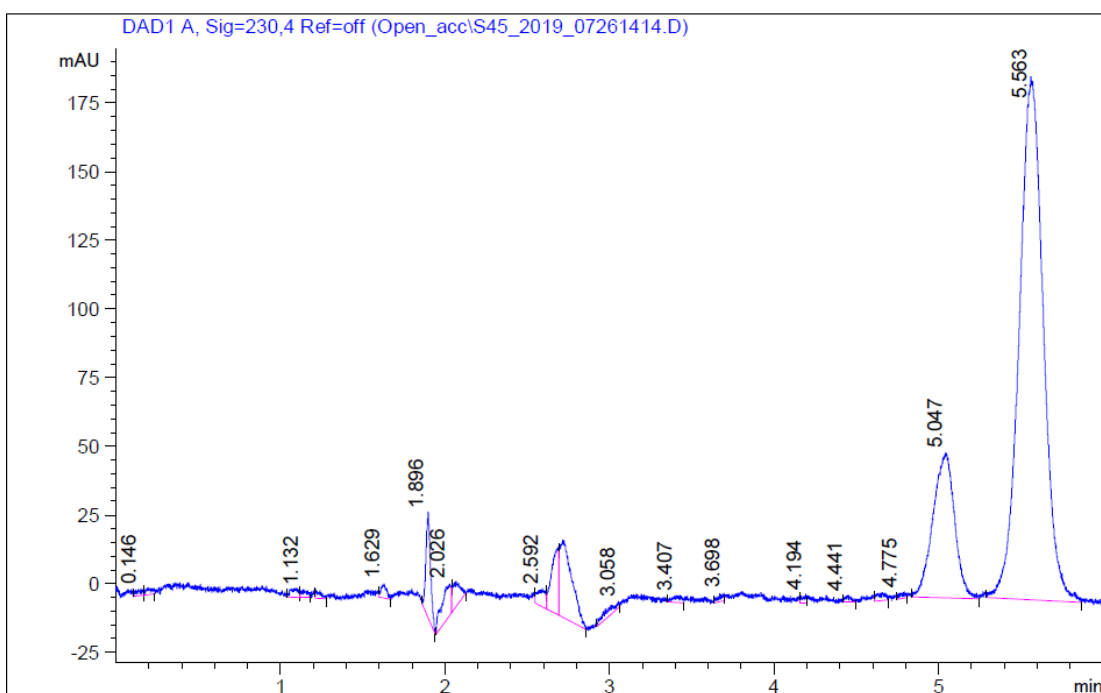
98:2 e.r. using modified conditions
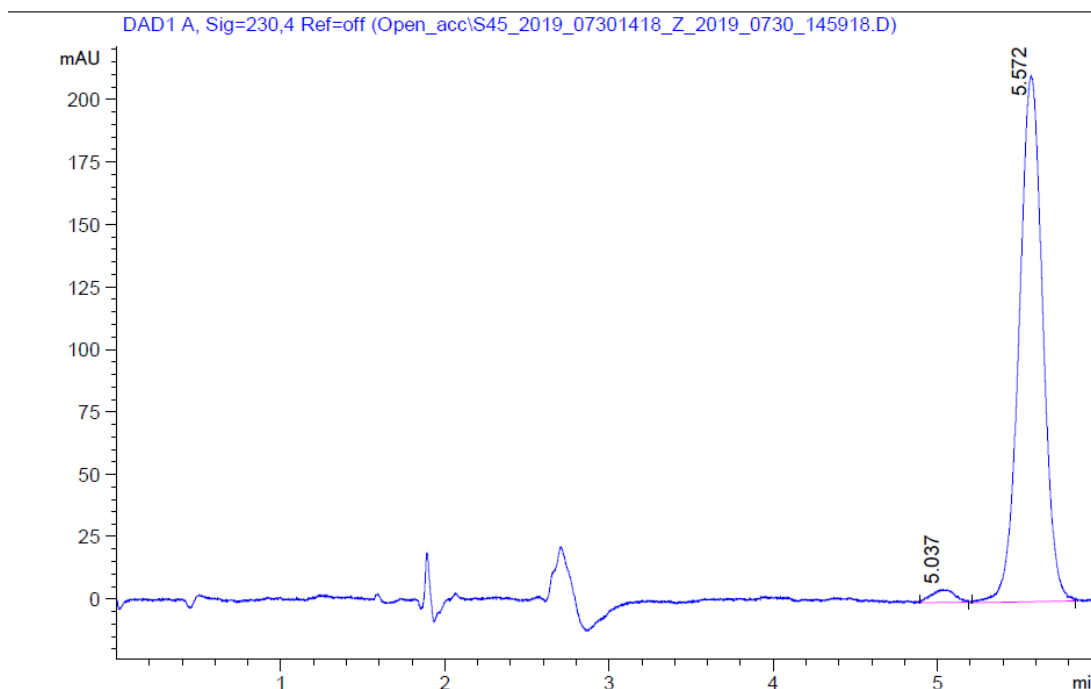
Synthesis of triazole 144 on gram-scale

1-Cyclohexyl-4-methyl-1,2,3-triazole (144) (7g scale)
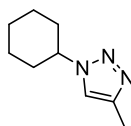
To a round-bottomed flask containing 1,1-dimethoxypropan-2-one (6.67 g, 56.5 mmol, 1.02 equiv) in methanol (140 mL) under nitrogen was added 4-methylbenzenesulfonohydrazide (10.28 g, 55.2 mmol, 1 equiv) at room temperature. The reaction was stirred for 5 minutes before addition of cyclohexylamine (6.07 g, 61.2 mmol, 1.11 equiv) and triethylamine (6.17 g, 61.2 mmol, 1.11 equiv) before heating under reflux. After 16 hours the reaction was cooled to room temperature and concentrated *in vacuo* to yield a yellow solid which was portioned between CH_2Cl_2 (100 mL) and water (100 mL). The layers were separated, and the remaining aqueous portion was extracted with CH_2Cl_2 (2 × 50 mL) before combining the organic portions, washing with brine (50 mL), drying over a hydrophobic frit and concentrating *in vacuo*. The

crude material was purified by chromatography (25–75% EtOAc in heptane) to give 1-cyclohexyl-4-methyl-1,2,3-triazole (**144**) as a white solid. (7.43 g, 44.9 mmol, 81%).

Analytical data consistent with those recorded previously.
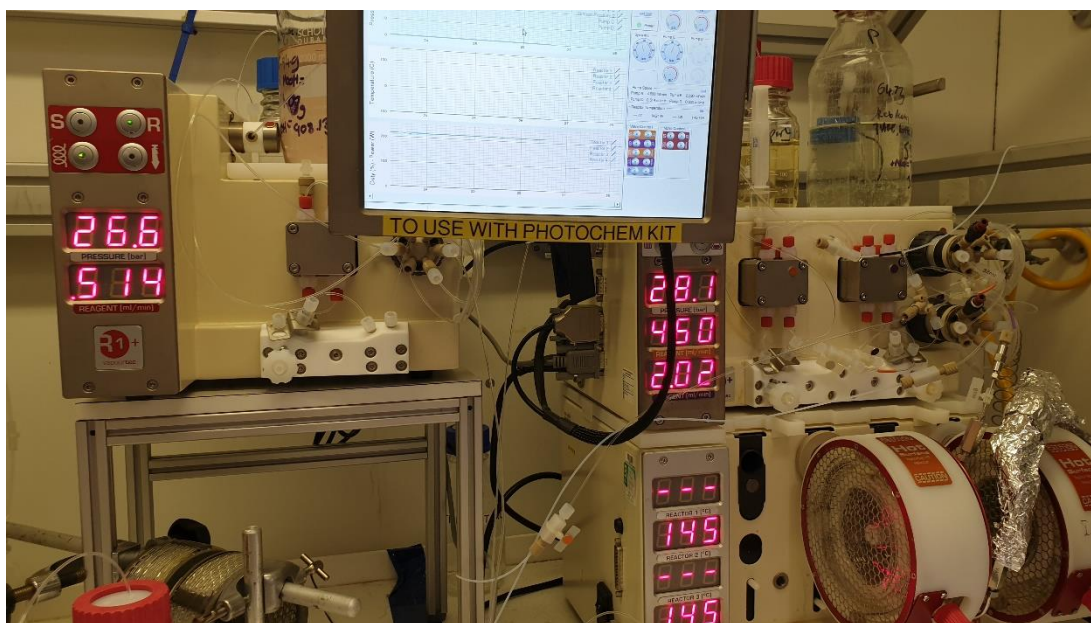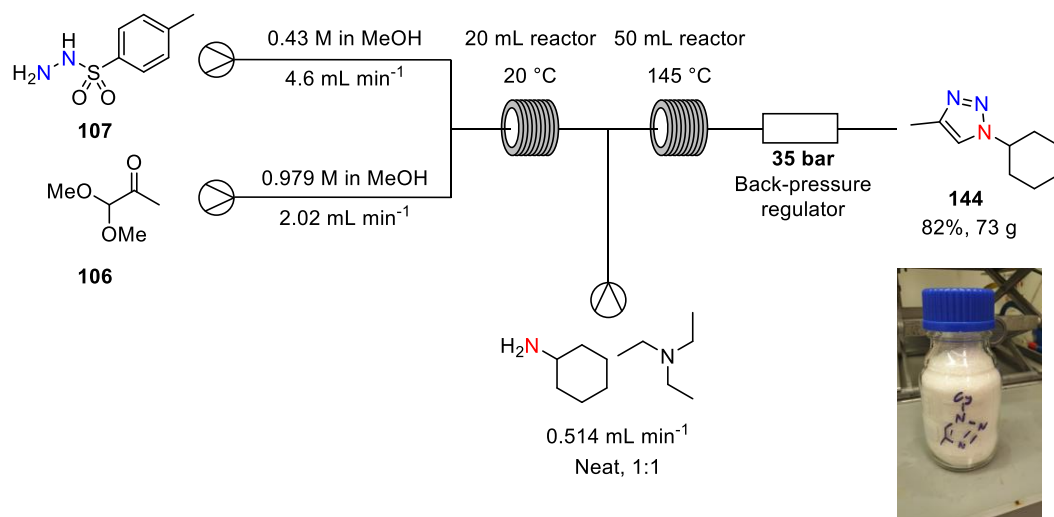
Figure 37: Flow set-up. Top left, R1+ pump for cyclohexylamine and triethylamine. Right, R2+ pump for 107 and 106. Right, 2 × 25 mL Vapourtec high temperature stainless steel coil reactors. Bottom left, 2 × 10 mL PFA loops.

Solutions of 4-methylbenzenesulfonohydrazide (**107**) (100.17 g, 538 mmol, 1 equiv) in methanol (1250 mL total volume) and 1,1-dimethoxypropan-2-one (**106**) (64.77 g, 548 mmol,

1.02 equiv) in methanol (560 mL total volume) were combined at flow rates of 4.60 mL min^{-1} and 2.02 mL min^{-1} in 1/16" OD PFA tubing through a Peek T-piece using the Vapourtec R2+ pump (1.979 mmol min^{-1} and 1.977 mmol min^{-1}). The solution was passed through 2 × 10 mL PFA loops at 20 °C. A solution of cyclohexylamine (80.11 g, 808 mmol, 1.50 equiv) and triethylamine (82.13 g, 812 mmol, 1.51 equiv) was pumped through 1/16" OD PFA tubing using the Vapourtec R1+ pump at a flow rate of 0.514 mL min^{-1} (1.982 mmol min^{-1}) and combined with the hydrazone solution through a Peek T-piece. The combined solution was then passed through 2 × 25 mL Vapourtec high temperature stainless steel coil reactors heated by the Vapourtec R4 to 145 °C (combined flow rate of 7.13 mL min^{-1}). After the 2 × 25 mL loop, the solution was passed through a 1 mL stainless steel cooling loop before passing through 2 × 17.2 bar Kinesis back-pressure regulators. The output solution was consistently monitored by HPLC and the production and quality of triazole **144** remained consistent throughout the 4.5-hour processing period. The output solution was concentrated *in vacuo* in batches of 50−100 mL until the feed solution of 4-methylbenzenesulfonohydrazide had been consumed. The combined crude reaction mixture was concentrated *in vacuo* until an off-white precipitate formed. The precipitate was portioned between EtOAc (800 mL) and water (800 mL) and the organic layer separated. The aqueous solution was extracted with EtOAc (3 × 400 mL) and the combined organic layer washed with saturated sodium bicarbonate (200 mL), brine (200 mL) and dried over anhydrous MgSO$_4$. The organic portion was concentrated *in vacuo* such that ~50 mL EtOAc remained. To the white suspension was added heptane (500 mL) and the slurry was vigorously stirred at 0 °C for 1 hour. The white crystalline material was filtered and dried in a vacuum oven at 40 °C for 16 hours to give 1-cyclohexyl-4-methyl-1,2,3-triazole (**144**) as a white crystalline solid (61.73 g, 374 mmol, 70%). The residual organic portion was recrystalised in the same manner to give a second crop of 1-cyclohexyl-4-methyl-1,2,3-triazole (**144**) as an off-white crystalline solid (11.44 g, 69 mmol, 13%). The two crops combined yielded 1-cyclohexyl-4-methyl-1,2,3-triazole (**144**) (73.17 g, 443 mmol, 82%).

Analytical data consistent with those recorded previously.

**Synthesis of *α*-ketoacetals**

1,1-Diethoxypent-4-en-2-one (171)
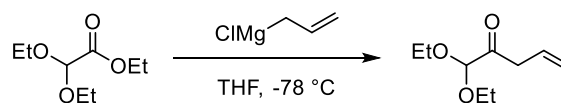
Using the reported procedure.[105] To a −78 °C solution of ethyl 2,2-diethoxyacetate (1.762 g, 10.0 mmol) in dry THF (40 mL) was added allyl magnesium chloride (2 M in THF, 5.1 mL, 10.2 mmol, 1.0 equiv) dropwise over 15 minutes. After the addition was complete, the reaction was left for 2 hours at −78 °C, quenched with 20% NH_4Cl (20 mL) and allowed to warm to room temperature. Water (50 mL) and EtOAc (100 mL) were added, the organic layer separated and the aqueous portion extracted with EtOAc (3 × 100 mL). The combined organic extracts were washed with brine (50 mL), dried over anhydrous $MgSO_4$ and concentrated *in vacuo*. The resultant oil was purified by chromatography (0–15% EtOAc in heptane) to give 1,1-diethoxypent-4-en-2-one (**171**) as a colourless oil (809 mg, 4.7 mmol, 47%).

Appearance: Colourless oil

^1H NMR (400 MHz, $CDCl_3$) δ ppm 5.94 (1H, ddt, *J* = 17.1, 10.2, 7.0, 7.0 Hz), 5.18 (2H, m), 4.60 (1H, s), 3.71 (2H, m), 3.58 (2H, m), 3.38 (2H, m), 1.25 (6H, t, *J* = 7.0 Hz)

^{13}C NMR (101 MHz, $CDCl_3$) δ ppm 203.9, 129.7, 118.5, 102.4, 63.4, 41.6, 15.1

The spectroscopic data is concurrent with the literature..[105]

1,1-Diethoxyhex-5-en-2-one (172)
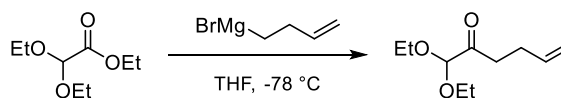
Using the reported procedure.[105] To a −78 °C solution of ethyl 2,2-diethoxyacetate (4.000 g, 22.7 mmol) in dry THF (80 mL) was added but-3-en-1-ylmagnesium bromide (0.5 M in THF, 45.0 mL, 22.50 mmol, 1.1 equiv) at a rate of 25 mL/hour. After the addition was complete, the

reaction was left for 2 hours at −78 °C, quenched with 20% NH$_4$Cl (50 mL) and allowed to warm to room temperature. Water (100 mL) and EtOAc (250 mL) were added, the organic layer separated and the aqueous portion extracted with EtOAc (2 × 150 mL). The combined organic extracts were washed with brine (75 mL), dried over anhydrous MgSO$_4$ and concentrated *in vacuo*. The resultant oil was purified by chromatography (0–15% EtOAc in heptane) to give 1,1-diethoxyhex-5-en-2-one (**172**) as a colourless oil (2.210 g, 11.87 mmol, 58%).

Appearance: Colourless oil

ν (neat): 2979, 1729, 1642, 1404, 1319, 1059 cm^{-1}

^{1}H NMR (400 MHz, CDCl$_3$) δ ppm 5.82 (1H, ddt, *J* = 17.0, 10.4, 7.4 Hz), 4.94–5.10 (2H, m), 4.56 (1H, s), 3.70 (2H, dq, *J* = 9.5, 7.1 Hz), 3.56 (2H, dq, *J* = 9.5, 7.1 Hz), 2.70 (2H, t, *J* = 7.4 Hz), 2.30–2.37 (2H, m), 1.25 (6H, t, *J* = 7.1 Hz)

^{13}C NMR (101 MHz, CDCl$_3$) δ ppm 205.4, 137.1, 115.0, 102.7, 63.3, 35.9, 26.9, 15.1

HRMS (ESI Orbitrap) *m/z*: Calcd for C$_{10}$H$_{19}$O$_3$ [M+H]$^+$ 187.1329; found [M+H]$^+$ 187.1337

1-Cyclohexyl-2,2-diethoxyethanone (174)
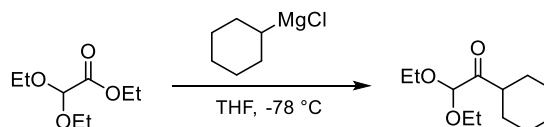
Using the reported procedure.[105] To a −78 °C solution of ethyl 2,2-diethoxyacetate (4.000 g, 22.7 mmol) in dry THF (80 mL) was added cyclohexylmagnesium chloride (2 M in Et$_2$O, 11.4 mL, 22.70 mmol, 1.0 equiv) at a rate of 25 mL/hour. After the addition was complete, the reaction was left for 2 hours at −78 °C, quenched with 20% NH$_4$Cl (50 mL) and allowed to warm to room temperature. Water (100 mL) and EtOAc (250 mL) were added, the organic layer separated and the aqueous portion extracted with EtOAc (2 × 150 mL). The combined organic extracts were washed with brine (75 mL), dried over anhydrous MgSO$_4$ and concentrated *in vacuo*. The resultant oil was purified by chromatography

(0–5% EtOAc in heptane) to give 1-cyclohexyl-2,2-diethoxyethanone (**174**) as a colourless oil (2.397 g, 11.18 mmol, 49%).

Appearance: Colourless oil

ν (neat): 2930, 2855, 1719, 1449, 1060 cm^{-1}

^{1}H NMR (400 MHz, CDCl$_3$) δ ppm 4.65 (1H, s), 3.68 (2H, dq, J = 9.5, 7.1 Hz), 3.56 (2H, dq, J = 9.5, 7.1 Hz), 2.76–2.87 (1H, m), 1.72–1.87 (4H, m), 1.63–1.71 (1H, m), 1.27–1.42 (5H. m), 1.24 (6H, t, J = 7.1 Hz)

^{13}C NMR (101 MHz, CDCl$_3$) δ ppm 208.7, 102.1, 63.1, 45.3, 28.5, 25.8, 25.6, 15.2

HRMS (ESI Orbitrap) *m/z*: Calcd for C$_{12}$H$_{23}$O$_3$ [M+H]$^+$ 215.1642; found [M+H]$^+$ 215.1640

1,1-Diethoxy-4-phenylbutan-2-one (175)
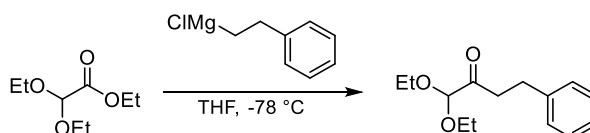
Using the reported procedure.[105] To a −78 °C solution of ethyl 2,2-diethoxyacetate (1.714 g, 9.73 mmol, 1 equiv) in dry THF (40 mL) was added phenethylmagnesium chloride (1M in THF, 11 mL, 11.00 mmol, 1.1 equiv) at a rate of 25 mL/hour. After the addition was complete, the reaction was left for 2 hours at −78 °C, quenched with 20% NH$_4$Cl (50 mL) and allowed to warm to room temperature. Water (50 mL) and EtOAc (150 mL) were added, the organic layer separated and the aqueous portion with EtOAc (2 × 150 mL). The combined organic extracts were washed with brine (50 mL), dried over anhydrous MgSO$_4$ and concentrated *in vacuo*. The resultant oil was purified by chromatography (10% EtOAc in heptane) to give 1,1-diethoxy-4-phenylbutan-2-one **175** as a colourless oil (1.471 g, 6.22 mmol, 64%).

Appearance: Colourless oil

ν (neat): 2978, 1728, 1497, 1454, 1059 cm^{-1}

^{1}H NMR (400 MHz, *CD₃CN*) δ ppm 7.14–7.31 (5H, m), 4.59 (1H, s), 3.62 (2H, dq, *J* = 9.5, 7.1 Hz), 3.51 (2H, dq, *J* = 9.5, 7.1 Hz), 2.80–2.91 (4H, m), 1.16 (6H, t, *J* = 7.1 Hz)

^{13}C NMR (101 MHz, *CD₃CN*) δ ppm 206.5, 142.9, 129.7, 129.7, 127.3, 103.6, 64.4, 39.8, 30.0, 15.9

HRMS (ESI Orbitrap) *m/z*: *Unable to detect mass*

Synthesis of 4-substituted triazoles

4-Allyl-1-benzyl-1,2,3-triazole (177) and (*E*)-1-Benzyl-4-(pro*p*-1-en-1-yl)-1,2,3-triazole (178a) and (*Z*)-1-Benzyl-4-(pro*p*-1-en-1-yl)-1,2,3-triazole (178b)

177   **178a**   **178b**

E : Z
4 : 1
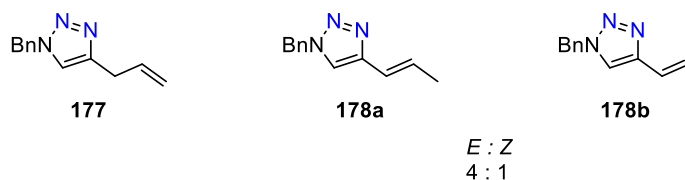
Following a modification of General Procedure 1 with 1,1-diethoxypent-4-en-2-one (**171**) (146 mg, 0.85 mmol, 1.1 equiv) in MeOH (2.1 mL) with 4-methylbenzenesulfonohydrazide (149 mg, 0.80 mmol, 1 equiv), the reaction was stirred at room temperature for 10 minutes (at which point consumption of 4-methylbenzenesulfonohydrazide was observed) before addition of benzylamine (94 mg, 0.88 mmol, 1.1 equiv) and triethylamine (89 mg, 0.88 mmol, 1.1 equiv. After 5 minutes at 140 °C and cooling to room temperature, the reaction mixture was portioned between CH₂Cl₂:water (40 mL, 1:1) and the organic layer separated. The aqueous layer was extracted with CH₂Cl₂ (2 × 15 mL) and the combined organic extracts washed with brine (20 mL) and dried over a hydrophobic frit before concentrating *in vacuo* to a yellow oil. The crude material was purified by chromatography (25–100% EtOAc in heptane) to give a colourless oil (121 mg). The oil was re-purified by MDAP (15–55% MeCN in H₂O with 0.05% ammonium bicarbonate buffer). The fractions containing the products were concentrated under reduced pressure to remove the volatile organics and the resulting aqueous portion was extracted into CH₂Cl₂ (3 × 15 mL), which were dried over a hydrophobic frit and concentrated *in vacuo* to give 4-allyl-1-benzyl-1,2,3-triazole (**177**) as a white solid (62 mg, 0.31 mmol, 39%) and (*E*)-1-

benzyl-4-(pro*p*-1-en-1-yl)-1,2,3-triazole (**178a**) and (*Z*)-1-benzyl-4-(pro*p*-1-en-1-yl)-1,2,3-triazole (**178b**) as a white solid in a 4:1 ratio by ^{1}H NMR analysis (39 mg, 0.20 mmol, 24%).

4-Allyl-1-benzyl-1,2,3-triazole (177)
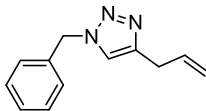
Appearance: White solid

M.pt: 40–41 °C

ν (neat): 3122, 3063, 1647, 1450, 1430, 1213, 1051, 922, 705 cm^{-1}

^{1}H NMR (400 MHz, CDCl$_3$) δ ppm 7.25–7.44 (5H, m), 7.22 (1H, s), 5.97 (1H, ddt, *J* = 16.9, 10.2, 6.7, 6.8 Hz), 5.51 (2H, s), 5.02–5.21 (2H, m), 3.50 (2H, d, *J* = 6.7 Hz)

^{13}C NMR (101 MHz, CDCl$_3$) δ ppm 146.8, 135.0, 134.9, 129.1, 128.6, 128.0, 121.0, 116.7, 54.1, 30.4

HRMS (ESI Orbitrap) *m/z*: Calcd for C$_{12}$H$_{14}$N$_3$ [M+H]$^+$ 200.1182; found [M+H]$^+$ 200.1181

(*E*)-1-Benzyl-4-(pro*p*-1-en-1-yl)-1,2,3-triazole (178a) and (*Z*)-1-Benzyl-4-(pro*p*-1-en-1-yl)-1,2,3-triazole (178b)
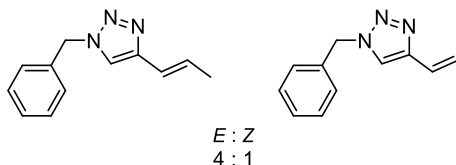
Appearance: White solid

ν (neat): 3037, 2910, 1493, 1454, 1432, 1221, 1052, 1027, 964 cm^{-1}

^{1}H NMR (400 MHz, CDCl$_3$) δ ppm (<u>*E* isomer</u>) 7.86 (1H, s), 7.24–7.51 (5H, m), 6.22–6.50 (2H, m), 5.55 (2H, s), 1.83–1.89 (3 H, m) (<u>*Z* isomer</u>) 7.99 (1H, s), 7.17–7.49 (5H, m), 6.22–6.50 (1H, m), 5.89 (1H, dq, *J* = 11.6, 7.1 Hz), 5.60 (2H, s), 1.91 (3H, dd, *J* = 7.1, 1.7 Hz)

^{13}C NMR (101 MHz, CDCl$_3$) δ ppm 146.4, 144.8, 135.5, 135.4, 128.6, 128.4, 128.2, 128.1, 128.1, 127.6, 127.6, 122.5, 120.4, 118.9, 118.2, 53.5, 53.4, 17.1, 14.0

HRMS (ESI Orbitrap) *m/z*: Calcd for C$_{12}$H$_{14}$N$_3$ [M+H]$^+$ 200.1182; found [M+H]$^+$ 200.1179

1-Benzyl-4-(but-3-en-1-yl)-1,2,3-triazole (181)
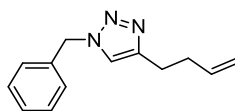
Following a modification of General Procedure 1 with 1,1-diethoxyhex-5-en-2-one (**172**) (292 mg, 1.57 mmol, 1.0 equiv) in methanol (3.9 mL) with 4-methylbenzenesulfonohydrazide (280 mg, 1.51 mmol, 1 equiv), the reaction was stirred at room temperature for 25 minutes (at which point consumption of 4-methylbenzenesulfonohydrazide was observed) before addition of benzylamine (186 mg, 1.74 mmol, 1.2 equiv) and triethylamine (167 mg, 1.65 mmol, 1.1 equiv). After 5 minutes at 140 °C and cooling to room temperature, the reaction mixture was portioned between CH$_2$Cl$_2$:water (40 mL, 1:1) and the organic layer separated. The aqueous layer was extracted with CH$_2$Cl$_2$ (2 × 15 mL) and the combined organic extracts washed with brine (20 mL) and dried over a hydrophobic frit before concentrating *in vacuo* to a yellow oil. The crude material was purified by preparative high-performance liquid chromatography (30–85% MeCN in water, 0.05% ammonium bicarbonate buffer). The fractions containing product were concentrated under reduced pressure to remove the volatile organics and the resulting aqueous portion was extracted into CH$_2$Cl$_2$ (3 × 50 mL). The combined organics were washed with brine (50 mL) and dried over a hydrophobic frit to yield **181** as a colourless oil (241 mg, 1.13 mmol, 75%).

Appearance: Colourless oil

ν (neat): 1641, 1551, 1497, 1435, 1217, 1049, 912, 728 cm^{-1}

^{1}H NMR (400 MHz, CD$_3$OD) δ ppm 7.72 (1H, s), 7.34–7.41 (3H, m), 7.28–7.34 (2H, m), 5.85 (1H, ddt, J = 17.0, 10.3, 6.6), 5.56 (2H, s), 4.94–5.07 (2H, m), 2.79 (2H, t, J = 7.6 Hz), 2.35–2.45 (2H, m)

^{13}C NMR (101 MHz, CD$_3$OD) δ ppm 147.5, 137.1, 135.5, 128.6, 128.1, 127.5, 121.9, 114.5, 53.4, 33.1, 24.5

HRMS (ESI Orbitrap) *m/z*: Calcd for C$_{13}$H$_{16}$N$_3$ [M+H]$^+$ 214.1339; found [M+H]$^+$ 214.1343

4-(But-3-en-1-yl)-1-phenyl-1,2,3-triazole (182)
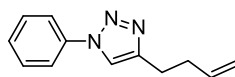
Following a modification of General Procedure 1 with 1,1-diethoxyhex-5-en-2-one (**172**) (295 mg, 1.58 mmol, 1.0 equiv) in methanol (3.9 mL) with 4-methylbenzenesulfonohydrazide (284 mg, 1.52 mmol, 1 equiv), the reaction was stirred at room temperature for 20 minutes (at which point consumption of 4-methylbenzenesulfonohydrazide was observed) before addition of aniline (163 mg, 1.75 mmol, 1.1 equiv) and triethylamine (174 mg, 1.72 mmol, 1.1 equiv). After 5 minutes at 140 °C and cooling to room temperature, the reaction mixture was portioned between CH_2Cl_2:water (40 mL, 1:1) and the organic layer separated. The aqueous layer was extracted with CH_2Cl_2 (2 × 15 mL) and the combined organic extracts washed with brine (20 mL) and dried over a hydrophobic frit before concentrating *in vacuo* to a yellow oil. The crude material was purified by chromatography (0–25% EtOAc in heptane) to yield **182** as a white solid (246 mg, 1.24 mmol, 81%).

Appearance: White solid

M.pt: 44–45 °C

ν (neat): 1639, 1599, 1501, 1228, 1047, 910, 754, 685 cm^{-1}

^{1}H NMR (400 MHz, CD$_3$OD) δ ppm 8.31 (1H, s), 7.79–7.88 (2H, m), 7.55–7.63 (2H, m), 7.43–7.53 (1H, m), 5.93 (1H, ddt, J = 17.0, 10.3, 6.6 Hz), 4.98–5.16 (2H, m), 2.90 (2H, t, J = 7.5 Hz), 2.44–2.57 (2H, m)

^{13}C NMR (101 MHz, CD$_3$OD) δ ppm 148.0, 137.1, 129.5, 128.5, 120.1, 120.0, 114.7, 33.0, 24.5. One signal missing.

HRMS (ESI Orbitrap) *m/z*: Calcd for C$_{12}$H$_{14}$N$_3$ [M+H]$^+$ 200.1182; found [M+H]$^+$ 200.1188

4-(But-3-en-1-yl)-1-methyl-1,2,3-triazole (183)
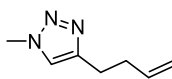
Following a modification of General Procedure 1 with 1,1-diethoxyhex-5-en-2-one (**172**) (291 mg, 1.56 mmol, 1.0 equiv) in methanol (3.9 mL) with 4-methylbenzenesulfonohydrazide (280 mg, 1.51 mmol, 1 equiv), the reaction was stirred at room temperature for 20 minutes (at which point consumption of 4-methylbenzenesulfonohydrazide was observed) before addition of methylamine (40 wt% solution in water, 0.15 mL, 1.73 mmol, 1.2 equiv) and triethylamine (167 mg, 1.65 mmol, 1.1 equiv). After 5 minutes at 140 °C and cooling to room temperature, the reaction mixture was portioned between CH_2Cl_2:water (40 mL, 1:1) and the organic layer separated. The aqueous layer was extracted with CH_2Cl_2 (2 × 15 mL) and the combined organic extracts washed with brine (20 mL) and dried over a hydrophobic frit before concentrating *in vacuo* to a yellow oil. The crude material was purified by preparative high-performance liquid chromatography (15–55% MeCN in water, 0.05% ammonium bicarbonate buffer). The fractions containing product were concentrated under reduced pressure to remove the volatile organics and the resulting aqueous portion was extracted into CH_2Cl_2 (3 × 50 mL). The combined organics were washed with brine (50 mL) and dried over a hydrophobic frit to yield **183** as a colourless oil (170 mg, 1.24 mmol, 82%).

Appearance: Colourless oil

ν (neat): 2926 (m), 1641 (m), 1552 (m), 1436 (m), 1216 (s), 1052 (s), 913 (vs)

^{1}H NMR (400 MHz, CD_3OD) δ ppm 7.69 (1H, s), 5.78–5.94 (1H, m), 4.95–5.11 (2H, m), 4.07 (3H, s), 2.80 (2H, t, *J* = 7.5 Hz), 2.38–2.47 (2H, m)

^{13}C NMR (101 MHz, CD_3OD) δ ppm 148.9, 138.7, 124.4, 116.1, 37.0, 34.7, 26.0

HRMS (ESI Orbitrap) *m/z*: Calcd for $C_7H_{12}N_3$ [M+H]$^+$ 138.1026; found [M+H]$^+$ 138.1029

4-(But-3-en-1-yl)-1-cyclohexyl-1,2,3-triazole (184)
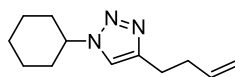
Following a modification of General Procedure 1 with 1,1-diethoxyhex-5-en-2-one (**172**) (295 mg, 1.59 mmol, 1.1 equiv) in methanol (3.9 mL) with 4-methylbenzenesulfonohydrazide (279 mg, 1.50 mmol, 1 equiv), the reaction was stirred at room temperature for 25 minutes (at which point consumption of 4-methylbenzenesulfonohydrazide was observed) before addition of cyclohexylamine (173 mg, 1.75 mmol, 1.2 equiv) and triethylamine (174 mg, 1.72 mmol, 1.2 equiv. After 5 minutes at 140 °C and cooling to room temperature, the reaction mixture was portioned between CH_2Cl_2:water (40 mL, 1:1) and the organic layer separated. The aqueous layer was extracted with CH_2Cl_2 (2 × 15 mL) and the combined organic extracts washed with brine (20 mL) and dried over a hydrophobic frit before concentrating *in vacuo* to a yellow oil. The crude material was purified by chromatography (0–25% EtOAc in heptane) to yield **184** as a white solid (259 mg, 1.26 mmol, 84%).

Appearance: White solid

M.pt: 61–62 °C

ν (neat): 2932, 2856, 1639, 1450, 1214, 1053, 908 cm^{-1}

^{1}H NMR (400 MHz, CDCl$_3$) δ ppm 7.28 (1H, s), 5.87 (1H, ddt, J = 17.0, 10.3, 6.5), 4.96–5.12 (2H, m), 4.41 (1H, tt, J = 11.8, 3.8 Hz), 2.82 (2H, t, J = 7.6 Hz), 2.38–2.50 (2H, m), 2.11–2.27 (2H, m), 1.87–1.98 (2H, m), 1.62–1.82 (3H, m), 1.46 (2H, qt, J = 13.0, 3.4 Hz), 1.16–1.35 (1H, m)

^{13}C NMR (101 MHz, CDCl$_3$) δ ppm 147.0, 137.7, 118.3, 115.3, 59.9, 33.6, 33.4, 25.3, 25.2, 25.2

HRMS (ESI Orbitrap) *m/z*: Calcd for $C_{12}H_{20}N_3$ [M+H]$^+$ 206.1652; found [M+H]$^+$ 206.1658

4-(But-3-en-1-yl)-1H-1,2,3-triazole (185)
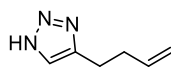
Following a modification of General Procedure 1 with 1,1-diethoxyhex-5-en-2-one (**172**) (292 mg, 1.57 mmol, 1.05 equiv) in methanol (3.5 mL) with 4-methylbenzenesulfonohydrazide (280 mg, 1.50 mmol, 1 equiv), the reaction was stirred at room temperature for 2 hours (at which point consumption of 4-methylbenzenesulfonohydrazide was observed) before addition of ammonia (7 M solution in MeOH) (0.47 mL, 3.31 mmol, 2.2 equiv) *note triethylamine omitted to aid isolation.* After 5 minutes at 140 °C and cooling to room temperature, the reaction mixture was portioned between CH$_2$Cl$_2$:water (40 mL, 1:1) and the organic layer separated. The aqueous layer was extracted with CH$_2$Cl$_2$ (2 × 15 mL) and the combined organic extracts washed with brine (20 mL) and dried over a hydrophobic frit before concentrating *in vacuo* to a yellow oil. The crude material was purified by preparative high-performance liquid chromatography (15–55% MeCN in water, 0.05% ammonium bicarbonate buffer). The fractions containing product were concentrated under reduced pressure to remove the volatile organics and the resulting aqueous portion was extracted into CH$_2$Cl$_2$ (3 × 50 mL). The combined organics were washed with brine (50 mL) and dried over a hydrophobic frit to yield **185** as a colourless oil (139 mg, 1.13 mmol, 75%).

Appearance: Colourless oil

ν (neat): 3137, 2922, 2854, 1641, 1440, 1111, 995, 912 cm^{-1}

^{1}H NMR (400 MHz, CDCl$_3$) δ ppm 14.2 (1H, *br.* s), 7.56 (), 5.85 (1H, ddt, *J* = 17.1, 10.3, 6.5 Hz), 4.95–5.13 (2H, m), 2.88 (2H, t, *J* = 7.5 Hz), 2.39–2.56 ppm (2H, m)

^{13}C NMR (101 MHz, CDCl$_3$) δ ppm 144.8, 137.0, 129.4, 115.7, 33.0, 24.1

HRMS (ESI Orbitrap) *m/z*: Calcd for C$_6$H$_{10}$N$_3$ [M+H]$^+$ 124.0869; found [M+H]$^+$ 124.0875

4-Butyl-1-methyl-1H-1,2,3-triazole (186)

183 **186** **186**

13 : 1
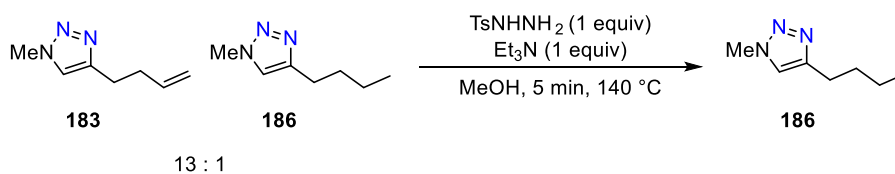
To the mixture of **183** and **186** (49 mg, 0.36 mmol, 1 equiv) was added methanol (0.9 mL) and 4-methylbenzenesulfonohydrazide (74 mg, 0.40 mmol, 1.1 equiv). The vial was sealed, and the reaction was heated to 140 °C for 5 minutes before concentrating *in vacuo*. The crude material was portioned between CH_2Cl_2:water (10 mL, 1:1) and the organic layer separated. The aqueous layer was extracted with CH_2Cl_2 (2 × 5 mL) and the combined organic extracts washed with brine (10 mL) and dried over a hydrophobic frit before concentrating *in vacuo* to yield 4-butyl-1-methyl-1*H*-1,2,3-triazole **186** as a white crystalline solid (49 mg, 0.36 mmol, 100%).

Appearance: White crystalline solid

M.pt: 50–51 °C

ν (neat): 3061, 2958, 2926, 1567, 1497, 1311, 1215, 1162 cm^{-1}

^{1}H NMR (400 MHz, CDCl$_3$) δ ppm 7.24 (1H, s), 4.03 (3H, s), 2.68 (2H, t, *J* = 7.5 Hz), 1.62 (2H, q, *J* = 7.5 Hz), 1.36 (2H, q, *J* = 7.5 Hz), 0.91 (3H, t, *J* = 7.5 Hz)

^{13}C NMR (101 MHz, CDCl$_3$) δ ppm 148.7, 121.6, 36.4, 31.6, 25.3, 22.2, 13.8

HRMS (ESI Orbitrap) *m/z*: Calcd for $C_7H_{14}N_3$ [M+H]$^+$ 140.1182; found [M+H]$^+$ 140.1189

1-Benzyl-4-phenyl-1,2,3-triazole (189)
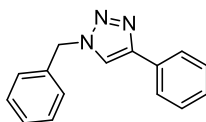
Following a modification of General Procedure 1 with 2,2-diethoxy-1-phenylethanone (**173**) (438 mg, 2.10 mmol, 1.0 equiv) in methanol (5.3 mL) with 4-methylbenzenesulfonohydrazide

(377 mg, 2.02 mmol, 1 equiv), the reaction was stirred at room temperature for 2 hours (at which point consumption of 4-methylbenzenesulfonohydrazide was observed) before addition of benzylamine (238 mg, 2.22 mmol, 1.1 equiv) and triethylamine (225 mg, 2.22 mmol, 1.1 equiv). After 5 minutes at 140 °C and cooling to room temperature, the reaction mixture was portioned between CH_2Cl_2:water (40 mL, 1:1) and the organic layer separated. The aqueous layer was extracted with CH_2Cl_2 (2 × 15 mL) and the combined organic extracts washed with brine (20 mL) and dried over a hydrophobic frit before concentrating *in vacuo* to a yellow solid. The crude material was purified by chromatography (25–50% EtOAc in heptane) to yield **189** as a white solid (341 mg, 1.50 mmol, 72%).

Appearance: White solid

M.pt: 130–131 °C

ν (neat): 1465, 1456, 1353, 1219, 1048, 763, 724, 693 cm^{-1}

^{1}H NMR (400 MHz, CDCl$_3$) δ ppm 7.81 (2H, d, *J* = 7.4 Hz), 7.67 (1H, s), 7.36–7.45 (5H, m), 7.29–7.36 (3H, m), 5.59 (2H, s)

^{13}C NMR (101 MHz, CDCl$_3$) δ ppm 148.3, 134.7, 130.6, 129.2, 128.8, 128.2, 128.1, 125.7, 119.5, 54.3. One aromatic signal missing.

HRMS (ESI Orbitrap) *m/z*: Calcd for $C_{15}H_{14}N_3$ [M+H]$^+$ 236.1182; found [M+H]$^+$ 236.1179

1,4-Diphenyl-1,2,3-triazole (190)
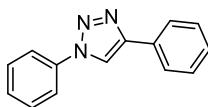
Following a modification of General Procedure 1 with 2,2-diethoxy-1-phenylethanone (**173**) (442 mg, 2.12 mmol, 1.0 equiv) in methanol (5.3 mL) with 4-methylbenzenesulfonohydrazide (377 mg, 2.03 mmol, 1 equiv), the reaction was stirred at room temperature for 2 hours (at which point consumption of 4-methylbenzenesulfonohydrazide was observed) before addition of aniline (208 mg, 2.30 mmol, 1.1 equiv) and triethylamine (226 mg, 2.30 mmol, 1.1 equiv).

After 5 minutes at 140 °C and cooling to room temperature, the reaction mixture was portioned between CH_2Cl_2:water (40 mL, 1:1) and the organic layer separated. The aqueous layer was extracted with CH_2Cl_2 (2 × 15 mL) and the combined organic extracts washed with brine (20 mL) and dried over a hydrophobic frit before concentrating *in vacuo* to give an off-white solid. The crude material was purified by chromatography (25–50% EtOAc in heptane) to yield **190** as a white crystalline solid (298 mg, 1.35 mmol, 67%).

Appearance: White crystals

M.pt: 183–184 °C

ν (neat): 3048, 1597, 1502, 1465, 1228, 755, 688 cm^{-1}

^{1}H NMR (400 MHz, CDCl$_3$) δ ppm 8.22 (1H, s), 7.90–7.98 (2H, m), 7.76–7.87 (2H, m), 7.54–7.61 (2H, m), 7.45–7.53 (3H, m), 7.37–7.44 (1H, m)

^{13}C NMR (101 MHz, CDCl$_3$) δ ppm 148.4, 137.1, 130.3, 129.8, 128.9, 128.8, 128.4, 125.9, 120.6, 117.6

HRMS (ESI Orbitrap) *m/z*: Calcd for $C_{14}H_{12}N_3$ [M+H]$^+$ 222.1026; found [M+H]$^+$ 222.1022

1-Methyl-4-phenyl-1,2,3-triazole (191)
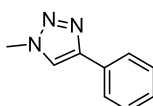
Following a modification of General Procedure 1 with 2,2-diethoxy-1-phenylethanone (**173**) (438 mg, 2.10 mmol, 1.0 equiv) in methanol (5.3 mL) with 4-methylbenzenesulfonohydrazide (376 mg, 2.02 mmol, 1 equiv), the reaction was stirred at room temperature for 2 hours (at which point consumption of 4-methylbenzenesulfonohydrazide was observed) before addition of methylamine (40 wt% solution in water, 0.19 mL, 2.22 mmol, 1.1 equiv) and triethylamine (225 mg, 2.22 mmol, 1.1 equiv). After 5 minutes at 140 °C and cooling to room temperature, the reaction mixture was portioned between CH_2Cl_2:water (40 mL, 1:1) and the organic layer separated. The aqueous layer was extracted with CH_2Cl_2 (2 × 15 mL) and the combined

organic extracts washed with brine (20 mL) and dried over a hydrophobic frit before concentrating *in vacuo* to a yellow solid. The crude material was purified by chromatography (25–50% EtOAc in heptane) to yield **191** as a white solid (277 mg, 1.74 mmol, 86%).

Appearance: White solid

M.pt: 121–122 °C

ν (neat): 1471, 1413, 1218, 1191, 839, 767, 700 cm^{-1}

^{1}H NMR (400 MHz, CDCl$_3$) δ ppm 7.83 (2H, d, *J* = 7.4 Hz), 7.74 (1H, s), 7.40–7.46 (2H, m), 7.31–7.37 (1H, m), 4.15 (3H, s)

^{13}C NMR (101 MHz, CDCl$_3$) δ ppm 148.1, 130.6, 128.8, 128.2, 125.7, 120.5, 36.8

HRMS (ESI Orbitrap) *m/z*: Calcd for C$_9$H$_{10}$N$_3$ [M+H]$^+$ 160.0869; found [M+H]$^+$ 160.0867

1-Cyclohexyl-4-phenyl-1,2,3-triazole (192)
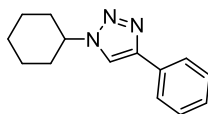
Following a modification of General Procedure 1 with 2,2-diethoxy-1-phenylethanone (**173**) (441 mg, 2.12 mmol, 1.0 equiv) in methanol (5.3 mL) with 4-methylbenzenesulfonohydrazide (379 mg, 2.04 mmol, 1 equiv), the reaction was stirred at room temperature for 2 hours (at which point consumption of 4-methylbenzenesulfonohydrazide was observed) before addition of cyclohexylamine (222 mg, 2.24 mmol, 1.1 equiv) and triethylamine (227 mg, 2.24 mmol, 1.1 equiv). After 5 minutes at 140 °C and cooling to room temperature, the reaction mixture was portioned between CH$_2$Cl$_2$:water (40 mL, 1:1) and the organic layer separated. The aqueous layer was extracted with CH$_2$Cl$_2$ (2 × 15 mL) and the combined organic extracts washed with brine (20 mL) and dried over a hydrophobic frit before concentrating *in vacuo* to a yellow solid. The crude material was purified by chromatography (25–50% EtOAc in heptane) to yield **192** as a white solid (339 mg, 1.49 mmol, 73%).

Appearance: White solid

M.pt: 102–103 °C

ν (neat): 2938, 2852, 1433, 1055, 828, 762, 693 cm^{-1}

^{1}H NMR (400 MHz, CDCl$_3$) δ ppm 7.82–7.93 (2H, m), 7.78 (1H, s), 7.44 (2H, t, J = 7.5 Hz), 7.32–7.38 (1H, m), 4.52 (1H, tt, J = 11.8, 3.9 Hz), 2.29 (2H, dd, J = 12.8, 2.0 Hz), 1.92–2.02 (2H, m), 1.76–1.89 (3H, m), 1.51 (2H, qt, J = 12.9, 3.2 Hz), 1.23–1.41 (1H, m)

^{13}C NMR (101 MHz, CDCl$_3$) δ ppm 147.3, 130.9, 128.8, 128.0, 125.6, 117.2, 60.2, 33.6, 25.2, 25.2

HRMS (ESI Orbitrap) m/z: Calcd for C$_{14}$H$_{18}$N$_3$ [M+H]$^+$ 228.1495; found [M+H]$^+$ 228.1492

4-Phenyl-1H-1,2,3-triazole (193)
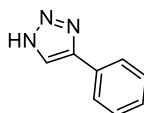
Following a modification of General Procedure 1 with 2,2-diethoxy-1-phenylethanone (**173**) (332 mg, 1.60 mmol, 1.0 equiv) in methanol (3.5 mL) with 4-methylbenzenesulfonohydrazide (284 mg, 1.53 mmol, 1 equiv), the reaction was stirred at room temperature for 2 hours (at which point consumption of 4-methylbenzenesulfonohydrazide was observed) before addition of ammonia (7 M solution in MeOH) (0.48 mL, 3.36 mmol, 2.2 equiv) *note triethylamine omitted to aid isolation*. After 5 minutes at 140 °C and cooling to room temperature, the reaction mixture was portioned between CH$_2$Cl$_2$:water (40 mL, 1:1) and the organic layer separated. The aqueous layer was extracted with CH$_2$Cl$_2$ (2 × 15 mL) and the combined organic extracts washed with brine (20 mL) and dried over a hydrophobic frit before concentrating *in vacuo* to a yellow solid. The crude material was purified by chromatography (0–50% EtOAc in heptane) to yield **193** as colourless oil (164 mg, 1.13 mmol, 74%).

Appearance: Colourless oil

^{1}H NMR (400 MHz, CD$_3$OD) δ ppm 8.17 (1H, s), 7.80–7.90 (2H, m), 7.42–7.51 (2H, m), 7.33–7.41 ppm (1H, m)

^{13}C NMR (101 MHz, CD$_3$OD) δ ppm 149.2, 136.4, 133.9, 132.6, 132.1, 129.5

The spectroscopic data is concurrent with the literature.[315]

1-Benzyl-4-cyclohexyl-1,2,3-triazole (195)
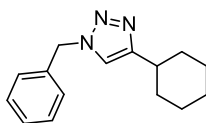
Following a modification of General Procedure 1 with 1-cyclohexyl-2,2-diethoxyethanone (**174**) (339 mg, 1.58 mmol, 1.0 equiv) in methanol (4.0 mL) with 4-methylbenzenesulfonohydrazide (287 mg, 1.54 mmol, 1 equiv), the reaction was stirred at room temperature for 90 minutes (at which point consumption of 4-methylbenzenesulfonohydrazide was observed) before addition of benzylamine (186 mg, 1.74 mmol, 1.1 equiv) and triethylamine (174 mg, 1.72 mmol, 1.1 equiv). After 5 minutes at 140 °C and cooling to room temperature, the reaction mixture was portioned between CH$_2$Cl$_2$:water (40 mL, 1:1) and the organic layer separated. The aqueous layer was extracted with CH$_2$Cl$_2$ (2 × 15 mL) and the combined organic extracts washed with brine (20 mL) and dried over a hydrophobic frit before concentrating *in vacuo* to a yellow oil. The crude material was purified by chromatography (25–50% EtOAc in heptane) to yield **195** as a fluffy white solid (313 mg, 1.30 mmol, 84%).

Appearance: Fluffy white solid

M.pt: 111–112 °C

ν (neat): 2920, 2852, 1540, 1451, 1208, 1051, 722, 701 cm^{-1}

^{1}H NMR (400 MHz, CDCl$_3$) δ ppm 7.32–7.42 (3H, m), 7.24–7.29 (2H, m), 7.15 (1H, s), 5.49 (2H, s), 2.68–2.82 (1H, m), 1.97–2.11 (2H, m), 1.65–1.86 (3H, m), 1.32–1.46 (4H, m), 1.11–1.30 (1H, m)

^{13}C NMR (101 MHz, CDCl$_3$) δ ppm 154.2, 135.0, 129.0, 128.6, 128.0, 119.1, 54.0, 35.4, 33.0, 26.1, 26.0

HRMS (ESI Orbitrap) *m/z*: Calcd for C$_{15}$H$_{20}$N$_3$ [M+H]$^+$ 242.1652; found [M+H]$^+$ 242.1649

4-Cyclohexyl-1-phenyl-1,2,3-triazole (196)
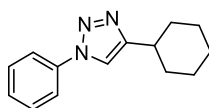
Following a modification of General Procedure 1 with 1-cyclohexyl-2,2-diethoxyethanone (**174**) (336 mg, 1.57 mmol, 1.0 equiv) in methanol (4.0 mL) with 4-methylbenzenesulfonohydrazide (286 mg, 1.54 mmol, 1 equiv), the reaction was stirred at room temperature for 90 minutes (at which point consumption of 4-methylbenzenesulfonohydrazide was observed) before addition of aniline (158 mg, 1.70 mmol, 1.1 equiv) and triethylamine (171 mg, 1.70 mmol, 1.1 equiv). After 5 minutes at 140 °C and cooling to room temperature, the reaction mixture was portioned between CH_2Cl_2:water (40 mL, 1:1) and the organic layer separated. The aqueous layer was extracted with CH_2Cl_2 (2 × 15 mL) and the combined organic extracts washed with brine (20 mL) and dried over a hydrophobic frit before concentrating *in vacuo* to a yellow solid. The crude material was purified by chromatography (0–30% EtOAc in heptane) to yield an off-white solid that was triturated with cold heptane (5 mL) to give **196** as a white solid (242 mg, 1.07 mmol, 69%).

Appearance: White solid

M.pt: 102–103 °C

ν (neat): 2929, 2846, 1599, 1504, 1222, 1444, 754, 691 cm^{-1}

^{1}H NMR (400 MHz, CDCl$_3$) δ ppm 7.71–7.77 (2H, m), 7.69 (1H, s), 7.46–7.55 (2H, m), 7.37–7.45 (1H, m), 2.86 (1H, ddt, J = 11.1, 7.5, 3.6, 3.6 Hz), 2.06–2.25 (2H, m), 1.80–1.92 (2H, m), 1.70–1.80 (1H, m), 1.36–1.54 (4H, m), 1.19–1.35 (1H, m)

^{13}C NMR (101 MHz, CDCl$_3$) δ ppm 154.4, 137.4, 129.6, 128.3, 120.4, 117.5, 35.3, 33.0, 26.2, 26.1

HRMS (ESI Orbitrap) *m/z*: Calcd for $C_{14}H_{18}N_3$ [M+H]$^+$ 228.1495; found [M+H]$^+$ 228.1491

4-Cyclohexyl-1-methyl-1,2,3-triazole (197)
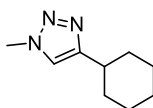
Following a modification of General Procedure 1 with 1-cyclohexyl-2,2-diethoxyethanone (**174**) (336 mg, 1.57 mmol, 1.0 equiv) in methanol (4.0 mL) with 4-methylbenzenesulfonohydrazide (286 mg, 1.54 mmol, 1 equiv), the reaction was stirred at room temperature for 2 hours (at which point consumption of 4-methylbenzenesulfonohydrazide was observed) before addition of methylamine (40 wt% solution in water, 0.16 mL, 1.85 mmol, 1.2 equiv) and triethylamine (171 mg, 1.69 mmol, 1.1 equiv). After 5 minutes at 140 °C and cooling to room temperature, the reaction mixture was portioned between CH_2Cl_2:water (40 mL, 1:1) and the organic layer separated. The aqueous layer was extracted with CH_2Cl_2 (2 × 15 mL) and the combined organic extracts washed with brine (20 mL) and dried over a hydrophobic frit before concentrating *in vacuo* to a yellow solid. The crude material was purified by chromatography (30–70% EtOAc in heptane) to yield **197** as a fluffy white solid (229 mg, 1.38 mmol, 90%).

Appearance: Fluffy white solid

M.pt: 97–98 °C

ν (neat): 2916, 2852, 1549, 1447, 1216, 1156, 1055, 845 cm^{-1}

^{1}H NMR (400 MHz, CDCl$_3$) δ ppm 7.22 (1H, s), 4.06 (3H, s), 2.70–2.83 (1H, m), 2.05 (2H, dd, *J* = 5.7, 1.7 Hz), 1.67–1.87 (3H, m), 1.34–1.50 (4H, m), 1.18–1.33 (1H, m)

^{13}C NMR (101 MHz, CDCl$_3$) δ ppm 154.0, 120.3, 36.5, 35.3, 33.1, 26.2, 26.1

HRMS (ESI Orbitrap) *m/z*: Calcd for C$_9$H$_{16}$N$_3$ [M+H]$^+$ 166.1339; found [M+H]$^+$ 166.1336

1,4-Dicyclohexyl-1,2,3-triazole (198)
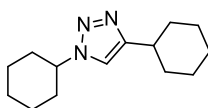
Following a modification of General Procedure 1 with 1-cyclohexyl-2,2-diethoxyethanone (**174**) (340 mg, 1.59 mmol, 1.0 equiv) in methanol (4.0 mL) with 4-methylbenzenesulfonohydrazide (288 mg, 1.55 mmol, 1 equiv), the reaction was stirred at room temperature for 90 minutes (at which point consumption of 4-methylbenzenesulfonohydrazide was observed) before addition of cyclohexylamine (173 mg, 1.75 mmol, 1.1 equiv) and triethylamine (174 mg, 1.72 mmol, 1.1 equiv). After 5 minutes at 140 °C and cooling to room temperature, the reaction mixture was portioned between CH_2Cl_2:water (40 mL, 1:1) and the organic layer separated. The aqueous layer was extracted with CH_2Cl_2 (2 × 15 mL) and the combined organic extracts washed with brine (20 mL) and dried over a hydrophobic frit before concentrating *in vacuo* to a yellow solid. The crude material was purified by chromatography (0–25% EtOAc in heptane) to yield **198** as a fluffy white solid (305 mg, 1.31 mmol, 85%).

Appearance: Fluffy white solid

M.pt: 151–152 °C

ν (neat): 3124, 2922, 2850, 1541, 1447, 1338, 1266, 1050 cm^{-1}

^1H NMR (400 MHz, $CDCl_3$) δ ppm 7.23 (1H, s), 4.41 (1H, tt, J = 11.8, 3.8 Hz), 2.76 (1H, m), 2.20 (2H, m), 2.06 (2H, m), 1.91 (2H, m), 1.77 (6H, m), 1.43 (6H, m), 1.23 (2H, m)

^{13}C NMR (101 MHz, $CDCl_3$) δ ppm 153.2, 116.7, 59.8, 35.4, 33.6, 33.1, 26.2, 26.1, 25.2, 25.2

HRMS (ESI Orbitrap) *m/z*: Calcd for $C_{14}H_{24}N_3$ $[M+H]^+$ 234.1965; found $[M+H]^+$ 234.1962

4-Cyclohexyl-1*H*-1,2,3-triazole (199)
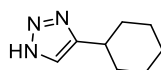
Following a modification of General Procedure 1 with 1-cyclohexyl-2,2-diethoxyethanone (**174**) (295 mg, 1.38 mmol, 1.1 equiv) in methanol (3.1 mL) with 4-methylbenzenesulfonohydrazide (242 mg, 1.30 mmol, 1 equiv), the reaction was stirred at room temperature for 2 hours (at which point consumption of 4-methylbenzenesulfonohydrazide was observed) before addition of ammonia (7 M solution in MeOH) (0.41 mL, 2.87 mmol, 2.2 equiv) *note triethylamine omitted to aid isolation*. After 5 minutes at 140 °C and cooling to room temperature, the reaction mixture was portioned between CH_2Cl_2:water (40 mL, 1:1) and the organic layer separated. The aqueous layer was extracted with CH_2Cl_2 (2 × 15 mL) and the combined organic extracts washed with brine (20 mL) and dried over a hydrophobic frit before concentrating *in vacuo* to a yellow solid. The crude material was purified by chromatography (0–50% EtOAc in heptane) to yield **199** as colourless oil (114 mg, 0.75 mmol, 58%).

Appearance: Colourless oil

ν (neat): 3150, 3117, 2925, 2853, 1727, 1548, 1450, 1378, 989, 876 cm^{-1}

^{1}H NMR (400 MHz, CDCl$_3$) δ ppm 13.42 (1H, *br.* s), 7.52 (1H, s), 2.81 (1H, tt, *J* = 11.1, 3.6 Hz), 2.00–2.10 (2H, m), 1.78–1.86 (2H, m), 1.68–1.77 (1H, m), 1.34–1.53 (4H, m), 1.20–1.34 ppm (1H, m)

^{13}C NMR (101 MHz, CDCl$_3$) δ ppm 150.2, 128.1, 34.5, 32.8, 26.0, 25.8

HRMS (ESI Orbitrap) *m/z*: Calcd for $C_8H_{14}N_3$ [M+H]$^+$ 152.1182; found [M+H]$^+$ 152.1188

1-Benzyl-4-phenethyl-1,2,3-triazole (201)
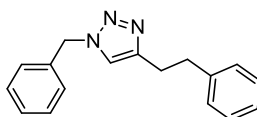
Following a modification of General Procedure 1 with 1,1-diethoxy-4-phenylbutan-2-one (**175**) (265 mg, 1.12 mmol, 1.0 equiv) in methanol (2.8 mL) with 4-methylbenzenesulfonohydrazide (202 mg, 1.08 mmol, 1 equiv), the reaction was stirred at room temperature for 5 minutes (at which point consumption of 4-methylbenzenesulfonohydrazide was observed) before addition of benzylamine (128 mg, 1.19 mmol, 1.1 equiv) and triethylamine (123 mg, 1.22 mmol, 1.1 equiv). After 5 minutes at 140 °C and cooling to room temperature, the reaction mixture was portioned between CH_2Cl_2:water (40 mL, 1:1) and the organic layer separated. The aqueous layer was extracted with CH_2Cl_2 (2 × 15 mL) and the combined organic extracts washed with brine (20 mL) and dried over a hydrophobic frit before concentrating *in vacuo* to a yellow solid. The crude material was purified by chromatography (25–100% EtOAc in heptane) to yield **201** as a white solid (238 mg, 0.90 mmol, 83%).

Appearance: White solid

M.pt: 74–75 °C

ν (neat): 1496, 1451, 1331, 1206, 1073, 1052, 696 cm^{-1}

^{1}H NMR (400 MHz, CDCl$_3$) δ ppm 7.35–7.42 (3H, m), 7.12–7.27 (7H, m), 7.04 (1H, s), 5.49 (2H, s), 2.95–3.09 (4H, m)

^{13}C NMR (101 MHz, CDCl$_3$) δ ppm 147.7, 141.2, 135.0, 129.0, 128.6, 128.5, 128.4, 127.9, 126.1, 121.1, 53.9, 35.6, 27.6

HRMS (ESI Orbitrap) *m/z*: Calcd for $C_{17}H_{18}N_3$ [M+H]$^+$ 264.1495; found [M+H]$^+$ 264.1493

4-Phenethyl-1-phenyl-1,2,3-triazole (202)
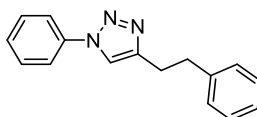
Following a modification of General Procedure 1 with 1,1-diethoxy-4-phenylbutan-2-one (**175**) (247 mg, 1.04 mmol, 1.0 equiv) in methanol (2.6 mL) with 4-methylbenzenesulfonohydrazide (186 mg, 1.00 mmol, 1 equiv), the reaction was stirred at room temperature for 5 minutes (at which point consumption of 4-methylbenzenesulfonohydrazide was observed) before addition of aniline (102 mg, 1.10 mmol, 1.1 equiv) and triethylamine (109 mg, 1.08 mmol, 1.1 equiv). After 5 minutes at 140 °C and cooling to room temperature, the reaction mixture was portioned between CH_2Cl_2:water (40 mL, 1:1) and the organic layer separated. The aqueous layer was extracted with CH_2Cl_2 (2 × 15 mL) and the combined organic extracts washed with brine (20 mL) and dried over a hydrophobic frit before concentrating *in vacuo* to a yellow solid. The crude material was purified by chromatography (25–100% EtOAc in heptane) to yield **202** as a white solid (193 mg, 0.77 mmol, 77%).

Appearance: White solid

M.pt: 104–105 °C

ν (neat): 1596, 1493, 1224, 1039, 753, 694 cm^{-1}

^{1}H NMR (400 MHz, CDCl$_3$) δ ppm 7.66–7.71 (2H, m), 7.56 (1H, s), 7.48–7.54 (2H, m), 7.39–7.45 (1H, m), 7.28–7.35 (2H, m), 7.19–7.26 (3H, m), 3.04–3.20 (4H, m)

^{13}C NMR (101 MHz, CDCl$_3$) δ ppm 148.0, 141.1, 137.2, 129.7, 128.5, 128.5, 128.5, 126.2, 120.4, 119.2, 35.5, 27.5

HRMS (ESI Orbitrap) *m/z*: Calcd for $C_{16}H_{16}N_3$ [M+H]$^+$ 250.1339; found [M+H]$^+$ 250.1335

1-Methyl-4-phenethyl-1,2,3-triazole (203)
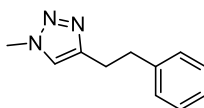
Following a modification of General Procedure 1 with 1,1-diethoxy-4-phenylbutan-2-one (**175**) (245 mg, 1.04 mmol, 1.0 equiv) in methanol (2.6 mL) with 4-methylbenzenesulfonohydrazide (188 mg, 1.01 mmol, 1 equiv), the reaction was stirred at room temperature for 5 minutes (at which point consumption of 4-methylbenzenesulfonohydrazide was observed) before addition of methylamine (40 wt% solution in water, 0.1 mL, 1.16 mmol, 1.2 equiv) and triethylamine (109 mg, 1.08 mmol, 1.1 equiv). After 5 minutes at 140 °C and cooling to room temperature, the reaction mixture was portioned between CH_2Cl_2:water (40 mL, 1:1) and the organic layer separated. The aqueous layer was extracted with CH_2Cl_2 (2 × 15 mL) and the combined organic extracts washed with brine (20 mL) and dried over a hydrophobic frit before concentrating *in vacuo* to give an orange oil. The crude material was purified by chromatography (25–100% EtOAc in heptane) to yield **203** as a white solid (166 mg, 0.88 mmol, 88%).

Appearance: White solid

M.pt: 70–71 °C

ν (neat): 3074, 2947, 1562, 1455, 1209, 1058, 742, 697 cm^{-1}

^{1}H NMR (400 MHz, CDCl$_3$) δ ppm 7.26–7.33 (2H, m), 7.17–7.24 (3H, m), 7.11 (1H, s), 4.03 (3H, s), 2.97–3.11 (4H, m)

^{13}C NMR (101 MHz, CDCl$_3$) δ ppm 147.6, 141.2, 128.5, 128.4, 126.1, 121.9, 36.5, 35.6, 27.4

HRMS (ESI Orbitrap) *m/z*: Calcd for $C_{11}H_{14}N_3$ [M+H]$^+$ 188.1182; found [M+H]$^+$ 188.1180

1-Cyclohexyl-4-phenethyl-1,2,3-triazole (204)
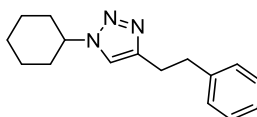
Following a modification of General Procedure 1 with 1,1-diethoxy-4-phenylbutan-2-one (**175**) (247 mg, 1.05 mmol, 1.1 equiv) in methanol (2.6 mL) with 4-methylbenzenesulfonohydrazide (187 mg, 1.00 mmol, 1 equiv), the reaction was stirred at room temperature for 5 minutes (at which point consumption of 4-methylbenzenesulfonohydrazide was observed) before addition of cyclohexylamine (113 mg, 1.14 mmol, 1.1 equiv) and triethylamine (109 mg, 1.08 mmol, 1.1 equiv). After 5 minutes at 140 °C and cooling to room temperature, the reaction mixture was portioned between CH_2Cl_2:water (40 mL, 1:1) and the organic layer separated. The aqueous layer was extracted with CH_2Cl_2 (2 × 15 mL) and the combined organic extracts washed with brine (20 mL) and dried over a hydrophobic frit before concentrating *in vacuo* to a yellow solid. The crude material was purified by chromatography (25–100% EtOAc in heptane) to yield **204** as a white solid (218 mg, 0.85 mmol, 85%).

Appearance: White solid

M.pt: 98–99 °C

ν (neat): 2932, 2857, 1450, 1209, 1057, 751, 701 cm^{-1}

^{1}H NMR (400 MHz, CDCl$_3$) δ ppm 7.28–7.34 (2H, m), 7.16–7.25 (3H, m), 7.12 (1H, s), 4.41 (1H, tt, J = 11.7, 3.9 Hz), 2.96–3.10 (4H, m), 2.13–2.23 (2H, m), 1.88–1.97 (2H, m), 1.73–1.82 (1H, m), 1.64–1.73 (2H, m), 1.46 (2H, qt, J = 12.8, 3.5 Hz), 1.28 (1H, qt, J = 12.8, 3.4 Hz)

^{13}C NMR (101 MHz, CDCl$_3$) δ ppm 146.8, 141.4, 128.5, 128.3, 126.0, 118.5, 59.9, 35.7, 33.6, 27.7, 25.2, 25.2

HRMS (ESI Orbitrap) *m/z*: Calcd for $C_{16}H_{22}N_3$ [M+H]$^+$ 256.1808; found [M+H]$^+$ 256.1806

4-Phenethyl-1H-1,2,3-triazole (205)
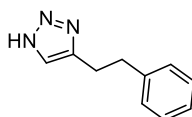
Following a modification of General Procedure 1 with 1,1-diethoxy-4-phenylbutan-2-one (**175**) (130 mg, 0.55 mmol, 1.0 equiv) in methanol (1.2 mL) with 4-methylbenzenesulfonohydrazide (98 mg, 0.53 mmol, 1 equiv), the reaction was stirred at room temperature for 5 minutes (at which point consumption of 4-methylbenzenesulfonohydrazide was observed) before addition of ammonia (7 M solution in MeOH) (0.17 mL, 1.19 mmol, 2.3 equiv) *note triethylamine omitted to aid isolation*. After 5 minutes at 140 °C and cooling to room temperature, the reaction mixture was portioned between CH_2Cl_2:water (40 mL, 1:1) and the organic layer separated. The aqueous layer was extracted with CH_2Cl_2 (2 × 15 mL) and the combined organic extracts washed with brine (20 mL) and dried over a hydrophobic frit before concentrating *in vacuo* to a yellow solid. The crude material was purified by chromatography (0–50% EtOAc in heptane) to yield **205** as colourless oil (75 mg, 0.43 mmol, 82%).

Appearance: Colourless oil

ν (neat): 3375, 2925, 2802, 1556, 1495, 1452, 1233, 1137, 968 cm^{-1}

^{1}H NMR (400 MHz, CDCl$_3$) δ ppm 7.46 (1H, s), 7.11–7.36 (5H, m), 3.08–3.16 (2H, m), 2.98–3.07 ppm (2H, m)

^{13}C NMR (101 MHz, CDCl$_3$) δ ppm 145.3, 140.8, 130.1, 128.5, 128.4, 126.3, 35.4, 26.8

HRMS (ESI Orbitrap) *m/z*: Calcd for C$_{10}$H$_{12}$N$_3$ [M+H]$^+$ 174.1026; found [M+H]$^+$ 174.1032

Synthesis of 1,5-substituted triazoles

Synthesis of aldehyde 211

Ethyl 2,2-diethoxypropanoate (210)
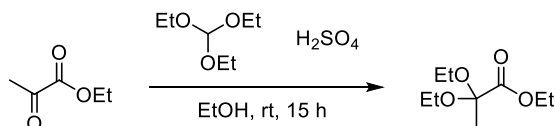
To a solution of ethyl 2-oxopropanoate (28.54 g, 0.246 mol, 1 equiv) in absolute ethanol (100 mL) was added triethyl*ortho*formate (89.00 g, 0.601 mol, 2.4 equiv) and sulfuric acid (0.92 g, 9.38 mmol, 0.04 equiv). The reaction was stirred under nitrogen for 15 hours before diluting with diethylether (200 mL) and saturated sodium bicarbonate (100 mL$_{(aq)}$). The portions were separated and the aqueous extracted with diethylether (2 × 100 mL), the combined organics washed with brine (100 mL) and dried over anhydrous MgSO$_4$ before concentrating *in vacuo* to yield ethyl 2,2-diethoxypropanoate (**210**) as a colourless oil (43.54 g, 0.229 mol, 93%).

Appearance: Colourless oil

^{1}H NMR (400 MHz, CDCl$_3$) δ ppm 4.27 (2H, qd, *J* = 7.1, 1.4 Hz), 3.56–3.65 (2H, m), 3.44–3.55 (2H, m), 1.55 (3H, s), 1.33 (3H, *app..* td, *J* = 7.1, 1.3 Hz), 1.25 (6H, *app.* td, *J* = 7.1, 1.3 Hz)

^{13}C NMR (101 MHz, CDCl$_3$) δ ppm 170.1, 99.6, 61.4, 58.0, 22.0, 15.2, 14.2

The spectroscopic data is concurrent with the literature.[108]

2,2-Diethoxypropanal (211)
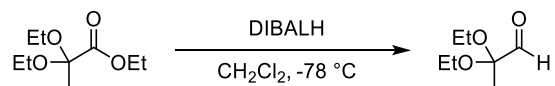
To a solution of ethyl 2,2-diethoxypropanoate (**210**) (4.97 g, 26.1 mol, 1 equiv) in CH$_2$Cl$_2$ (50 mL) at −78 °C under nitrogen was added diisobutylaluminium hydride (1M solution in hexanes, 58 mL, 58 mmol, 2.2 equiv) dropwise over the course of 60 minutes. After a further 20 minutes at −78 °C, MeOH (3 mL, 74.2 mmol, 2.8 equiv) was added over 20 minutes followed by saturated potassium sodium tartrate (50 mL$_{(aq)}$) and diethylether (50 mL). The reaction was

vigorously stirred and allowed to warm to room temperature where it was stirred for 5 hours. After the emulsions had broken up, the layers were separated, and the aqueous portion extracted with diethylether (2 × 100 mL). The combined organic portions were washed with brine (50 mL) and dried over anhydrous $MgSO_4$ before concentrating *in vacuo*. The crude product was purified by vacuum distillation (Kugelrohr, 10 mbar, 45 °C) to give 2,2-diethoxypropanal (**211**) as a colourless oil (1.65 g, 11.3 mmol, 43%).

Appearance: Colourless oil

^{1}H NMR (400 MHz, CDCl$_3$) δ ppm 9.51 (1H, s), 3.47–3.69 (4H, m), 1.38 (3H, s), 1.25 (6H, t, *J* = 7.0 Hz)

^{13}C NMR (101 MHz, CDCl$_3$) δ ppm 199.7, 100.4, 57.7, 18.8, 15.4

The spectroscopic data is concurrent with the literature.[108]

1,5-substituted triazoles

1-Benzyl-5-methyl-1,2,3-triazole (213)
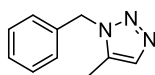
Following a modification of General Procedure 1 with 2,2-diethoxypropanal (**211**) (195 mg, 1.33 mmol, 1.1 equiv) in methanol (3.3 mL) with 4-methylbenzenesulfonohydrazide (223 mg, 1.20 mmol, 1 equiv), the reaction was stirred at room temperature for 5 minutes (at which point consumption of 4-methylbenzenesulfonohydrazide was observed) before addition of benzylamine (147 mg, 1.37 mmol, 1.1 equiv) and triethylamine (138 mg, 1.36 mmol, 1.1 equiv). After 5 minutes at 140 °C and cooling to room temperature, the reaction mixture was portioned between CH_2Cl_2:water (40 mL, 1:1) and the organic layer separated. The aqueous layer was extracted with CH_2Cl_2 (2 × 15 mL) and the combined organic extracts washed with brine (20 mL) and dried over a hydrophobic frit before concentrating *in vacuo* to a yellow oil. The crude

material was purified by chromatography (50–70% EtOAc in heptane) to yield 1-benzyl-5-methyl-1,2,3-triazole (**213**) as a white solid. (150 mg, 0.86 mmol, 72%).

Appearance: White solid

^{1}H NMR (400 MHz, CDCl$_3$) δ ppm 7.49 (1H, s), 7.30–7.41 (3H, m), 7.11–7.22 (2H, m), 5.52 (2H, s), 2.20 (3H, s)

^{13}C NMR (101 MHz, CDCl$_3$) δ ppm 134.8, 133.5, 132.7, 129.0, 128.3, 127.1, 51.6, 8.5

The spectroscopic data is concurrent with the literature.[316]

1-Cyclohexyl-5-methyl-1,2,3-triazole (214)
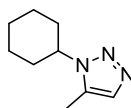
Following a modification of General Procedure 1 with 2,2-diethoxypropanal (**211**) (196 mg, 1.34 mmol, 1.1 equiv) in methanol (3.3 mL) with 4-methylbenzenesulfonohydrazide (225 mg, 1.21 mmol, 1 equiv), the reaction was stirred at room temperature for 5 minutes (at which point consumption of 4-methylbenzenesulfonohydrazide was observed) before addition of cyclohexylamine (130 mg, 1.31 mmol, 1.1 equiv) and triethylamine (138 mg, 1.36 mmol, 1.1 equiv). After 5 minutes at 140 °C and cooling to room temperature, the reaction mixture was portioned between CH$_2$Cl$_2$:water (40 mL, 1:1) and the organic layer separated. The aqueous layer was extracted with CH$_2$Cl$_2$ (2 × 15 mL) and the combined organic extracts washed with brine (20 mL) and dried over a hydrophobic frit before concentrating *in vacuo* to a yellow oil. The crude material was purified by chromatography (40–60% EtOAc in heptane) to yield 1-cyclohexyl-5-methyl-1,2,3-triazole (**214**) as a colourless oil. (153 mg, 0.93 mmol, 77%).

Appearance: Colourless oil

ν (neat): 2933, 2857, 1557, 1452, 1415, 1234, 973, 819 cm^{-1}

^{1}H NMR (400 MHz, CDCl$_3$) δ ppm 7.44 (1H, s), 4.06–4.16 (1H, m), 2.33 (3H, s), 1.94–2.15 (6H, m), 1.74–1.83 (1H, m), 1.28–1.53 (3H, m)

^{13}C NMR (101 MHz, CDCl$_3$) δ ppm 132.7, 131.3, 57.8, 32.8, 25.6, 25.1, 8.5

HRMS (ESI Orbitrap) *m/z*: Calcd for C$_9$H$_{16}$N$_3$ [M+H]$^+$ 166.1339; found [M+H]$^+$ 166.1346

5-Methyl-1-(pro*p*-2-yn-1-yl)-1,2,3-triazole (215)
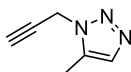
Following a modification of General Procedure 1 with 2,2-diethoxypropanal (**211**) (217 mg, 1.48 mmol, 1.1 equiv) in methanol (3.3 mL) with 4-methylbenzenesulfonohydrazide (245 mg, 1.32 mmol, 1 equiv), the reaction was stirred at room temperature for 5 minutes (at which point consumption of 4-methylbenzenesulfonohydrazide was observed) before addition of propargylamine (80 mg, 1.45 mmol, 1.1 equiv) and triethylamine (147 mg, 1.50 mmol, 1.1 equiv). After 5 minutes at 140 °C and cooling to room temperature, the reaction mixture was portioned between CH$_2$Cl$_2$:water (40 mL, 1:1) and the organic layer separated. The aqueous layer was extracted with CH$_2$Cl$_2$ (2 × 15 mL) and the combined organic extracts washed with brine (20 mL) and dried over a hydrophobic frit before concentrating *in vacuo* to a yellow oil. The crude material was purified by chromatography (40–80% EtOAc in heptane) to yield 5-methyl-1-(pro*p*-2-yn-1-yl)-1,2,3-triazole (**215**) as a colourless oil. (120 mg, 0.99 mmol, 75%).

Appearance: Colourless oil

^{1}H NMR (400 MHz, CDCl$_3$) δ ppm 7.49 (1H, s), 5.12 (2H, d, *J* = 2.5 Hz), 2.47 (1H, t, *J* = 2.5 Hz), 2.43 ppm (3H, s)

^{13}C NMR (101 MHz, CDCl$_3$) δ ppm 133.4, 132.8, 75.3, 74.6, 37.6, 8.4

The spectroscopic data is concurrent with the literature.[317]

5-Methyl-1-phenyl-1,2,3-triazole (216)

Following a modification of General Procedure 1 with 2,2-diethoxypropanal (**211**) (218 mg, 1.49 mmol, 1.1 equiv) in methanol (3.3 mL) with 4-methylbenzenesulfonohydrazide (244 mg, 1.31 mmol, 1 equiv), the reaction was stirred at room temperature for 5 minutes (at which point consumption of 4-methylbenzenesulfonohydrazide was observed) before addition of aniline (134 mg, 1.44 mmol, 1.1 equiv) and triethylamine (146 mg, 1.44 mmol, 1.1 equiv). After 5 minutes at 140 °C and cooling to room temperature, the reaction mixture was portioned between CH_2Cl_2:water (40 mL, 1:1) and the organic layer separated. The aqueous layer was extracted with CH_2Cl_2 (2 × 15 mL) and the combined organic extracts washed with brine (20 mL) and dried over a hydrophobic frit before concentrating *in vacuo* to a yellow oil. The crude material was purified by chromatography (10–50% EtOAc in heptane) to yield 5-methyl-1-phenyl-1,2,3-triazole (**216**) as an off-white solid. (142 mg, 0.89 mmol, 68%).

Appearance: Off-white solid

M.pt: 108–110 °C

^{1}H NMR (400 MHz, CDCl$_3$) δ ppm 7.45–7.65 (6H, m), 2.32 (3H, s)

^{13}C NMR (101 MHz, CDCl$_3$) δ ppm 136.4, 133.4, 133.2, 129.5, 129.3, 124.9, 9.4

The spectroscopic data is concurrent with the literature.[316]

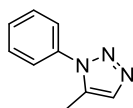**1-(*Tert*-butyl)-5-methy-1,2,3-triazole (217)**
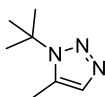
Following a modification of General Procedure 1 with 2,2-diethoxypropanal (**211**) (230 mg, 1.57 mmol, 1.2 equiv) in methanol (3.3 mL) with 4-methylbenzenesulfonohydrazide (247 mg, 1.33 mmol, 1 equiv), the reaction was stirred at room temperature for 5 minutes (at which point consumption of 4-methylbenzenesulfonohydrazide was observed) before addition of *tert-*

butylamine (107 mg, 1.46 mmol, 1.1 equiv) and triethylamine (148 mg, 1.46 mmol, 1.1 equiv). After 5 minutes at 140 °C and cooling to room temperature, the reaction mixture was portioned between CH$_2$Cl$_2$:water (40 mL, 1:1) and the organic layer separated. The aqueous layer was extracted with CH$_2$Cl$_2$ (2 × 15 mL) and the combined organic extracts washed with brine (20 mL) and dried over a hydrophobic frit before concentrating *in vacuo* to a yellow oil. The crude material was purified by chromatography (0–40% EtOAc in heptane) to yield 1-(*tert*-butyl)-5-methy-1,2,3-triazole (**217**) as a colourless oil. (143 mg, 1.03 mmol, 77%).

Appearance: Colourless oil

ν (neat): 3435, 2983, 1552, 1463, 1384, 1371, 1232, 1133, 1098 cm^{-1}

^{1}H NMR (400 MHz, CDCl$_3$) δ 7.39–7.46 (1H, m), 2.48 (3H, s), 1.69–1.78 ppm (9H, m)

^{13}C NMR (101 MHz, CDCl$_3$) δ 135.3, 131.9, 60.4, 29.6, 11.4

HRMS (ESI Orbitrap) *m/z*: Calcd for C$_7$H$_{14}$N$_3$ [M+H]$^+$ 140.1182; found [M+H]$^+$ 140.1177

Bond angle calculations for substrate 226 and 228

115.1 °
226

Faster
-HOR

227

Slower
-HOR

115.6 °
228

229

Thorpe-Ingold effect
Favoured intramolecuar H-bonding interaction with ketoketals
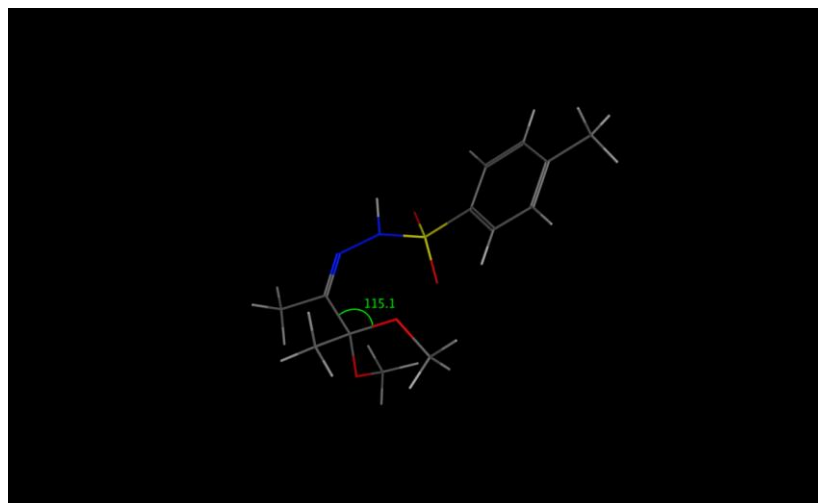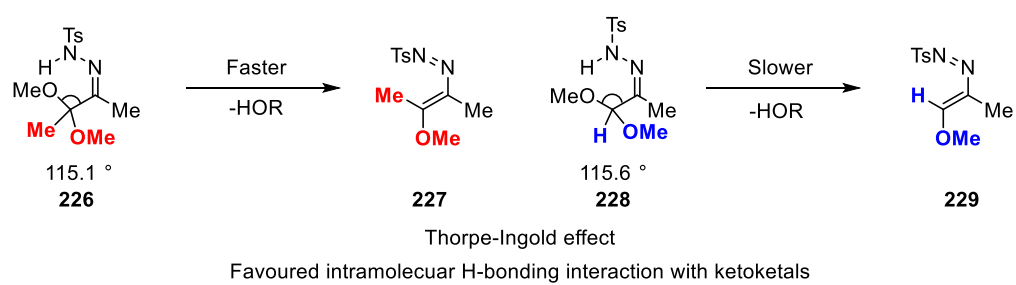
226 bond-angle calculation
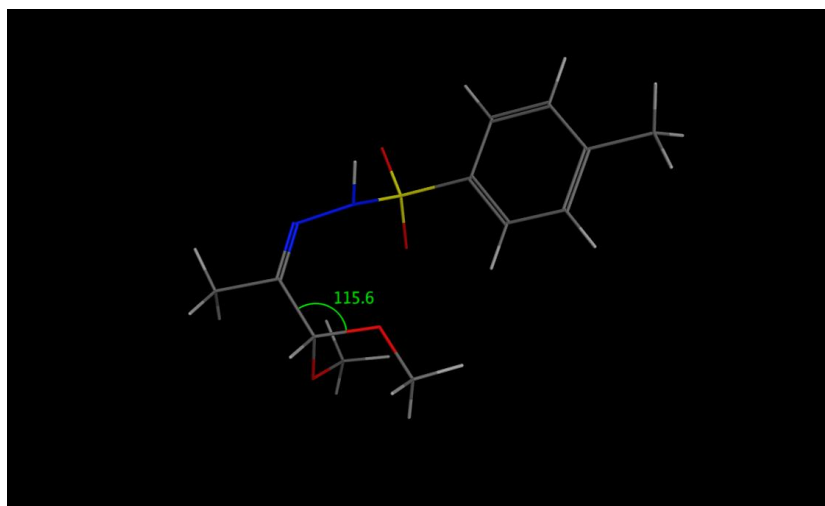
228 bond-angle calculation

Synthesis of 1,4,5-trisubstituted triazoles

Acyclic systems

1-Benzyl-4,5-dimethyl-1,2,3-triazole (234)
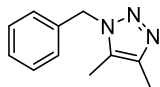
Following a modification of General Procedure 1 with 3,3-dimethoxybutan-2-one (266 mg, 2.01 mmol, 2.0 equiv) in methanol (2.5 mL) and 4-methylbenzenesulfonohydrazide (192 mg, 1.03 mmol, 1 equiv). The reaction was stirred at room temperature for 1 minute before addition of benzylamine (245 mg, 2.29 mmol, 2.2 equiv). After 5 minutes at 140 °C and cooling to room temperature, the reaction mixture was portioned between CH_2Cl_2:water (40 mL, 1:1) and the organic layer separated. The aqueous layer was extracted with CH_2Cl_2 (2 × 15 mL) and the combined organic extracts washed with brine (20 mL) and dried over a hydrophobic frit before concentrating *in vacuo* to give an orange oil. The oil was purified by chromatography (50–100% EtOAc in heptane) to give 1-benzyl-4,5-dimethyl-1,2,3-triazole (**234**) as an off-white solid. (143 mg, 0.77 mmol, 75%).

Appearance: Off-white solid

M.pt: 108–110 °C

ν (neat): 1588, 1495, 1202, 732, 710, 694 cm^{-1}

^{1}H NMR (400 MHz, CD$_3$OD) δ ppm 7.29–7.40 (3H, m), 7.19 (2H, d, *J* = 6.9 Hz), 5.54 (2H, s), 2.24 (3H, s), 2.16 (3H, s)

^{13}C NMR (101 MHz, CD$_3$OD) δ ppm 140.6, 135.3, 130.2, 128.6, 127.9, 126.9, 51.3, 8.5, 6.3

HRMS (ESI Orbitrap) *m/z*: Calcd for $C_{11}H_{14}N_3$ [M+H]$^+$ 188.1182; found [M+H]$^+$ 188.1187

4,5-Dimethyl-1-phenyl-1,2,3-triazole (235)
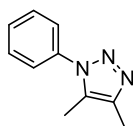
Following a modification of General Procedure 1 with 3,3-dimethoxybutan-2-one (393 mg, 2.97 mmol, 2.0 equiv) in methanol (3.8 mL) and 4-methylbenzenesulfonohydrazide (281 mg, 1.51 mmol, 1 equiv). The reaction was stirred at room temperature for 1 minute before addition of aniline (306 mg, 3.29 mmol, 2.2 equiv). After 5 minutes at 140 °C and cooling to room temperature, the reaction mixture was portioned between CH_2Cl_2:water (40 mL, 1:1) and the organic layer separated. The aqueous layer was extracted with CH_2Cl_2 (2 × 15 mL) and the combined organic extracts washed with brine (20 mL) and dried over a hydrophobic frit before concentrating *in vacuo* to give an orange oil. The oil was purified by chromatography (10–50% EtOAc in heptane) to give 4,5-dimethyl-1-phenyl-1,2,3-triazole (**235**) as an off-white solid. (238 mg, 1.37 mmol, 91%).

Appearance: Off-white solid

^{1}H NMR (400 MHz, CDCl$_3$) δ ppm 7.41–7.59 (5H, m), 2.37 (3H, s), 2.28 ppm (3H, s)

^{13}C NMR (101 MHz, CDCl$_3$) δ ppm 141.1, 136.9, 129.6, 129.4, 129.1, 124.9, 10.4, 8.8

The spectroscopic data is concurrent with the literature.[318]

Synthesis of α-ketoketals

4,4-Diethoxy-1-phenylpentan-3-one (244)
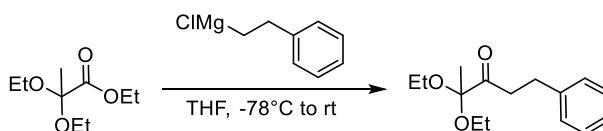
To a solution of 2,2-diethoxypropanoate (4.23 g, 22.2 mmol, 1 equiv) in THF (50 mL) at −78 °C under nitrogen was added homobenzyl magnesium chloride (1M solution in THF, 23.6 mL, 23.6 mmol, 1.1 equiv) dropwise over 60 minutes. The reaction was gradually allowed to warm

to room temperature, and after 16 hours the reaction was quenched with NH₄Cl (20% aqueous solution, 200 mL). The mixture was extracted into EtOAc (3 × 100 mL), the combined organics washed with brine (50 mL) and dried over anhydrous MgSO₄ before concentrating *in vacuo*. The crude material was purified by chromatography (5% EtOAc in heptane) to give 4,4-diethoxy-1-phenylpentan-3-one (**244**) as a colourless oil (552 mg, 2.20 mmol, 10%).

Appearance: Colourless oil

^{1}H NMR (400 MHz, CDCl₃) δ ppm 7.13–7.38 (5H, m), 3.46–3.56 (2H, m), 3.35–3.45 (2H, m), 2.87–3.00 (4H, m), 1.35 (3H, s), 1.21 (6H, t, *J* = 7.1 Hz)

^{13}C NMR (101 MHz, CDCl₃) δ ppm 208.8, 141.4, 128.5, 128.4, 126.0, 102.3, 57.6, 39.8, 29.5, 20.7, 15.3

The spectroscopic data is concurrent with the literature.[319]

(*E*)-4,4-Dimethoxy-1-phenylpent-1-en-3-one (251)
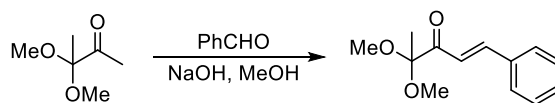
To a solution of 3,3-dimethoxybutan-2-one (10.07 g, 76 mmol, 1 equiv) in MeOH (200 mL) was added benzaldehyde (8.17 g, 77 mmol, 1.01 equiv) and NaOH (10M, 38 mL, 380 mmol, 4.98 equiv). The reaction was stirred at room temperature for 14 hours, before water (40 mL) was added and the reaction concentrated *in vacuo*. The resultant biphasic solution was extracted with CH₂Cl₂ (3 × 70 mL), the organics washed with brine (70 mL), dried over a hydrophobic frit and concentrated *in vacuo* to give (*E*)-4,4-dimethoxy-1-phenylpent-1-en-3-one (**251**) as a brown oil (15.95 g, 72.4 mmol, 95% *corrected for residual benzaldehyde*). The material was clean enough to be used in the following transformation, but analytically clean was material was obtained through purifying by chromatography (20% EtOAc in heptane).

Appearance: Colourless oil

^{1}H NMR (400 MHz, CDCl$_3$) δ ppm 7.82 (1H, d, J = 15.9 Hz), 7.60–7.68 (2H, m), 7.39–7.47 (3H, m), 7.29 (1H, d, J = 15.9 Hz), 3.33 (6H, s), 1.49 (3H, s)

^{13}C NMR (101 MHz, CDCl$_3$) δ ppm 196.9, 144.9, 134.7, 130.7, 128.9, 128.7, 120.4, 102.4, 49.9, 20.1

The spectroscopic data is concurrent with the literature.[320]

4,4-Dimethoxy-1-phenylpentan-3-one (250)
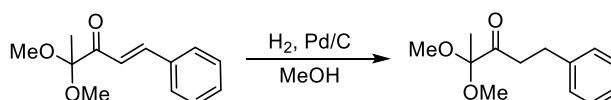
To a solution of (*E*)-4,4-dimethoxy-1-phenylpent-1-en-3-one (**251**) (1.986 g, 9.02 mmol, 1 equiv) in MeOH (27 mL) was added palladium on carbon (10% Pd loading, 2.5% Pd/C, 3.853 g, 0.91 mmol, 0.1 equiv). The reaction was exposed to vacuum and flushed with H$_2$ for 3 cycles before being stirred under 4 bar H$_2$ at room temperature for 4 hours. The reaction was filtered over a celite pad, concentrated *in vacuo* and purified by chromatography (0–50% EtOAc in heptane). The fractions containing product were re-purified by preparative high-performance liquid chromatography (30–55% MeCN in water, 0.05% ammonium bicarbonate buffer). The fractions containing product were concentrated under reduced pressure to remove the volatile organics and the resulting aqueous portion was extracted into CH$_2$Cl$_2$ (3 × 50 mL). The combined organics were washed with brine (50 mL) and dried over a hydrophobic frit to yield 4,4-dimethoxy-1-phenylpentan-3-one (**251**) as a colourless oil (859 mg, 3.87 mmol, 43%).

Appearance: Colourless oil

ν (neat): 2941, 1727, 1454, 1368, 1189, 1127, 1042 cm^{-1}

^{1}H NMR (400 MHz, CDCl$_3$) δ ppm 7.15–7.36 (5H, m), 3.22 (6H, s), 2.85–3.00 (4H, m), 1.30–1.37 (3H, m)

^{13}C NMR (101 MHz, CDCl$_3$) δ ppm 208.2, 141.2, 128.5, 128.4, 126.1, 102.6, 49.7, 39.8, 29.4, 19.7

HRMS (ESI Orbitrap) *m/z*: An accurate HRMS of this compound could not be obtained.

Cyclic systems

2,2-Dimethoxycyclohexanone (257)
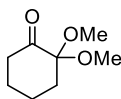
To a round-bottomed flask containing MeOH (100 mL) was added trimethylsilyl chloride (10.75 g, 99 mmol, 1 equiv). To this solution was added cyclohexane-1,2-dione (11.1 g, 99 mmol, 1.0 equiv). The reaction was stirred at room temperature for 2.5 hours before water (200 mL) was added and the solution extracted with diethylether (2 × 100 mL). The combined organics were washed with brine (80 mL), dried over anhydrous MgSO$_4$ and concentrated *in vacuo.* The crude material was purified by chromatography (0–20% EtOAc in heptane) to yield 2,2-dimethoxycyclohexanone (**257**) as a colourless oil (3.69 g, 23.34 mmol, 24%).

^{1}H NMR (400 MHz, CDCl$_3$) δ ppm 3.26 (6H, s), 2.53 (2H, t, *J* = 6.4 Hz), 1.93–2.00 (2H, m), 1.74–1.88 (5H, m)

^{13}C NMR (101 MHz, CDCl$_3$) δ ppm 207.1, 100.7, 49.2, 40.0, 35.3, 27.4, 21.9

The spectroscopic data is concurrent with the literature.[113]

1-Benzyl-4,5,6,7-tetrahydro-benzo[*d*][1,2,3]triazole (259)
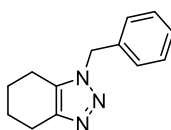
Following a modification of General Procedure 1 with 2,2-dimethoxycyclohexanone (**257**) (176 mg, 1.11 mmol, 1.1 equiv) in methanol (2.6 mL) with 4-methylbenzenesulfonohydrazide (188 mg, 1.01 mmol, 1 equiv), the reaction was stirred at room temperature for 10 minutes (at which point consumption of 4-methylbenzenesulfonohydrazide was observed) before addition of benzylamine (119 mg, 1.11 mmol, 1.1 equiv) and triethylamine (109 mg, 1.08 mmol, 1.1 equiv). After 5 minutes at 140 °C and cooling to room temperature, the reaction mixture was portioned between CH$_2$Cl$_2$:water (40 mL, 1:1) and the organic layer separated. The

aqueous layer was extracted with CH_2Cl_2 (2 × 15 mL) and the combined organic extracts washed with brine (20 mL) and dried over a hydrophobic frit before concentrating *in vacuo* to give an orange oil. The crude material was purified by chromatography (30–70% EtOAc in heptane) to yield 1-benzyl-5-methyl-1,2,3-triazole (**259**) as a white solid. (169 mg, 0.79 mmol, 79%).

Appearance: White solid

M.pt: 81–82 °C

ν (neat): 2941, 1588, 1496, 1454, 1307, 1194, 735 cm⁻¹

¹H NMR (400 MHz, CDCl₃) δ ppm 7.30–7.38 (3H, m), 7.14–7.23 (2H, m), 5.43 (2H, s), 2.67–2.79 (2H, m), 2.36–2.47 (2H, m), 1.71–1.84 (4H, m)

¹³C NMR (101 MHz, CDCl₃) δ ppm 143.9, 135.0, 132.0, 128.9, 128.2, 127.5, 51.8, 22.5, 22.4, 21.9, 20.1

HRMS (ESI Orbitrap) *m/z*: Calcd for $C_{13}H_{16}N_3$ [M+H]⁺ 214.1339; found [M+H]⁺ 214.1345

The spectroscopic data is concurrent with the literature.[115]

4,5,6,7-Tetrahydro-1H-benzo[*d*][1,2,3]triazole (260)
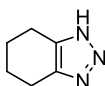
Following a modification of General Procedure 1 with 2,2-dimethoxycyclohexanone (**257**) (256 mg, 1.67 mmol, 1.1 equiv) in methanol (3.7 mL) with 4-methylbenzenesulfonohydrazide (280 mg, 1.50 mmol, 1 equiv), the reaction was stirred at room temperature for 5 minutes (at which point consumption of 4-methylbenzenesulfonohydrazide was observed) before ammonia (7 M solution in MeOH) (0.47 mL, 3.30 mmol, 2.2 equiv) was added. *Note triethylamine omitted to aid isolation.* After 5 minutes at 140 °C and cooling to room temperature, the reaction mixture was portioned between CH_2Cl_2:water (40 mL, 1:1) and the organic layer separated. The aqueous layer was extracted with CH_2Cl_2 (2 × 15 mL) and the combined organic extracts washed with brine (20 mL) and dried over a hydrophobic frit before concentrating *in vacuo* to

a yellow oil. The crude material was purified by chromatography (0–50% EtOAc in heptane) to yield 4,5,6,7-tetrahydro-1*H*-benzo[*d*][1,2,3]triazole (**260**) as an off-white solid. (161 mg, 1.31 mmol, 87%).

Appearance: Off-white solid

^{1}H NMR (400 MHz, CDCl$_3$) δ ppm 12.98 (1H, *br.* s), 2.69–2.83 (4H, m), 1.80–1.92 ppm (4H, m)

^{13}C NMR (101 MHz, CDCl$_3$) δ ppm 141.7, 23.0, 21.3

The spectroscopic data is concurrent with the literature.[321]

Synthesis of 1-substituted triazoles

To a 5 mL microwave vial containing methanol (2.6 mL) was added the quantity of **265** shown in the table below. **265** was used as a 60% solution in water, explaining why volume is quoted. The specified quantity of 4-methylbenzenesulfonohydrazide **107** was then added and the reaction stirred at room temperature for 2 hours. If necessary, the hydrazone formation was monitored by removing 5 μL and diluting into 1.5 mL acetonitrile and analysing by LCMS. The hydrazone formation was complete after 2 hours. To each reaction was then added benzylamine (123 mg, 1.16 mmol, 1.1 equiv) and the specified additives. The reaction was then sealed and heated to the specified temperature for the stated reaction time, after which the reaction was concentrated *in vacuo*. To each crude reaction was added the stated quantity of 1,3,5-trimethoxybenzene. The crude reaction was homogenised with CD$_3$OD (~3 mL) and analysed by quantitative ^{1}H NMR to give the yields shown in Table 4 and below. When isolation was stated (Entry 6), it was purified by chromatography (30–70% EtOAc in heptane). Analytical data for triazole **269** is given below.
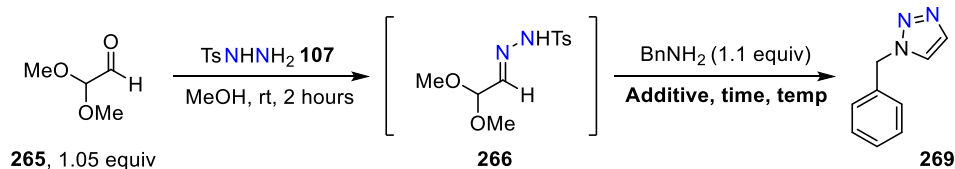
Entry	265 / µL (mmol)	107 / mg (mmol)	Additive / mg *or* µL (mmol)	Temp / °C	Time / hours	1,3,5-TMB / mg	Yield
1	165 (1.10)	195 (1.05)	Et₃N 116 mg (1.15)	75	16	54.9	57%
2	164 (1.10)	194 (1.05)	None	75	16	55.4	65%
3	165 (1.10)	194 (1.05)	AcOH 3 µL (0.05)	75	16	52.9	69%
4	166 (1.10)	196 (1.05)	AcOH 6 µL (0.10)	75	16	53.6	72%
5	167 (1.10)	196 (1.05)	AcOH 12 µL (0.20)	75	16	52.9	76%
6	165 (1.10)	195 (1.05)	AcOH 61 µL (1.00)	75	16	56.8	78% (76%)
7	166 (1.10)	198 (1.05)	AcOH 183 µL (3.00)	75	16	56.3	79%
8	165 (1.10)	197 (1.05)	AcOH 305 µL (5.00)	75	16	54.7	74%
9	166 (1.10)	196 (1.05)	AcOH 61 µL (1.00)	40	72	56.5	60%
10	166 (1.10)	196 (1.05)	AcOH 61 µL (1.00)	30	72	57.5	54%
11	166 (1.10)	198 (1.05)	MsOH 98 µL (1.00)	75	16	57.9	2%
12	166 (1.10)	197 (1.05)	MsOH 293 µL (5.00)	75	16	56.2	0%
13	166 (1.10)	196 (1.05)	MsOH 489 µL (5.00)	75	16	52.7	0%
14	167 (1.10)	198 (1.05)	PFP 193 mg (1.00)	75	16	55.9	76%
15	166 (1.10)	196 (1.05)	HFIP 112 µL (1.00)	75	16	57.9	72%

HFIP = hexafluoroisopropanol, PFP = pentafluorophenol, TMB = trimethoxybenzene

General procedure 2 for 1-substituted triazole synthesis
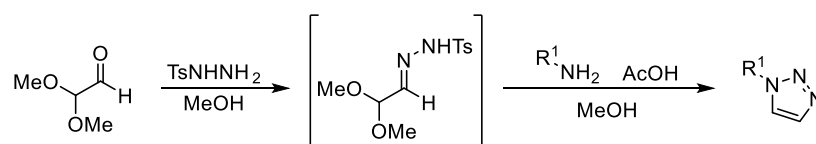
To a solution of 4-methylbenzenesulfonohydrazide (1.0 equiv) in MeOH was added 2,2-dimethoxyacetaldehyde (60% solution in water, 1.05 equiv). The reaction was stirred at room temperature for 2 hours before the desired amine (1.1 equiv) and acetic acid (1.0 equiv) were added, the reaction vial was sealed and then heated to 75 °C for 16 hours in a DrySyn. The reaction mixture was cooled to room temperature and concentrated *in vacuo*. The crude residue was homogenised in CH_2Cl_2, washed with water, 10% K_2CO_3 solution and dried before being concentrated in vacuo. The crude material was purified by chromatography to afford the desired triazole.

1-Benzyl-1,2,3-triazole (269)
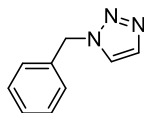
Using General Procedure 2 with 4-methylbenzenesulfonohydrazide (1.146 g, 6.15 mmol, 1 equiv), 2,2-dimethoxyacetaldehyde (1.02 mL, 6.77 mmol, 1.10 equiv) in MeOH (13 mL), with benzylamine (725 mg, 6.77 mmol, 1.1 equiv) and acetic acid (352 µL, 6.15 mmol, 1.0 equiv). After 16 hours at 75 °C, the reaction mixture was concentrated *in vacuo* and portioned between CH_2Cl_2:water (40 mL, 1:1). The organic layer was separated and washed with K_2CO_3 (5% aq, 10 mL), brine (10 mL) and concentrated *in vacuo*. The crude material was purified by chromatography (30–70% EtOAc in heptane) to give 1-benzyl-1,2,3-triazole (**269**) as a beige solid (740 mg, 4.65 mmol, 76%).

Appearance: Beige solid

M.pt: 59–60 °C

ν (neat): 3106, 2973, 1606, 1495, 1113, 721, 691 cm^{-1}

^{1}H NMR (400 MHz, CDCl$_3$) δ ppm 7.72 (1H, d, J = 0.7 Hz), 7.48 (1H, d, J = 0.7 Hz), 7.35–7.42 (3H, m), 7.23–7.31 (2H, m), 5.58 (2H, s)

^{13}C NMR (101 MHz, CD$_3$OD) δ ppm 135.4, 133.3, 128.6, 128.2, 127.7, 124.4, 53.3

HRMS (ESI Orbitrap) m/z: calcd [M+H]$^+$ for C$_9$H$_9$N$_3$ 160.0869; found [M+H]$^+$ 160.0876

The spectroscopic data is concurrent with the literature.[322]

1-(Pro*p*-2-yn-1-yl)-1,2,3-triazole (270)
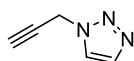
Using General Procedure 2 with 4-methylbenzenesulfonohydrazide (300 mg, 1.61 mmol, 1 equiv), 2,2-dimethoxyacetaldehyde (0.25 mL, 1.69 mmol, 1.05 equiv) in MeOH (3.9 mL), with propargylamine (98 mg, 1.77 mmol, 1.1 equiv) and acetic acid (92 µL, 1.61 mmol, 1.0 equiv). After 16 hours at 75 °C, the reaction mixture was concentrated *in vacuo* and portioned between CH$_2$Cl$_2$:water (40 mL, 1:1). The organic layer was washed with water (3 × 5 mL), K$_2$CO$_3$ (2 × 5 mL) and brine (10 mL) before being concentrated *in vacuo*. The crude material was purified by chromatography (10–50% EtOAc in heptane) to give 1-(pro*p*-2-yn-1-yl)-1,2,3-triazole (**270**) was isolated as a colourless oil (57 mg, 0.53 mmol, 33%).

Appearance: Colourless oil

ν (neat): 3288, 3130, 2129, 1627, 1218, 1071, 786, 750 cm^{-1}

^{1}H NMR (400 MHz, CDCl$_3$) δ ppm 7.81 (1H, s), 7.76 (1H, s), 5.22 (2H, d, J = 2.7 Hz), 2.59 (1H, t, J = 2.7 Hz)

^{13}C NMR (101 MHz, CDCl$_3$) δ ppm 134.2, 123.2, 75.9, 75.1, 39.7

HRMS (ESI Orbitrap) m/z: Calcd for C$_5$H$_6$N$_3$ [M+H]$^+$ 108.0556; found [M+H]$^+$ 108.0554

1-Cyclohexyl-1,2,3-triazole (271)
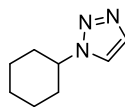
Using General Procedure 2 with 4-methylbenzenesulfonohydrazide (310 mg, 1.67 mmol, 1 equiv), 2,2-dimethoxyacetaldehyde (0.26 mL, 1.75 mmol, 1.05 equiv) in MeOH (3.9 mL), with cyclohexylamine (182 mg, 1.83 mmol, 1.1 equiv) and acetic acid (95 µL, 1.62 mmol, 1.0 equiv). After 16 hours at 75 °C, the reaction mixture was concentrated *in vacuo* and portioned between CH_2Cl_2:water (40 mL, 1:1). The organic layer was separated and washed with K_2CO_3 (5% aq, 10 mL), brine (10 mL) and concentrated *in vacuo*. The crude material was purified by chromatography 30–70% EtOAc in heptane) to give 1-cyclohexyl-1,2,3-triazole (**271**) as a yellow solid (136 mg, 0.90 mmol, 54%).

Appearance: Yellow crystals

M.pt: 60–61 °C

ν (neat): 3113, 2927, 2857, 1615, 1448, 1286, 1072, 799 cm^{-1}

^{1}H NMR (400 MHz, CD_3OD) δ ppm 8.02 (1H, d, *J* = 0.7 Hz), 7.71 (1H, d, *J* = 0.7 Hz), 4.54 (1H, tt, *J* = 11.8, 4.4 Hz), 2.12–2.24 (2H, m), 1.90–1.99 (2H, m), 1.83–1.89 (2H, m), 1.75–1.83 (1H, m), 1.54 (2H, qt, *J* = 13.5, 3.4 Hz), 1.36 (1H, qt, *J* = 12.8, 3.7 Hz)

^{13}C NMR (101 MHz, CD_3OD) δ ppm 132.6, 122.3, 60.0, 33.1, 24.9 Two overlapping signals at 24.9 ppm resolved by HSQC

HRMS (ESI Orbitrap) *m/z*: Calcd for $C_8H_{13}N_3$ [M+H]$^+$ 152.1182; found [M+H]$^+$ 152.1189

1-Hexyl-1,2,3-triazole (272)
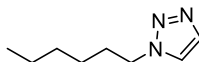
Using General Procedure 2 with 4-methylbenzenesulfonohydrazide (305 mg, 1.64 mmol, 1 equiv), 2,2-dimethoxyacetaldehyde (0.26 mL, 1.72 mmol, 1.05 equiv) in MeOH (3.9 mL), with hexylamine (182 mg, 1.80 mmol, 1.1 equiv) and acetic acid (94 µL, 1.64 mmol, 1.0 equiv). After 16 hours at 75 °C, the reaction mixture was concentrated *in vacuo* and portioned between

CH$_2$Cl$_2$:water (40 mL, 1:1). The organic layer was washed with water (10 mL), K$_2$CO$_3$ (5%, 10 mL), brine (10 mL), and concentrated *in vacuo*. The crude material was purified by chromatography (30–70% EtOAc in heptane to give 1-hexyl-1,2,3-triazole (**272**) was isolated as a yellow oil (143 mg, 0.93 mmol, 57%).

Appearance: Yellow oil

ν (neat): 3122, 2929, 2869, 1466, 1215, 1072 cm^{-1}

^{1}H NMR (400 MHz, CDCl$_3$) δ ppm 7.71 (1H, d, *J* = 0.5 Hz), 7.54 (1H, d, *J* = 0.5 Hz), 4.39 (2H, t, *J* = 7.3 Hz), 1.84–1.98 (2H, m), 1.21–1.38 (6 H, m), 0.82–0.94 (3H, m)

^{13}C NMR (101 MHz, CDCl$_3$) δ ppm 133.8, 123.2, 50.3, 31.2, 30.3, 26.2, 22.5, 14.0

HRMS (ESI Orbitrap) *m/z*: calcd. for C$_8$H$_{15}$N$_3$ [M+H]+ 154.1339; found [M+H]$^+$ 154.1345

The spectroscopic data is concurrent with the literature.[323]

1-Phenyl-1,2,3-triazole (273)
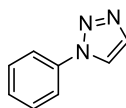
Using General Procedure 2 with 4-methylbenzenesulfonohydrazide (311 mg, 1.67 mmol, 1 equiv), 2,2-dimethoxyacetaldehyde (0.26 mL, 1.75 mmol, 1.05 equiv) in MeOH (3.9 mL), with aniline (174 mg, 1.84 mmol, 1.1 equiv) and acetic acid (96 μL, 1.67 mmol, 1.0 equiv). After 16 hours at 75 °C, the reaction mixture was concentrated *in vacuo* and portioned between CH$_2$Cl$_2$:water (40 mL, 1:1). The organic layer was separated and washed with K$_2$CO$_3$ (5% aq, 10 mL), brine (10 mL) and concentrated *in vacuo*. The crude material was purified by chromatography (10–50% EtOAc in heptane) to give 1-phenyl-1,2,3-triazole (**273**) was isolated as a pale yellow solid (235 mg, 1.62 mmol, 97%).

Appearance: Pale-yellow solid

M.pt: 54–55 °C

ν (neat): 3147, 3065, 1597, 1503, 1038, 759, 683 cm^{-1}

^{1}H NMR (400 MHz, CDCl$_3$) δ ppm 8.01 (1H, d, J = 1.0 Hz), 7.86 (1H, d, J = 1.0 Hz), 7.73–7.78 (2H, m), 7.52–7.58 (2H, m), 7.42–7.49 (1H, m)

^{13}C NMR (101 MHz, CD$_3$OD) δ ppm 138.6, 135.5, 131.2, 130.3, 124.4, 121.9

HRMS (ESI Orbitrap) *m/z*: Calcd for C$_8$H$_7$N$_3$ [M+H]$^+$ 146.0713; found [M+H]$^+$ 146.0720

The spectroscopic data is concurrent with the literature.[324]

1-(4-Fluorophenyl)-1,2,3-triazole (274)
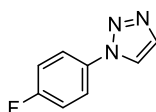
Using General Procedure 2 with 4-methylbenzenesulfonohydrazide (302 mg, 1.62 mmol, 1 equiv), 2,2-dimethoxyacetaldehyde (0.26 mL, 1.70 mmol, 1.05 equiv) in MeOH (3.9 mL), with 4-fluoroaniline (198 mg, 1.78 mmol, 1.1 equiv) and acetic acid (95 µL, 1.62 mmol, 1.0 equiv). After 16 hours at 75 °C, the reaction mixture was concentrated *in vacuo* and portioned between CH$_2$Cl$_2$:water (40 mL, 1:1). The organic layer was separated and washed with water (10 mL), brine (10 mL) and concentrated *in vacuo*. The crude material was purified by chromatography (10–50% EtOAc in heptane) to give 1-(4-fluorophenyl)-1,2,3-triazole (**274**) was isolated as a beige solid (218 mg, 1.34 mmol, 82%).

Appearance: Beige solid

M.pt: 74–75 °C

ν (neat): 3139, 3114, 1606, 1513, 1226, 1039, 836, 789 cm^{-1}

^{1}H NMR (400 MHz, CDCl$_3$) δ ppm 7.96 (1H, d, J = 1.1 Hz), 7.86 (1H, d, J = 1.1 Hz), 7.70–7.76 (2H, m), 7.21–7.27 (2H, m)

^{19}F (376 MHz, CD$_3$OD) δ ppm -114.24 (1 F, s)

^{13}C NMR (101 MHz, CD$_3$OD) δ ppm 162.4 (d, J = 247.2 Hz), 133.9, 133.3, 122.9, 122.4 (d, J = 9.2 Hz), 116.3 (d, J = 24.4 Hz)

HRMS (ESI Orbitrap) *m/z*: Calcd for C$_8$H$_6$FN$_3$ [M+H]$^+$ 164.0619; found [M+H]$^+$ 164.0626

The spectroscopic data is concurrent with the literature.[59]

1-(4-Chlorophenyl)-1,2,3-triazole (275)
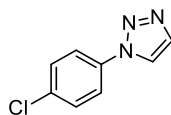
Using General Procedure 2 with 4-methylbenzenesulfonohydrazide (303 mg, 1.63 mmol, 1 equiv), 2,2-dimethoxyacetaldehyde (0.26 mL, 1.71 mmol, 1.05 equiv) in MeOH (3.9 mL), with 4-chloroaniline (236 mg, 1.84 mmol, 1.1 equiv) and acetic acid (93 μL, 1.62 mmol, 1.0 equiv). After 16 hours at 75 °C, the reaction mixture was concentrated *in vacuo* and portioned between CH$_2$Cl$_2$:water (40 mL, 1:1). The organic layer was separated and washed with K$_2$CO$_3$ (5% aq, 10 mL), brine (10 mL) and concentrated *in vacuo*. The crude material was purified by chromatography (10–50% EtOAc in heptane) to give 1-(4-chlorophenyl)-1,2,3-triazole (**275**) as a light brown powder (222 mg, 1.22 mmol, 75%).

Appearance: Light-brown solid

M.pt: 112–114 °C

ν (neat): 3129, 3102, 1497, 1127, 825, 794 cm^{-1}

^{1}H NMR (400 MHz, CDCl$_3$) δ ppm 7.98 (1H, d, *J* = 1.0 Hz), 7.87 (1H, d, *J* = 1.0 Hz), 7.68–7.75 (2H, m), 7.50–7.55 (2H, m)

^{13}C NMR (101 MHz, CD$_3$OD) δ ppm 133.7, 134.3, 134.0, 129.6, 122.8, 121.7

HRMS (ESI Orbitrap) *m/z*: Calcd for C$_8$H$_7$^{35}ClN$_3$ [M+H]$^+$ 180.0323; found [M+H]$^+$ 180.0319

The spectroscopic data is concurrent with the literature.[59]

1-(4-Bromophenyl)-1,2,3-triazole (276)
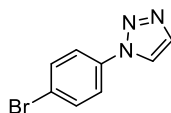
Using General Procedure 2 with 4-methylbenzenesulfonohydrazide (311 mg, 1.67 mmol, 1 equiv), 2,2-dimethoxyacetaldehyde (0.27 mL, 1.80 mmol, 1.08 equiv) in MeOH (3.9 mL), with 4-bromoaniline (332 mg, 1.87 mmol, 1.1 equiv) and acetic acid (95 μL, 1.62 mmol, 1.0 equiv). After 16 hours at 75 °C, the reaction mixture was concentrated *in vacuo* and portioned between

CH$_2$Cl$_2$:water (40 mL, 1:1). The organic layer was separated and washed with water (10 mL),

saturated NaHCO$_3$ (2 × 20 mL), brine (10 mL) and concentrated *in vacuo*. The crude material

was purified by chromatography (0−50% EtOAc in heptane) to give 1-(4-bromophenyl)-1,2,3-

triazole (**276**) as a brown powder (282 mg, 1.26 mmol, 75%).

Appearance: Brown powder

M.pt: 138–143 °C

ν (neat): 3126, 1594, 1489, 1227, 816, 788, 507 cm^{-1}

^{1}H NMR (400 MHz, CDCl$_3$) δ ppm 7.99 (1H, d, J = 1.0 Hz), 7.84 (1H, d, J = 1.0 Hz), 7.59–7.68

(4H, m)

^{13}C NMR (101 MHz, (CD$_3$)$_2$SO) δ ppm 136.3, 135.1, 133.2, 123.7,122.5, 121.7

HRMS (ESI Orbitrap) *m/z*: Calcd for C$_8$H$_7$^{79}BrN$_3$ [M+H]$^+$ 223.9818; found [M+H]$^+$ 223.9810

1-(4-Iodophenyl)-1,2,3-triazole (277)
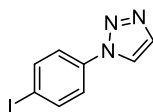
Using General Procedure 2 with 4-methylbenzenesulfonohydrazide (304 mg, 1.63 mmol, 1

equiv), 2,2-dimethoxyacetaldehyde (0.26 mL, 1.71 mmol, 1.05 equiv) in MeOH (3.9 mL), with

4-iodoaniline (395 mg, 1.81 mmol, 1.1 equiv) and acetic acid (95 µL, 1.62 mmol, 1.0 equiv).

After 16 hours at 75 °C, the reaction was cooled to room temperature whereby the resultant

solid was filtered to give 1-(4-iodophenyl)-1*H*-1,2,3-triazole (**277**) as a beige solid (345 mg,

1.27 mmol, 78%).

Appearance: Beige solid

M.pt: 179–180 °C

ν (neat): 3147, 3128, 1501, 1487, 1225, 816, 787 cm^{-1}

^{1}H NMR (400 MHz, CD$_3$OD) δ ppm 8.83 (1H, d, J = 1.0 Hz), 7.97 (1H, d, J = 1.0 Hz), 7.94 (2H,

d, J = 8.6 Hz), 7.73 (2H, d, J = 8.6 Hz)

^{13}C NMR (101 MHz, CD$_3$OD) δ ppm 139.0, 136.8, 135.1, 123.6, 122.5, 94.6

HRMS (ESI Orbitrap) *m/z*: Calcd for C$_8$H$_7$IN$_3$ [M+H]$^+$ 271.9679; found [M+H]$^+$ 271.9692

1-(4-Methoxyphenyl)-1H-1,2,3-triazole (278)
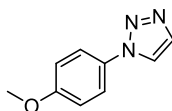
Using General Procedure 2 with 4-methylbenzenesulfonohydrazide (303 mg, 1.66 mmol, 1 equiv), 2,2-dimethoxyacetaldehyde (0.26 mL, 1.71 mmol, 1.05 equiv) in MeOH (3.9 mL), with 4-methoxyaniline (231 mg, 1.88 mmol, 1.15 equiv) and acetic acid (95 µL, 1.66 mmol, 1.0 equiv). After 16 hours at 75 °C, the reaction mixture was concentrated *in vacuo* and portioned between CH$_2$Cl$_2$:water (40 mL, 1:1). The organic layer was separated and washed with water (3 × 5 mL), before the organic portions were washed with brine (10 mL) and concentrated *in vacuo*. The crude material was purified by chromatography (10−50% EtOAc in heptane) to give 1-(4-methoxyphenyl)-1,2,3-triazole (**278**) as a pale yellow solid (255 mg, 1.46 mmol, 90%).

Appearance: Pale-yellow powder

M.pt: 78–80 °C

ν (neat): 3141, 3126, 2947, 2837, 1610, 1592, 1508, 1226, 1027, 834, 812, 789

^{1}H NMR (400 MHz, CD$_3$OD) δ ppm 8.31 (1H, d, *J* = 0.8 Hz), 7.83 (1H, d, *J* = 0.8 Hz), 7.62 (2H, d, *J* = 9.2 Hz), 6.97 (2H, d, *J* = 9.2 Hz), 3.77 (3H, s)

^{13}C NMR (101 MHz, CD$_3$OD) δ ppm 160.0, 133.7, 130.2, 122.7, 121.8, 114.5, 54.8

HRMS (ESI Orbitrap) *m/z*: Calcd for C$_9$H$_9$N$_3$O [M+H]+ 176.0818; found [M+H]$^+$ 176.0826

N,N-dimethyl-4-(1,2,3-triazol-1-yl)aniline (279)
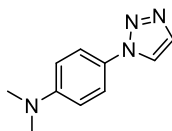
Using General Procedure 2 with 4-methylbenzenesulfonohydrazide (308 mg, 1.65 mmol, 1 equiv), 2,2-dimethoxyacetaldehyde (0.26 mL, 1.74 mmol, 1.05 equiv) in MeOH (3.9 mL), with 4-dimethylaminoaniline (251 mg, 1.84 mmol, 1.1 equiv) and acetic acid (95 µL, 1.58 mmol, 1.0 equiv). After 16 hours at 75 °C, the reaction mixture was concentrated *in vacuo* and portioned between CH_2Cl_2:water (40 mL, 1:1). The organic layer was separated the aqueous portion extracted with CH_2Cl_2 (3 × 15 mL). The combined organic portions were washed with brine (10 mL) and concentrated *in vacuo.* The crude material was purified by chromatography (15−60% EtOAc in heptane) to give *N,N*-dimethyl-4-1,2,3-triazol-1-yl)aniline (**279**) as a pale yellow solid (243 mg, 1.29 mmol, 78%).

Appearance: Pale-yellow powder

M.pt: 101–102 °C

ν (neat): 3150, 2890, 2819, 1605, 1518, 1007, 812, 802, 771 cm^{-1}

^{1}H NMR (400 MHz, CD$_3$OD) δ ppm 8.28 (1H, d, *J* = 1.0 Hz), 7.82 (1H, d, *J* = 1.0 Hz), 7.53–7.59 (2H, m), 6.78–6.85 (2H, m), 2.97 (6H, s)

^{13}C NMR (101 MHz, CD$_3$OD) δ ppm 151.0, 133.4, 126.5, 122.5, 121.5, 112.1, 39.2

HRMS (ESI Orbitrap) *m/z*: Calcd for $C_{10}H_{12}N_4$ [M+H]+ 189.1335; found [M+H]$^+$ 189.1144

1-(4-(1,2,3-Triazol-1-yl)phenyl)ethan-1-one (280)
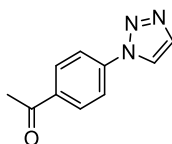
Using General Procedure 2 with 4-methylbenzenesulfonohydrazide (282 mg, 1.52 mmol, 1 equiv), 2,2-dimethoxyacetaldehyde (0.24 mL, 1.59 mmol, 1.05 equiv) in MeOH (3.8 mL), with

1-(4-aminophenyl)ethan-1-one (227 mg, 1.68 mmol, 1.1 equiv) and acetic acid (90 µL, 1.57 mmol, 1.0 equiv). After 16 hours at 75 °C, the reaction mixture was concentrated *in vacuo* and portioned between CH_2Cl_2:water (40 mL, 1:1). The organic layer was separated and the aqueous extracted with CH_2Cl_2 (2 × 15 mL), before the combined organic portions were washed with brine (10 mL), dried over a hydrophobic frit and concentrated *in vacuo*. The crude material was purified by chromatography (0−50% EtOAc in heptane) to give 1-(4-(1,2,3-triazol-1-yl)phenyl)ethenone (**280**) as a beige solid (271 mg, 1.48 mmol, 95%).

Appearance: Beige solid

M.pt: 166–170 °C

ν (neat): 3153, 3115, 1671, 1517, 1234, 1028, 836, 786 cm^{-1}

^{1}H NMR (400 MHz, $(CD_3)_2SO$) δ ppm 8.98 (1H, d, *J* = 1.0 Hz), 8.18 (2H, d, *J* = 8.7 Hz), 8.10 (2H, d, *J* = 8.7 Hz), 8.03 (1H, d, *J* = 1.0 Hz), 2.64 (3H, s)

^{13}C NMR (101 MHz, $(CD_3)_2SO$) δ ppm 197.4, 140.1, 136.8, 135.3, 130.5, 123.9, 120.3, 27.3

HRMS (ESI Orbitrap) *m/z*: Calcd for $C_{10}H_{10}N_3O$ [M+H]$^+$ 188.0818; found [M+H]$^+$ 188.0826

The spectroscopic data is concurrent with the literature.[325]

Methyl 4-(1,2,3-triazol-1-yl)benzoate (281)
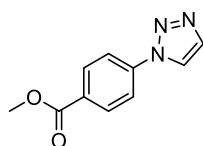
Using General Procedure 2 with 4-methylbenzenesulfonohydrazide (283 mg, 1.52 mmol, 1 equiv), 2,2-dimethoxyacetaldehyde (0.24 mL, 1.59 mmol, 1.05 equiv) in MeOH (3.8 mL), with methyl 4-aminobenzoate (257 mg, 1.70 mmol, 1.1 equiv) and acetic acid (90 µL, 1.57 mmol, 1.0 equiv). After 16 hours at 75 °C, the reaction mixture was concentrated *in vacuo* and portioned between CH_2Cl_2:water (40 mL, 1:1). The organic layer was separated and the aqueous extracted with CH_2Cl_2 (2 × 15 mL), before the combined organic portions were washed with brine (10 mL), dried over a hydrophobic frit and concentrated *in vacuo*. The crude

material was purified by chromatography (10–50% EtOAc in heptane) to give methyl 4-(1,2,3-triazol-1-yl)benzoate (**281**) as a brown powder (303 mg, 1.49 mmol, 98%).

Appearance: Brown powder

M.pt: 171–172 °C

ν (neat): 3138, 3122, 1712, 1608, 1282, 767 cm^{-1}

^{1}H NMR (400 MHz, (CD$_3$)$_2$SO) δ ppm 8.97 (1H, d, J = 1.2 Hz), 8.15–8.20 (2H, m), 8.09–8.14 (2H, m), 8.03 (1H, d, J = 1.2 Hz), 3.89 (3H, s)

^{13}C NMR (101 MHz, (CD$_3$)$_2$SO) δ ppm 165.9, 140.4, 135.3, 131.5, 129.7, 123.9, 120.5, 52.7

HRMS (ESI Orbitrap) m/z: Calcd for C$_{10}$H$_{10}$N$_3$O$_2$ [M+H]$^+$ 204.0768; found [M+H]$^+$ 204.0776

1-(4-Nitrophenyl)-1,2,3-triazole (282)
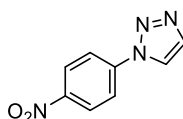
Using General Procedure 2 with 4-methylbenzenesulfonohydrazide (301 mg, 1.62 mmol, 1 equiv), 2,2-dimethoxyacetaldehyde (0.26 mL, 1.70 mmol, 1.05 equiv) in MeOH (3.9 mL), with 4-nitroaniline (249 mg, 1.80 mmol, 1.1 equiv) and acetic acid (95 µL, 1.62 mmol, 1.0 equiv). After 16 hours at 75 °C, the reaction mixture was concentrated *in vacuo* and portioned between CH$_2$Cl$_2$:water (40 mL, 1:1). The organic layer was separated and washed with water (10 mL), brine (10 mL) and concentrated *in vacuo*. The crude material was purified by chromatography (0–50% EtOAc in heptane) to give 1-(4-nitrophenyl)-1,2,3-triazole (**282**) as a brown solid (259 mg, 1.31 mmol, 81%).

Appearance: Brown powder

M.pt: 204–205 °C

ν (neat): 3128, 3056, 1595, 1509, 1235, 855, 799, 748 cm^{-1}

^{1}H NMR (400 MHz, CDCl$_3$) δ ppm 8.41–8.48 (2H, m), 8.13 (1H, d, J = 1.0 Hz), 7.98–8.05 (2H, m), 7.93 (1H, d, J = 1.0 Hz)

^{13}C NMR (101 MHz, CD$_3$OD) δ ppm 147.1, 141.4, 135.5, 126.0, 124.2, 121.1

HRMS (ESI Orbitrap) *m/z*: Calcd for $C_8H_6N_4O_2$ [M+H]+ 191.0564; found [M+H]+ 191.0573

The spectroscopic data is concurrent with the literature.[326]

1-(2,6-Dimethylphenyl)-1H-1,2,3-triazole (283)
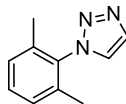
Using General Procedure 2 with 4-methylbenzenesulfonohydrazide (305 mg, 1.64 mmol, 1 equiv), 2,2-dimethoxyacetaldehyde (0.26 mL, 1.72 mmol, 1.05 equiv) in MeOH (3.9 mL), with 2,6-dimethylaniline (218 mg, 1.80 mmol, 1.1 equiv) and acetic acid (95 µL, 1.62 mmol, 1.0 equiv). After 16 hours at 75 °C, the reaction mixture was concentrated *in vacuo* and portioned between CH_2Cl_2:water (40 mL, 1:1). The organic layer was separated and washed with saturated $NaHCO_3$ (2 × 5 mL), brine (10 mL) and concentrated *in vacuo*. The crude material was purified by chromatography (0−40% EtOAc in heptane) to yield 1-(2,6-dimethylphenyl)-1,2,3-triazole (**283**) as a white solid (231 mg, 1.34 mmol, 82%).

Appearance: White solid

M.pt: 73–74 °C

ν (neat): 3147, 3121, 2953, 2924, 1490, 1468, 1230, 1027, 799, 786 cm^{-1}

^{1}H NMR (400 MHz, CD$_3$OD) δ ppm 8.13 (1H, d, *J* = 1.0 Hz), 7.97 (1H, d, *J* = 1.0 Hz), 7.32–7.40 (1H, m*H*), 7.20–7.28 (2H, m), 1.95 (6H, s)

^{13}C NMR (101 MHz, CD$_3$OD) δ ppm 137.4, 136.8, 134.9, 131.6, 129.9, 128.2, 17.7

HRMS (ESI Orbitrap) *m/z*: Calcd for $C_{10}H_{11}N_3$ [M+H]+ 174.1026; found [M+H]+ 174.1033

2-(1,2,3-Triazol-1-yl)phenol (284)
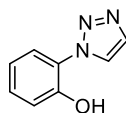
Using General Procedure 2 with 4-methylbenzenesulfonohydrazide (308 mg, 1.65 mmol, 1 equiv), 2,2-dimethoxyacetaldehyde (0.26 mL, 1.74 mmol, 1.05 equiv) in MeOH (3.9 mL), with

2-aminophenol (200 mg, 1.84 mmol, 1.1 equiv) and acetic acid (95 µL, 1.62 mmol, 1.0 equiv). After 16 hours at 75 °C, the reaction mixture was concentrated *in vacuo* and portioned between CH_2Cl_2:water (40 mL, 1:1). The organic layer was separated and washed with K_2CO_3 (5% aq, 10 mL), brine (10 mL) and concentrated *in vacuo*. The crude material was purified by chromatography (0–50% EtOAc in heptane) to give 2 (1,2,3-triazol-1-yl)phenol (**284**) as a beige powder (223 mg, 1.38 mmol, 84%).

Appearance: Beige powder

M.pt: 149–151 °C

ν (neat): 3031, 1602, 1438, 1224, 781, 738 cm^{-1}

^{1}H NMR (400 MHz, CDCl$_3$) δ ppm 9.88 (1H, s), 8.15 (1H, d, J = 1.1 Hz), 7.95 (1H, d, J = 1.1 Hz), 7.45 (1H, dd, J = 8.1, 1.5 Hz), 7.31 – 7.37 (1H, m), 7.24 (1H, dd, J = 8.1, 1.5 Hz), 7.04 (1H, ddd, J = 8.1, 7.1, 1.5 Hz)

^{13}C NMR (101 MHz, CD$_3$OD) δ ppm 149.7, 132.6, 130.0, 126.2, 124.7, 124.6, 119.6, 116.7

HRMS (ESI Orbitrap) *m/z*: Calcd for $C_8H_7N_3O$ [M+H]$^+$ 162.0662; found [M+H]$^+$ 162.0669

The spectroscopic data is concurrent with the literature.[327]

2-(1,2,3-Triazol-1-yl)pyridine (285)
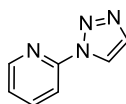
Using General Procedure 2 with 4-methylbenzenesulfonohydrazide (303 mg, 1.63 mmol, 1 equiv), 2,2-dimethoxyacetaldehyde (0.26 mL, 1.71 mmol, 1.05 equiv) in MeOH (3.9 mL), with 2-aminopyridine (168 mg, 1.79 mmol, 1.1 equiv) and acetic acid (95 µL, 1.62 mmol, 1.0 equiv). After 16 hours at 75 °C, the reaction mixture was concentrated *in vacuo* and portioned between CH_2Cl_2:water (40 mL, 1:1) and the pH of the aqueous increased to 13 with NaOH (2 M). The organic layer was separated and extracted with HCl (2 M, 3 × 10 mL), before basifying the aqueous with NaOH (2 M) to pH 13 and re-extracting with CH_2Cl_2 (3 × 15 mL). The organic portions were washed with brine (10 mL) and concentrated *in vacuo*. The crude material was

purified by chromatography (0−50% EtOAc in heptane) to give 2-(1,2,3-triazol-1-yl)pyridine (**285**) as a white solid (91 mg, 0.62 mmol, 38%).

Appearance: White crystals

M.pt: 87–88 °C

ν (neat): 3144, 1577, 1466, 1047, 778 cm^{-1}

^{1}H NMR (400 MHz, CDCl$_3$) δ ppm 8.61 (1H, d, J = 1.0 Hz), 8.52 (1H, m), 8.23 (1H, d, J = 8.4 Hz), 7.93 (1H, td, J = 7.5 Hz, 1.2 Hz), 7.85 (1H, d, J = 1.0 Hz), 7.36 (1H, ddd, J = 7.5, 4.8, 1.0 Hz)

^{13}C NMR (101 MHz, CDCl$_3$) δ 149.3, 148.6, 139.2, 134.2, 123.6, 121.0, 114.0

HRMS (ESI Orbitrap) m/z: Calcd for C$_7$H$_6$N$_4$ [M+H]$^+$ 147.0665; found [M+H]$^+$ 147.0672

3-(1,2,3-Triazol-1-yl)pyridine (286)
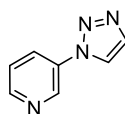
Using General Procedure 2 with 4-methylbenzenesulfonohydrazide (302 mg, 1.62 mmol, 1 equiv), 2,2-dimethoxyacetaldehyde (0.26 mL, 1.71 mmol, 1.05 equiv) in MeOH (3.9 mL), with 3-aminopyridine (171 mg, 1.82 mmol, 1.1 equiv) and acetic acid (95 μL, 1.62 mmol, 1.0 equiv). After 16 hours at 75 °C, the reaction mixture was concentrated *in vacuo* and portioned between CH$_2$Cl$_2$:water (40 mL, 1:1) and the pH of the aqueous increased to 13 with NaOH (2 M). The organic layer was separated and extracted with HCl (2 M, 3 × 10 mL), before basifying the aqueous with NaOH (2 M) to pH 13 and re-extracting with CH$_2$Cl$_2$ (3 × 15 mL). The organic portions were washed with brine (10 mL) and concentrated *in vacuo*. The crude material was purified by chromatography (10−50% EtOAc in heptane) to give 3-(1,2,3-triazol-1-yl)pyridine (**286**) as pale-yellow crystals (159 mg, 1.09 mmol, 67%).

Appearance: Pale-yellow crystals

M.pt: 89–90 °C

ν (neat): 3111, 3093, 1584, 1430, 1223, 797, 700 cm^{-1}

^{1}H NMR (400 MHz, CDCl$_3$) δ ppm 9.01–9.05 (1H, m), 8.73 (1H, dd, J = 4.7, 1.5 Hz), 8.17 (1H, ddd, J = 8.2, 2.7, 1.5 Hz), 8.07 (1H, d, J = 1.1 Hz), 7.92 (1H, d, J = 1.1 Hz), 7.53 (1H, ddd, J = 8.2, 4.7, 0.5 Hz)

^{13}C NMR (101 MHz, CD$_3$OD) δ ppm 150.7, 142.6, 135.8, 135.6, 130.1, 126.1, 124.6

HRMS (ESI Orbitrap) *m/z*: Calcd for C$_7$H$_7$N$_4$ [M+H]$^+$ 147.0665; found [M+H]$^+$ 147.0661

The spectroscopic data is concurrent with the literature.[328]

1-(2-Fluoro-5-methylphenyl)-1,2,3-triazole (287)
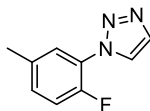
Using General Procedure 2 with 4-methylbenzenesulfonohydrazide (302 mg, 1.62 mmol, 1 equiv), 2,2-dimethoxyacetaldehyde (0.26 mL, 1.70 mmol, 1.05 equiv) in MeOH (3.9 mL), with 2-fluoro-5-methylaniline (223 mg, 1.78 mmol, 1.1 equiv) and acetic acid (93 µL, 1.62 mmol, 1.0 equiv). After 16 hours at 75 °C, the reaction mixture was concentrated *in vacuo* and portioned between CH$_2$Cl$_2$:water (40 mL, 1:1). The organic layer was separated and washed with K$_2$CO$_3$ (5% aq, 10 mL), brine (10 mL) and concentrated *in vacuo*. The crude material was purified by chromatography (0–50% EtOAc in heptane) to give 1-(2-fluoro-5-methylphenyl)-1,2,3-triazole (**287**) as a pale red solid (258 mg, 1.46 mmol, 90%).

Appearance: Pale-red powder

M.pt: 49–50 °C

ν (neat): 3113, 2928, 1611, 1516, 1475, 1242, 1211, 1028, 825, 793, 763 cm^{-1}

^{1}H NMR (400 MHz, CD$_3$OD) δ ppm 8.35 (1H, dd, J = 2.5, 1.3 Hz), 7.92 (1H, d, J = 1.0 Hz), 7.62 (1H, dd, J = 7.1, 1.3 Hz), 7.30–7.36 (1H, m), 7.21–7.29 (1H, m), 2.39 (3H, s)

^{13}C NMR (101 MHz, CD$_3$OD) δ ppm 152.2 (d, *J* = 248.7 Hz), 135.4, 133.4, 131.1 (d, *J* = 7.6 Hz), 125.8 (d, *J* = 6.1 Hz), 125.3, 124.4 (d, *J* = 10.7 Hz), 116.4 (d, *J* = 19.8 Hz), 19.2

HRMS (ESI Orbitrap) *m/z*: Calcd for C$_9$H$_8$FN$_3$ [M+H]$^+$ 178.0775; found [M+H]$^+$ 178.0783

1-(4-Chloro-2-nitrophenyl)-1H-1,2,3-triazole (288)
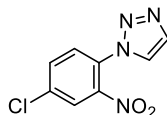
Using General Procedure 2 with 4-methylbenzenesulfonohydrazide (294 mg, 1.58 mmol, 1 equiv), 2,2-dimethoxyacetaldehyde (0.25 mL, 1.66 mmol, 1.05 equiv) in MeOH (3.9 mL), with 4-chloro-2-nitroaniline (300 mg, 1.74 mmol, 1.1 equiv) and acetic acid (90 µL, 1.58 mmol, 1.0 equiv). After 16 hours at 75 °C, the reaction mixture was concentrated *in vacuo* and portioned between CH$_2$Cl$_2$:water (40 mL, 1:1). The organic layer was separated the aqueous portion extracted with CH$_2$Cl$_2$ (3 × 15 mL). The combined organic portions washed with K$_2$CO$_3$ (5%, 2 × 10 mL), brine (10 mL) and concentrated *in vacuo*. The crude material was purified by chromatography (0−50% EtOAc in heptane) to give 1-(4-chloro-2-nitrophenyl)-1,2,3-triazole (**288**) as a yellow solid (86 mg, 0.38 mmol, 24%).

Appearance: Yellow powder

M.pt: 127–129 °C

ν (neat): 3134, 2981, 1531, 1359, 1024, 837, 522 cm^{-1}

^{1}H NMR (400 MHz, CD$_3$OD) δ ppm 8.43 (1H, d, *J* = 1.2 Hz), 8.28 (1H, d, *J* = 2.2 Hz), 7.93–7.93 (2H, m), 7.80 (1H, d, *J* = 7.9 Hz)

^{13}C NMR (101 MHz, CD$_3$OD) δ ppm 144.9, 136.3, 133.7, 128.8, 128.4, 126.1, 125.5 Two overlapping signals at 133.7 ppm resolved by HSQC.

HRMS (ESI Orbitrap): Unable to detect mass

Methyl 4-(1,2,3-triazol-1-yl)benzoate (281)
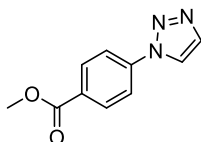
On larger scale

To a solution of 4-methylbenzenesulfonohydrazide (14.40 g, 77.0 mmol, 1 equiv) in methanol (187 mL) was added 2,2-dimethoxyacetaldehyde (12.2 mL, 81.0 mmol, 1.05 equiv). The reaction was stirred for 2 hours before addition of further 2,2-dimethoxyacetaldehyde (2.08 mL, 13.8 mmol, 0.18 equiv). After a further 2 hours, methyl 4-aminobenzoate (12.86 g, 85.0 mmol, 1.1 equiv) and acetic acid (4.43 mL, 77.0 mmol, 1.0 equiv) were added and the reaction heated under reflux. After 16 hours, the reaction was concentrated *in vacuo* to give a brown slurry. tBME (100 mL) was added and the mixture stirred for 1 hour. The solids were filtered, washed with tBME (2 × 25 mL) and dried in a vacuum oven at 45 °C to give methyl 4-(1,2,3-triazol-1-yl)benzoate (**281**) as a brown crystalline solid (13.35 g, 65.7 mmol, 85%).

Analytical data consistent with those recorded previously.

9.3.10 Synthesis of *N*-methyltosylhydrazide

***N*,4-dimethylbenzenesulfonohydrazide (289)**
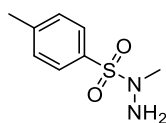
To a solution of methyl hydrazine (4.38 g, 95 mmol, 3 equiv) in water (25 mL) was added 4-toluenesulfonyl chloride (6.04 g, 31.7 mmol, 1 equiv) in toluene (22 mL) over 10 minutes. The reaction was stirred at room temperature for 40 minutes before removing the volatiles *in vacuo*. The resultant solid was filtered and washed with cold water (3 × 10 mL) to yield *N*,4-dimethylbenzenesulfonohydrazide (**289**) as a fluffy white solid (5.11 g, 25.5 mmol, 81%).

Appearance: White fluffy solid

^{1}H NMR (400 MHz, CDCl$_3$) δ ppm 7.75 (2H, d, *J* = 8.0 Hz), 7.41 (2H, d, *J* = 8.0 Hz), 3.48, (2H, *br*. s), 2.85 (3H, s), 2.48 (3H, s)

^{13}C NMR (101 MHz, CDCl$_3$) δ ppm 140.1, 136.6, 129.7, 124.5, 36.9, 21.4

The spectroscopic data is concurrent with the literature.[329]

Comparison in rate of triazole formation using hydrazones 108 and 310
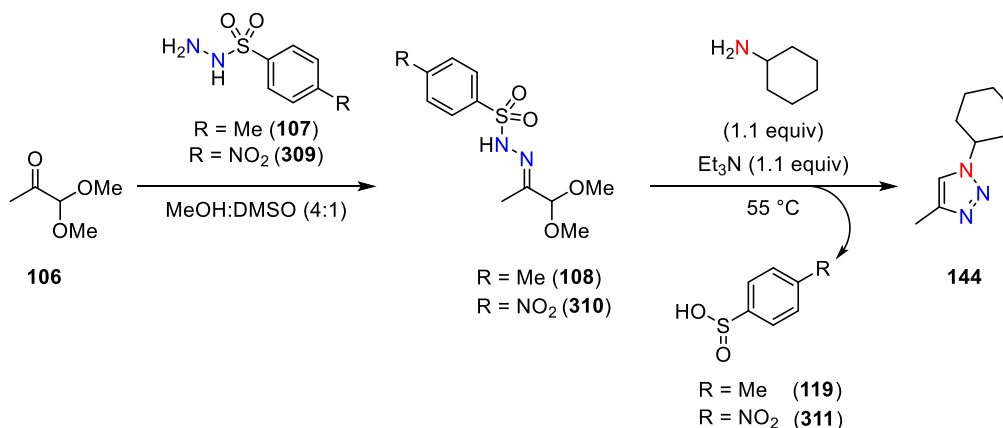
To two separate round-bottom flasks was added the shown quantity of **106** which was then dissolved in methanol (7.5 mL). To reaction 1 was added the shown quantity of **107** and to reaction 2 was added the shown quantity of **309**. After 1 minute, a precipitate formed in reaction 2 which proved to be hydrazone **310** by LCMS analysis. To each reaction was added methanol (10 mL) and DMSO (4 mL), at which point the precipitate in reaction 2 dissolved. Ansiole (98 μL) was added to both reactions as an internal standard.

Reaction	**106** / mg (mmol)	**107** / mg (mmol)	**309** / mg (mmol)	**Anisole** (int. s) / μL
1	375 (3.18)	561 (3.01)	–	98
2	377 (3.19)	–	660 (3.04)	98

The reactions were heated to 55 °C and sampled for HPLC analysis at 10, 20, 40, 60, 110 and 180 minutes by diluting 5 μL of reaction mixture into 1.5 mL acetonitrile. The relative ratio of HPLC area % of triazole **144**:anisole (shown below) was then plotted over time to give Figure 18.
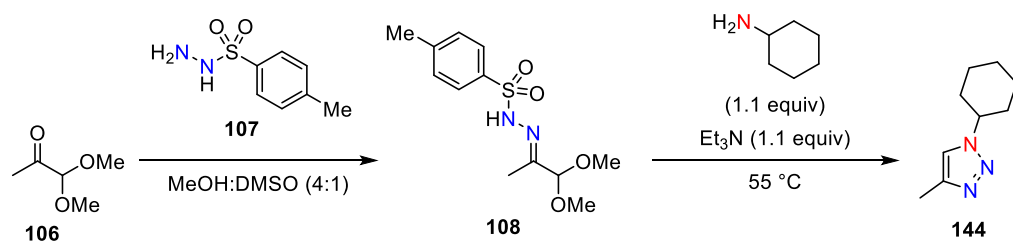
Time	Triazole **144** area %	Anisole area %	**144:**anisole
10	0.673	14.711	0.046
20	1.501	14.627	0.103
40	2.868	14.072	0.204
60	4.328	14.197	0.305
110	7.586	13.278	0.571
180	11.057	12.394	0.892
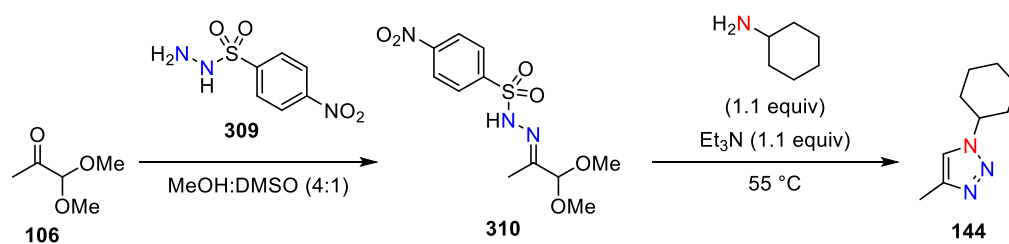
Time	Triazole **144** area %	Anisole area %	**144:**anisole
10	1.420	22.244	0.064
20	2.217	22.141	0.100
40	4.035	20.937	0.193
60	5.936	20.223	0.2942
110	10.768	18.822	0.572
180	16.543	18.121	0.913

9.3.9 Chemoselective triazole synthesis

4-(2-(4-Methyl-1,2,3-triazol-1-yl)ethyl)aniline (322)
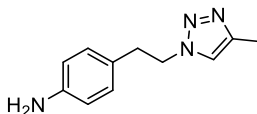
Following a modification of General Procedure 1 using 1,1-dimethoxypropan-2-one (185 mg, 1.57 mmol, 1.05 equiv) in methanol (3.8 mL) with 4-methylbenzenesulfonohydrazide (280 mg, 1.50 mmol, 1 equiv), 4-(2-aminoethyl)aniline (207 mg, 1.52 mmol, 1.0 equiv) and triethylamine (167 mg, 1.65 mmol, 1.1 equiv). After 5 minutes at 140 °C and cooling to room temperature, the reaction mixture was concentrated *in vacuo* to give an orange oil. The oil was portioned between CH$_2$Cl$_2$:water (40 mL, 1:1) and the organic layer separated. The aqueous was extracted with CH$_2$Cl$_2$ (2 × 15 mL) and the combined organic extracts washed with brine (20 mL), dried over a hydrophobic frit and concentrated *in vacuo* to give an orange oil. The crude material was purified by chromatography (40–100% EtOAc in heptane) to yield **322** as a white solid (252 mg, 1.25 mmol, 83%).

Appearance: White solid

M.pt: 121–123 °C

ν (neat): 3421, 3329, 3225, 1636, 1609, 1517, 1283, 817, 794 cm^{-1}

^{1}H NMR (400 MHz, CD$_3$OD) δ ppm 7.47 (1H, s), 6.85–6.91 (2H, m), 6.63–6.68 (2H, m), 4.52 (2H, t, J = 7.1 Hz), 3.05 (2H, t, J = 7.1 Hz), 2.24–2.31 (3H, m)

^{13}C NMR (101 MHz, CD$_3$OD) δ ppm 146.1, 142.4, 129.0, 126.7, 122.4, 115.4, 51.5, 35.4, 8.97

HRMS (ESI Orbitrap) *m/z*: Calcd for C$_{11}$H$_{15}$N$_4$ [M+H]$^+$ 203.1291; found [M+H]$^+$ 203.1285

2-(4-(1,2,3-Triazol-1-yl)phenyl)ethan-1-amine (326)
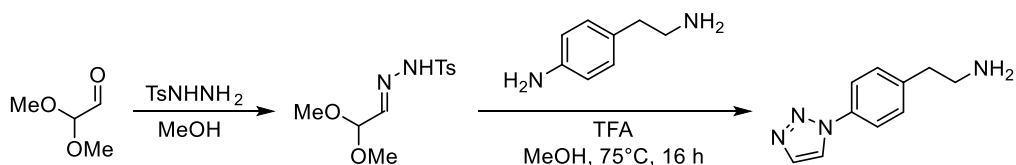
To a solution of 4-methylbenzenesulfonohydrazide (279 mg, 1.50 mmol, 1 equiv) in MeOH (3.8 mL) in a microwave vial was added 2,2-dimethoxyacetaldehyde (0.25 mL, 1.66 mmol, 1.10 equiv). The reaction was stirred at room temperature for 2 hours before addition of 4-(2-aminoethyl)aniline (227 mg, 1.67 mmol, 1.10 equiv) and trifluoroacetic acid (178 mg, 0.12 mL, 1.56 mmol, 1.05 equiv). The reaction was sealed and heated to 75 °C for 16 hours before concentrating *in vacuo*. The crude material was portioned between CH_2Cl_2:water (40 mL, 1:1) and the pH of the aqueous increased to 14 with NaOH (2M). The organic layer was separated and the aqueous was extracted with CH_2Cl_2 (3 × 20 mL). The combined organics were washed with brine (30 mL) and dried over a hydrophobic frit before concentrating *in vacuo*. The crude product was purified by chromatography (0–5% MeOH in CH_2Cl_2 with 2% Et_3N in the CH_2Cl_2 portion) to give 2-(4-(1,2,3-triazol-1-yl)phenyl)ethan-1-amine (**326**) as a white solid (228 mg, 1.21 mmol, 81%).

Appearance: White powder

M.pt: 121–123 °C

ν (neat): 3515, 3369, 3112, 2920, 1627, 1558, 1520, 1469, 1335, 1229, 1033 cm^{-1}

^{1}H NMR (400 MHz, $CDCl_3$) δ ppm 7.98 (1H, d, $J = 1.2$ Hz), 7.83 (1H, d, $J = 1.2$ Hz), 7.60–7.71 (2H, m), 7.34–7.39 (2H, m), 3.01 (2H, t, $J = 7.0$ Hz), 2.82 (2H, t, $J = 7.0$ Hz). Note NH_2 signals missing. The presence of a broad, large water peak is potentially obscuring these signals.

^{13}C NMR (101 MHz, CD_3OD) δ ppm 140.2, 135.5, 133.8, 129.9, 122.7, 120.5, 42.1, 36.9

HRMS (ESI Orbitrap) *m/z*: Calcd for $C_{10}H_{13}N_4$ [M+H]$^+$ 189.1135; found [M+H]$^+$ 189.1129

2-(4-(4-Methyl-1H-1,2,3-triazol-1-yl)phenyl)ethan-1-amine (329)
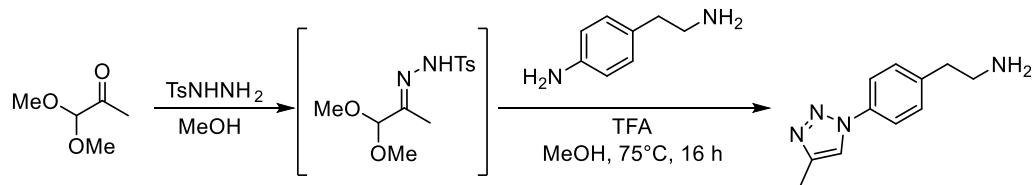
To a solution of 1,1-dimethoxypropan-2-one (186 mg, 1.57 mmol, 1.05 equiv) in MeOH (3.8 mL) was added 4-methylbenzenesulfonohydrazide (279 mg, 1.50 mmol, 1 equiv). The reaction

was stirred at room temperature for 5 minutes before addition of 4-(2-aminoethyl)aniline (207 mg, 1.52 mmol, 1.0 equiv) and trifluoroacetic acid (178 mg, 0.12 mL, 1.56 mmol, 1.05 equiv) and the reaction was heated to 75 °C. After 14 hours, the reaction was concentrated *in vacuo* and the crude material portioned between CH_2Cl_2:water (40 mL, 1:1). The pH of the aqueous increased to 12 with NaOH (2M) and the organic layer separated, before extracting the aqueous with CH_2Cl_2 (5 × 15 mL). The combined organics were washed with brine (30 mL) and dried over a hydrophobic frit before concentrating *in vacuo*. The crude product was purified by chromatography (0–5% MeOH in CH_2Cl_2 with 2% Et_3N in the CH_2Cl_2 portion) to give 2-(4-(4-methyl-1H-1,2,3-triazol-1-yl)phenyl)ethan-1-amine (**329**) as an off-white solid (264 mg, 1.31 mmol, 87%).

Appearance: Off-white powder

M.pt: 105–107 °C

ν (neat): 3346, 3136, 2925, 2866, 1559, 1519, 1438, 1335, 1224, 1048, 813 cm^{-1}

^{1}H NMR (400 MHz, CD$_3$OD) δ ppm 8.23 (1H, s), 7.73–7.79 (2H, m), 7.41–7.47 (2H, m), 2.93–2.99 (2H, m), 2.84–2.91 (2H, m), 2.41 (3H, s)

^{13}C NMR (101 MHz, CD$_3$OD) δ ppm 142.2, 139.0, 134.0, 128.3, 118.8, 118.7, 40.9, 36.2, 7.6

HRMS (ESI Orbitrap) *m/z*: Calcd for $C_{11}H_{15}N_4$ [M+H]$^+$ 203.1291; found [M+H]$^+$ 203.1285

1-(4-(1,2,3-Triazol-1-yl)phenethyl)-4-methyl-1,2,3-triazole (330)
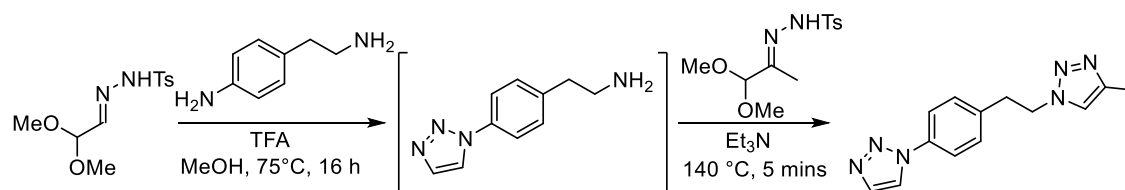
To a solution of 4-methylbenzenesulfonohydrazide (279 mg, 1.50 mmol, 1 equiv) in MeOH (3.8 mL) in a microwave vial was added 2,2-dimethoxyacetaldehyde (0.25 mL, 1.66 mmol, 1.10 equiv). The reaction was stirred at room temperature for 2 hours before addition of 4-(2-aminoethyl)aniline (207 mg, 1.52 mmol, 1.0 equiv) and trifluoroacetic acid (178 mg, 0.12 mL, 1.56 mmol, 1.05 equiv). The reaction was sealed and heated to 75 °C for 16 hours. To a

separate vial containing 1,1-dimethoxypropan-2-one (189 mg, 1.57 mmol, 1.05 equiv) in MeOH (3.8 mL) was added 4-methylbenzenesulfonohydrazide (179 mg, 1.50 mmol, 1 equiv) and the reaction was stirred at room temperature. After 5 minutes, triethylamine (334 mg, 3.30 mmol, 2.2 equiv) and the previous reaction mixture were added, the vial was sealed and heated to 140 °C for 5 minutes. On cooling to room temperature, the reaction mixture was concentrated *in vacuo* and the crude material portioned between CH_2Cl_2:water (40 mL, 1:1). The organic layer was separated, and the aqueous portion extracted with CH_2Cl_2 (3 × 20 mL). The combined organic portions were washed with brine (50 mL) and dried over a hydrophobic frit before concentrating *in vacuo* and purifying by chromatography (50–100% EtOAc in heptane) to give 1-(4-(1,2,3-triazol-1-yl)phenethyl)-4-methyl-1,2,3-triazole (**330**) as a beige powder (263 mg, 1.03 mmol, 69%).

Appearance: Beige powder

M.pt: 145–146 °C

ν (neat): 3117, 3070, 1521, 1451, 1231, 1034, 818, 799 cm^{-1}

^{1}H NMR (400 MHz, CDCl$_3$) δ ppm 7.98 (1H, d, J = 1.0 Hz), 7.83 (1H, d, J = 1.0 Hz), 7.64–7.69 (2H, m), 7.22–7.27 (2H, m), 7.09 (1H, s), 4.58 (2H, t, J = 7.1 Hz), 3.28 (2H, t, J = 7.1 Hz), 2.30 (3H, s)

^{13}C NMR (101 MHz, CDCl$_3$) δ ppm 143.2, 138.1, 136.0, 134.5, 130.1, 121.7, 121.5, 121.0, 51.0, 36.2, 10.8

HRMS (ESI Orbitrap) *m/z*: Calcd for $C_{13}H_{15}N_6$ [M+H]$^+$ 255.1353; found [M+H]$^+$ 255.1344

9.4 Chapter Two Experimental

9.4.1 Synthesis of Guanidine Starting Materials

General procedure 3 for guanidine synthesis

To a dry round-bottom flask was added a 60% suspension of sodium hydride (1.2 equiv) which was slurried in anhydrous DMSO (0.5 mL/mmol of NaH). The flask was exposed to vacuum and back-filled with nitrogen for 3 cycles before cooling the flask to 0 °C and adding the aniline (1.0 equiv) dropwise as a solution in anhydrous DMSO (0.33 mL/mmol of aniline). The reaction was stirred at 0 °C for 15 minutes before addition of the cyanamide (1.2 equiv), at which point the reaction was gradually allowed to warm to room temperature. After the stated time, the reaction was carefully quenched with water (~3 mL/mmol of sodium hydride used) and extracted into tBME (3 washes of equal volume of the water solution). The combined organic extracts were washed with water (3 washes of 0.33 × total organic volume), brine (1 wash of 0.33 × total organic volume), dried over anhydrous MgSO4 and concentrated in vacuo. The crude product was either purified by crystallisation or chromatography to yield the desired guanidine.

2-(3-Methoxyphenyl)-1,1-dimethylguanidine (454)
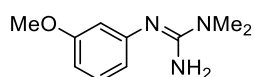
Using General Procedure 3 with 3-methoxyaniline (6.61 g, 53.7 mmol, 1 equiv), sodium hydride (2.53 g, 63.4 mmol, 1.2 equiv) and dimethylcyanamide (4.44 g, 63.4 mmol, 1.2 equiv). After 3.5 hours and the standard work up, the crude material was purified by recrystalisation from heptane/EtOAc. The resultant crystals were washed with cold tBME (10 mL) to give. 2-(3-methoxyphenyl)-1,1-dimethylguanidine (**454**) as a pale-orange crystalline solid (5.42 g, 28.0 mmol, 52%).

Appearance: Pale-orange crystals.

M.pt: 134–136 °C

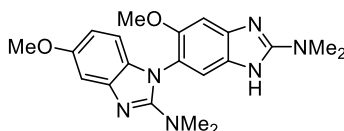ν (neat): 3409, 3131 (br), 1653, 1544, 1485, 1396 cm^{-1}

^{1}H NMR (400 MHz, CD$_3$OD) δ ppm 7.19 (1H, t, J = 8.1 Hz), 6.59 (1H, ddd, J = 8.1, 2.2, 0.9 Hz), 6.52 (1H, dd, J = 2.2, 0.9 Hz), 6.48–6.50 (1H, m), 3.78 (3H, s), 2.99 (6H, s)

^{13}C NMR (101 MHz, CD$_3$OD) δ ppm 162.2, 157.1, 152.6, 130.9, 117.6, 110.9, 109.0, 55.6, 38.1

HRMS (ESI Orbitrap) *m/z*: Calcd for C$_{10}$H$_{16}$N$_3$O [M+H]$^+$, 194.1288; found [M+H]$^+$ 194.1280

5,6'-Dimethoxy-*N²,N²,N²',N²'*-tetramethyl-3'*H*-[1,5'-bibenzo[*d*]imidazole]-2,2'-diamine (456)

To a vial containing 2-(3-methoxyphenyl)-1,1-dimethylguanidine (**454**) (1.00 g, 5.17 mmol, 1 equiv), copper(I) acetate (634 mg, 5.17 mmol, 1.0 equiv) & pivalic acid (529 mg, 5.17 mmol) was added NMP (17 mL). The reaction was heated to 80 °C in the CAT96 pressure reactor under 6 bar compressed air for 16 hours. On cooling to room temperature, the solution was flushed through an SCX-2 ion exchange cartridge with MeOH (100 mL), followed by a 7N methanolic ammonia (50 mL). The methanolic ammonia solution was concentrated in vacuo and purified by chromatography (0–10% MeOH in CH$_2$Cl$_2$ with 2% triethylamine modifier in the CH$_2$Cl$_2$ portion) to yield 126 mg of a brown solid. The brown solid was then re-purified by preparative HPLC (15–55% MeCN/H$_2$O, NH$_4$HCO$_3$ modifier at 0.1%), the volatiles were removed under reduced pressure, the aqueous extracted with CH$_2$Cl$_2$ (3 × 30 mL), before drying over a hydrophobic frit and concentrating in vacuo to yield 5,6'-dimethoxy-*N²,N²,N²',N²'*-tetramethyl-3'*H*-[1,5'-bibenzo[*d*]imidazole]-2,2'-diamine *(**454**)* as a white solid (63 mg, 0.17 mmol, 3%).

Appearance: White solid

^{1}H NMR (400 MHz, CD$_3$OD) δ ppm 7.14 (1H, s), 7.09 (1H, s), 6.97 (1H, d, *J* = 1.2 Hz), 6.53–6.60 (2H, m), 3.79 (3H, s), 3.76 (3H, s), 3.15 (6H, s), 2.84 (6H, s)

^{13}C NMR (101 MHz, CD$_3$OD) δ ppm 158.4, 158.0, 156.0, 150.8, 141.6, 131.8, 118.3, 108.8, 107.5, 99.7, 96.5, 55.4, 54.9, 39.3, 37.2. *Multiple signals missing from 13C NMR.*

HRMS (ESI Orbitrap) *m/z*: Calcd for C$_{20}$H$_{24}$N$_6$O$_2$ [M+H]$^+$ 380.1960; found [M+H]$^+$ 380.1963

5-Methoxy-*N,N*-dimethyl-1H-benzo[d]imidazol-2-amine (455)
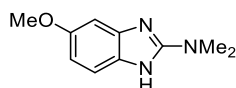
To a dry schlenk tube was added 2-(3-methoxyphenyl)-1,1-dimethylguanidine (**454**) (97 mg, 0.5 mmol, 1 equiv), pivalic acid (50 mg, 0.5 mmol, 1.0 equiv), copper(I) acetate (60 mg, 48.9 mmol, 1.0 equiv) and a stir bar. The schlenk tube was fitted with a septum and the vessel exposed to vacuum before being back-filled with nitrogen. This process was repeated 3 times, and the reaction remained exposed to nitrogen. To the schlenk tube was added freeze-pump thawed degassed NMP (2 mL). The sealed schlenk tube was then placed in a silicone oil bath which had been preheated to 80 °C. After 21 hours, the reaction was removed from the oil bath and the septum taken out, allowing the solution to cool to room temperature. Water (10 mL), tBME (10 mL) and EDTA$_{(aq)}$ solution (6 mL, 0.1 M, 0.6 mmol, 1.2 equiv w.r.t copper(I) acetate) were added and the organic portion separated. The aqueous layer was extracted a further two times with tBME (2 × 15 mL) and the combined organic extracts were washed with water (2 × 15 mL) and brine (1 × 10 mL). The combined water and brine washes were back-extracted with tBME (2 × 10 mL), and the combined tBME extracts were concentrated *in vacuo*. The crude reaction mixture was purified by column chromatography (0–10% MeOH in CH$_2$Cl$_2$) to yield 5-methoxy-*N,N*-dimethyl-1*H*-benzo[*d*]imidazol-2-amine (**455**) as a white solid. (62 mg, 0.3 mmol, 64%).

Appearance: White solid

^{1}H NMR (400 MHz, CD$_3$OD) δ ppm 7.08 (1H, d, J = 8.6 Hz), 6.82 (1H, d, J = 2.4 Hz), 6.60 (1H, dd, J = 8.6, 2.4 Hz), 3.77 (3H, s), 3.09 (6H, s)

^{13}C NMR (101 MHz, CD$_3$OD) δ ppm 158.5, 156.0, 155.5, 118.0, 111.5, 108.5, 98.0, 56.5, 38.5 ppm

The spectroscopic data is concurrent with the literature.[330]

1,1-Dimethyl-2-(3-(trifluoromethyl)phenyl)guanidine (458)
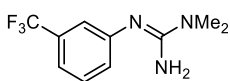
Using General Procedure 3 with 3-(trifluoromethyl)aniline (3.00 g, 31.0 mmol, 1 equiv), sodium hydride (1.49 g, 37.2 mmol, 1.2 equiv) and dimethylcyanamide (2.61 g, 37.2 mmol, 1.2 equiv). After a 45-minute reaction time, a precipitate formed on addition of water, which was filtered, the liquors extracted and combined with the filtered solid. The crude material was purified by recrystalisation from boiling heptane to give pale-yellow crystals, which were rinsed with cold tBME (5 mL) to give 1,1-dimethyl-2-(3-(trifluoromethyl)phenyl) guanidine (**458**) as an off-white crystalline solid (4.66 g, 20.2 mmol, 65%).

Appearance: Off-white crystals

M.pt: 102–104 °C

ν (neat): 3450, 3122 (br), 1637, 1566, 1334 cm^{-1}

^{1}H NMR (400 MHz, CD$_3$OD) δ ppm 7.40 (1H, t, J = 7.9 Hz), 7.18–7.22 (1H, m), 7.09–7.14 (2H, m), 2.98 (6H, s)

^{13}C NMR (101 MHz, CD$_3$OD) δ ppm 157.3, 152.8, 132.6 (q, J = 31.7 Hz), 131.0, 128.8, 125.9 (q, J = 271.4 Hz), 121.7 (q, J = 3.8 Hz), 119.1 (q, J = 3.8 Hz), 38.0

^{19}F NMR (377 MHz, CD$_3$OD) δ ppm -64.14 (1 F, s)

HRMS (ESI Orbitrap) *m/z*: Calcd for C$_{10}$H$_{13}$F$_3$N$_3$ [M+H]$^+$ 232.1056; found [M+H]$^+$ 232.1047

5-Trifluoromethyl-*N,N*-dimethyl-1Hbenzo[d]imidazol-2-amine (459)

To a dry schlenk tube was added 1,1-dimethyl-2-(3-(trifluoromethyl)phenyl)guanidine (**458**) (115 mg, 0.5 mmol, 1 equiv), pivalic acid (51 mg, 0.5 mmol, 1.0 equiv), copper(I) acetate (61 mg, 0.5 mmol, 1.0 equiv) and a stir bar. The schlenk tube was fitted with a septum and the vessel exposed to vacuum before being back-filled with nitrogen. This process was repeated 3 times, and the reaction remained exposed to nitrogen. To the schlenk tube was added freeze-pump thawed degassed NMP (2 mL). The sealed schlenk tube was then placed in a silicone oil bath which had been preheated to 80 °C. After 2 days, the reaction was removed from the oil bath and the septum taken out, allowing the solution to cool to room temperature. Water (10 mL) was added, causing a precipitate to form. tBME (10 mL) and EDTA$_{(aq)}$ solution (6 mL, 0.1 M, 0.6 mmol, 1.2 equiv w.r.t copper(I) acetate) were added. The aqueous layer was extracted a further two times with tBME (2 x 15 mL) and the combined organic extracts washed with water (2 x 15 mL) and brine (1 x 10 mL). The combined water and brine washes were back-extracted with tBME (2 x 10 mL), and the combined tBME extracts were concentrated *in vacuo*. The crude reaction mixture was purified by column chromatography (0–10% MeOH in CH$_2$Cl$_2$) to yield 5-trifluoromethyl-*N,N*-dimethyl-1Hbenzo[d]imidazol-2-amine (**459**) as a yellow solid. (20 mg, 0.09 mmol, 17%).

Appearance: Yellow solid

M.pt: 210–211 °C

ν (neat): 3073 (br), 2925 (br), 1639, 1611, 1320

^{1}H NMR (400 MHz, CD$_3$OD) δ ppm 7.45 (1H, s), 7.24–7.33 (2H, m), 3.15 (6H, s)

^{13}C NMR (101 MHz, CD$_3$OD) δ ppm 157.8, 141.1, 138.2, 125.3 (t, J = 270.1 Hz), 121.9 (q, J = 31.3 Hz), 116.9 (q, J = 3.8 Hz), 111.2, 108.2, 37.1

^{19}F NMR (376 MHz, CD$_3$OD) δ ppm −61.8 (s)

HRMS (ESI Orbitrap) *m/z*: Calcd for C$_{10}$H$_{10}$F$_3$N$_3$ [M+H]$^+$ 230.0900; found [M+H]$^+$ 230.0893

1,1-Dimethyl-2-(pyridin-4-yl)guanidine (461)
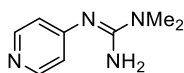
Using a modification of General Procedure 3 with 4-aminopyridine (2.50 g, 26.6 mmol, 1 equiv), sodium hydride (1.38 g, 34.5 mmol, 1.3 equiv) and dimethylcyanamide (2.20 g, 31.3 mmol, 1.2 equiv). After 3 hours, the reaction was quenched with water (80 mL). The pH was adjusted to 2 using 2 M HCl$_{aq}$ and flushed through an SCX-2 cartridge. The cartridge was flushed with methanol (50 mL) and then methanolic ammonia (2 M, 20 mL). The ammonia solution was concentrated *in vacuo* to give 1,1-dimethyl-2-(pyridin-4-yl)guanidine (**461**) as an orange solid(0.44 g, 2.65 mmol, 10%).

Appearance: Orange solid

M.pt: 82–85 °C

ν (neat): 3061 (br), 1656, 1493, 1396 cm^{-1}

^{1}H NMR (400 MHz, CD$_3$OD) δ ppm 8.16–8.18 (2H, m), 6.85–6.88 (2H, m), 3.00 (6H, s)

^{13}C NMR (101 MHz, CD$_3$OD) δ ppm 160.8, 158.1, 150.2, 119.7, 38.0

HRMS (ESI Orbitrap) *m/z*: Calcd for C$_8$H$_{12}$N$_4$ [M+H]$^+$ 165.1135; found [M+H]$^+$ 165.1126

High throughput screen of copper sources, solvents and additives

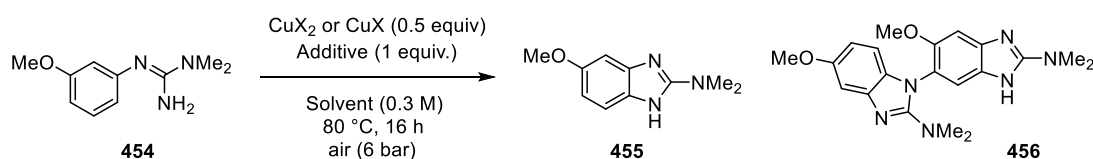To 0.5 mL glass vials were weighed the below masses of copper source and to the reactions containing basic additives added NaOAc/NaOPiv using the automated weighing platform Quantos QX96. To each vial was added 2-(3-methoxyphenyl)-1,1-dimethylguanidine (**454**, as a 0.2 mL of a stock solution in the quoted solvent) such that each 0.2 mL delivers 25 mg / 0.13 mmol of **454**. To the reactions containing acidic additives was added a further 0.2 mL of a stock solution of the desired acid in the quoted solvent such that the 0.2 mL delivers 1 equivalent of the desired acidic additive with respect to **454**. To the remaining reactions in which the basic additive was added as a solid, a further 0.2 mL of the quoted solvent was added to make the total reaction volume up to 0.4 mL (0.32 M with respect to substrate **454**). All reactions were then stirred with a magnetic flea and heated to 80 °C under 6 bar of compressed air in a CAT96 reactor for 16 hours before filtering and analysing by HPLC and LCMS. Displayed below are the dispensed masses of solid reagents and the HPLC peak area % data of starting material **454**, product **455** and undesired dimeric product **456**.

Catalyst / Solvent / Additive	[Cu] / mg	Additive / mg	**454** / HPLC %	**455** / HPLC %	**456** / HPLC %
CuOAc / Sulfolane / PivOH	7.91	s.s	30	45	5
CuOAc / Sulfolane / AcOH	8.06	s.s	33	42	6
CuOAc / Sulfolane / NaOPiv	8.02	16.02	79	9	1
CuOAc / Sulfolane / NaOAc	7.89	10.57	72	15	1
CuOAc / DMSO / PivOH	7.95	s.s	45	19	6
CuOAc / DMSO / AcOH	7.89	s.s	42	16	7
CuOAc / DMSO / NaOPiv	7.92	15.96	78	3	0.4
CuOAc / DMSO / NaOAc	7.92	10.57	80	5	0.8
CuOAc / NMP / PivOH	7.91	s.s	25	33	13
CuOAc / NMP / AcOH	7.92	s.s	27	32	12
CuOAc / NMP / NaOPiv	7.93	16.83	74	8	2
CuOAc / NMP / NaOAc	7.95	10.72	66	14	3
CuTC / Sulfolane / PivOH	11.95	s.s	34	27	7

Catalyst / Solvent / Additive	[Cu] / mg	Additive / mg	**454** / HPLC %	**455** / HPLC %	**456** / HPLC %
CuTC / Sulfolane / AcOH	12.59	*s.s*	38	44	3
CuTC / Sulfolane / NaOPiv	12.09	15.79	82	8	0.3
CuTC / Sulfolane / NaOAc	11.81	10.58	51	19	7
CuTC / DMSO / PivOH	12.58	*s.s*	66	17	2.4
CuTC / DMSO / AcOH	11.72	*s.s*	67	17	2
CuTC / DMSO / NaOPiv	11.85	15.88	71	9	1.6
CuTC / DMSO / NaOAc	15.70	10.60	75	5	1.4
CuTC / NMP / PivOH	12.82	*s.s*	37	30	7.5
CuTC / NMP / AcOH	12.29	*s.s*	34	25	10
CuTC / NMP / NaOPiv	11.66	16.07	70	11	2
CuTC / NMP / NaOAc	15.72	10.60	57	18	4
CuEH$_2$ / Sulfolane / PivOH	23.00	*s.s*	63	30	0.5
CuEH$_2$ / Sulfolane / AcOH	23.07	*s.s*	53	35	1.5
CuEH$_2$ / Sulfolane / NaOPiv	23.24	15.86	60	27	2.5
CuEH$_2$ / Sulfolane / NaOAc	23.30	10.61	39	33	8
CuEH$_2$ / DMSO / PivOH	23.08	*s.s*	68	17	2
CuEH$_2$ / DMSO / AcOH	23.17	*s.s*	69	16	2
CuEH$_2$ / DMSO / NaOPiv	23.52	15.88	72	9	2
CuEH$_2$ / DMSO / NaOAc	23.09	10.70	75	6	1
CuEH$_2$ / NMP / PivOH	23.55	*s.s*	47	35	4
CuEH$_2$ / NMP / AcOH	23.22	*s.s*	46	30	5
CuEH$_2$ / NMP / NaOPiv	23.04	15.90	66	14	5
CuEH$_2$ / NMP / NaOAc	22.60	10.58	59	17	6
Cu 3-MeSal / Sulfolane / PivOH	13.93	*s.s*	55	29	0.8
Cu 3-MeSal / Sulfolane / AcOH	13.99	*s.s*	71	19	0
Cu 3-MeSal / Sulfolane / NaOPiv	14.01	15.93	91	2.5	0
Cu 3-MeSal / Sulfolane / NaOAc	13.97	10.67	55	10	4
Cu 3-MeSal / DMSO / PivOH	13.99	*s.s*	76	13	0
Cu 3-MeSal / DMSO / AcOH	14.00	*s.s*	62	11	2.5
Cu 3-MeSal / DMSO / NaOPiv	14.00	15.95	70	7	2
Cu 3-MeSal / DMSO / NaOAc	14.01	10.60	75	5	1
Cu 3-MeSal / NMP / PivOH	14.00	*s.s*	54	20	3.5
Cu 3-MeSal / NMP / AcOH	14.34	*s.s*	54	20	4
Cu 3-MeSal / NMP / NaOPiv	13.89	15.96	62	13	4
Cu 3-MeSal / NMP / NaOAc	13.94	10.70	67	10	3
Cu(II)(acacF$_6$)$_2$ / Sulfolane / PivOH	30.94	*s.s*	68	17	0.5
Cu(II)(acacF$_6$)$_2$ / Sulfolane / AcOH	30.96	*s.s*	78	14	0
Cu(II)(acacF$_6$)$_2$ / Sulfolane / NaOPiv	30.98	16.00	70	20	0.5
Cu(II)(acacF$_6$)$_2$ / Sulfolane / NaOAc	31.24	10.61	74	9	0.5
Cu(II)(acacF$_6$)$_2$ / DMSO / PivOH	31.65	*s.s*	94	1	0
Cu(II)(acacF$_6$)$_2$ / DMSO / NaOPiv	32.02	15.99	57	12	2.4
Cu(II)(acacF$_6$)$_2$ / DMSO / NaOAc	30.96	10.92	54	11	4

Catalyst / Solvent / Additive	[Cu] / mg	Additive / mg	454 / HPLC %	455 / HPLC %	456 / HPLC %
Cu(II)(acacF$_6$)$_2$ / NMP / PivOH	31.55	*s.s*	82	7	0
Cu(II)(acacF$_6$)$_2$ / NMP / AcOH	30.83	*s.s*	84	7	0
Cu(II)(acacF$_6$)$_2$ / NMP / NaOPiv	30.87	16.00	45	25	4
Cu(II)(acacF$_6$)$_2$ / NMP / NaOAc	32.10	10.79	53	19	4
Cu(II)(EAA)$_2$ / Sulfolane / PivOH	20.95	*s.s*	25	54	2
Cu(II)(EAA)$_2$ / Sulfolane / AcOH	20.98	*s.s*	31	49	2
Cu(II)(EAA)$_2$ / Sulfolane / NaOPiv	21.02	15.98	80	9	0
Cu(II)(EAA)$_2$ / Sulfolane / NaOAc	21.11	10.45	71	9	0
Cu(II)(EAA)$_2$ / DMSO / PivOH	21.02	*s.s*	41	32	0
Cu(II)(EAA)$_2$ / DMSO / NaOPiv	21.04	16.00	44	13	0.5
Cu(II)(EAA)$_2$ / DMSO / NaOAc	21.07	10.83	81	2	0
Cu(II)(EAA)$_2$ / NMP / PivOH	21.04	*s.s*	10	43	0.4
Cu(II)(EAA)$_2$ / NMP / AcOH	21.05	*s.s*	15	43	1
Cu(II)(EAA)$_2$c / NMP / NaOPiv	21.18	16.00	56	19	0.5
Cu(II)(EAA)$_2$ / NMP / NaOAc	21.13	10.48	46	22	0

s.s = dispensed in stock solution of solvent. Mass accuracy given to 2 decimal places as weighing was performed on a 4 decimal point mg balance.

Design of Experiments optimisation procedure
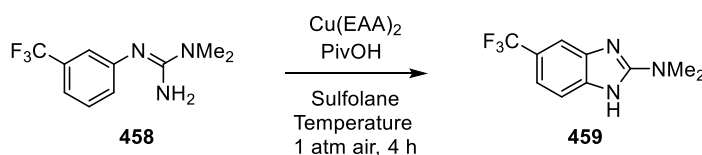
To 4 mL glass vials were added **458**, Cu(EAA)$_2$ and pivalic acid where the respective masses and loading of each is shown below, relative to the amount of **458**. Each 4 mL glass vial was then fitted with a stir bar and sulfolane (1 mL). To minimise mass-transfer effects of air, constant volume experiments were designed, hence the varying quantity of **458**. 25 µL samples were taken at 4 h and 21 h, diluted into acetonitrile (500 µL), filtered and analysed by HPLC and LCMS. Heating was performed with a heating mantle set to the specified temperature. Raw HPLC data was then used to calculate HPLC area % which is then shown in Table 9 (4 hour) and Table 10 (21 hour).

Reaction number	458 / mg	Cu(EAA)$_2$ / mg	PivOH / mg	Cu(EAA)$_2$ / mol%	PivOH / eq	Temperature / °C
1	23.06	1.56	10.53	5	1	100
2	23.28	8.01	10.82	25	1	130
3	23.07	1.67	20.39	5	2	130
4	93.44	32.15	83.19	25	2	130
5	24.09	24.09	21.44	25	2	100
6	57.92	12.14	28.49	15	1.5	115
7	93.66	6.43	82.89	5	2	100
8	92.45	32.21	40.82	25	1	100
9	58.34	12.07	38.63	15	1.5	115
10	92.53	6.44	40.63	5	1	130

Mass accuracy given to 2 decimal places as weighing was performed on a 4.d.p mg balance.

Statistical analysis of 4-hour data after processing in DX10.

Centre Points Detected: The ANOVA is presented in two ways:

Adjusted model: The factorial model includes a curvature term, which separates the curvature from the lack-of-fit sum of squares. The adjusted model provides the factorial model coefficients you'd get if there were no centre points and is used for diagnostics (by default).

Unadjusted model: The model coefficients are fit using all the data (including the centre points) without a curvature term. The unadjusted model is used to create the model graphs and for optimization predictions.

ANOVA Summary

	Adjusted Model			Unadjusted Model		
	F-value	p-value		F-value	p-value	
Model	110.16	< 0.0001	significant	10.80	0.0073	significant
Curvature	65.43	0.0002	significant			
Lack of Fit	94.11	0.0781		935.36	0.0250	Curvature appears significant. Augment to RSM if you want to explain what is causing the curvature or if curvature is in a desirable direction for your goal.

Model Summary

Factor	Adjusted Model Coefficient Estimate	p-value	Unadjusted Model Coefficient Estimate	p-value
Intercept	44.66		50.68	
C-Catalyst	24.23	< 0.0001	24.23	0.0026
D-Temp	4.64	0.0316	4.64	0.4113
Ctr Pt 1	30.06	0.0002		

The following ANOVA is for a model that does not adjust for curvature.
ANOVA for selected factorial model
Analysis of variance table [Partial sum of squares - Type III]

Source	Sum of Squares	df	Mean Square	F Value	p-value Prob > F	
Model	4869.88	2	2434.94	10.80	0.0073	significant
C-Catalyst	*4697.76*	*1*	*4697.76*	*20.83*	*0.0026*	
D-Temp	*172.12*	*1*	*172.12*	*0.76*	*0.4113*	
Residual	1578.71	7	225.53			
Lack of Fit	*1578.43*	*6*	*263.07*	*935.36*	*0.0250*	*significant*
Pure Error	*0.28*	*1*	*0.28*			
Cor Total	6448.59	9				

The following ANOVA is for a model that adjusts for curvature.
This is the default model used for the diagnostic plots.
This model is also used for prediction and model plots.
ANOVA for selected factorial model
Analysis of variance table [Partial sum of squares - Type III]

Source	Sum of Squares	df	Mean Square	F Value	p-value Prob > F	
Model	4869.88	2	2434.94	110.16	< 0.0001	significant
C-Catalyst	*4697.76*	*1*	*4697.76*	*212.54*	*< 0.0001*	
D-Temp	*172.12*	*1*	*172.12*	*7.79*	*0.0316*	
Curvature	1446.09	1	1446.09	65.43	0.0002	
Residual	132.62	6	22.10			

Std. Dev.	4.70	R-Squared	0.9735
Mean	50.68	Adj R-Squared	0.9647
C.V. %	9.28	Pred R-Squared	0.9321
PRESS	339.91	Adeq Precision	19.820
-2 Log Likelihood	54.23	BIC	61.14
		AICc	64.23

The "Pred R-Squared" of 0.9321 is in reasonable agreement with the "Adj R-Squared" of 0.9647; i.e. the difference is less than 0.2. "Adeq Precision" measures the signal to noise ratio. A ratio greater than 4 is desirable. The ratio of 19.820 indicates an adequate signal. This model can be used to navigate the design space.

Factor	Coefficient Estimate	df	Standard Error	95% CI Low	95% CI High	VIF
Intercept	44.66	1	1.66	40.60	48.73	
C-Catalyst	24.23	1	1.66	20.17	28.30	1.00
D-Temp	4.64	1	1.66	0.57	8.71	1.00
Ctr Pt 1	30.06	1	3.72			

Final Equation in Terms of Coded Factors:

Product %	=
+44.66	
+24.23	* C
+4.64	* D

The equation in terms of coded factors can be used to make predictions about the response for given levels of each factor. By default, the high levels of the factors are coded as +1 and the low levels of the factors are coded as -1. The coded equation is useful for identifying the relative impact of the factors by comparing the factor coefficients.
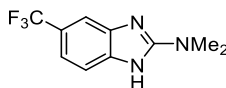
Final Equation in Terms of Actual Factors:

Product %	=
-21.23251	
+2.42326	* Catalyst
+0.30923	* Temp

General procedure 4 for aerobic copper catalysed dehydrogenative cyclisation to form benzimidazoles
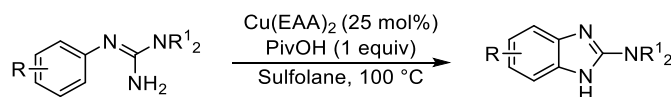
Aryl guanidine, pivalic acid (1 equiv) and copper(II) ethylacetoacetate (25 mol%) were placed in a round bottom flask fitted with a magnetic stirring flea. Sulfolane was warmed using a heated water bath and the desired volume was dispensed by syringe to make up to a reaction concentration of 0.4 M. The reaction was stirred and heated to 100 °C by heating mantle with the round bottom flask open to air. Reactions were monitored by both HPLC and LCMS analysis and were cooled to room temperature after the stated time. The reaction mixture was loaded directly onto an SCX-2 ion-exchange cartridge and homogenised with MeOH, after which the cartridge was flushed with a further 15 column volumes of MeOH. The cartridge was then flushed with 2 column volumes of a 2 M methanolic ammonia solution to elute the product, which was then concentrated *in vacuo* and purified by flash column chromatography (0–4% MeOH in CH$_2$Cl$_2$ in most cases unless stated otherwise) to yield the product.

5-Trifluoromethyl-*N,N*-dimethyl-1Hbenzo[d]imidazol-2-amine (459)

1-Dimethyl-2-(3-(trifluoromethyl)phenyl) guanidine (**458**) (370 mg, 1.6 mmol, 1 equiv), pivalic acid (163 mg, 1.6 mmol, 1.0 equiv) and copper(II) 2-ethylacetoacetate (129 mg, 0.4 mmol, 0.25 equiv) were placed in a round bottomed flask that was fitted with a stir bar. Sulfolane (4 mL) was added, and the reaction heated to 100 °C. After 24 hours, the reaction was removed from the hotplate and allowed to cool to room temperature, at which point water (20 mL), EDTA$_{(aq)}$ (5 mL, 0.1 M, 0.5 mmol, 1.2 equiv w.r.t copper.) and tBME (20 mL) was added. The organic layer was separated, the aqueous layer extracted a further 2 times (2 × 15 mL), before the combined organic extracts were washed with water (3 × 10 mL) and brine (1 × 20 mL). The water and brine washes were then back-extracted with tBME (1 × 15 mL). The combined organic extracts were then concentrated *in vacuo* and purified by column chromatography (0−10% MeOH in CH$_2$Cl$_2$) to yield (**458**) as an orange solid (196 mg, 0.9 mmol, 54%).

Appearance: Orange solid

Analytical data consistent with those recorded previously.

1,1-Dimethyl-2-phenylguanidine (463)
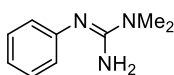
Using General Procedure 3 with aniline (1.00 g, 10.7 mmol, 1 equiv), sodium hydride (0.52 g, 12.9 mmol, 1.2 equiv) and dimethylcyanamide (0.90 g, 12.9 mmol, 1.20 equiv) was reacted for 5 hours before addition of a further portion of dimethylcyanamide (0.26 g, 3.7 mmol, 0.35 equiv) and the reaction stirred at room temperature for 14 hours. After the standard work up, the product was purified by chromatography (Biotage K*P*-NH silica, EtOAc) and the fractions containing product were recrystallised from EtOAc to yield 1,1-dimethyl-2-phenylguanidine (**463**) as a white crystalline solid (943 mg, 5.8 mmol, 54%).

Appearance: White crystals

M.pt: 91–93 °C

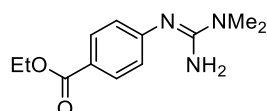ν (neat): 3429, 3144 (br), 1635, 1561, 1484 cm^{-1}

^{1}H NMR (400 MHz, CD$_3$OD) δ ppm 7.26–7.32 (2H, m), 7.00 (1H, dt, J = 14.8, 1.2 Hz), 6.90–6.94 (2H, m), 2.99 (6H, s)

^{13}C NMR (101 MHz, CD$_3$OD) δ ppm 157.1, 151.3, 130.3, 125.3, 123.3, 38.1

HRMS (ESI Orbitrap) m/z: Calcd for C$_9$H$_{14}$N$_3$ [M+H]$^+$ 164.1188; found [M+H]$^+$ 164.1183

The spectroscopic data is concurrent with the literature.[331]

Ethyl 4-((amino(dimethylamino)methylene)amino) benzoate (464)

Using General Procedure 3 with ethyl 4-aminobenzoate (1.00 g, 6.1 mmol, 1 equiv), sodium hydride (0.32 g, 8.0 mmol, 1.3 equiv) and dimethylcyanamide (0.51 g, 7.3 mmol, 1.2 equiv), after 2 hours, ethyl 4-((amino(dimethyl- amino)methylene) amino)benzoate (**464**) was isolated as a white solid by chromatography (Biotage K*P*-NH silica 0–10% MeOH in CH$_2$Cl$_2$) (136 mg, 0.6 mmol, 10%).

Appearance: White solid

M.pt: 89–92 °C

ν (neat): 3455, 3124 (br), 1703, 1624, 1551, 1493, 1401 cm^{-1}

^{1}H NMR (400 MHz, CD$_3$OD) δ ppm 7.87–7.96 (2H, m), 6.93–7.01 (2H, m), 4.33 (2H, q, J = 7.1 Hz), 3.01 (6H, s), 1.39 (3H, t, J = 7.1 Hz)

^{13}C NMR (101 MHz, CD$_3$OD) δ ppm 168.5, 157.4, 157.1, 132.1, 124.3, 124.0, 61.7, 38.1, 14.8

HRMS (ESI Orbitrap) m/z: Calcd for C$_{12}$H$_{18}$N$_3$O$_2$ [M+H]$^+$ 236.1394; found [M+H]$^+$ 236.1384

Tert-butyl 3-((amino(dimethylamino)methylene)amino)benzoate (465)
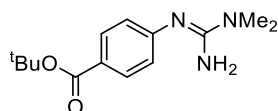
Using General Procedure 3 with *tert*-butyl 4-aminobenzoate (2.52 g, 13.1 mmol, 1 equiv), sodium hydride (0.77 g, 19.3 mmol, 1.5 equiv) and dimethylcyanamide (1.13 g, 16.1 mmol, 1.2 equiv), after 16 hours and the standard work-up, the resultant crude solid was washed with heptane (15 mL) and recrystallised from heptane/EtOAc to afford *tert*-butyl 3-((amino(dimethylamino)methylene) amino)benzoate (**465**) as a white crystalline solid (2.61 g, 9.9 mmol 76%).
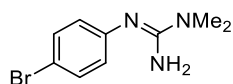
Appearance: White crystals

M.pt: 104–107 °C

ν (neat): 3446, 2982 (br), 1701, 1563, 1368, 1289 cm^{-1}

^{1}H NMR (400 MHz, CD$_3$OD) δ ppm 7.86 (2H, d, J = 8.4 Hz), 6.95 (2H, d, J = 8.4 Hz), 3.01 (6H, s), 1.60 (9H, s)

^{13}C NMR (101 MHz, CD$_3$OD) δ ppm 166.5, 155.7, 155.2, 130.4, 124.4, 123.0, 80.2, 36.6, 27.1

HRMS (ESI Orbitrap) *m/z*: Calcd for C$_{13}$H$_{22}$N$_3$O$_2$ [M+H]$^+$ 264.1707; found [M+H]$^+$ 264.2698

2-(4-Bromophenyl)-1,1-dimethylguanidine (466)

Using General Procedure 3 with 4-bromoaniline (4.00 g, 23.3 mmol, 1 equiv), sodium hydride (1.21 g, 30.3 mmol, 1.3 equiv) and dimethylcyanamide (1.91 g, 27.2 mmol, 1.20 equiv), after 16 hours, following the standard work-up the resultant yellow solid was purified by recrystallisation from hot EtOAc and washing the resultant crystals with cold heptane to yield 2-(4-bromophenyl)-1,1-dimethylguanidine (**466**) as a yellow crystalline solid (2.19 g, 9.1 mmol, 39%).

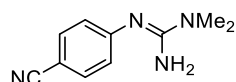Appearance: Yellow crystals

M.pt: 92–94 °C

ν (neat): 3540, 3190 (br), 1693, 1633, 1593, 1556 cm^{-1}

^{1}H NMR (400 MHz, CD$_3$OD) δ ppm 7.37–7.42 (2H, m), 6.81–6.85 (2H, m), 2.99 (6H, s)

^{13}C NMR (101 MHz, CD$_3$OD) δ ppm 157.1, 151.0, 133.2, 127.1, 115.5, 38.0

HRMS (ESI Orbitrap) *m/z*: Calcd for C$_9$H$_{13}$^{79}BrN$_3$ [M+H]$^+$ 242.0297; found [M+H]$^+$ 242.0280

2-(4-Cyanophenyl)-1,1-dimethylguanidine (467)

Using General Procedure 3 with 4-aminobenzonitrile (3.00 g, 25.4 mmol, 1 equiv), sodium hydride (1.32 g, 33.0 mmol, 1.3 equiv) and dimethylcyanamide (2.14 g, 30.5 mmol, 1.2 equiv), after 16 hours 2-(4-cyanophenyl)-1,1-dimethylguanidine (**467**) was isolated as a white crystalline solid after recrystallisation from EtOAc (1.412 g, 7.5 mmol, 30%).

Appearance: White crystals

M.pt: 125–127 °C

ν (neat): 3370, 2216, 1631, 1514, 1404, cm^{-1}

^{1}H NMR (400 MHz, CD$_3$OD) δ ppm 7.53–7.60 (2H, m), 6.98–7.04 (2H, m), 3.02 (6H, s)

^{13}C NMR (101 MHz, CD$_3$OD) δ ppm 157.6, 157.4, 134.4, 125.3, 121.0, 103.9, 38.0

HRMS (ESI Orbitrap) *m/z*: Calcd for C$_{10}$H$_{13}$N$_3$ [M+H]$^+$ 189.1135; found [M+H]$^+$ 189.1136

2-(2-Fluorophenyl)-1,1-dimethylguanidine (468)
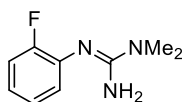
Using General Procedure 3 with 2-fluoroaniline (2.00 g, 18.0 mmol, 1 equiv), sodium hydride (0.87 g, 21.9 mmol, 1.2 equiv) and dimethylcyanamide (1.51 g, 21.6 mmol, 1.2 equiv). After 15 hours and the standard work up, the crude material was purified by column chromatography

(5% MeOH in CH$_2$Cl$_2$ with 2% triethylamine in the CH$_2$Cl$_2$ portion) to give 2-(2-fluorophenyl)-1,1-dimethylguanidine (**468**) as an off-white solid (2.02 g, 11.2 mmol, 62%).

Appearance: Off-white solid

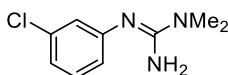M.pt: 86–88 °C

ν (neat): 3458, 3134 (br), 1636, 1566, 1481 cm^{-1}

^{1}H NMR (400 MHz, CD$_3$OD) δ ppm 7.03–7.11 (2H, m), 6.95–7.03 (2H, m), 3.02 (6H, s)

^{13}C NMR (101 MHz, CD$_3$OD) δ ppm 157.4, 157.6 (d, J = 242.4 Hz), 139.0 (d, J = 12.8 Hz), 128.1 (d, J = 2.5 Hz), 125.7 (d, J = 3.6 Hz), 124.4 (d, J = 7.4 Hz), 116.9 (d, J = 20.8 Hz), 38.1.

^{19}F NMR (377 MHz, CD$_3$OD) δ ppm −126.93 (s)

HRMS (ESI Orbitrap) *m/z*: Calcd for C$_{11}$H$_{13}$FN$_3$ [M+H]$^+$ 182.1088; found [M+H]$^+$ 182.1079

3-(3-Chlorophenyl)-1,1-dimethylguanidine (469)

Using General Procedure 3 with 3-chloroaniline (1.51 g, 11.8 mmol, 1 equiv), sodium hydride (0.58 g, 14.5 mmol, 1.2 equiv) and dimethylcyanamide (1.00 g, 14.2 mmol, 1.2 equiv), after 2.5 hours, 3-(3-chlorophenyl)-1,1-dimethylguanidine (**469**) was isolated as a white solid after chromatography (0–10% MeOH in CH$_2$Cl$_2$) (1.06 g, 5.4 mmol, 46%).
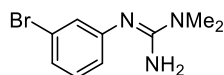
Appearance: White solid

M.pt: 89–91 °C

ν (neat): 3437, 3122 (br), 1637, 1553, 1398, 1302 cm^{-1}

^{1}H NMR (400 MHz, (CD$_3$)$_2$SO) δ ppm 7.19 (1H, t, J = 7.9 Hz), 6.83–6.87 (1H, m), 6.76 (1H, t, J = 2.0 Hz), 6.68–6.72 (1H, m), 5.81 (2H, *br.* s), 2.89 (6H, s)

^{13}C NMR (101 MHz, (CD$_3$)$_2$SO) δ ppm 153.4, 152.0, 133.1, 130.3, 122.6, 121.7, 119.9, 37.4

HRMS (ESI Orbitrap) *m/z*: Calcd for C$_9$H$_{13}$^{35}ClN$_3$ [M+H]$^+$ 198.0793; found [M+H]$^+$ 198.0785

3-(3-Bromophenyl)-1,1-dimethylguanidine (470)

Using General Procedure 3 with 3-bromoaniline (3.00 g, 17.4 mmol, 1 equiv), sodium hydride (0.84 g, 20.9 mmol, 1.2 equiv) and dimethylcyanamide (1.47 g, 20.9 mmol, 1.2 equiv), after 16 hours and the standard work-up procedure the crude product was purified by reverse-phase chromatography (kP-C$_{18}$-HS cartridge 15–55% water/acetonitrile with 0.1% NH$_4$HCO$_3$ buffer). The fractions containing product were evaporated to remove the acetonitrile and the aqueous pH increased to ~10 with NH$_4$OH, which was then extracted with tBME (3 × 50 mL). The organic portion was then washed with brine, dried over anhydrous MgSO$_4$ and concentrated *in vacuo* to afford 3-(3-bromophenyl)-1,1-dimethylguanidine (**470**) as an off-white solid (883 mg, 3.7 mmol, 21%).

Appearance: Off-white solid

M.pt: 104–106 °C

ν (neat): 3437, 3128 (br), 1637, 1598, 1551, 1465, 1398 cm^{-1}

^{1}H NMR (400 MHz, CD$_3$OD) δ ppm 7.15 (1H, t, J = 7.8 Hz), 7.09 (1H, ddd, J = 7.8, 2.0, 1.2 Hz), 7.04 (1H, t, J = 2.0 Hz), 6.84 (1H, ddd, J = 7.8, 2.0, 1.2 Hz), 2.96 (6H, s)

^{13}C NMR (101 MHz, CD$_3$OD) δ ppm 157.2, 153.7, 131.7, 128.2, 125.8, 124.1, 123.7, 38.0

HRMS (ESI Orbitrap) *m/z*: Calcd for C$_9$H$_{13}$^{79}BrN$_3$ [M+H]$^+$ 242.0287; found [M+H]$^+$ 242.0275

2-(Benzo[*d*][1,3]dioxol-5-yl)-1,1-dimethylguanidine (471)
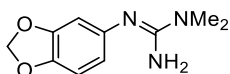
Using General Procedure 3 with benzo[d][1,3]dioxol-5-amine (2.49 g, 29.5 mmol, 1 equiv), sodium hydride (1.58 g, 39.6 mmol, 1.3 equiv) and dimethylcyanamide (2.49 g, 35.5 mmol, 1.2 equiv), after 16 hours and the standard work-up, the resultant solid was washed with cold heptane and then EtOAc, and purified by chromatography (0–6% MeOH in CH$_2$Cl$_2$, Biotage KP-NH silica) to afford 2-(benzo[d][1,3]dioxol-5-yl)-1,1-dimethylguanidine (**471**) as a fluffy grey solid (2.63 g, 12.7 mmol, 43%).
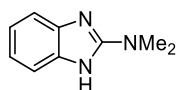
Appearance: Grey solid

M.pt: 137–138 °C

ν (neat): 3435, 3192 (br), 2898, 1634, 1574, 1437 cm^{-1}

^{1}H NMR (400 MHz, CD$_3$OD) δ ppm 6.75 (1H, d, J = 8.2 Hz), 6.43 (1H, d, J = 2.1 Hz), 6.36 (1H, dd, J = 8.2, 2.1 Hz), 5.91 (2H, s), 2.97 (6H, s)

^{13}C NMR (101 MHz, CD$_3$OD) δ ppm 157.4, 149.7, 145.4, 144.5, 117.4, 109.4, 106.7, 102.2, 38.1 HRMS (ESI Orbitrap) m/z: Calcd for C$_{10}$H$_{14}$N$_3$O$_2$ [M+H]$^+$ 208.1081; found [M+H]$^+$ 208.1070

N,N-dimethyl-1H-benzo[d]imidazol-2-amine (472)

Using General Procedure 4 for benzimidazole formation was performed with 1,1-dimethyl-2-phenylguanidine (**463**) (201 mg, 1.2 mmol), Cu(EAA)$_2$ (98 mg, 0.3 mmol, 0.25 equiv) and pivalic acid (125 mg, 1.2 mmol, 1.0 equiv) for 24 hours to yield *N,N*-dimethyl-1*H*-benzo[*d*]imidazol-2-amine (**472**) as an off-white solid. (129 mg, 0.8 mmol, 65%).

Appearance: Off-white solid

M.pt: 202–204 °C

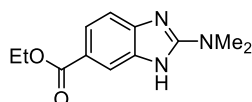ν (neat): 2918, 1634, 1603, 1575 (br), 1425, 1411 cm^{-1}

^{1}H NMR (400 MHz, CD$_3$OD) δ ppm 7.24 (2H, dd, J = 5.8, 3.3 Hz), 6.99 (2H, dd, J = 5.8, 3.3 Hz), 3.08 - 3.25 (6H, s)

^{13}C NMR (101 MHz, CD$_3$OD) δ ppm 156.6, 138.1 (*br*), 119.8, 111.2 (*br*), 37.2

HRMS (ESI Orbitrap) m/z: Calcd for C$_9$H$_{12}$N$_3$ [M+H]$^+$ 162.1031; found [M+H]$^+$ 162.1033

The spectroscopic data is concurrent with the literature.[209]

Ethyl 2-(dimethylamino)-1H-benzo[d]imidazole-6-carboxylate (473)

Using General Procedure 4 for benzimidazole formation was performed with ethyl 4-((amino(dimethylamino)methylene)amino)benzoate (**464**) (50 mg, 0.2 mmol), Cu(EAA)$_2$ (18 mg, 0.06 mmol, 0.27 equiv) and pivalic acid (22 mg, 0.2 mmol, 1.0 equiv) for 14.5 hours to yield ethyl 2-(dimethylamino)-1*H*-benzo[*d*]imidazole-6-carboxylate (**473**) as an off-white solid. (31 mg, 0.13 mmol, 63%).

Appearance: Off-white solid

M.pt: 210–212 °C

ν (neat): 3193, 2981, 1693, 1638, 1602, 1297 cm^{-1}

^{1}H NMR (400 MHz, CD$_3$OD) δ ppm 7.75 (1H, d, *J* = 1.5 Hz), 7.62 (1H, dd, *J* = 8.2, 1.5 Hz), 7.12 (1H, d, *J* = 8.2 Hz), 4.22 (2H, q, *J* = 7.1 Hz), 3.02 (6H, s), 1.27 (3H, t, *J* = 7.1 Hz)

^{13}C NMR (101 MHz, CD$_3$OD) δ ppm 169.2, 159.6, 145.2, 138.5, 123.9, 123.0, 113.7, 112.7, 61.7, 38.5, 14.8

HRMS (ESI Orbitrap) *m/z*: Calcd for C$_{12}$H$_{16}$N$_3$O$_2$ [M+H]$^+$ 234.1237; found [M+H]$^+$ 234.1227

Tert-butyl 2-(dimethylamino)-1*H*-benzo[*d*]-imidazole-5-carboxylate (474)
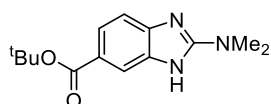
Using General Procedure 4 for benzimidazole formation was performed with *tert*-butyl 4-((amino(dimethylamino)methylene)amino)benzoate (**465**) (259 mg, 1.0 mmol), Cu(EAA)$_2$ (81 mg, 0.25 mmol, 0.26 equiv) and pivalic acid (102 mg, 1.0 mmol, 1.0 equiv) for 25 hours to yield *tert*-butyl 2-(dimethylamino)-1*H*-benzo[*d*]imidazole-5-carboxylate (**474**) as a brown solid. (137 mg, 0.52 mmol, 53%).

Appearance: Brown solid

M.pt: 216–218 °C

ν (neat): 2981, 1695, 1635, 1605, 1574 cm^{-1}

^{1}H NMR (400 MHz, CD$_3$OD) δ ppm 7.83 (1H, s), 7.69 (1H, dd, J = 8.3, 1.1 Hz), 7.23 (1H, d, J = 8.3 Hz), 3.15 (6H, s), 1.61 (9H, s)

^{13}C NMR (101 MHz, CD$_3$OD) δ ppm 167.1, 123.2, 122.3, 112.0, 111.0, 80.1, 37.1, 27.2

Not all signals are present by NMR. 1 × aliphatic carbon missing from spectra and 1 × quaternary carbon. NMR sample was saturated (~100 mg in solution) and number of scans set to 10,000

HRMS (ESI Orbitrap) m/z: Calcd for C$_{14}$H$_{20}$N$_3$O$_2$ [M+H]$^+$ 262.1550; found [M+H]$^+$ 262.1539

5-Bromo-*N,N*-dimethyl-1*H*-benzo[*d*]imidazol-2-amine (475)
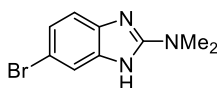
Using General Procedure 4 for benzimidazole formation was performed with 2-(4-bromophenyl)-1,1-dimethylguanidine (**466**) (174 mg, 0.72 mmol), Cu(EAA)$_2$ (59 mg, 0.18 mmol, 0.25 equiv) and pivalic acid (74 mg, 0.72 mmol, 1.0 equiv) for 14.5 hours to yield 5-bromo-*N,N*-dimethyl-1*H*-benzo[*d*]imidazol-2-amine (**475**) as an off-white solid. (100 mg, 0.42 mmol, 58%).

Appearance: Off-white solid

M.pt: 244–245 °C

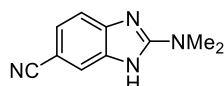ν (neat): 2981, 1630, 1602, 1568, 1459, 1408 cm^{-1}

^{1}H NMR (400 MHz, CD$_3$OD) δ ppm 7.34 (1H, s), 7.06–7.14 (2H, m), 3.13 (6H, s)

^{13}C NMR (101 MHz, CD$_3$OD) δ ppm 158.7, 141.8, 138.1, 123.9, 116.0, 113.8, 113.6, 38.6

HRMS (ESI Orbitrap) m/z: Calcd for C$_9$H$_{11}$N$_3$^{79}Br [M+H]$^+$ 240.0131; found [M+H]$^+$ 240.0121.

The spectroscopic data is concurrent with the literature.[332]

2-(Dimethylamino)-1*H*-benzo[*d*]imidazole-6-carbo-nitrile (476)

Using General Procedure 4 for benzimidazole formation was performed with 2-(4-cyanophenyl)-1,1-dimethylguanidine (**466**) (292 mg, 1.6 mmol), Cu(EAA)$_2$ (115 mg, 0.4 mmol, 0.25 equiv) and pivalic acid (158 mg, 1.6 mmol, 1.0 equiv) for 24 hours to yield 2-(dimethylamino)-1*H*-benzo[*d*]imidazole-6-carbonitrile (**476**) as a brown solid (114 mg, 0.61 mmol, 40%).

Appearance: Brown solid
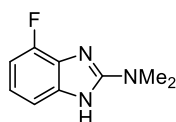
ν (neat): 2978, 2210 (CN), 1639, 1599, 1574, 1470 cm^{-1}

^{1}H NMR (400 MHz, CD$_3$OD) δ ppm 7.49 (1H, s), 7.28–7.38 (2H, m), 3.18 (6H, s)

^{13}C NMR (101 MHz, CD$_3$OD) δ ppm 159.9, 140.2, 139.1, 126.0, 121.9, 113.8, 103.0, 38.7

HRMS (ESI Orbitrap) *m/z*: Calcd for C$_{10}$H$_{11}$N$_4$ [M+H]$^+$ 187.0978; found [M+H]$^+$ 187.0972

The spectroscopic data is concurrent with the literature.[333]

4-Fluoro-*N,N*-dimethyl-1*H*-benzo[*d*]imidazol-2-amine (477)

Using General Procedure 4 for benzimidazole formation was performed with 2-(2-fluorophenyl)-1,1-dimethylguanidine (**468**) (201 mg, 1.1 mmol), Cu(EAA)$_2$ (89 mg, 0.3 mmol, 0.25 equiv) and pivalic acid (114 mg, 1.1 mmol, 1.0 equiv) for 19 hours to yield 4-fluoro-*N,N*-dimethyl-1*H*-benzo[*d*]imidazol-2-amine (**477**) as an off-white solid. (92 mg, 0.5 mmol, 46%).

Appearance: Off-white solid
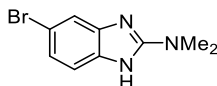
M.pt: 232–234 °C

ν (neat): 2921, 1634, 1578, 1509,1415cm^{-1}

^{1}H NMR (400 MHz, CD$_3$OD) δ ppm 7.01–7.06 (1H, m), 6.90–6.96 (1H, m), 6.76 (1H, ddd, *J* = 10.9, 8.2, 0.6 Hz), 3.16 (6H, s)

^{13}C NMR (101 MHz, CD$_3$OD) δ ppm 158.5, 151.6 (d, J = 243.2 Hz), 141.0, 129.1, 121.2 (d, J = 7.1 Hz), 107.9, 107.6 (d, J = 17.7 Hz), 38.7
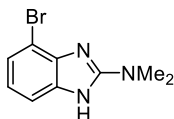
^{19}F NMR (376 MHz, CD$_3$OD) δ ppm −135.4

HRMS (ESI Orbitrap) m/z: Calcd for C$_9$H$_{11}$FN$_3$ [M+H]$^+$ 180.0937; found [M+H]$^+$ 180.0938

## 5-Bromo-*N,N*-dimethyl-1*H*-benzo[*d*]imidazol-2-amine (475)

4-Bromo-*N,N*-dimethyl-1*H*-benzo[*d*]imidazol-2-amine (478)

Using General Procedure 4 for benzimidazole formation was performed with 2-(3-bromophenyl)-1,1-dimethylguanidine (**470**) (201 mg, 0.83 mmol), Cu(EAA)$_2$ (67 mg, 0.21 mmol, 0.25 equiv) and pivalic acid (86 mg, 0.84 mmol, 1.0 equiv) for 18 hours. 5-bromo-*N,N*-dimethyl-1*H*-benzo[*d*]imidazol-2-amine (**475**) was isolated as a brown solid (130 mg, 0.54 mmol, 66%). The fractions containing impure 4-bromo-*N,N*-dimethyl-1*H*-benzo[*d*]imidazol-2-amine (**478**) were re-purified by chromatography (3% MeOH in CH$_2$Cl$_2$) to yield 4-bromo-*N,N*-dimethyl-1*H*-benzo[d]imidazol-2-amine (**478**) as a brown foam (49 mg, 0.21 mmol, 25%).

5-Bromo-*N,N*-dimethyl-1*H*-benzo[*d*]imidazol-2-amine (475)
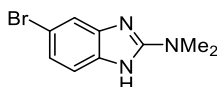
Appearance: Brown solid

M.pt: 244–246 °C

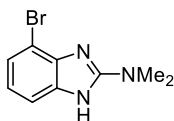ν (neat): 2921, 2859, 1628, 1603, 1578, 1459, 1409, 1278.

^{1}H NMR (400 MHz, CD$_3$OD) δ ppm 7.32 (1H, d, J = 1.1 Hz), 7.05–7.12 (2H, m), 3.12 (6H, s)

^{13}C NMR (101 MHz, CD$_3$OD) δ ppm 158.7, 141.8, 138.1, 123.9, 116.0, 113.8, 113.6, 38.6

HRMS (ESI Orbitrap) m/z: Calcd for C$_9$H$_{11}$N$_3$Br [M+H]$^+$ 240.0131; found [M+H]$^+$ 240.0143

The spectroscopic data is concurrent with the literature.[332]

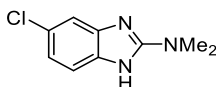**4-Bromo-*N,N*-dimethyl-1*H*-benzo[*d*]imidaz-ol-2-amine (478)**

Appearance: Brown foam

^{1}H NMR (400 MHz, CD$_3$OD) δ ppm 7.18 (1H, dd, *J* = 7.9, 0.8 Hz), 7.15 (1H, dd, *J* = 7.9, 0.8 Hz), 6.89 (1H, d, *J* = 7.9 Hz), 3.18 (6H, s)
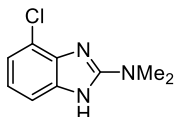
^{13}C NMR (101 MHz, CD$_3$OD) δ ppm. Low sample quantity and rapid tautomerisation meant multiple peaks were missing from the ^{13}C NMR

HRMS (ESI Orbitrap) *m/z*: Calcd for C$_9$H$_{11}$N$_3$Br [M+H]$^+$ 240.0131; found [M+H]$^+$ 240.0144

5-Chloro-*N,N*-dimethyl-1*H*-benzo[*d*]imidazol-2-amine (479)

4-Chloro-*N,N*-dimethyl-1*H*-benzo[*d*]imid- azol-2-amine (480)

Using General Procedure 4 for benzimidazole formation was performed with 2-(3-chlorophenyl)-1,1-dimethylguanidine (**469**) (203 mg, 1.02 mmol), Cu(EAA)$_2$ (82 mg, 0.25 mmol, 0.25 equiv) and pivalic acid (104 mg, 1.02 mmol, 1.0 equiv) for 22 hours. The reaction was worked-up as described General Procedure 2, and purified by chromatography (60–100% EtOAc in Heptane) to isolate 5-chloro-*N,N*-dimethyl-1*H*-benzo[*d*]imidazol-2-amine (**479**) as a white solid (61 mg, 0.31 mmol, 30%). The fractions containing impure 4-chloro-*N,N*-dimethyl-1*H*-benzo[*d*]imidazol-2-amine (**480**) were re-purified by chromatography (3% MeOH in CH$_2$Cl$_2$) to yield 4-chloro-*N,N*-dimethyl-1*H*-benzo[*d*]imidazol-2-amine (**480**) as a white solid (10 mg, 0.05 mmol, 5%).

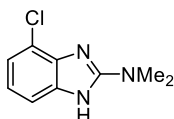**5-Chloro-*N*,*N*-dimethyl-1*H*-benzo[*d*]imidazol-2-amine (479)**
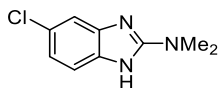
Appearance: White solid

M.pt: 245–247 °C

^{1}H NMR (400 MHz, CD$_3$OD) δ ppm 7.17 (1H, d, *J* = 1.9 Hz), 7.13 (1H, d, *J* = 8.4 Hz), 6.94 (1H, dd, *J* = 8.4, 1.9 Hz), 3.11 (6H, s)

HRMS (ESI Orbitrap) *m/z*: Calcd for C$_9$H$_{11}$N$_3$Cl [M+H]$^+$ 196.0636; found [M+H]$^+$ 196.0645

The spectroscopic data is concurrent with the literature.[334]

4-Chloro-*N*,*N*-dimethyl-1*H*-benzo[*d*]imidazol-2-amine (480)


Appearance: White solid

^{1}H NMR (400 MHz, CD$_3$OD) δ ppm 7.12 (1H, dd, *J* = 8.0, 1.1 Hz), 6.97 (1H, dd, *J* = 8.0, 1.1 Hz), 6.91 (1H, d, *J* = 8.0 Hz), 3.15 (6H, s)

^{13}C NMR (101 MHz, CD$_3$OD) δ ppm 159.0, 121.8 (*br*), 39.1.

Multiple signals missing from spectra. It is likely that the quaternary carbons are the non-observable signals and the lack of material meant a more resolved spectrum was not obtained.

HRMS (ESI Orbitrap) *m/z*: Calcd for C$_9$H$_{11}$N$_3$Cl [M+H]$^+$ 196.0636; found [M+H]$^+$ 196.0646

**N,N-dimethyl-5*H*-[1,3]dioxolo[4',5':4,5]benzo[1,2-*d*]imidazol-6-amine (481)**
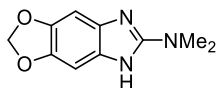
N,N-dimethyl-8H-[1,3]dioxolo[4',5':3,4]benzo[1,2-d]imidazol-7-amine (482)
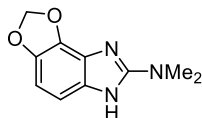
Using General Procedure 4 for benzimidazole formation was modified to 90 °C but otherwise identical with 2-(benzo[d][1,3]dioxol-5-yl)-1,1-dimethylguanidine (**471**) (50 mg, 0.24 mmol), Cu(EAA)$_2$ (19 mg, 0.06 mmol, 0.25 equiv) and pivalic acid (25 mg, 0.24 mmol, 1.0 equiv) for 12 hours. The products were purified by chromatography using the standard method to yield *N,N*-dimethyl-5*H*-[1,3]dioxolo[4',5':4,5]benzo[1,2-*d*]imidazol-6-amine (**481**) as an off-white solid (14 mg, 0.07 mmol, 28%) and *N,N*-dimethyl-8*H*-[1,3]dioxolo[4',5':3,4]benzo[1,2-*d*]imidazol-7-amine (**482**) as an off white solid (26 mg, 0.13 mmol, 53%).

N,N-dimethyl-8H-[1,3]dioxolo[4',5':3,4]benzo[1,2-d]imidazol-7-amine (482)
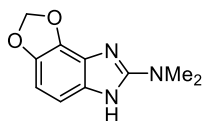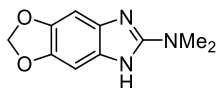

Appearance: Off-white solid

M.pt: 110–112 °C

ν (neat): 3357, 3126 (br), 1664, 1622, 1603, 1463 cm^{-1}

^{1}H NMR (400 MHz, CD$_3$OD) δ ppm 6.55 (1H, d, *J* = 8.2 Hz), 6.43 (1H, d, *J* = 8.2 Hz), 5.80 (2H, s), 2.99 (6H, s)

^{13}C NMR *an informative ^{13}C spectra could not be obtained due to the low sample quantity and multiple peaks were not present in the spectra. All the available material was loaded into the NMR tube, despite this, the signals were not detectable above the baseline, even when increasing the number of scans to 8192.*

HRMS (ESI Orbitrap) *m/z*: Calcd for C$_{10}$H$_{12}$N$_3$O$_2$ [M+H]$^+$ 206.0924; found [M+H]$^+$ 206.0916

N,N-dimethyl-5H-[1,3]dioxolo[4',5':4,5]benzo[1,2-d]imidazol-6-amine (481)

324

Appearance: Off-white solid

M.pt: > 400 °C

ν (neat): 2981, 2867, 1623, 1601, 1496, 1463, 1423 cm^{-1}

^{1}H NMR (400 MHz, CD$_3$OD) δ ppm 6.64 (2H, s), 5.73 (2H, s), 2.96 (6H, s)

^{13}C NMR *an informative ^{13}C spectra could not be obtained due to the low sample quantity and multiple peaks were not present in the spectra. Sample saturation was performed (as above) to afford a more informative spectrum.*

HRMS (ESI Orbitrap) *m/z*: Calcd for C$_{10}$H$_{12}$N$_3$O$_2$ [M+H]$^+$ 206.0924; found [M+H]$^+$ 206.0915

1,1-Diethyl-2-phenylguanidine (484)
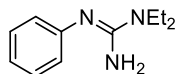
Using General Procedure 3 with aniline (1.50 g, 16.1 mmol, 1 equiv), sodium hydride (0.869 g, 21.7 mmol, 1.4 equiv) and diethylcyanamide (1.74 g, 17.7 mmol, 1.1 equiv), after 24 hours using the standard work-up and purification by chromatography (0–10% MeOH in CH$_2$Cl$_2$) yielded 1,1-diethyl-2-phenylguanidine (**484**) as a white solid (1.09 g, 5.7 mmol, 35%).

Appearance: White solid

M.pt: 59–61 °C

ν (neat): 3441, 3074, 2976, 1637, 1543 cm^{-1}

^{1}H NMR (400 MHz, CD$_3$OD) δ ppm 7.25–7.33 (2H, m), 7.00 (1H, tt, *J* = 7.4, 1.2 Hz), 6.89–6.95 (2H, m), 3.41 (4H, q, *J* = 7.1 Hz), 1.22 (6H, t, *J* = 7.1 Hz)

^{13}C NMR (101 MHz, CD$_3$OD) δ ppm 153.8, 150.2, 128.9, 124.0, 121.8, 41.6, 12.5

HRMS (ESI Orbitrap) *m/z*: Calcd for C$_{11}$H$_{18}$N$_3$ [M+H]$^+$ 192.1495; found [M+H]$^+$ 192.1488

2-(4-Bromophenyl)-1,1-diethylguanidine (485)
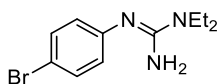
Using General Procedure 3 with 4-bromoaniline (2.44 g, 14.2 mmol, 1 equiv), sodium hydride (0.732 g, 18.3 mmol, 1.3 equiv) and diethylcyanamide (1.61 g, 16.4 mmol, 1.2 equiv) after 24 hours at room temperature was added further diethylcyanamide (0.42 g, 4.3 mmol, 0.3 equiv). After a further 5 hours using the standard work-up was isolated 2-(4-bromophenyl)-1,1-diethylguanidine (**485**) as a white crystalline solid by chromatography (1% MeOH/EtOAc w/ 1% triethylamine in EtOAc portions) and subsequent recrystallisation (heptane/EtOAc) (700 mg, 2.6 mmol, 18%).

Appearance: White crystals

M.pt: 53–54 °C

ν (neat):=3453, 3139, 2976 cm^{-1}

^{1}H NMR (400 MHz, CD$_3$OD) δ ppm 7.28–7.44 (2H, m), 6.70–6.88 (2H, m), 3.37 (4H, q, J = 7.1 Hz), 1.17 (6H, t, J = 7.1 Hz)

^{13}C NMR (101 MHz, CD$_3$OD) δ ppm 153.8, 149.7, 131.8, 125.8, 114.0, 41.6, 12.4

HRMS (ESI Orbitrap) *m/z*: Calcd for C$_{11}$H$_{17}$^{79}BrN$_3$ [M+H]$^+$ 270.0600; found [M+H]$^+$ 270.0599

N-phenylpiperidine-1-carboximidamide (486)

Using General Procedure 3 with aniline (1.23 g, 13.2 mmol, 1 equiv), sodium hydride (0.643 g, 16.1 mmol, 1.2 equiv) and piperidine-1-carbonitrile (1.41 g, 12.8 mmol, 1.0 equiv) after 16 hours and the standard work-up was isolated *N*-phenylpiperidine-1-carboximidamide (**486**) as a white solid by chromatography (1% triethylamine in EtOAc) (555 mg, 2.7 mmol, 21%).
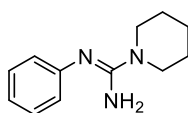
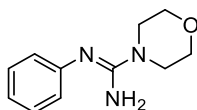Appearance: White solid

M.pt: 74–76 °C

ν (neat): 3435, 2857, 1637 cm⁻¹

^{1}H NMR (400 MHz, CD$_3$OD) δ ppm 7.25–7.33 (2H, m), 7.00 (1H, tt, J = 7.4, 1.2 Hz), 6.87–6.94 (2H, m), 3.37–3.45 (4H, m), 1.57–1.76 (6H, m)

^{13}C NMR (101 MHz, CD$_3$OD) δ ppm 155.6, 149.7, 128.9, 123.5, 121.9, 46.4, 25.5, 24.4

HRMS (ESI Orbitrap) m/z: Calcd for C$_{12}$H$_{18}$N$_3$ [M+H]$^+$ 204.1495; found [M+H]$^+$ 204.1486

N-phenylmorpholine-4-carboximidamide (487)

Using General Procedure 3 with aniline (1.00 g, 10.7 mmol, 1 equiv), sodium hydride (0.589 g, 14.7 mmol, 1.4 equiv) and morpholine-4-carbonitrile (1.26 g, 11.3 mmol, 1.1 equiv) after 24 hours and the standard work-up was isolated N-phenylmorpholine-4-carboximidamide (**487**) as a white solid by chromatography (80–100% EtOAc in heptane with 2% triethylamine in EtOAc portions). (752 mg, 3.6 mmol, 34%).

Appearance: White solid

M.pt: 131–133 °C

ν (neat): 3453, 3354, 2848 cm⁻¹

^{1}H NMR (400 MHz, CD$_3$OD) δ ppm 7.31 (2H, tt, J = 7.6, 1.2 Hz), 7.02 (1H, tt, J = 7.6, 1.2 Hz), 6.88–6.94 (2H, m), 3.72–3.78 (4H, m), 3.37–3.41 (4H, m)

^{13}C NMR (101 MHz, CD$_3$OD) δ ppm 155.7, 149.4, 129.0, 123.4, 122.2, 66.4, 45.9

HRMS (ESI Orbitrap) m/z: Calcd for C$_{11}$H$_{16}$N$_3$O [M+H]$^+$ 206.1288; found [M+H]$^+$ 206.1278

N-(4-bromophenyl)morpholine-4-carboximidamide (488)
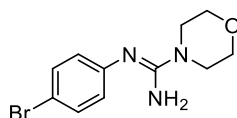
Using General Procedure 3 with 4-bromoaniline (2.46 g, 14.3 mmol, 1 equiv), sodium hydride (0.78 g, 19.6 mmol, 1.4 equiv) and morpholine 4-carbonitrile (1.76 g, 15.7 mmol, 1.1 equiv) after 16 hours and chromatography (1–3% MeOH in EtOAc w/ 1% triethylamine in EtOAc portion) was isolated *N*-phenylmorpholine-4-carboximidamide (**488**) as an off-white solid (2.84 g, 10.0 mmol, 70%).
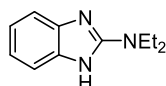
Appearance: White solid

M.pt: 110–112 °C

ν (neat): 3447, 3069, 2852, 1635, 1589, 1560, 1433 cm^{-1}

^{1}H NMR (400 MHz, CD$_3$OD) δ ppm 7.38–7.44 (2H, m), 6.79–6.86 (2H, m), 3.74 (4H, t, *J* = 4.8 Hz), 3.38 (4H, t, *J* = 4.8 Hz)

^{13}C NMR (101 MHz, CD$_3$OD) δ ppm 155.6, 149.1, 131.9, 125.3, 114.4, 66.3, 45.8

HRMS (ESI Orbitrap) *m/z*: Calcd for C$_{11}$H$_{15}$^{79}BrN$_3$O [M+H]$^+$ 284.0393; found [M+H]$^+$ 284.0384

N,N-diethyl-1H-benzo[d]imidazol-2-amine (489)

Using General Procedure 4 for benzimidazole formation was performed with 1,1-diethyl-2-phenylguanidine (**484**) (256 mg, 1.34 mmol), Cu(EAA)$_2$ (108 mg, 0.34 mmol, 0.25 equiv) and pivalic acid (139 mg, 1.36 mmol, 1.0 equiv) for 19 hours to yield *N,N*-diethyl-1*H*-benzo[*d*]imidazol-2-amine (**484**) as a pale orange solid. (118 mg, 0.62 mmol, 46%).

Appearance: Pale-orange solid

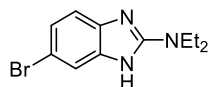M.pt: 202–204 °C

ν (neat): 2964, 2871, 1625, 1599, 1567 cm^{-1}

^{1}H NMR (400 MHz, CD$_3$OD) δ ppm 7.22 (2H, dd, J = 5.5, 3.2 Hz), 6.97 (2H, dd, J = 5.5, 3.2 Hz), 3.51 (4H, q, J = 7.0 Hz), 1.24 (6H, t, J = 7.0 Hz)

^{13}C NMR (101 MHz, CD$_3$OD) δ ppm 155.1, 138.2, 119.7, 111.2, 42.6, 12.3

HRMS (ESI Orbitrap) m/z: Calcd for C$_{11}$H$_{16}$N$_3$ [M+H]$^+$ 190.1339; found [M+H]$^+$ 190.1331

6-Bromo-*N,N*-diethyl-1*H*-benzo[*d*]imidazol-2-amine (490)

Using General Procedure 4 for benzimidazole formation was performed with 2-(4-bromophenyl)-1,1-diethylguanidine (**485**) (217 mg, 0.80 mmol), Cu(EAA)$_2$ (66 mg, 0.20 mmol, 0.25 equiv) and pivalic acid (84 mg, 0.82 mmol, 1.0 equiv) for 18 hours to yield 6-bromo-*N,N*-diethyl-1*H*-benzo[*d*]imidazol-2-amine (**490**) as an off-white solid. (159 mg, 0.59 mmol, 74%).

Appearance: Off-white solid

M.pt: 190–192 °C

ν (neat): 2971, 2929, 1625, 1560, 1463 cm^{-1}

^{1}H NMR (400 MHz, CD$_3$OD) δ ppm 7.33 (1H, d, J = 1.0 Hz), 7.04 - 7.13 (2H, m), 3.54 (4H, q, J = 7.1 Hz), 1.27 (6H, t, J = 7.1 Hz)

^{13}C NMR (101 MHz, CD$_3$OD) δ ppm 155.7, 122.2, 114.3, 112.2, 111.8, 42.7, 12.2 Two signals missing from spectra.

HRMS (ESI Orbitrap) m/z: Calcd for C$_{11}$H$_{15}$^{79}BrN$_3$ [M+H]$^+$ 268.0444; found [M+H]$^+$ 268.0445

2-(Piperidin-1-yl)-1*H*-benzo[*d*]imidazole (491)
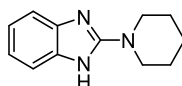
Using General Procedure 4 for benzimidazole formation was performed with *N*-phenylpiperidine-1-carboximidamide (**486**) (263 mg, 1.29 mmol), Cu(EAA)$_2$ (101 mg, 0.32

mmol, 0.25 equiv) and pivalic acid (137 mg, 1.34 mmol, 1.0 equiv) for 24 hours to yield 2-(piperidin-1-yl)-1H-benzo[d]imidazole (**491**) as a pale orange solid. (108 mg, 0.54 mmol, 41%).

Appearance: Pale-orange solid

M.pt: 276–278 °C

ν (neat): 2947, 2849, 1625, 1565, 1542 cm^{-1}

^{1}H NMR (400 MHz, CD$_3$OD) δ ppm 7.23 (2H, dd, J = 5.6, 3.1 Hz), 6.99 (2H, dd, J = 5.6, 3.1 Hz), 3.47–3.58 (4H, m), 1.65–1.77 (6H, m)

^{13}C NMR (101 MHz, CD$_3$OD) δ ppm 156.5, 120.0, 111.7 (br.), 47.0, 25.0, 23.9. One ^{13}C signal is missing from the spectra, presumably due to rapid interconversion by tautomerisation around the benzimidazole*.*

HRMS (ESI Orbitrap) *m/z*: Calcd for C$_{12}$H$_{16}$N$_3$ [M+H]$^+$ 202.1339; found [M+H]$^+$ 202.1329

The spectroscopic data is concurrent with the literature.[335]

4-(1H-Benzo[*d*]imidazol-2-yl)morpholine (492)

Using General Procedure 4 for benzimidazole formation was performed with *N*-phenylmorpholine-1-carboximidamide (**487**) (250 mg, 1.22 mmol), Cu(EAA)$_2$ (98 mg, 0.31 mmol, 0.25 equiv) and pivalic acid (126 mg, 1.23 mmol, 1.0 equiv) for 24 hours to yield 4-(1H-benzo[d]imidazol-2-yl)morpholine (**492**) as an off-white solid. (129 mg, 0.64 mmol, 52%).
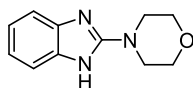
Appearance: Off-white solid

M.pt: 286–287 °C

ν (neat): 2981, 2848, 1625, 1560, 1451 cm^{-1}
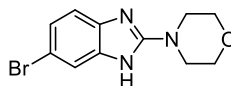
^{1}H NMR (400 MHz, CD$_3$OD) δ ppm 7.28 (2H, dd, J = 5.3, 3.2 Hz), 7.03 (2H, dd, J = 5.3, 3.2 Hz), 3.76–3.85 (4H, m), 3.44–3.54 (4H, m)

^{13}C NMR (101 MHz, CD$_3$OD) δ ppm 156.3 (br), 137.6 (br), 120.4, 112.0, 65.9, 46.3

HRMS (ESI Orbitrap) *m/z*: Calcd for $C_{11}H_{14}N_3O$ [M+H]$^+$ 204.1131; found [M+H]$^+$ 204.1121.

The spectroscopic data is concurrent with the literature.[209]

4-(6-Bromo-1*H*-benzo[*d*]imidazol-2-yl)morpholine (493)

Using General Procedure 4 for benzimidazole formation was performed with *N*-(4-bromophenyl)morpholine-4-carboximidamide (**488**) (269 mg, 0.95 mmol), Cu(EAA)$_2$ (78 mg, 0.24 mmol, 0.26 equiv) and pivalic acid (99 mg, 0.97 mmol, 1.0 equiv) for 21 hours to yield (**493**) as a brown solid. (157 mg, 0.56 mmol, 59%).

Appearance: Brown solid

M.pt: 235–236 °C

ν (neat): 3476 (br), 2976, 2842, 1626, 1557, 1441 cm^{-1}

^{1}H NMR (400 MHz, CD$_3$OD) δ ppm 7.39 (1H, s), 7.09–7.19 (2H, m), 3.79–3.87 (4H, m), 3.48−3.55 (4H, m)

^{13}C NMR (101 MHz, CDCl$_3$) δ ppm 156.4, 123.9, 113.8, 66.1, 46.6. *4 signals missing from the spectra*

HRMS (ESI Orbitrap) *m/z*: Calcd for $C_{11}H_{13}{}^{79}BrN_3O$ [M+H]$^+$ 282.0237; found [M+H]$^+$ 282.0233

N-(2-bromophenyl)piperidine-1-carboximidamide (494)
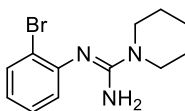
Using General Procedure 3 with 2-bromoaniline (2.00 g, 11.6 mmol, 1 equiv), sodium hydride (0.66 g, 16.5 mmol, 1.4 equiv) and piperidine 1-carbonitrile (1.33 g, 12.1 mmol, 1.05 equiv) after 16 hours and chromatography (EtOAc:heptane, 1:1, w/ 2% triethylamine in EtOAc portion) was isolated a white solid. The solid was then recrystalised from TBME to yield *N*-(2-

bromophenyl)piperidine-1-carboximidamide (**494**) as a white crystalline solid (1.41 g, 5.0 mmol, 43%).

Appearance: White crystals

M.pt: 104–105 °C

ν (neat): 3458, 3160, 2848, 1623, 1550, 1491, 1447 cm^{-1}

^{1}H NMR (400 MHz, CD$_3$OD) δ ppm 7.58 (1H, dd, J = 8.0, 1.3 Hz), 7.27 (1H, td, J = 7.6, 1.3 Hz), 6.98 (1H, dd, J = 8.0, 1.5 Hz), 6.92 (1H, td, J = 7.6, 1.5 Hz), 3.42–3.49 (4H, m), 1.61–1.75 (6H, m)

^{13}C NMR (101 MHz, CD$_3$OD) δ ppm 154.9, 148.5, 132.7, 128.0, 125.6, 123.4, 119.3, 46.5, 25.4, 24.4

HRMS (ESI Orbitrap) *m/z*: Calcd for C$_{12}$H$_{17}$^{79}BrN$_3$ [M+H]$^+$ 282.0600; found [M+H]$^+$ 282.0596

N-(2-bromophenyl)morpholine-4-carboximidamide (495)

Using General Procedure 3 with 2-bromoaniline (2.00 g, 11.6 mmol, 1 equiv), sodium hydride (0.61 g, 15.1 mmol, 1.3 equiv) and morpholine 4-carbonitrile (1.44 g, 12.9 mmol, 1.1 equiv) after 16 hours and chromatography (EtOAc:heptane, 1:1, w/ 2% triethylamine in EtOAc portion) was isolated a white solid. The solid was then recrystalised from TBME to yield *N*-(2-bromophenyl)morpholine-4-carboximidamide (**495**) as a white crystalline solid (1.48 g, 5.2 mmol, 45%).
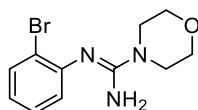
Appearance: White crystals

M.pt: 98–100 °C

ν (neat): 3458, 3150 (br), 2974, 1630, 1546, 1426, 1275 cm^{-1}
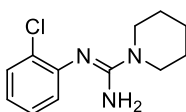
^{1}H NMR (400 MHz, CD$_3$OD) δ ppm 7.59 (1H, dd, J = 8.0, 1.4 Hz), 7.29 (1H, td, J = 7.6, 1.4 Hz), 6.98 (1H, dd, J = 8.0, 1.6 Hz), 6.94 (1H, td, J = 7.6, 1.6 Hz), 3.74–3.79 (4H, m), 3.41–3.47 (4H, m)

^{13}C NMR (101 MHz, CD$_3$OD) δ ppm 155.1, 148.2, 132.8, 128.1, 125.3, 123.7, 118.9, 66.4, 46.0

HRMS (ESI Orbitrap) m/z: Calcd for C$_{11}$H$_{15}$^{79}BrN$_3$O [M+H]$^+$ 284.0393; found [M+H]$^+$ 284.0384

N-(2-chlorophenyl)piperidine-1-carboximidamide (496)

Using General Procedure 3 with 2-chloroaniline (2.00 g, 15.7 mmol, 1 equiv), sodium hydride (0.82 g, 20.5 mmol, 1.3 equiv) and piperidine 1-carbonitrile (1.82 g, 16.5 mmol, 1.05 equiv) after 16 hours and chromatography (EtOAc:heptane, 1:1, w/ 2% triethylamine in EtOAc portion) was isolated a white solid. The solid was then recrystalised from TBME to yield *N*-(2-chlorophenyl)piperidine-1-carboximidamide (**496**) as a white crystalline solid (1.34 g, 5.6 mmol, 36%).

Appearance: White crystals

M.pt: 111–113 °C

ν (neat): 3463, 3151, 2934, 1628, 1590, 1550, 1434, 1308 cm^{-1}

^{1}H NMR (400 MHz, CD$_3$OD) δ ppm 7.36–7.42 (1H, m), 7.22 (1H, td, J = 7.6, 1.4 Hz), 6.95−7.02 (2H, m), 3.41–3.52 (4H, m), 1.60–1.77 (6H, m)

^{13}C NMR (101 MHz, CD$_3$OD) δ ppm 155.1, 147.2, 129.6, 128.5, 127.4, 125.8, 123.1, 46.5, 25.5, 24.4

HRMS (ESI Orbitrap) m/z: Calcd for C$_{12}$H$_{17}$^{35}ClN$_3$ [M+H]$^+$ 238.1106; found [M+H]$^+$ 238.1097

2-(Piperidin-1-yl)-1*H*-benzo[d]imidazole (491)
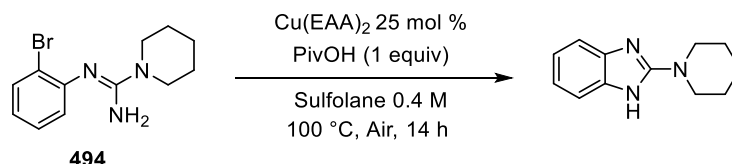
Using General Procedure 4 for benzimidazole formation was performed with *N*-(2-bromophenyl)piperidine-1-carboximidamide (**494**) (303 mg, 1.08 mmol), Cu(EAA)$_2$ (87 mg, 0.27 mmol, 0.25 equiv) and pivalic acid (113 mg, 1.11 mmol, 1.0 equiv) for 14 hours to give 2-(piperidin-1-yl)-1*H*-benzo[d]imidazole (**491**) as an off-white solid. (160 mg, 0.79 mmol, 74%).

Appearance: Off-white solid

Analytical data consistent with those recorded previously.

The spectroscopic data is concurrent with the literature.[335]

4-(1*H*-Benzo[*d*]imidazol-2-yl)morpholine (492)
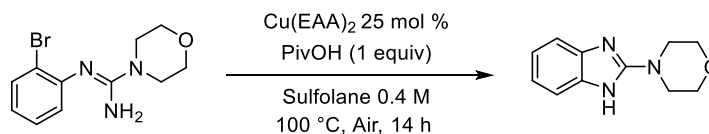
Using General Procedure 4 for benzimidazole formation was performed with *N*-(2-bromophenyl)morpholine-4-carboximidamide (**495**) (304 mg, 1.07 mmol), Cu(EAA)$_2$ (87 mg, 0.27 mmol, 0.25 equiv) and pivalic acid (109 mg, 1.07 mmol, 1.0 equiv) for 14 hours to give 4-(1*H*-benzo[*d*]imidazole-2-yl)morpholine (**492**) as an off-white solid. (155 mg, 0.76 mmol, 71%).

Appearance: Off-white solid

Analytical data consistent with those recorded previously.

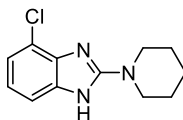*The spectroscopic data is concurrent with the literature.*[209]

4-Chloro-2-(piperidin-1-yl)-1*H*-benzo[*d*]imidazole (499)

Using an adaption of General Procedure 4 for benzimidazole formation was performed with *N*-(2-chlorophenyl)piperidine-1-carboximidamide (**496**) (242 mg, 1.02 mmol), Cu(EAA)$_2$ (82 mg, 0.26 mmol, 0.26 equiv) and pivalic acid (104 mg, 1.02 mmol, 1.0 equiv) for 24 hours. After flushing through the SCX cartridge, the crude material was purified by preparative high-performance liquid chromatography (30−75% MeCN in water, 0.05% ammonium bicarbonate buffer). The fractions containing product were concentrated under reduced pressure to remove the volatile organics and the resulting aqueous portion was extracted into CH$_2$Cl$_2$ (3 × 50 mL). The combined organics were washed with brine (50 mL) and dried over a hydrophobic frit to yield 4-chloro-2-(piperidin-1-yl)-1H-benzo[d]imidazole (**499**) as a brown solid. (123 mg, 0.51 mmol, 51%).

Appearance: Off-white solid

M.pt: 301–303 °C

ν (neat): 2940, 2856, 1624, 1545, 1468, 1438, 1401, 1313, 1259 cm^{-1}

^{1}H NMR (400 MHz, CD$_3$OD) δ ppm 7.13 (1H, d, *J* = 7.9 Hz), 6.99 (1H, d, *J* = 7.9 Hz), 6.93 (1H, t, *J* = 7.9 Hz), 3.51–3.63 (4H, m), 1.62–1.78 (6H, m)

^{13}C NMR (101 MHz, CD$_3$OD) δ ppm 156.9, 130.0, 127.8, 127.2, 120.5, 120.1, 109.2, 47.0, 25.0, 23.8

HRMS (ESI Orbitrap) *m/z*: Calcd for C$_{12}$H$_{15}$^{35}ClN$_3$ [M+H]$^+$ 236.0949; found [M+H]$^+$ 236.0941

1-Dimethyl-2-phenyl(D$_5$)guanidine (500)
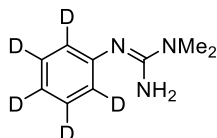
Using General Procedure 3 with aniline-D$_5$ (1.09 g, 11.1 mmol, 1 equiv), sodium hydride (0.51 g, 12.7 mmol, 1.15 equiv) and dimethylcyanamide (0.91 g, 13.0 mmol, 1.2 equiv) was reacted for 5 hours before addition of a further portion of dimethylcyanamide (0.17 g, 0.22 equiv) and the reaction stirred at room temperature overnight. After the standard work up, the product was purified by chromatography (Biotage K*P*-NH silica, EtOAc) and the fractions containing product were recrystallised from EtOAc to yield 1,1-dimethyl-2-(phenyl-D$_5$)guanidine (**500**) as a white crystalline solid (461 mg, 2.7 mmol, 25%).

Appearance: White crystals

^{1}H NMR (400 MHz, CD$_3$OD) δ ppm 2.96 (6H, s)

^{13}C NMR (101 MHz, CD$_3$OD) δ ppm 157.1, 151.1, 129.8 (t, J = 25.0 Hz), 124.9 (t, J = 24.0 Hz), 122.8 (t, J = 23.8 Hz), 38.1

^{2}H NMR (92 MHz, (CD$_3$)$_2$SO) δ ppm 7.4 (2 D, s), 7.1 (1 D, s), 7.1 (2 D, s)

Internal standard calculations for 463 and 500

$$K_x = \frac{\%_{Int.Std.}/\%_{x.}}{Wt_{Int.Std.}/Wt_{x.}}$$

*K_x value calculation from stock solutions of known amount of biphenyl and **X** where X = **463***

*or **500***

Two solutions of *N,N*-dimethyl-1*H*-benzo[*d*]imidazol-2-amine (**463**) and biphenyl (internal standard) were made up to a 25 mL solution in acetonitrile in a volumetric flask. The masses used are shown in the below table with the HPLC area percentages. 3 samples of each volumetric flask were analysed by HPLC analysis and Kx calculations were performed using the above equation with HPLC peak area response % (PAR%).
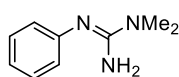
463
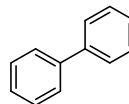
Biphenyl / mg	**463** / mg	**463** / HPLC %	Biphenyl / PAR%	*Kx*
18.2	20.5	61.872	38.128	0.694
18.2	20.5	61.996	38.004	0.690
18.2	20.5	61.911	38.089	0.692
17.3	21.8	64.857	35.143	0.682
17.3	21.8	64.815	35.185	0.684
17.3	21.8	64.850	35.150	0.683
		Kx average:		**0.688**

463 Kx calculations. Masses were recorded on a 5-figure balance.

Two solutions of 1-dimethyl-2-phenyl(D5)guanidine (**500**) and biphenyl (internal standard) were made up to a 25 mL solution in acetonitrile in a volumetric flask. The masses used are shown in the below table with the HPLC area percentages. 3 samples of each volumetric flask were analysed by HPLC analysis and Kx calculations were performed using the above

equation with HPLC peak area response % (PAR%). Masses were recorded on a 5-figure balance.
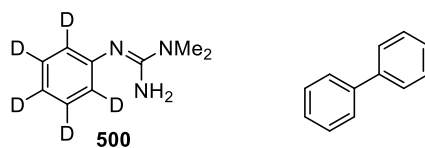
Biphenyl / mg	**500** / mg	**500** / HPLC %	Biphenyl / PAR%	Kx
17.4	21.7	63.981	36.019	0.702
17.4	21.7	64.007	35.993	0.701
17.4	21.7	63.988	36.012	0.702
21.7	18.8	61.647	38.353	0.700
21.7	18.8	61.618	38.382	0.701
21.7	18.8	61.702	38.298	0.699
		Kx average:		**0.701**

500 Kx calculations. Masses were recorded on a 5-figure balance.

Kinetic isotope effect experiment
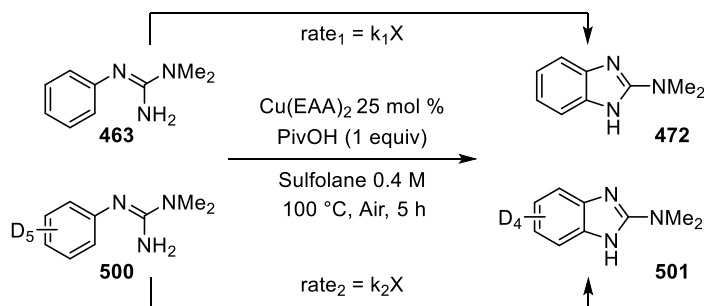
Two four separate round-bottomed flasks were added the following:

Reaction	**463** / mg (mmol)	**500** / mg (mmol)	Biphenyl / mg	Cu(EAA)$_2$ / mg (mmol)	PivOH / mg (mmol)
1	65 (0.40)	–	25	32 (0.10)	42 (0.41)
2	65 (0.40)	–	26	32 (0.10)	42 (0.41)
3	–	67 (0.40)	26	32 (0.10)	42 (0.41)
4	–	67 (0.40)	26	32 (0.10)	42 (0.41)

Each reaction was then dissolved in sulfolane (1 mL) and the reactions heated to 100 °C for 300 minutes. The reactions were sampled at 9, 21, 31, 45, 60, 135, 180, 210, 240, 270 and 300 minutes for HPLC analysis. Using the Kx values and calculation in the above section, the remaining quantity of **463**/**500** was plotted against time to give the plots shown in Figure 30 and Figure 31.

Internal standard calculations for 458

$$K_x = \frac{\%_{Int.Std.}/\%_{458}}{Wt_{Int.Std.}/Wt_{458}}$$

K_x value calculation from stock solutions of known amount of 4,4'-di-tertbutyl-1,1'-biphenyl

*and **458***

Four solutions of 1,1-dimethyl-2-(3-(trifluoromethyl)phenyl)guanidine (**458**) and 4,4'-di-tertbutyl-1,1'-biphenyl (internal standard) were made up to a 25 mL solution in acetonitrile in a volumetric flask. The masses used are shown in the below table with the HPLC area percentages. 2 samples of each volumetric flask were analysed by HPLC analysis and Kx calculations were performed using the above equation with HPLC peak area response % (PAR%).
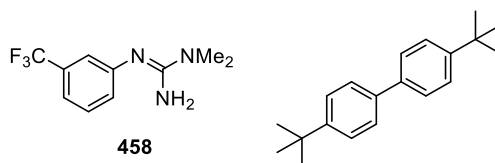

4,4'-di-tertbutyl-1,1'-biphenyl / mg	**458** / mg	**458** / HPLC %	4,4'-di-tertbutyl-1,1'-biphenyl / PAR%	*Kx*
8.9	18.9	66.91	33.09	1.050
8.9	18.9	66.89	33.11	1.051
8.6	27.0	74.79	25.21	1.058
8.6	27.0	74.87	25.14	1.054
8.5	23.4	72.59	27.41	1.040
8.5	23.4	72.56	27.44	1.041
8.2	22.8	72.40	27.60	1.060
8.2	22.8	72.48	27.52	1.056
		Kx average:		**1.051**

***458** Kx calculations. Masses were recorded on a 5-figure balance.*

Internal standard calculations for 459

$$K_x = \frac{\%_{Int.Std.}/\%_{459}}{Wt_{Int.Std.}/Wt_{459}}$$

K_x value calculation from stock solutions of known amount of 4,4'-di-tertbutyl-1,1'-biphenyl

and 459

Two solutions of 5-trifluoromethyl-*N,N*-dimethyl-1*H*-benzo[d]imidazol-2-amine (**459**) and 4,4'-di-tertbutyl-1,1'-biphenyl (internal standard) were made up to a 25 mL solution in acetonitrile in a volumetric flask. The masses used are shown in the below table with the HPLC area percentages. 2 samples of each volumetric flask were analysed by HPLC analysis and Kx calculations were performed using the above equation with HPLC peak area response % (PAR%).
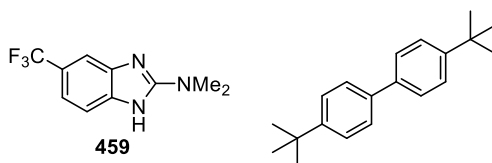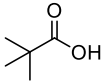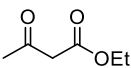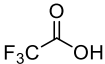
4,4'-di-tertbutyl-1,1'-biphenyl / mg	**459** / mg	**459** / HPLC %	4,4'-di-tertbutyl-1,1'-biphenyl / PAR%	*Kx*
28.5	26.7	79.368	20.632	0.243
28.5	26.7	79.241	20.759	0.245
27.6	26.7	79.761	20.339	0.244
27.6	25.7	79.700	20.300	0.244
		Kx average:		**0.244**
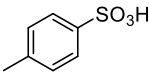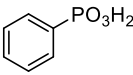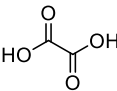
459 Kx calculations. Masses were recorded on a 5-figure balance.
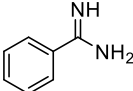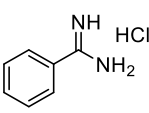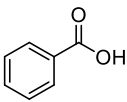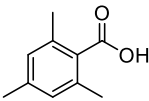
Procedure for reaction additive screening
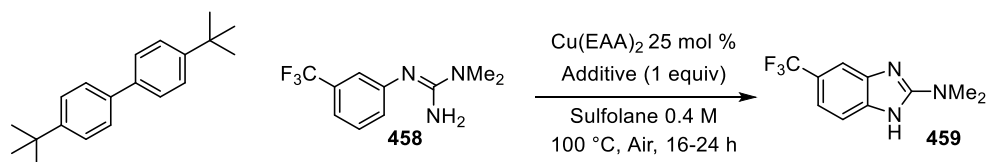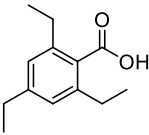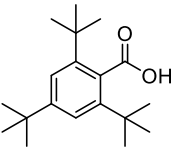
To 1.5 mL glass vials were added the following masses of **458**, Cu(EAA)$_2$ and the respective additive. To each reaction was added sulfolane (0.5 mL) and a stirring flea. The reactions were heated to 100 °C and at the times shown Table 11, Scheme 196, Table 12 and Scheme 200, 5 µL of the reaction was diluted into 1.5 mL acetonitrile and analysed by HPLC analysis. The solution yield was calculated using the above Kx calculation to quantify the amount of **458** and **459** in solution.

Entry	**458** / mg (mmol)	Cu(EAA)$_2$ / mg (mmol)	Additive	Additive / mg (mmol)	4,4'-di-tertbutyl-1,1'-biphenyl / mg (mmol)
1	47.2 (0.21)	16 (0.05)	None	–	15 (0.06)
2	46.1 (0.20)	16 (0.05)	Pivalic acid	24 (0.23)	15 (0.06)
3	47.5 (0.21)	16 (0.05)	Ethyl acetoacetate	27 (0.21)	15 (0.06)
4	50.0 (0.22)	17 (0.05)	Acetic acid	12 µL (0.22)	15 (0.06)
5	50.0 (0.22)	17 (0.05)	Trifluoroacetic acid	17 µL (0.22)	15 (0.06)

Entry	458 / mg (mmol)	Cu(EAA)$_2$ / mg (mmol)	Additive	Additive / mg (mmol)	4,4'-di-tertbutyl-1,1'-biphenyl / mg (mmol)
6	46.6 (0.20)	16 (0.05)	Methane sulfonic acid	19 (0.20)	15 (0.06)
7	45.5 (0.20)	16 (0.05)	*p*-toluene sulfonic acid monohydrate	59 (0.31)	15 (0.06)
8	46.2 (0.20)	16.0 (0.05)	Phenyl phosphonic acid	32 (0.20)	15 (0.06)
9	45.9 (0.20)	16 (0.05)	Oxalic acid	19 (0.21)	15 (0.06)
10	45.7 (0.20)	16 (0.05)	Lactic acid	18 (0.20)	15 (0.06)
11	46.1 (0.20)	16 (0.05)	Alanine	19 (0.21)	15 (0.06)
12	47.0 (0.20)	16 (0.05)	2-aminoisobutyric acid	23 (0.22)	15 (0.06)

Entry	**458** / mg (mmol)	Cu(EAA)$_2$ / mg (mmol)	Additive	Additive / mg (mmol)	4,4'-di-tertbutyl-1,1'-biphenyl / mg (mmol)
13	50.0 (0.22)	17 (0.05)	Phenol	20 (0.22)	15 (0.06)
14	50.0 (0.22)	17 (0.05)	2-hydroxypyridine	21 (0.22)	15 (0.06)
15	50.0 (0.22)	17 (0.05)	Benzamidine	26 (0.22)	15 (0.06)
16	50.0 (0.22)	17 (0.05)	Benzamidine hydrochloride	34 (0.22)	15 (0.06)
17	45.9	16 (0.05)	Benzoic acid	26 (0.21)	15 (0.06)
18	46.0 (0.20)	16 (0.05)	2,4,6-trimethylbenzoic acid	35 (0.21)	15 (0.06)

Entry	**458** / mg (mmol)	Cu(EAA)₂ / mg (mmol)	Additive	Additive / mg (mmol)	4,4'-di-tertbutyl-1,1'-biphenyl / mg (mmol)
19	45.9 (0.20)	16 (0.05)	2,4,6-triethylbenzoic acid	41 (0.20)	12 (0.04)
20	50.1 (0.22)	17 (0.05)	2,4,6-tri-*tert*-butyl benzoic acid	64 (0.22)	12 (0.05)

2-Bromo-1,3,5-triethylbenzene (518)
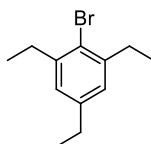
To a solution of 1,3,5-triethylbenzene (1.00 g, 6.16 mmol, 1 equiv) in chloroform (3 mL) was added iron powder (32 mg, 0.57 mmol, 0.09 equiv). The reaction was cooled to 0 °C, the flask wrapped in aluminium foil and dibromine (0.985 g, 6.16 mmol, 1.00 equiv) was added dropwise over 60 minutes under vigorous stirring. The reaction was stirred at room temperature for 14 hours, at which point, CH_2Cl_2 (20 mL) was added and the organic solution washed with water (2 × 15 mL), NaOH (2M, 20 mL) and a further portion of water (20 mL). The organic portion was dried over anhydrous $MgSO_4$, concentrated *in vacuo* and purified by chromatography (heptane) to give 2-bromo-1,3,5-triethylbenzene (**518**) as a colourless oil (1.30 g, 5.39 mmol, 88%).

Appearance: Colourless oil

^{1}H NMR (400 MHz, CDCl$_3$) δ ppm 6.95 (2H, s), 2.81 (4H, q, *J* = 7.5 Hz), 2.62 (2H, q, *J* = 7.5 Hz), 1.27 (9H, *app.* t, *J* = 7.5 Hz)

^{13}C NMR (101 MHz, CDCl$_3$) δ ppm 143.6, 143.1, 126.6, 123.2, 30.2, 28.3, 15.6, 14.4

The spectroscopic data is concurrent with the literature.[336]

2,4,6-Triethylbenzoic acid (519)
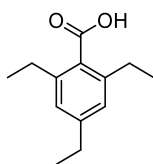
To a round-bottomed flask containing dry diethylether (5 mL) and magnesium turnings (102 mg, 4.19 mmol, 1.04 equiv) was added a solution of 2-bromo-1,3,5-triethylbenzene (**518**) (0.98 g, 4.05 mmol, 1 equiv) in dry diethylether (5 mL) dropwise over the course of 30 minutes. After which, one drop of 1,2-dibromoethane was added and the reaction stirred for 3 hours. The reaction was cooled to 0 °C and carbon dioxide was bubbled into the reaction. After being allowed to warm to room temperature for 14 hours, diethylether (5 mL) was added and the reaction mixture poured into ice-water (4 mL) containing ammonium chloride (0.4 g) and HCl (10 M, 0.1 mL). The organic layer was separated and washed with HCl (0.25 M, 2 × 2 mL), before washing the resultant aqueous layers with diethylether (2 × 5 mL). The combined organic portions were washed with NaOH (2 M, 3 × 2 mL), and the basic layers were acidified with HCl to pH 0 and re-extracted into diethylether (3 × 10 mL). The organic layer was washed with brine (5 mL), dried over anhydrous MgSO$_4$ and concentrated *in vacuo* to give 2,4,6-triethylbenzoic acid (**519**) as a white crystalline solid. (432 mg, 2.10 mmol, 52%).

Appearance: White crystals

^{1}H NMR (400 MHz, CDCl$_3$) δ ppm 10.93 (1H, *br.* s), 6.98 (2H, s), 2.78 (4H, q, *J* = 7.5 Hz), 2.67 (2H, q, *J* = 7.5 Hz), 1.29 (9H, m)

^{13}C NMR (101 MHz, CDCl$_3$) δ ppm 175.5, 146.3, 141.5, 129.1, 125.9, 28.8, 27.1, 15.6

The spectroscopic data is concurrent with the literature.[336]

2,4,6-Tri-*tert*-butylbenzoic acid (521)
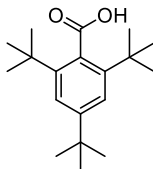
To a solution of 2-bromo,1-3-5-tri-*tert*-butylbenzene (496 mg, 1.53 mmol, 1 equiv) in dry tetrahydrofuran (2 mL) was added *n*-BuLi (2.5 M, 0.64 mL, 1.60 mmol, 1.05 equiv) dropwise over the course of 60 minutes after which, carbon dioxide was bubbled into the reaction and the reaction stirred at room temperature for 14 hours. The reaction was quenched with water (15 mL) and acidified with HCl (2 M, 5 mL), before being extracted into EtOAc. The combined organic portions were washed with NaOH (2 M, 3 × 5 mL), and the basic layers were acidified with HCl to pH 0 and re-extracted into EtOAc (3 × 20 mL). The organic layer was washed with brine (5 mL), dried over anhydrous MgSO$_4$ and concentrated *in vacuo* to give 2,4,6-tri-*tert*-butylbenzoic acid (**521**) as a white crystalline solid (117 mg, 0.40 mmol, 26%).

Appearance: White crystals

^{1}H NMR (400 MHz, CDCl$_3$) δ ppm 10.97 (1H, *br.* s), 7.46 (2H, s), 1.49 (18H, s), 1.34 (9H, s)

^{13}C NMR (101 MHz, CDCl$_3$) δ ppm 178.9, 150.7, 146.4, 127.4, 122.2, 37.0, 35.1, 32.2, 31.3

The spectroscopic data is concurrent with the literature.[337]

Note the authors in the above reference observed no carboxylic acid −OH peak. A broad singlet at 10.97 ppm was observed which has been attributed to this signal.

N-methyl-N-phenylcyanamide (529)
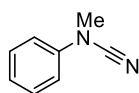
To a room temperature solution of cyanogen bromide (1.510 g, 14.2 mmol, 1 equiv) in Et$_2$O:THF (1:1, 25 mL) was added N-methylaniline (2.277 g, 21.3 mmol, 1.49 equiv). The reaction was stirred for 5 hours before being quenched with NaOH (2 M, 50 mL) and extracted into EtOAc (2 × 40 mL). The combined organic portions were washed with water (30 mL) and brine (30 mL) before being dried over anhydrous MgSO$_4$, concentrating in vacuo and purifying by chromatography (25–50% EtOAc in heptane) to give N-methyl-N-phenylcyanamide (**529**) as an off-white solid (1.392 g, 10.5 mmol, 74%).

Appearance: Off-white solid

^{1}H NMR (400 MHz, (CD$_3$)$_2$SO) δ ppm 7.40–7.49 (2H, m), 7.12–7.18 (3H, m), 3.35 (2H, s)

^{13}C NMR (101 MHz, (CD$_3$)$_2$SO) δ ppm 140.9, 130.1, 123.5, 115.2, 114.4, 37.0

The spectroscopic data is concurrent with the literature.[338]

1,1-Diethyl-3-methyl-3-phenylguanidine (524)
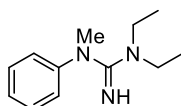
To a solution of N-methyl-N-phenylcyanamide (**529**) (498 mg, 3.76 mmol, 1 equiv) in CH$_2$Cl$_2$ (10 mL) was added aluminium chloride (542 mg, 4.06 mmol, 1.08 equiv). The reaction was stirred at room temperature for 5 minutes before careful addition of diethylamine (848 mg, 11.6 mmol, 3.1 equiv). After 60 minutes, water (10 mL) and the pH adjusted to 14 with NaOH (2 M) was added, before extracting with CH$_2$Cl$_2$ (3 × 20 mL). The organic portion was washed with brine (20 mL), dried over a hydrophobic frit and concentrated in vacuo. The product was

isolated by chromatography (0–10% MeOH in EtOAc) to give 1,1-diethyl-3-methyl-3-phenylguanidine (**524**) as a colourless oil (251 mg, 1.22 mmol, 33%).

Appearance: Colourless oil

ν (neat): 3313, 2970, 2929, 2865, 1591, 1578, 1498, 1294 cm^{-1}

^{1}H NMR (400 MHz, CD$_3$OD) δ ppm 7.26–7.35 (2H, m), 6.98–7.06 (3H, m), 3.21 (4H, q, *J* = 7.1 Hz), 3.18 (3H, s), 1.04 (6H, t, *J* = 7.1 Hz)

^{13}C NMR (101 MHz, CD$_3$OD) δ ppm 163.5, 147.1, 128.8, 122.1, 120.2, 42.1, 38.2, 11.7

HRMS (ESI Orbitrap) *m/z*: Calcd for C$_{12}$H$_{20}$N$_3$ [M+H]$^+$ 206.1657; found [M+H]$^+$ 206.1667

Substrates designed to probe the coordination to the catalyst

N-cyano-4-methyl-N-phenylbenzenesulfonamide (530)
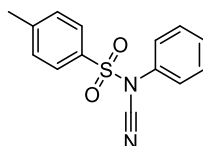
To a solution of phenylurea (1.15 g, 8.4 mmol, 1 equiv) in pyridine (54 mL) under nitrogen was added *p*-toluenesulfonylchloride (5.99 g, 31.4 mol, 3.7 equiv). The reaction was stirred at room temperature for 20 minutes before ice-water (400 mL) was added and the resultant suspension was warmed to room temperature under vigorous stirring. The solid was filtered and purified by chromatography (10% EtOAc in heptane) to yield *N*-cyano-4-methyl-*N*-phenylbenzenesulfonamide (**530**) as a white solid (1.67 g, 6.1 mmol, 73%).

Appearance: White solid

^{1}H NMR (400 MHz, CDCl$_3$) δ ppm 7.66 (2H, d, *J* = 8.4 Hz), 7.34–7.48 (5H, m), 7.18–7.25 (2H, m), 2.50 (3H, s)

^{13}C NMR (101 MHz, CDCl$_3$) δ ppm 146.8, 134.5, 132.3, 130.2, 130.0, 129.9, 128.4, 126.5, 108.7, 21.8

The spectroscopic data is concurrent with the literature.[339]

N-cyano-N-phenylbenzamide (534)
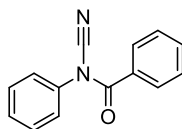
To a round bottomed flask containing KHMDS (1M solution in THF, 9 mL, 1.13 equiv) at −10 °C was added isothiocyanatobenzene (1.08 g, 8 mmol, 1 equiv) dropwise as a solution in THF (12 mL). The reaction was gradually warmed to room temperature and after 3 hours the volatiles were removed under reduced pressure. To the resultant off-white solid was added CH$_2$Cl$_2$ (35 mL) and the suspension stirred at −10 °C for 20 minutes, at which point benzoyl chloride (1.15 g, 8.2 mmol, 1.03 equiv) was added dropwise. After warming to room temperature and stirring for 18 hours, the reaction was concentrated in vacuo. The resultant yellow solid was purified by chromatography (0–20% EtOAc in heptane) to give N-cyano-N-phenylbenzamide (**534**) as a fluffy white solid (658 mg, 3.0 mmol, 37%).

Appearance: Fluffy white solid

^{1}H NMR (400 MHz, CDCl$_3$) δ ppm 7.86–7.92 (2H, m), 7.65 (1H, tt, J = 7.4, 1.2 Hz), 7.41–7.58 (7H, m)

^{13}C NMR (101 MHz, CDCl$_3$) δ ppm 168.0, 135.7, 133.5, 130.7, 129.9, 129.1, 129.0, 128.7, 125.4, 110.3

The spectroscopic data is concurrent with the literature.[300]

N-benzyl-N-phenylcyanamide (538)
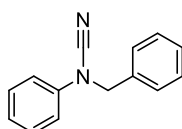
To a round-bottomed flask containing benzyl alcohol (0.180 g, 1.67 mmol, 1 equiv), tetrabutylammonium iodide (68 mg, 0.18 mmol, 0.11 equiv) and sodium *tert*-pentoxide (0.375 g, 3.41 mmol, 2.05 equiv) was added THF (10 mL). The reaction was stirred at room

temperature before addition of *N*-cyano-4-methyl-*N*-phenylbenzenesulfonamide (**530**) (0.500 g, 1.84 mmol, 1.10 equiv). After 30 minutes, the reaction was quenched by addition of saturated ammonium chloride (15 mL) and water (25 mL). The reaction was extracted into EtOAc (3 × 15 mL), the organic portion washed with brine (20 mL), dried over anhydrous MgSO$_4$ and concentrated in vacuo. Purification by chromatography (10% EtOAc in heptane) gave *N*-benzyl-*N*-phenylcyanamide (**538**) as a white solid (251 mg, 1.20 mmol, 72%).

Appearance: White solid

^{1}H NMR (400 MHz, CDCl$_3$) δ ppm 7.32–7.47 (7H, m), 7.15–7.21 (2H, m), 7.12 (1H, tt, *J* = 7.6, 1.0 Hz), 4.84 (2H, s)

^{13}C NMR (101 MHz, CDCl$_3$) δ ppm 139.8, 134.3, 129.7, 129.1, 128.5, 127.4, 123.7, 116.1, 113.9, 53.8

The spectroscopic data is concurrent with the literature.[299]

1-Benzyl-3,3-diethyl-1-phenylguanidine (525)
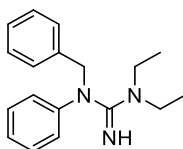
To a solution of *N*-benzyl-*N*-phenylcyanamide (**538**) (163 mg, 0.78 mmol, 1 equiv) in CH$_2$Cl$_2$ (3.3 mL) was added aluminium chloride (120 mg, 0.90 mmol, 1.16 equiv). The reaction was stirred at room temperature for 10 minutes before careful addition of diethylamine (354 mg, 4.83 mmol, 6.2 equiv). After 5 minutes, water (20 mL) and NaOH (2M, 3 mL) was added, before extracting with CH$_2$Cl$_2$ (3 × 30 mL). The organic portion was washed with brine (20 mL), dried over a hydrophobic frit and concentrated in vacuo. The product was isolated by chromatography (1% Et$_3$N in EtOAc) to give 1-benzyl-3,3-diethyl-1-phenylguanidine (**525**) as a colourless oil (209 mg, 0.74 mmol, 95%).

Appearance: Colourless oil

^{1}H NMR (400 MHz, CD$_3$OD) δ ppm 7.22–7.40 (7H, m), 7.00–7.10 (3H, m), 4.89 (2H, s), 3.22 (4H, q, J = 7.1 Hz), 0.97 (6H, t, J = 7.1 Hz)

^{13}C NMR (101 MHz, CD$_3$OD) δ ppm 162.6, 146.5, 138.7, 128.8, 128.1, 127.4, 126.8, 122.7, 121.5, 55.2, 41.9, 11.4

HRMS (ESI Orbitrap) m/z: Calcd for C$_{18}$H$_{24}$N$_3$ [M+H]$^+$ 282.1965; found [M+H]$^+$ 285.1950

HRMS experiments

The HRMS used was the Thermo Orbitrap Velos, equipped with a heated electrospray source (HESI-II), connected to an Agilent 1290 Liquid chromatography system. The system was operated by flow injection analysis (FIA) using 90% acetonitrile 10% (water + 0.1% formic acid) as a commutation solvent. Instrument control and data processing were performed using Themo Xcalibur 2.2 software. The instrument was calibrated on the day of data acquisition and will maintain a mass accuracy of better than 5 ppm over a 24-hour period. The source conditions were adjusted to provide a suitable signal.
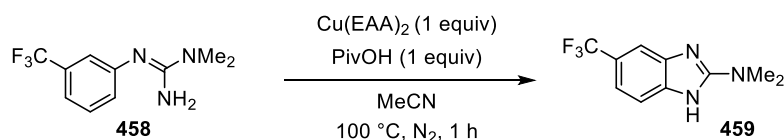
To a vial was added 1,1-dimethyl-2-(3-(trifluoromethyl)phenyl)guanidine **458** (102 mg, 0.44 mmol, 1 equiv), Cu(EAA)$_2$ (142 mg, 0.44 mmol, 1 equiv) and pivalic acid (45 mg, 0.44 mmol, 1 equiv) and a stirring bar, the reaction was placed under nitrogen and evacuated to vacuum. This process was repeated 3 times. To the vial was added freeze-pump-thaw degassed acetonitrile (1.1 mL) and the reaction heated to 100 °C for 60 minutes. The reaction was cooled to room temperature where a solid precipitated and was filtered (22 mg). 10 μL of the solution was diluted into 1 mL acetonitrile and analysed by HRMS under the conditions shown above to give the mass spectra shown below containing *m/z* = 525.1241 and 523.1085. 5 mg of the filtered solid was dissolved in 1 mL acetonitrile and analysed by HRMS under the conditions shown above to give the mass spectra shown below containing *m/z* = 521.0957.
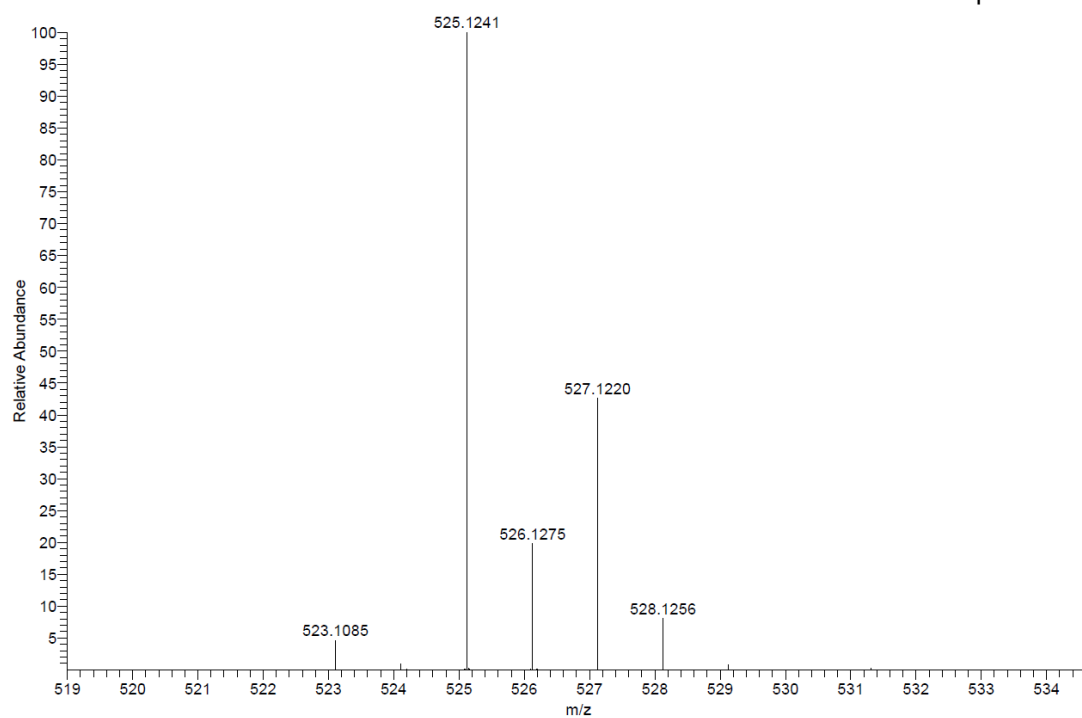
HRMS of the solution. Observed mass-ion of m/z = 525.1241 and 523.1085
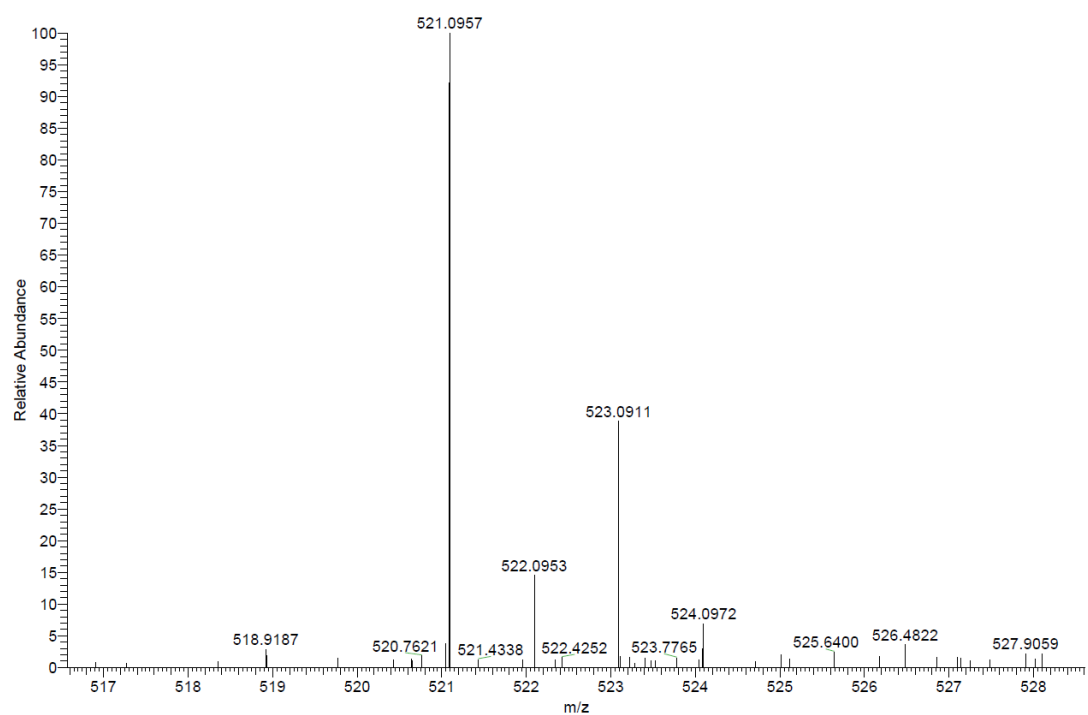
Filtered solid HRMS. Observed mass-ion of m/z = 521.0957
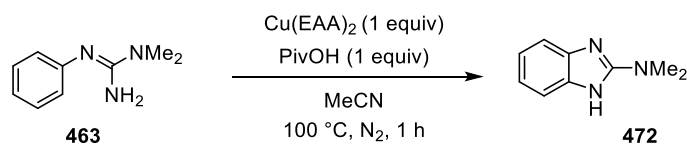
To a vial was added 1,1-dimethyl-2-phenylguanidine **463** (97 mg, 0.59 mmol, 1 equiv), Cu(EAA)$_2$ (197 mg, 0.61 mmol, 1 equiv) and pivalic acid (67 mg, 0.66 mmol, 1.1 equiv) and a stirring bar, the reaction was placed under nitrogen and evacuated to vacuum. This process was repeated 3 times. To the vial was added freeze-pump-thaw degassed acetonitrile (1.5 mL) and the reaction heated to 100 °C for 60 minutes. The reaction was cooled to room temperature and 10 μL was diluted into 1 mL acetonitrile and analysed by HRMS under the conditions shown above. The observed mass-spectra is shown below.
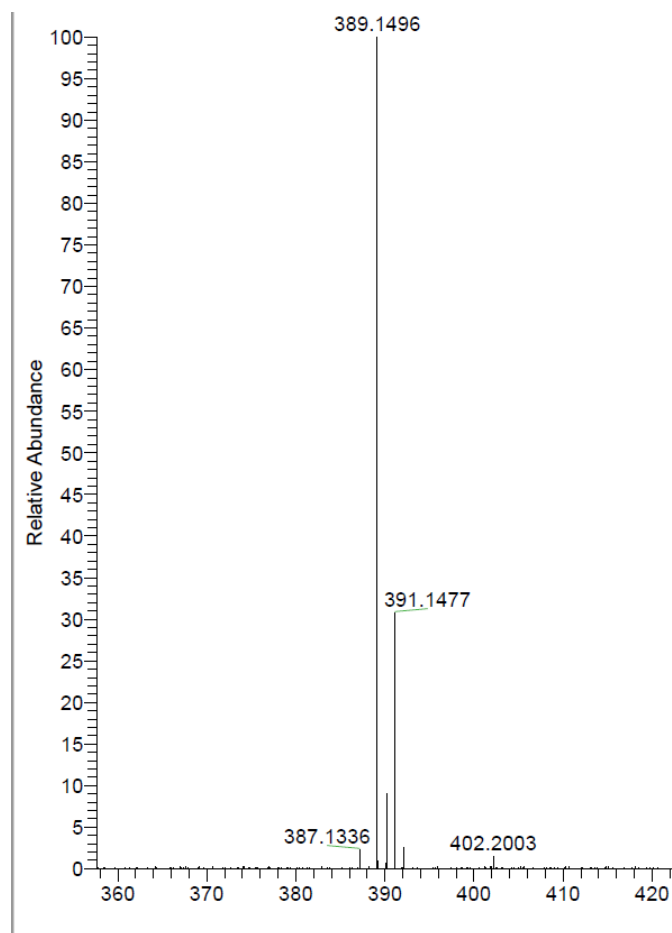
Observed mass-ion of m/z = 389.1496

Emedastine synthesis

4-Cyano-1,4-diazepane-1-carboxylate (553)
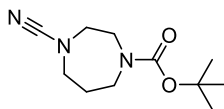
To an ice-cooled solution of cyanogen bromide (3.15 g, 29.7 mmol, 1 equiv) in chloroform (35 mL) was added *tert*-butyl 1,4-diazepane-1-carboxylate (6.17 g, 30.8 mmol, 1.04 equiv) dropwise as a solution in chloroform (20 mL). Diisopropylethylamine (4.00 g, 30.9 mmol, 1.04 equiv) was added and the reaction was gradually allowed to warm to room temperature. After 4 hours, NaOH (2M, 50 mL) was added and the biphasic mixture extracted with CH_2Cl_2 (3 × 40 mL). The combined organic extracts were washed with brine (40 mL) and dried over anhydrous $MgSO_4$ before concentrating *in vacuo* and purifying by chromatography (20% EtOAc in heptane) to yield 4-cyano-1,4-diazepane-1-carboxylate (**553**) as a colourless oil (4.67 g, 20.7 mmol, 70%).

Appearance: Colourless oil

^{1}H NMR (400 MHz, CDCl$_3$) δ ppm 3.33–3.50 (4H, m), 3.19–3.25 (2H, m), 3.13–3.18 (2H, m), 1.79–1.92 (2H, m), 1.37 (9H, s)

^{13}C NMR (101 MHz, CDCl$_3$) δ ppm 154.8, 154.5, 117.8, 117.7, 80.1, 80.0, 52.1, 50.3, 47.5, 47.4, 46.3, 45.7, 28.3, 27.6, 27.6. *Observed as a mixture of rotamers.*

The spectroscopic data is concurrent with the literature.[340]

Tert-butyl 4-(N'-phenylcarbamimidoyl)-1,4-diazepane-1-carboxylate (552)
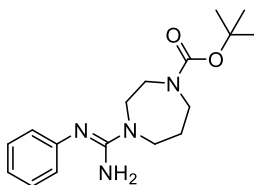
To a stirred suspension of 60% sodium hydride (0.620 g, 15.5 mmol, 1.1 equiv) in DMSO (10 mL) was added aniline (1.33 g, 14.3 mmol, 1 equiv) as a solution in DMSO (9 mL) dropwise.

After 15 minutes, *tert*-butyl 4-cyano-1,4-diazepane-1-carboxylate (**553**) (3.00 g, 13.3 mmol, 0.93 equiv) was added as a solution in DMSO (10 mL) and the reaction stirred at room temperature for 24 hours, at which point a further portion of *tert*-butyl 4-cyano-1,4-diazepane-1-carboxylate (**553**) (0.500 g, 2.2 mmol, 0.16 equiv) was added as a solution in DMSO (5 mL). After a further 60 minutes, the reaction was quenched with water (50 mL) and extracted into tBME (3 × 50 mL). The combined organic extracts were washed with water (3 × 50 mL) and brine (1 × 30 mL) before being purified by chromatography (50–100% EtOAc in heptane with 2% triethylamine in the EtOAc and heptane portions) to yield an off white solid (3.17 g, 9.6 mmol, 96.7% purity by HPLC analysis, 67% *based on aniline*). The off-white solid was recrystallised from tBME to yield 2.65 g of analytically pure **552** of > 99% purity by HPLC analysis which was used in the subsequent dehydrogenative cyclisation.

Appearance: White crystals

M.pt: 107–108 °C

ν (neat): 3485, 3395, 2979, 1680, 1618, 1575 cm⁻¹

^{1}H NMR (400 MHz, CD$_3$OD) δ ppm 7.29 (2H, t, *J* = 7.6 Hz), 7.01 (1H, t, *J* = 7.6 Hz), 6.91 (2H, d, *J* = 7.6 Hz), 3.60–3.67 (4H, m), 3.55 (2H, t, *J* = 5.9 Hz), 3.49 (2H, t, *J* = 5.9 Hz), 1.87–1.98 (2H, m), 1.52 (9H, s). *Observed as a mixture of rotomers.*

^{13}C NMR (101 MHz, (CD$_3$)$_2$SO) δ ppm 154.9, 151.9, 151.3, 151.2, 129.3, 123.5, 120.5, 78.9, 78.8, 48.6, 48.2, 47.4, 47.1, 46.8, 46.6, 46.2, 45.8, 28.6, 27.1.

HRMS (ESI Orbitrap) *m/z*: Calcd for C$_{17}$H$_{27}$N$_4$O$_2$ [M+H]$^+$ 319.2129; found [M+H]$^+$ 319.2116

Tert-butyl 4-(1*H*-benzo[*d*]imidazol-2-yl)-1,4-diazepane-1-carboxylate (551)
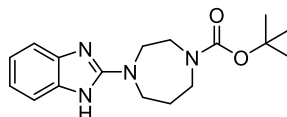
To a round bottom flask was added *tert*-butyl 4-(*N*-phenylcarbamimidoyl)-1,4-diazepane-1-carboxylate (**552**) (2.415 g, 7.6 mmol, 1 equiv), Cu(EAA)$_2$ (303 mg, 0.94 mmol, 0.12 equiv) and pivalic acid (776 mg, 7.6 mmol, 1.03 equiv) prior to the addition of a stir bar and sulfolane

(20 mL). The reaction was heated to 100 °C for 30 hours at which point it was then cooled to room temperature. The resultant solid was suspended between water (100 mL) and tBME (100 mL) before addition of EDTA$_{(aq)}$ (20 mL, 0.1 M). The organic portion was separated and the aqueous washed with further tBME (3 × 75 mL). The resultant aqueous solution (~100 mL) was then saturated with NaCl and then extracted with tBME (1 × 50 mL). The combined organic extracts were then washed with water (5 × 50 mL), the water washes back-extracted with tBME (2 × 50 mL) and the combined organic portions washed with brine. The brown organic solution was reduced in volume to ~30 mL at which point a white solid precipitated. The mixture was cooled in an ice bath and the solid was filtered to yield a white solid (1.410 g). The organic solution was then concentrated *in vacuo* and purified by chromatography (0–3% MeOH in CH$_2$Cl$_2$) to yield 305 mg of a white solid. The two solids were combined, homogenised with MeOH and evaporated to give *tert*-butyl 4-(1H-benzo[*d*]imidazol-2-yl)-1,4-diazepane-1-carboxylate (**551**) as a white solid (1.715 g, 5.4 mmol, 71%).

Appearance: White solid

M.pt: 219–220 °C

ν (neat): 2970, 1686, 1626, 1597, 1566, 1461 cm^{-1}

^{1}H NMR (400 MHz, CD$_3$OD) δ ppm 7.19–7.26 (2H, m), 6.95–7.02 (2H, m), 3.63–3.81 (6H, m), 3.38–3.48 (2H, m), 1.88–2.08 (2H, m), 1.38 (4H, s), 1.30 (5H, s). *Observed as a mixture of rotomers.*

^{13}C NMR (101 MHz, CD$_3$OD) δ ppm 155.6, 155.4, 154.7, 119.9, 111.6, 79.8, 50.6, 48.6, 48.3, 47.9, 46.5, 46.2, 45.9, 45.5, 27.3, 27.2, 27.0, 26.2, 26.1, 22.3.

HRMS (ESI Orbitrap) *m/z*: Calcd for C$_{17}$H$_{25}$N$_4$O$_2$ [M+H]$^+$ 317.1972; found [M+H]$^+$ 317.1867

1-Ethoxy-2-iodoethane (558)
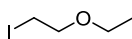
To a solution of sodium iodide (20.07 g, 68.3 mmol, 1.96 equiv) in acetone (100 mL) was added 1-chloro-2-ethoxyethane (7.42 g, 68.3 mmol) and the reaction was heated to reflux under nitrogen for 16 hours. After cooling to room temperature, the reaction was filtered and concentrated *in vacuo*. The resultant solid was triturated with CH_2Cl_2 (3 × 50 mL), the organic portions washed with brine (50 mL), dried over anhydrous $MgSO_4$ and the concentrated *in vacuo* to give 1-ethoxy-2-iodoethane (**558**) as a brown oil (2.60 g, 13.0 mmol, 19%).

Appearance: Brown oil

^{1}H NMR (400 MHz, $CDCl_3$) δ ppm 3.72 (2H, t, *J* = 6.9 Hz), 3.58 (2H, q, *J* = 7.0 Hz), 3.28 (2H, t, *J* = 6.9 Hz), 1.25 ppm (3H, t, *J* = 7.0 Hz)

^{13}C NMR (101 MHz, $CDCl_3$) δ ppm 71.2, 66.3, 15.1, 3.1

Tert-butyl   4-(1-(2-ethoxyethyl)-1*H*-benzo[d]imidazol-2-yl)-1,4-diazepane-1-carboxylate (550)
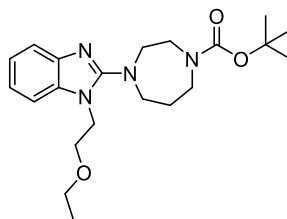
To a suspension of *tert*-butyl 4-(1H-benzo[*d*]imidazol-2-yl)-1,4-diazepane-1-carboxylate (**551**) (1.320 g, 4.2 mmol, 1.0 equiv) in THF (30 mL) was added 60% sodium hydride suspension (0.220 g, 5.5 mmol, 1.3 equiv) in 5 separate portions over a period of 15 minutes. The resultant solution was stirred for 15 minutes before addition of 1-(2-iodoethoxy)ethane (**558**) (1.155 g, 5.8 mmol, 1.4 equiv) as a solution in THF (2 mL). The reaction was heated to reflux for 18 hours under nitrogen before a second addition of 1-(2-iodoethoxy)ethane (**558**) (0.162 g, 0.81 mmol, 0.2 equiv). After a further 60 minutes the reaction was cooled to room temperature,

quenched with water and the volatiles removed under reduced pressure. The resultant aqueous was extracted into CH_2Cl_2 (3 × 30 mL), the combined organic portions washed with brine, dried over a hydrophobic frit and concentrated *in vacuo.* The crude material was purified by chromatography (40–100% EtOAc in heptane) to yield *tert*-butyl 4-(1-(2-ethoxyethyl)-1*H*-benzo[*d*]imidazol-2-yl)-1,4-diazepane-1-carboxylate (**550**) as a colourless oil (1.443 g, 3.7 mmol, 89%).

Appearance: Colourless oil

ν (neat): 2971, 2871, 1688, 1527, 1436, 1408 cm^{-1}

^{1}H NMR (400 MHz, CDCl$_3$) δ ppm 7.52–7.61 (1H, m), 7.26–7.33 (1H, m), 7.10–7.23 (2H, m), 4.21 (2H, t, J = 5.8 Hz), 3.81 (2H, t, J = 5.8 Hz), 3.64–3.75 (2H, m), 3.53–3.64 (5H, m), 3.47 (3H, q, J = 6.9 Hz), 1.91–2.08 (2H, m), 1.50 (4.5H, s), 1.49 (4.5H, s), 1.16 (3H, t, J = 6.9 Hz). *Observed as a mixture of rotomers.*

^{13}C NMR (101 MHz, CDCl$_3$) δ ppm 159.0, 158.8, 155.5, 155.3, 141.6, 141.5, 135.4, 135.3, 121.8, 121.1, 121.0, 117.8, 117.8, 109.3, 79.6, 79.5, 68.3, 68.2, 66.9, 54.5, 54.2, 53.1, 52.7, 48.3, 47.7, 45.9, 45.4, 44.7, 44.6, 28.6, 28.5, 28.2, 15.1.

HRMS (ESI Orbitrap) *m/z*: Calcd for C$_{21}$H$_{33}$N$_4$O$_3$ [M+H]$^+$ 389.2547; found [M+H]$^+$ 389.2534

2-(1,4-Diazepan-1-yl)-1-(2-ethoxyethyl)-1*H*-benzo[*d*]imidazole (559)
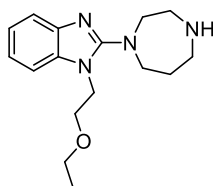
To a dry round bottomed flask containing *tert*-butyl 4-(1-(2-ethoxyethyl)-1H-benzo[*d*]imidazol-2-yl)-1,4-diazepane-1-carboxylate (**550**) (1.397 g, 3.6 mmol, 1.0 equiv) was added HCl as a solution in EtOAc (1M, 20 mL, 20 mmol, 5.6 equiv). The reaction was stirred at room temperature for 64 hours before quenching with saturated NaHCO$_3$ (50 mL) and diluting with CH_2Cl_2 (30 mL). The organic layer was separated and the resultant aqueous portion washed a further 2 times with CH_2Cl_2 (2 × 10 mL). The combined organics were washed with brine (10

mL), dried over a hydrophobic frit and concentrated *in vacuo* to yield 2-(1,4-diazepan-1-yl)-1-(2-ethoxyethyl)-1H-benzo[*d*]imidazole (**559**) as a pale-yellow oil (962 mg, 3.3 mmol, 93%)

Appearance: Pale-yellow oil

ν (neat): 3400 (*br*), 2970, 2872, 1528, 1464, 1408, 1285 cm^{-1}

^{1}H NMR (400 MHz, CDCl$_3$) δ ppm 7.52–7.57 (1H, m), 7.24–7.29 (1H, m), 7.08–7.20 (2H, m), 4.20 (2H, t, *J* = 6.0 Hz), 3.79 (2H, t, *J* = 6.0 Hz), 3.59–3.64 (4H, m), 3.47 (2H, q, *J* = 7.0 Hz), 3.10–3.15 (2H, m), 3.04–3.08 (2H, m), 2.30 (1H, *br.* s), 1.94 (2H, quin, *J* = 5.9 Hz), 1.15 (3H, t, *J* = 7.0 Hz)

^{13}C NMR (101 MHz, CDCl$_3$) δ ppm 159.2, 141.7, 135.5, 121.7, 120.8, 117.6, 109.1, 68.3, 66.9, 55.8, 52.7, 49.8, 48.2, 44.7, 31.1, 15.1

HRMS (ESI Orbitrap) *m/z*: Calcd for C$_{16}$H$_{25}$N$_4$O [M+H]$^+$ 289.2023; found [M+H]$^+$ 289.2012

The spectroscopic data is concurrent with the literature.[341]

2-(4-Methyl-1,4-diazepan-1-yl)-1-(2-ethoxyethyl)-1*H*-benzo[d]imidazole, Emedastine (361)
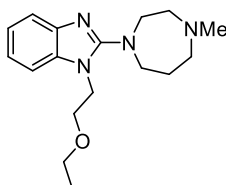
To a dry round bottomed flask containing 2-(1,4-diazepan-1-yl)-1-(2-ethoxyethyl)-1H-benzo[*d*]imidazole (**559**) (915 mg, 3.2 mmol, 1.0 equiv) was added formaldehyde (13.0 mL, 37 wt% aq, 175.0 mmol, 55 equiv) and formic acid (1.80 g, 1.50 mL, 39.1 mmol, 12.3 equiv). The reaction was stirred and heated to 80 °C for 30 minutes before diluting into water (50 mL), basifying with NaOH to pH 10 (2 M aq) and extracting with CH$_2$Cl$_2$ (5 × 40 mL). The combined organic extracts were washed with brine (20 mL), dried over a hydrophobic frit and concentrated *in vacuo* to yield an orange oil, which was purified by chromatography (0–10% MeOH in CH$_2$Cl$_2$ w/ 1% Et$_3$N in the CH$_2$Cl$_2$ portion) to yield 2-(4-methyl-1,4-diazepan-1-yl)-1-

(2-ethoxyethyl)-1H-benzo[*d*]imidazole (Emedastine, **361**) as a pale yellow oil (824 mg, 2.7 mmol, 86%).

Appearance: Pale-yellow oil

ν (neat): 2910, 2803, 1611, 1532, 1470 cm^{-1}

^{1}H NMR (400 MHz, CDCl$_3$) δ ppm 7.55 (1H, m), 7.26 (1H, s), 7.15 (2H, m), 4.21 (2H, t, J = 6.0 Hz), 3.80 (2H, t, J = 6.0 Hz), 3.71 (2H, m), 3.67 (2H, t, J = 6.2 Hz), 3.48 (2H, q, J = 6.9 Hz), 2.79 (4H, m), 2.45 (3H, s), 2.06 (2H, br. s.), 1.17 (3H, t, J = 7.0 Hz)

^{13}C NMR (101 MHz, CDCl$_3$) δ ppm 141.8, 135.6, 121.7, 120.7, 117.5, 110.0, 109.1, 77.2, 68.3, 66.9, 58.6, 57.6, 51.9, 46.8, 44.9, 28.0, 15.1

HRMS (ESI Orbitrap) *m/z*: Calcd for C$_{17}$H$_{27}$N$_4$O [M+H]$^+$ 303.2179; found [M+H]$^+$ 303.2173

The spectroscopic data is concurrent with the literature.[342]

10. References

(1)   Watson, J. D.; Crick, F. H. C. *Nature* **1953**, *171*, 737.

(2)   Rich, A.; Stevens, C. F. *Nature* **2004**, *430*, 845.

(3)   Yamada, K. In *Interrelations between Essential Metal Ions and Human Diseases*; Sigel, A., Sigel, H., Sigel, R. K. O., Eds.; Springer Netherlands: Dordrecht, 2013, p 295.

(4)   Brown, M. J.; Beier, K. *Vitamin B6 Deficiency (Pyridoxine)*; StatPearls Publishing, Treasure Island (FL), 2018.

(5)   Vitaku, E.; Smith, D. T.; Njardarson, J. T. *J. Med. Chem.* **2014**, *57*, 10257.

(6)   Baumann, M.; Baxendale, I. R.; Ley, S. V.; Nikbin, N. *Billstein. J. Org. Chem.* **2011**, *7*, 442.

(7)   Weed, R. I.; Reed, C. F.; Berg, G. *J. Clin. Invest.* **1963**, *42*, 581.

(8)   Kopple, J. D.; Swendseid, M. E. *J. Clin. Invest.* **1975**, *55*, 881.

(9)   Zhang, C.; Sun, C.; Hu, B.; Yu, C.; Lu, M. *Science* **2017**, *355*, 374.

(10)   McGrath, N. A.; Brichacek, M.; Njardarson, J. T. *J. Chem. Ed.* **2010**, *87*, 1348.

(11)   *Lancet* **2013**, *382*, 769.

(12)   Riss, J.; Cloyd, J.; Gates, J.; Collins, S. *Acta Neurol. Scand.* **2008**, *118*, 69.

(13)   Yang, Y.; Rasmussen, B. A.; Shlaes, D. M. *Pharmacol. Ther.* **1999**, *83*, 141.

(14)   Sanford, M.; Plosker, G. L. *Drugs* **2008**, *68*, 1319.

(15)   Pfeffer, M. A.; Swedberg, K.; Granger, C. B.; Held, P.; McMurray, J. J. V.; Michelson, E. L.; Olofsson, B.; Östergren, J.; Yusuf, S. *Lancet* **2003**, *362*, 759.

(16)   Rostovtsev, V. V.; Green, L. G.; Fokin, V. V.; Sharpless, K. B. *Angew. Chem. Int. Ed.* **2002**, *41*, 2596.

(17)   Tornøe, C. W.; Christensen, C.; Meldal, M. *J. Org. Chem.* **2002**, *67*, 3057.

(18)   Kantheti, S.; Narayan, R.; Raju, K. V. S. N. *RSC Adv.* **2015**, *5*, 3687.

(19)   Huo, J.; Hu, H.; Zhang, M.; Hu, X.; Chen, M.; Chen, D.; Liu, J.; Xiao, G.; Wang, Y.; Wen, Z. *RSC Adv.* **2017**, *7*, 2281.

(20)   Kukwikila, M.; Gale, N.; El-Sagheer, A. H.; Brown, T.; Tavassoli, A. *Nat. Chem.* **2017**, *9*, 1089.

(21)   Kharb, R.; Sharma, P. C.; Yar, M. S. *J. Enzyme Inhib. Med. Chem.* **2011**, *26*, 1.

(22)   Alam, S.; Hamid, H. *Inflamm. Cell Signal.* **2014**, *1*.

(23)   Dheer, D.; Singh, V.; Shankar, R. *Bioorg. Chem.* **2017**, *71*, 30.

(24)   Agalave, S. G.; Maujan, S. R.; Pore, V. S. *Chem. Asian. J.* **2011**, *6*, 2696.

(25)   Zhang, B. *Eur. J. Med. Chem.* **2019**, *168*, 357.

(26)   Bonandi, E.; Christodoulou, M. S.; Fumagalli, G.; Perdicchia, D.; Rastelli, G.; Passarella, D. *Drug Discov. Today* **2017**, *22*, 1572.

(27)   Mohammed, I.; Kummetha, I. R.; Singh, G.; Sharova, N.; Lichinchi, G.; Dang, J.; Stevenson, M.; Rana, T. M. *J. Med. Chem.* **2016**, *59*, 7677.

(28)   Thirumurugan, P.; Matosiuk, D.; Jozwiak, K. *Chem. Rev.* **2013**, *113*, 4905.

(29)   Zheng, T.; Rouhanifard, S. H.; Jalloh, A. S.; Wu, P. *Top Heterocycl Chem* **2012**, *28*, 163.

(30)   Hein, C. D.; Liu, X.-M.; Wang, D. *Pharm. Res.* **2008**, *25*, 2216.

(31)   Moses, J. E.; Moorhouse, A. D. *Chem. Soc. Rev.* **2007**, *36*, 1249.

(32)   Kim, E.; Koo, H. *Chem. Sci.* **2019**, *10*, 7835.

(33)   McKay, Craig S.; Finn, M. G. *Cell Chem. Biol.* **2014**, *21*, 1075.

(34)   Dimroth, O. *Ber. Dtsch. Chem. Ges.* **1902**, *35*, 1029.

(35)   Dimroth, O. *Liebigs Ann.* **1909**, *364*, 183.

(36)   Dimroth, O.; Michaelis, W. *Liebigs Ann.* **1927**, *459*, 39.

(37)   Smith, L. I. *Chem. Rev.* **1938**, *23*, 193.

(38)   *Proc. Chem. Soc.* **1961**, 357.

(39)   Huisgen, R. *Angew. Chem. Int. Ed. Engl.* **1963**, *2*, 565.

(40)   Huisgen, R. *Angew. Chem. Int. Ed. Engl.* **1963**, *2*, 633.

(41)   Boren, B. C.; Narayan, S.; Rasmussen, L. K.; Zhang, L.; Zhao, H.; Lin, Z.; Jia, G.; Fokin, V. V. *J. Am. Chem. Soc.* **2008**, *130*, 8923.

(42)   Himo, F.; Lovell, T.; Hilgraf, R.; Rostovtsev, V. V.; Noodleman, L.; Sharpless, K. B.; Fokin, V. V. *J. Am. Chem. Soc.* **2005**, *127*, 210.

(43)   Moen, A.; Nicholson, D. G. *Journal of the Chemical Society, Faraday Transactions* **1995**, *91*, 3529.

(44)   Rodionov, V. O.; Fokin, V. V.; Finn, M. G. *Angew. Chem. Int. Ed.* **2005**, *44*, 2210.

(45)   Wang, X.; Song, Y.; Qu, J.; Luo, Y. *Organometallics* **2017**, *36*, 1042.

(46)   Kuang, G.-C.; Guha, P. M.; Brotherton, W. S.; Simmons, J. T.; Stankee, L. A.; Nguyen, B. T.; Clark, R. J.; Zhu, L. *J. Am. Chem. Soc.* **2011**, *133*, 13984.

(47)   Rodionov, V. O.; Presolski, S. I.; Díaz Díaz, D.; Fokin, V. V.; Finn, M. G. *J. Am. Chem. Soc.* **2007**, *129*, 12705.

(48)   Worrell, B. T.; Malik, J. A.; Fokin, V. V. *Science* **2013**, *340*, 457.

(49) Ben El Ayouchia, H.; Bahsis, L.; Anane, H.; Domingo, L. R.; Stiriba, S.-E. *RSC Adv.* **2018**, *8*, 7670.

(50) Zhang, L.; Chen, X.; Xue, P.; Sun, H. H. Y.; Williams, I. D.; Sharpless, K. B.; Fokin, V. V.; Jia, G. *J. Am. Chem. Soc.* **2005**, *127*, 15998.

(51) Johansson, J. R.; Beke-Somfai, T.; Said Stålsmeden, A.; Kann, N. *Chem. Rev.* **2016**, *116*, 14726.

(52) Majireck, M. M.; Weinreb, S. M. *J. Org. Chem.* **2006**, *71*, 8680.

(53) Pribut, N.; Veale, C. G. L.; Basson, A. E.; van Otterlo, W. A. L.; Pelly, S. C. *Bioorg. Med. Chem. Lett.* **2016**, *26*, 3700.

(54) Kauer, J. C.; Carboni, R. A. *J. Am. Chem. Soc.* **1967**, *89*, 2633.

(55) R. J. Lewis; Sax, N. I. *Sax's Dangerous Properties of Industrial Materials*; Van Nostrand Reinhold: New York, 1992.

(56) Wu, L.-Y.; Xie, Y.-X.; Chen, Z.-S.; Niu, Y.-N.; Liang, Y.-M. *Synlett* **2009**, *2009*, 1453.

(57) Fletcher, J. T.; Walz, S. E.; Keeney, M. E. *Tetrahedron Lett.* **2008**, *49*, 7030.

(58) Xu, M.; Kuang, C.; Wang, Z.; Yang, Q.; Jiang, Y. *Synthesis* **2011**, *2011*, 223.

(59) Liu, Y.; Han, C.; Ma, X.; Yang, J.; Feng, X.; Jiang, Y. *Tetrahedron Lett.* **2018**, *59*, 650.

(60) Jiang, Y.; Kuang, C.; Yang, Q. *Synlett* **2009**, *2009*, 3163.

(61) Giel, M.-C.; Smedley, C. J.; Mackie, E. R. R.; Guo, T.; Dong, J.; Soares da Costa, T. P.; Moses, J. E. *Angew. Chem. Int. Ed.* **2020**, *59*, 1181.

(62) Scriven, E. F. V.; Turnbull, K. *Chem. Rev.* **1988**, *88*, 297.

(63) Gribanov, P. S.; Topchiy, M. A.; Golenko, Y. D.; Lichtenstein, Y. I.; Eshtukov, A. V.; Terekhov, V. E.; Asachenko, A. F.; Nechaev, M. S. *Green Chem.* **2016**, *18*, 5984.

(64) Liu, Q.; Tor, Y. *Org. Lett.* **2003**, *5*, 2571.

(65) Meng, G.; Guo, T.; Ma, T.; Zhang, J.; Shen, Y.; Sharpless, K. B.; Dong, J. *Nature* **2019**, *574*, 86.

(66) L'Abbe, G. *Chem. Rev.* **1969**, *69*, 345.

(67) Urben, P. G. *Bretherick's Handbook of Reactive Chemical Hazards*; 7th ed.; Academic Press: Oxford, 2007; Vol. 1.

(68) Keicher, T.; Löbbecke, S. *Organic Azides* **2009**, 1.

(69) Richardson, S. G.; Giles, C.; Swan, C. H. *J. Clin. Pathol.* **1975**, *28*, 350.

(70) Karlsson, S.; Cook, C.; Emtenäs, H.; Fan, K.; Gillespie, P.; Mohamed, M. *Org. Process. Res. Dev.* **2017**, *21*, 1668.

(71) Wang, Q.; Han, J.; Zhang, Y.; Yan, Z.; Velasco, E.; Yang, L.; Wang, B.; Zang, S.-Q. *ACS Appl. Mater. Interfaces* **2019**, *11*, 8081.

(72)   Wang, Q.; Feng, X.; Wang, S.; Song, N.; Chen, Y.; Tong, W.; Han, Y.; Yang, L.; Wang, B. *Adv. Mater.* **2016**, *28*, 5837.

(73)   *Chem. Eng. News* **1976**, *54*, 6.

(74)   Cartwright, M.; Wilkinson, J. *Propellants Explos. Pyrotech.* **2010**, *35*, 326.

(75)   Kalliokoski, T. *ACS Comb. Sci.* **2015**, *17*, 600.

(76)   Cai, Z.-J.; Lu, X.-M.; Zi, Y.; Yang, C.; Shen, L.-J.; Li, J.; Wang, S.-Y.; Ji, S.-J. *Org. Lett.* **2014**, *16*, 5108.

(77)   Chen, Z.; Yan, Q.; Liu, Z.; Zhang , Y. *Chem. Eur. J.* **2014**, *20*, 17635.

(78)   Chen, Z.; Yan, Q.; Liu, Z.; Xu, Y.; Zhang, Y. *Angew. Chem. Int. Ed.* **2013**, *52*, 13324.

(79)   Chen, Z.; Yan, Q.; Yi, H.; Liu, Z.; Lei, A.; Zhang, Y. *Chem. Eur. J.* **2014**, *20*, 13692.

(80)   Bai, H.-W.; Cai, Z.-J.; Wang, S.-Y.; Ji, S.-J. *Org. Lett.* **2015**, *17*, 2898.

(81)   Sakai, K.; Hida, N.; Kondo, K. *Bull. Chem. Soc. Jpn.* **1986**, *59*, 179.

(82)   van Berkel, S. S.; Brauch, S.; Gabriel, L.; Henze, M.; Stark, S.; Vasilev, D.; Wessjohann, L. A.; Abbas, M.; Westermann, B. *Angew. Chem. Int. Ed.* **2012**, *51*, 5343.

(83)   Gravestock, M. B.; Barry, M.; Hales, N. J.; Reck, F.; Zhou, F.; Fleming, P. J.; Carcanague, D. R.; Girardot, M. M.; Organization, W. I. P., Ed. 2003 Vol. WO 03/072575 At.

(84)   Hanselmann, R.; Job, G. E.; Johnson, G.; Lou, R.; Martynow, J. G.; Reeve, M. M. *Org. Process. Res. Dev.* **2010**, *14*, 152.

(85)   D'Oyley, J. M.; Aliev, A. E.; Sheppard, T. D. *Angew. Chem. Int. Ed.* **2014**, *53*, 10747.

(86)   Harada, K.; Oda, M.; Matsushita, A.; Shirai, M. *Heterocycles* **1970**, *48*, 695.

(87)   Harada, K.; Oda, M.; Matsushita, A.; Shirai, M. *ChemInform* **1998**, *29*.

(88)   Singh, I. P.; Spevak, P.; Palak, B.; Amedjo, S.; Micetich, R. G. United States Patent, 1996; Vol. US005527920.

(89)   Kolb, H. C.; Finn, M. G.; Sharpless, K. B. *Angew. Chem. Int. Ed.* **2001**, *40*, 2004.

(90)   Lima, C. G. S.; Ali, A.; van Berkel, S. S.; Westermann, B.; Paixão, M. W. *Chem. Comm.* **2015**, *51*, 10784.

(91)   Brown, O. C.; Baguña Torres, J.; Holt, K. B.; Blower, P. J.; Went, M. J. *Dalton Trans.* **2017**, *46*, 14612.

(92)   Bamford, W. R.; Stevens, T. S. *Journal of the Chemical Society (Resumed)* **1952**, 4735.

(93)   Shapiro, R. H.; Lipton, M. F.; Kolonko, K. J.; Buswell, R. L.; Capuano, L. A. *Tetrahedron Lett.* **1975**, *16*, 1811.

(94)   Hall, H. K. *J. Am. Chem. Soc.* **1957**, *79*, 5441.

(95)   Sayer, J. M.; Peskin, M.; Jencks, W. P. *J. Am. Chem. Soc.* **1973**, *95*, 4277.

(96)   Schreiber, J.; Felix, D.; Eschenmoser, A.; Winter, M.; Gautschi, F.; Schulte-Elte, K. H.; Sundt, E.; Ohloff, G.; Kalovoda, J.; Kaufmann, H.; Wieland, P.; Anner, G. *Helv. Chim. Acta* **1967**, *50*, 2101.

(97)   *Comprehensive Organic Name Reactions and Reagents* **2010**, 1005.

(98)   Bissell, E. R.; Finger, M. *J. Org. Chem.* **1959**, *24*, 1256.

(99)   Sebest, F.; Casarrubios, L.; Rzepa, H. S.; White, A. J. P.; Díez-González, S. *Green Chem.* **2018**, *20*, 4023.

(100)   Yadav, J. S.; Reddy, G. S. K. K.; Sabitha, G.; Krishna, A. D.; Prasad, A. R.; Hafeez, U. R. R.; Vishwaswar Rao, K.; Bhaskar Rao, A. *Tetrahedron: Asymmetry* **2007**, *18*, 717.

(101)   Rouf, A.; Gupta, P.; Aga, M. A.; Kumar, B.; Parshad, R.; Taneja, S. C. *Tetrahedron: Asymmetry* **2011**, *22*, 2134.

(102)   Ayala-Mata, F.; Barrera-Mendoza, C.; Jiménez-Vázquez, H. A.; Vargas-Díaz, E.; Zepeda, L. G. *Molecules* **2012**, *17*, 13864.

(103)   Campbell, A.; Kenyon, J. *Journal of the Chemical Society (Resumed)* **1947**, 436.

(104)   Creary, X. *J. Org. Chem.* **1987**, *52*, 5026.

(105)   Adamczyk, M.; Johnson, D. D.; Mattingly, P. G.; Pan, Y.; Reddy, R. E. *Syn. Comm.* **2002**, *32*, 3199.

(106)   J. Clayden; N. Greeves; Warren, S. *Organic Chemistry*; Second ed.; Oxford University Press.

(107)   Pasto, D. J.; Taylor, R. T. *Organic Reactions* **2004**, 91.

(108)   Trost, B. M.; Fettes, A.; Shireman, B. T. *J. Am. Chem. Soc.* **2004**, *126*, 2660.

(109)   Shaw, B. L. *J. Am. Chem. Soc.* **1975**, *97*, 3856.

(110)   Miller, R. D.; McKean, D. R. *Tetrahedron Lett.* **1982**, *23*, 323.

(111)   Yoshidomi, S.; Abe, M. *J. Am. Chem. Soc.* **2019**, *141*, 3920.

(112)   Jencks, W. P.; Carriuolo, J. *J. Am. Chem. Soc.* **1960**, *82*, 1778.

(113)   Gregoire, B.; Carre, M. C.; Caubere, P. *J. Org. Chem.* **1986**, *51*, 1419.

(114)   Atanes, N.; Escudero, S.; Pérez, D.; Guitián, E.; Castedo, L. *Tetrahedron Lett.* **1998**, *39*, 3039.

(115)   Medina, J. M.; McMahon, T. C.; Jiménez-Osés, G.; Houk, K. N.; Garg, N. K. *J. Am. Chem. Soc.* **2014**, *136*, 14706.

(116)   Sloan Devlin, A.; Du Bois, J. *Chem. Sci.* **2013**, *4*, 1059.

(117)   Fife, T. H.; Natarajan, R. *J. Am. Chem. Soc.* **1986**, *108*, 8050.

(118)   Jones, K. *Encyclopedia of Reagents for Organic Synthesis* **2001**.

(119) Apffel, A.; Chakel, J. A.; Fischer, S.; Lichtenwalter, K.; Hancock, W. S. *Anal. Chem.* **1997**, *69*, 1320.

(120) Perrin, D. D. *Dissociation constants of organic bases in aqueous solution*; Butterworths: London, 1965.

(121) Bott, K. *Chem. Ber.* **1975**, *108*, 402.

(122) Zhou, J.; Wakchaure, V.; Kraft, P.; List, B. *Angew. Chem. Int. Ed.* **2008**, *47*, 7656.

(123) Clark, P. R.; Williams, G. D.; Hayes, J. F.; Tomkinson, N. C. O. *Angew. Chem. Int. Ed.* **2020**, *59*, 6740.

(124) Audi, S.; Burrage, D. R.; Lonsdale, D. O.; Pontefract, S.; Coleman, J. J.; Hitchings, A. W.; Baker, E. H. *Br. J. Clin. Pharmacol.* **2018**, *84*, 2562.

(125) Figueiras, A.; Sarraguça, J. M. G.; Carvalho, R. A.; Pais, A. A. C. C.; Veiga, F. J. B. *Pharm. Res.* **2007**, *24*, 377.

(126) World Health, O. *World Health Organization model list of essential medicines: 21st list 2019*, World Health Organization, 2019.

(127) McClellan, K. J.; Markham, A. *Drugs* **1998**, *56*, 1039.

(128) Smiley, R. A. *Ullmann's Encyclopedia of Industrial Chemistry* **2000**.

(129) Damm, M.; Glasnov, T. N.; Kappe, C. O. *Org. Process. Res. Dev.* **2010**, *14*, 215.

(130) Lee, Y.-S.; Cho, Y.-H.; Lee, S.; Bin, J.-K.; Yang, J.; Chae, G.; Cheon, C.-H. *Tetrahedron* **2015**, *71*, 532.

(131) Alaqeel, S. I. *J. Saudi Chem. Soc.* **2017**, *21*, 229.

(132) Reddy, K. S.; Srinivasan, N.; Reddy, C. R.; Kolla, N.; Anjaneyulu, Y.; Venkatraman, S.; Bhattacharya, A.; Mathad, V. T. *Org. Process. Res. Dev.* **2007**, *11*, 81.

(133) Uchida, M.; Morita, S.; Chihiro, M.; Kanbe, T.; Yamasaki, K.; Yabuuchi, Y.; Nakagawa, K. *Chem. Pharm. Bull.* **1989**, *37*, 2109.

(134) Tingle, J. B.; Blanck, F. C. *J. Am. Chem. Soc.* **1908**, *30*, 1395.

(135) Bielory, L.; Lien, K. W.; Bigelsen, S. *Drugs* **2005**, *65*, 215.

(136) Gyurik, R. J.; Theodorides, V. J.; Google Patents: 1975.

(137) Dold, C.; Holland, C. V. *Microb. Infect.* **2011**, *13*, 632.

(138) Isabel, H.; Tatiana, G. *Infect. Disord. Drug. Targets.* **2010**, *10*, 349.

(139) Gustavsen, K. M.; Bradley, M. H.; Wright, A. L. *Ann. Trop. Med. Parasit.* **2009**, *103*, 11.

(140) GlaxoSmithKline ups albendazole worm drug donation, https://www.telegraph.co.uk/finance/newsbysector/pharmaceuticalsandchemicals/8062194/GlaxoSmithKline-ups-albendazole-worm-drug-donation.html 28-November-2016.

(141) Ramalingam, S.; Sinniah, B.; Krishnan, U. *Am. J. Trop. Med. Hyg.* **1983**, *32*, 984.

(142) Spasov, A. A.; Chernikov, M. V.; Yakovlev, D. S.; Anisimova, V. A. *Pharm. Chem. J.* **2006**, *40*, 603.

(143) Zhukovskaya, O. N.; Anisimova, V. A.; Spasov, A. A.; Yakovlev, D. S.; Gurova, N. A.; Kucheryavenko, A. F.; Salaznikova, O. A.; Kuznetsova, V. A.; Mal'tsev, D. V.; Brigadirova, A. A.; Morkovina, Y. V.; Solov'eva, O. A.; Gurova, V. V.; Reznikov, E. V. *Pharm. Chem. J.* **2017**, *51*, 182.

(144) Özden, S.; Atabey, D.; Yıldız, S.; Göker, H. *Eur. J. Med. Chem.* **2008**, *43*, 1390.

(145) Zhang, G.; Ren, P.; Gray, N. S.; Sim, T.; Liu, Y.; Wang, X.; Che, J.; Tian, S.-S.; Sandberg, M. L.; Spalding, T. A.; Romeo, R.; Iskandar, M.; Chow, D.; Martin Seidel, H.; Karanewsky, D. S.; He, Y. *Bioorg. Med. Chem. Lett.* **2008**, *18*, 5618.

(146) Kim, R. M.; Chang, J.; Lins, A. R.; Brady, E.; Candelore, M. R.; Dallas-Yang, Q.; Ding, V.; Dragovic, J.; Iliff, S.; Jiang, G.; Mock, S.; Qureshi, S.; Saperstein, R.; Szalkowski, D.; Tamvakopoulos, C.; Tota, L.; Wright, M.; Yang, X.; Tata, J. R.; Chapman, K.; Zhang, B. B.; Parmee, E. R. *Bioorg. Med. Chem. Lett.* **2008**, *18*, 3701.

(147) Bonfanti, J.-F.; Meyer, C.; Doublet, F.; Fortin, J.; Muller, P.; Queguiner, L.; Gevers, T.; Janssens, P.; Szel, H.; Willebrords, R.; Timmerman, P.; Wuyts, K.; van Remoortere, P.; Janssens, F.; Wigerinck, P.; Andries, K. *J. Med. Chem.* **2008**, *51*, 875.

(148) Shao, B.; Huang, J.; Sun, Q.; Valenzano, K. J.; Schmid, L.; Nolan, S. *Bioorg. Med. Chem. Lett.* **2005**, *15*, 719.

(149) Ognyanov, V. I.; Balan, C.; Bannon, A. W.; Bo, Y.; Dominguez, C.; Fotsch, C.; Gore, V. K.; Klionsky, L.; Ma, V. V.; Qian, Y.-X.; Tamir, R.; Wang, X.; Xi, N.; Xu, S.; Zhu, D.; Gavva, N. R.; Treanor, J. J. S.; Norman, M. H. *J. Med. Chem.* **2006**, *49*, 3719.

(150) Barber, G. N. *Nat. Rev. Immunol.* **2015**, *15*, 760.

(151) Ramanjulu, J. M.; Pesiridis, G. S.; Yang, J.; Concha, N.; Singhaus, R.; Zhang, S.-Y.; Tran, J.-L.; Moore, P.; Lehmann, S.; Eberl, H. C.; Muelbaier, M.; Schneck, J. L.; Clemens, J.; Adam, M.; Mehlmann, J.; Romano, J.; Morales, A.; Kang, J.; Leister, L.; Graybill, T. L.; Charnley, A. K.; Ye, G.; Nevins, N.; Behnia, K.; Wolf, A. I.; Kasparcova, V.; Nurse, K.; Wang, L.; Puhl, A. C.; Li, Y.; Klein, M.; Hopson, C. B.; Guss, J.; Bantscheff, M.; Bergamini, G.; Reilly, M. A.; Lian, Y.; Duffy, K. J.; Adams, J.; Foley, K. P.; Gough, P. J.; Marquis, R. W.; Smothers, J.; Hoos, A.; Bertin, J. *Nature* **2018**, *564*, 439.

(152) Li, T.; Chen, Z. J. *J. Exp. Med.* **2018**, *215*, 1287.

(153) Corrales, L.; McWhirter, S. M.; Dubensky, T. W., Jr.; Gajewski, T. F. *J. Clin. Invest.* **2016**, *126*, 2404.

(154) P. Pierron *Ann. Chim. Phys.* **1908**, *15*, 189.

(155) Mandel, L. R.; Porter, C. C.; Kuehl, F. A.; Jensen, N. P.; Schmitt, S. M.; Windholz, T. B.; Beattie, T. R.; Carty, J. A.; Christensen, B. G.; Shen, T.-Y. *J. Med. Chem.* **1970**, *13*, 1043.

(156) Joseph, L. *J. Med. Chem.* **1963**, *6*, 601.

(157) Leonard, N. J.; Curtin, D. Y.; Beck, K. M. *J. Am. Chem. Soc.* **1947**, *69*, 2459.

(158) Ogura, H.; Takayanagi, H.; Yamazaki, Y.; Yonezawa, S.; Takagi, H.; Kobayashi, S.; Kamioka, T.; Kamoshita, K. *J. Med. Chem.* **1972**, *15*, 923.

(159) Deasy, R. E.; Slattery, C. N.; Maguire, A. R.; Kjell, D. P.; Hawk, M. K. N.; Joo, J. M.; Gu, R. L.; Moynihan, H. *J. Org. Chem.* **2014**, *79*, 3688.

(160) Simonov, A. M.; Anisimova, V. A. *Chem. Heterocycl. Com.* **1979**, *15*, 705.

(161) Janssens, F.; Torremans, J.; Janssen, M.; Stokbroekx, R. A.; Luyckx, M.; Janssen, P. A. J. *J. Med. Chem.* **1985**, *28*, 1943.

(162) Cee, V. J.; Downing, N. S. *Tetrahedron Lett.* **2006**, *47*, 3747.

(163) P. Lugosi, B. A., G. Hornyak *Periodica Polytechnica Chemical Engineering* **1975**, *19*, 307.

(164) Zhu, T.-H.; Wang, S.-Y.; Wang, G.-N.; Ji, S.-J. *Chem. Eur. J.* **2013**, *19*, 5850.

(165) Kym, O.; Ratner, L. *Ber. Dtsch. Chem. Ges.* **1912**, *45*, 3238.

(166) Hadole, C.; Rajput, J.; Bendre, R. *Org. Chem. Curr. Res.* **2018**, *7*, 1.

(167) Goldstein, S. W.; Bill, A.; Dhuguru, J.; Ghoneim, O. *J. Chem. Ed.* **2017**, *94*, 1388.

(168) Gallego, M. G.; Sierra, M. A. In *Organic Reaction Mechanisms: 40 Solved Cases*; Gallego, M. G., Sierra, M. A., Eds.; Springer Berlin Heidelberg: Berlin, Heidelberg, 2004, p 217.

(169) Kwan, E. E.; Zeng, Y.; Besser, H. A.; Jacobsen, E. N. *Nat. Chem.* **2018**, *10*, 917.

(170) Ueda, S.; Buchwald, S. L. *Angew. Chem. Int. Ed.* **2012**, *51*, 10364.

(171) Hunger, A.; Kebrle, J.; Rossi, A.; Hoffmann, K. *Helv. Chim. Acta* **1961**, *44*, 1273.

(172) Charaschanya, M.; Bogdan, A. R.; Wang, Y.; Djuric, S. W. *Tetrahedron Lett.* **2016**, *57*, 1035.

(173) Hong, Y.; Tanoury, G. J.; Wilkinson, H. S.; Bakale, R. P.; Wald, S. A.; Senanayake, C. H. *Tetrahedron Lett.* **1997**, *38*, 5607.

(174) Louie, J.; Hartwig, J. F. *Tetrahedron Lett.* **1995**, *36*, 3609.

(175) Guram, A. S.; Rennels, R. A.; Buchwald, S. L. *Angew. Chem. Int. Ed. Engl.* **1995**, *34*, 1348.

(176) Velagapudi, U. K.; Langelier, M.-F.; Delgado-Martin, C.; Diolaiti, M. E.; Bakker, S.; Ashworth, A.; Patel, B. A.; Shao, X.; Pascal, J. M.; Talele, T. T. *J. Med. Chem.* **2019**, *62*, 5330.

(177) Timsina, Y. N.; Gupton, B. F.; Ellis, K. C. *ACS. Catal.* **2018**, 5732.

(178) Park, Y.; Kim, Y.; Chang, S. *Chem. Rev.* **2017**, *117*, 9247.

(179) Hazelard, D.; Nocquet, P.-A.; Compain, P. *Org. Chem. Front.* **2017**, *4*, 2500.

(180) Chichibabin, A. E.; Zeide, O. A. *Zhur. Russ. Fiz. Kim. Obshch.* **1914**, *46*, 1216.

(181) McGill, C. K.; Rappa, A. In *Advances in Heterocyclic Chemistry*; Katritzky, A. R., Ed.; Academic Press: 1988; Vol. 44, p 1.

(182) Preston, P. N. *Chem. Rev.* **1974**, *74*, 279.

(183) Buncel, E.; Menon, B. *J. Organomet. Chem.* **1977**, *141*, 1.

(184) Das, R.; Banerjee, M.; Rai, R. K.; Karri, R.; Roy, G. *Org. Biomol. Chem.* **2018**, *16*, 4243.

(185) Bunnett, J. F.; Garbisch, E. W.; Pruitt, K. M. *J. Am. Chem. Soc.* **1957**, *79*, 385.

(186) Bunnett, J. F. *J. Am. Chem. Soc.* **1957**, *79*, 5969.

(187) Shreve, R. N.; Riechers, E. H.; Rubenkoenig, H.; Goodman, A. H. *Ind. Eng. Chem. Res.* **1940**, *32*, 173.

(188) Monguchi, D.; Fujiwara, T.; Furukawa, H.; Mori, A. *Org. Lett.* **2009**, *11*, 1607.

(189) Wagh, Y. S.; Bhanage, B. M. *Tetrahedron Lett.* **2012**, *53*, 6500.

(190) Wang, Q.; Schreiber, S. L. *Org. Lett.* **2009**, *11*, 5178.

(191) Xu, J.; Li, J.; Wei, Z.; Zhang, Q.; Shi, D. *RSC Adv.* **2013**, *3*, 9622.

(192) McDonald, S. L.; Hendrick, C. E.; Wang, Q. *Angew. Chem. Int. Ed.* **2014**, *53*, 4667.

(193) Matsuda, N.; Hirano, K.; Satoh, T.; Miura, M. *Org. Lett.* **2011**, *13*, 2860.

(194) Miyasaka, M.; Hirano, K.; Satoh, T.; Kowalczyk, R.; Bolm, C.; Miura, M. *Org. Lett.* **2011**, *13*, 359.

(195) Cho, S. H.; Kim, J. Y.; Lee, S. Y.; Chang, S. *Angew. Chem. Int. Ed.* **2009**, *48*, 9127.

(196) Guo, S.; Qian, B.; Xie, Y.; Xia, C.; Huang, H. *Org. Lett.* **2011**, *13*, 522.

(197) Li, Y.; Xie, Y.; Zhang, R.; Jin, K.; Wang, X.; Duan, C. *J. Org. Chem.* **2011**, *76*, 5444.

(198) Wang, J.; Hou, J.-T.; Wen, J.; Zhang, J.; Yu, X.-Q. *Chem. Comm.* **2011**, *47*, 3652.

(199) Xu, D.; Wang, W.; Miao, C.; Zhang, Q.; Xia, C.; Sun, W. *Green Chem.* **2013**, *15*, 2975.

(200) Pal, P.; Giri, A. K.; Singh, H.; Ghosh, S. C.; Panda, A. B. *Chem. Asian. J.* **2014**, *9*, 2392.

(201) Joseph, J.; Kim, J. Y.; Chang, S. *Chem. Eur. J.* **2011**, *17*, 8294.

(202) Froehr, T.; Sindlinger, C. P.; Kloeckner, U.; Finkbeiner, P.; Nachtsheim, B. J. *Org. Lett.* **2011**, *13*, 3754.

(203) Lamani, M.; Prabhu, K. R. *J. Org. Chem.* **2011**, *76*, 7938.

(204) Wertz, S.; Kodama, S.; Studer, A. *Angew. Chem. Int. Ed.* **2011**, *50*, 11511.

(205) Wagh, Y. S.; Tiwari, N. J.; Bhanage, B. M. *Tetrahedron Lett.* **2013**, *54*, 1290.

(206) Wang, R.; Liu, H.; Yue, L.; Zhang, X.-k.; Tan, Q.-y.; Pan, R.-l. *Tetrahedron Lett.* **2014**, *55*, 2233.

(207) Evindar, G.; Batey, R. A. *Org. Lett.* **2003**, *5*, 133.

(208) Saha, P.; Ramana, T.; Purkait, N.; Ali, M. A.; Paul, R.; Punniyamurthy, T. *J. Org. Chem.* **2009**, *74*, 8719.

(209) Deng, X.; McAllister, H.; Mani, N. S. *J. Org. Chem.* **2009**, *74*, 5742.

(210) Lv, X.; Bao, W. *J. Org. Chem.* **2009**, *74*, 5618.

(211) J. Sheehan; P. Cruickshank *Org. Synth.* **1968**, *48*.

(212) Wang, F.; Cai, S.; Liao, Q.; Xi, C. *J. Org. Chem.* **2011**, *76*, 3174.

(213) Shen, G.; Bao, W. *Adv. Synth. Catal.* **2010**, *352*, 981.

(214) Ho, T.-L.; Fieser, M.; Fieser, L.; Danheiser, R.; Roush, W. *Fieser and Fieser's Reagents for Organic Synthesis* **2009**, 000.

(215) Vajpayee, V.; Moon, M. E.; Lee, S.; Ravikumar, S.; Kim, H.; Ahn, B.; Choi, S.; Hong, S. H.; Chi, K.-W. *Tetrahedron* **2013**, *69*, 3511.

(216) Sandmeyer, T. *Ber. Dtsch. Chem. Ges.* **1884**, *17*, 1633.

(217) Sandmeyer, T. *Ber. Dtsch. Chem. Ges.* **1884**, *17*, 2650.

(218) Gattermann, L. *Ber. Dtsch. Chem. Ges.* **1890**, *23*, 1218.

(219) Booth, G. *Ullmann's Encyclopedia of Industrial Chemistry* **2000**.

(220) Held, P.; Gross, M.; Schubert, H. *Z. Chem.* **1973**, *13*, 292.

(221) Partridge, M. W.; Turner, H. A. *Journal of the Chemical Society (Resumed)* **1958**, 2086.

(222) Esser, F.; Ehrengart, P.; Peter Ignatow, H. *J. Chem. Soc., Perkin Trans. 1.* **1999**, 1153.

(223) Goliński, J.; Makosza, M. *Tetrahedron Lett.* **1978**, *19*, 3495.

(224) Esser, F.; Pook, K.-H. *Synthesis* **1992**, *1992*, 596.

(225) Chi, Y.; Zhang, W.-X.; Xi, Z. *Org. Lett.* **2014**, *16*, 6274.

(226) He, H.-F.; Wang, Z.-J.; Bao, W. *Adv. Synth. Catal.* **2010**, *352*, 2905.

(227) Tran, L. Q.; Li, J.; Neuville, L. *J. Org. Chem.* **2015**, *80*, 6102.

(228) Li, W.; Nelson, D. P.; Jensen, M. S.; Hoerrner, R. S.; Cai, D.; Larsen, R. D.; Reider, P. J. *J. Org. Chem.* **2002**, *67*, 5394.

(229) Ishiyama, T.; Takagi, J.; Ishida, K.; Miyaura, N.; Anastasi, N. R.; Hartwig, J. F. *J. Am. Chem. Soc.* **2002**, *124*, 390.

(230) Ishiyama, T.; Murata, M.; Miyaura, N. *J. Org. Chem.* **1995**, *60*, 7508.

(231) O'Donovan, M. R.; Mee, C. D.; Fenner, S.; Teasdale, A.; Phillips, D. H. *Mutation Research/Genetic Toxicology and Environmental Mutagenesis* **2011**, *724*, 1.

(232) Hansen, M. M.; Jolly, R. A.; Linder, R. J. *Org. Process. Res. Dev.* **2015**, *19*, 1507.

(233) Elwell, C. E.; Gagnon, N. L.; Neisen, B. D.; Dhar, D.; Spaeth, A. D.; Yee, G. M.; Tolman, W. B. *Chem. Rev.* **2017**, *117*, 2059.

(234) Redox Reactions, wiley.com, https://www.wiley.com/college/boyer/0470003790/reviews/redox/redox.htm, 7th October 2019.

(235) Barnwell, C. N. *Fundamentals of Molecular Spectroscopy*; McGRAW HILL Book Company (UK) Limited: Maidenhead, England, 1983.

(236) T. Engel; Reid, P. *Physical Chemistry*; Pearson Benjamin-Cummings, 2006.

(237) Constable, D. J. C.; Dunn, P. J.; Hayler, J. D.; Humphrey, G. R.; Leazer, J. J. L.; Linderman, R. J.; Lorenz, K.; Manley, J.; Pearlman, B. A.; Wells, A.; Zaks, A.; Zhang, T. Y. *Green Chem.* **2007**, *9*, 411.

(238) Huang, J.; Huang, J.; Liu, X.; Li, C.; Ding, L.; Yu, H. *Sci. Bull.* **2018**, *63*, 1180.

(239) Cavani, F.; Teles, J. H. *Chem. Sus. Chem.* **2009**, *2*, 508.

(240) Chen, J.-R. *Process Safety Progress* **2004**, *23*, 72.

(241) Crescitelli, S.; Meli, S.; Russo, G.; Tufano, V. *J. Hazard. Mater.* **1980**, *3*, 293.

(242) Allen, S. E.; Walvoord, R. R.; Padilla-Salinas, R.; Kozlowski, M. C. *Chem. Rev.* **2013**, *113*, 6234.

(243) Ye, X.; Johnson, M. D.; Diao, T.; Yates, M. H.; Stahl, S. S. *Green Chem.* **2010**, *12*, 1180.

(244) Fischer, J.; Liebner, C.; Hieronymus, H.; Klemm, E. *Chem. Eng. Sci.* **2009**, *64*, 2951.

(245) Ochen, A.; Whitten, R.; Aylott, H. E.; Ruffell, K.; Williams, G. D.; Slater, F.; Roberts, A.; Evans, P.; Steves, J. E.; Sanganee, M. J. *Organometallics* **2019**, *38*, 176.

(246) McCann, S. D.; Stahl, S. S. *Acc. Chem. Res.* **2015**, *48*, 1756.

(247) Solomon, E. I.; Heppner, D. E.; Johnston, E. M.; Ginsbach, J. W.; Cirera, J.; Qayyum, M.; Kieber-Emmons, M. T.; Kjaergaard, C. H.; Hadt, R. G.; Tian, L. *Chem. Rev.* **2014**, *114*, 3659.

(248) Jira, R. *Angew. Chem. Int. Ed.* **2009**, *48*, 9034.

(249) Eckert, M.; Fleischmann, G.; Jira, R.; Bolt, H. M.; Golka, K. *Ullmann's Encyclopedia of Industrial Chemistry* **2006**.

(250) Goodman, B. R.; Hass, K. C.; Schneider, W. F.; Adams, J. B. *J. Phys. Chem. B* **1999**, *103*, 10452.

(251) Santra, S.; Archipov, T.; Ene, A. B.; Komnik, H.; Stoll, H.; Roduner, E.; Rauhut, G. *Phys. Chem. Chem. Phys.* **2009**, *11*, 8855.

(252) Roduner, E.; Kaim, W.; Sarkar, B.; Urlacher, V. B.; Pleiss, J.; Gläser, R.; Einicke, W.-D.; Sprenger, G. A.; Beifuß, U.; Klemm, E.; Liebner, C.; Hieronymus, H.; Hsu, S.-F.; Plietker, B.; Laschat, S. *ChemCatChem* **2013**, *5*, 82.

(253) Milazzo, G.; Caroli, S.; Sharma, V. K. *Tables of Standard Electrode Potentials*; Wiley: Chichester, 1978.

(254) Bard, A. J.; Parsons, R.; Jordan, J. *Standard Potentials in Aqueous Solutions*; Marcel Dekker: New York, 1985.

(255) Lam, P. Y. S.; Clark, C. G.; Saubern, S.; Adams, J.; Winters, M. P.; Chan, D. M. T.; Combs, A. *Tetrahedron Lett.* **1998**, *39*, 2941.

(256) Vantourout, J. C.; Miras, H. N.; Isidro-Llobet, A.; Sproules, S.; Watson, A. J. B. *J. Am. Chem. Soc.* **2017**, *139*, 4769.

(257) Chan, D. M. T.; Monaco, K. L.; Wang, R.-P.; Winters, M. P. *Tetrahedron Lett.* **1998**, *39*, 2933.

(258) Lam, P. Y. S.; Vincent, G.; Bonne, D.; Clark, C. G. *Tetrahedron Lett.* **2003**, *44*, 4927.

(259) Hoover, J. M.; Stahl, S. S. *J. Am. Chem. Soc.* **2011**, *133*, 16901.

(260) Hoover, J. M.; Steves, J. E.; Stahl, S. S. *Nat. Protoc.* **2012**, *7*, 1161.

(261) Hoover, J. M.; Ryland, B. L.; Stahl, S. S. *J. Am. Chem. Soc.* **2013**, *135*, 2357.

(262) Brasche, G.; Buchwald, S. L. *Angew. Chem. Int. Ed.* **2008**, *47*, 1932.

(263) Raju, R.; Prasad, K. *Tetrahedron* **2012**, *68*, 1341.

(264) Chemler, S. R.; Casavant, B. J. In *Encyclopedia of Reagents for Organic Synthesis*; John Wiley & Sons, Ltd: 2001.

(265) Parish, E. J.; Li, S. *Encyclopedia of Reagents for Organic Synthesis* **2001**.

(266) Barclay, G. A.; Cooper, A. *Journal of the Chemical Society (Resumed)* **1965**, 3746.

(267) Farahat, A. A.; Boykin, D. W. *Tetrahedron Lett.* **2014**, *55*, 3049.

(268) Zhang, S.; Zhang, D.; Liebeskind, L. S. *J. Org. Chem.* **1997**, *62*, 2312.

(269) Isac-García, J.; Dobado, J. A.; Calvo-Flores, F. G.; Martínez-García, H. In *Experimental Organic Chemistry*; Isac-García, J., Dobado, J. A., Calvo-Flores, F. G., Martínez-García, H., Eds.; Academic Press: 2016, p 145.

(270) Tilstam, U. *Org. Process. Res. Dev.* **2012**, *16*, 1273.

(271) Steeno, G. S. In *Chemical Engineering in the Pharmaceutical Industry*; John Wiley & Sons, Inc.: 2010, p 597.

(272) S. Polotis, P. C., G. Colombo, D. Rekkas *Drug. Dev. Ind. Pharm.* **2017**, *43*, 889.

(273) Sambiagio, C.; Marsden, S. P.; Blacker, A. J.; McGowan, P. C. *Chem. Soc. Rev.* **2014**, *43*, 3525.

(274) Ueda, S.; Nagasawa, H. *J. Org. Chem.* **2009**, *74*, 4272.

(275) Simmons, E. M.; Hartwig, J. F. *Angew. Chem. Int. Ed.* **2012**, *51*, 3066.

(276) Ben, S.; Zhao, J.; Rabczuk, T. *Phys. Chem. Chem. Phys.* **2015**, *17*, 20990.

(277) Gómez-Gallego, M.; Sierra, M. A. *Chem. Rev.* **2011**, *111*, 4857.

(278) Tang, S.; Gong, T.; Fu, Y. *Sci. Chin. Chem.* **2013**, *56*, 619.

(279) Winstein, S.; Traylor, T. G. *J. Am. Chem. Soc.* **1955**, *77*, 3747.

(280) Gorelsky, S. I.; Lapointe, D.; Fagnou, K. *J. Am. Chem. Soc.* **2008**, *130*, 10848.

(281) Bruce, M. I. *Angew. Chem. Int. Ed. Engl.* **1977**, *16*, 73.

(282) Ryabov, A. D. *Chem. Rev.* **1990**, *90*, 403.

(283) Vicente, J.; Saura-Llamas, I. *Comment. Inorg. Chem.* **2007**, *28*, 39.

(284) Ryabov, A. D.; Sakodinskaya, I. K.; Yatsimirsky, A. K. *Journal of the Chemical Society, Dalton Transactions* **1985**, 2629.

(285) Angamuthu, R.; Byers, P.; Lutz, M.; Spek, A. L.; Bouwman, E. *Science* **2010**, *327*, 313.

(286) Serjeant, E. P.; Dempsey, B. *Ionization Constants of Organic Acids in Aqueous Solution*; Pergamon: Oxford, 1979.

(287) Lugo, M. L.; Lubes, V. R. *J. Chem. Eng. Data* **2007**, *52*, 1217.

(288) Fiol, S.; Brandariz, I.; Herrero, R. F.; Vilarino, T.; Sastre de Vicente, M. E. *J. Chem. Eng. Data* **1995**, *40*, 117.

(289) Perrin, D. D. *Journal of the Chemical Society (Resumed)* **1958**, 3125.

(290) Baldini, L.; Cacciapaglia, R.; Casnati, A.; Mandolini, L.; Salvio, R.; Sansone, F.; Ungaro, R. *J. Org. Chem.* **2012**, *77*, 3381.

(291) Frenna, V.; Vivona, N.; Consiglio, G.; Spinelli, D. *Journal of the Chemical Society, Perkin Transactions 2* **1985**, 1865.

(292) Pratt, D. A.; Pesavento, R. P.; van der Donk, W. A. *Org. Lett.* **2005**, *7*, 2735.

(293) Albert, A.; Hampton, A. *Journal of the Chemical Society (Resumed)* **1954**, 505.

(294) Albert, A.; Goldacre, R.; Phillips, J. *Journal of the Chemical Society (Resumed)* **1948**, 2240.

(295) Feng, Y.; Wang, Y.; Landgraf, B.; Liu, S.; Chen, G. *Org. Lett.* **2010**, *12*, 3414.

(296) Bühl, M.; DaBell, P.; Manley, D. W.; McCaughan, R. P.; Walton, J. C. *J. Am. Chem. Soc.* **2015**, *137*, 16153.

(297) Lapointe, D.; Fagnou, K. *Chem. Lett.* **2010**, *39*, 1118.

(298) Narayana Murthy, V.; Nikumbh, S. P.; Praveen Kumar, S.; Vaikunta Rao, L.; Raghunadh, A. *Tetrahedron Lett.* **2015**, *56*, 5767.

(299) Ayres, J. N.; Ashford, M. W.; Stöckl, Y.; Prudhomme, V.; Ling, K. B.; Platts, J. A.; Morrill, L. C. *Org. Lett.* **2017**, *19*, 3835.

(300) Maestri, G.; Larraufie, M.-H.; Ollivier, C.; Malacria, M.; Fensterbank, L.; Lacôte, E. *Org. Lett.* **2012**, *14*, 5538.

(301) Szymański, P.; Frączek, T.; Markowicz, M.; Mikiciuk-Olasik, E. *BioMetals* **2012**, *25*, 1089.

(302) Oeser, E. A.; Tuck, J. L. *Nature* **1937**, *139*, 1110.

(303) Cui, X.-Y.; Tan, C.-H.; Leow, D. *Org. Biomol. Chem.* **2019**, *17*, 4689.

(304) Gray, A.; Tsybizova, A.; Roithova, J. *Chem. Sci.* **2015**, *6*, 5544.

(305) Saget, T.; Lemouzy Sébastien, J.; Cramer, N. *Angew. Chem. Int. Ed.* **2012**, *51*, 2238.

(306) Finkelstein, H. *Ber. Dtsch. Chem. Ges.* **1910**, *43*, 1528.

(307) Eschweiler, W. *Ber. Dtsch. Chem. Ges.* **1905**, *38*, 880.

(308) Iemura, R.; Kawashima, T.; Fukuda, T.; Ito, K.; Tsukamoto, G. *J. Med. Chem.* **1986**, *29*, 1178.

(309) Clark, P. R.; Williams, G. D.; Tomkinson, N. C. O. *Org. Biomol. Chem.* **2019**, *17*, 7943.

(310) Taber, D. F.; Ruckle, R. E.; Hennessy, M. J. *J. Org. Chem.* **1986**, *51*, 4077.

(311) Wang, Y.; Deng, L.; Deng, Y.; Han, J. *J. Org. Chem.* **2018**, *83*, 4674.

(312) Rodríguez-Rodríguez, M.; Gras, E.; Pericàs, M. A.; Gómez, M. *Chem. Eur. J.* **2015**, *21*, 18706.

(313) Cailleux, P.; Piet, J. C.; Benhaoua, H.; Carrié, R. *Bull. Soc. Chim. Belg.* **1996**, *105*, 45.

(314) Wang, T.; Ueda, Y.; Zhang, Z.; Yin, Z.; Matiskella, J.; Pearce, B. C.; Yang, Z.; Zheng, M.; Parker, D. D.; Yamanaka, G. A.; Gong, Y.-F.; Ho, H.-T.; Colonno, R. J.; Langley, D. R.; Lin, P.-F.; Meanwell, N. A.; Kadow, J. F. *J. Med. Chem.* **2018**, *61*, 6308.

(315) Kamijo, S.; Huo, Z.; Jin, T.; Kanazawa, C.; Yamamoto, Y. *J. Org. Chem.* **2005**, *70*, 6389.

(316) Cheng, G.; Zeng, X.; Shen, J.; Wang, X.; Cui, X. *Angew. Chem. Int. Ed.* **2013**, *52*, 13265.

(317) Jana, S.; Thomas, J.; Dehaen, W. *J. Org. Chem.* **2016**, *81*, 12426.

(318) Wang, L.; Peng, S.; Danence, L. J. T.; Gao, Y.; Wang, J. *Chem. Eur. J.* **2012**, *18*, 6088.

(319) Fredrich, S.; Göstl, R.; Herder, M.; Grubert, L.; Hecht, S. *Angew. Chem. Int. Ed.* **2016**, *55*, 1208.

(320) Muxfeldt, H.; Weigele, M.; Rheenen, V. V. *J. Org. Chem.* **1965**, *30*, 3573.

(321) Thomas, J.; Jana, S.; Liekens, S.; Dehaen, W. *Chem. Comm.* **2016**, *52*, 9236.

(322) Hu, H.; Ohno, A.; Sato, T.; Mase, T.; Uozumi, Y.; Yamada, Y. M. A. *Org. Process. Res. Dev.* **2019**, *23*, 493.

(323) Reeder, Z. K.; Adler, A. M.; Miller, K. M. *Tetrahedron Lett.* **2016**, *57*, 206.

(324) Nagaradja, E.; Bentabed-Ababsa, G.; Scalabrini, M.; Chevallier, F.; Philippot, S.; Fontanay, S.; Duval, R. E.; Halauko, Y. S.; Ivashkevich, O. A.; Matulis, V. E.; Roisnel, T.; Mongin, F. *Bioorg. Med. Chem.* **2015**, *23*, 6355.

(325) Zhang, N.-N.; Sun, C.; Jiang, X.-M.; Xing, X.-S.; Yan, Y.; Cai, L.-Z.; Wang, M.-S.; Guo, G.-C. *Chem. Comm.* **2017**, *53*, 9269.

(326) Yamajala, K. D. B.; Patil, M.; Banerjee, S. *J. Org. Chem.* **2015**, *80*, 3003.

(327) Medaer, B. P.; Van Aken, K. J.; Hoornaert, G. J. *Tetrahedron* **1996**, *52*, 8813.

(328) Galli, U.; Mesenzani, O.; Coppo, C.; Sorba, G.; Canonico, P. L.; Tron, G. C.; Genazzani, A. A. *Eur. J. Med. Chem.* **2012**, *55*, 58.

(329) Greulich, T. W.; Daniliuc, C. G.; Studer, A. *Org. Lett.* **2015**, *17*, 254.

(330) F. Ke, C. L., J. Xu, X. Chen, S. Xu, Y. Xu China, 2018; Vol. CN107954939.

(331) Gross, M.; Held, P.; Schubert, H. *J. Prakt. Chem.* **1974**, *316*, 434.

(332) J. Diaz, D. H., J. Speake,C. Zhang, W. Mills, P. Spearing, D. Cowan, G. Green. 2010; Vol. US222345.

(333) Montalvão, S.; Leino, T. O.; Kiuru, P. S.; Lillsunde, K.-E.; Yli-Kauhaluoma, J.; Tammela, P. *Archiv der Pharmazie* **2016**, *349*, 137.

(334) Joseph, L.; Albert, A. H. *J. Het. Chem.* **1966**, *3*, 107.

(335) Zhu, J.; Wu, C.-F.; Li, X.; Wu, G.-S.; Xie, S.; Hu, Q.-N.; Deng, Z.; Zhu, M. X.; Luo, H.-R.; Hong, X. *Bioorg. Med. Chem.* **2013**, *21*, 4218.

(336) Clayden, J.; Pink, J. H.; Westlund, N.; Frampton, C. S. *J. Chem. Soc., Perkin Trans. 1.* **2002**, 901.

(337) Wagner, P. J.; Park, B.-S.; Sobczak, M.; Frey, J.; Rappoport, Z. *J. Am. Chem. Soc.* **1995**, *117*, 7619.

(338) S. Bradamante; S. Colombo; G. A. Pagani; Roelens, S. *Gazz. Chim. Ital.* **1981**, *111*, 357.

(339) Ayres, J. N.; Williams, M. T. J.; Tizzard, G. J.; Coles, S. J.; Ling, K. B.; Morrill, L. C. *Org. Lett.* **2018**, *20*, 5282.

(340) Liang, H.; Bao, L.; Du, Y.; Zhang, Y.; Pang, S.; Sun, C. *Synlett* **2017**, *28*, 2675.

(341) Iemura, R.; Hori, M.; Ohtaka, H. *Chem. Pharm. Bull.* **1989**, *37*, 962.

(342) R. Iemura, T. K., F. Toshikazu, K. Ito, T. Nose, G. Tsukamoto 1982; Vol. US4430343.